VOLCANIC AND SEDIMENTARY PROCESSES IN PHREATOMAGMATIC VOLCANOES

by

CLYDE ANDREW LEYS

A thesis submitted in fulfilment of the requirements
for the degree of Doctor of Philosophy

The University of Leeds, Department of Earth Sciences

October, 1982

ABSTRACT

Phreatomagmatic volcanoes form when ascending magma explosively interacts with surface or groundwater at shallow depths. Three types of phreatomagmatic activity are recognised- phreatic, phreatomagmatic (s.s.) and surtseyan - based on the degree of involvement of magma with water and the depth of the interaction. Phreatic maars and phreatomagmatic tuff-rings are underlain by pipe-like diatremes but these structures are poorly-developed or absent in surtseyan tuff-rings. Comparisons of phreatomagmatic volcanoes with their eroded diatreme equivalents, which contain subsided subaerially-deposited material, allow a model for activity of this type to be constructed.

The Saefell tuff-ring, SW Iceland, is a surtseyan-type structure whose crater remained open to the sea during most of its activity, allowing easy access of water to the magma. Base-surges, sourced partly from directed blasts, formed large dunes with internal structures indicating deposition by density currents whose flow-power decreased with time and with distance from the vent. Syndepositional slumping and minor en masse collapse of crater deposits formed a pile of massive tuffs above which subsequent surge and airfall activity deposited a nested, inner crater rim.

The Medano tuff-ring, Tenerife, is a phreatomagmatic-type structure whose crater contains reworked tuffs deposited during subsidence into the underlying diatreme. Initial activity ejected much country rock material as magma contacted groundwater at depth but with time eruptions became more strombolian, as water was used up or failed to gain access to the vent. Surges were less common than in the Saefell eruption because the Medano water:magma ratio and explosion depth less often fulfilled the optimum conditions for surge production.

The East Lothian diatremes in Scotland are subdivided into two groups on the basis of their infilling. The Red group diatremes contain high proportions of sediment and

represent the subsided products of phreatic maars which erupted into a pile of water-rich, poorly-consolidated alluvial plain sediments. The later Green group diatremes contain mainly juvenile basalt fragments and formed as phreatomagmatic or sometimes surtseyan tuff-rings, due to magma contacting water at shallow depths or in marginal lakes respectively. The Parade diatreme, Dunbar, contains over 300m of largely base-surge tuffs thought to represent the subsided inner flank deposits of a large maar.

The Heads of Ayr and the East Fife diatremes expose different levels in subsided phreatomagmatic tuff-rings due to collapse and erosion. Deep levels, such as that exposed at Lundin Links, contain unbedded tuffs and abundant intrusive material. Shallower levels, such as at Elie Ness, contain high proportions of bedded tuffs which are often centroclinally orientated. Base-surge, airfall, slumped and reworked tuffs in the Scottish diatremes are directly comparable to deposits in the modern tuff-rings studied, proving their origin.

A model for the formation of surtseyan tuff-rings is presented, with phreatomagmatic explosions resulting from steam expansion jets which disrupt an already vesiculating magma as it engulfes subsiding water-laden ash. A base-surge model is also presented, involving deposition of tuffs with characteristic bedforms and structures by the head, body and tail of each surge, analogous to turbidity currents. Cooling of hot, dry steam to cool, moist steam towards the rear of surge pulses leads to lag breccias and progressive dune deposits being succeeded by regressive dunes and plastering structures with time.

Juvenile sideromelane fragments erupted by phreatomagmatic volcanoes rapidly alter to palagonite as heated pore-waters circulate through the newly-deposited tuffs. Palagonitization results in cation mobility within unstable glass and precipitation of authigenic minerals in voids. Non-equilibrium growth of such minerals results in variable compositions and crystal forms. Subsequent alteration occurs slowly as a weathering process whose rate is greatly reduced as authigenic precipitation closes pore

spaces within the tuffs. On diagenesis, unstable alteration products are commonly replaced by chlorite, calcite and clay. Reddening of some tuffs occurs by in situ breakdown of iron-bearing minerals and release of Fe to solution, although groundwater exchange with red country rock sediments may also occur.

Unless present in diatremes, phreatomagmatic products have a low preservation potential due to :- extreme alteration, rapid syn- and post-volcanic reworking, low ejecta volumes and breaching and burial beneath later lavas. In contrast, the sedimentary structures, petrography, morphology and grain size characteristics of diatreme tuffs are shown to be often sufficiently well preserved to permit the identification of their original surface volcanoes and their eruptive histories.

ACKNOWLEDGEMENTS

First of all I would like to thank the joint supervisors of this project, Howel Francis and Mike Leeder. I thank Howel for introducing me to the Scottish diatremes and for improving the geology and the English in this and other reports. Mike has always proved ready to listen to my often garbled thoughts and I especially thank him for discussing and simplifying many of the research problems.

In the field many people have provided constructive criticism and advice about the project. Steve Sparks introduced me to the field study of pyroclastics on the V.S.G. Italy trip in 1979. Volker Lorenz kindly acted as a guide to the Eifel volcanics and inspired some of the ideas in this thesis. In Iceland and Scotland the "Yobs" : Peter Kokelaar, Malcolm Howells, Chris Stillman, Richie Bevins, Bob Roach, Graham Durant and Roger Suthren provided helpful comments on tuff-rings and diatremes. Discussions with Peter Kokelaar in particular have improved my ideas on magma:water interaction and I thank him for all his advice and criticism of my work.

In Leeds, various people have patiently listened to my thoughts and for this I thank in particular : Russell Alexander, Kevin Downing, Ian Luff, Richard Morgan, Pete Nixon, Marge Powell and Pete Ruxton. On the technical side I thank Finlay Johnston for all his help and humourous advice, Alan Gray for XRF analyses and David Bailey for photographic assistance. Thanks also to Eric Condliffe for guiding me in the use of the microprobe and for suggesting the benefits of the Digimap facility. Special mention must be made of the thin section technicians who made excellent slides from often difficult material.

For logistical aid I thank Gordon Ridley, whose B.S.A.C. trip to Iceland enabled me to visit Surtsey, and to the Surtsey Research Council for permission to do so.

Love and thanks are especially due to Marion, who typed this tome and put up with me during the many evenings spent drawing diagrams and maps.

Finally I acknowledge the funding for this project given by the Natural Environmental Research Council.

CONTENTS

CHAPTER 1
INTRODUCTION

1.1. Aims of the Study

This study was initiated to determine the volcanic and sedimentary processes which occur during the formation and evolution of phreatomagmatic volcanoes. Such volcanoes generally consist of a surface expression - a maar or a tuff-ring, and a sub-surface structure - a diatreme. During and after volcanic activity surface products subside into the diatreme which underlies the volcano. Diatreme deposits thus contain much information about the depositional processes which formed their now eroded surface expressions, and their study also indicates the nature of sub-surface volcanic processes which can never be directly observed.

Recent tuff-rings on Iceland and Tenerife were studied to characterise the range of primary volcanic and sedimentary reworking processes which affect these pyroclastic volcanoes. Numerous diatremes in Scotland were studied to determine their origin and to examine the types of sub-surface processes which formed them.

Comparisons between modern and ancient examples of phreatomagmatic volcanoes allow an idealised model to be constructed for activity of this type. Differences between the model and specific volcanoes may be interpreted in terms of variations in geological setting, eruption style and collapse history. Such a model can also be used to indicate the possible variations in modern activity of this type and to provide information useful in identifying phreatomagmatic deposits in the geological record.

1.2. Methods of Study

The Recent tuff-rings were mapped in detail using aerial photographs and enlarged base maps at scales of 1:10,000 to 1:20,000. The diatremes, for which some detailed base maps already exist, were mapped at scales of 1:2500 to 1:3500 from aerial photographs. Mapping was supplemented by logging of much of the bedded tuff sequences and examination of the sedimentary structures

to determine their depositional mechanism.

Representative samples were collected for petrographic examination, which included modal and grain-size analyses of the tuffs. Grain morphology was quantitatively studied in thin section and in more detail by S.E.M. Limited microprobe analyses were carried out on selected mineral phases, especially on alteration products. Microprobe element variation maps were used to study the movement of cations during the alteration of sideromelane to palagonite.

1.3. Previous Work

Studies of tuff-rings, maars and diatremes have been carried out since the last century but it was not until recently that the role of groundwater in their formation was recognised. Lorenz et al. (1970), in a broad-based review of these volcanoes, summarised much of the previous literature along with many of their own field observations. They were amongst the first authors to discuss and relate both surface and sub-surface volcanic features.

The literature on observed phreatic and phreatomagmatic eruptions has greatly increased in recent years with the advent of improved communications, which allow geologists easier access to often remote volcanoes. The most recent example is that of Mt. St. Helens which involved intermittent steam-blast eruptions (Christiansen & Peterson, 1981). These observations may be used to indicate the types of processes which occur during volcanism.

Various aspects of phreatomagmatic (s.l.) activity have been the study of more detailed recent work. Base-surge deposits and their relevance to surge dynamics and processes have been extensively studied (Moore, 1967; Waters & Fisher, 1971; Schmincke et al., 1973; Sheridan & Updike, 1975; Fisher, 1977). The alteration of basaltic glass, although not confined to phreatomagmatic deposits, is nevertheless an important process in their post-eruptive history. Such alteration has been studied in historic eruptive products, such as Surtsey, Iceland (Jakobsson, 1978) and in more ancient tuff-rings, such as Oahu, Hawaii (Hay & Iijima, 1968).

1.4. Layout of Thesis

In a comparative study of this type the volcanoes from each area are treated separately. Each chapter is thus complete in itself although the diatreme studies draw heavily on information presented in the chapters on Recent tuff-rings. Important features of each area are discussed in the appropriate chapter although general considerations about the origin and evolution of phreatomagmatic volcanoes are presented as a model for this type of activity.

A brief review of observed phreatomagmatic activity is presented in Chapter 4 as a summary of the processes known to occur. The final chapter (Chapter 8) is a summary of the more important conclusions drawn from each data chapter as well as the main points of the review and model chapters. The appendices contain details of the analytical methods used and the pocket at the back of the thesis contains a general lithological key to the diatreme maps and the logs for bedded tuff sequences throughout the thesis.

1.5. Definitions

Since the terminology of pyroclastic deposits is as yet ill-defined it is thought necessary to define much of the nomenclature used in this thesis. The definitions used largely come from Lorenz et al. (1970), Lorenz (1973), Wright et al. (1980) and Schmid (1981).

Diatreme :- A pipe-like volcanic conduit filled with pyroclastic debris and brecciated wall rocks, which are often cut by intrusions.

Fluidization :- A process in which a mixture of particles (solid or liquid) is suspended by an upward escaping fluid phase (liquid or gas) so that the frictional force between the fluid and the particles counterbalances the weight of the particles and the whole mass behaves as a fluid.

Hyaloclastite:- A glassy clastic rock formed by the non-explosive quench granulation of magma on contact with water.

Hyalotuff :- A glassy pyroclastic rock formed by the explosive interaction of magma and water at shallow depths where volatile exsolution has already partly fragmented the magma.

Maar :- A large volcanic crater cut into country rock below general ground level and possessing a low rim composed of pyroclastic debris. Approximate dimensions are - 100 to 200m wide, 30 to 200m deep, with a rim height of 10 to 100m.

Phreatic eruption :- Eruptive activity caused by steam explosions due to heating of water, generally by magmatic intrusions or extrusions. The magma acts purely as a heat source and is not intimately involved in the eruption. Comminuted country rock material is commonly ejected by these explosions.

Phreatomagmatic eruption :- An eruption similar to phreatic activity except that magma is intimately involved in the eruption and chilled juvenile material is ejected. In its wider sense (sensu lato) it is used to describe all types of pyroclastic eruptions resulting from the contact of water with magma.

Pyroclastic surge :- A low-concentration tephra flow that travels outwards from a volcanic vent as time-transient pulses in which the kinetic energy rapidly decays. Base-surges are a particular form of these flows which result from phreatomagmatic eruptions, and are highly charged with steam.

Scoria :- Vesiculated fragments of basalt or basaltic andesite composition which are the basic analogues of pumice. Many fragments are glassy and consist largely of tachylite. Blocky, sparsely-vesicular phreatomagmatic tephra composed largely of sideromelane is distinct from scoria although it has as yet no short descriptive term.

Strombolian :- A type of eruption which involves ejection of liquid magma droplets by volatile exsolution and bubble coalescence. Eruptions typically form small scoria cones.

Surtseyan :- A type of eruption which is characterised by phreatomagmatic activity (s.l.) and the formation of a tuff-ring. In this thesis the term is restricted to those tuff-rings formed as a result of phreatomagmatic activity when water contacted shallow surface water bodies.

Tuffisite :- Intrusive tuff composed of juvenile and lithic fragments mobilised by gas-streaming and injected into fissures.

Tuffite :- A mixed pyroclastic/epiclastic rock containing between 25% and 75% of epiclastic material. The term is the mixed tuff-epiclastic analogue of pyroclastic and is subdivided by average clast size into tuffaceous shales to tuffaceous conglomerates.

Tuff-ring :- A large volcanic crater above general ground level surrounded by a ring-like rim of phreatomagmatic debris and similar in size to maars.

CHAPTER 2
THE SAEFELL TUFF-RING, ICELAND

2.1. Introduction and Geological Setting

The Saefell tuff-ring occurs on Heimaey, the largest of the Westmann Islands which lie off the SW coast of Iceland (Fig. 2.1a). The islands constitute part of the Pleistocene to Recent Vestmannaeyjar volcanic system, situated at the SE end of Iceland's Eastern Volcanic Zone. This system is characterised by the eruption of mildly alkaline olivine basalt, although most recently (1973) Eldfell on Heimaey has erupted hawaiites (Jakobsson, 1979). Most of the islands are eroded tuff-rings, some of which have later scoria cones associated with them. Heimaey is composed of lavas and tuffs of various ages and origins (Jakobsson, 1968).

On Heimaey (Fig. 2.1b) the oldest formations (>10,000yrs. B.P.) occur in the N of the island and are partly of sub-glacial origin, formed before the last major glacial retreat. The Storhofdi volcano in the S of the island was formed next and consists of a tuff-ring with late-stage lava extrusion; ^{14}C dating of peat immediately overlying these lavas gives an age of about 5400 B.P. (Kjartansson, 1967). This was shortly followed by the Saefell phreatomagmatic activity and soon afterwards by the formation of Helgafell, a composite scoria cone whose lavas form the central section of the island. No further activity occurred until the formation of the Eldfell scoria cone in 1973 whose lavas added a substantial area onto the NE coast of the island.

Although the Surtsey eruption has been well documented the only published work on Saefell is by Jakobsson (1968) who recognised its phreatomagmatic origin and briefly mentioned its age and petrographic character.

2.2. Structure and Products

The tuff-ring (Fig. 2.2) presently has a maximum basal diameter of ca.2·9km, a maximum height of 188m and a maximum crater diameter of ca.1·4km. The crater rim is a

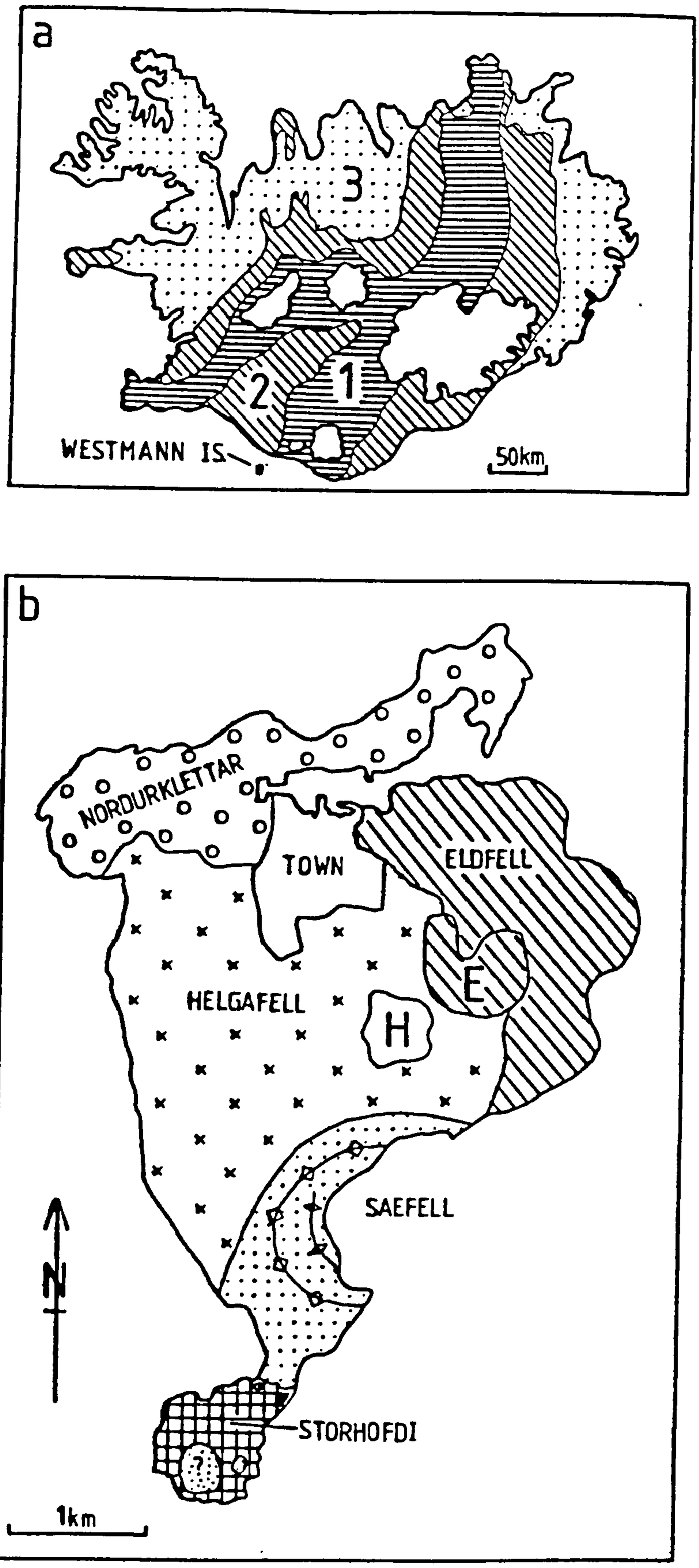

Fig. 2.1 a) Map of Iceland showing position of Westmann Is.

1: Postglacial Volcanic zone
2: Plio-Pleistocene formations
3: Tertiary formations

b) Geological map of Heimaey.

simple anticlinal structure in the youngest tuffs which occurs where indipping crater tuffs bend over and pass into the outdipping, flank succession. The indipping tuffs are more steeply inclined (up to 40°) than the outdipping beds (up to 30°) due to syndepositional slumping steepening the depositional surface onto which crater tuffs were deposited, and to later collapse processes.

2.2.1 Crater tuffs

Only the western crater wall tuffs are presently exposed, erosion, especially by marine processes, having removed the eastern rim and most of the crater centre deposits. Two small islands about 600m offshore provide the only exposures of eastern crater tuffs. In the N the crater deposits are thin (<30m) or may occur as isolated veneers overlying the face of the outdipping tuffs exposed on the crater wall (Fig. 2.2). A minor nested rim occurs within the crater in the W, sub-concentric with the main rim. It seems to have formed by deposition of younger tuffs over a pile of collapsed crater deposits.

2.2.2 Flank tuffs

The flank tuffs are well exposed in the coastal cliffs to the NE, S and SW of the crater. The flank tuffs are presently asymmetrically distributed about the crater, the youngest tuffs occuring mainly to the W and SW. To the N and W the tuffs are overlain by Helgafell lavas as they thin away from the crater and their distal equivalents are thus not exposed. To the SW the most distal tuffs are preserved and outcrop above the Storhofdi lavas. The present day topography largely follows the upper bedding surfaces of the youngest flank tuffs though outcrops inland are poor due to a thin soil and grass cover.

2.2.3 Crater rim

The crater rim is a ridge-like anticlinal feature defining the passage from the indipping crater tuffs to the outdipping flank tuffs along the crest of the tuff-ring.

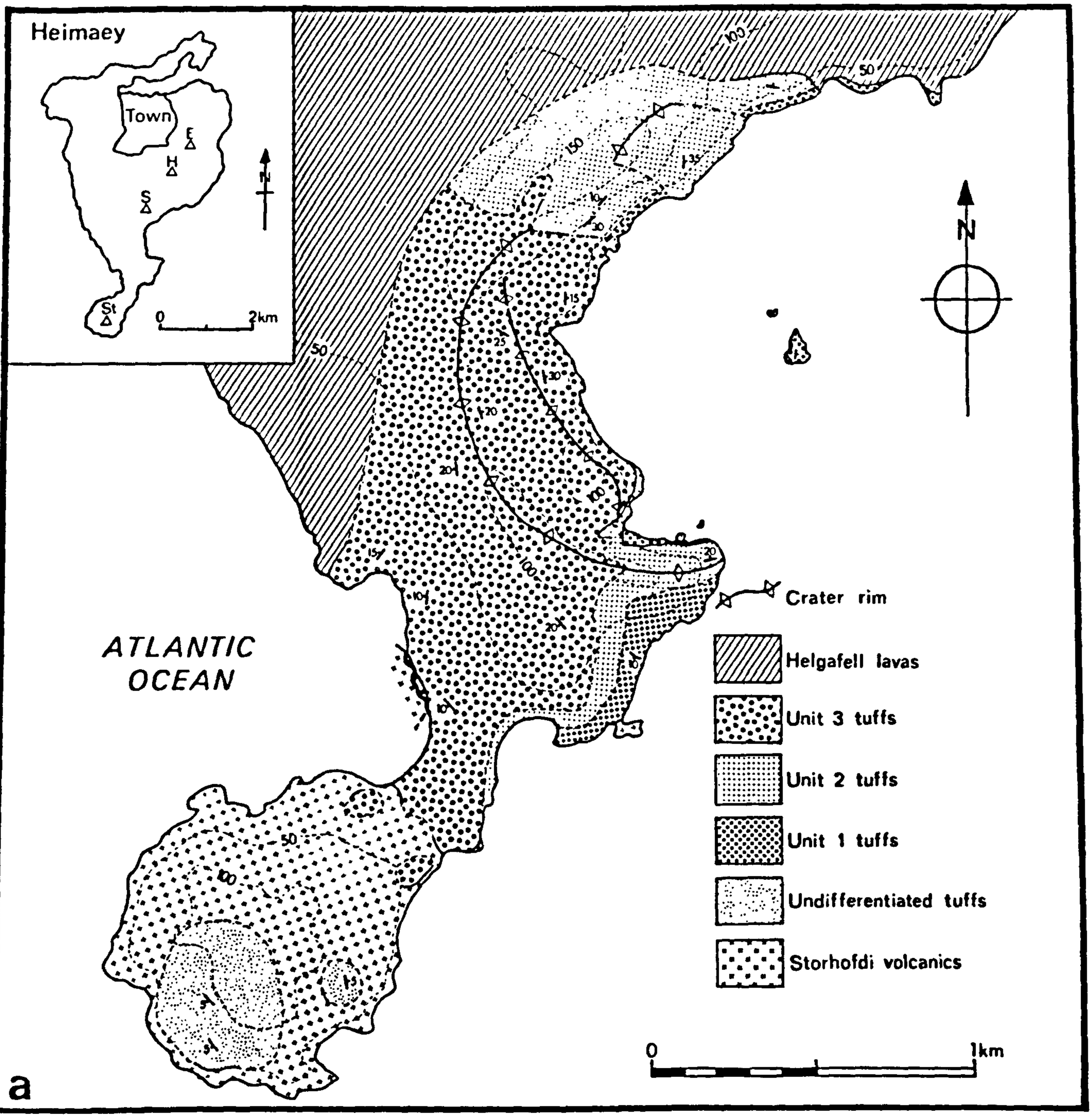

Fig. 2.2 a)Geological map of the Saefell tuff-ring.
b)Cross-sections of Saefell showing Units 1, 2 and 3 (stippled). a: Main crater rim b: Inner crater rim

At deeper structural levels the contact of the crater and flank tuffs is an unconformity caused by slippage of indipping tuffs down the crater wall. At the lowest exposed structural level the contact is a 3-5m zone of blocky, shattered tuffs indicating that fault subsidence has occured. These blocky tuffs may originally have been debris flows since they wedge out upslope (Fig. 2.3) and have a broadly conformable, unfaulted upper contact with the overlying bedded indipping tuffs. Ring-fault subsidence occured after lithification of the blocky deposits and caused the shattering of the matrix and the break up of blocks within them.

2.2.4 Individual units

The tuffs have been subdivided into three units on the basis of their field relationships as seen on the southern side of the crater rim (Figs. 2.2, 2.3). Each unit unconformably overlies the unit below in the crater rim sequence, mainly because of syndepositional slumping of poorly consolidated tuffs into the crater along with minor erosion. Outwards from the crater all the units are conformable and are difficult to distinguish because of lithological similarity. The schematic cross-section (Fig. 2.2b) summarises the stratigraphic relationships between each unit.

Unit 1

This oldest exposed unit is composed of ca.40m of bedded tuffs which dip away from the crater at 5-10°. Their indipping equivalent has slumped into the crater and is not now exposed. Unit 1 is exposed along the SE coastline of Heimaey but could only be definitely recognised S of the crater by tracing it away from the rim where it thins to < 1m thick at a distance of 600m. The basal tuffs overlie eroded, columnar-jointed lava flows of the Storhofdi complex and are largely of base-surge origin with well developed plastering structures and ripples. A soil horizon (maximum thickness of 1m) occurs within some hollows in the lava top. It consists of an approximately 30cm thick basal orange-brown layer rich in rootlets and

altered scoria lapilli overlain by a buff-coloured fine dust horizon which contains many desiccation cracks. The top of the soil consists of a thin (<10cm) peaty layer rich in twigs, rootlets and leaf remains which passes into scoria layers in a matrix of grey, fine ash. This soil is only developed at the top of the lava cliffs some 20-40m above sea-level. It is not present where the Saefell tuffs - Storhofdi lava contact occurs near the present day sea-level. Here, joints in the lava surface are partly filled by unbedded impure tuff rich in sediment and scoriaceous material and overlain by thinly bedded ash which is often plastered against the sides of the cracks.

Above the soil horizon and the joint infilling material exposed on the wave-cut platform on the SW coast of Heimaey there is a thin (<10cm) layer of fine ash full of broken up fossilised grass stems. These grass stems are often aligned and plastered against the sides of lava joint faces and blocks, and will be further described in the section on base-surge structures (Section 2.3.2). These grass-rich layers are not found in the basal Saefell tuffs where these are exposed ca.500m SW of the southern crater rim on the SW coast of Heimaey (Fig. 2.4). This is because the grass grew on soil developed on the subaerially exposed Storhofdi lavas to the NW and W of this outcrop. Surges which deposited tuffs there had not yet entrained any stems.

The Unit 1 tuffs above the basal layers consist mainly of base-surge material with interbedded airfall deposits. One now greatly eroded scoria cone erupted through the thin distal flank tuffs 1100m SW of the crater centre. To the S the scoria layer rests on the older underlying lavas whereas the northern deposit is underlain by at least 6m of bedded tuffs (Fig. 2.5). The section indicates that erosion of an originally much larger scoria deposit, sourced near the welded spatter in the S would account for the present outcrops of scoria. Removal of scoria which originally mantled the buried lava hill formed the present break in the deposits. The scoria layers consist of a small area of welded spatter along

with lapilli and bombs of plagioclase-phyric basalt, although some rare accessory lithic lava blocks occur in places.

The maximum exposed thickness of scoria is <10m but because of erosion this is probably much less than the original maximum thickness. U-shaped channels which cut the top 1m of the scoria indicate that some reworking by base surges occurred but such examples are only patchily developed. The bulk of the reworking, causing rapid lateral thickness variations and much interfingering of scoria with thin tuff layers is thought to have been caused by fluvial activity.

The scoria formed during a break in the phreatomagmatic activity. Perhaps lateral migration of magma away from the main chamber initiated the flank eruptions. The absence or exclusion of water allowed strombolian activity to occur, probably because the parasitic vents erupted subaerially on the previously formed Storhofdi island (Fig. 2.4).

The Unit 1 tuffs above the scoria reach up to 40m thick in the southern crater rim and are well-bedded throughout. In the northern crater wall sequence Unit 1 tuffs probably form at least the lower 40m of the deposits. Due to the lack of correlatable horizons their existance and thickness cannot be proven.

Unit 2

This sequence of well-bedded tuffs unconformably overlies Unit 1 in the crater rim (Figs. 2.2, 2.3). Infilling of hollows in the partly collapsed crater rim of Unit 1 causes the lower beds of the Unit 2 outdipping sequence (Fig. 2.3, 2a) to thicken laterally by as much as 30m. The indipping equivalents of these lower beds (Fig. 2.3, 2b) have slumped and are represented by debris flow fan deposits which wedge out up the slip plane. The upper part of the indipping sequence (Fig. 2.3) consists of ca. 45m of bedded tuffs. These conformably overlie the slumped indipping deposits, drape the crater rim and rest conformably on the lower Unit 2 tuffs of the outer flank sequence.

Fig. 2.3 Southern crater rim tuffs exposed on E coast of Heimaey. See text for description.

Well-bedded indipping tuffs of the southern crater wall sequence (Fig. 2.3, 2b) pass to the N into structureless blocky tuffs of >40m thickness (Fig. 2.3, St). Near the margin of the structureless pile the bedded tuffs are cut by sub-vertical faults with displacements up to 5m into the crater centre. These faults bound the structureless pile which contains faint traces of bedding broadly continuous with the well-bedded sequence to the SW. The pile is thought to have formed by differential movements on concentric faults within the originally well-bedded crater sequence. Some upthrow motions, perhaps due to minor resurgence, are invoked to explain the great thickness and severe bedding disruption within the pile. It is also possible that the pile is a relic of the collapsed crater centre sequence which has been agitated by explosions.

To the S of the crater rim, Unit 2 is generally poorly exposed. The Unit 2 tuffs are much better exposed in the cliffs along the northern crater wall. Here,

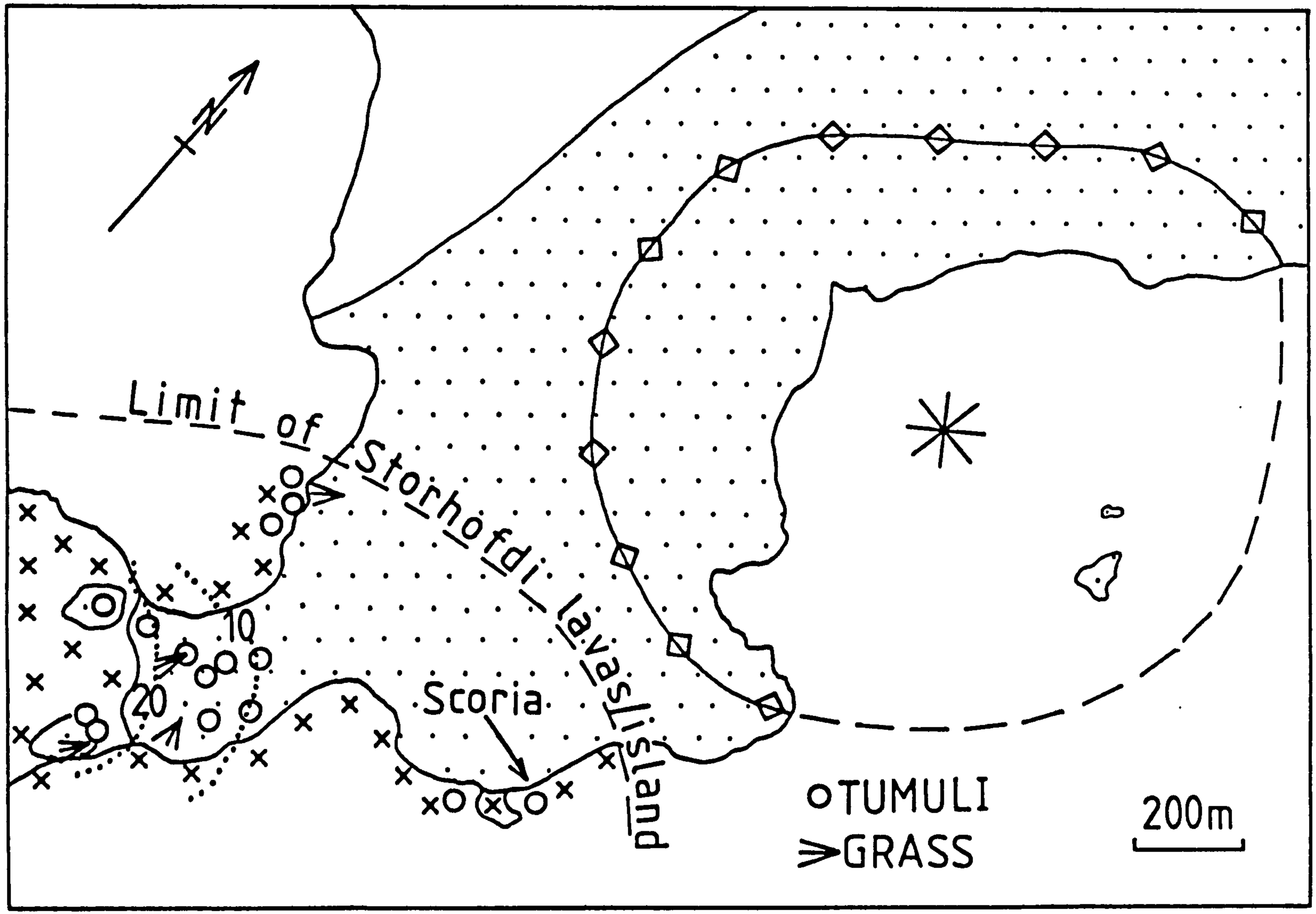

Fig. 2.4 Map of Saefell showing approximate shoreline of the Storhofdi lava island before burial beneath Saefell tuffs. Surge-transported grass stems found only where Storhofdi lavas were subaerially exposed W of the emerging tuff-ring.

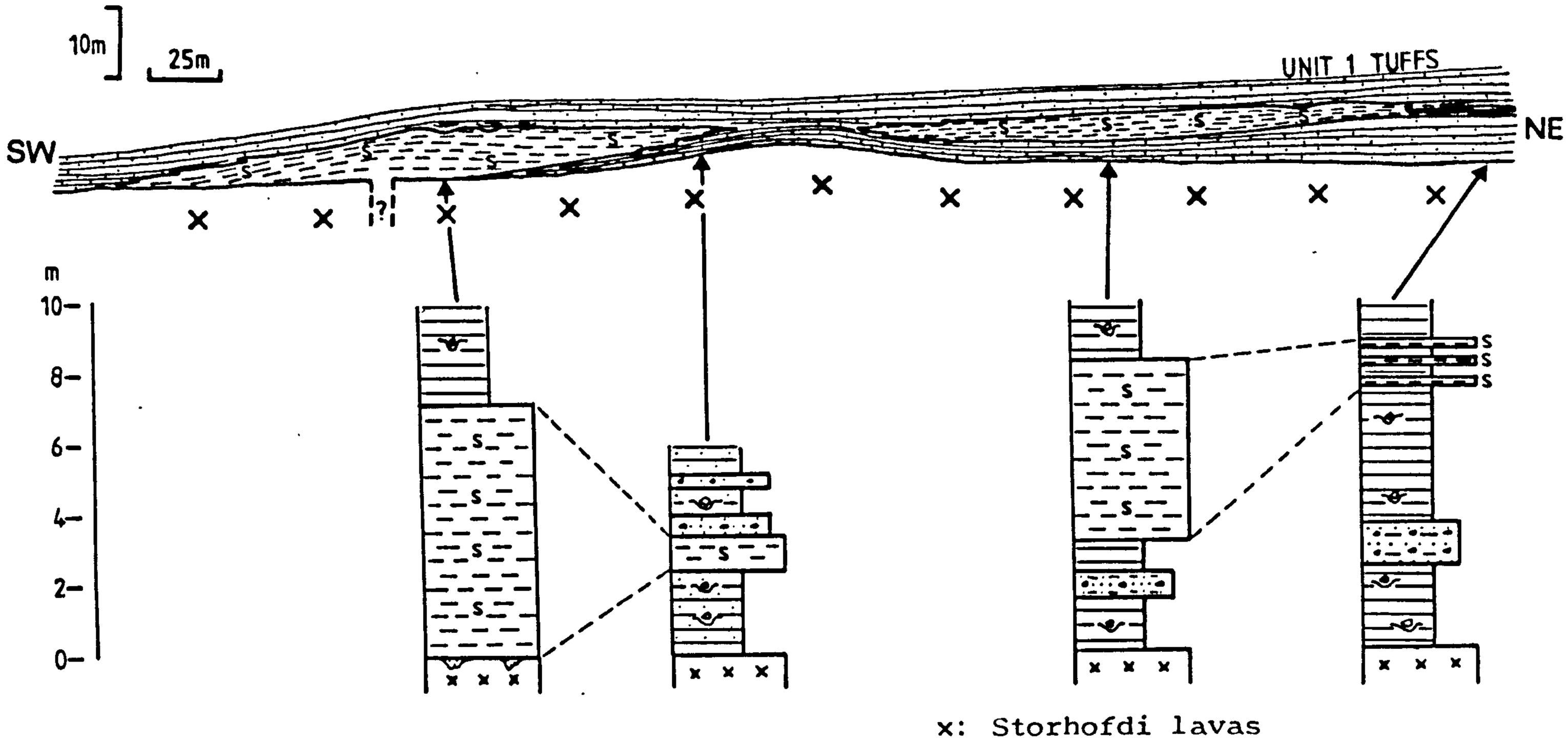

Fig. 2.5 Section of Unit 1 tuffs 500m S of the southern crater rim. Scoria (s) deposits wedge out over a lava mound mantled by tuffs to the NE of the presumed scoria source vent. Further NE the scoria deposits wedge out and interfinger with Unit 1 tuffs. Note exaggeration of vertical scale. See insert in back pocket of thesis for key to lithological logs.

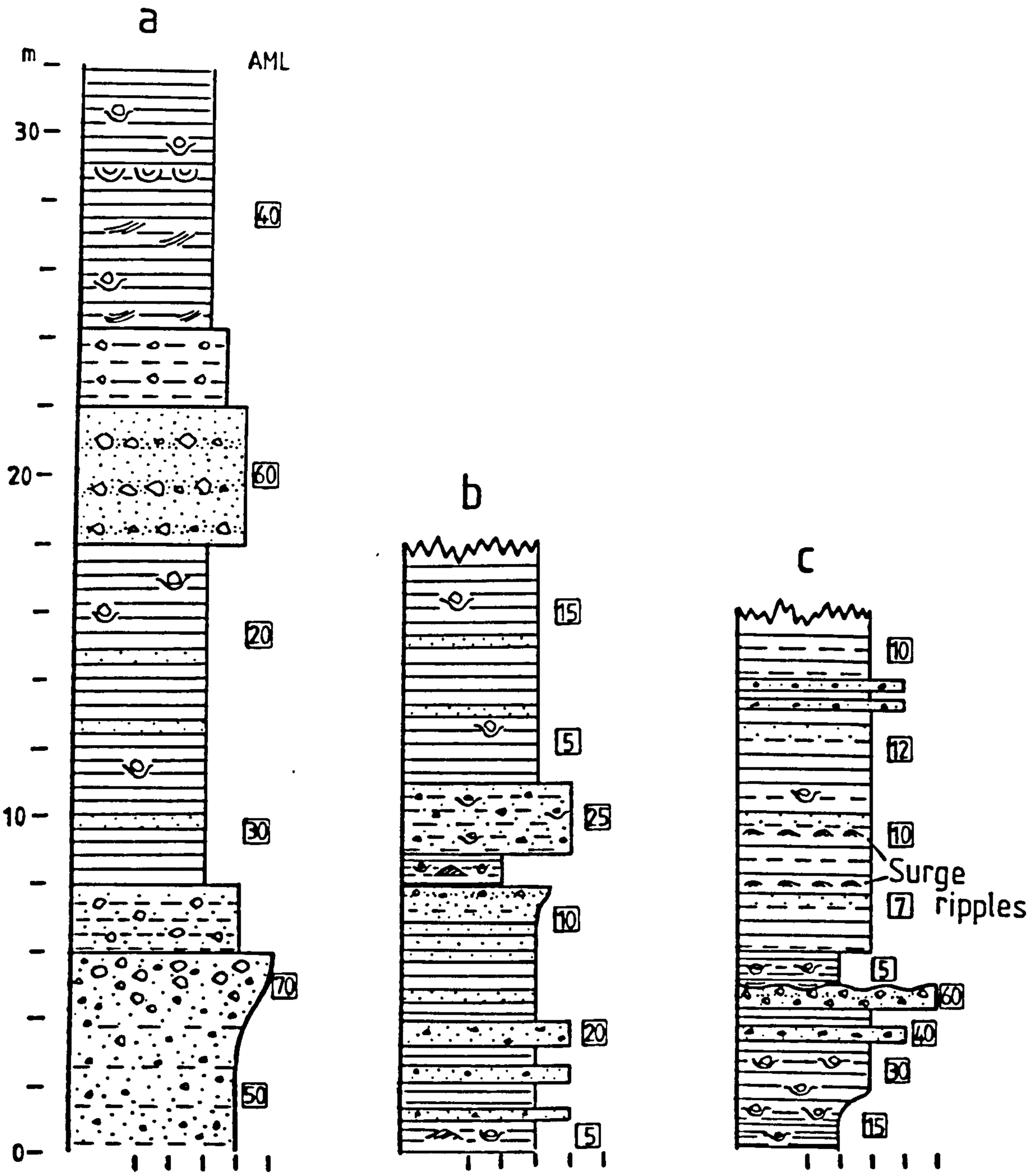

Fig. 2.6 Logs of Saefell tuffs.
a: Unit 2 indipping tuffs in southern part of crater
b: Unit 2 indipping tuffs in northern part of crater
c: Unit 3 tuffs within the crater
See insert in back pocket of thesis for key to lithological logs.

assuming Unit 1 to be 40m thick, the outdipping sequence of Unit 2 is ca.140m thick whereas in the southern crater rim it is ca.60m thick. This increased thickness is partly due to a lack of erosion in the N but may be partly the effect of SW-directed blasts. These increased the areal extent of Unit 2 to the SW and correspondingly reduced the topographic height of the rim in this direction.

In the N the Unit 2 outdipping tuffs form a monotonous pile of well-bedded, occasionally cross-bedded tuffs which vary from fine ash to blocky agglomerate in grain size (Fig. 2.6). Near the top of the unit a 4m scoria horizon occurs which is cut into by a >60m wide curved shear surface caused by slumping of tuffs into the crater (Fig. 2.7).

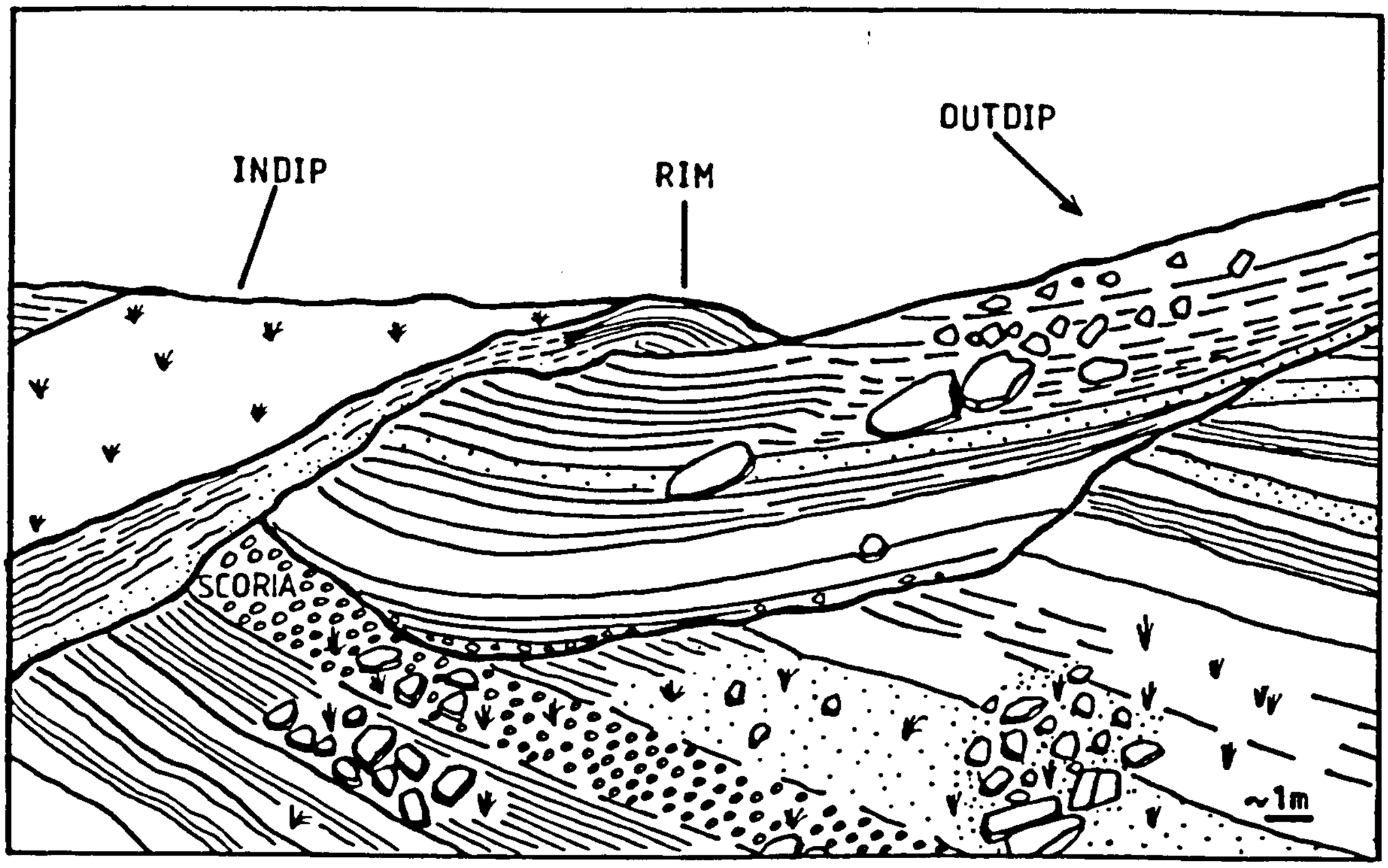

Fig. 2.7 Slump scar on northern crater rim, now partly mantled by Unit 2 indipping tuffs.

The base of the slumped material contains many blocks and some scoria fragments and is overlain by block-sagged layers bedded parallel to the margins of the shear surface. Mass movement must have occurred soon after deposition of the scoria whilst the overlying tuffs were moist and unconsolidated, giving rise to the curved shear plane similar to that seen in slumped clays. Deposition of the

succeeding tuffs infilled the slump scar and was accompanied by slumping of their indipping equivalents down the crater wall. The origin of the scoria layer is uncertain. Since it is completely conformable with the surrounding tuffs it was probably formed by very short-lived strombolian activity of the Saefell vent itself due to isolation of water from the magma. Such mixed activity has recently been described on Capelinhos, Azores by Camus et al.(1981).

Other slump scars exposed further to the E are more recent and are infilled by debris flows and occasionally by later lava flows. These Helgafell lavas flowed S over the eroded, scarred cliff face of the northern crater rim. They now drape the rim (Fig. 2.8), their high viscosity enabling them to dip at up to 40°. Collapse oversteepening of the crater tuffs and the later lavas may, however, have occurred.

Unit 3

This unit, well-bedded throughout, unconformably mantles eroded underlying collapsed tuffs within the crater (Fig. 2.3) where it has built a small, nested concentric rim inside the main rim (Fig. 2.2). The nested rim is a purely constructional feature built up as Unit 3 beds bend over from indipping to outdipping above the pile of collapsed tuffs below.

The unit occurs SW of the main Saefell summit and extends out to at least 1100m from the crater rim. From a maximum thickness of ca.40m within the crater, Unit 3 thins to <3m at its most distal exposure in the SW. The deposits contain some small internal unconformities in their oversteepened crater sequence but are usually conformable.

Mixed airfall and surge deposits near the crater give way to mainly surge derived material in the distal tuffs. Occasional blocky units beneath cross-bedded layers represent the coarse airfall components of the surge-forming eruptions which out-distanced the surges further from the vent and were deposited before them. Unit 3 tuffs do not persist to the N of the main Saefell summit, due to erosion and to SW-directed blasts (Section 2.3.3). Some

thin, indipping tuffs high up on the northern crater wall may belong to Unit 3, as may some of the younger debris flows at the foot of the crater wall, which were probably derived from them (Fig. 2.3).

Well-bedded sub-horizontal tuffs, at least 9m thick, are exposed on the SW of the island some 2·5km from the crater. The tuffs overlie the Storhofdi lavas and cover an area of at least 0·25km^2. They consist of well-bedded, occasionally blocky, lapilli-rich deposits containing highly vesicular basaltic bombs. These bombs are unlike any found in the Saefell ejecta and often reach 25cm in size, associated with blocks up to 1·5m diameter. No directional data are preserved. The thickness of the tuffs this distance from the vent, the nature of the bombs and the large size of the blocks suggest that these deposits were derived from a nearby additional volcano, perhaps to the S.

On the SW coast of Heimaey the Unit 3 tuffs are overlain by Helgafell lavas, with no intervening soil. The absence of any erosive features in the youngest tuffs and their conformable contact with the lavas indicate that the Helgafell eruption shortly followed the cessation of the Saefell activity. This is in agreement with soil profiles from the Westmann Islands (Jakobsson, 1968) which show the similarity in age of the two volcanoes.

Summary

The units are separated by unconformities on and within the crater rim. These discordances are largely the result of syndepositional slumping of material into the crater. This, together with the lack of any evidence of depositional breaks in the outer flank sequence suggests that the three units were deposited in rapid succession. Similar relationships on Surtsey, where pyroclastic deposits built a similar structure in less than three years (Thorarinsson, 1967), support this conclusion.

2.3. Pyroclastic Facies

The tuff-ring deposits are subdivided into pyroclastic and resedimented facies. The pyroclastic facies consist of

Fig. 2.8 Blocky Helgafell lavas which flowed over the eroded Saefell northern crater rim and now overlie slumped Unit 2 crater tuffs.

Fig. 2.9 Block impact craters in distal Unit 3 tuffs SW of the crater. The crater on the left is surrounded by radial cracks due to dewatering and fracturing of moist ash. The right-hand crater is surrounded by a rim of tuff ejected plastically on block impact. Hammer measures 30cm.

airfall and base-surge tuffs. The resedimented facies comprise debris flows, slumped tuffs and aeolian reworked deposits.

2.3.1 Airfall tuffs

Deposition of airfall ejecta occurred throughout the activity of Saefell, interspersed with periodic base-surge events. The proportion of airfall material in any unit is difficult to estimate. It changes laterally outwards from the vent but is probably >70% near the vent and <30% in distal tuffs. Typical logs of the airfall ejecta are shown in Fig. 2.6.

Some of the most prominent features of airfall deposits are block impact craters. These often deeply penetrate moist, bedded phreatomagmatic tuffs, forming prominent sags in cross-section. Many of the distal, fine-grained surge tuffs are deformed by block impacts, which may be asymmetric due to inclined impact angles. When seen on exhumed bedding surfaces some of the craters are surrounded by radially oriented cracks whilst others have raised rims of material partly ejected from the sag crater (Fig. 2.9).

The cracks, which are similar to those figured by Camus et al.(1981, Fig. 9), may have formed by fracturing of rapidly drying fine tuffs on impact. Alternatively, if the tuffs were still moist, impact dewatering may have forced water outwards from the crater along radial fissures which have now preferentially weathered out. The raised rims were formed by partial ejection of more cohesive ash from the crater. The better consolidation and preservation of the rims may be ascribed to improved packing of grains within them because of their secondary flowage.

Block impact structures, as well as being occasionally asymmetric and thus indicating their direction of origin, may also be used to determine the cohesiveness of the underlying tuffs at the time of impact. As at Medano, Tenerife (Chapter 3) the most cohesive tuffs tend to be the distal, fine-grained surge deposits. These are most deeply deformed (Fig. 2.10) by block impacts. The fallout

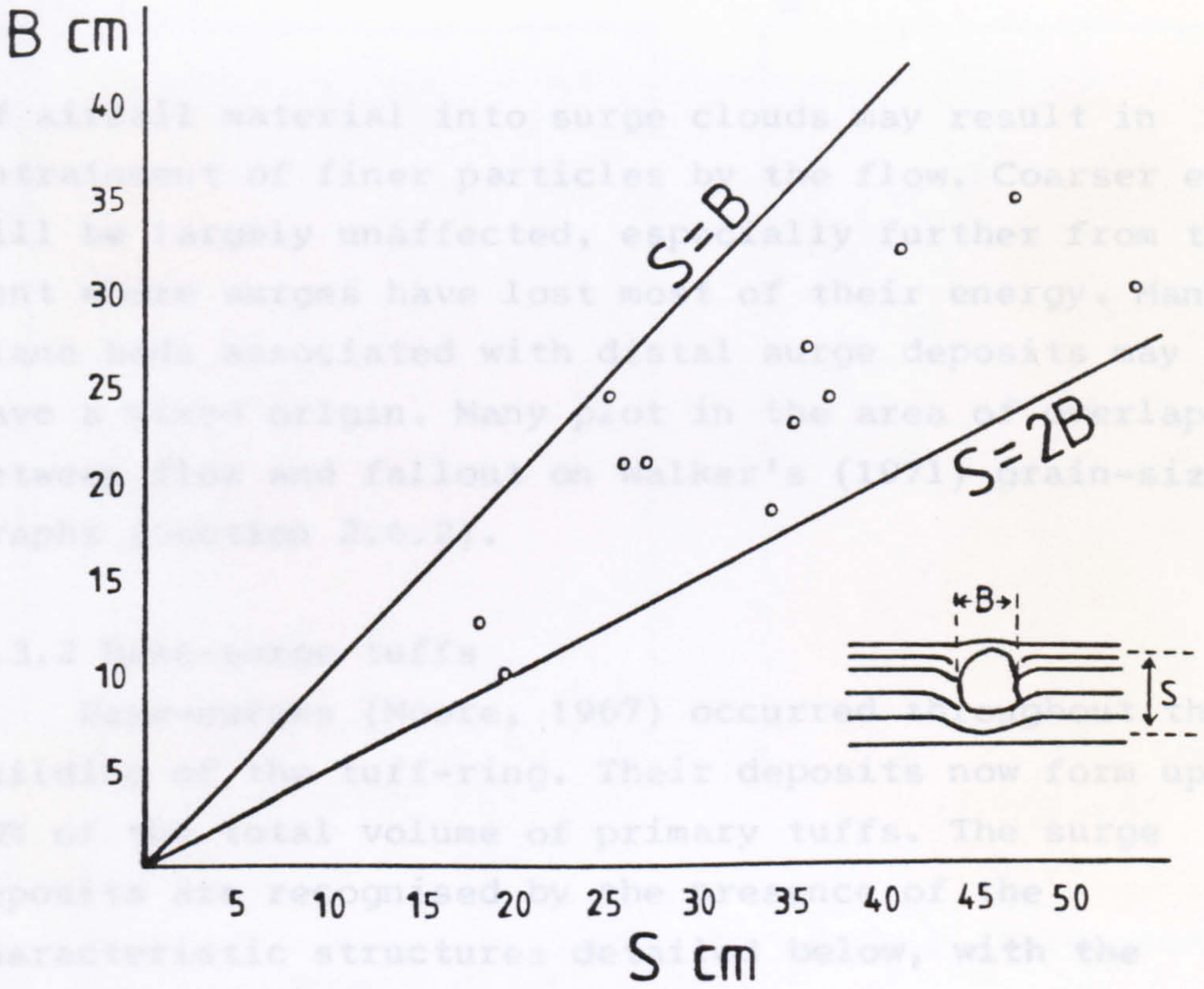

Fig. 2.10 Block sag impact measurements from all units of the tuff-ring. Blocks penetrate deeply into the moist, cohesive phreatomagmatic tuffs.

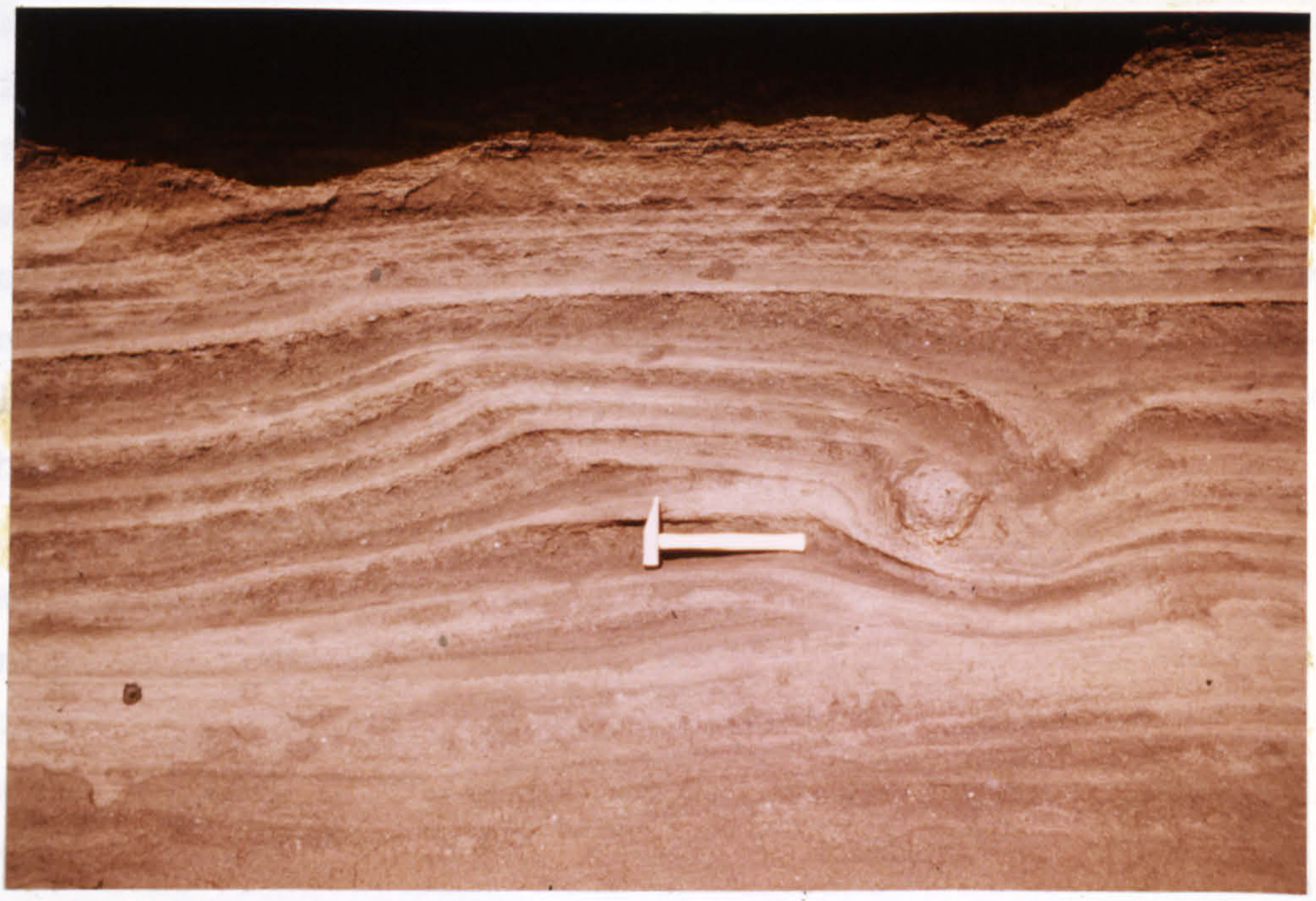

Fig. 2.11 Unit 3 surge antidune structure exhibiting downflow-migrating crests. See text for description. Flow from right to left. During impact, the block which deformed the antidune had the same direction of movement as the surge. Hammer measures 30cm.

of airfall material into surge clouds may result in entrainment of finer particles by the flow. Coarser ejecta will be largely unaffected, especially further from the vent where surges have lost most of their energy. Many plane beds associated with distal surge deposits may thus have a mixed origin. Many plot in the area of overlap between flow and fallout on Walker's (1971) grain-size graphs (Section 2.6.2).

2.3.2 Base-surge tuffs

Base-surges (Moore, 1967) occurred throughout the building of the tuff-ring. Their deposits now form up to 30% of the total volume of primary tuffs. The surge deposits are recognised by the presence of the characteristic structures detailed below, with the addition of structures rarely described in the literature :- small ripples of varying asymmetry.

Antidunes

a) Description

The antidunes have heights up to 3m and wavelengths up to 15m. They contain lee-side laminae deposited at dip angles less than the angle of repose, abundant stoss-side laminae and regular sinuous profiles (Fig. 2.11). Similar features, characteristic of antidunes preserved in subaqueous supercritical flows, were noted by Fisher & Waters (1970) in base-surge deposits of Ubehebe, California. Wave height tends to increase with wavelength (Fig. 2.12a) similar to surge dunes formed in other tuff-rings (Crowe & Fisher, 1973).

The antidunes commonly exhibit internal climbing cross-laminations with predominantly downflow crest migration at climb angles of between 15° and 35°. These features are similar to the subaqueous ripple laminae Type C of Reineck & Singh (1973), though on a larger scale. Plots of these stoss-side versus lee-side dips (Fig. 2.12b) indicate that stoss-side slopes increase as lee-side slopes decrease similar to other base-surge dunes (Crowe & Fisher, 1973). Individual laminae tend to thin over the antidune crests, and dip angles of both stoss and lee-side laminae

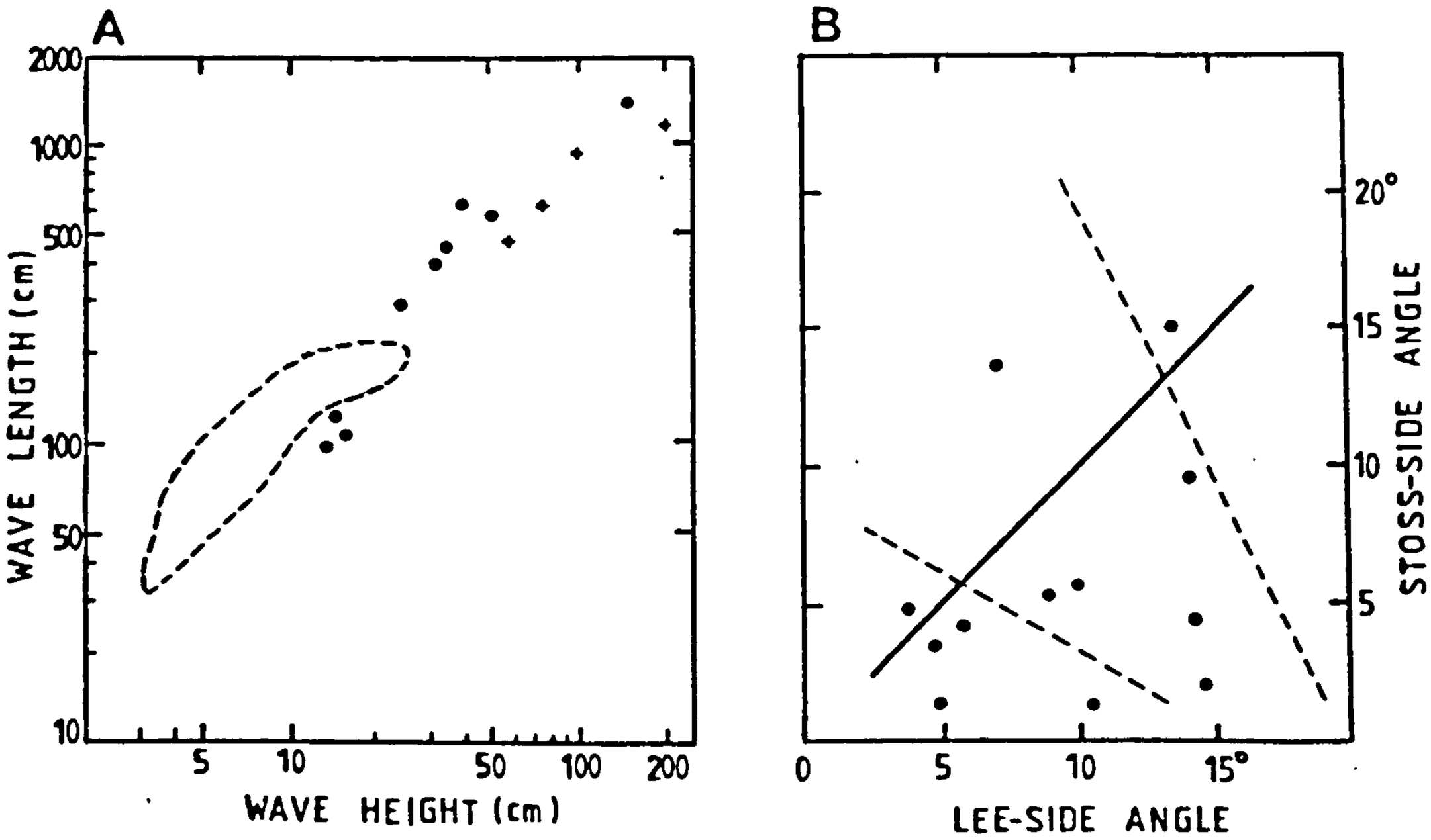

Fig. 2.12 A Wave height vs wave length for surge dunes from Saefell (filled circles), Taal Volcano (crosses) and Ubehebe (dashed field) from Crowe & Fisher (1971).
B Lee-side angle vs stoss-side dip angle with dashed lines marking field of Ubehebe dunes. Solid line marks where lee-side dip = stoss-side dip.

increase upwards in any individual structure. Lee-side laminae are coarser and sigmoidal in shape whereas those on the stoss-side are planar (Fig. 2.11).

One antidune in Unit 1 has a wave height of 1·5m and a wavelength of 15m and has built up over gently undulating well-bedded tuffs (Fig. 2.13). The structure grew on the downflow side of the crest of a gentle undulation, with the lower bedding set (a) consisting of upflow migrating crests at a climb angle of 30-50°. Stoss-side laminae dip at 15° and lee-side at 5-8° in this set. Both are of similar grain size, although isolated larger clasts lie along many of the upflow dipping laminae. Upwards in the set the dip angles of the stoss and lee-side laminae increase and the crest of the antidune becomes more peaked.

At a peak height of about 60cm, a thin, fine, mantling layer (b) was deposited, followed by a coarser lapilli horizon which is much thicker on the stoss-side of the dune crest and thins rapidly away from it. Above, the laminae of the upper bedding set (c) are finer and more prominent than any of the underlying antidune tuffs. They exhibit downflow climbing crest migration at an angle of 30°.

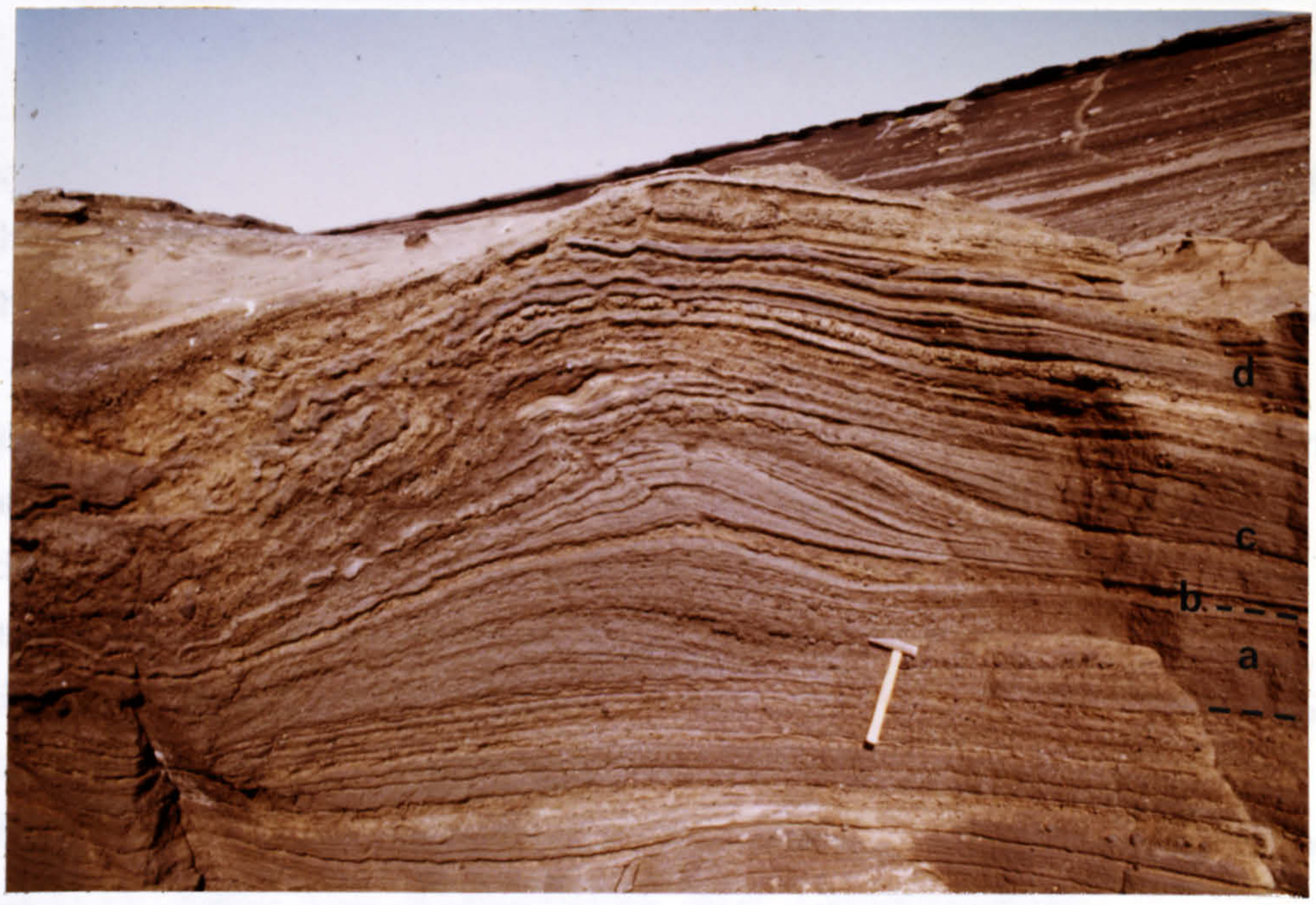

Fig. 2.13 Slumped antidune in Unit 1 outer flank tuffs 500m S of the southern crater rim. See text for description. Hammer measures 30cm.

Some of these laminae thicken over the crest although those near the top surface of the antidune thin markedly and in places wedge out. The whole structure is capped by about 75cm of thin, well-bedded tuffs (d) which, together with the lee-side laminae, slumped down its lee face. Some of these upper tuffs are thought to have formed part of the migrating antidune but slumping has obscured their relationship to it. A small thrust which cuts up through the downflow migrating bedform crests and dies out in the slumped material may be an example of drag thrusting due to frictional stress exerted by the overhead motion of the surge. The structure is analogous with thrusts in turbidite sequences described by Ballance (1964) but has probably been aided by gravity slip along bedding planes. It is thought that shearing of the unstable peaked crest initiated drag thrusting and slumping, and obliterated much of the earlier structure of the dune.

b) Interpretation

Theoretical profiles of sinusoidal "dune" growth (Exner, 1920; Leliavsky, 1955) show that an increasingly peaked, overturned crest is developed with time as a dune migrates (Fig. 2.14). Such a peak is not normally seen in sediments due to grain avalanching processes, but in this

case deposition of the slightly cohesive ash was so rapid that the overturned peak became fully developed before being slumped. Slumping was facilitated by the instability of the structure and the moist nature of the tuffs. Further examples of base-surge antidunes (Fig. 2.14) have been figured by Lorenz & Buchel (1980, Fig. 42) and by Fisher & Waters (1970, Fig. 5). These antidunes represent better preserved examples of until now theoretically predicted structures. Both sets of authors suggest that the structures were formed by strong shearing of an originally symmetrical antidune by base-surges. However, it is difficult to envisage how a surge could exert sufficient shear stress to deform rather cohesive tuffs, especially when the structures are large-scale.

The sudden upwards change from upflow to downflow crest migration and decrease in grain size in the bedding sets indicate more than one base-surge event, each having a different flow power and depositing material of different grain size. The lower bedding set of antidune type is succeeded by a thin plane bed perhaps as flow power decreased within the base-surge. This was then followed by another surge of lower flow power whose power changed with time to form the megaripples and capping plane beds.

Another high flow regime structure associated with the antidunes is upflow-dipping backset bedding probably of chute-and-pool flow origin. These beds dip at up to 45°, are planar to sigmoidal in shape and closely resemble the Type 1 dunes of Schmincke et al.(1973).

Plastering structures

These occur only at the base of Unit 1 and are moderately well laminated grey ash deposits which have adhered to vertical and overhanging joint faces in the underlying lavas (Fig. 2.15). They bank up against lava blocks and fill up crevices in the underlying deposits. At the base a 2-10cm thick, unbedded reverse-graded layer is succeeded by coarser, bedded, reverse-to-ungraded tuffs up to 70cm thick. Cracks in the lava surface which are sub-parallel to the surge motion are filled by plastering tuffs whereas others oblique to this contain only

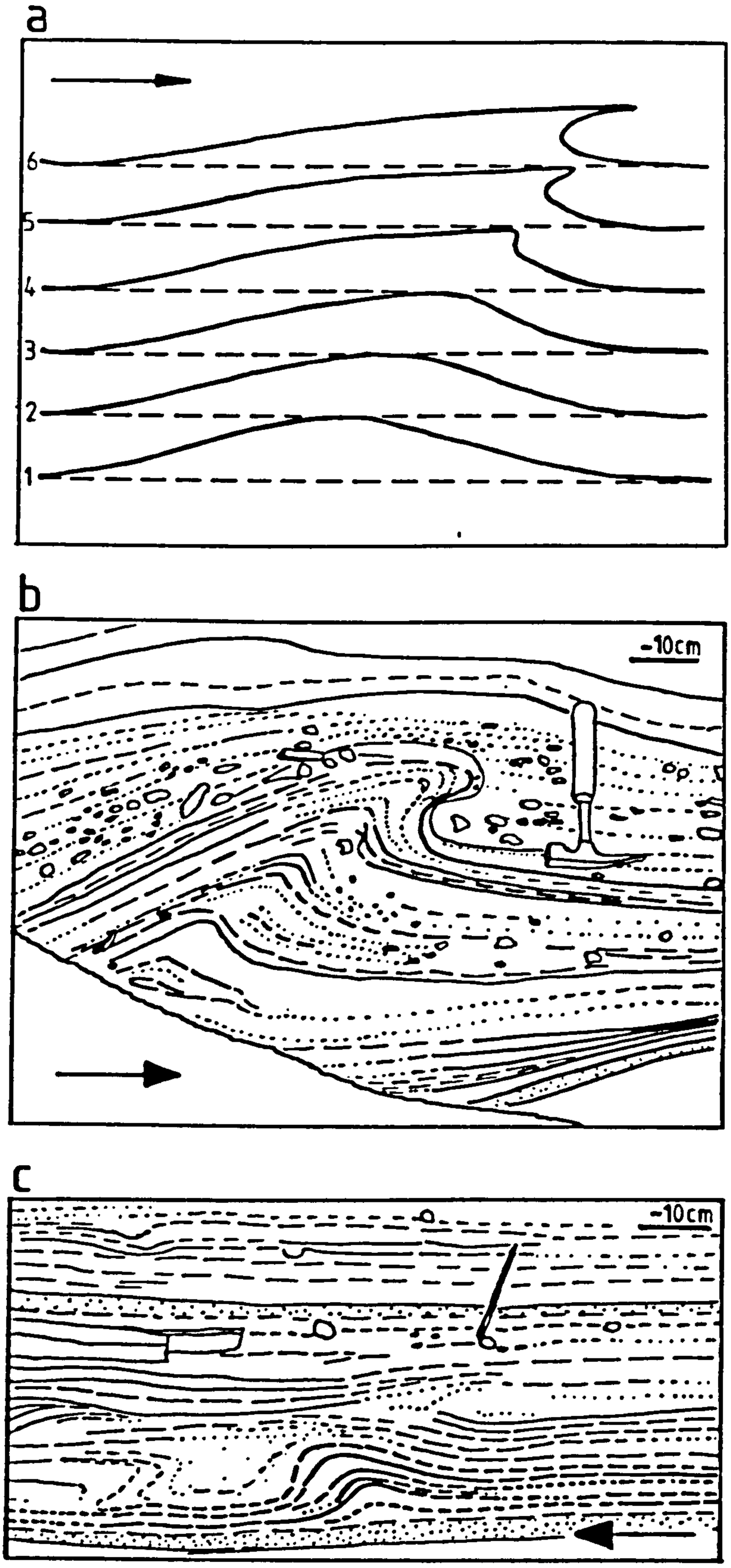

Fig. 2.14 a) Theoretical profiles of subaqueous dune growth, after Exner (1920).
b) Peaked, overturned surge dune, from Lorenz & Buchel (1980).
c) Peaked surge dune, from Fisher & Waters (1970).
Arrows indicate flow direction.

Fig. 2.15 Unit 1 surge tuffs plastered against jointed, eroded Storhofdi lavas. Surge motion towards the bottom of the photograph. Hammer measures 30cm.

Fig. 2.16 Casts of broken up grass stems in basal Unit 1 tuffs. Note hematite-stained scoria mounds at top of photograph. Surge motion from right to left. Knife measures 8cm.

horizontally bedded ash which may have fallen out of the main body of the surge as it passed overhead.

The initial plaster layer contains comminuted plant material throughout and, in places, flow-aligned fossilised grass stems occur in discrete layers at its base (Fig. 2.16). The grass stems, which are now replaced, are broken into 1-5cm long fragments and are thought to have been transported and aligned within base-surges. The grass fragments occur within a thin layer of fine grey ash above a soil horizon containing scoria lapilli which form elongate mounds sub-parallel to the alignment of the stems (Fig. 2.17a). Base-surges reworked the top of the soil horizon, aggregated the older scoria lapilli in elongate mounds and plastered ash and grass over these.

The grass itself consists mainly of flattened, broken stems with fine ribs parallel to their length and most have been split lengthways so that only one side of the stem is preserved. Occasionally, complete tubular stems with cellular interior structures occur and these are filled with fine ash. Grass seeds are also sometimes found. The stems are replaced by light grey, soft and fibrous slightly lustrous material which powders easily and is possibly gypsum. Some stems are reddish-brown in places, probably due to hematitic pigment, and are overgrown by a white, fibrous radiating soft mineral which is possibly a zeolite. The ash matrix contains many small black scoria fragments and feldspar crystals but predominantly consists of unaltered sideromelane.

The stems are generally well aligned within a small area (Fig. 2.17b) but this trend varies greatly over short distances due to topographic channelling and to turbulence within the surge. In some areas vertical lava joints have been plastered by ash containing the stems. Loose lava blocks are surrounded by plastered ash with the stems indicating flowage around the block sides.

The grass stems were broken and entrained whilst brittle indicating that the surges were hot and dry, probably containing superheated steam. Cooling of the steam allowed condensation of water and cohesive plaster tuffs

a

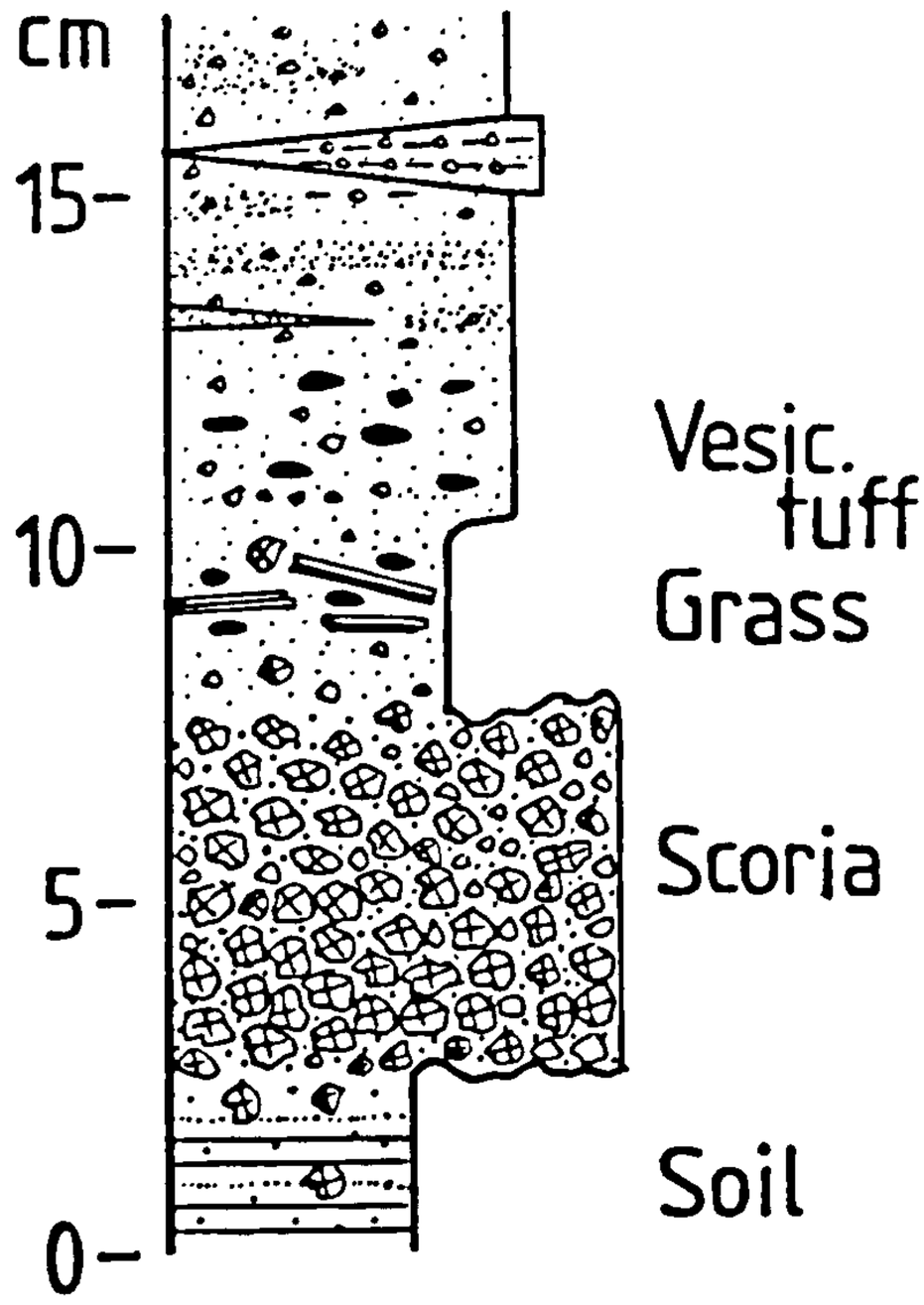

b

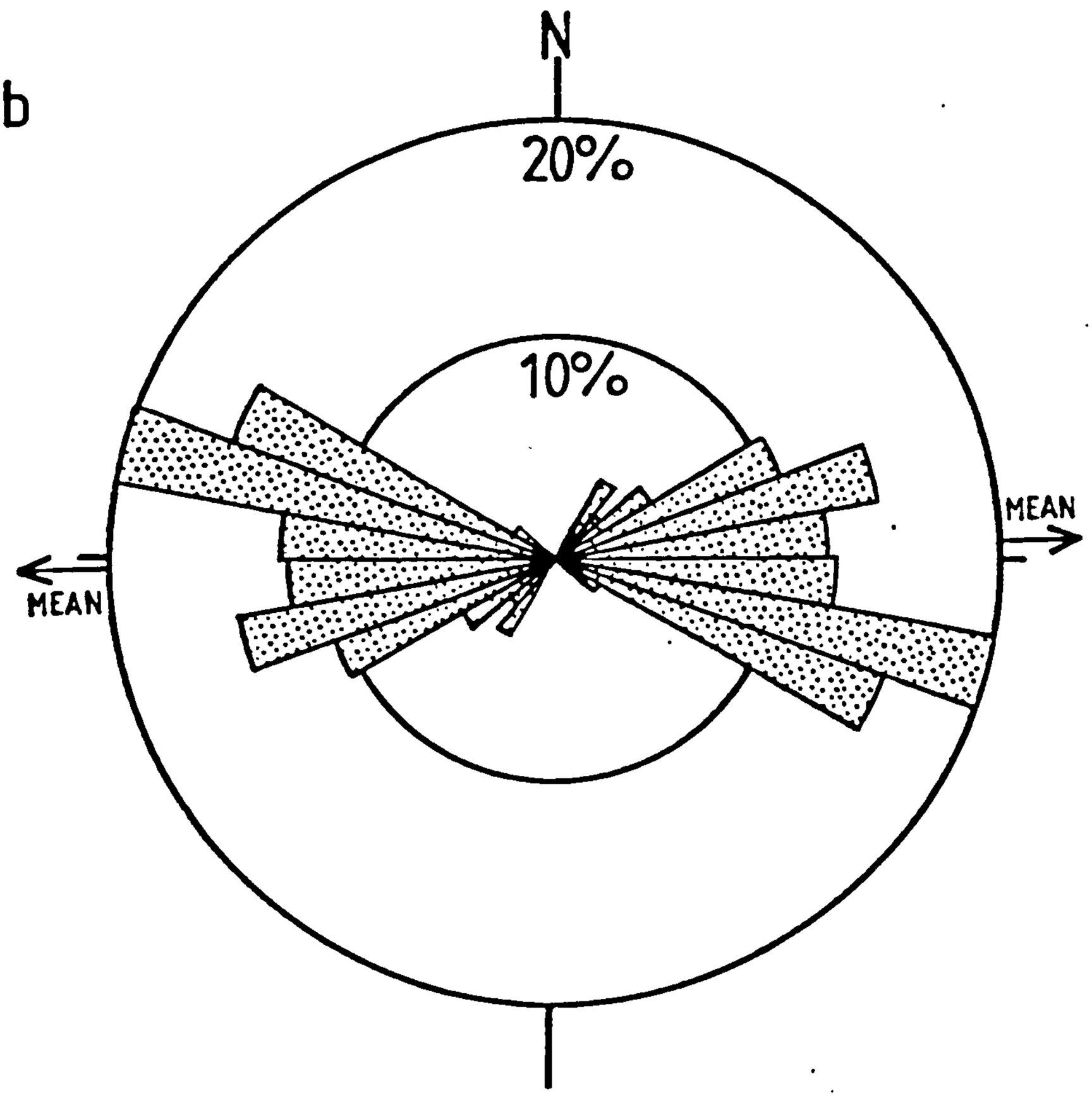

Fig. 2.17 a) Log of basal Saefell tuff on southern flank of tuff-ring. Note vesiculated tuff above layer containing grass stems.
b) Current-rose of grass stem orientations in basal Unit 1 tuffs, showing spread of values about an E-W mean.

were deposited. Rapid burial of the stems prevented oxidation and rotting and the organic material was replaced due to percolation of solutions through the tuffs.

Thickness variations

Marked thinning of plane-bedded horizons over positive topographic features, and thickening into depressions occur throughout all the Saefell surge tuffs. The most common depressions are block sag craters and channels and these are infilled by surge beds which thicken and coarsen into the centre of the hollows. The most prominent topographic rises are tumuli which protrude from the underlying lava flows, and the surge dunes themselves. Pinch-and-swell bedding within surge tuffs is not due to irregularities in the underlying surface but is related to the formation of low profile dunes.

Vesiculated tuffs

These rare features consist of thin fine-grained tuffs with flattened vesicles. They formed by entrapment of gas bubbles in water-rich cohesive surge deposits (Lorenz, 1974a). Many of the plaster tuffs at the base of the tuff-ring deposits contain vesicles which are often flattened in the plane of the bedding and elongate in the surge direction. These formed by surge shearing of the cohesive tuffs and compaction of the deposits. Vesiculated accretionary lapilli are sometimes associated with these tuffs and also presumably formed within the surge.

Accretionary lapilli

Accretionary lapilli are often found associated with base-surge deposits. Most of the small juvenile and lithic fragments in the tuffs are rimmed by 1-3mm thick layers of fine ash which may be concentrically layered. Occasionally, small spherical accretions of ash contain no larger nuclei and are poorly banded or internally structureless. The accretionary rims are generally composed of poorly sorted ash and are much coarser than the delicately banded rims described by Moore & Peck (1962). They may better be described as armoured lapilli (Womer et al., 1980) and probably formed rapidly in the lower part

of the eruption column where particle sorting was poorer. The abundance of such structures in all the Saefell tuffs has important consequences for grain-size analyses by sieving methods. Disaggregation of the composite lapilli will occur and result in more fine-skewed distributions than are actually present. The further consequences of these results will be discussed in the section on petrography (Section 2.6).

U-shaped channels

U-shaped channels with radial orientation to the crater rim occur throughout the tuff-ring deposits but are never abundant. The best exposed examples occur within a 2m thick horizon of the well-bedded indipping Unit 2 succession. Here, at least three closely-spaced episodes of channel erosion are indicated by crosscutting relationships (Fig. 2.18).

The maximum shoulder width of the channels is 210cm and depth 50cm. The average dimensions of eight measured channels are 130cm width and 30cm depth. Some channels have moderately flat-bottomed profiles and all are filled by surge deposits which thicken and coarsen into the centre of the troughs. Many have a fine ash layer plastered onto their sides whilst other channel walls have slumped, forming small marginal slump folds. The profiles of the channels are all symmetrical and their bases roughly follow the bedding planes of the tuffs which they cut.

A meandering mudflow channel of box-shaped cross-section is exposed on a bedding surface beneath one of the channelled zones. A surge channel which developed immediately above the mudflow channel (Fig. 2.19) has deposited a thin plastered layer over its inside walls. The meander wavelength of the mudflow channel is about 2m and is similar to modern mudflow channels which erode the outer flank tuffs on Surtsey.

The mudflow channel presumably provided an irregularity in the topography sub-parallel to the surge motion, which then deposited plane beds above the channel and subsequently eroded them. Surge erosion probably developed because the

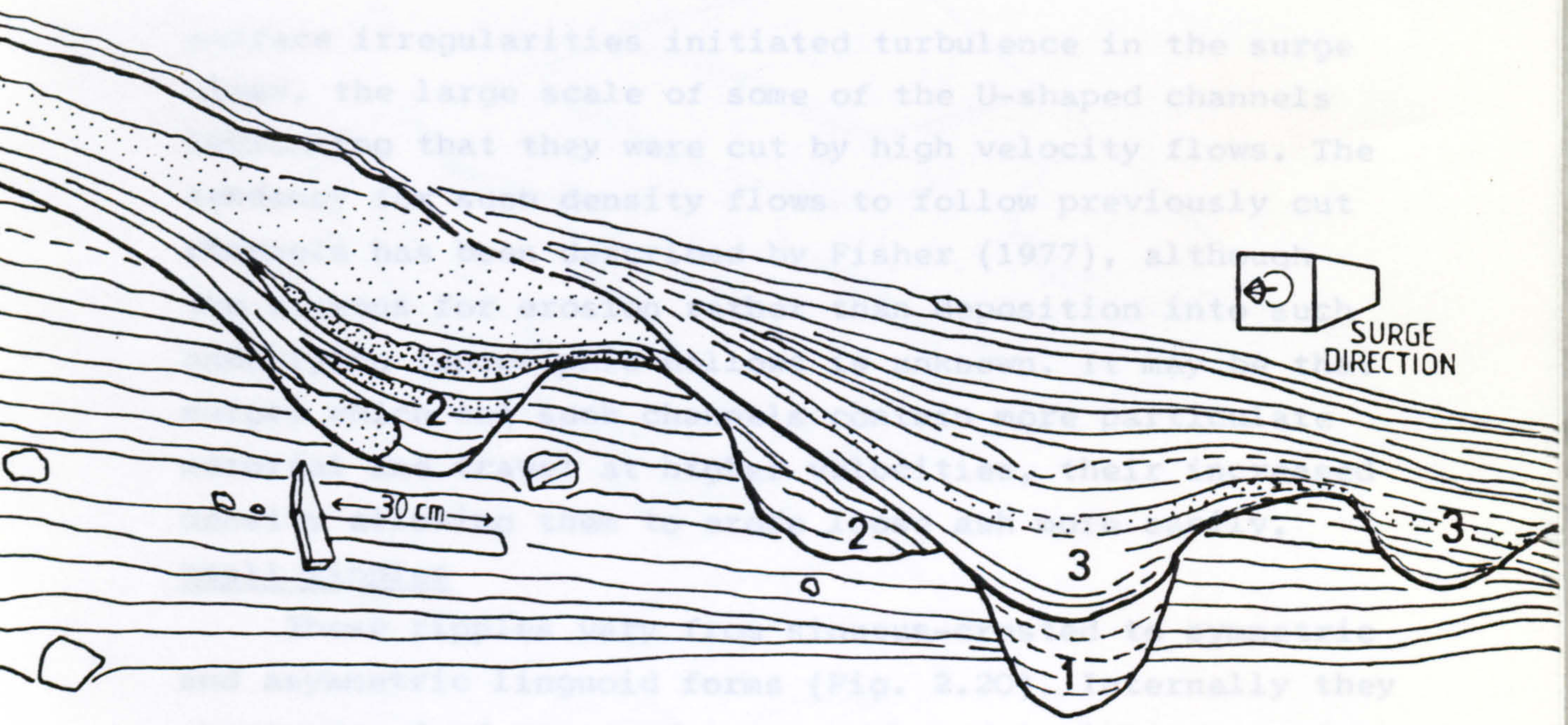

Fig. 2.18 Surge U-shaped channels cutting Unit 2 crater tuffs near the southern part of the crater rim. Evidence for the three phases of surge erosion indicated was derived from localities outside the diagram.

Fig. 2.19 Broad U-shaped surge channel cuts bedded tuffs at the top of the photograph and follows the course of a meandering mudflow channel in which the hammer lies. Same locality as Fig. 2.18.

surface irregularities initiated turbulence in the surge cloud, the large scale of some of the U-shaped channels indicating that they were cut by high velocity flows. The tendency for such density flows to follow previously cut channels has been described by Fisher (1977), although the reasons for erosion rather than deposition into such underlying topographic hollows is unknown. It may be that surges which cut such channels contain more particulate material and travel at higher velocities, their increased density allowing them to erode loose ash more easily.

Small ripples

These ripples vary from sinuous-crested to symmetric and asymmetric linguoid forms (Fig. 2.20). Internally they are composed of cores of coarse ash and lapilli covered by finer layers 1-3cm thick. They commonly have heights up to 5cm, chord lengths up to 12cm and are often found on the surfaces of larger surge dune structures. Some nucleated on larger clasts which now have parabolic ash tails on their upflow sides whereas others consist of convex-upward ash laminae which overlie irregularly-shaped lapilli clumps.

Internally the ripples are either structureless, composed of poorly sorted coarse ash or comprise faint convex-upwards-to-irregular laminations of better sorted fine ash. The ripples are thought to have formed partly in a similar way to antiripplets or adhesion ripples (van Straaten, 1953) which develop when dry wind-borne sand is blown over a smooth, moist sediment surface. However, since the pyroclastic material is transported by base-surges which contain a high proportion of water vapour, plastering as well as adhesion processes can occur, giving rise to a wide variety of ripple shapes. Ripple irregularity is due to variations in the direction of flow in the surge cloud and to whether plastering or adhesion processes were dominant. Occasional vesicles within the finer, rippled tuffs indicate that these layers were deposited by plastering of cohesive ash.

Similar structures, composed of fine ash with faint convex-upwards laminations are found in the upper Surtur I outdipping tuffs on Surtsey. In section parallel to the

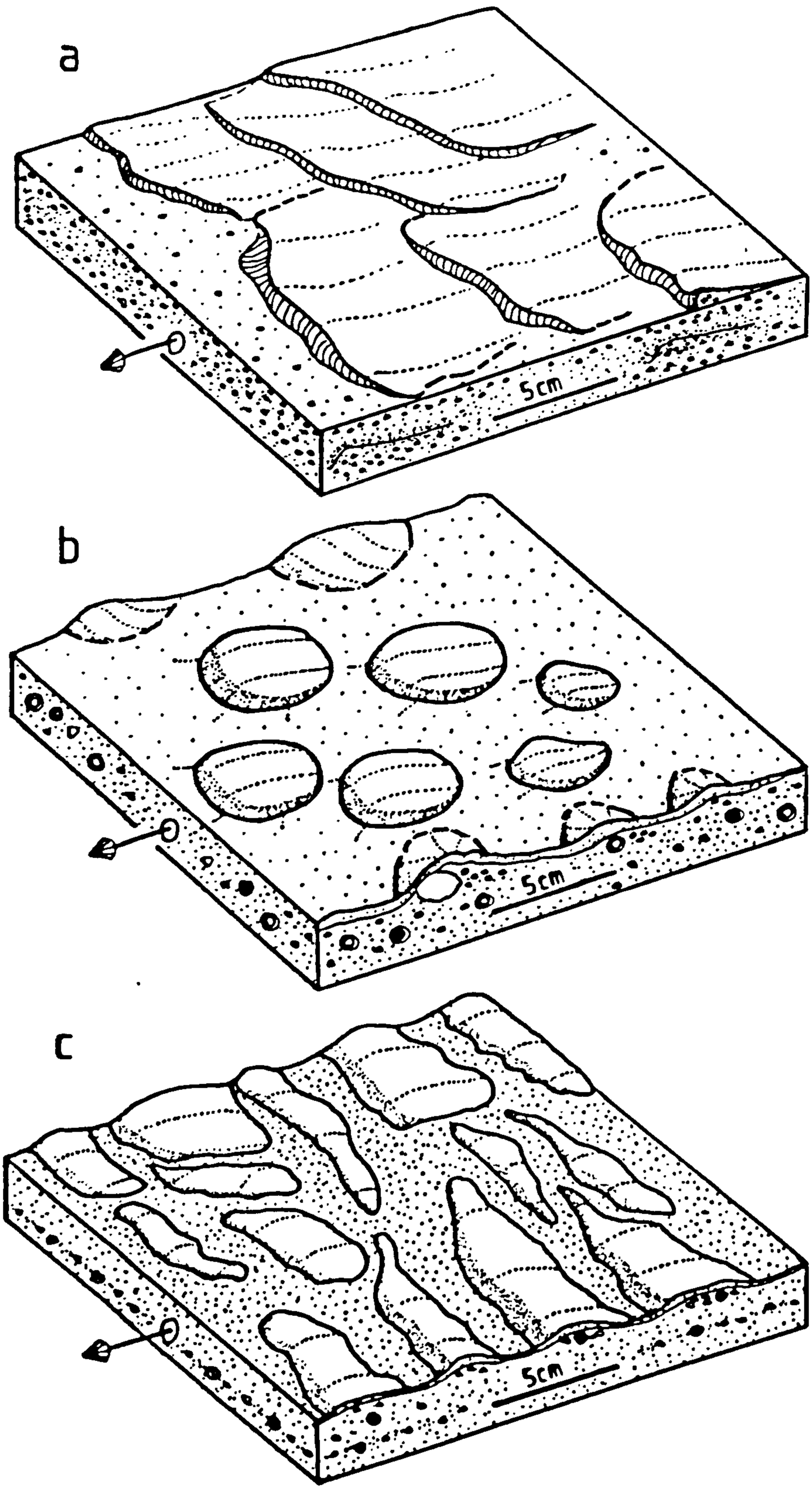

Fig. 2.20 Small surge ripples.
a) Sinuous-crested ripples partly formed by adhesion.
b) Linguoid ripples developed over lapilli clumps.
c) Irregular ripples formed by plastering and adhesion

presumed current direction the adhesion ripples (Fig. 2.21a) consist of undulating laminae with staggered crests and narrow troughs between. The ripples grew by upflow accretion with steep stoss and more gently dipping lee-sides. In some inclined tuffs on Surtsey and Saefell gravity flowage has formed small ripples or deformed previously deposited surge ripples. The gravity flowage structures are often difficult to distinguish from surge ripples since both types are small, fine-grained and lack internal foresets.

Often, small scale surge ripples occur on the upper surfaces of large surge dunes or pinch-and-swell structures, and may be interbedded with such large scale features. It is thought that the ripples may be the deposits of the "tail" of surge clouds which are more expanded and carry smaller amounts of material than the "head" region. This would explain their small size, plaster origin (since most of the steam in the tail of a surge would probably be cooler and more condensed) and their association with much larger surge structures possibly deposited by the head and body of the surge.

Similar ripples have been described only once before (Lorenz, 1974b), perhaps because their more irregular forms have been confused with complex differential erosion patterns, which they may superficially resemble. Whenever more regular examples are seen, however, their depositing current directions are consistently radially outward from the crater confirming their surge origin. Deflection of the surges by larger dunes results in an increased spread of palaeocurrent data derived from them (Fig. 2.21b). Only the general sense of movement of the surges may be deduced from such examples.

2.3.3 Directional data

Many of the base-surge deposits contain structures which may be used to determine the direction of the depositing flows (Fig. 2.22a). These directions indicate derivation from the crater, although some anomalous directions are recorded in the smaller-scale structures

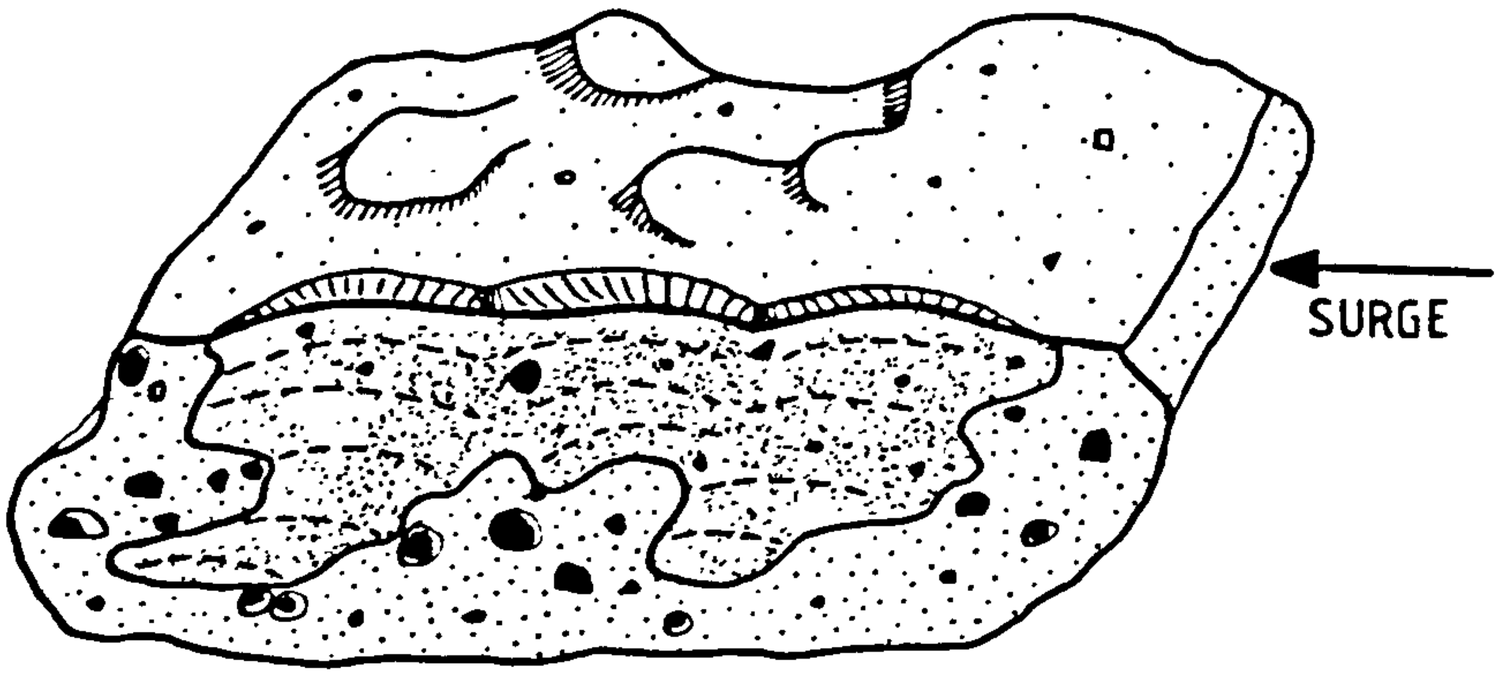

Fig. 2.21 a) Surge adhesion ripple found on Surtsey. Note upflow migration of ripple crests and knobbly projections on upper surface of the block.

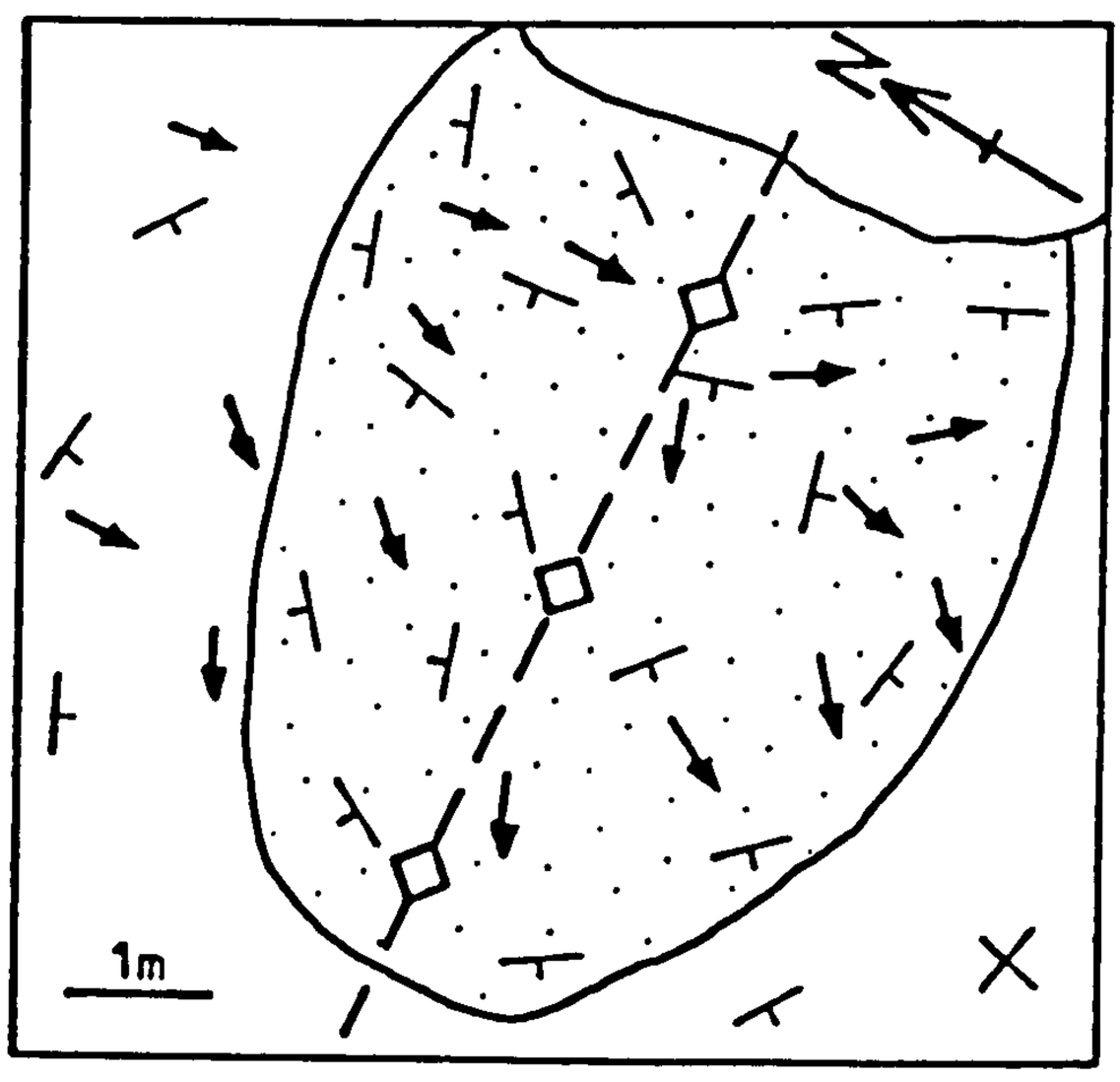

Fig. 2.21 b) Plan view of large Saefell surge dune with smaller ripples superimposed on its surface. Arrows indicate surge movement direction as shown by small ripples. Large dune deposited by surges which moved from N to S.

such as block sag craters, small ripples, current lineations and parabolic plaster coatings. The smaller structures were presumably deposited by surges which were more deflected by topography and wind action. Some of the NW-SE orientated lineations were undoubtedly formed solely by paleowinds since they trend at 90° to the radial surge flow direction. The lack of directional data to the N of the crater is due to poor exposure.

Directed blasts may also have influenced the measured surge directional data. Figure 2.22b is a contour map of the average maximum lithic size distribution for a block rich bed 1-2m below the top of Unit 3. This layer was deposited by SSW-directed blasts which ejected 25cm blocks to a distance of 1600m from the geometrical centre of the crater (which is close to the inferred source of the explosions). The directed blasts may also explain the distribution of Unit 3 itself which is best developed SW of the crater. The present topography of the ring consists of high ground to the N and NW and lower areas to the S and SW and was probably controlled by these directed blasts. Whether high ground to the N deflected the eruptive blasts through a notch in the rim to the SW, or primary SW-directed blasts reduced the height of the rim in this direction is unclear. Since the block distribution is clearly asymmetric and Unit 3 is absent to the N on the crater walls it is thought that the latter, directed blast hypothesis is the more likely.

2.3.4 Surge depositional processes

Base-surges vary in their physical properties and this variation results in the formation of different depositional structures. The concept of various types of surge has been previously proposed by Crowe & Fisher (1973) and Sheridan & Updike (1975). It is important to note that surges change in character as they travel away from the vent (Wohletz & Sheridan, 1979), becoming cooler, more expanded and slower moving. Cooling of initially superheated steam results in hot, dry steam changing to cool, wet vapour with time.

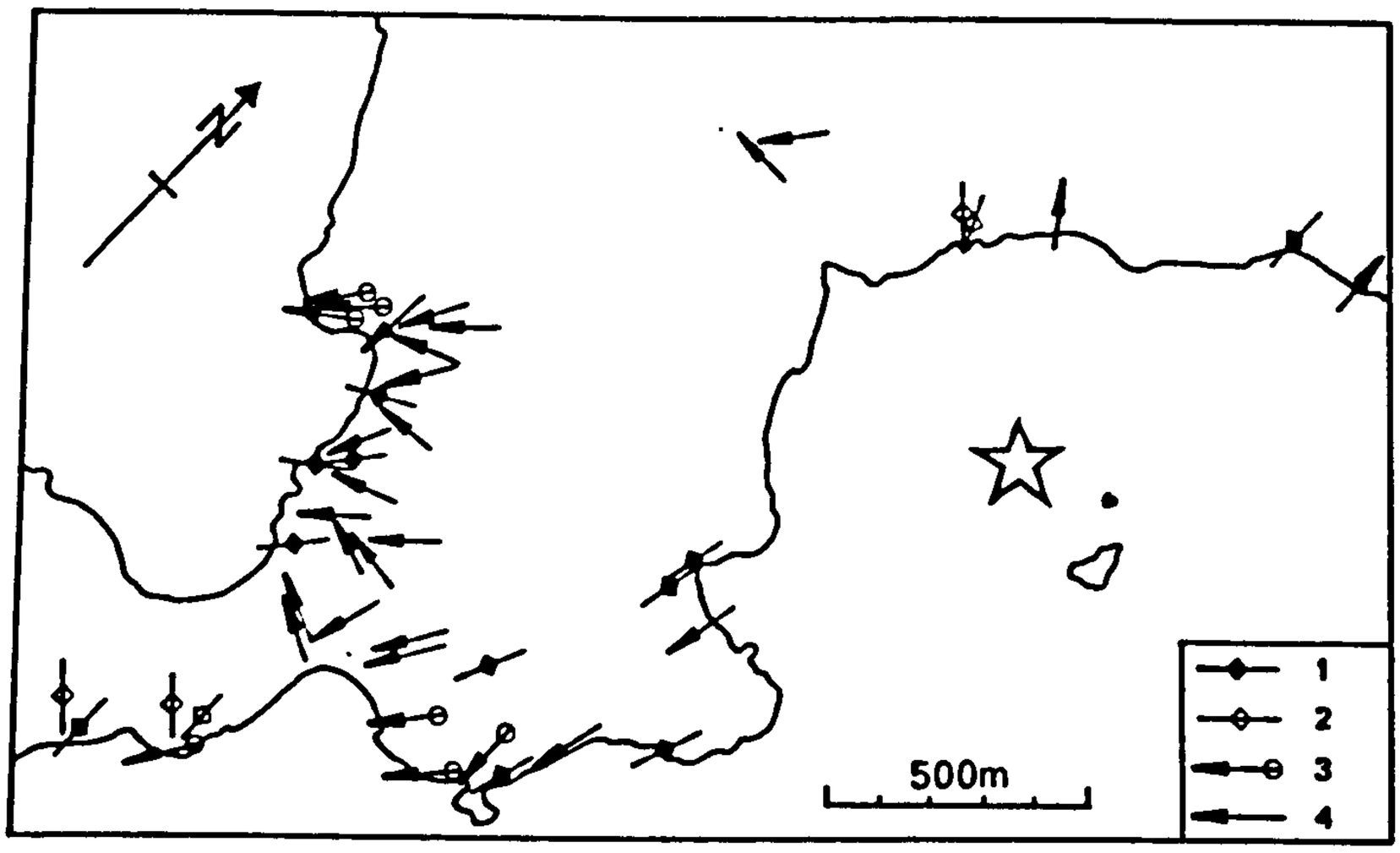

Fig. 2.22 a) Directional data from Saefell structures.
1: surge channels
2: lineations
3: surge cross-beds
4: grass stems, plaster ripples, asymmetric block sags

Star indicates approximate vent position suggested by directional structures.

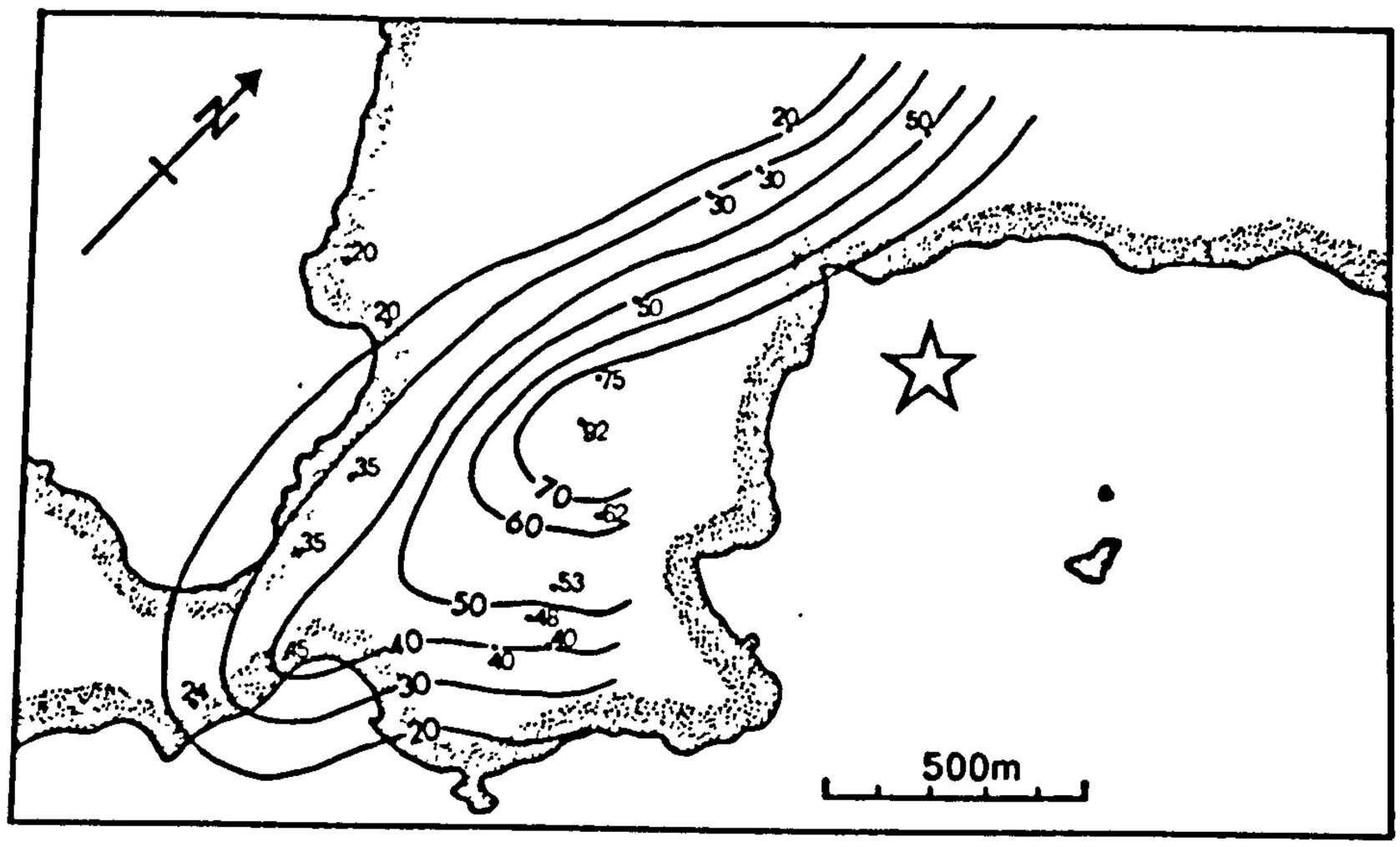

Fig. 2.22 b) Contoured average maximum lithic clast diameter map of the upper Unit 3 tuffs.

Star indicates approximate vent position suggested by block size distributions.

The large-scale antidune structures are thought to have been deposited by rapidly moving, concentrated surges which had low proportions of wet steam relative to superheated dry steam. The similarity in form of these surge structures to antidunes developed in subaqueous sedimentary environments (Skipper, 1971), suggests that rapid deposition rather than cohesive ash plastering was the dominant process. The large scale of these structures, and the climbing cross-laminations indicate deposition by heavily particle-laden, fast moving flows. This is supported by the occurrence of the peaked, overturned dune crest described above (Section 2.3.2). Other large-scale structures such as U-shaped channels and marked lateral thickness variations were probably formed by such high velocity, dry, concentrated flows.

Plastering structures, vesiculated tuffs and small ripples contain abundant evidence of cohesive ash deposition. These structures are small, indicating dilute surges lacking in tephra. Their depositing surges tend to be deflected by positive topographic features and winds, indicating low-velocity flows. This suggests that they were formed by slow-moving, dilute, wet steam flows. Ideally, one surge could deposit all the above structures at different distances from the vent, these distances depending on the initial properties of the surge. Moore (1967) referred to strong sandblasting of trees near the vent of Taal Volcano, the Philippines whereas further out the trees were plastered with mud coatings. This is thought to be due to the effects of superheated steam clouds near the vent, which cooled and condensed outwards, depositing cohesive ash.

The concept of flow power to describe the relative characteristics of surges seems appropriate. At a given distance from a vent a surge which deposits large-scale antidunes has higher flow power than one which deposits only vesiculated tuffs. Outward from the vent, surges deposit structures of decreasing flow regime such as at Taal where surge dunes decreased in size further from the vent (Waters & Fisher, 1971). Deposition at any one point

in space reflects the deceleration of a single surge (Crowe & Fisher, 1973) and results in a decrease in flow power upwards in a bedding set. It must be stressed, however, that surges are not discrete events, but are pulse-like in nature. This is due to fluctuations in the eruptive activity, a common feature of phreatomagmatic volcanicity (Tazieff, 1959; Thorarinsson et al., 1964).

The head of one surge pulse may thus overtake the tail of the one preceding it and mixing will occur. This could explain why large-scale surge structures are rarely overlain by smaller structures, which might have been expected to form as a surge cloud loses energy and deposits lower flow power structures. Mixing of surge pulses increases the complexity of a simple flow regime model. The idealised sequence of decreasing flow regime upwards in a bedding set is thus only rarely developed (Crowe & Fisher, 1973).

Another factor which complicates analogies with flow regime studies in sedimentology is the cooling of steam in the surge. The transition from hot, dry steam to cool, wet steam will, by clumping of moist particles, lead to instantaneous fallout of variously-sized aggregates of ash and plastering onto underlying surfaces. These processes are not analogous to deposition of sediment from an aqueous medium, although some interparticle (cohesive) forces do occur especially between fine grained sediments. These factors result in more complex relationships between flow power, sediment size and bedform structures.

2.4. Resedimented Pyroclastic Facies

Syn-eruptive reworking of airfall and surge tuffs occurred throughout the formation of Saefell and post-eruptive reworking has continued up to the present.

2.4.1 Debris flows

Many of the indipping crater tuffs consist of massive, blocky units, 1-3m thick, with irregular top surfaces. The mainly basalt blocks reach up to 50cm diameter and are often concentrated towards the top of the

individual debris flow units, forming inverse coarse-tail grading. Their common alignment in trails defines a crude internal stratification. Often, well-bedded indipping tuffs become slump-folded downslope with occasional small thrust imbricate structures. These tuffs pass downdip into debris flows which form a pile at least 10m thick at the base of the crater wall. The pile unconformably overlies the outdipping tuffs exposed in the crater wall and contains rafts of originally more lithified bedded tuff up to 20m across and 4m thick. These rafts occur at the top of debris flow units and are broadly conformable with them. The rafts were emplaced by slumping of less consolidated underlying deposits.

Some of the debris flows have not moved very far, indicated by the downslope transition from bedded to massive tuffs. Others may have flowed down the crater wall, since many debris flows thicken downslope to form a wedge-shaped pile. One scoria-rich debris flow at the base of the crater wall probably represents the slumped equivalent of a scoria horizon exposed near the top of the outdipping Unit 2 sequence to the N of the crater. This relationship suggests flowage up to a maximum of 110m.

Some of the debris flows overlie a thin, fine grained layer which is occasionally well-bedded and contains accretionary lapilli. This layer is thought to have been deposited as a cohesive layer over the crater wall, with subsequent coarser material sliding downslope over this basal moist horizon. In places, coarse blocks at the base of the overlying debris flows have scoured this fine horizon, forming grooves and scour pits. Where this fine basal horizon is absent, blocks projecting from the underlying tuffs often have a "tail" of tuff on their downslope side. The tails formed as the debris flows passed over and around the block, rather like glacial "crag-and-tail" structures.

Debris flows which occurred during volcanism are overlain by well-bedded tuffs and were formed by slumping of poorly consolidated, probably moist, tephra. These debris flows clearly originated from curved slump scars

which dissect much of the northern crater wall. The scars cut back into the outdipping flank sequence and their hanging walls are often overlain by younger, probably post-volcanic debris flows. In places the scars acted as channels for the later Helgafell lavas which flowed over the eroded cliff face. Further evidence of post-volcanic debris flows is scarce but some thick, blocky deposits which drape over the ring fault in the N of the crater probably post-date the volcanism, since they were emplaced after extensive erosion of the crater tuffs.

2.4.2 Disturbed bedding

Disturbed bedding occurs occasionally in the outer flank tuffs, and forms units up to 2m thick interbedded with well-stratified, predominantly surge tuffs. One particular unit, 1-2m thick, occurs 500m SW of the southern crater rim in a sequence which dips SW at 5° (Fig. 2.23). The base of the unit is essentially planar and is overlain by a 5-20cm thick ash layer. This layer is often injected into the coarser unit above, forming flame structures up to 15cm high. The top of the unit is irregular and hummocky and is overlain by surge tuffs which thicken into the hollows in the top of the disturbed tuffs.

The unit was formed by gravity slumping of lapilli-rich beds over a basal finer horizon. Rotation and imbrication of these moderately well consolidated tuff blocks during slumping led to breakdown of some of the coarser beds which now largely form the unit. Slump folding of some of the more elongate slabs also occurred. Movement occurred largely before deposition of the overlying surge beds which infill the irregular top surface. Minor movement after this is indicated by one slab which penetrates up into the bedded surge tuffs and slightly deforms them.

A thin ash layer some 15-20cm below the base of the disturbed unit has a rippled top surface (Fig. 2.24). These asymmetric, regularly-spaced ripples contain no internal stratification and are often overturned down dip. The dip slope is also the downflow movement direction of

Fig. 2.23 Gravity slumped Unit 3 tuffs on the southern flank of the tuff-ring. Downslope slump movements from right to left broke up bedded tuffs and caused rucking up of finer tuffs below. Knife measures 8cm.

Fig. 2.24 Gravity slump ripples in fine tuffs from same locality as Fig. 2.23. Downslope movement occurred from left to right and the ripples were subsequently deformed by surges which moved in the same direction. See text for description. Tape measures 20cm.

the base-surges which deposited the bulk of the surrounding tuffs. The crests of the structures are rounded to sharp and are overlain by a 15cm thick layer which is inversely graded and is rich in accretionary lapilli. In places, coarser lapilli are banked up against the overturned side of the ripples whereas their other sides are overlain by finer grained tuff.

The rounded, downslope overturned form of many of these ripples, the lack of internal stratification and their similarity to small scale slump folds suggest that these ripples were initiated by gravity slumping of moist, fine tuffs. However, the passage of surges overhead has sheared out some of the slump folds and deposited coarser material on their downflow sides. Similar structures were described by Crowe & Fisher (1973, Fig. 7) as current sheared flame structures, but it is difficult to envisage how surges could affect injection structures developed in sub-surface deposits.

Both the disturbed beds and the sheared slump structures are developed in base-surge tuffs of Unit 3 age. The structures were formed by gravity slumping of (presumably) moist tuffs on slopes of $<5^{\circ}$. Small contorted bedding structures are also developed in some of these surge tuffs. They may have a primary origin similar to contorted laminations described by Coleman (1969) in channel deposits of the Brahmaputra River. These were thought to have formed by turbulence associated with the abrupt transition between the lower and upper flow regimes. The transition caused an increased shear stress on the bed of the river and subsequently formed convolute bedding. Base-surges might form similar structures due to transitions of flow regime. However, these would probably be on a small scale due to the inability of pyroclastic flows to exert as great a shear stress on the surface beds.

2.4.3 Eolian and fluvial reworking

a) Eolian

Strong winds often affect the distribution of tephra from pyroclastic volcanoes and may also erode and redeposit

tuffs during and after eruptive activity. Loose, blocky rubble which covers many of the upper tuffs SW of the crater has probably been formed by wind deflation removing finer material. During eruption this deflation is thought to have formed some blocky, coarse-skewed particle distributions. However, since phreatomagmatic tuffs are generally strongly fine-skewed, this effect is rarely discernable. Gullies were cut by wind and rain action in the initial crater rim of Unit 1 age. Similar features are presently cut into poorly consolidated distal tuffs SW of the crater.

Strong winds are presently eroding the Surtsey tuffs and strongly wind-sculpted tuffs are well exposed on the NW cliffs of the island. Some recent wind blown deposits on Surtsey are banked up against the SE cliffs. They are almost indistinguishable from primary fine tuffs except that they contain many parabolic wind tails on the lee-faces of upstanding clasts. Similar features are common in exposed poorly consolidated Saefell tuffs and also on the bedding surfaces of more indurated tuffs. Such structures continue beneath overlying tuff beds and were formed during the eruption, as were ridges and grooves along the bedding surfaces. Directional measurements of these structures indicate that the palaeowinds responsible were mainly from the E or NE.

b) Fluvial

Many recent tuff-rings such as Surtsey and Hverfjall are extensively eroded by fluvial and mudflow channels. Saefell has few exposures of these features, apart from the previously mentioned meandering mudflow channel. This is partly due to the poor exposures of bedding surfaces and sections concentric to the crater rim. However, although there was some fluvial erosion of the Surtsey tuffs during eruption, most occurred after the end of the tephra-producing activity and is thus restricted to the youngest tuff beds. These beds are largely grass covered or wind eroded on Saefell so are seldom exposed. Those that are sometimes contain fluvial channels.

2.5. Volcanic History

A brief history of the Saefell activity is useful as a comparison with modern observed eruptions of this type.

1. Rising magma interacts with water contained in the upper crust and sea-floor sediments, probably at water depths of <100m (the average water depth on the continental shelf round Heimaey). A subaqueous pile of tuffs was built up until the volcano broke the water surface where airfall and base-surge processes formed a tuff-ring. This tuff-ring was probably soon breached on its eastern side, allowing constant water access to the vent. Minor parasitic scoria eruptions occurred due to brief lateral migration of magma.

2. Syndepositional slumping and collapse of the Unit 1 indipping tephra was followed by prolonged Unit 2 deposition with continued oversteepening and slumping of indipping material. Some indipping tuffs survived slumping but were partly downfaulted into the crater to form a structureless pile.

3. Unit 3 was then deposited, predominantly by base-surges, over the collapsed and eroded tuffs below. A nested inner rim was formed over the largely structureless crater pile of Unit 2. Outcrop distribution was controlled by SSW-directed blasts.

4. Erosion of the inactive tuff-ring then followed before the strombolian activity of Helgafell. Later lavas flowed over the eroded Unit 2 cliffs on the N side of the crater. Erosion removed most of the remaining indip succession particularly by tidal processes, perhaps aided by further minor crater collapse. Outer flank tuffs were not eroded to the same extent, but were affected by wind deflation.

2.6. Petrography, Morphology and Alteration

2.6.1 Petrography

The Saefell tuffs are predominantly composed of ash and lapilli of basaltic glass (sideromelane) and tachylite with clasts of basalt, scoria and sediment mainly derived from older, underlying deposits. Some basaltic clasts

may have been derived by brecciation of more slowly cooled magma at depth beneath the volcano and would thus be of cognate origin. No means of distinguishing between these and shattered accessory basaltic clasts has been found. Subordinate crystals of olivine and plagioclase occur along with rare opaque grains. The location of all the samples studied is given in Fig. 2.25.

a) Sideromelane

Most of the pale brown sideromelane grains are vesicular and have blocky, often equant shapes. The more vesicular grains have highly irregular margins due to breakage across vesicles whereas poorly vesicular grains tend to have straight or slightly curved margins. Vesicles are spherical or sub-spherical and any one grain generally contains a variety of vesicle sizes, up to a maximum of 0·5mm. Microlites of plagioclase, which grew after most of the vesicles had formed, are found in the sideromelane along with phenocrysts of plagioclase, olivine (up to 1cm diameter) and rare Ti-augite.

Some rare, elongate sideromelane grains with stretched vesicles and flow-aligned microlites occur (Fig. 2.26). These formed by flowage of more viscous magma simultaneously with volatile exsolution prior to quenching. Most grains formed by explosive granulation due to chilling of vesiculating, fluid magma.

Occasionally, sideromelane grains may be enclosed within rims of further sideromelane (Fig. 2.27). The first non-vesicular grain probably fell back into the vent and was caught up in a subsequent eruption and rimmed by a rapidly quenched magma droplet. Other grains have irregular curved cracks due to shattering of the glass during rapid quenching. These cracks are most abundant in the non-vesicular grains and perhaps indicate that such fragments suffered the most intense quenching, or more probably that they have been severely abraded since their formation.

b) Tachylite

Although not as abundant as sideromelane, dark brown to black tachylite occurs in all units of the tuff-ring in variable proportions (Table 2.1). Tachylite grains are

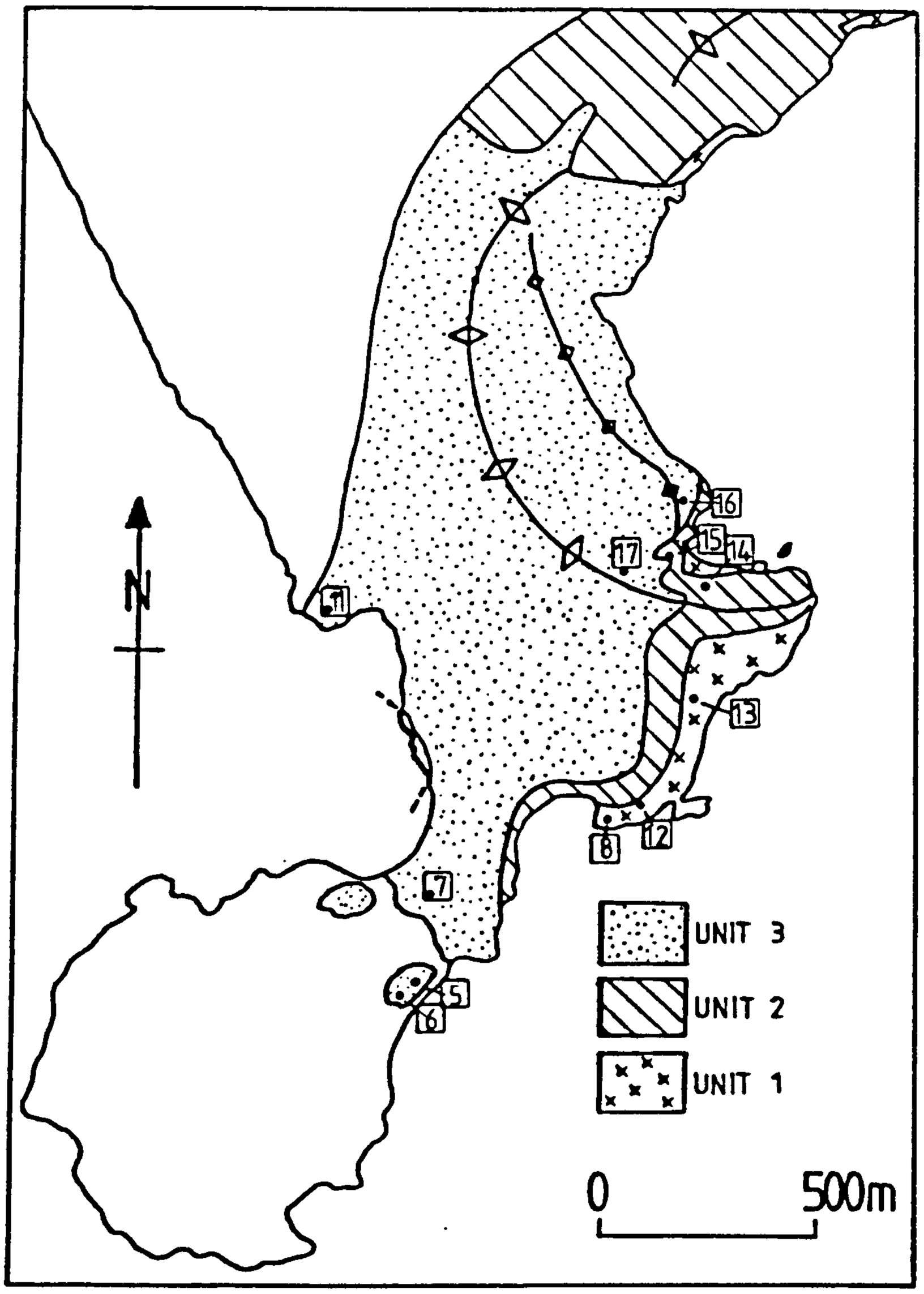

Fig. 2.25 Location map of samples which are numbered as they appear in the text.

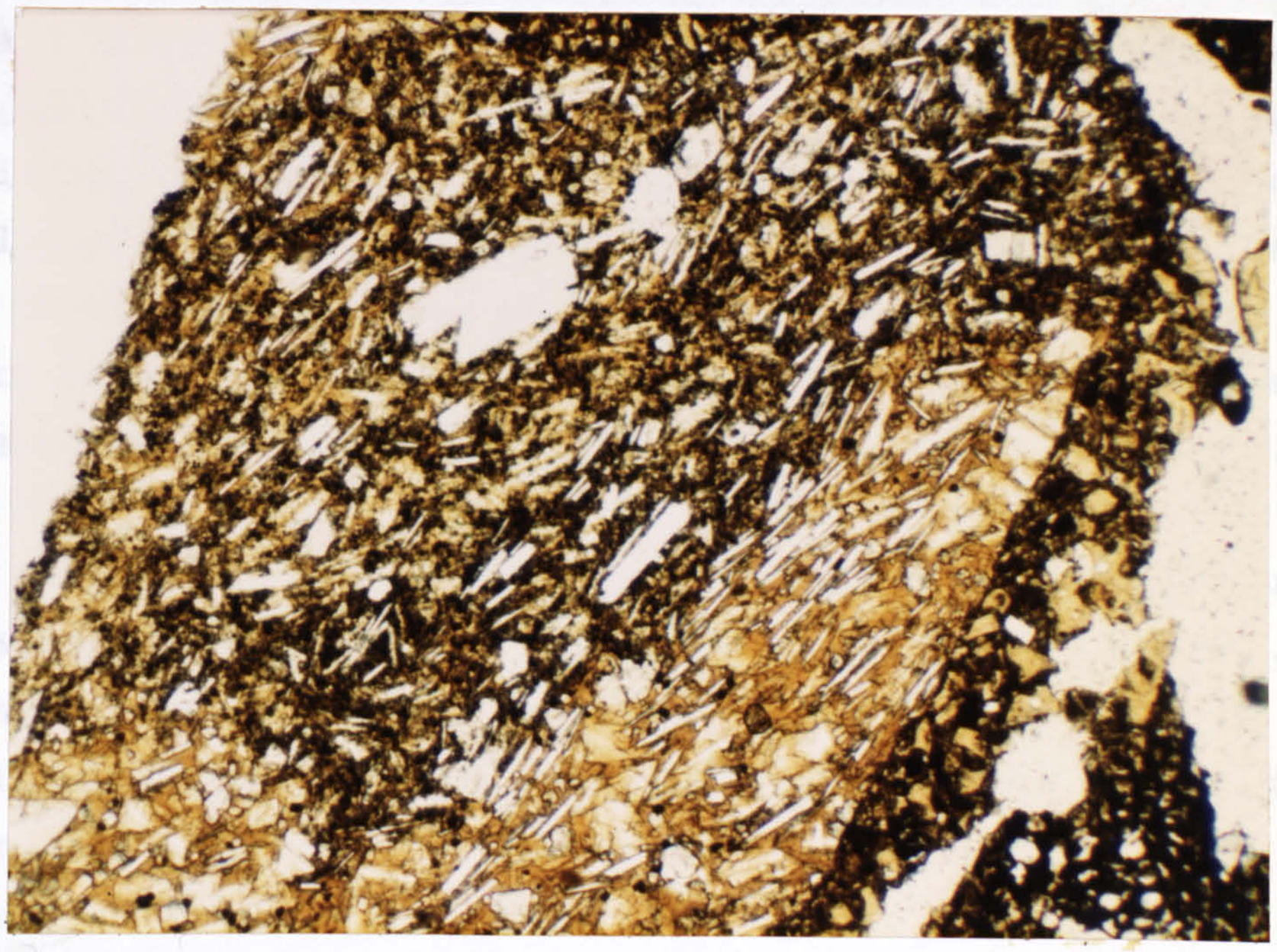

Fig. 2.26 Flow-aligned plagioclase microlites in partly tachylitic sideromelane lapillus. Plane polarised light. x10.

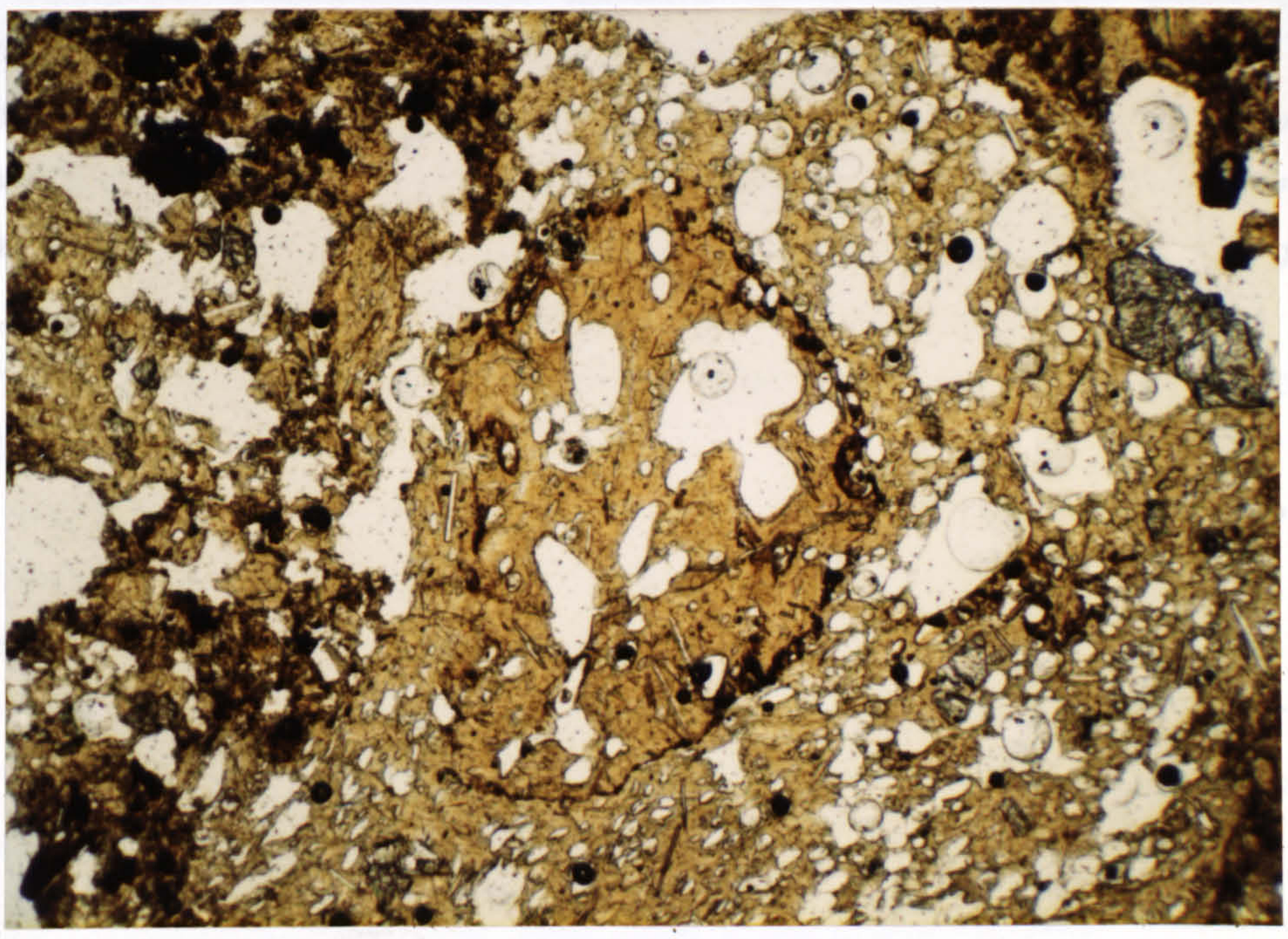

Fig. 2.27 Slightly altered sideromelane lapillus enclosed within pale vesicular glass. Plane polarised light. x10.

generally more vesicular than sideromelane and have more irregular though still sub-spherical vesicles. These are in places smaller near grain margins due to more rapid chilling. Grain shapes are roughly equant or elliptical with small irregularities because of breakage across vesicles. Many grains have lobate or ragged margins as magma droplets plastically flowed during slow cooling.

Plagioclase microlites up to 0•2mm are common in most tachylite grains and, especially in the larger grains, are aligned parallel to vesicle elongation directions. In grains which have spherical vesicles, the microlites are still well-aligned indicating slow flowage of fluid magma before disruption. The microlites grew before cooling of the magma since many are sharply truncated by grain margins and no decrease in their size towards tachylite margins is seen. Some grains have microlite alignment and vesicle elongation parallel to their margins, perhaps indicating spinning of still fluid magma droplets during ejection.

Rarely, sideromelane grains have developed tachylite patches due to the rapid chilling of magma which was beginning to crystallize iron oxides. Other grains develop variable amounts of iron oxide ranging from pure tachylite to pure sideromelane, depending on the rate of cooling. Some grains consist of sideromelane with enclosing tachylite rims (or vice-versa) due to recycling of earlier eruptive products.

Although highly variable in size and vesicularity, many of the grains being being scoriaceous, the tachylite is generally coarser than sideromelane in any deposit, often reaching 1cm diameter. It is probable that the rapid chilling of the sideromelane more effectively fragmented the magma, producing finer particles. In some samples tachylite-cored accretionary lapilli completely dominate particular horizons (Fig. 2.28) indicating less water-influenced eruptions.

c) Vesicle size

In common with most pyroclastic deposits the sideromelane ash fragments do not contain an abundance

of very small vesicles. They are dominated by vesicles with radii in the range 0·02-0·1mm. Sparks (1978) noted that vesicles with dimensions less than the critical bubble radius for expansion (R*) should not be preserved, and most should be considerably larger than this. For scoria R* is generally about 5μm which is close to the minimum Saefell vesicle size. However, the average size of the Saefell vesicles is rather less than the average for basaltic scoria which is 1-10mm (Sparks, op.cit.). This is due to the different eruption mechanisms of surtseyan and strombolian volcanoes.

In strombolian activity, magma rises freely to the surface and is disrupted by bursting of relatively large bubbles. In surtseyan activity, magma rises to near-surface depths and explosively interacts with water, causing quenching. The mass of surface overburden imposes a hydrostatic pressure on the magma, retarding free vesiculation. This effect is slightly enhanced by the flashing of water into steam, which imposes additional retarding pressures. The vesicle sizes thus depend to some extent on the depth below surface at which the magma contacts water, and the amount of steam produced.

The small size of the Saefell vesicles is thought to be at least partly due to the effects of pressure on the magma. Sparks (1978) modelled the growth of bubbles as a function of depth below magma surface for various magma parameters. Fig. 2.29 shows two of his graphs for varying magma ascent rate and water content. The effect of explosively quenching magma at depth below overburden is comparable to arresting magma vesiculation when bubbles are some depth below its upper surface. Because the overburden material is likely to be less dense than basaltic magma, direct comparison between depth values on Sparks' theoretical curves and surtseyan eruption depths is not possible. It must be stressed that overburden pressures will influence only the decompressional growth of bubbles, diffusional growth is dependant on the physical properties of the magma.

In the Saefell tuffs the vesicle sizes preserved are

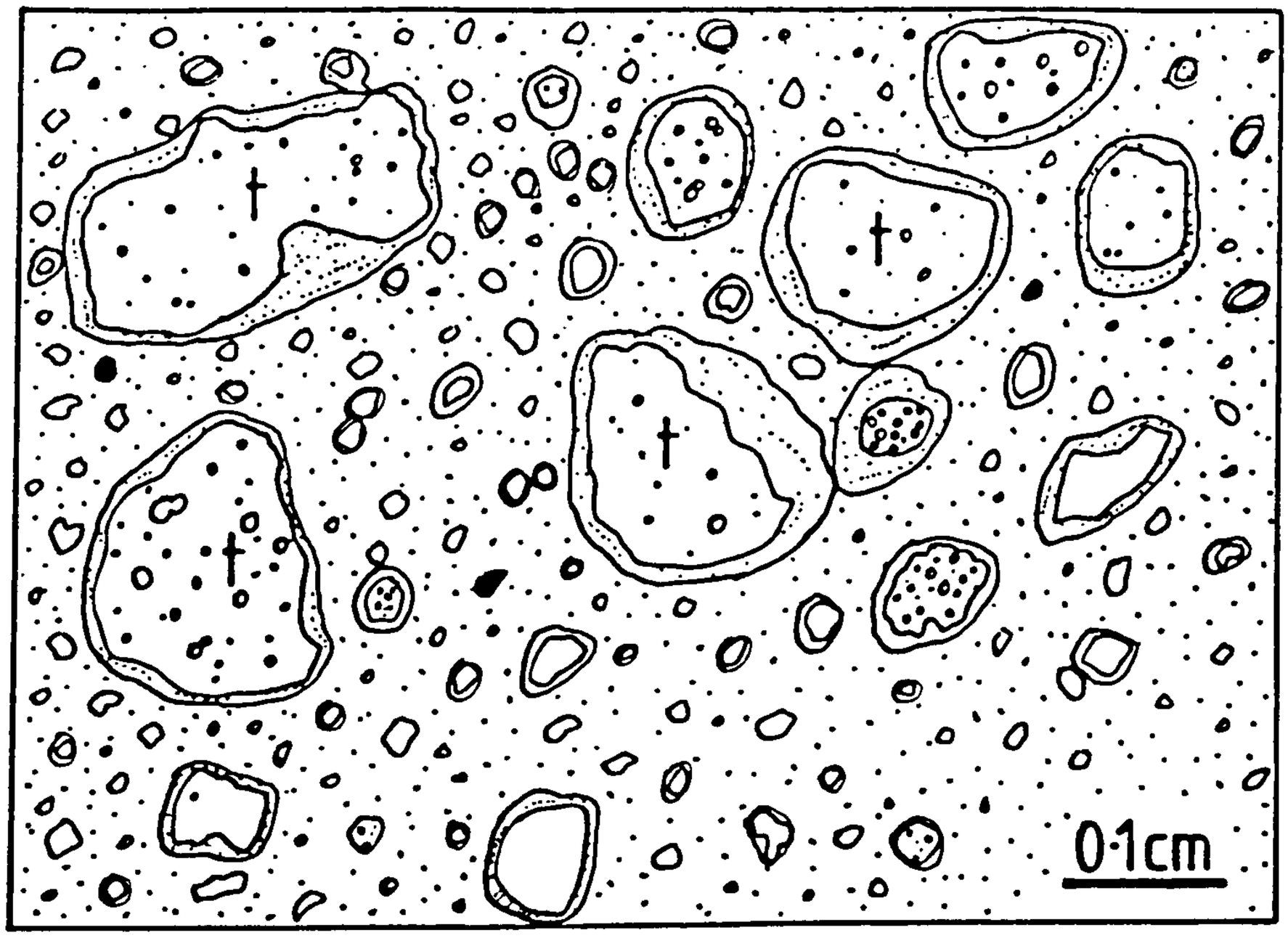

Fig. 2.28 Tachylite(t)-cored accretionary lapilli from sample I12 (Unit 1).

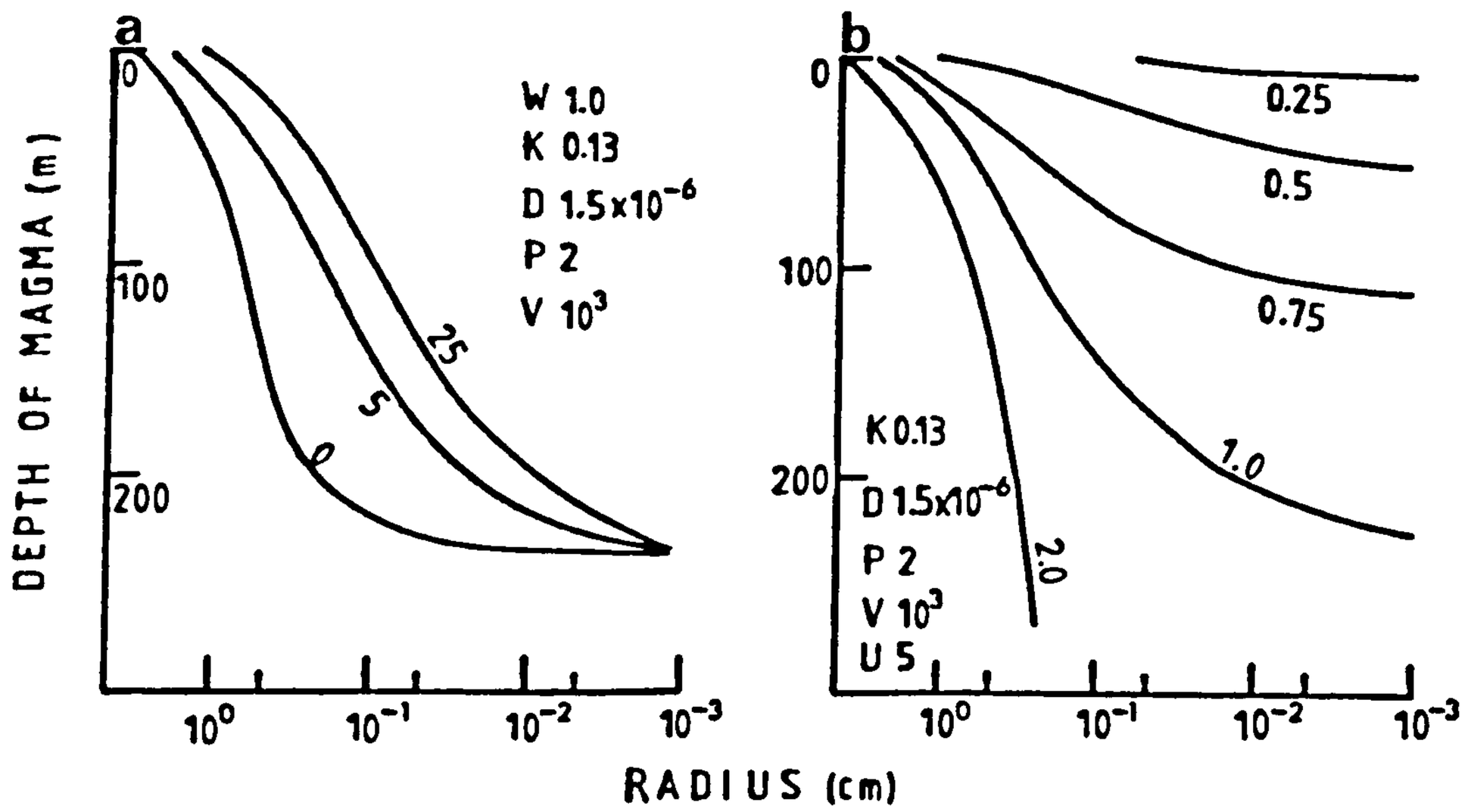

K: solubility constant D: diffusion coefficient(cm s^{-1})
P: supersaturation pressure(bar) V: viscosity(poise)

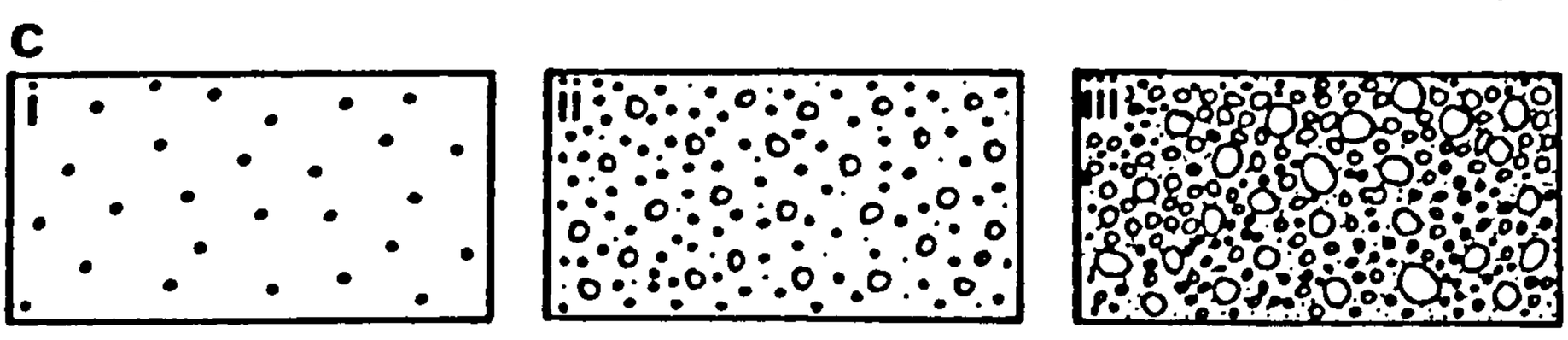

Fig. 2.29 a) Variation in vesicle radius with magma ascent rate (U cm s^{-1}).
b) Variation in vesicle radius with wt% H_2O (W) content of magma.
c) Progressive bubble growth as magma nears surface. Chilling of the Saefell magma occurred between stages ii) and iii).

0·02-0·1mm. In the more scoriaceous lapilli vesicle sizes reach 0·4mm. Since sideromelane fragments are smaller than scoria from the same horizon, it seems likely that larger bubbles are not preserved within them due to shattering of the glass on quenching. The concave embayments in many sideromelane fragments support this conclusion. By reference to Sparks' (1978) diagrams the range of vesicles in the Saefell tuffs can be used to estimate the depth below surface of magma:water interaction. Assuming magma parameters to be the same as in Fig. 2.29b and dissolved water content to be 1% the 0·1-0·4mm vesicle size range would be preserved by quenching at depths of <100m. The state of vesiculation of the Saefell magma is thought to be as indicated in Fig. 2.29c, with only minor disruption due to bursting of large bubbles.

These results are in general agreement with the similar type of eruptions on Surtsey. Here, the tuff-ring built up a 130m thick pile of hyaloclastic and pyroclastic debris above the sea-floor. Water percolating down through the vent material from the breached crater of the tuff-ring could contact magma at shallow depths. In conclusion, it may be seen that vesicle size ranges can be qualitatively used to compare eruption mechanisms. Further discussion of this evidence will follow in later chapters.

d) Fines

All the Saefell tuffs contain a high proportion of fine ash which generally forms a matrix between coarser particles. For practical purposes the matrix was defined in thin section as those particles <0·2mm and this was found to constitute between 35 and 75% of each sample (Table 2.1). Although altered in many samples the matrix is generally composed of sideromelane grains. These are largely less vesicular than the coarser grains because many represent the broken up glass between the vesicles of coarser particles.

In many of the lapilli-tuffs much of the fine material exists as accretionary rims around cores of coarser particles (Fig. 2.30). In some cases all the fine material in a particular lapilli horizon is found within

TABLE 2.1 MODAL ANALYSES OF SAEFELL AND SURTSEY TUFFS

Sample number	I5	I6	I7	I11	I12	I13	I14	I15	I16	I17	I9	I10
Vesicular sideromelane	14•9	18•2	23•7	12•4	40•0	11•9	29•0	40•0	23•4	24•4	39•1	31•1
Non-vesicular sideromelane	4•8	6•0	4•0	1•7	2•5	7•0	1•6	2•9	3•7	8•6	3•5	4•4
Matrix	59•9	49•2	50•0	76•7	37•0	45•0	46•0	49•2	57•6	50•4	46•8	58•9
Olivine/ pyroxene	2•0	1•2	1•0	0•6	1•5	0•4	0•1	0•1	0•4	0•8	1•6	2•6
Lithics	0•2	2•1	1•5	0•3	4•0	17•5	2•2	0•6	0•1	0•2	0•1	0•1
Tachylite	15•2	18•2	18•5	7•4	12•6	15•0	19•0	5•5	11•5	13•6	8•3	2•5
Opaques	1•0	2•2	0•1	0•7	0•3	0•4	0	0•5	1•2	0•8	0•2	0•3
Plagioclase	1•6	2•6	0•8	0•2	1•6	1•2	1•1	1•2	2•1	1•2	0•4	0•1
Authigenics	0•2	0•1	0	0	0•5	1•4	0	0	0	0	0	0
% Palagonite in rock	4•5	0	0	15•0	22•3	16•5	1•5	2•5	0•5	0	0•2	4•3

these rims. Such horizons contain a high proportion of void space between the large, composite grains. Typically, the rims are 0·1-1mm thick and contain fragments <0·2mm in diameter which are poorly sorted and either coarsen towards the outer rim margin or are ungraded. Elongate rim fragments lie with their long axes concentric to the core of the lapilli but this is rarely sufficiently well developed to form even faint concentric banding. The rims vary in thickness between deposits but tend to be of similar size in any one bed, and form around any particles larger than the rim grain size. All lapilli contain a particle nucleus with a diameter greater than half the total diameter, which may be a juvenile, lithic or crystal fragment.

The rims vary in thickness around irregularly-shaped grains so as to smooth out such irregularities. This is best displayed by lapilli which stuck together during growth and subsequently accreted a common rim. The largest lapillus found has a diameter of 15mm with a rim thickness of 2mm. The majority lie between 1 and 5mm and occur in thin, well-sorted beds or more usually scattered throughout massive, poorly-sorted thicker units.

The rimmed lapilli are different to most accretionary lapilli described from pyroclastic deposits, which generally have fine, concentric laminae around a central core of coarser, structureless ash (Moore & Peck, 1962). However, most of the latter lapilli formed by accretion in high eruption columns. Here, the abundance of fine material and small amounts of moisture favoured such relatively slow "onion-skin" growth as particles were buoyed up in the plume convective system. In contrast, small tuff-ring volcanoes, with their low, heavily particle laden eruption columns rich in steam would provide conditions favouring the rapid growth and fallout of lapilli rimmed by poorly sorted, coarse ash. The inverse grading seen in many of the rims was probably formed as lapilli fell through the lower, coarser regions of the eruption cloud. Similar accretionary lapilli have been found by the author in other Icelandic tuff-rings such as Hverfjall, Hrossaborg,

Ludent and Surtsey and are thus characteristic of the water-rich, poorly-developed eruption columns of tuff-rings.

e) Crystal and lithic fragments

Plagioclase, olivine and magnetite are the main crystal phases, along with rare clinopyroxene. Their compositions have been determined optically. The plagioclase is andesine-labradorite (An46-54) and is the most abundant phenocryst, reaching up to 2cm (and 4cm in the marginal scoria deposits within Unit 1). The plagioclase occurs either as separate crystals with broken, angular margins or is rimmed by basaltic glass. Such rimmed feldspars are commonly intergrown with the glass at their margins (Fig. 2.31) indicating that resorption and corrosion occurred just prior to quenching of the magma. Some feldspars have rounded patches of vesicular glass within them which may indicate that corrosion of early formed feldspars occurred with penetration of magma into cracks. Skeletal inclusions of acicular opaque crystals, possibly magnetite, are found in one feldspar grain.

Olivine, like plagioclase, occurs as single crystals up to 0·4mm but is more commonly associated with basaltic glass. The olivine is forsteritic in composition (Fo60-85) and sometimes contains small brown cubes similar to those which Jakobsson (1968) identified as Cr-spinel in olivines from other Westmann Island volcanics. Many of the olivines are deeply corroded by the surrounding glass although some subhedral fragments do exist within glass lapilli. Clinopyroxene is purplish to pale brown, often weakly pleochroic and is probably titanaugite. It rarely forms a separate crystal phase and is much more common in the basalt lithic clasts.

The lithic clasts consist almost entirely of alkali olivine basalt probably similar to the composition of the Saefell glass which has been analysed (Table 2.2). The most common lithic clast is a medium-grained holocrystalline basalt with plagioclase feldspars up to 0·5mm, olivine and intergranular titanaugite. These clasts were derived by

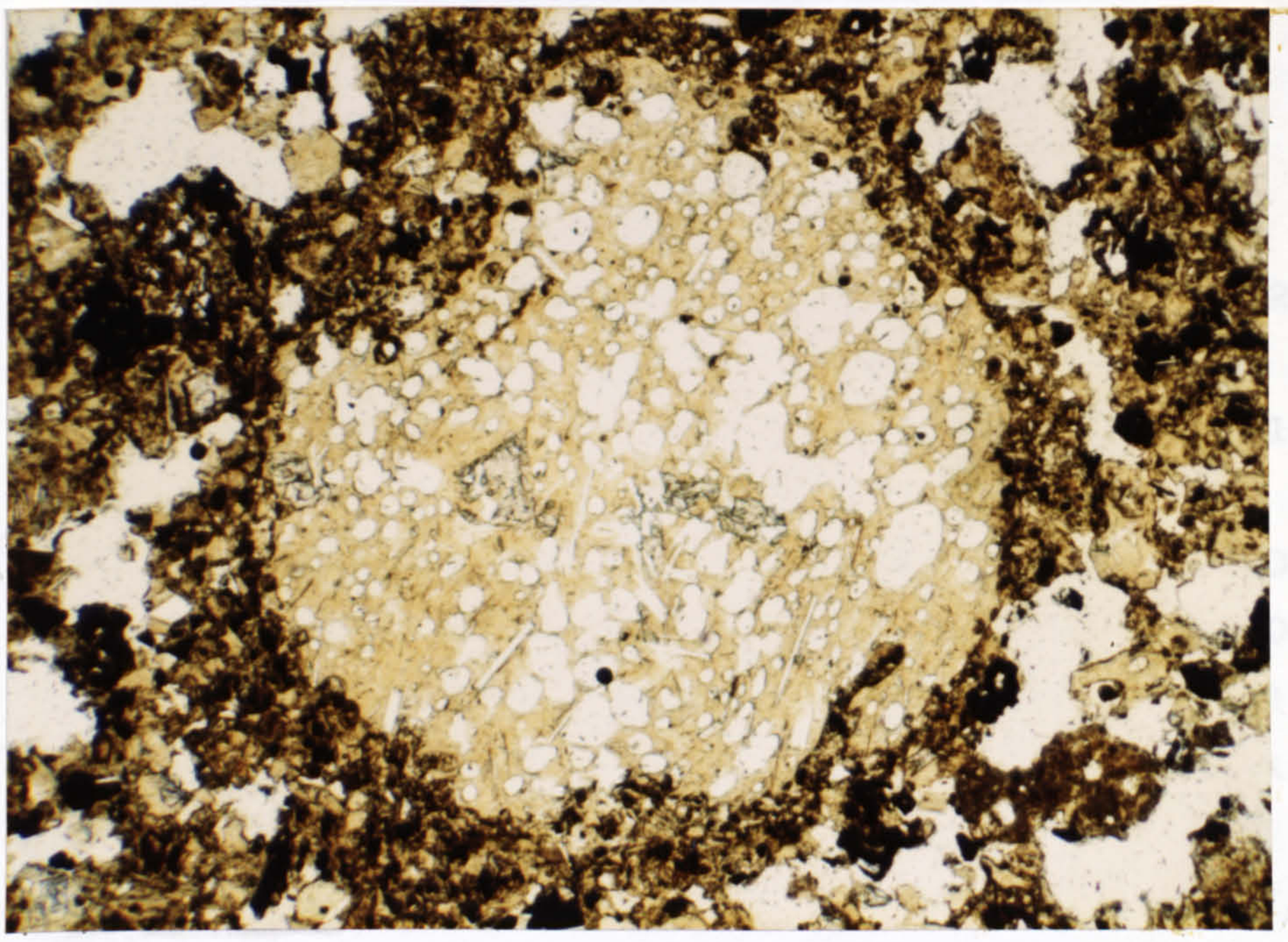

Fig. 2.30 Sideromelane lapillus with poorly-sorted accretionary rim. Plane polarised light. x10.

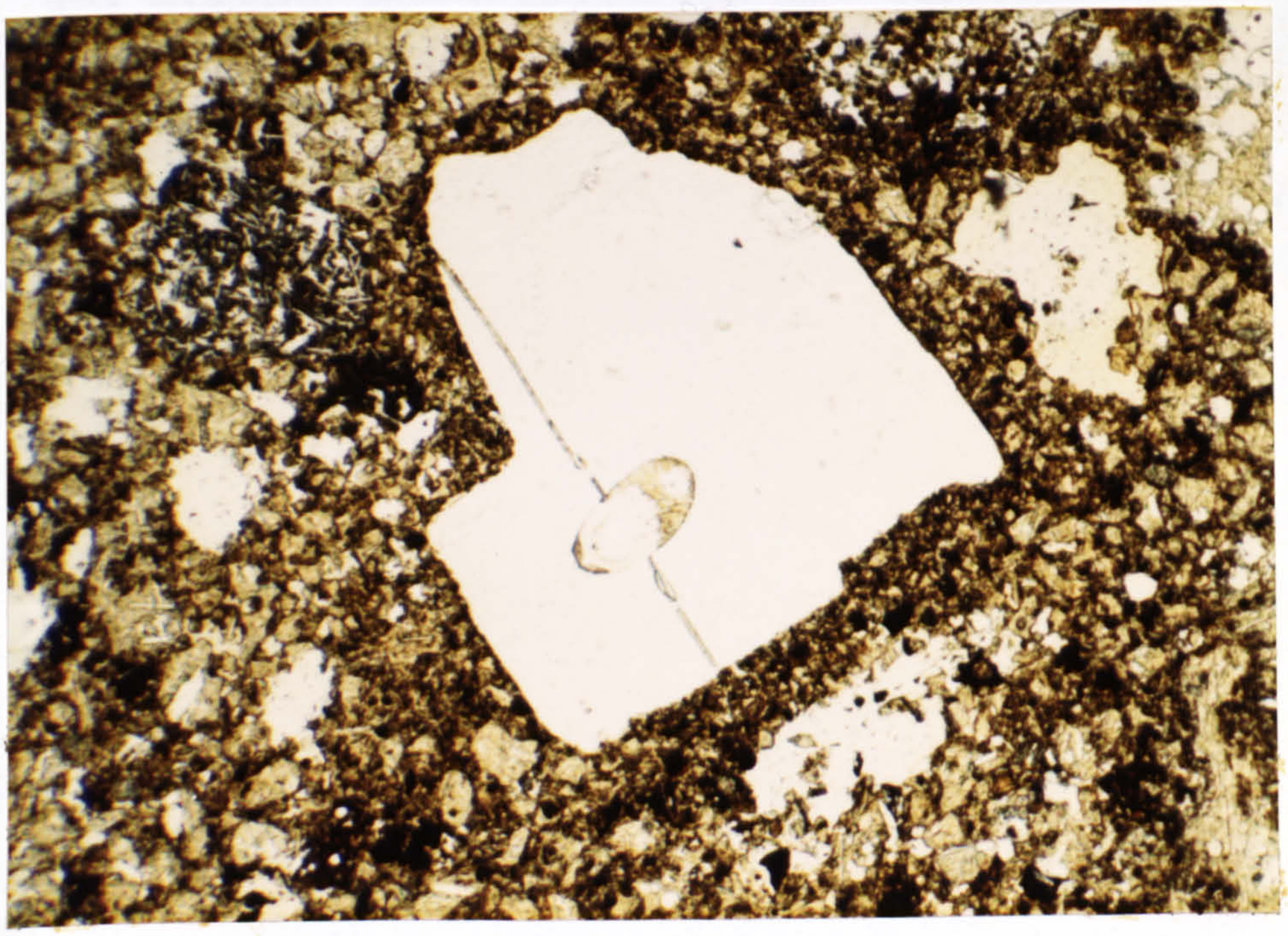

Fig. 2.31 Plagioclase crystal with sideromelane glass which has penetrated along a cleavage plane and corroded part of the grain. Plane polarised light. x10.

TABLE 2.2 SAEFELL GLASS AND MINERAL ANALYSES

	(1)	(2)	(3)	(4)	(5)	(6)
SiO_2	46·8	46·8	53·2	37·6	47·3	46·6
TiO_2	2·53	2·78	0·07	0·12	2·36	2·02
Al_2O_3	14·1	16·7	26·9	0·08	16·9	15·9
Fe_2O_3	-	-	-	-	2·66	1·61
FeO	12·1	12·7	0·52	20·6	9·10	10·3
MnO	0·22	0·28	-	0·38	0·15	0·20
MgO	6·59	6·12	-	39·4	5·38	9·00
CaO	12·2	9·51	10·5	0.30	10·4	10·51
Na_2O	3·04	4·01	5·02	0·59	3·63	3·21
K_2O	0·59	0·82	0·35	0·02	0·70	0·51
P_2O_5	-	-	-	-	0·37	0·26
Total	98·17	99·72	96·56	99·09	98·95	100.12

(1) Sideromelane lapillus from I12 (Unit 1).
(2) Sideromelane lapillus from I12.
(3) Plagioclase microlite from I12 lapillus.
(4) Olivine phenocryst from I12 lapillus.
(5) Helgafell lava (Jakobsson, 1968) for comparison with Saefell glass.
(6) Surtsey lava (April 1964) (Jakobsson, 1968).

Total Fe as FeO in samples (1) to (4) analysed by electron microprobe.

fragmentation of older underlying lavas.

f) Composition of the tuffs

The tuffs were point-counted in thin section to determine their modal composition (Table 2.1). The similarity in composition of the tuffs is indicated in Fig. 2.32 which displays the variation in composition up the Saefell sequence. No systematic changes in the tuff composition are found to occur although the exeptionally high matrix content of the Unit 3 samples may indicate the greater violence of the eruption at this time, causing intense granulation of the tephra.

2.6.2 Grain size and morphology

a) Grain size studies .

Although grain size studies have long been used in sedimentology to determine the origin and depositional mechanism of sediments this approach has only comparatively recently been quantitatively applied to pyroclastic deposits (Sheridan, 1971; Walker, 1971; Walker & Croasdale, 1971). Various size parameters have been used in an attempt to distinguish the eruption type, the depositional mechanism and the distance from the vent of tephra samples. Walker (op.cit.) used median diameter vs. sorting plots to distinguish between pyroclastic flow and fall deposits. Walker & Croasdale (1971) showed that such plots are effective in discriminating between strombolian and surtseyan activity. In a different approach, Sheridan (1971) used C (coarsest one percentile) - M (median diameter) plots to distinguish between various types of airfall, surge and flow deposits.

Many younger pyroclastic deposits have now been sieved to determine these parameters and comparison with the Saefell tuffs may be usefully made. Due to the indurated nature of many of the Saefell tuffs the grain size distribution was determined by thin section point counting techniques (see Appendix 1 for methods employed). Conversion of thin section data to equivalent sieve values was carried out by use of Harrell & Eriksson's (1979) equations (Appendix 1). The raw and converted data for the

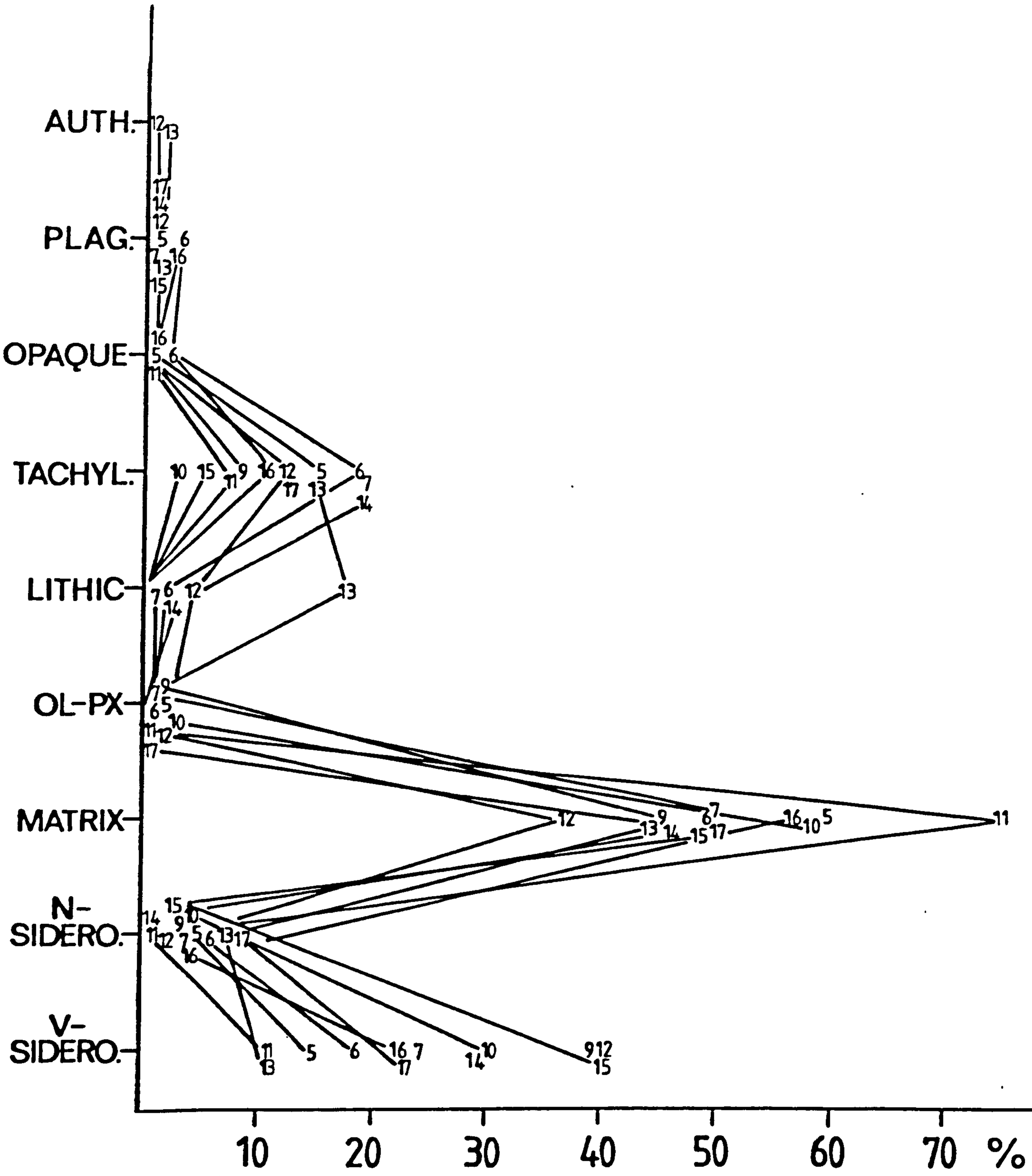

Fig. 2.32 Point count modal analyses of the Saefell tuffs. V: vesicular, N: non-vesicular lapilli.

samples is given in Table 2.3. No attempt was made to calculate skewness or kurtosis parameters because they cannot be accurately converted from thin section to sieve grain size measurements and are little used in pyroclastic studies.

When the 8 Saefell samples are plotted on an Mdø/σø diagram (Fig. 2.33) the samples lie within the surtseyan field or are more often slightly finer and less well-sorted. All the samples plot within Walker's (1971) flow field (Fig. 2.33) and some plot in the area of overlap with the airfall field, a characteristic of many base-surge deposits (Walker op.cit.). However, on a C-M diagram (Fig. 2.33) the samples fall into the fall, flow and surge fields of Sheridan (1971). This apparent diversity in origin may be explained by considering some of the features of the tuffs which are as follows :-

1. Many samples contain accretionary lapilli. Build up of poorly sorted rims of ash round coarser cores and subsequent fall out will result in much more poorly-sorted grain distributions. This is sufficient to cause airfall tephra to plot in the field of pyroclastic flow on an Mdø/σø diagram. Sample I7 is completely composed of large accretionary lapilli and plots in the flow field on an Mdø/σø diagram (Fig. 2.33) but in the airfall field on a C-M diagram. The presence of accretionary lapilli increases σø greatly and for such samples C-M plots are more meaningful since they are not dependant on sorting. The reason why many of the samples plot in the rhyolitic ash flow field is unclear. It may be connected with the extreme fines-enriched nature of most samples, causing them to have higher positive Mdø values.

2. Many samples, although dominantly composed of fine ash, contain isolated lapilli which greatly alter their C (coarsest one percentile) values. Such coarse fragments are very common in proximal deposits and may result by mixing of coarser material from a particular eruption with the finer, more slowly settling material from a preceding explosion. Also, the moisture-rich, dense, poorly-expanded eruption columns of surtseyan tuff-rings preclude any

a.

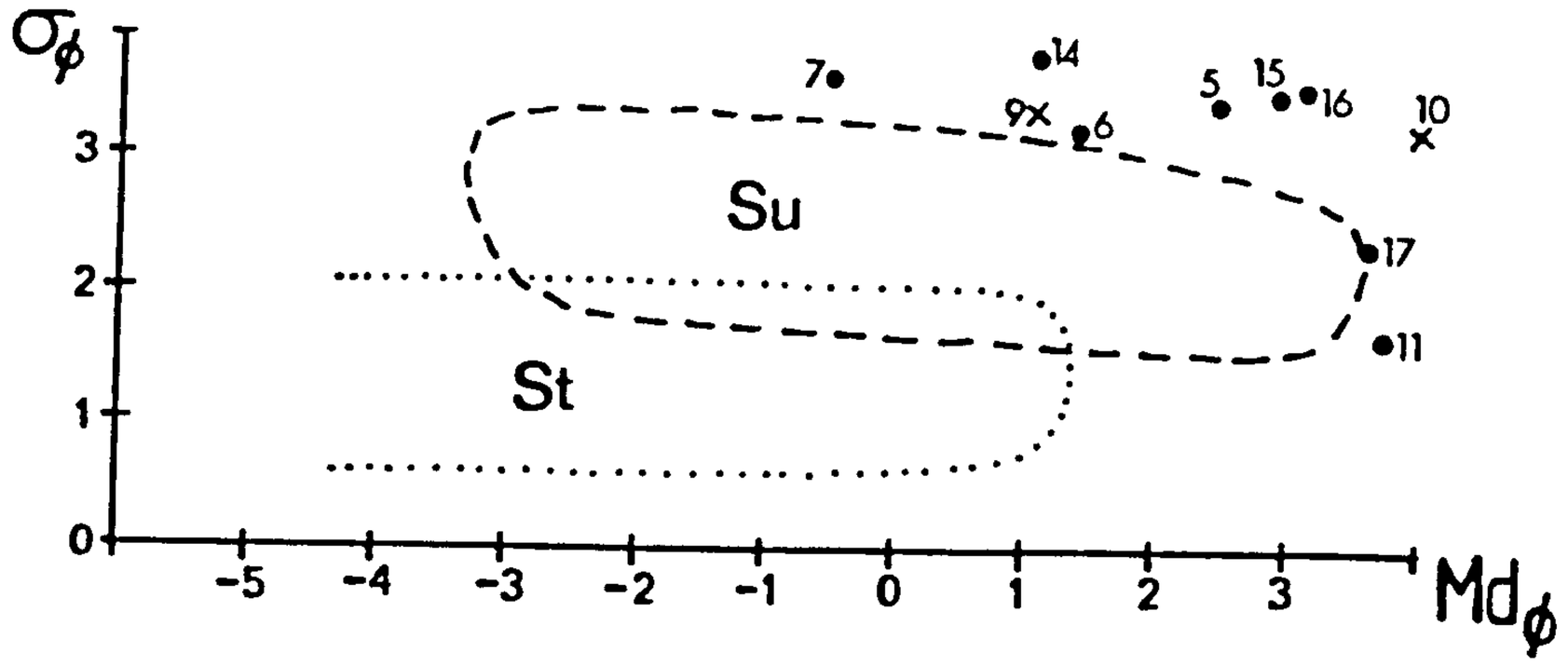

b.

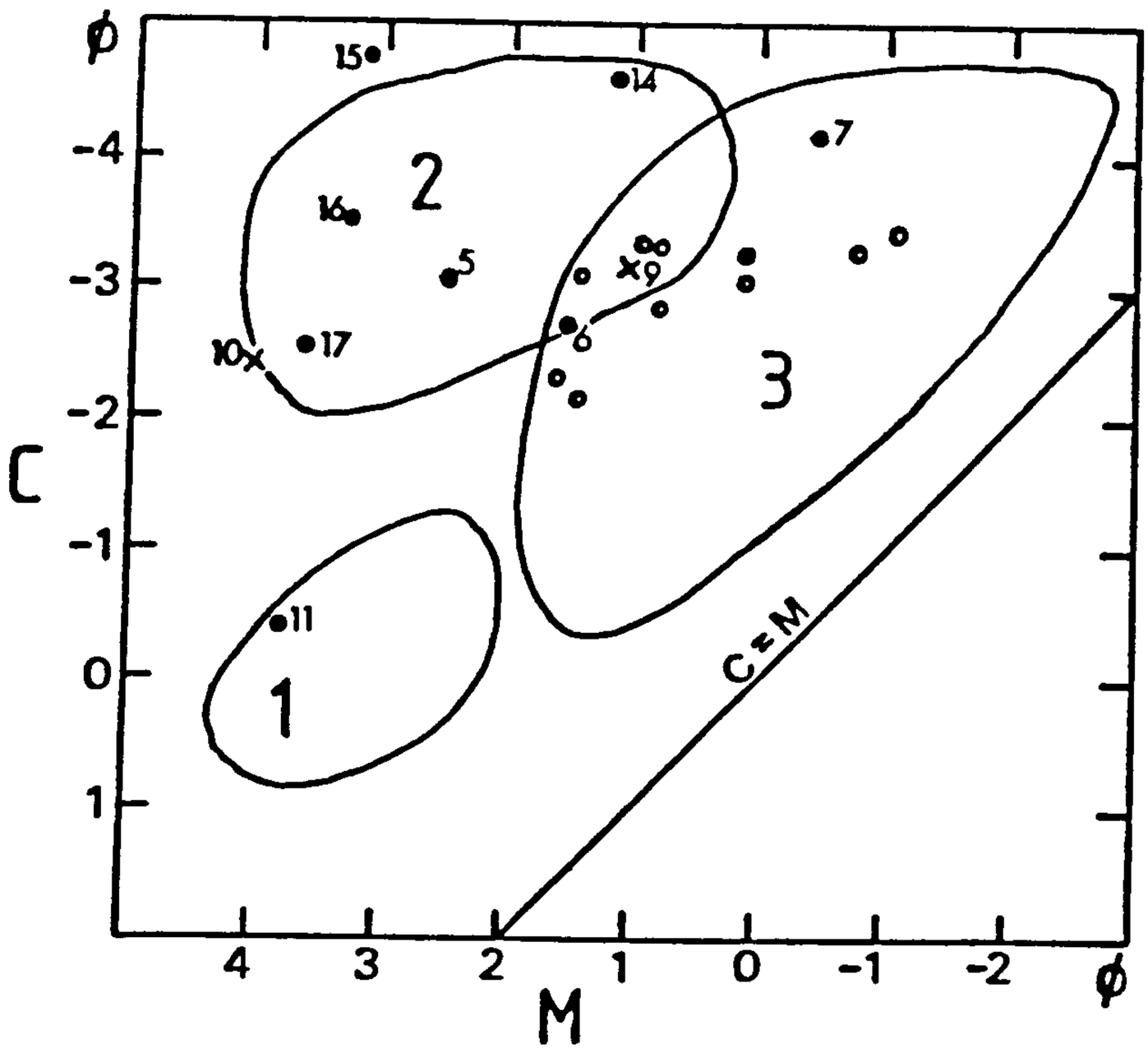

C.

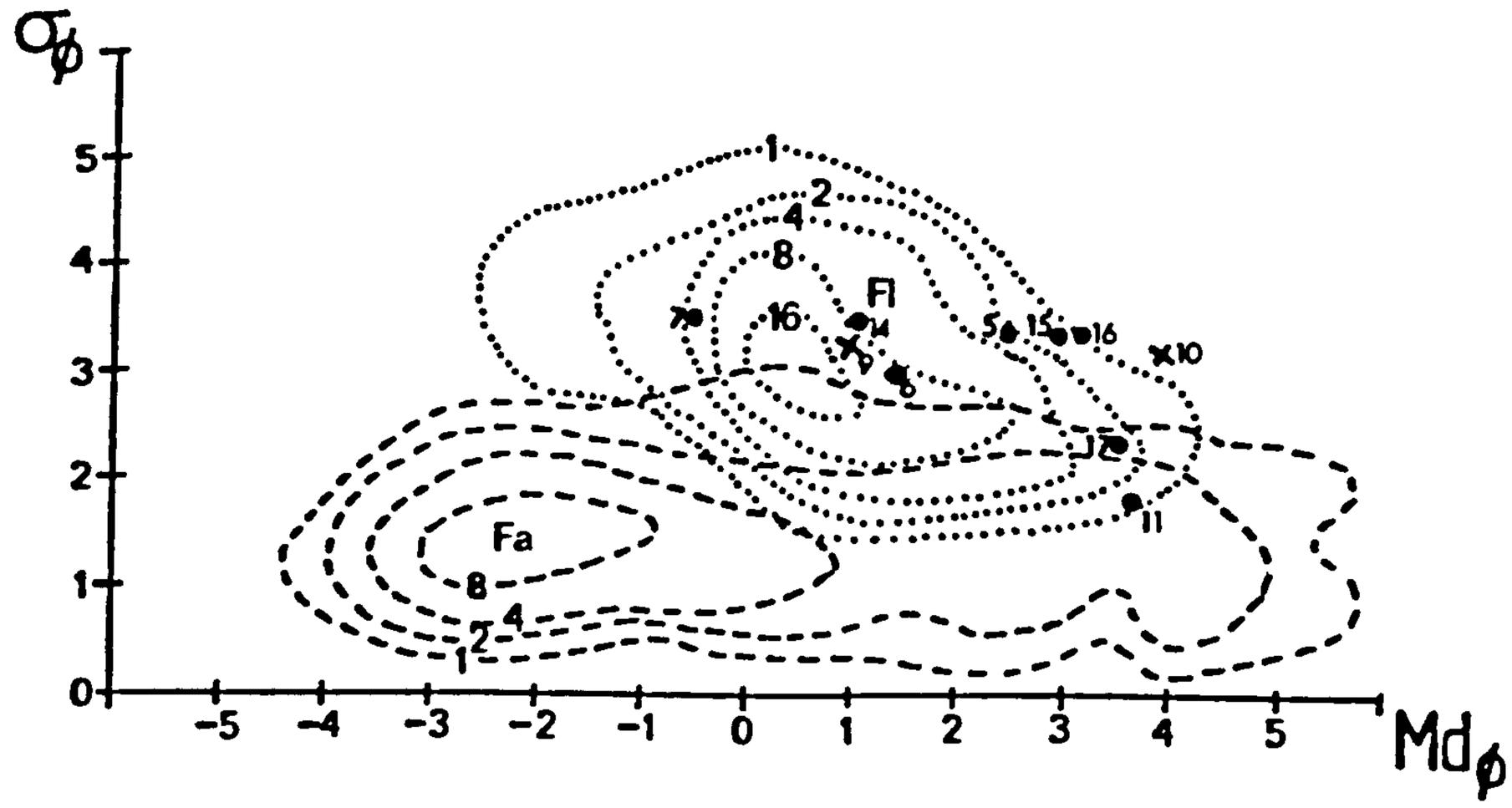

Fig. 2.33 Grain size plots of the Saefell and Surtsey tuffs. Filled circles: Saefell tuffs, crosses: Surtsey tuffs. See text for discussion.

TABLE 2.3 THIN SECTION GRAIN SIZE ANALYSES

Sample number	I5	I6	I7	I11	I14	I15	I16	I7	I9	I10
+6ø	30	28	22	41	27	33	26	30	20	40
+5	6	4	8	9	6	9	18	17	5	13
+4	12	8	9	17	5	10	10	14	9	9
+3	13	7	5	17	7	10	8	9	9	6
+2	11	9	2	7	9	9	7	10	12	7
+1	6	22	3	8	10	6	4	10	14	7
0	2	9	18	1	11	6	7	5	9	4
-1	18	12	23	0	12	10	14	5	18	14
-2*	2	1	8	0	8	4	6	0	4	0
-3	0	0	2	0	5	3	0	0	0	0

* Grain sizes coarser than -2ø (4mm) measured from slabs of tuff samples

marked sorting unless strong winds are blowing. These cause removal of fines and thus better sorting in proximal tephra.

3. Samples of Unit 3 from more distal tuffs are generally finer and better sorted than other deposits. This is thought to be the result of directed blasts during Unit 3 deposition sorting the tephra better than non-directed eruptions. This would explain the fine, well-sorted sample I11 which is thought on field evidence to be a distal base-surge deposit,and plots in the base surge dune area on a Sheridan C-M diagram (Fig. 2.33). Other distal Unit 3 deposits (I6 & I7) are much more poorly sorted, due to the presence of the previously mentioned accretionary lapilli.

When compared with cumulative curves for Surtsey tephra (Sheridan, 1971), all the Saefell samples have similar characteristics (Fig. 2.34). Sheridan argues that the Surtsey deposits have two modes of transport indicated by their coarse and fine fractions respectively. The coarse fraction has airfall and the fine fraction has suspended load characteristics on size-frequency diagrams. This is possibly because near the vent airfall tephra is continually falling into and mixing with base-surge deposits. The convergence of the Saefell (and Surtsey) curves towards the finer part of the distribution suggests coarse tail grading, indicative of high particle concentration flows (Middleton, 1966).

b) Morphology of tephra

Ash morphology was studied by SEM (see Appendix 2 for details) and quantitative measurements of grain shapes were carried out using the methods of Honnorez & Kirst (1975). Such studies are useful in distinguishing the mode of formation of pyroclastic deposits by comparison with the products of observed or better understood eruptions. A comprehensive atlas of ash morphology has been prepared by Heiken (1974).

SEM studies

SEM studies indicate that the Saefell tephra is typical blocky phreatomagmatic ash with grain shapes

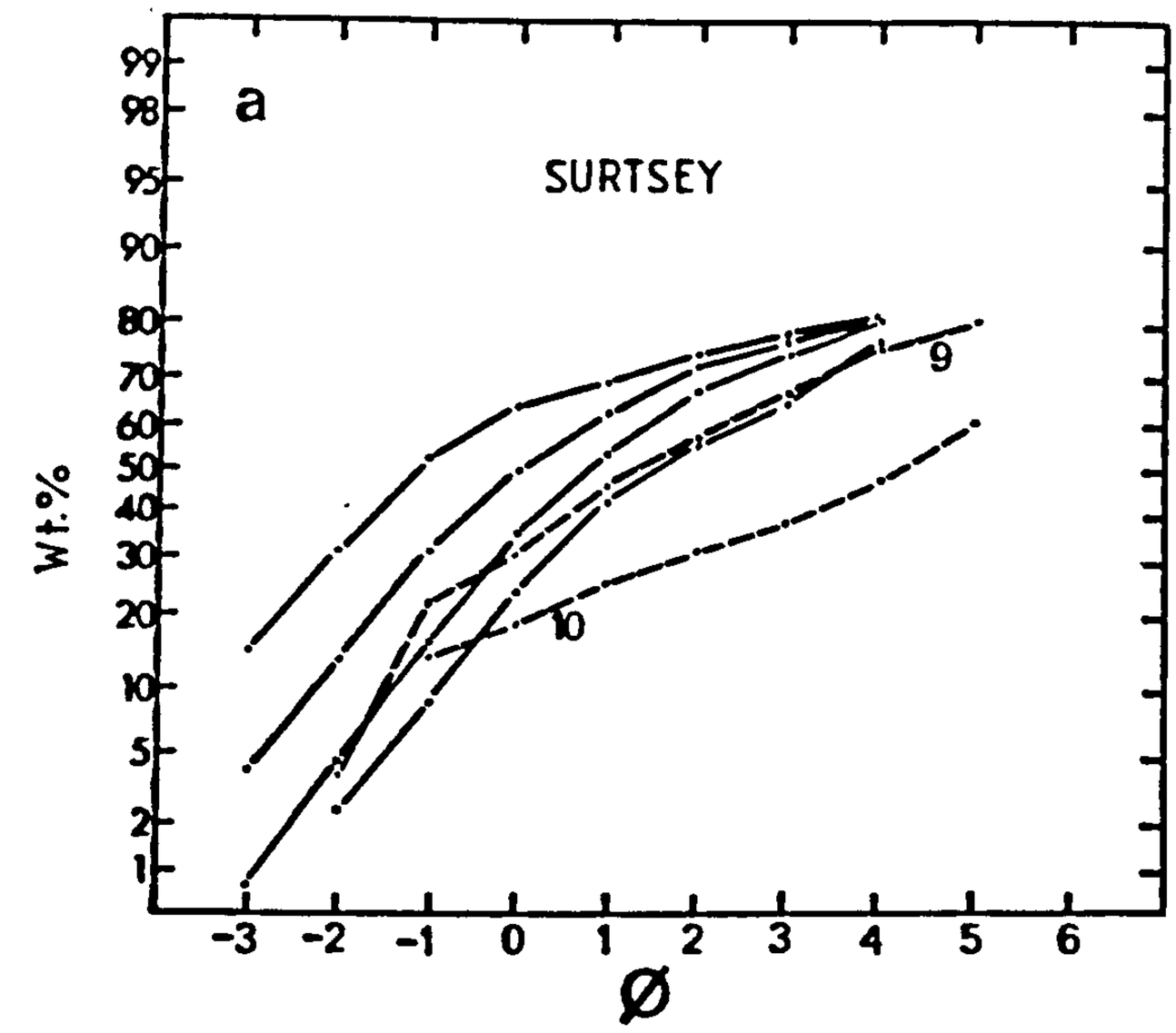

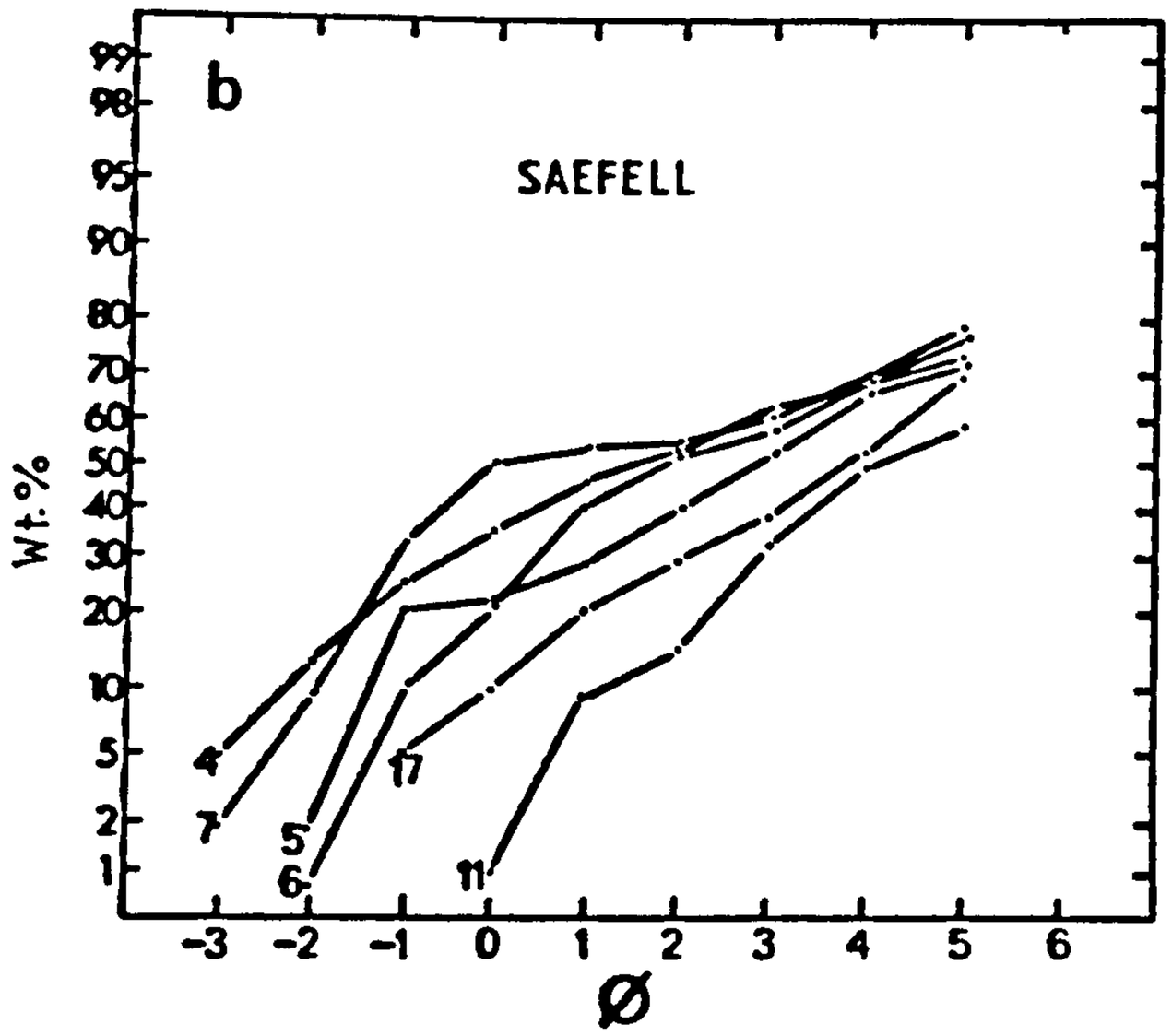

Fig. 2.34 Cumulative frequency curves of Surtsey and Saefell tuffs.
a) Surtsey tuffs (largely from Sheridan, 1971)
b) Saefell tuffs

controlled by fractures, and having generally low vesicle contents. Concave fracture surfaces and triangular impact pits (Fig. 2.35a) are common due to high velocity particle collisions which knock the sharp corners off most of the larger grains. Grain abrasion is probably aided by the internal thermal stress within the rapidly chilled glass which causes the particles to react in a more brittle manner than more slowly cooled glass. This process partly accounts for the lower proportion of fine tachylite grains in the matrix of the tuffs even though they have been subjected to similar impact effects. Finer glass grains tend to be more angular (Fig. 2.35b) and have been less abraded during eruption, a process noted in the wind transport of quartz grains (Kuenen, 1964). The main origin of the variously-sized tephra is of course primary granulation of slightly vesiculating fluid magma by explosive quenching. This forms the main , planar fracture surfaces which bound most grains and meet at nearly right angles. These are due to contraction of the glass after chilling and are characteristic of hyaloclastic ashes (Heiken, 1972). The abrasion process is a later effect superimposed on this and forms the smaller,curved fracture surfaces and impact pits.

Other features of the tuffs include :-

a) Spherical, smooth-surfaced projections (Fig. 2.35c) interpreted as vesicle infilling material exposed by breakage of altered grains during sample preparation.

b) Rare etch pits (Fig. 2.35d) which are probably due to dissolution by groundwater.

c) Growth of authigenic minerals; this feature is seen on most grain surfaces and will be discussed in the section on alteration.

Quantitative grain morphology

Measurements of the relative proportions of planar (P), convex (V) and concave (C) segments along grain perimeters were carried out on thin sections of the tuffs. Honnorez & Kirst (1975) developed such measurements to quantify the difference between non-explosive granulation of deep sea basaltic extrusive activity and explosive granulation of

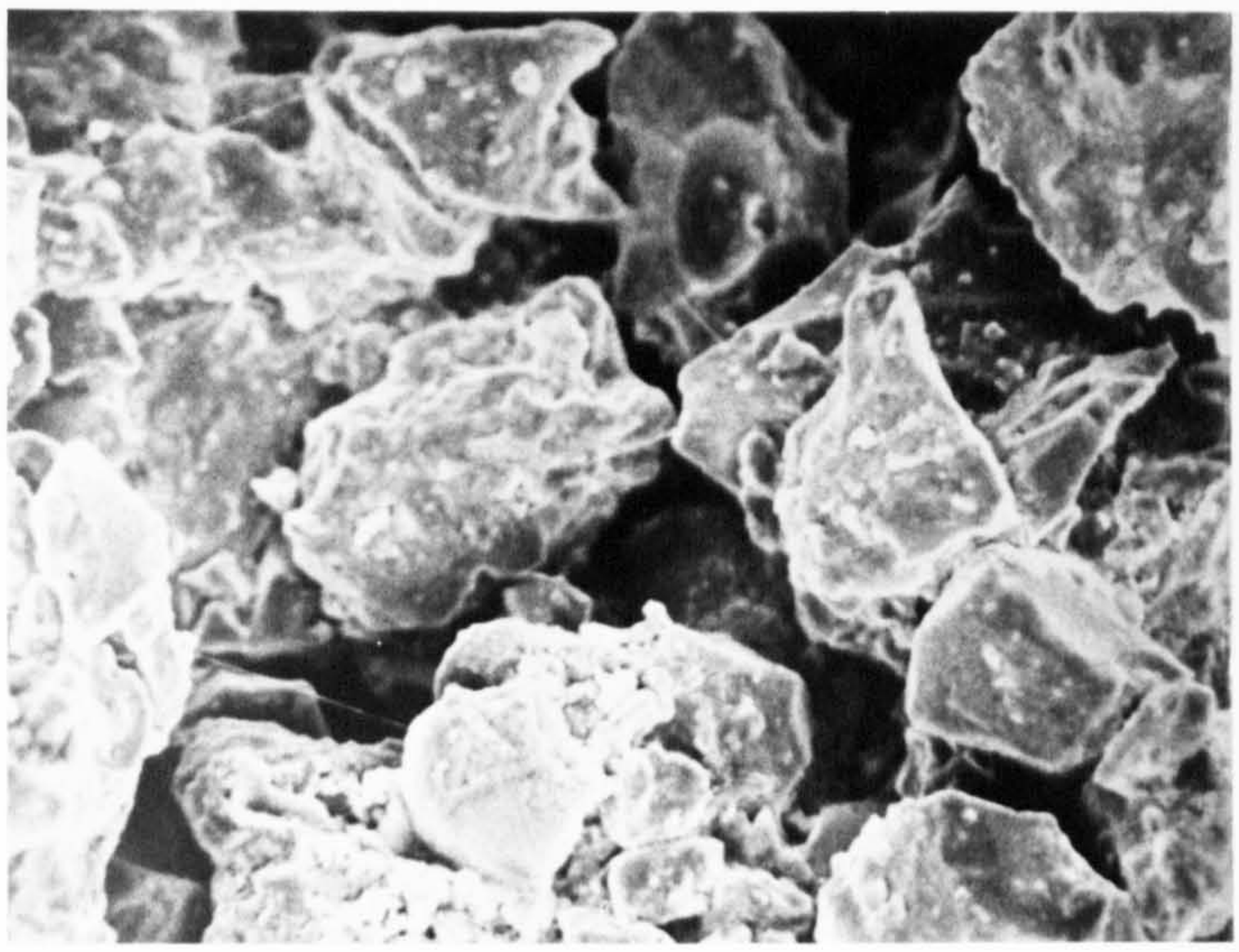

Fig. 2.35 a) SEM photograph of Saefell ash showing concave fracture surfaces, impact pits and small vesicles. x250.

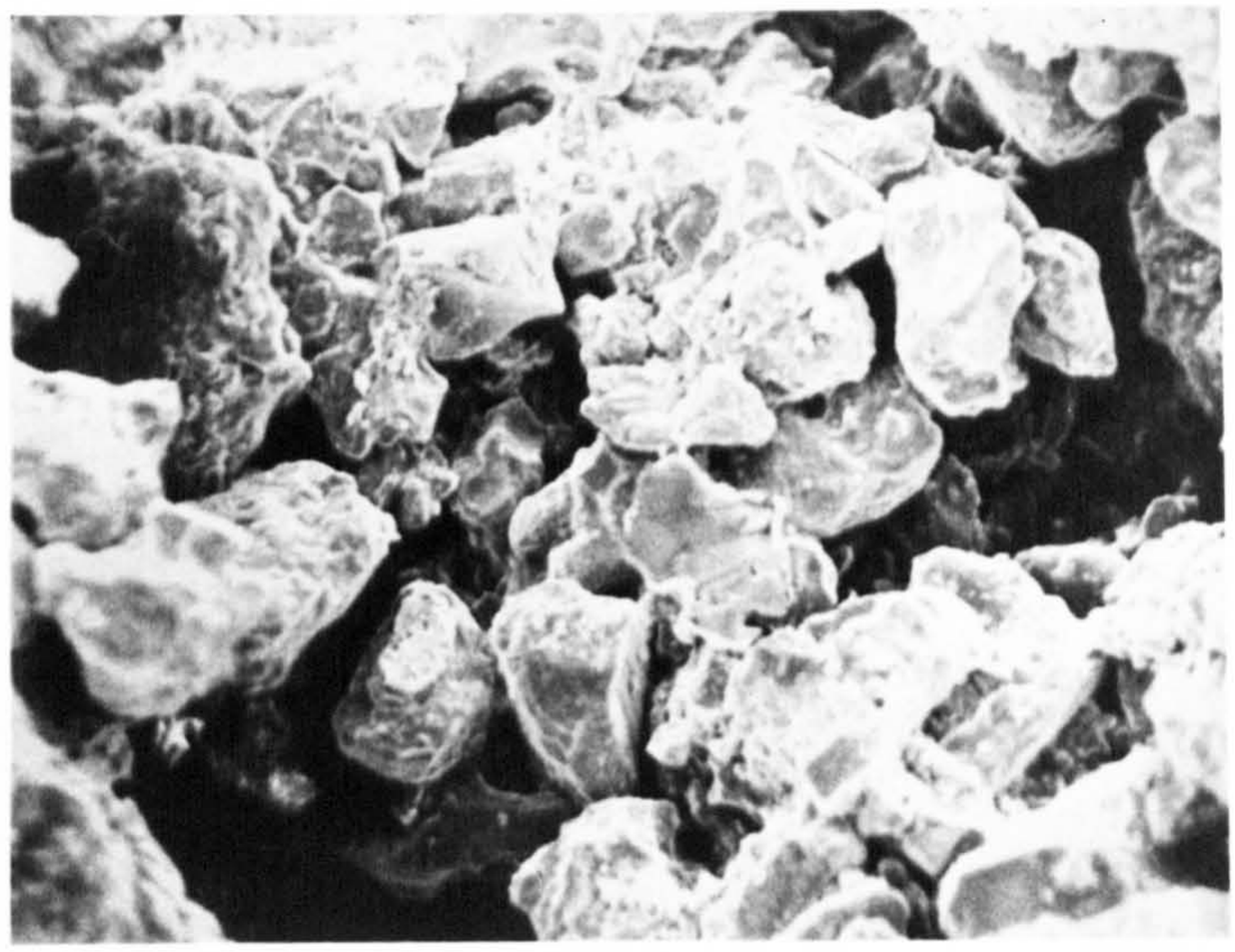

Fig. 2.35 b) SEM photograph showing blocky, angular, fine Saefell ash. x150.

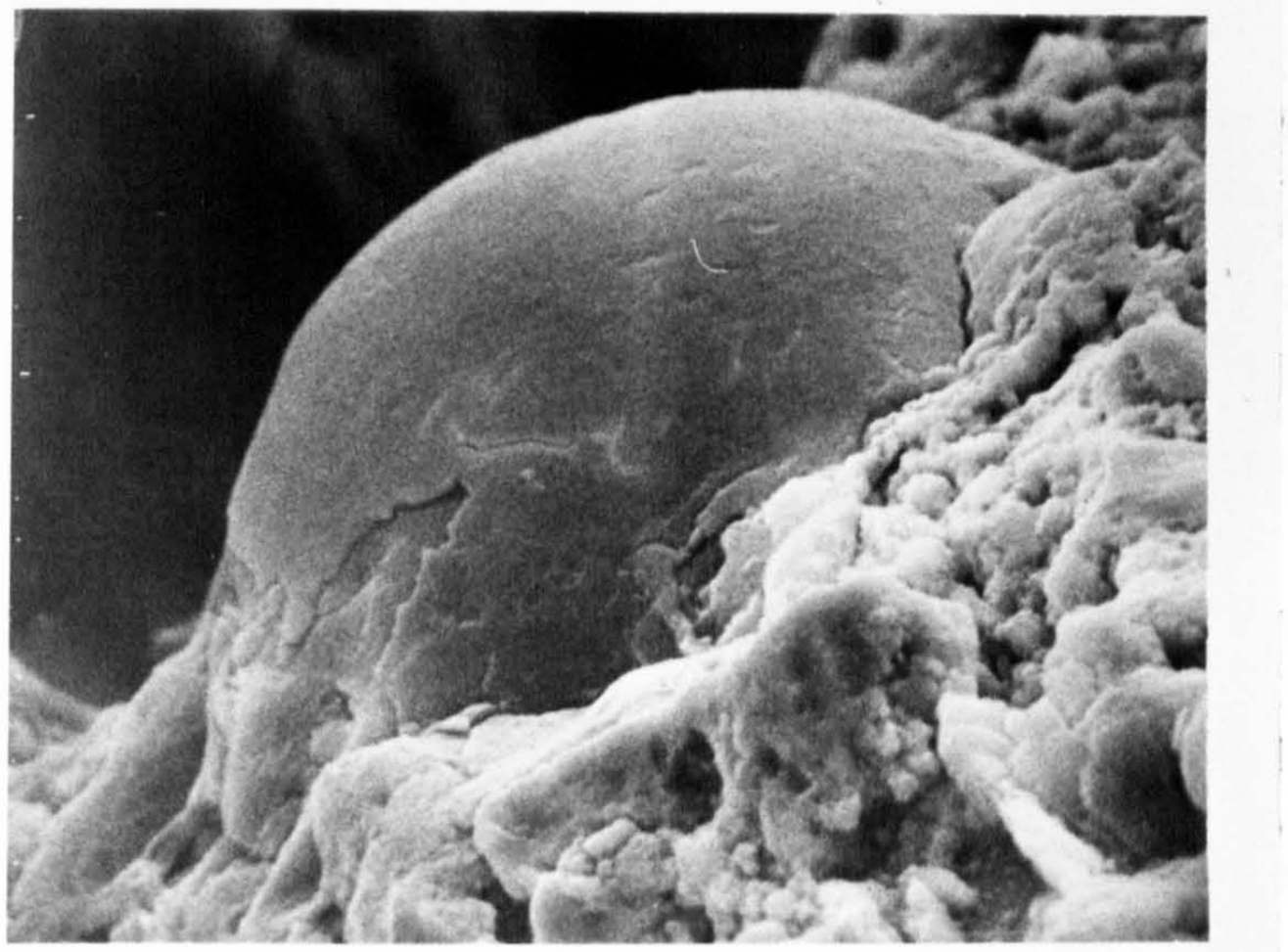

Fig. 2.35 c) SEM photograph of authigenic vesicle infill material exposed due to grain breakage. Note smooth surface of material in contrast to the irregular authigenic coatings on surrounding grain surfaces. x900.

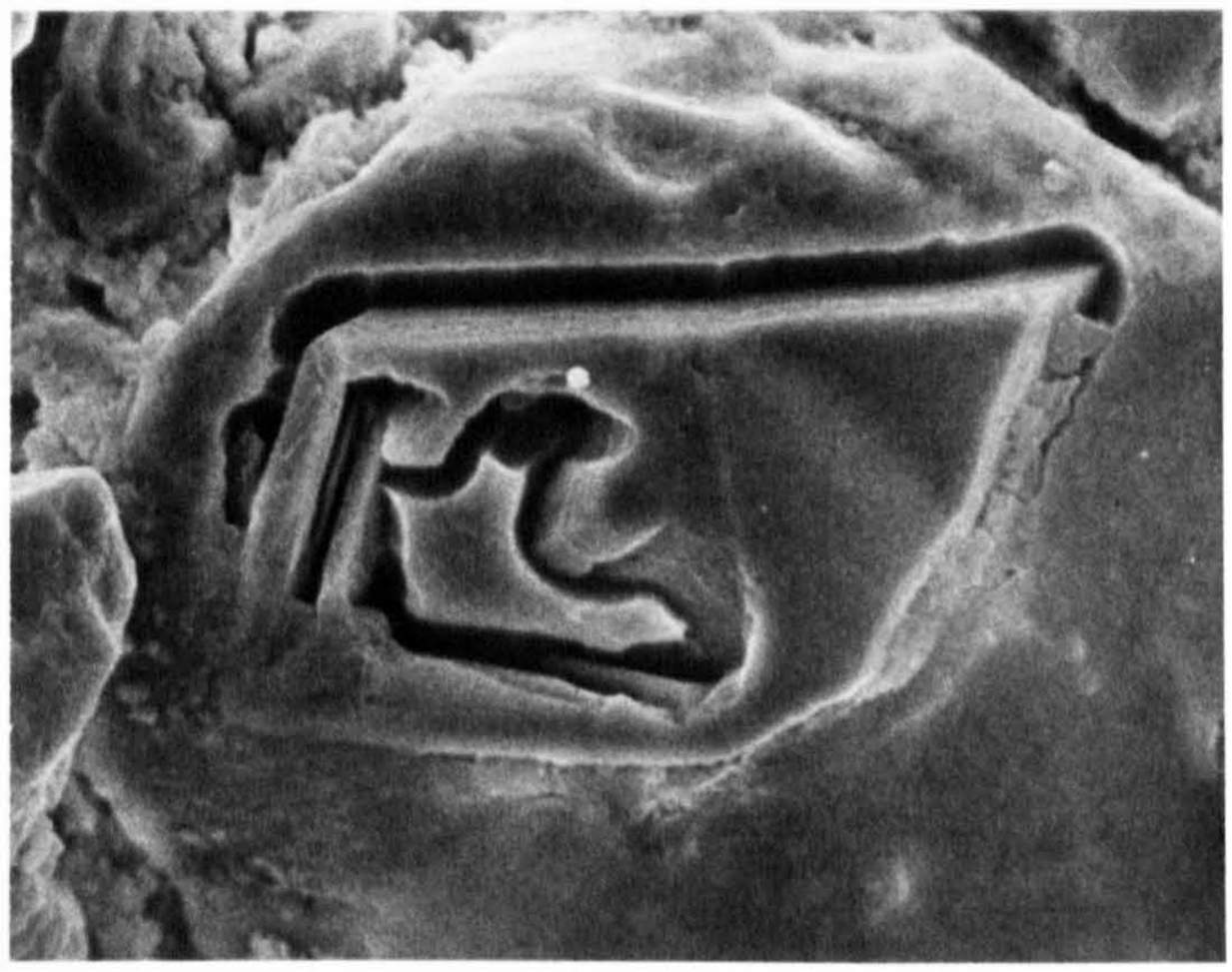

Fig. 2.35 d) SEM photograph of etch trails on sideromelane lapillus, probably due to dissolution by pore fluids. x800.

shallow water eruptions. Deep water extrusion of non-vesiculating magma forms hyaloclastic debris which is characterised by high proportions of planar grain boundaries. Shallow water activity, where the confining water pressure is insufficient to prevent vesiculation of the magma, forms hyalotuff debris characterised by high proportions of convex and concave grain boundaries. Some measure of the degree of vesicularity of the magma during any particular eruption episode can thus be made and may be related to the eruption type and the primary depositional mechanism of the tephra. Such studies also provide quantitative comparisons between modern and ancient volcanic products and aid in the recognition of ancient eruption types.

PVC plots of the Saefell tephra (and two Surtsey examples) are shown in Fig. 2.36 and compared to typical hyalotuff and hyaloclastic distributions taken from known eruptions of these types. In general the spread of the Saefell results reach much higher P values than Honnorez & Kirst's (1975) dividing boundary of P=20% for blocky hyaloclastites and irregular hyalotuff grains. This indicates a much more variable vesicularity of the Saefell magma on quenching which means simple conclusions are hard to make. As a general rule none of the grains analysed have P>50% and most have P<40% indicating that explosive fragmentation was the dominant process. As well as this, samples analysed have higher C proportions than V, because both intersection of planar fractures with vesicles and abrasion pits are concave. It is difficult to see how convex grain margins could be formed in such an explosive environment.

Variable vesicularity of closely spaced areas of the Saefell magma as it was chilled is thought to be the reason for the spread of PVC data. This variability need only be present on the scale of a few cm's to produce the total range in vesicularity found in the Saefell ash. Since the disruption of the magma does not depend on bubble coalescence (Section 2.6.1c) it becomes a chance factor whether any particular grain contains a vesicle or

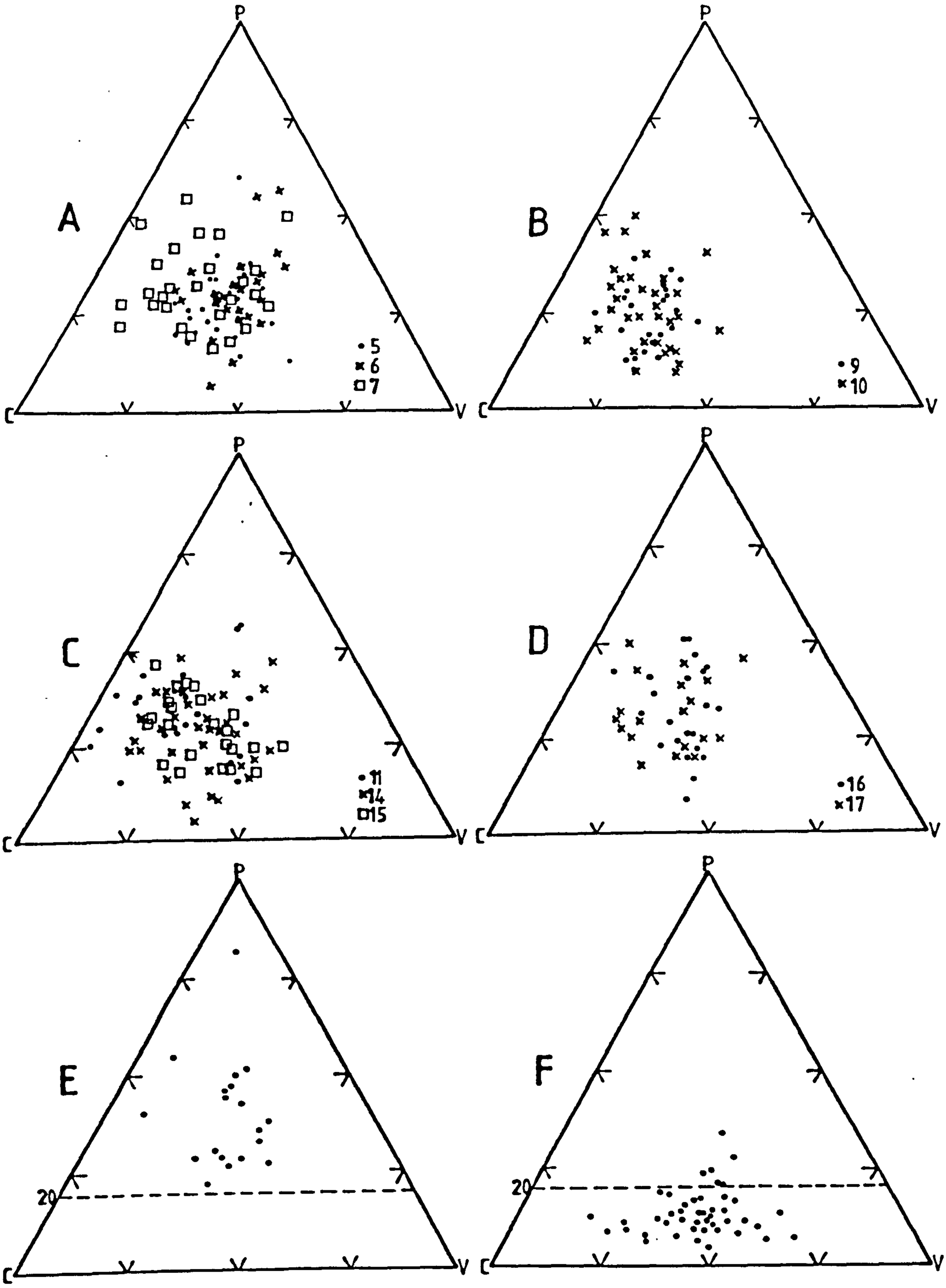

Fig. 2.36 PVC triangular diagrams of ash morphology.
A, C and D: Saefell ash B: Surtsey ash
E: hyaloclastite fragments
F: hyalotuff fragments
} Honnorez & Kirst (1975).

not. The state of the magma on chilling is thought to be as indicated in Fig. 2.29 where sparse, larger bubbles coexist with more abundant, smaller vesicles. The large bubbles are never preserved in the Saefell tephra because the size of the containing fragments is too large to be stable on quenching and subsequent abrasion.

Comparisons between the different Saefell samples, and also with the Surtsey examples, indicate few essential differences in the state of the magma and the eruption type. Average PVC values for all the tuffs are bounded by the area P23-40, V17-34 and C32-50. In general finer fragments tend to plot with higher P values, due to their smaller perimeters intersecting few or no vesicles.

A more effective plot for distinguishing hyalotuffs from hyaloclastites is a P vs N plot [where N= no. of inflexion points around grain perimeters (Honnorez & Kirst, op.cit.)]. On this diagram a line with slope 0·75 forms a boundary between hyaloclastite grains below and hyalotuff grains above the line. The Saefell grains (Fig. 2·37) are generally distributed on either side of the line with quite a wide scatter. For individual beds the proportion of grains in the hyalotuff field varies from 40 to 71%, but with only one exeption all the samples plot more towards the hyalotuff field. This exeption is sample I11, a probable distal base-surge tuff, which has a high proportion of fines. The finer particles (<0·5mm) in all the samples account for almost all the points which plot in the hyaloclastite field. This is not surprising, since fines have low N values (being small) and have fewer vesicles, giving them high P values. Thus I11, having more fines than any other sample, plots more in the hyaloclastite field. The two Surtsey samples plot with similar spreads to the Saefell grains (Fig. 2.37) except that I9 plots mainly in the hyalotuff field, although many fines lie close to the boundary line.

It is thought that the spread of results indicates that both explosive and non-explosive granulation of magma occurred throughout the Saefell activity. However, since many fines are probably derived by breakage of larger

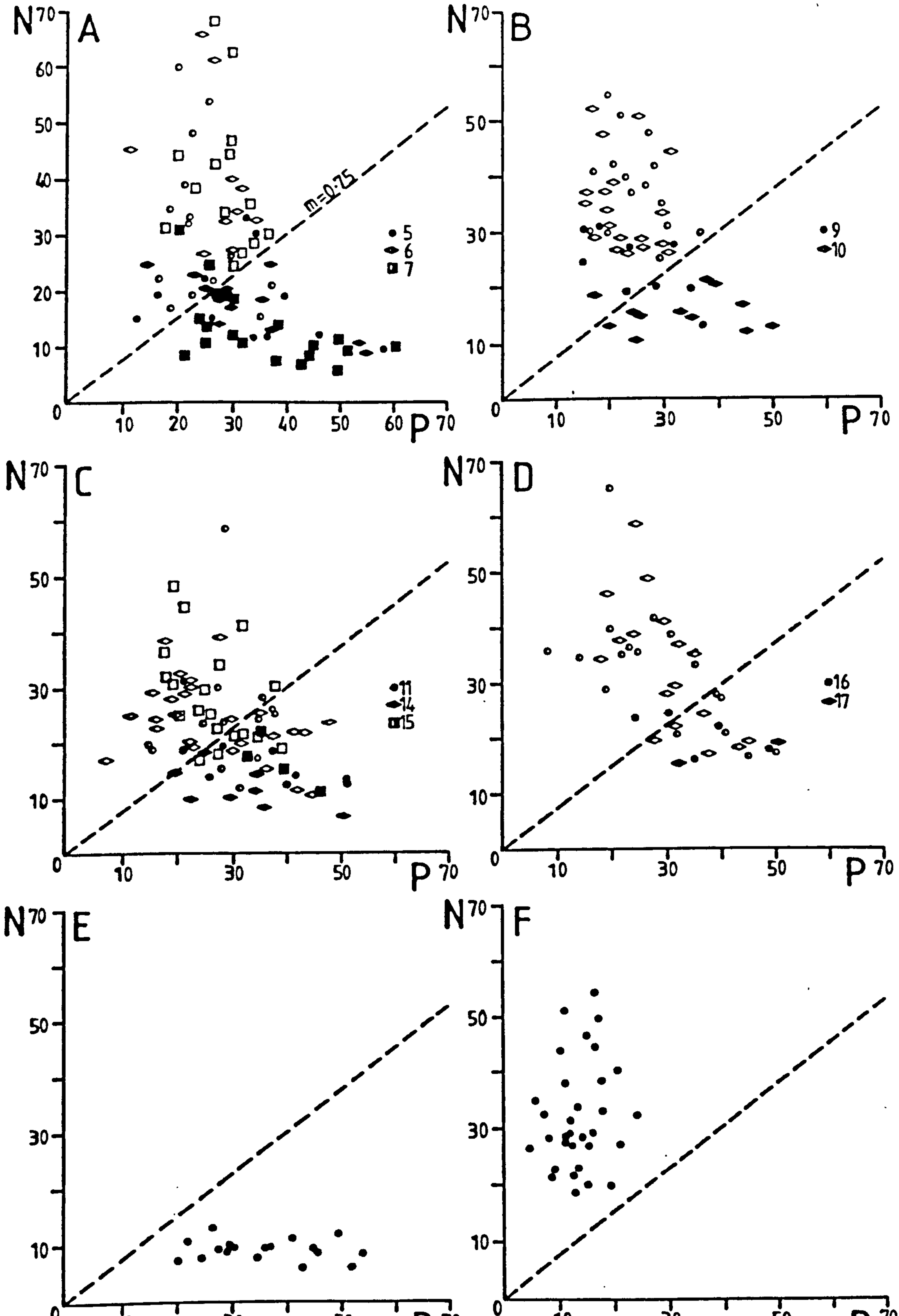

Fig. 2.37 P (% of planar grain edges) vs N (total number of inflection points on grain perimeter).
A, C and D: Saefell ash B: Surtsey ash
E: hyaloclastite fragments
F: hyalotuff fragments
} Honnorez & Kirst (1975).

grains, little can be said about the state of the Saefell magma except that it was vesiculating, but not disrupting due to bubble coalescence, when chilling occurred. Honnorez & Kirst (1975) conclude that most volcanogenic material is likely to be generated by more than one mechanism, a fact borne out by this study. Due to the marked difference in morphology of coarse and fine particles however, it is suggested that only grains larger than 0•5mm should be measured in attempts to identify the products of explosive and non-explosive subaqueous volcanism. These particles result almost entirely from the primary chilling of the magma and readily indicate its degree of vesicularity at that time.

2.6.3 Alteration of tuffs

a) Previous work

The alteration of sideromelane to palagonite is a microsolution:precipitation process (Jakobsson, 1979) which involves the movement of cations through the glass structure and their replacement by H_2O. Some workers, most recently Bonatti (1965), believed that palagonite could be formed simultaneously with the quench formation of sideromelane. It is now widely accepted, however, that the process is dependant on time, temperature and the pH of the water (Hay & Iijima, 1968b; Jakobsson, 1978). During alteration the main components leached out of the sideromelane are, in order on a volume basis: Na_2O, CaO, Al_2O_3, K_2O, SiO_2 and MgO (Jakobsson, 1979). H_2O enters the glass and ferrous iron is oxidised to ferric iron, staining the palagonite and the rock yellow to red-brown. These results were able to be obtained because the alteration of sideromelane to palagonite is essentially isovolumetric (Hay & Iijima, 1968a).

Microprobe analyses by other workers (Hay & Iijima, op.cit.; Harvey, 1974) indicate that the distribution of most cations in palagonite is variable and that of K_2O is highly variable. This is thought by Harvey (op.cit.) to be due to its high ionic radius preventing movement out of the sideromelane. Also, it is more mobile in the looser

palagonite structure but unable to leave the system completely. Such variability in distribution of cations within the palagonite contrasts markedly with the very sharp boundary between fresh and altered glass. This indicates that a microsolution front penetrates into the fresh glass,a slow process which causes the prominent banded nature of many altered glass rinds.

Most of the displaced cations go to form authigenic mineral growths close to the site of alteration, since percentages of palagonite and authigenic minerals are closely comparable within the scale of thin sections (Hay & Iijima, 1968a,b). Bulk analyses of altered and unaltered tuffs (Hay & Iijima, op.cit.) indicate that although extensive small-scale cation movement occurs at grain margins their mass movement through the rock is not extensive. These authigenic growths are mainly of zeolites and carbonates although opal and montmorillonite have also been described.

b) Saefell alteration

Palagonite

The first noticeable stage in the alteration of the Saefell tuffs is a darkening of the extremely fine material in the matrix which becomes muddy as individual grains lose their definition. This is followed by the development of thin rinds of orange-brown palagonite around grain margins and vesicles within the grains. Small amounts of zeolite are patchily developed in the pore spaces and vesicles and these increase with the increase in thickness of palagonite rinds. The most extreme alteration is found in one of the oldest samples from Unit 1. Within this, most grains smaller than 0·1mm are totally palagonitized and altered rinds of up to 0·05mm exist on the larger grains.

The first type of palagonite to form is clear, yellow, isotropic, and in places concentrically layered with no optically determinable crystalline phases. This is a form known as gelpalagonite (Peacock, 1926) and was also the first visible palagonite to form on Surtsey (Jakobsson, 1978). In some of the most altered Saefell samples the

gelpalagonite is replaced by a more brownish, translucent, birefringent form (Figs. 2.38, 2.39) which is occasionally fibrous. This is probably fibropalagonite (Peacock, 1926), the fibres of which have been found to consist of smectites (Nayudu, 1964; Hay & Iijima, 1968b). The gelpalagonite and fibropalagonite correspond respectively to the phases X and Y of Stokes (1971) who believed phase Y to be a crystalline form of phase X. The crystalline nature of the Saefell fibropalagonite is indicated by its fibrous form and by a ubiquitous length slow character normal to rind margins even where crystals cannot be optically detected.

Extreme variability in the thickness of palagonite rinds,even within the scale of a thin section, is common. In one of the more altered tuffs the thickness varies from 0·01-0·1mm in grains 2cm apart. On Surtsey, variations of this magnitude and greater were ascribed by Jakobsson (1968) to the inability of steam to permeate non-porous tuffs. This steam originated by convective heating of mixed sea and meteoric water and permeated through the tuffs within the craters. The most highly altered Saefell deposits occur within the crater but the palagonite thickness variations noted above occur in distal, outer flank Unit 1 tuffs. However, alteration in this area SW of the crater was probably enhanced by a thermal anomaly associated with the nearby parasitic scoria cone, as elsewhere the outer flank tuffs are moderately or completely unaltered. The more extreme crater tuff alteration is probably due to steam seepage associated with a crater thermal anomaly. This was not developed throughout the crater as indicated by the distribution and degree of palagonization of the Saefell tuffs (Fig. 2.40). This qualitative map shows that the tuffs on the N side of the crater are the most altered, due to preferential steam permeation in this area perhaps aided by an additional thermal input from the overlying Helgafell lavas. In general the older, outer flank tuffs are more altered because palagonitization has occurred slowly by subaerial weathering at low temperatures.

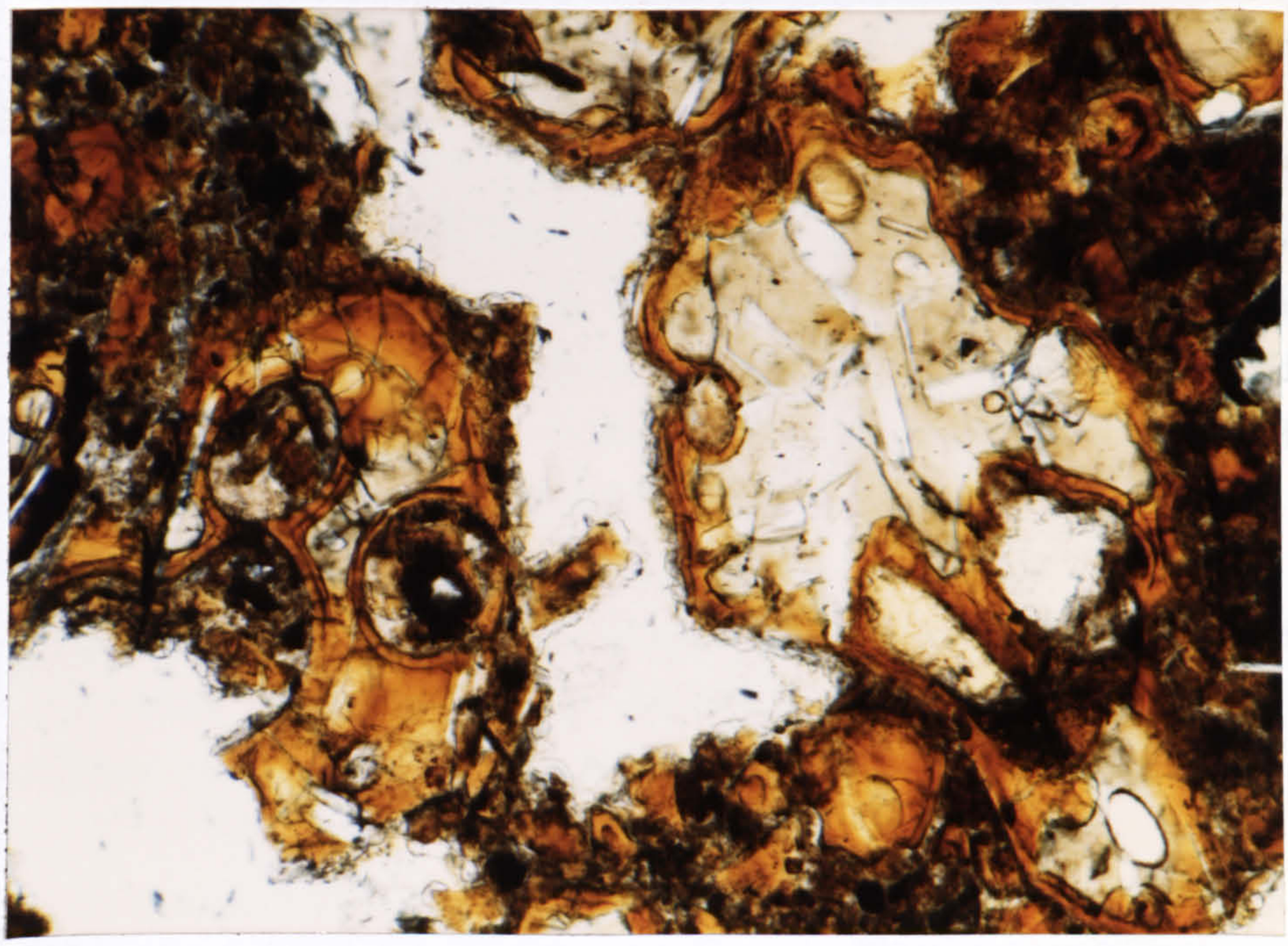

Fig. 2.38 Altered sideromelane ash with outer banded fibropalagonite rind and inner gelpalagonite. Plane polarised light. x25.

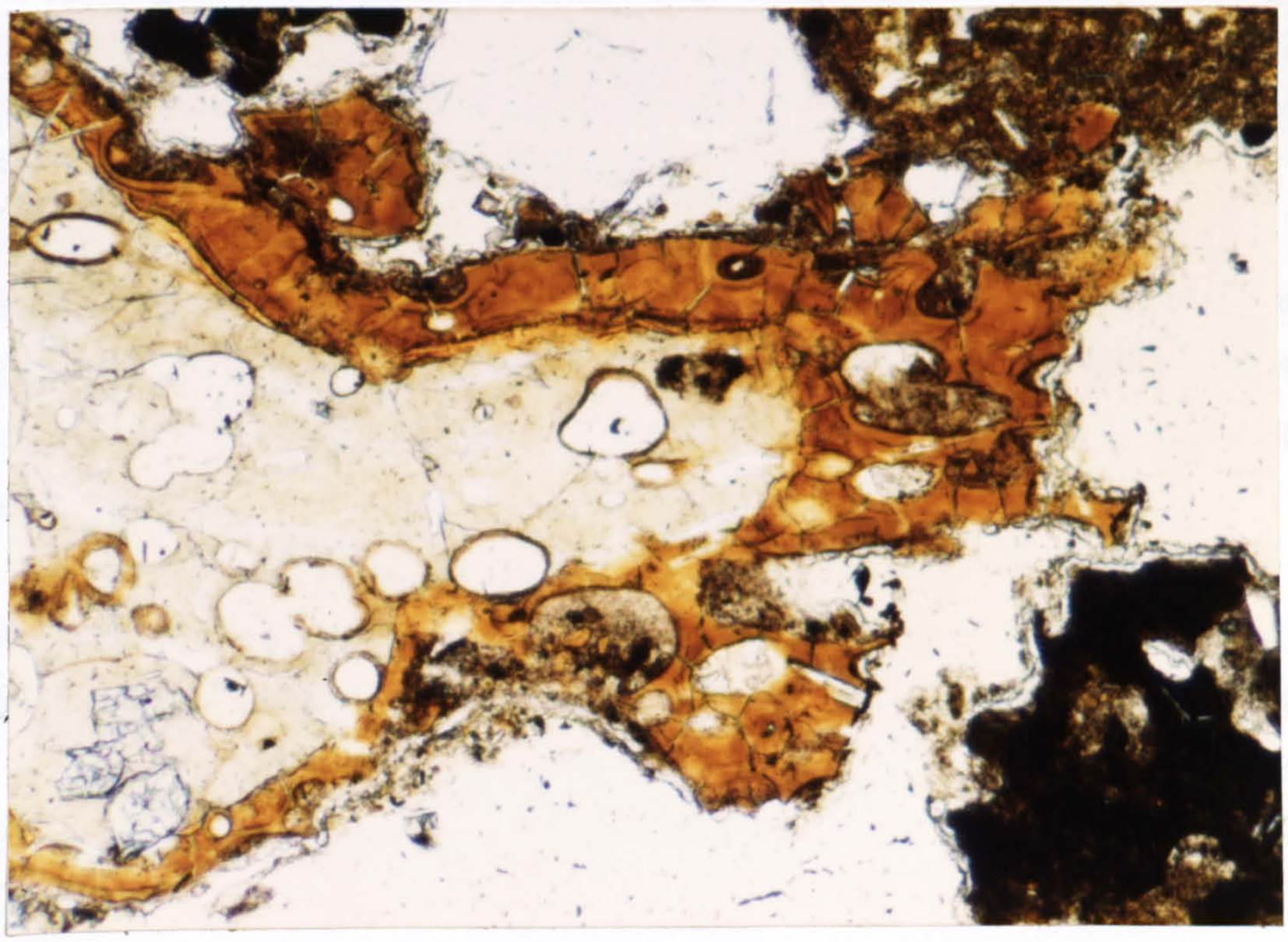

Fig. 2.39 Altered sideromelane lapillus with banded palagonite rind and thin accretionary ash rim. Clear, blocky zeolite around the composite fragment formed after partial removal of the tuff matrix. Plane polarised light. x40.

Chemically, the alteration of glass to palagonite in single grains was studied by electron microprobe (Table 2.4). Palagonite is depleted in SiO_2, Al_2O_3, CaO and Na_2O with respect to sideromelane. TiO_2, FeO and K_2O are relatively enriched in the palagonite, which is much more hydrous. MgO is slightly enriched in one palagonite sample and depleted in another. These results agree with those of Hay & Iijima (1968b) except for K_2O and MgO, which they indicate are depleted in palagonite within single grains. However, both cations are enriched in the above authors bulk analyses of palagonite, indicating variations in their distribution through the altered material.

Authigenic minerals

The authigenic minerals formed on palagonitization of sideromelane are present in small amounts but increase with increasing alteration. The most common authigenic minerals are zeolites which form thin irregular linings in the pore spaces or within vesicles. The minerals (Fig. 2.39) are of two types:-

1) Colourless, blocky crystal aggregates with moderate relief (n>balsam) and weak to nil birefringence. Their optical properties suggest that they may be chabazite or analcite.

2) Fine, radiating needle-like aggregates of low relief (n<balsam), low birefringence and length slow crystals. They are much less abundant than the blocky aggregates and are perhaps natrolite or phillipsite.

Limited semi-quantitative microprobe analyses of these authigenic minerals (Table 2.4) indicate that they are hydrous, inhomogeneous phases. The blocky aggregates have a significant Na content along with lesser amounts of Ca, Mg and Fe. Their chemistry varies over small distances, suggesting that ion diffusion has occurred. They may represent Na-zeolites such as analcite or natrolite which have exchanged cations with aqueous solutions. Zeolites are precipitated from cation-rich fluids which have leached the surrounding glass. The permeable structure of zeolites (Deer et al, 1975) would allow small amounts of

TABLE 2.4 PALAGONITE AND AUTHIGENIC ANALYSES

	(1)	(2)	(3)	(4)	(5)	(6)	(7)	(8)
SiO_2	45·7	38·6	31·9	38·2	44·4	44·4	45·4	44·4
TiO_2	2·71	4·13	4·39	4·35	0·14	0·14	0·01	0·16
Al_2O_3	16·1	11·0	8·49	11·2	19·5	19·6	20·2	19·7
FeO	12·4	19·9	20·1	20·5	1·07	0·85	0·25	0·61
MnO	0·19	0·18	0·23	0·16	0·11	0·03	0·02	-
MgO	6·20	4·90	6·33	5·18	1·87	0·05	0·14	0·52
CaO	9·72	3·38	1·15	3·29	1·24	1·29	0·74	1·49
Na_2O	3·90	1·13	1·37	1·67	4·18	5·12	5·00	5·16
K_2O	0·78	0·93	0·88	1·26	0·11	0·72	0·81	1·16
Total	97·70	84·15	74·84	85·81	72·62	73·20	72·57	73·20

(1) Sideromelane lapillus from I12 (Unit 1).
(2) Palagonite rind around above lapillus.
(3) Palagonite rind around lapillus from I12.
(4) Palagonite rind around vesicle in I12 tuffs.
(5) Blocky zeolite (?analcite) from I12 pore infill.
(6) Blocky zeolite (?analcite) from I12 pore infill.
(7) Fibrous zeolite from I12 vesicle infill.
(8) Fibrous zeolite from I12 vesicle infill.

"foreign" cations to enter its aluminosilicate framework. The high water content of the Saefell zeolites enhanced their capacity for cation exchange.

The fibrous aggregates have similar Na contents to the blocky material. They contain only minor traces of other cations and may thus be purer forms of analcite or, since they are fibrous, more probably natrolite. The low Na values compared with published zeolite analyses (Deer et al, 1975) may be partly due to loss of volatiles during microprobe analysis. The high water content was determined by difference and may have contributed by dilution to lower concentrations of the other elements. When recalculated on a water-free basis the cation contents are more like published analyses.

The ability of zeolite minerals to exchange cations readily with solutions has led to them being extensively used as ion or molecular sieves. The variable composition of the Saefell zeolites is largely due to this property.

The authigenic minerals, although generally more abundant in the most altered tuffs, do not increase proportionally with formation of palagonite (Table 2.1). This is thought to be because the tuffs have behaved as an open system on the scale of a hand specimen. The authigenic content of the tuffs is influenced either by removal of components expelled from the fresh glass or later dissolution of zeolites by percolating solutions. However, within vesicles in glass fragments there is less possible movement of solutions and the amount of authigenic minerals correlates well with the thickness of palagonite around the vesicle (Fig. 2.41). Furnes (1974) found a similar relationship, although as in Saefell removal of some of the leached components leads to generally less authigenic material than palagonite, which must remain in situ.

<u>Element distribution mapping</u>

As well as analysing associated sideromelane, palagonite and zeolite by electron microprobe, the relative changes in element concentration can be displayed by mapping. Previously this has been carried out using

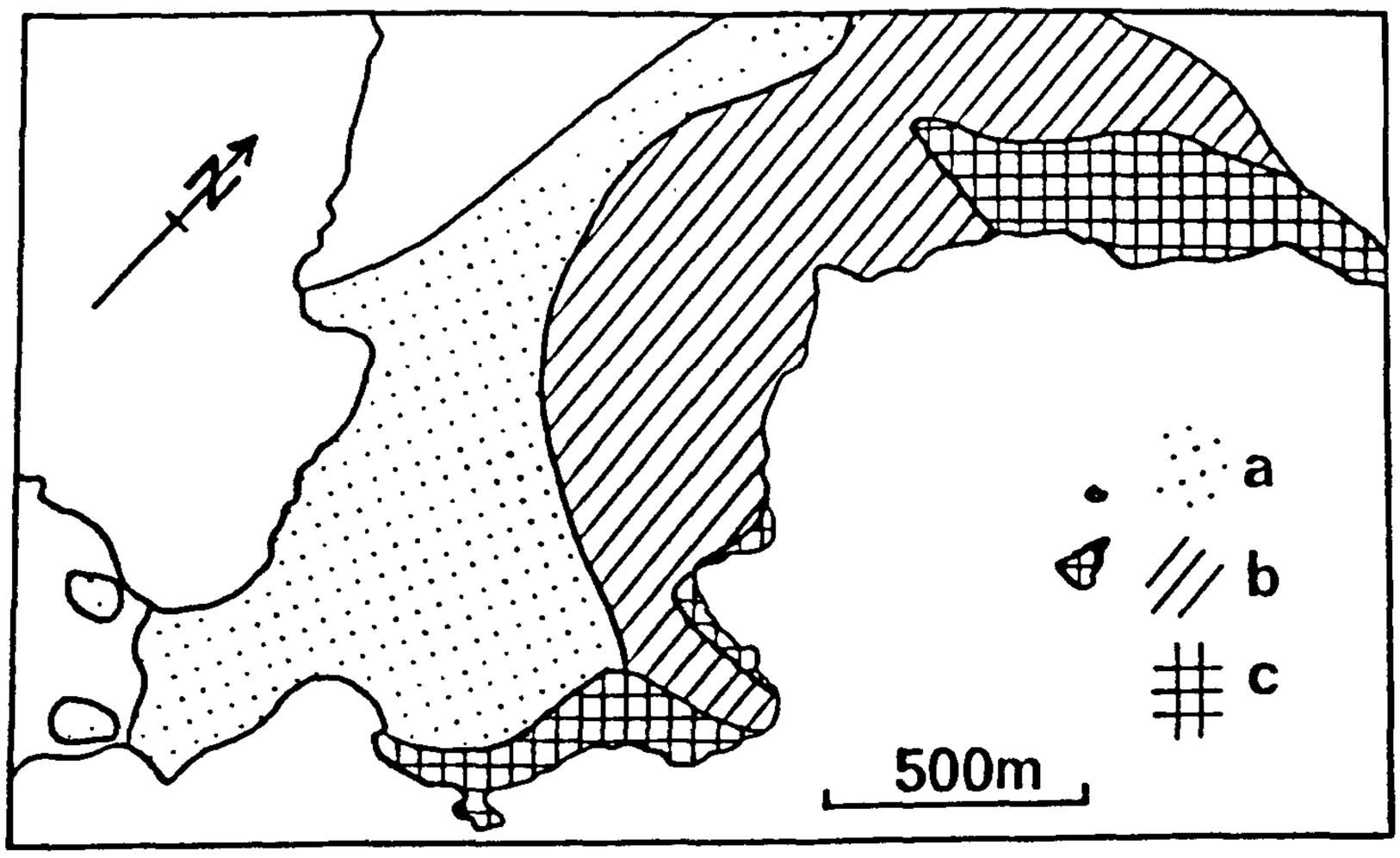

Fig. 2.40 Degree of alteration of Saefell tuffs.
a: no palagonite found
b: incipient to moderately palagonitized tuffs
c: moderate to highly palagonitized tuffs

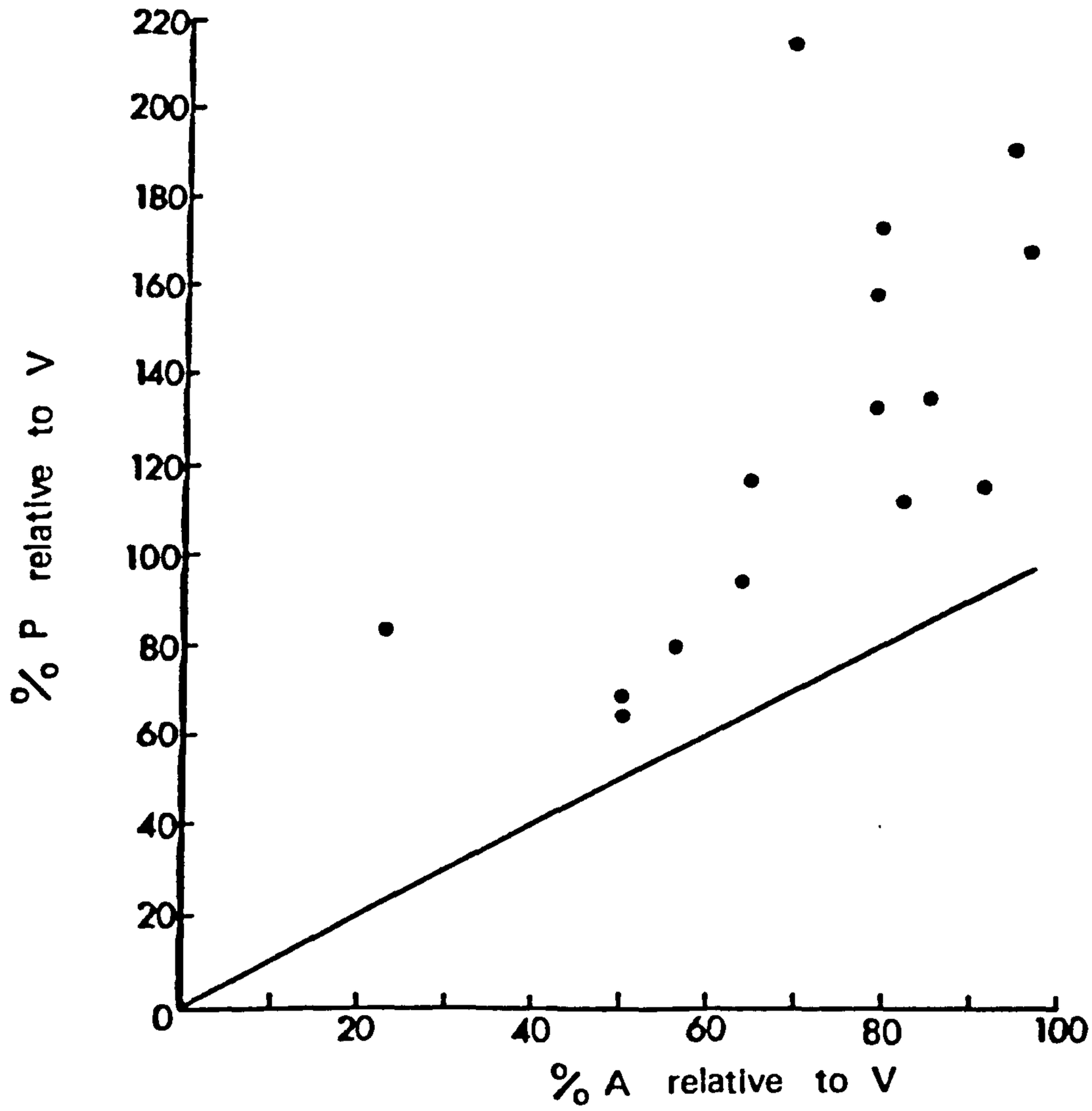

Fig. 2.41 Plot of A (authigenic material) vs P (palagonite) as volume % relative to the vesicles with which they are associated (after Furnes, 1974).

an SEM with attached X-ray spectrometers. The method used here involves digital area mapping using an EDS microprobe and attached minicomputer (Appendix 2).

Two areas around partly-filled vesicles in altered glass were mapped. The first area (Fig. 2.42a) consists of sideromelane with vesicles surrounded by palagonite rinds. One vesicle is partly filled with blocky zeolite. The mapping confirms that palagonite is depleted in SiO_2, Al_2O_3, CaO and Na_2O and enriched in TiO_2, FeO, K_2O and MgO relative to sideromelane (Fig.2.42b,c,d,e). The elements which are depleted in the palagonite have been leached out of the rind and have formed the zeolites in the vesicles. The element line-scans on each map indicate that the sideromelane: palagonite boundary is compositionally sharp. The distribution of certain elements, notably TiO_2 and MgO is shown to be irregular throughout the palagonite.

The second area (Fig. 2.43a) consists of a vesicle, partly filled with blocky zeolite, having a rind of concentrically zoned palagonite. In thin section the inner rind is orange-brown, fibrous and weakly birefringent whereas the outer rind is brown, structureless and isotropic. Other zones are visible under the microprobe backscattered electron image, suggesting they have slightly different compositions. The element maps (Fig. 2.43a,b,c,d) support this and show that the inner rind is depleted in SiO_2 and enriched in MgO, FeO and K_2O relative to the outer rind. Overall the palagonite is depleted in TiO_2, CaO and FeO and enriched in MgO, Al_2O_3 and SiO_2 relative to sideromelane.

The zoning is thought to be due to the replacement of gelpalagonite by fibropalagonite during continued leaching of the glass. Solution fronts moved concentrically outwards from vesicles and cracks in the glass, redistributing elements. The establishment of a crystalline palagonite phase expelled certain elements and concentrated others within it, aided by movement of solutions. The marked difference in the types of elements enriched or depleted in the palagonite relative to the sideromelane, compared with other grains, is difficult to

explain. One explanation may be that the sideromelane mapped here is itself partly leached and altered. The higher water content of sideromelane in the mapped grain supports this. Once significant amounts of water enter the glass, elements are able to move more readily.

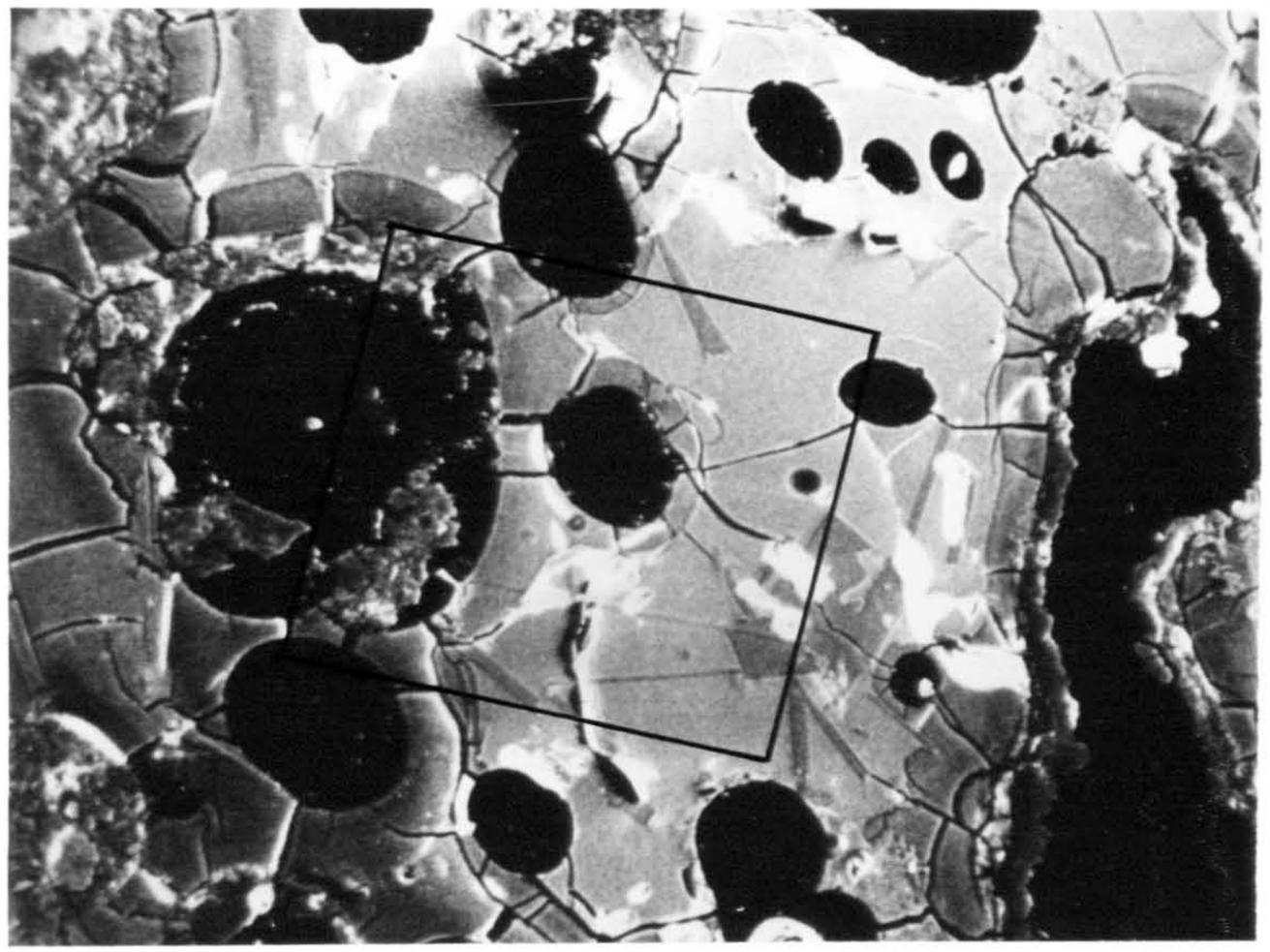

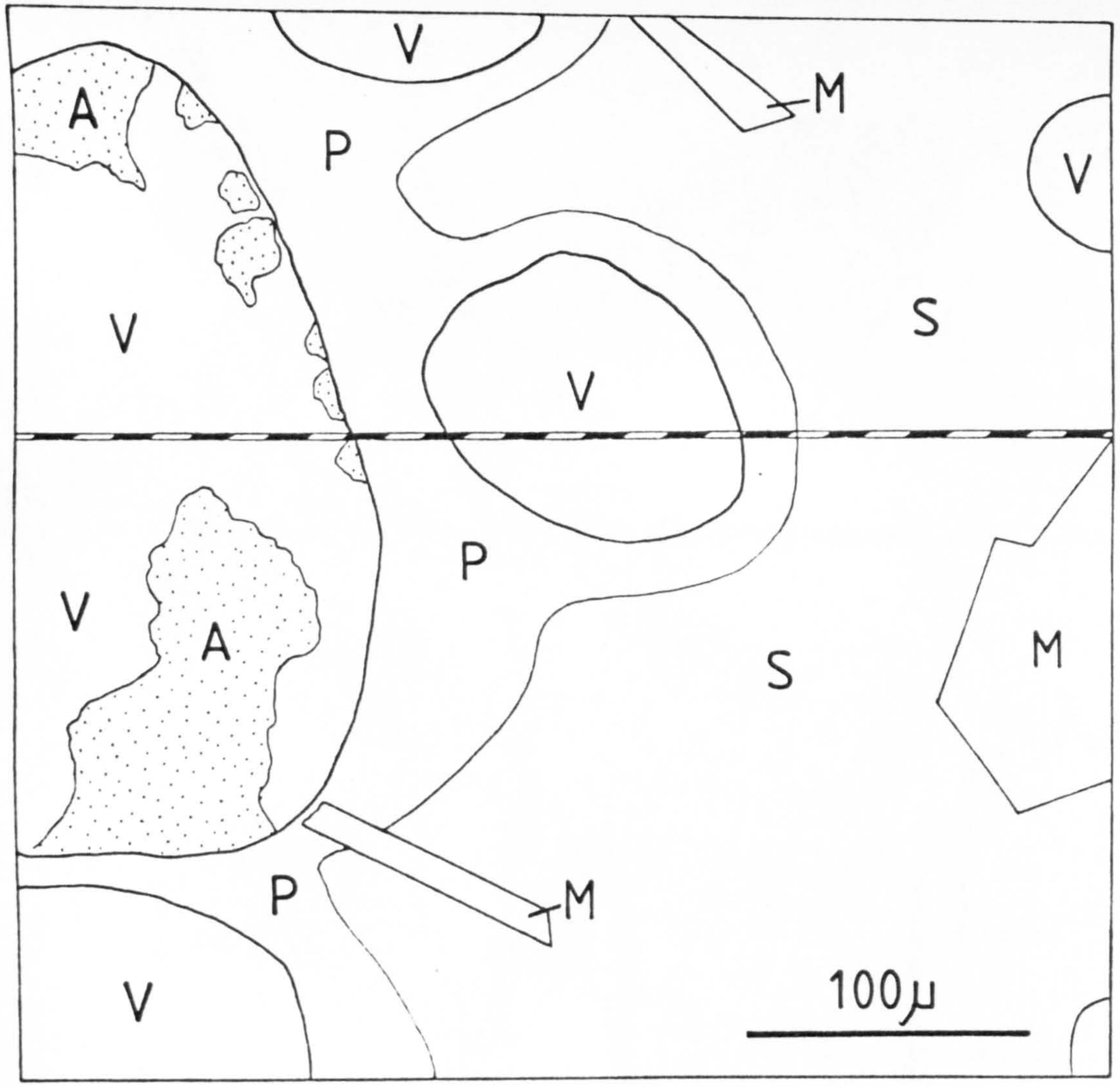

Fig. 2.42 a) BEI photograph and enlarged sketch of marked area of palagonitized lapillus used for element mapping.

A: authigenic material (zeolite)
M: microlite plagioclase
P: palagonite
S: sideromelane
V: vesicle void space

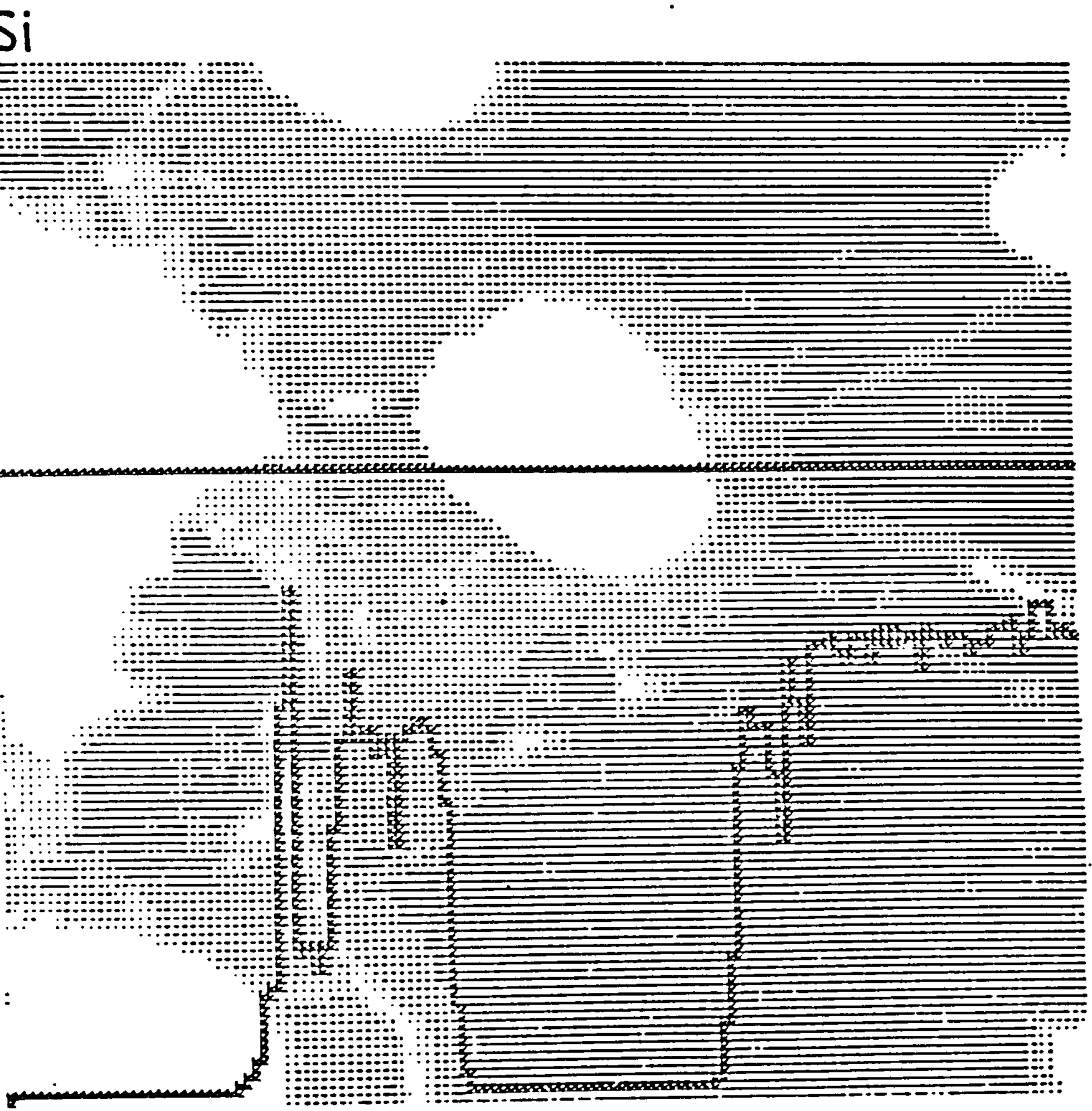

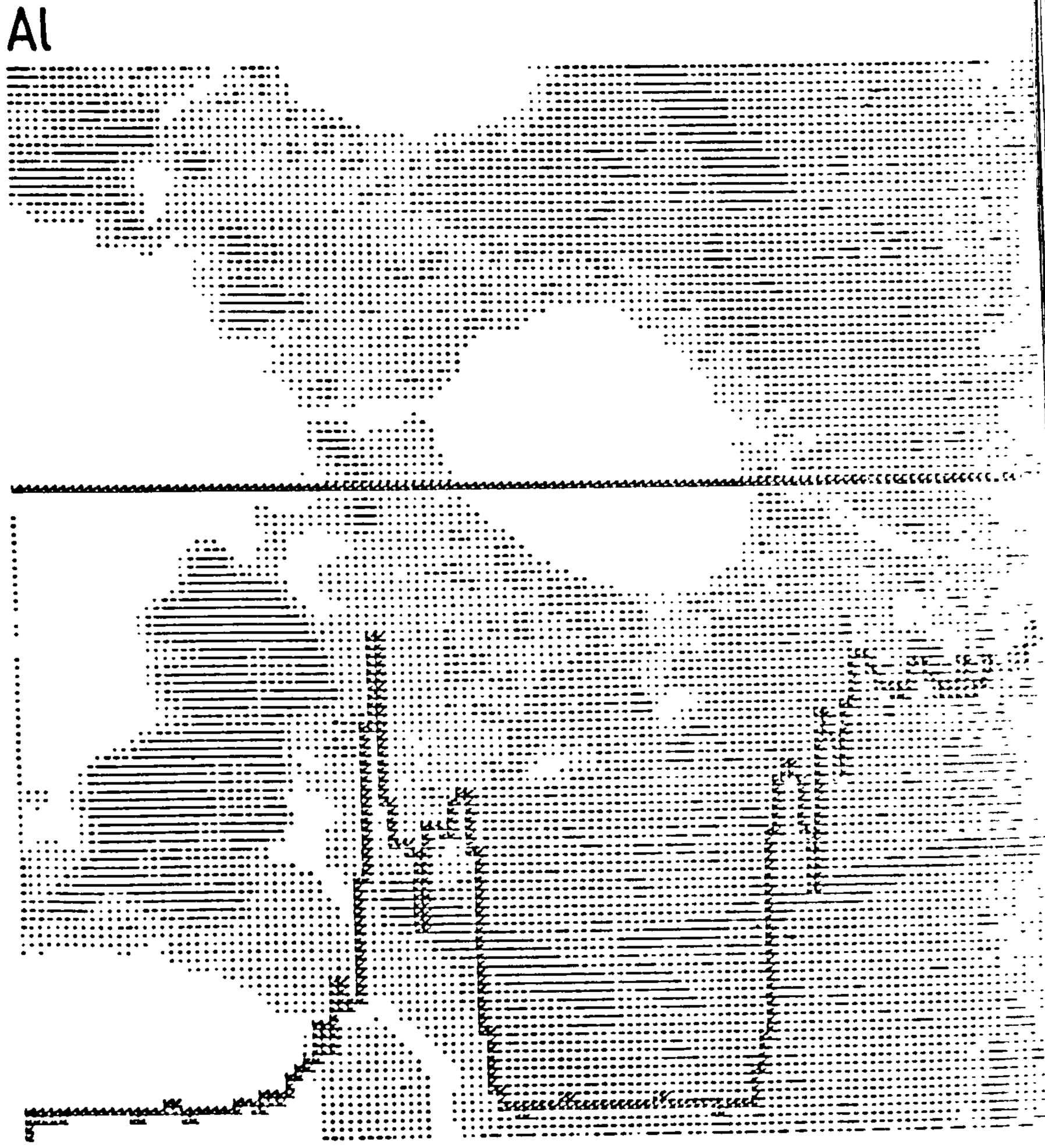

Fig. 2.42 b) Element distribution maps and linescans of Si and Al.

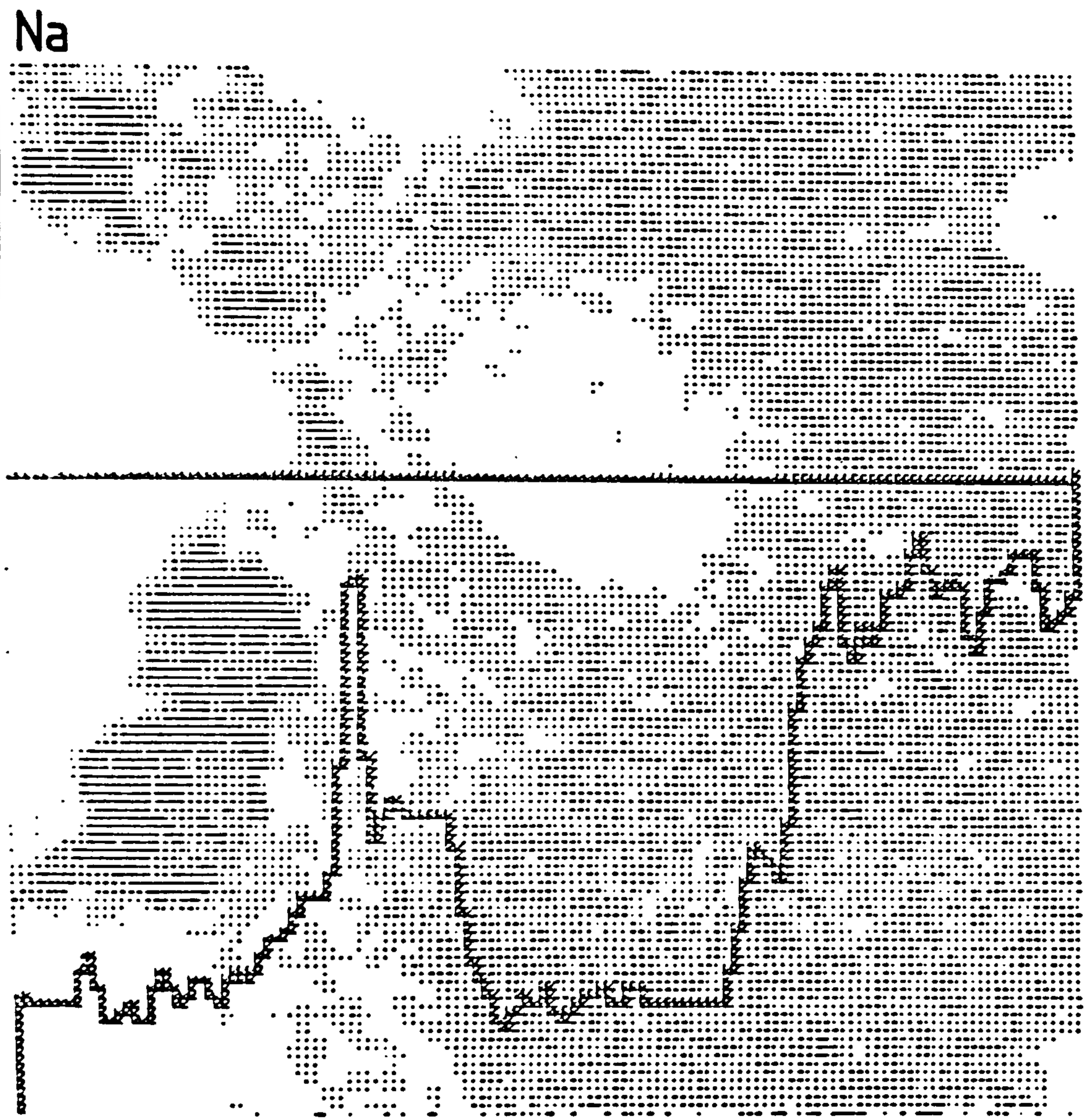

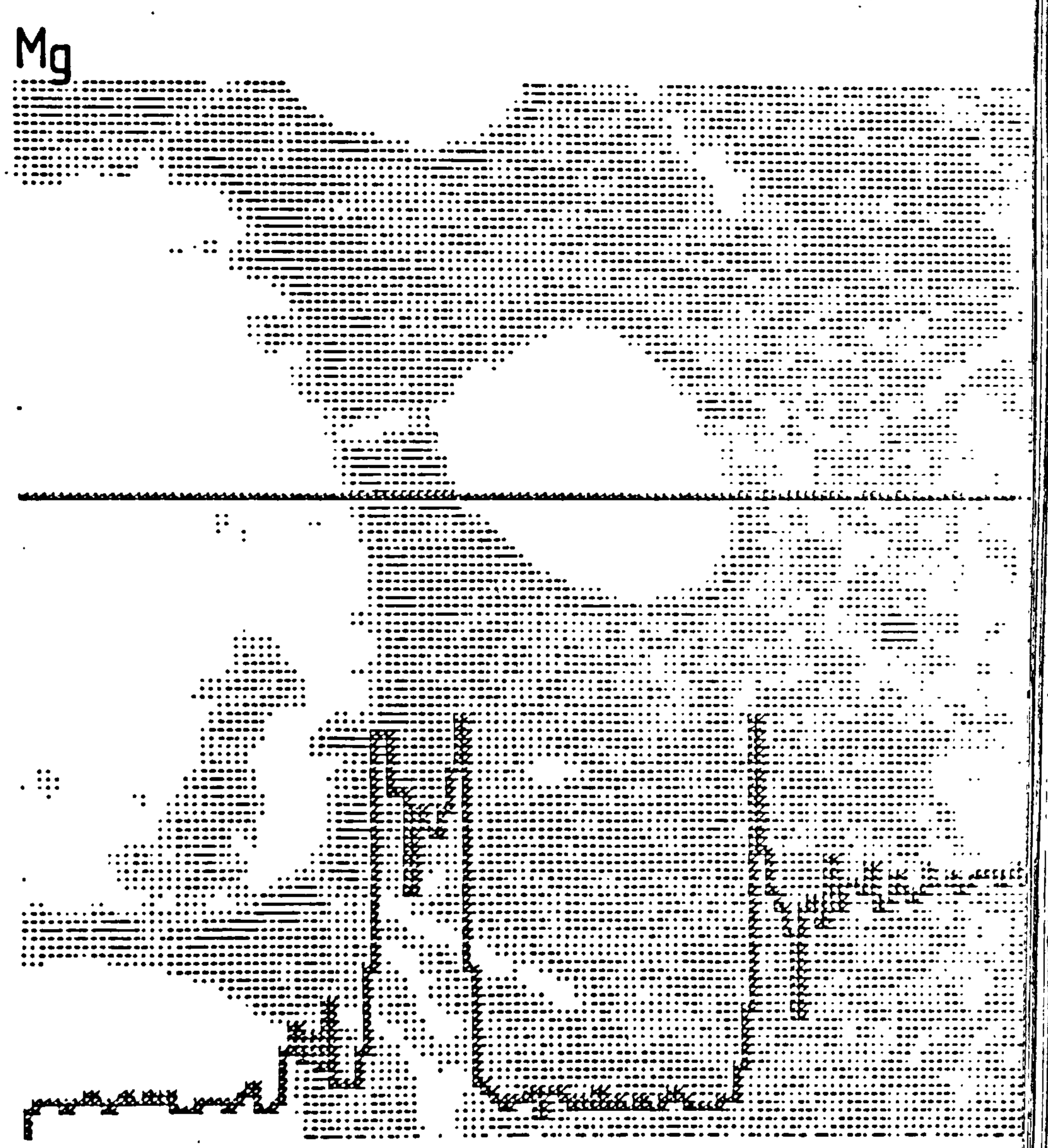

Fig. 2.42 c) Element distribution maps and linescans of Na and Mg.

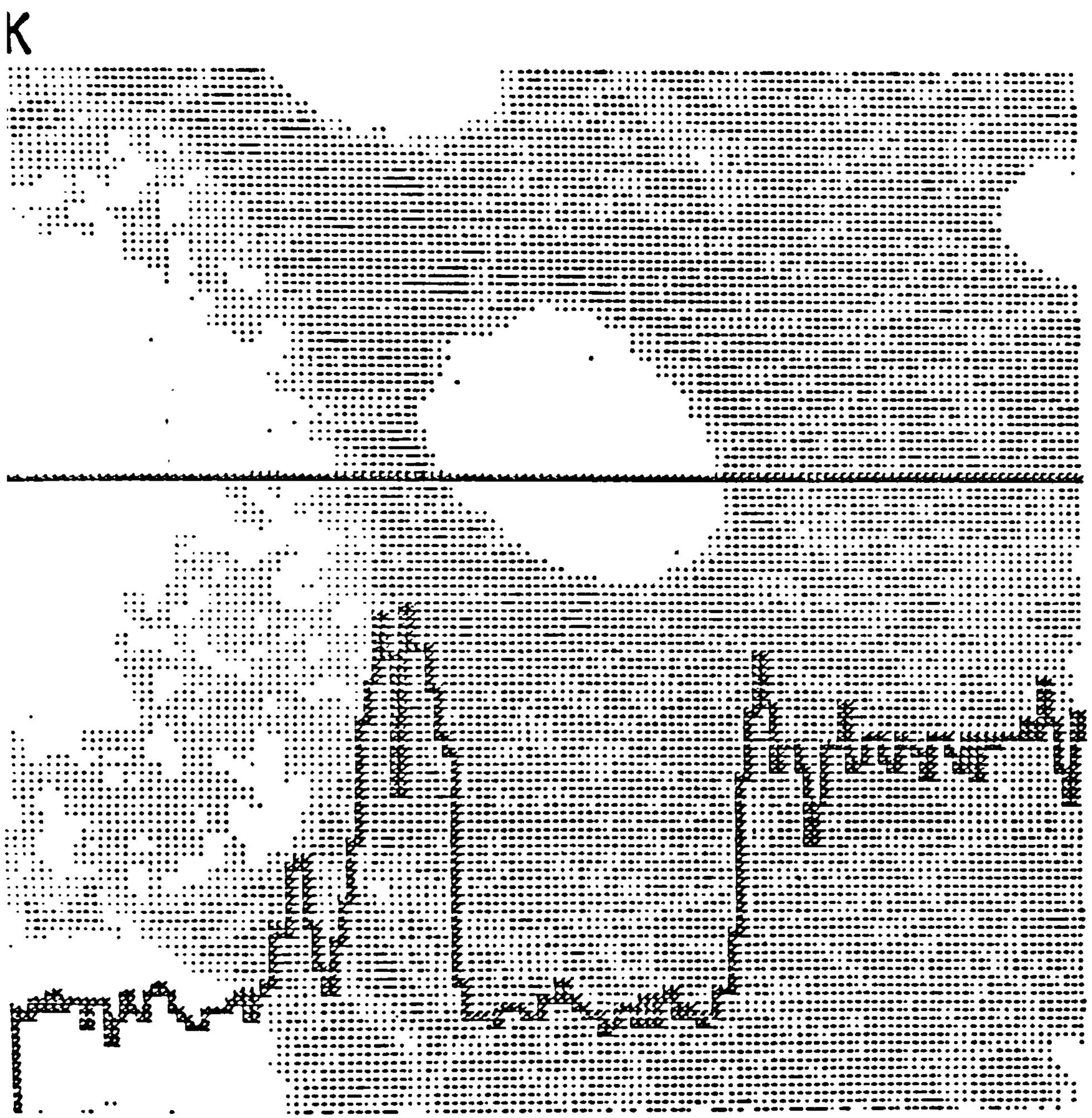

Fig. 2.42 d) Element distribution maps and linescans of K and Ca.

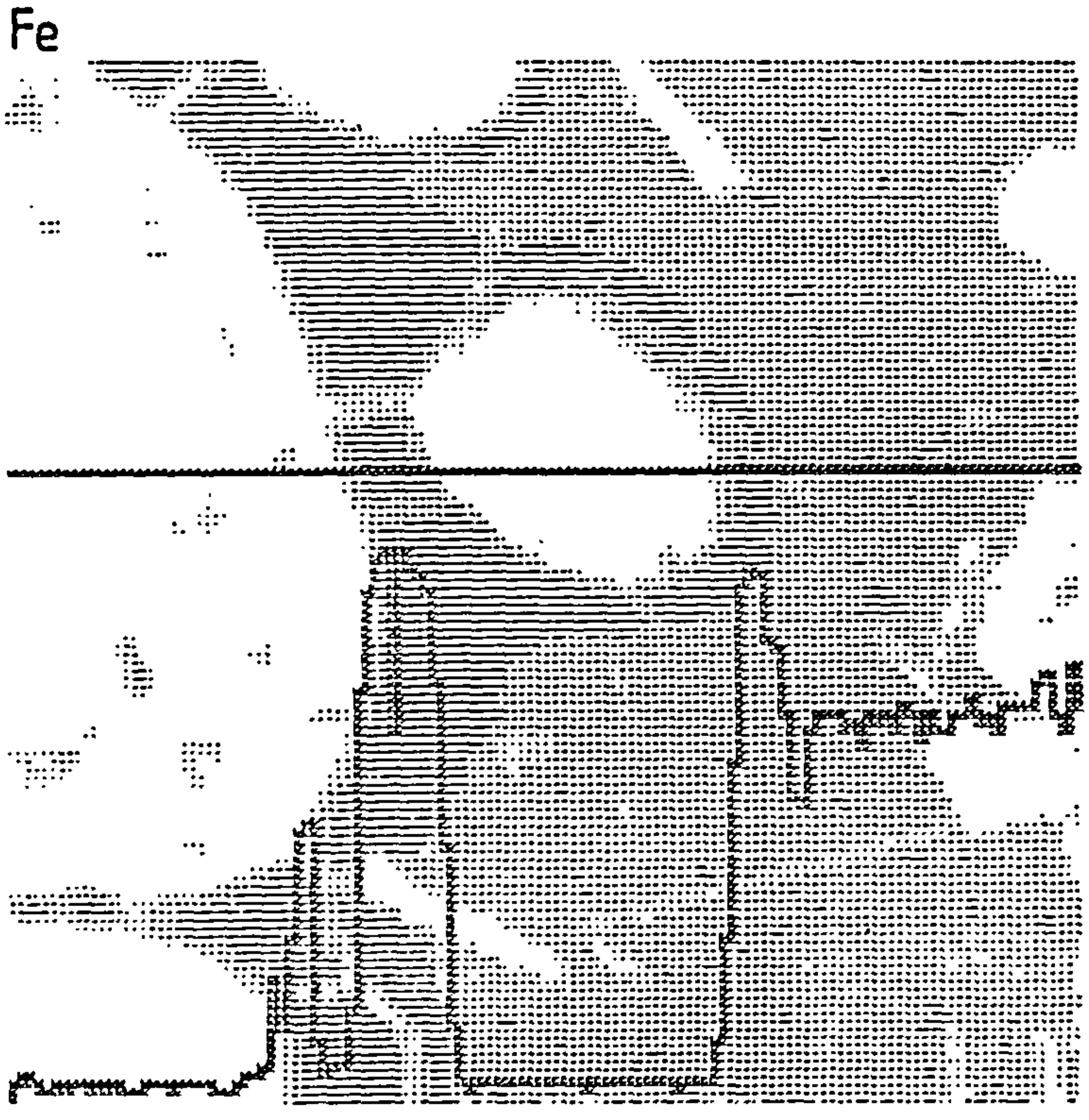

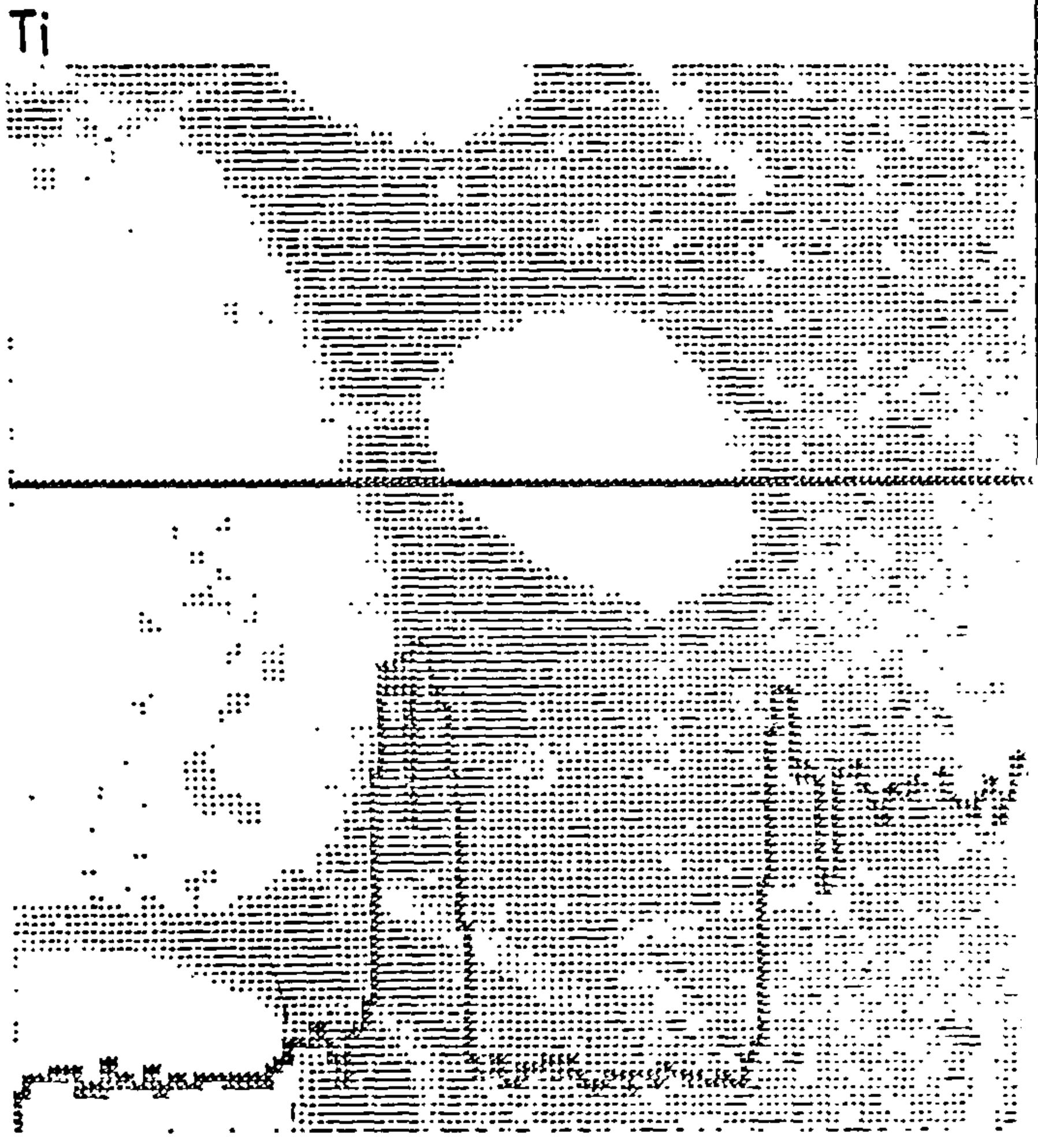

Fig. 2.42 e) Element distribution maps and linescans of Fe and Ti.

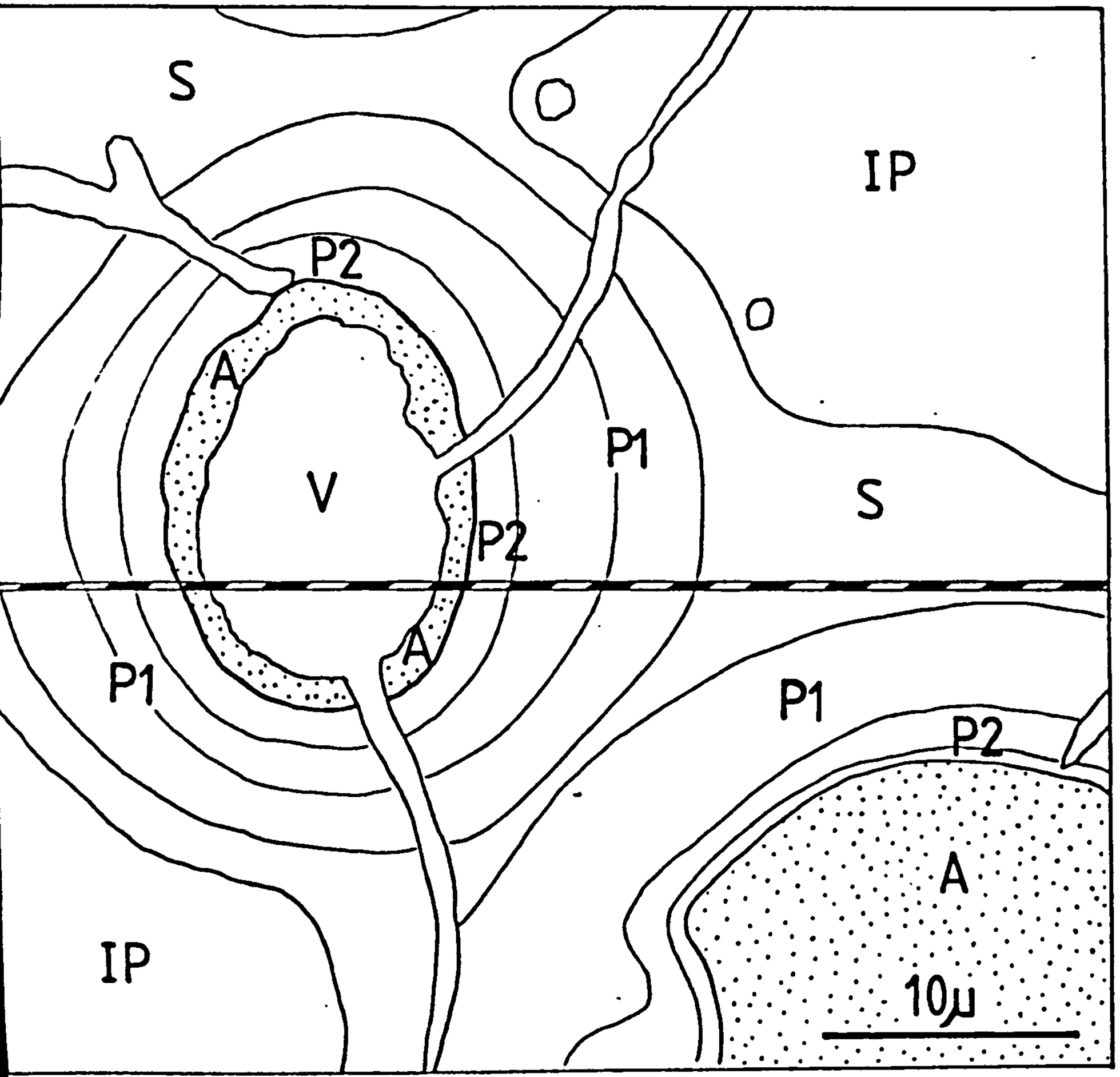

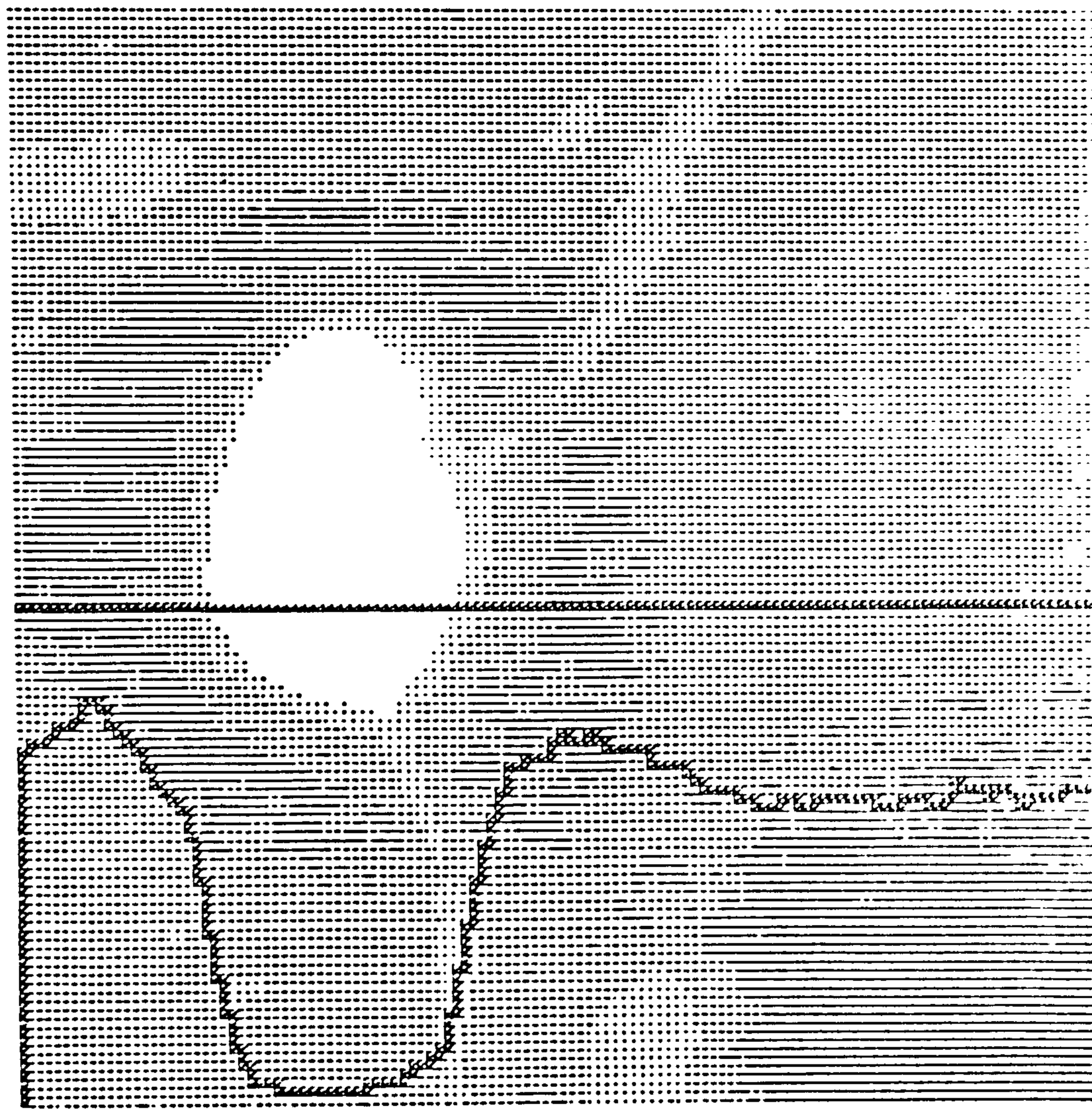

Fig. 2.43 a) Sketch and Si distribution map and linescan of palagonitized lapillus used for element mapping.
A: authigenic material IP: incipient palagonitization P1/P2: palagonite bands
S: sideromelane V: vesicle void space.

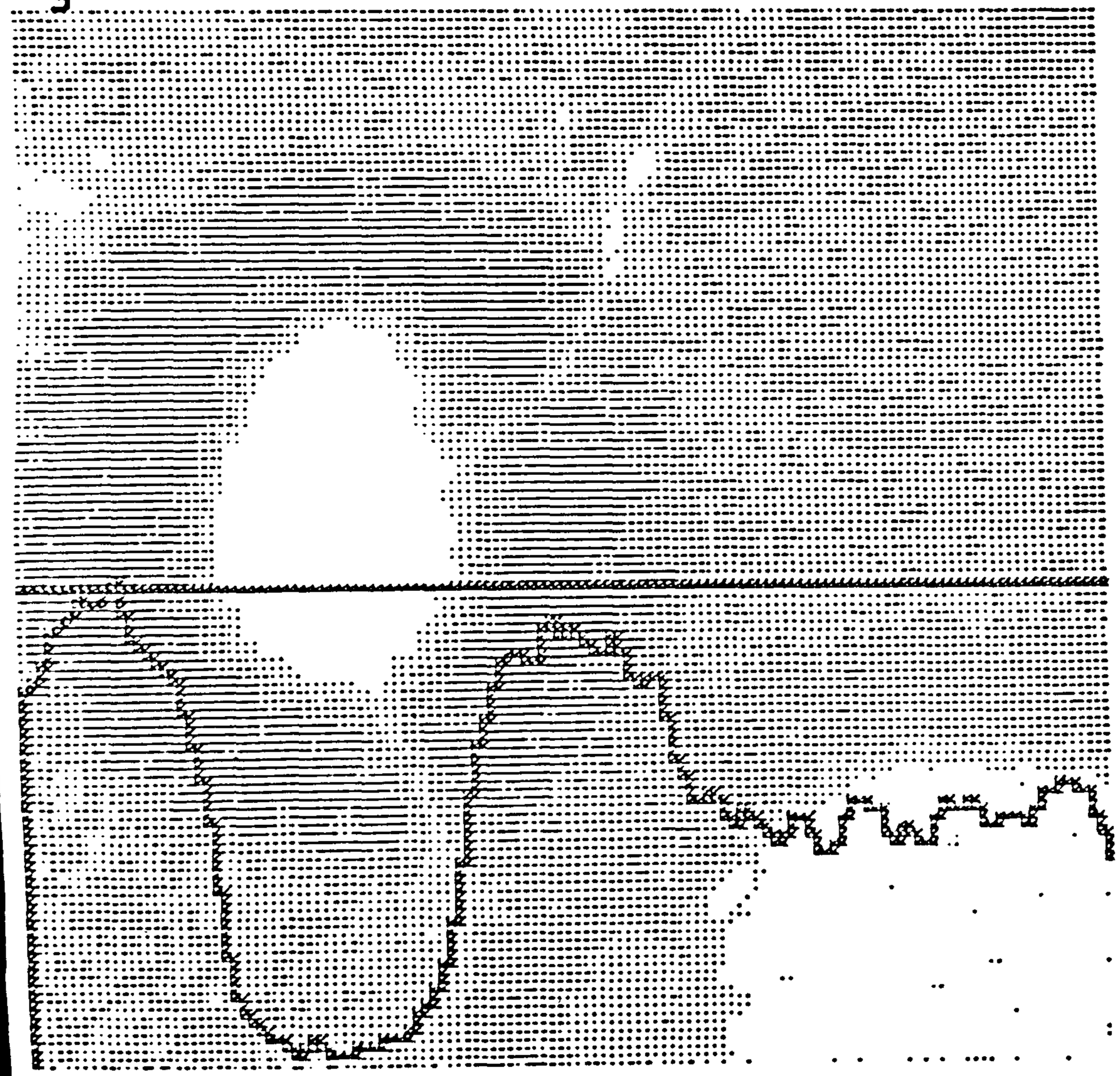

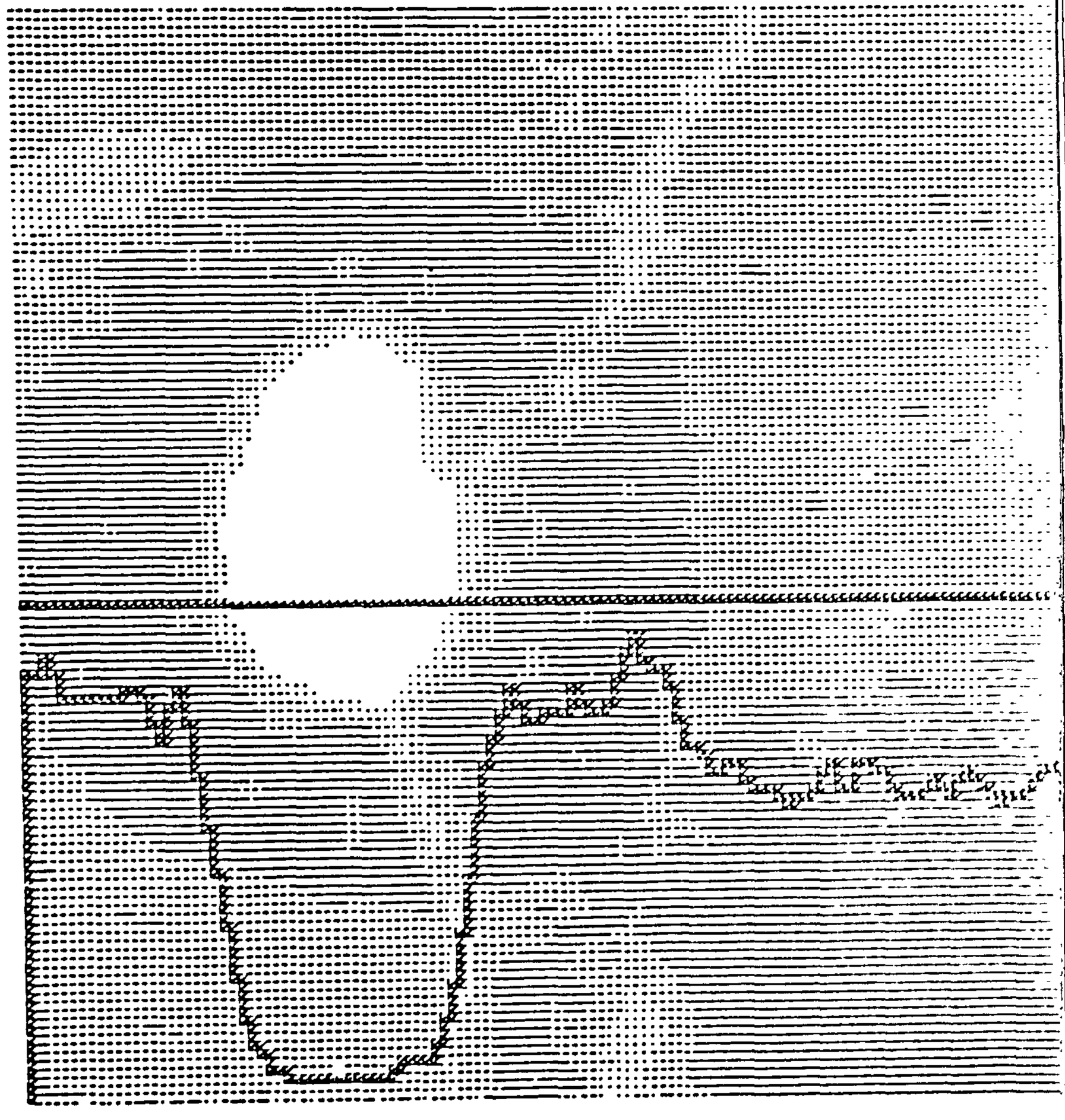

Fig. 2.43 b) Element distribution maps and linescans of Mg and Al.

K

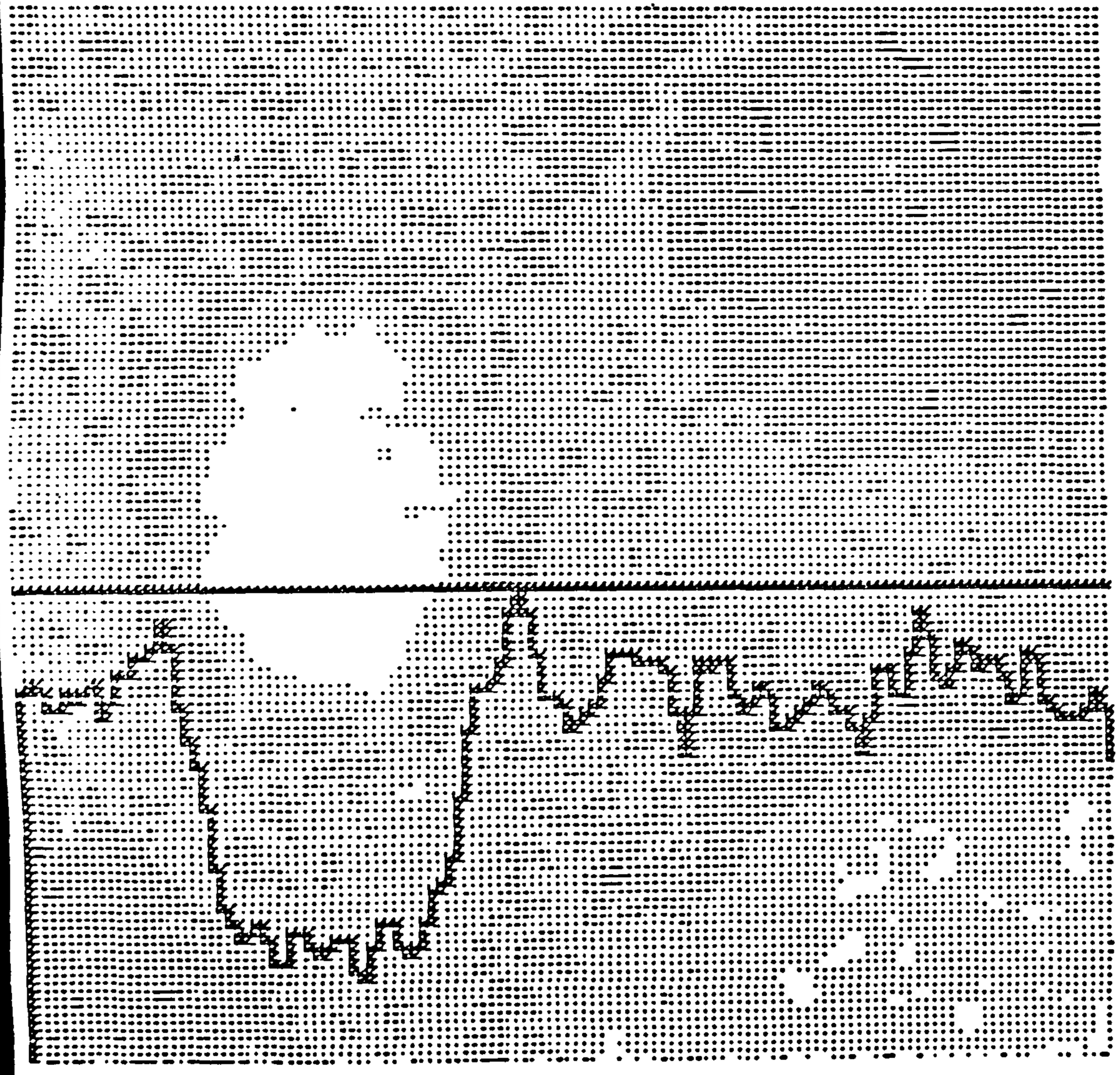

Ca

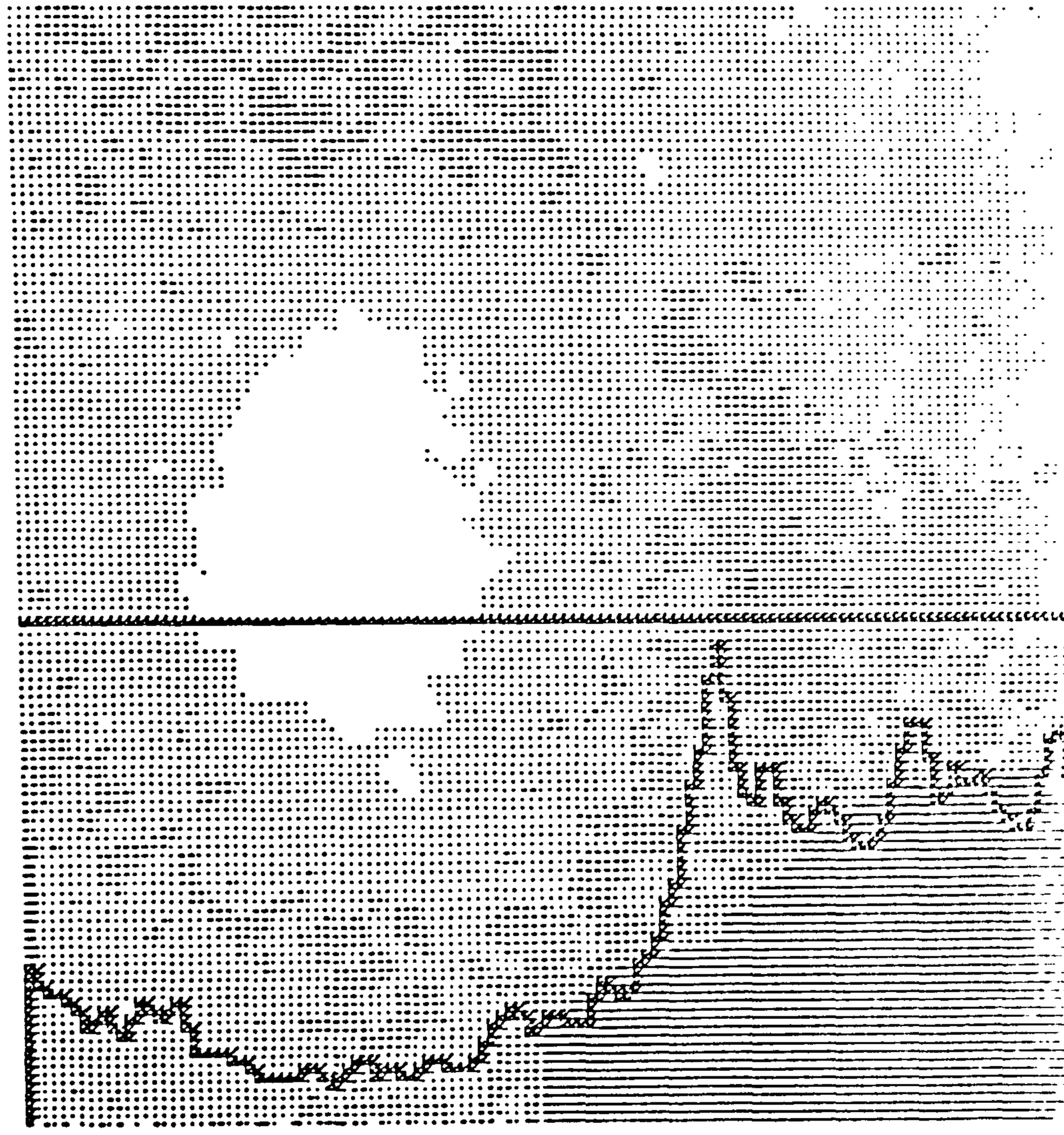

Fig. 2.43 c) Element distribution maps and linescans of K and Ca.

Fe

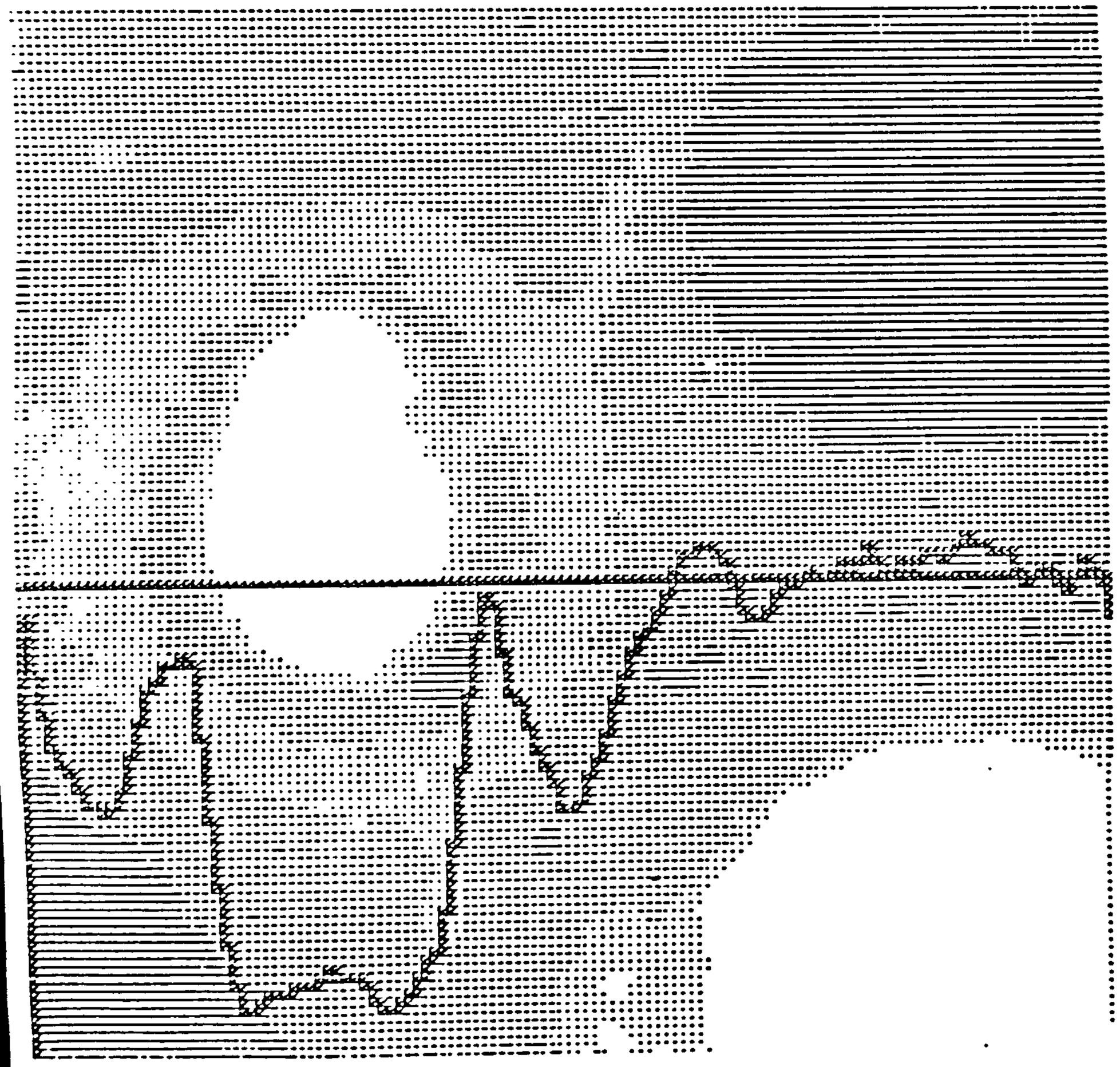

Ti

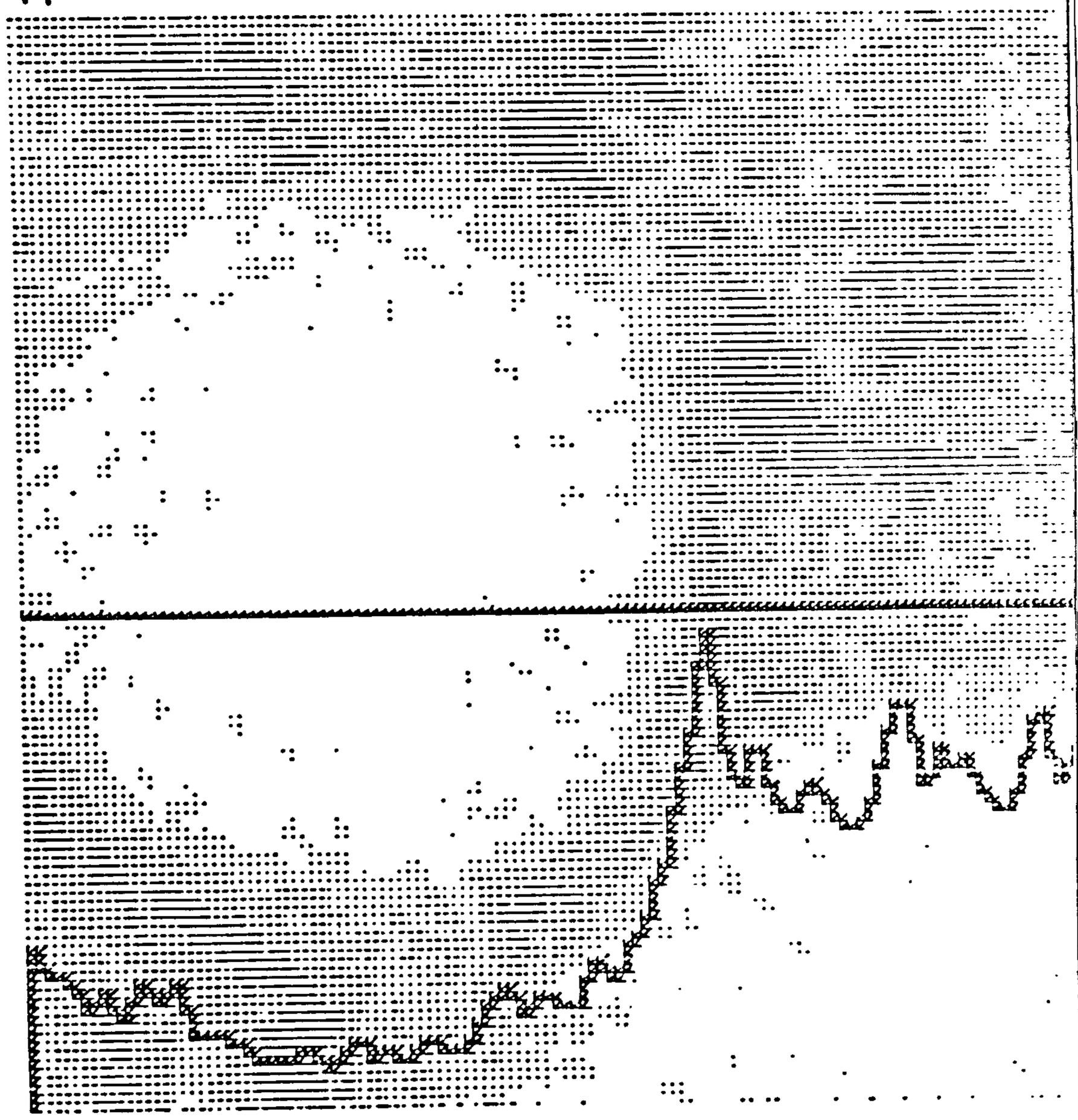

Fig. 2.43 d) Element distribution maps and linescans of Fe and Ti.

2.7. SUMMARY

1. The Saefell tuff-ring is closely similar to Surtsey and was dominated by rapid ring growth with syndepositional reworking processes affecting mainly crater tuffs. Crater subsidence on ring faults occurred at a late stage during its activity but displacements were minor.

2. Base-surges occurred throughout the volcanism, and formed many structures attesting to different types of surge. One large antidune contains evidence for the preservation of structures known formerly only from theoretical models and was deposited by surges of decreasing flow power.

3. Directed blasts affected the distribution of tephra and were sourced from eruptive vents which had moved laterally within the crater. These sourced base-surges and also destroyed much of formerly bedded crater tuffs.

4. Vesiculation of the alkali-olivine basalt magma was arrested by explosive chilling at depths of <100m. Although much of the tephra was formed by chilling of vesiculating magma a great deal of granulation occurred, in part due to quench shattering of larger glass fragments.

5. Accretionary lapilli are extremely abundant in the tuffs due to moist conditions in the poorly-expanded particle rich eruption columns. Capture of fines by accretion, and subsequent fallout, led to highly fine-skewed particle distributions at all distances from the vent. This process, along with mixing of airfall and surge deposits complicates conclusions on depositional processes based on grain size properties.

6. Alteration of the sideromelane to palagonite was probably initiated soon after volcanic activity ceased due to the formation of a thermal anomaly located mainly within the crater. At present the alteration is proceeding

slowly as a weathering process.

7. Palagonitization redistributed elements throughout the tuffs, and by promoting zeolite formation, reduced their permeability and porosity. Zeolite compositions are variable due to cation exchange processes.

8. Preservation of the newly-formed tuff-ring in the active marine environment was due to the proximity of a land mass and subsequently by rapid consolidation of the tuffs.

CHAPTER 3
THE MEDANO TUFF-RING, TENERIFE

3.1. Introduction and Geological Setting

The Medano tuff-ring occurs on the SE coast of Tenerife, the largest of the Canary Islands off NW Africa (Fig. 3.1). These islands, of Tertiary to Recent age, are truly oceanic in character, with no sialic material underlying them even though they occur well up on the African continental rise (Macfarlane & Ridley, 1968). The Canary Islands volcanics are characteristically alkaline and undersaturated, and belong to the basanite (alkali olivine basalt)-trachyte-phonolite suite (Ridley, 1970). The composition of the Tenerife volcanics includes all the members of the above suite in addition to more intermediate members such as trachybasalt and trachyandesite.

The oldest formation on Tenerife is a basement shield composed of basanite and ankaramite lavas and pyroclastics dated at 16-7.2my (Abdel-Monem et al.,1968). The Vilaflor volcanic complex was built up on this shield and suffered major caldera collapse in post-Pleistocene times (Ridley, 1970). Quaternary activity within the collapsed area built up the twin central volcanoes of Viejo and Teide which are the most prominent physiographic features on the island apart from the large semi-circular wall of the caldera. Volcanic activity on Tenerife has continued in historic times, the last recorded eruption being of Mtn. Chinyero in 1909 (Fuster et al.,1968).

The tuff-ring itself lies on the coast, 3km NE of Medano, near a cluster of scoria cones some of which probably erupted along fissures. Later lava flows, one from the nearest scoria cone, overlap onto the eroded flanks of the ring and these and the crater are partly covered by a plinian pumice fall deposit named the Granadilla pumice (Booth, 1973). This pumice fall was immediately succeeded by an ignimbrite which has ponded in the crater of the tuff-ring and was sourced in the Las Canadas caldera to the NW. Near Los Cristianos the ignimbrite contains carbonised plant material which has been dated at

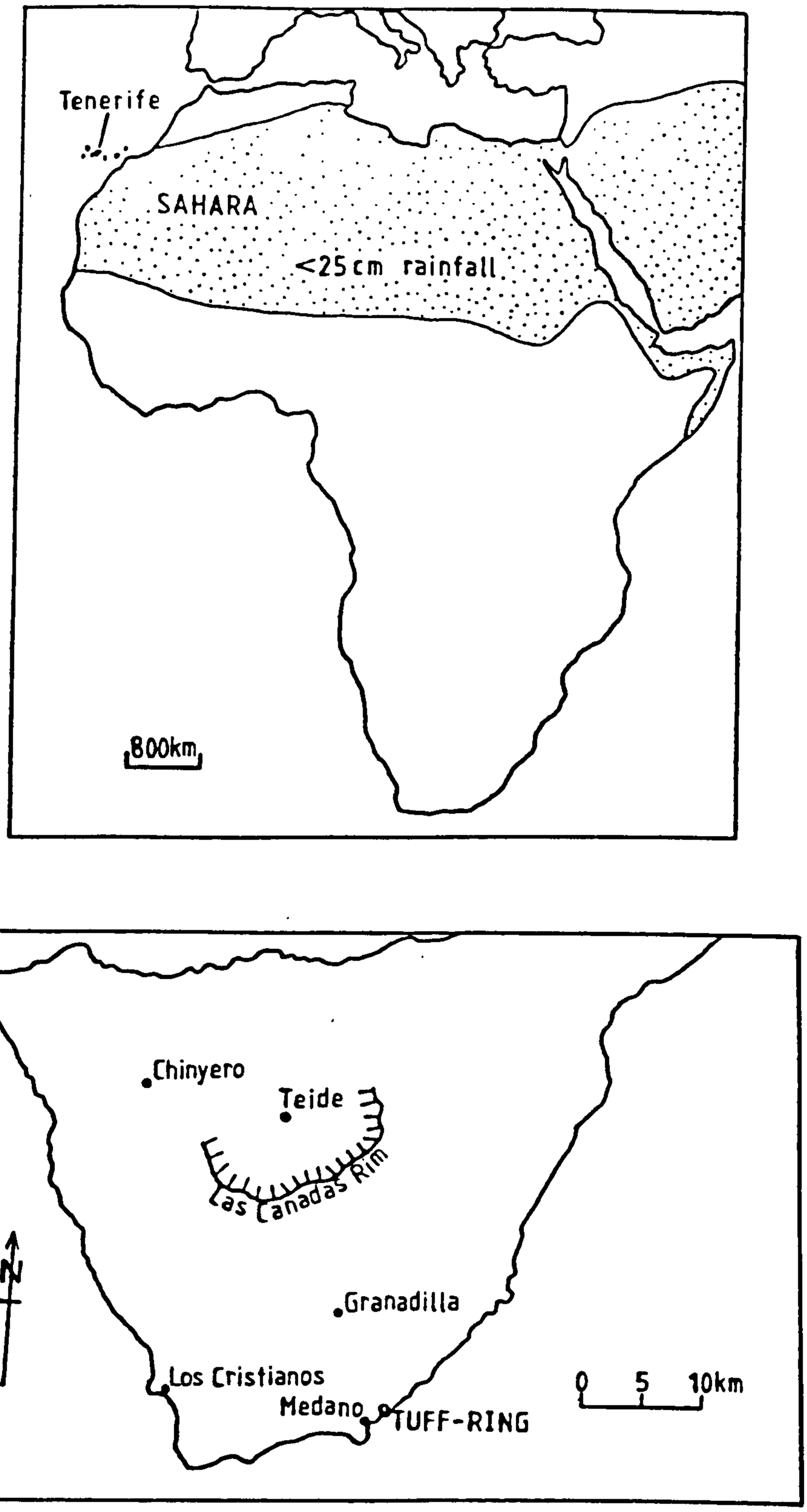

Fig. 3.1 Location maps of Tenerife and the Medano tuff-ring.

≥32,000yrs. B.P. (Shotton & Williams, 1971).

No previous work has been published on the tuff-ring although Fuster et al.(1968) referred to its "phreatic" origin and classified it with their Series 3 basalts which are succeeded only by Recent and historic activity.

3.2. Structure and Products

The tuff-ring has a basal diameter of 1.1 - 1.6km (Fig. 3.2) and is elongated NE-SW although the crater is approximately circular with a maximum diameter of 620m. The maximum height of the tuff-ring is approximately 110m on the SW part of the rim whereas it is only 80m in the NW, indicating prevailing SW directed eruptions or winds during volcanism (Fig. 3.3). The height:width ratio averages 1:20 comparable with most other tuff-rings which lie in the range 1:10 - 1:30 (Heiken, 1971).

The tuff-ring is at present partly eroded, especially on its SE flank which has been dissected by wave action. Flash floods due to intermittent heavy rains have cut many small gullies in the crater deposits and the outer flanks. Winds are presently removing fine material eroded by water-runoff thus preventing soil formation over much of the outer flanks. The crater contains much material eroded off the inner walls. Extensive vegetation (coarse grass, small bushes and cacti) causes poor exposure within the crater and outcrop is best on the seaward flank of the ring.

The structure of the tuff-ring is generally simple, with outwardly inclined tuffs dipping at up to 30° near the crater rim and decreasing outwards to <10° in the most distal beds. This regular quaquaversal structure is not found on the southern flank where in places the tuffs dip towards the crater at up to 25° or are horizontal (Fig. 3.2). The uppermost flank deposits in this area are horizontal or dip outwards at shallow angles. This, plus the lack of evidence of slumping or faulting suggests that the dip reversal is due to the burial of a small hill by the tuff-ring in this area.

The crater is filled to a maximum height of ca.70m

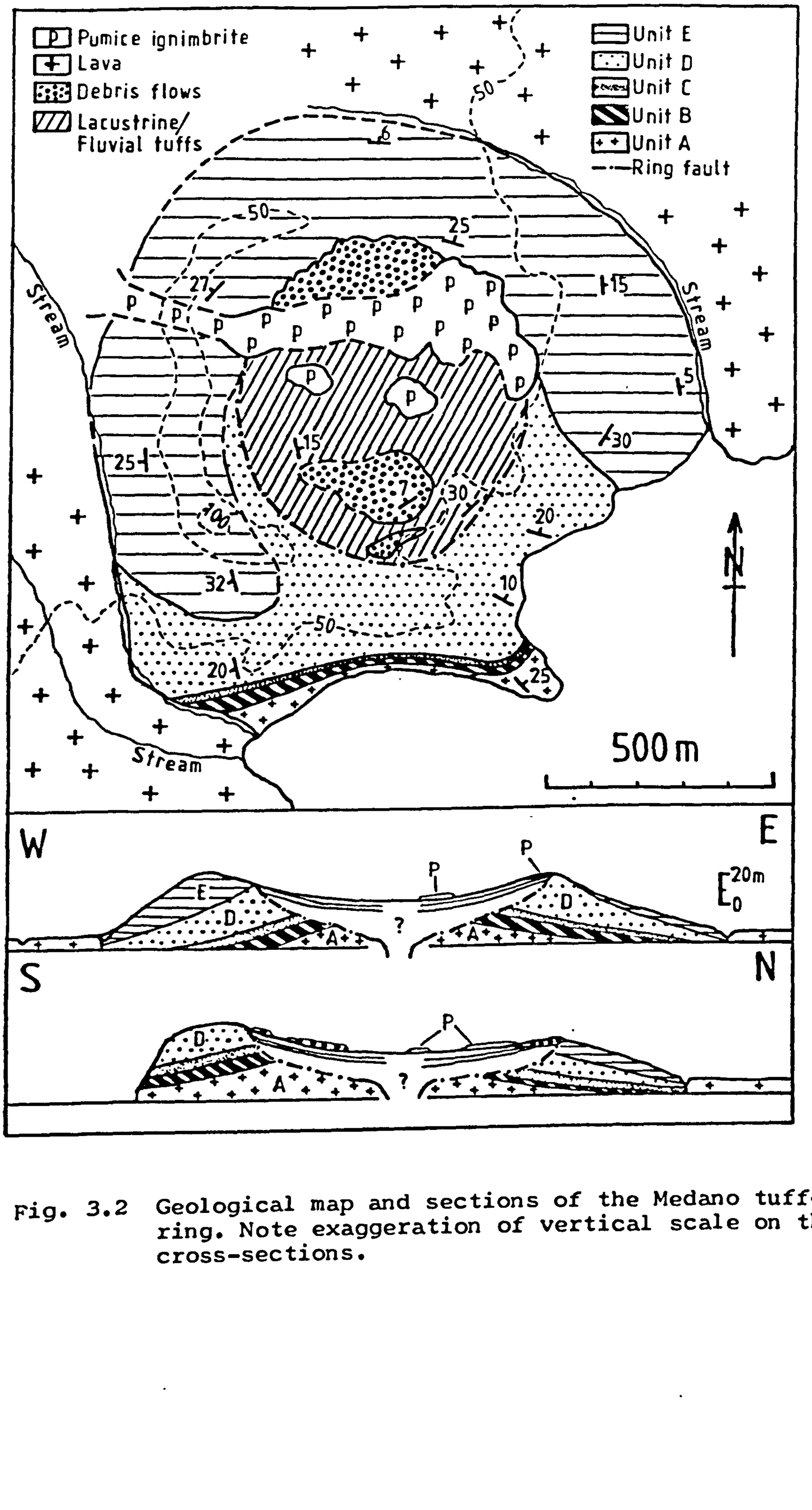

Fig. 3.2 Geological map and sections of the Medano tuff-ring. Note exaggeration of vertical scale on the cross-sections.

Fig. 3.3 Medano tuff-ring, looking to the SE, showing low, wide profile and higher rim in the S (right-hand side of photograph).

Fig. 3.4 Crater rim unconformity in the southwestern part of the tuff-ring. Crater tuffs dip to the right. Large block in centre of photograph measures 2·5m across.

a.s.l. with near horizontal tuffs and pumice deposits. Only near the crater rim are more steeply dipping tuffs exposed, inclined inwards at up to 40° and unconformably overlain by tuffs dipping at < 15° into the crater.

The crater rim is well exposed in tidally-enlarged gullies on the SE flank and consists of a sharp fault plane (Fig. 3.4) which dips into the crater at 40-50° and separates outwardly inclined tuffs from more steeply dipping crater tuffs. No beds may be traced across this junction, even at its highest topographic position, indicating that collapse and oversteepening of the crater tuffs has occurred. Erosion of the crater rim has been extensive, and has sourced the sequence of reworked tuffs now found within the crater. It is estimated from the thickness of the outdipping tuffs partially planed off by erosion on the crater flank that the rim height has been reduced by at least 30m. Simple calculations assuming the reworked crater tuffs to consist of a disc of radius 300m and thickness 20m, and the former rim of the ring to be a toroidal ring of square X-section, radius 300m, indicate removal of 55m thickness of rim beds to source the crater infill.

The amount of collapse is more difficult to estimate due to the lack of correlatable horizons across the fault. Collapse was greater in the crater centre than at the margins, causing rotational steepening of the marginal indipping tuffs. Steepening of lacustrine reworked tuffs, presumably deposited horizontally, to 30° inward dip at the margins of the crater involved subsidence of at least 50m in the centre.

The tuff-ring deposits may be subdivided into those of the outer flanks which are largely of primary origin, and those of the crater which have been entirely reworked.

3.2.1 Outer flank deposits

The tuffs may be further divided into five distinct lithofacies on the basis of field characteristics (Fig. 3.5) :-

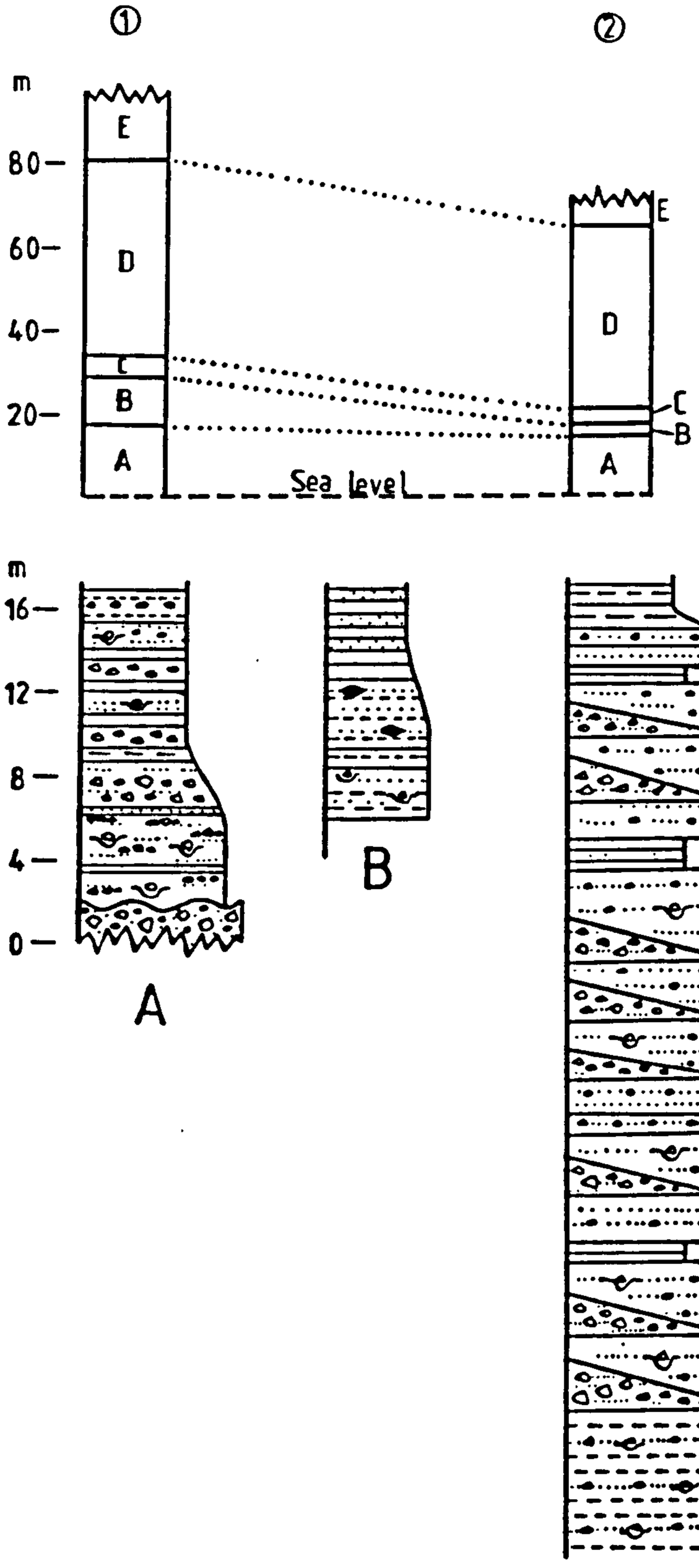

Fig. 3.5 Stratigraphy of the Medano tuff-ring.
Section (1): southern flank,
Section (2): western flank of tuff-ring.
A,B,D and E: logs of best-developed sections of respective units.
See insert in back pocket of thesis for key to lithological logs.

Unit A

This comprises the oldest exposed tuffs, found only along the wave-cut cliffs on the S flank of the tuff-ring. They consist of at least 17m of pale yellow, bedded, often blocky tuffs (Fig. 3.5). Most of the blocks consist of angular, slightly vesicular basalt, some of which have chilled margins suggesting they are cognate lithics. Other basalt blocks are poorly vesiculated, unchilled with abundant iddingsitised olivine and are probably accessory lithics. Less abundant accessory lithics consist of basalts derived from underlying lava flows (some large blocks exhibiting ropey flow structures), bedded tuffs, reddened palaeosols, plutonic syenites and rare fragments of gastropod-bearing limestone.

At the base of Unit A is a poorly stratified, coarse block-rich deposit at least 3m thick (base not exposed) which contains blocks up to 1.5m diameter. Crude internal stratification is defined by laterally impersistant trails of similarly-sized clasts although the matrix of the tuffs is massive. The coarse component fines upwards (coarse tail grading) from 50-150cm at the base to 20-40cm diameter at the top of the bed. Above this, less block-rich tuffs predominate with an upward decrease in the size and concentration of blocks. The tuffs above the basal bed contain internal matrix stratification on a centimetre scale with block sags beneath most of the clasts. Some of the block sag hollows are infilled by coarse, horizontally bedded layers (Fig. 3.6) in addition to the impacted block. These layers are generally thickest and coarsest in the centre of the hollow, fining and wedging out rapidly away from it. It is thought that base-surges deposited the coarse infill material, preferentially dropping part of their basal load into topographic "lows".

The bulk of the unit was deposited by airfall processes indicated by the abundant planar bedding and block sags, the moderate sorting and the lack of well developed surge features. Minor base-surge activity is thought to have occurred throughout deposition of Unit A. The basal coarse beds are thought to represent blocky debris flows because

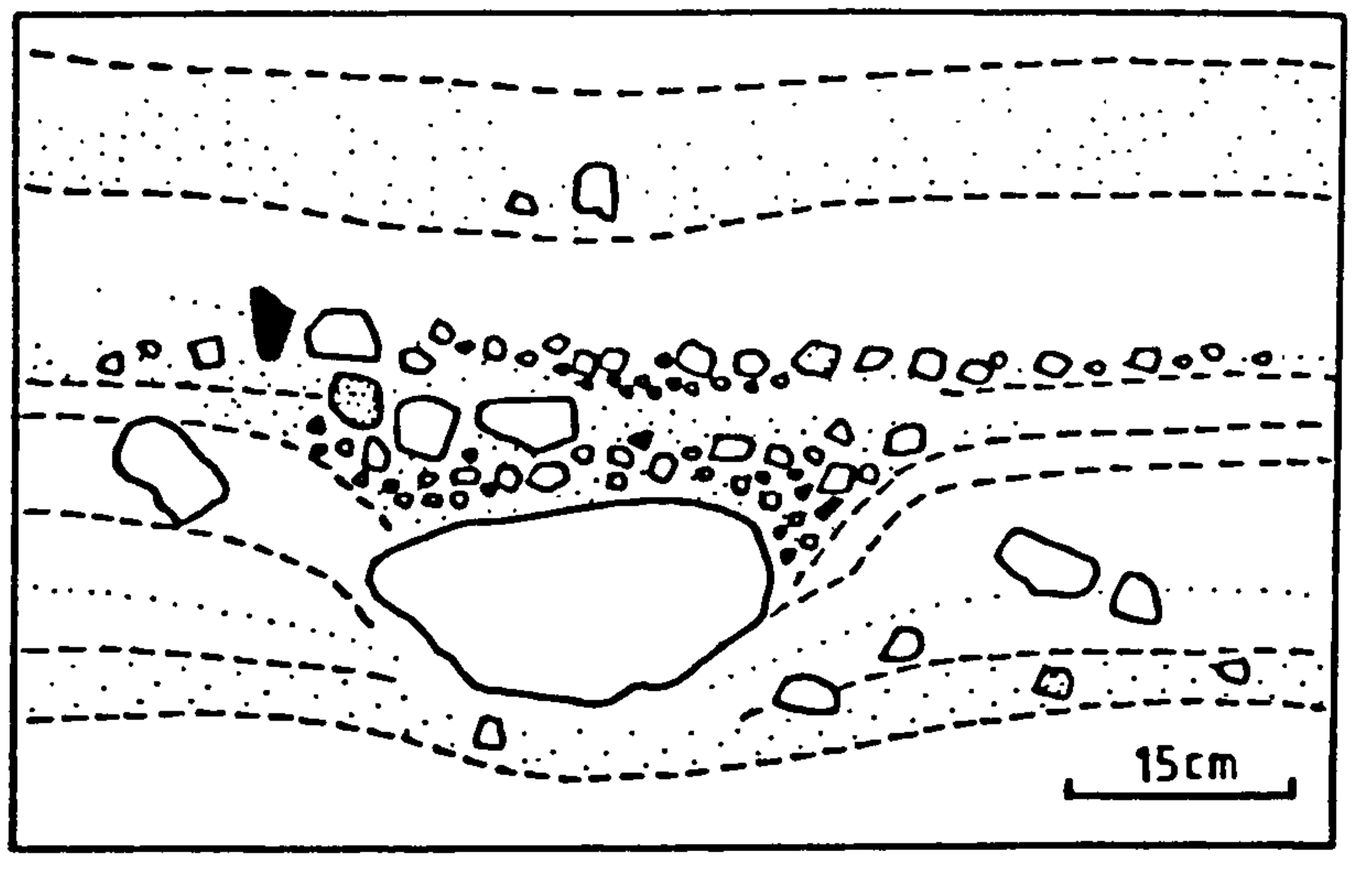

Fig. 3.6 Block within impact crater in Unit A which is infilled by coarse, horizontally bedded layers. This bedding may be a feature of surge deposition into topographic "lows".

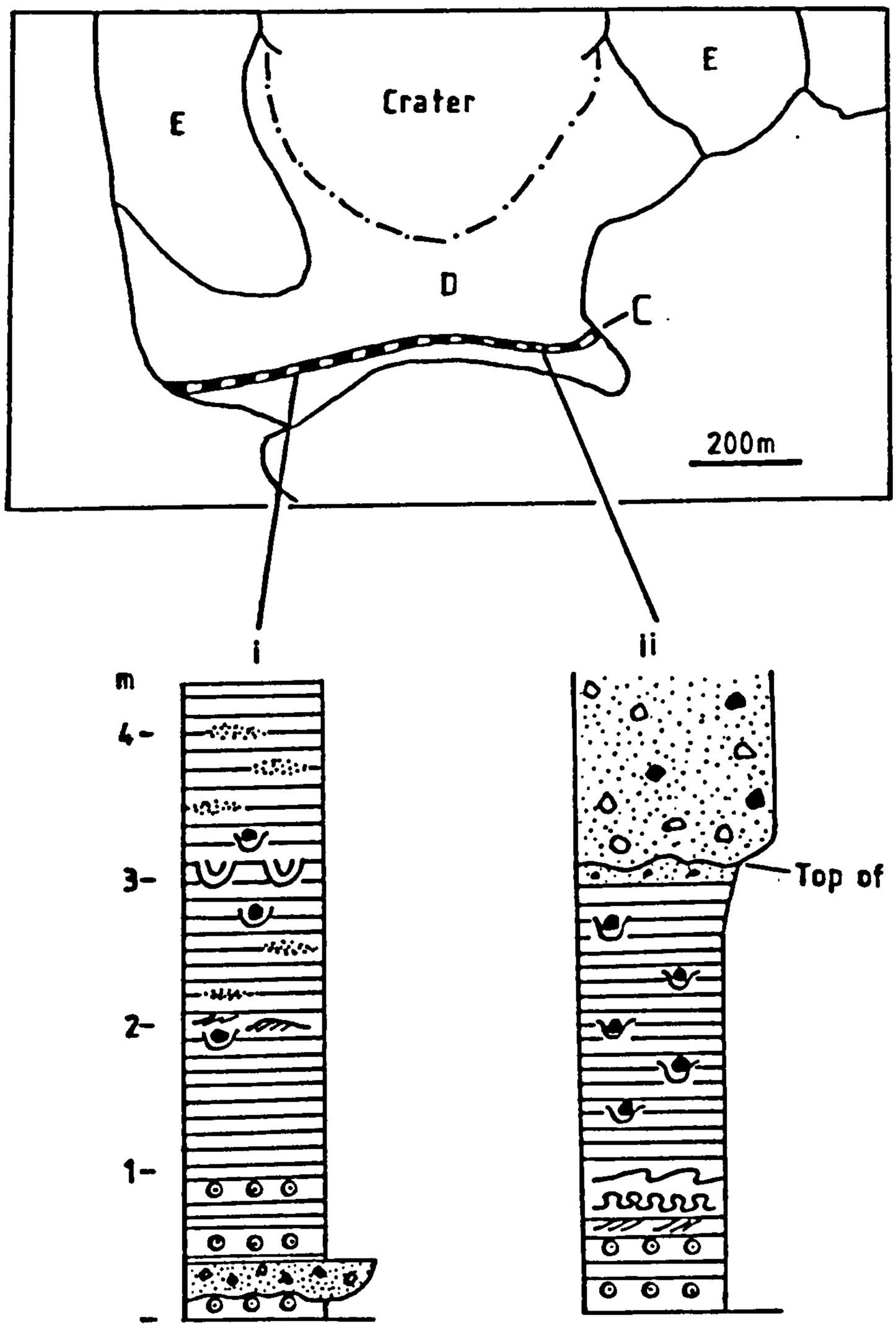

Fig. 3.7 Location of the two Unit C sections and logs of their main features. See insert in back pocket of thesis for key to lithological logs.

of their trains of blocks sitting in much finer massive tuff. It is possible that these coarse beds represent some proximal surge breccia similar to ignimbrite examples described by Wright & Walker (1977) but exposure is too poor to permit exact determination of their origin.

Unit B

This unit consists of well-bedded lapilli tuffs containing much fewer, smaller blocks than Unit A. Unit B thins along strike from 11.5m in the S to less than 3m thick to the E (Fig. 3.2). Beds range from 2-30cm thick and are well-sorted lapilli and ash tuffs, with the lapilli being more vesicular than those found in Unit A. Highly vesicular, sometimes breadcrusted basaltic bombs are found throughout the unit especially towards the top and these are occasionally flattened, indicating their molten plastic state on ejection.

Upwards in the unit the amount and size of accidental and cognate lithic clasts decrease as the number of bombs and the proportion of vesicular lapilli increases (Fig. 3.5). Near the top of the unit two 30cm thick beds occur, containing a high proportion of angular basalt lithic clasts. These contain no internal stratification and are inversely-graded, with almost entirely matrix-free clast supported layers at their tops. The beds appear to have a gradational contact with underlying well-bedded tuffs and are thought to be of surge origin since they infill hollows in the topography with coarse blocks. A 50cm well-bedded lapilli tuff layer separates the two clast-rich beds and appears to be of airfall origin.

Overall, Unit B consists of airfall tuffs although minor surge activity occurred during its final stages of deposition. The presence of true vesicular bombs and almost scoraceous lapilli indicates that more strombolian-like activity was occurring due to the inability of water to completely chill the magma. The paucity of scoriaceous tachylite throughout, however, indicates that true fire-fountaining did not occur.

Unit C

This unit is generally well-bedded, consisting of up

to 5m of pale grey ash with subordinate cognate and accessory lapilli and rare blocks up to 60cm. Although largely inaccessible it is well exposed in two localities about 500m apart on the S flank of the tuff-ring (Fig. 3.7). The Unit C tuffs contain many features which indicate deposition by base-surges but lateral variations between the two localities present important evidence of varying surge characteristics.

a) Section 1

This section (Fig. 3.7) lies 750m SSW of the geometrical centre of the tuff-ring and consists of 5m of SW dipping tuffs which are part of the irregularly-dipping non-quaquaversal tuffs on this southern flank. At the base, the tuffs are full of accretionary lapilli which reach 1cm diameter. These structures occur in smaller amounts throughout Unit C. Above this basal 10cm bed a 25cm thick, coarse lapilli tuff occurs which is laterally very discontinuous and wedges out completely in places. No internal stratification is present and it has a sharp, sometimes erosive base which along with its complete lack of size grading suggests it may be of debris flow origin. The slightly hummocky top of the coarse bed is overlain by 50cm of bedded accretionary lapilli-rich tuffs which pass upwards into 1-1.5m of well-bedded ash tuffs containing occasional cross-bedding, of low-angle tabular type.

A well exposed dune occurs at the top of the 1.5m thick well-bedded tuffs (Fig. 3.8) and overlies a 15cm basal block which has an asymmetric sag beneath it indicating R→L sense of motion on emplacement. The surge which formed the dune plastered coarse ash and lapilli over the upper faces of the block and built an asymmetric dune above the sag crater. The dune, or more properly antidune, has a wavelength of 150cm and a height of 16cm and exhibits rounded ripple crests initially, which become more peaked upwards. As in other dunes of surge origin (Crowe & Fisher, 1973) the stoss side beds are thinner and finer than those on the lee-side, although only a small amount of downflow crest migration has occurred.

Fig. 3.8 Unit C dune deposited by surges which moved R→L and out of the plane of the photograph, forming a ridge-like dune with its long axis normal to the surge direction. More steeply dipping (if no correction is made for the angle of the depositional slope) lee-side beds are laterally well developed, sometimes normally-graded and planar or slightly concave in shape. Hammer measures 30cm.

Erosion or non-deposition of the upper part of the original dune crest is indicated by truncated lee-side X-laminae of at least 10cm thickness. Continued surge deposition caused the overlying beds to thin markedly over the antidune and removed its effect on bed topography by 20cm above the crest.

The surge is thought to have deposited the antidune at this point because the block sag formed a major discontinuity on the bed which generated turbulence in the surge as it passed overhead, causing it to deposit material. A change in the physical properties of the surge pulses caused antidune deposition to cease and damping of topographic highs on the bed by rapid lateral thickness variation (+ ?erosion of highs).

Above the antidune beds a 25cm block occurs, also with an asymmetric sag indicating a SW-directed trajectory

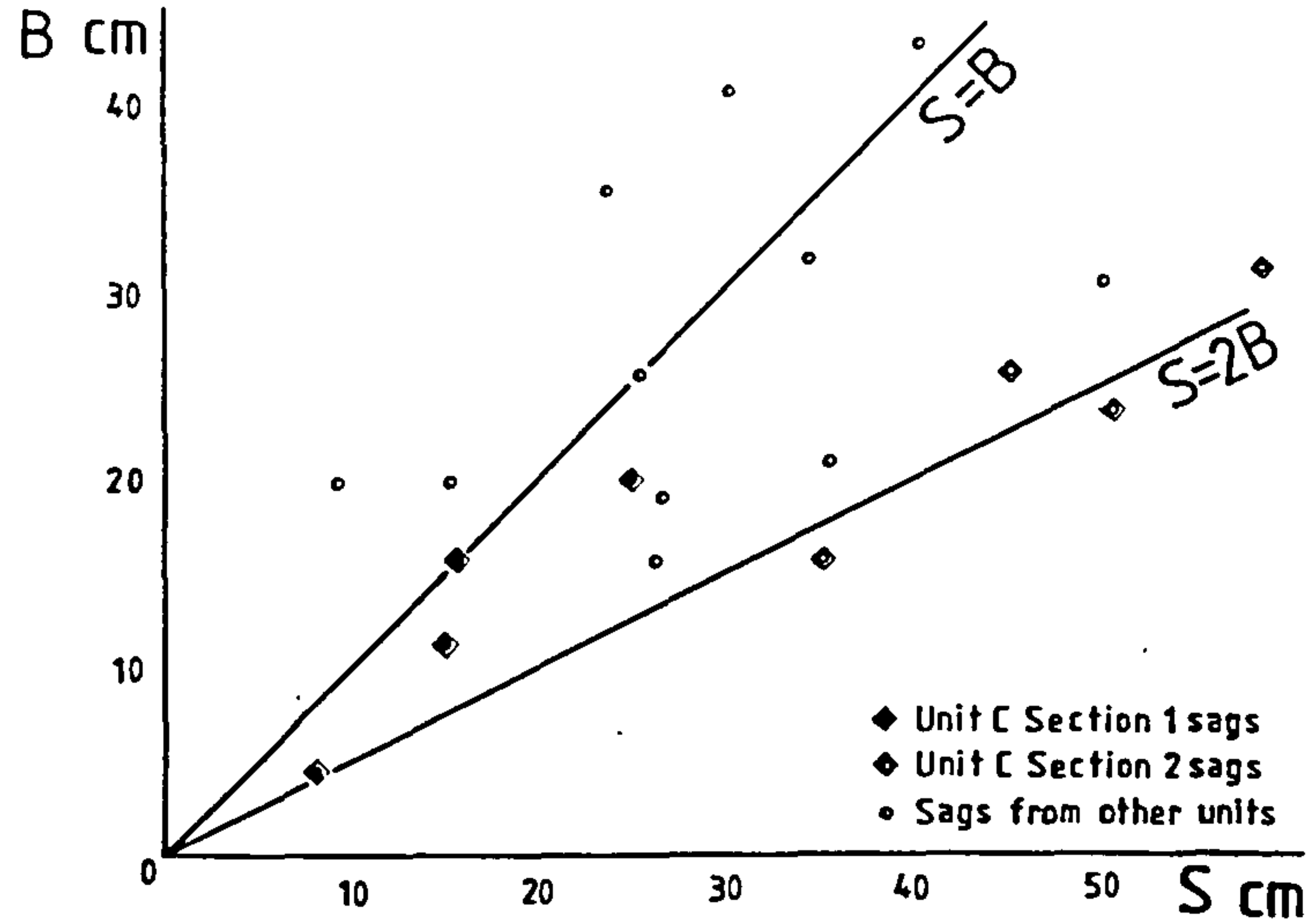

Fig. 3.9 Block impact sag data. B: block diameter S: impact depth

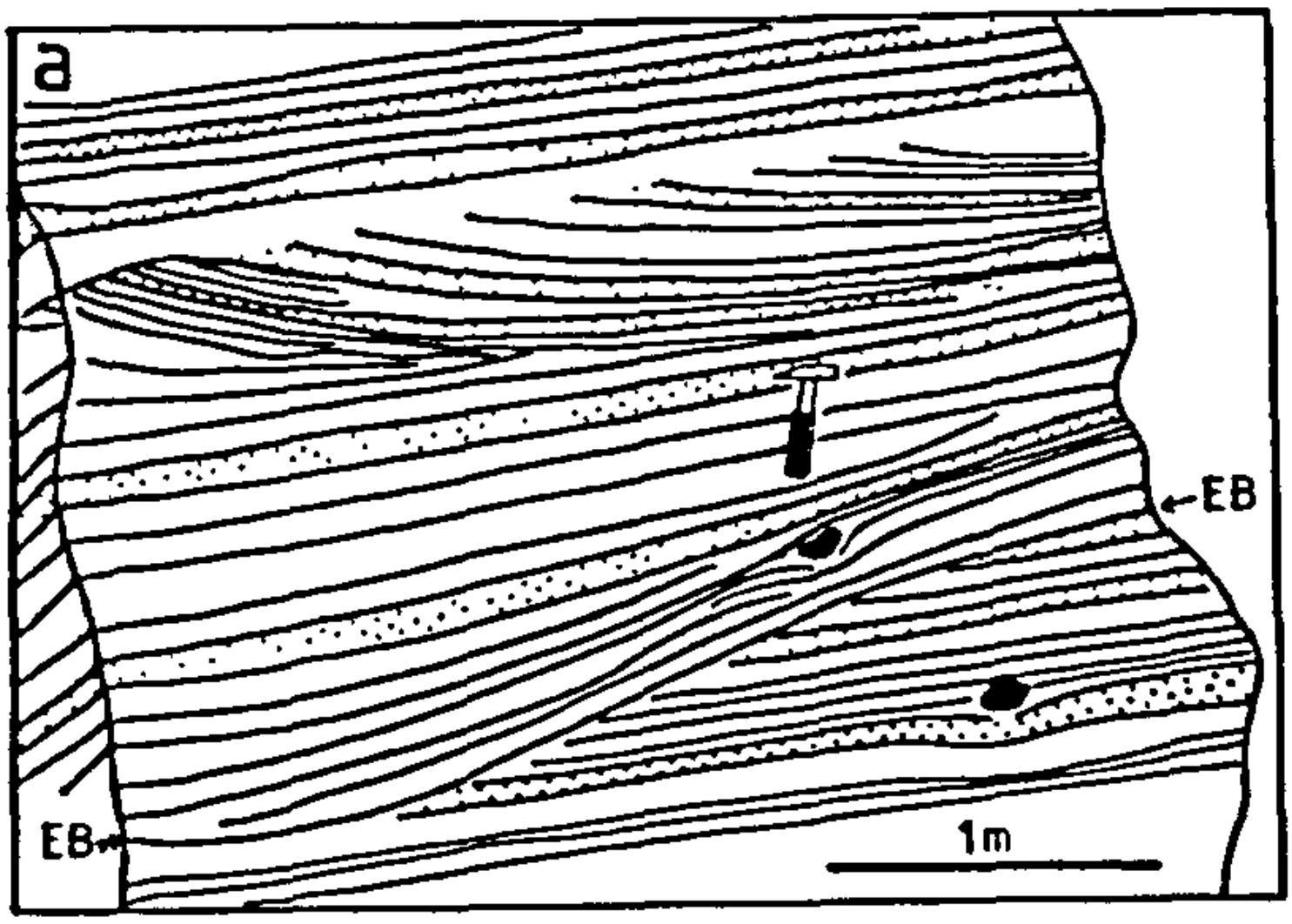

Fig. 3.10 a) Unit C surge channel with trough cross-bedding indicating banking of surges on the outside curve of a meander in its course (Fisher, 1977).
EB: erosive base of channel

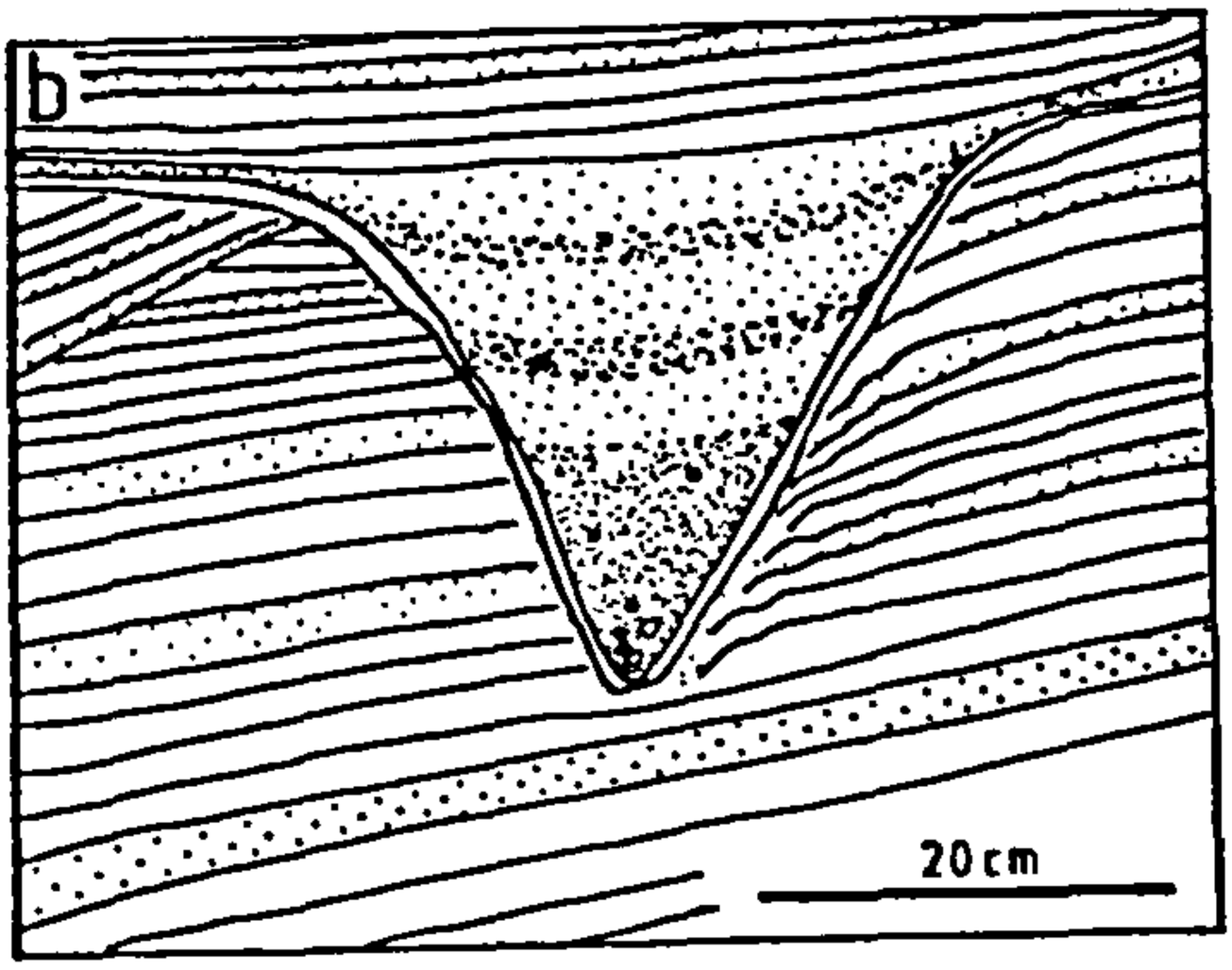

Fig. 3.10 b) V-shaped Unit C channel cut by fluvial action and infilled by surge tuffs which subsequently slumped.

similar to the block beneath the antidune. The sag of the upper block is filled with coarse blocky tuff on its crater-facing side and immediately overlain by a 40-50cm thick coarse bed which is poorly internally laminated and thins to the SW. The base of the bed consists of mixed block-and-ash tuff and the blocks decrease in size upwards from 25 to 5 cm. The internal lamination consists of lapilli lenses 2-5cm thick and block trains and these together with the downslope thinning, occasional clast imbrication and rare internal block sags indicate that the unit is possibly derived from the bedload of a powerful surge able to transport coarse material further from the vent than most of the surges which deposited Unit C.

The remainder of Unit C consists of ash tuffs with thin lapilli layers, or more often lenses, as well as rare coarser units. Isolated blocks often have very deep sags beneath them indicating that the underlying tuffs were moist and plastic. A plot of some of the blocks and the depth of their sags indicates that Unit C tuffs were more plastic than other tuff-ring deposits (Fig. 3.9). Two channels of different origin are found within this outcrop (Fig. 3.10) and will be further described :-

i) The first channel occurs near the top of Unit C and is 2m deep and at least 4m wide (Fig. 3.10a). It cuts plane-bedded tuffs and is well exposed, though its margins have been eroded away. The shape, size and internal structure of the channel indicate it was cut by surges and infilled by them, although an isolated block with associated sag was probably emplaced as an airfall product.

ii) The second channel cuts upper Unit C tuffs to the E of the first channel and is much smaller and of V-shaped cross-section (Fig. 3.10b). The shape of the channel and its small size suggest it was cut by the action of streams on consolidated tuffs. Modern stream channels on the crater walls have steep V-shaped profiles where they cut consolidated tuffs but much more flat-bottomed U-shapes where they cut loose tuffs. The origin of the poorly-bedded infilling tuff is unclear since bedding was destroyed by mass movements soon after deposition. However, the

marginal fine ash layer is thought to have been plastered onto the channel walls by surges. The surges then infilled the channel, the upper channel deposits passing out unaffected into the surrounding sequence of surge tuffs.

b) Section 2

This section (Fig. 3.7) crops out approximately the same distance from the centre of the crater as Section 1 and consists of 3m of surge deposits overlain and cut out to the E by coarse, unbedded blocky tuffs. The basal 50cm of Unit C contains >50% of accretionary lapilli in thin ash beds which are in places slump folded and contain convolute bedding. This basal layer overlies coarse Unit B beds which are highly contorted due to gravity slumping. Small-scale trough cross-beds occur immediately above the basal 50cm and are also often slumped.

The upper 2m of the unit consist of fine, well-bedded, sometimes cross-bedded tuffs which are highly block-sagged, some of the blocks reaching 50cm. The sags beneath these blocks (Fig. 3.11) are very marked and indicate the highly plastic nature of the tuffs on deposition (Fig. 3.9). The ash beds coarsen upwards towards the top of the unit, becoming poorly-laminated lapilli tuffs which are cut out by the overlying coarse deposits, although updip Unit C only reaches 3·5m thick and is conformably overlain by bedded, blocky tuffs. Downdip these blocky beds become massive and cut into the top 1m of Unit C as they grade into debris flows.

The various features of the two Unit C sections may be summarised as follows :-

Section 1	Section 2
Base rich in accretionary lapilli	Base rich in accretionary lapilli
Many lapilli layers and coarse lenses	Fine ash throughout, except for lapilli top
Large antidunes, cross-bedding and erosive channels	Small-scale trough cross-beds, abundant slumping and convolute bedding
Moderate sags beneath blocks	Very prominent sags beneath blocks
>4m thick	>4m thick even though cut out by debris flows

Fig. 3.11 Deep impact sag in Unit C Section (2) tuffs. Note plastic deformation of moist, cohesive tuffs. Hammer measures 30cm.

Fig. 3.12 Accretionary lapilli in Unit E. Parabolic plaster tails deposited by surges which moved from top to bottom of photograph.

The difference between Section 1 and Section 2 can be explained by their being deposited by surges with different physical properties. Section 2 contains abundant evidence of being deposited as fine, very moist tephra whereas Section 1 has much more coarse material, large antidunes and channels indicating that its depositing surges were concentrated in coarse debris and not particularly moisture-rich. It is suggested that Section 2 tuffs were deposited by expanded surges carrying only fine material and low temperature steam (i.e. moisture-rich), whereas Section 1 surges probably contained high temperature steam. A possible reason for this difference might be that some surge blasts were directed towards the SSW (towards Section 1) and thus surges reaching Section 2 would be more expanded and travelling at lower velocities.

Unit D

This unit, 47cm thick in the SW and < 30m thick in the SE, consists of poorly-bedded tuff with agglomeratic layers rich in blocks, especially near the base (Fig. 3.5). Bedding is crudely defined by clast rich lenses and layers up to 1·5m thick or by laterally impersistent coarse lapilli layers up to 30cm. The blocks are predominantly angular basalt and are mostly accessory lithics along with blocks of syenite, trachyte, bedded tuff, pink pumice, red scoria and some ignimbrite. Maximum block size reaches 1·5m but most are 15-40cm diameter, decreasing in abundance and average size upwards to less than 25cm at the top of the unit. Block sags are found where large clasts overlie thinly bedded lapilli layers but are generally absent due to poor bedding definition. Although largely block-rich the unit contains a high proportion of yellow glass shards of ash grade which form the matrix.

Rare (<5%) fine beds contain faint traces of low angle cross-bedding and are probably of surge origin. Towards the top the bedding in Unit D becomes much better defined, due to the reduction in size and abundance of lithic clasts and better sorting of the lapilli and ash in the matrix.

The moderate sorting, block sags, poor-to-moderate

bedding and the rare thin cross-bedded layers indicate that Unit D is a coarse airfall deposit which probably formed from a dense, poorly developed eruption column leading to lack of sorting of fine and coarse material. Intermittent minor surges occurred throughout the mainly airfall sequence. Some debris flow activity may have formed massive blocky beds found throughout the unit.

Unit E

This unit has a gradational contact with Unit D and the transition is marked by a 4m thick zone within which lithic clasts in Unit D fine to <10cm and decrease in abundance and are replaced by the incoming of vesicular bombs (Fig. 3.5). Unit E consists of up to 40m of well-bedded, blocky sideromelane lapilli in a yellow ash matrix of the same composition with scoriaceous, often broken ribbon and irregular bombs up to 20cm. These bombs have highly vesicular cores with an outer chilled margin 2-5cm thick and often broke up on impact, but never show any signs of flattening. The bombs are not abundant but occur throughout Unit E, associated with layers of more vesicular lapilli, some scoriaceous.

Unit E is well sorted with thin laminae of ash and lapilli often <2cm thick, which vary laterally in thickness and grain size within distances of <1m. Thin, fine-grained, often cross-bedded layers occur in places, reaching 40cm thickness but laterally impersistent. These often have large accretionary lapilli associated with them which occur towards the base of these surge horizons. The accretionary lapilli (Fig. 3.12) consist of poorly-sorted concentric rims of fine to coarse ash up to 2cm thick around cores of vesicular basalt or lithic clasts up to 4cm diameter. The thickest coatings are formed only around smaller lapilli cores. The maximum diameter of any complete lapillus is always <5cm and this may be associated with the flow power of the surges which are thought to have emplaced them (Section 3.3.2). Many of the accretionary lapilli are flattened parallel to bedding and rare examples deform fine layers producing small impact sags. Smaller accretionary, or more properly rimmed lapilli, which

consist of poorly-sorted ash up to only 4mm thick are abundant throughout Unit E and probably grew rapidly in the moisture-rich eruption column of the tuff-ring.

As well as this concentric coating of ash many of the larger accretionary lapilli, and other large clasts in the surge deposits < 5cm diameter, have parabolic-shaped ash coatings on their sides facing the crater centre (Fig. 3.12). Similar aerodynamic, layered, parabolic coatings have been described by Moore (1967) from the sides of trees facing the crater of Taal volcano. There, coatings 10cm thick were recorded 2·5km from the vent centre. In Unit E up to 9-layered coatings, with an overall maximum thickness of 17cm, are found 500m from the vent centre. As in Taal some of the coatings consist of reverse-graded layers up to 2cm thick individually, indicating initial deposition of moist fine ash which coarsens outwards in any layer. Some indication that surges have partly reworked underlying tephra is given by the association of clasts >8cm with coats only on their upflow sides with slightly smaller clasts which have been moved short distances and are coated with small parabolic tails on more than one side. The plastering structures were not found closer than 500m from the crater centre. Directional data from these structures and from surge channels (Fig. 3.13) indicate a consistent radial orientation to the crater. No evidence for topographic channelling or directed blasts is indicated.

Unit E also contains many channels of various origins (Fig. 3.14) which are well exposed because the Unit E tuffs are the youngest primary deposits of the tuff-ring and are thus not overlain by any other beds. The channels may be divided into four types, all found within the top 10m of the unit.

a) Small flat-bottomed U-to modified V-shaped channels (Fig. 3.14a) of shoulder width 20-80cm and depth 15-40cm occur along a single horizon within Unit E and are restricted to an outcrop length of less than 20m. The channels are spaced at intervals between 60 and 150 cm and their bases dip at 15-20°, cutting beds which dip SE at 10°. The channels are filled with lapilli and ash tuffs

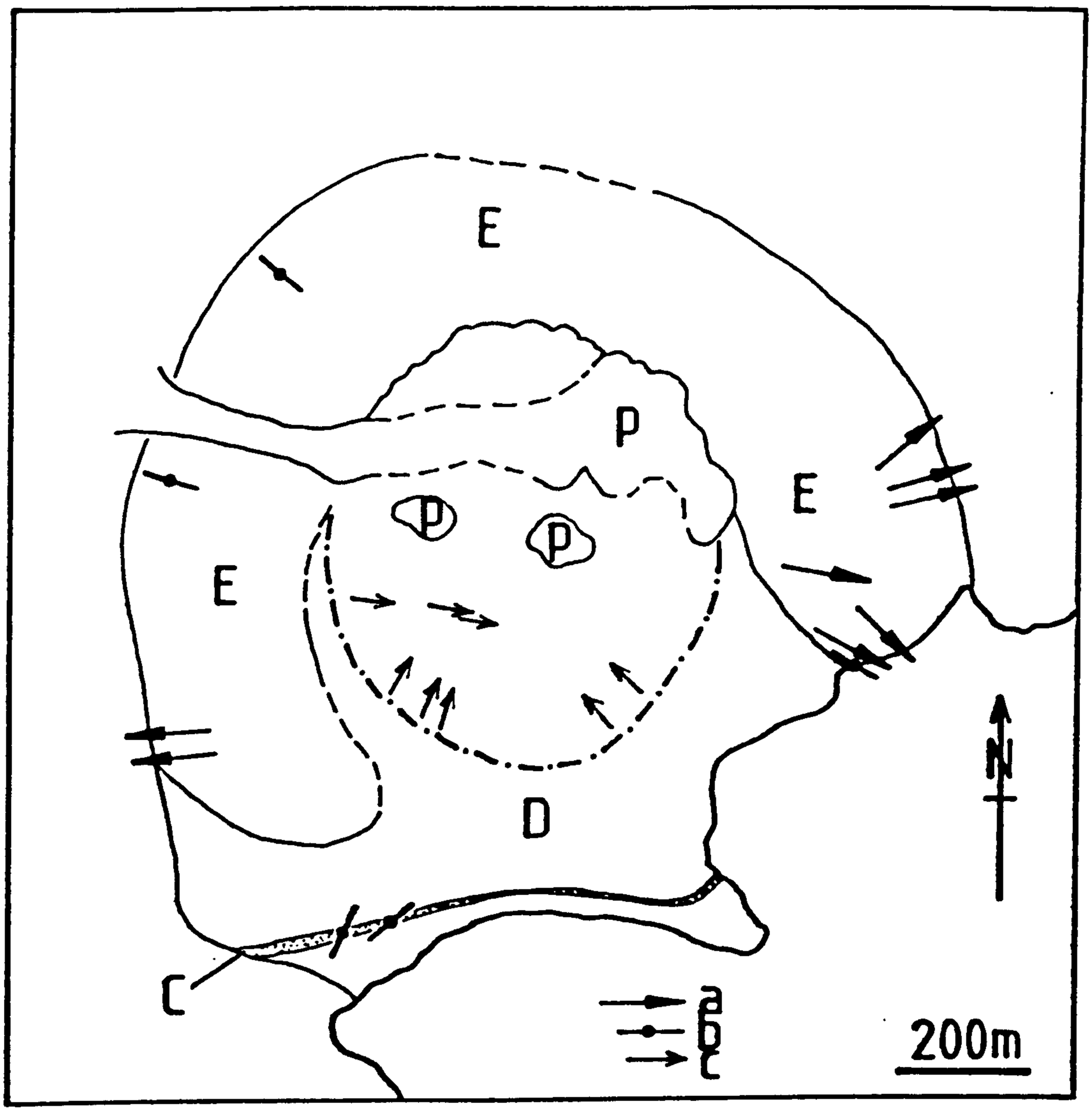

Fig. 3.13 Directional data from Medano tuff-ring.
a: plastering structures } surge direction
b: surge channels }
c: fluvial cross-beds and clast imbrication
p: pumiceous ignimbrite

which are finer and generally better sorted than the beds which the channels cut, although many channels contain isolated lithic clasts of up to 8cm diameter. The infilling tuffs are coarse and horizontally-bedded or massive at the channel base, becoming finer, better sorted, concave upward bedded tuffs towards the channel top. These upper beds may be traced out from the channels and form the lower part of a 30-40cm well-bedded surge deposit which contains low-angle trough cross-bedding, flame structures, pinch-and-swell and convolute bedding and is markedly finer than the airfall beds above and below. A 2-3cm thick, bedded ash layer often occurs parallel to the channel sides and may be traced out into the overlying tuffs.

The shape, small size and basal horizontally bedded or massive infilling tuffs are indicative of a fluvial origin for most of the channels. The major part of their infilling was, however, by base-surges which plastered ash onto the channel sides and deposited convex-upward laminae within them. Some of the original V-shapes of the channels have been enlarged by surges to more U-shaped profiles in their upper regions. Some contortion of bedding probably resulted from mass movement of moist tephra for short distances down the channel.

b) The southern margin of a large flat-bottomed channel (Fig. 3.14b) crops out on the side of a modern stream-cut gully on the NE flank of the tuff-ring. The width of the structure is unknown but its depth exceeds 2m and may be much greater. The channel margin is stepped and the basal infilling material is composed of well-bedded ash which abuts the near vertical margin at 10-15° and is overlain by massive, coarser lapilli tuffs. The upper channel infill consists of well-bedded tuffs which unconformably overlie the lower infilling material and dip into the channel centre at 30°. The channel is orientated NW-SE which is approximately concentric to the crater rim.

The lack of any surge features and the concentric orientation indicate the stepped channel is of fluvial origin, and was infilled by fluvial and debris flow material at the base before being subsequently eroded and

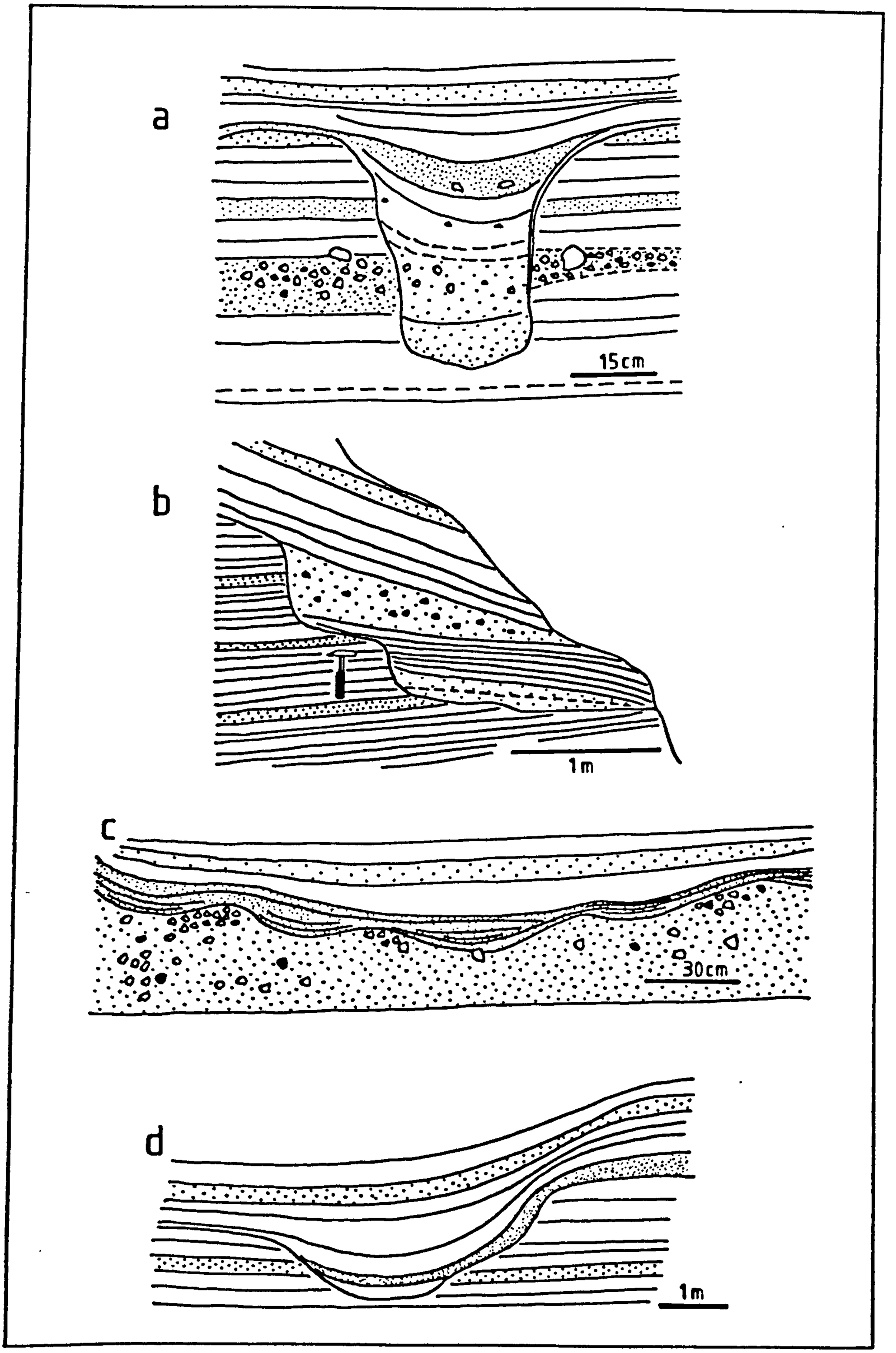

Fig. 3.14 Unit E fluvial and surge channels. See text for description and discussion.

infilled by airfall beds.

c) Small closely-spaced channels (Fig. 3.14c) of flat bottomed U-shape and measuring up to 40cm across and 15cm deep occur in the uppermost 5m of Unit E on the NE flank of the tuff-ring. They cut coarser poorly-bedded grey lapilli tuffs and are infilled at their base by 2-3cm of bedded ash parallel to their sides with horizontally bedded ash above. The beds immediately above the channels, which were all formed at the same time, consist of well-laminated ash containing pinch-and-swell bedding. These small channels occur as projections beneath a shallow depression, 2m wide, which existed before their formation.

The large channel was probably cut by surges and later modified by surges which cut the smaller channels and infilled the composite structure with tuffs which thicken and coarsen into the hollow. It is possible that a single surge lobe with closely spaced highly debris concentrated "streamers" within it (Fisher, 1977) could have simultaneously cut the large U-shaped channel and the small U-shaped notches at its base.

d) The final channel example occurs immediately below the eroded top of Unit E on the NW flank of the tuff-ring (Fig. 3.14d). The channel is a composite, asymmetric structure 2m deep and >6m wide. The base of the channel is a 1•3m wide flat-bottomed U-shaped structure which on its NE side passes into a steep-sided wall 1m high, but to the SW it passes into horizontally bedded tuffs. The infilling tuffs are banked up against the steep wall but pass into concave-upwards beds in the channel centre, and consist of well-bedded lapilli tuffs.

The channel was probably cut initially by surges and enlarged by them to form its slightly asymmetric shape. Infilling was by surge and airfall tuffs, forming many beds which thicken into the channel centre although lacking any other surge characteristics. Banking-up of deposits on the NE side of the channel may have been caused by surges which were moving across the channel or around a channel meander.

3.2.2 Crater tuffs

The crater tuffs are largely reworked and may be subdivided into three units on the basis of suspected depositional environment.

Lacustrine tuffs

A 2-4m thick bed of ash and lapilli tuff containing many fine-grained, discontinuous muddy tuff laminae and small cross-laminae is found immediately in contact with the ring fault inside the crater (Fig. 3.15). This unit is bedded parallel to the fault plane which forms its lower boundary, and dips into the crater at 30-45°. The muddy tuffs(Fig. 3.16) contain small lenses or ripples of fine tuff which in places are flaser-like. The lenticular laminae form beds up to 8cm thick separated by poorly-sorted lapilli tuff, and lenses of coarser ash and lapilli at times occur within these fine beds. Small-scale tabular cross-laminae with mud drapes occur within many of the finer beds. The ripples and flasers reach lengths of 4cm and heights of <1cm, the ripples having rounded crests and rarely exhibiting small-scale climbing-ripple lamination. Some of the muddy units contain small desiccation cracks of irregular shape.

The regular development of this unit against the fault indicates that the beds were deposited against its footwall after some collapse had occurred. The fine tuffs are interpreted as being the deposits of a short-lived crater lake which had an input of coarser material from inflowing streams and airfall ejecta. Evidence for the latter is indicated by some sags in the muddy layers beneath small clasts.

Fluvial tuffs

The lacustrine unit is conformably overlain by at least 24m of mainly fine-grained, well-bedded tuffs (Fig. 3.16) which are largely of airfall origin at the base but become more reworked towards the top. The lower 6m consists of bedded airfall tuffs with blocks and bombs up to 10cm, many underlain by sags. Thin, muddy layers occur but are associated with fluvial channels and are probably of overbank origin. Some poorly exposed 2-5m wide U-shaped

Fig. 3.15 Lacustrine tuffs near the southern crater edge with mud flasers and drapes on cross-laminae. Coin measures 2cm across.

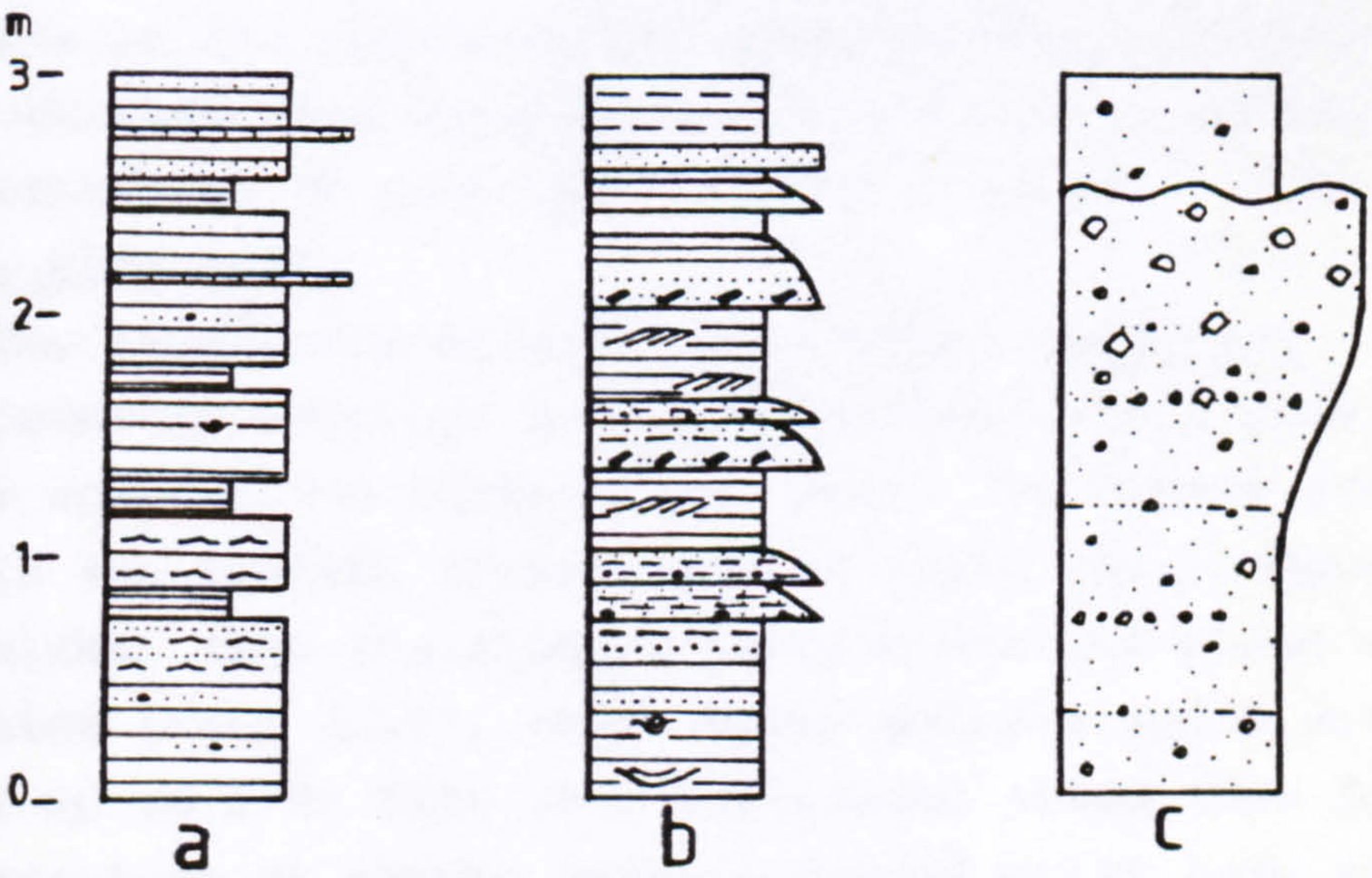

Fig. 3.16 Logs of reworked crater tuffs
a: lacustrine tuffs
b: fluvial tuffs
c: debris flow tuffs

channels may be of surge origin, and cut the airfall tuffs. The airfall tuffs are most similar to the Unit E tuffs in that they lack many blocks and have irregularly-shaped bombs, and may be their crater equivalents.

Upwards in the unit, and into the crater centre, the airfall tuffs become completely reworked by fluvial action. The upper deposits are almost horizontal, well-sorted bedded tuffs which contain rare clasts < 5cm diameter with no underlying sags. Individual beds fine into the crater and become better bedded with small-scale trough cross-bedding indicating flow into the crater. Clast imbrication generally agrees with this current direction although in places clasts lie along foreset bedding and care must be taken to identify their transport direction. Channels are very abundant in the upper 10cm of the deposit and palaeocurrent directions derived from them indicate that much of the crater fluvial tuffs were derived from the W side of the tuff-ring. (Fig. 3.13).

The deposits represent a sequence of airfall tuffs with increasing fluvial reworking with time, transporting material into the crater centre. Coarse braid-bar deposits at the crater rim pass laterally into alluvial plain deposits in the crater centre with an increased spread of palaeocurrent data derived from them, and an increase in the proportion of fine material and sorting.

Debris flow tuffs

The lacustrine airfall and fluvial tuffs are unconformably overlain by coarse, blocky, debris flow tuffs at the edge of the crater (Fig. 3.4). The debris flows overlie the tilted, eroded edge of these older deposits and thicken into the crater, forming massive piles up to 10m thick (Fig. 3.15). Very coarse massive tuffs with blocks up to 2·5m fine into the crater where they form structureless or weakly reverse-graded units 1-2m thick individually. These finer grained debris flows contain blocks up to 15cm, often arranged in pebble trains which dip radially inwards at up to 10°. Further into the crater centre the debris flows grade into fluvial deposits as they wedge out and become themselves reworked.

In the N the debris flows originated from curved slump scars which cut back into the outdipping Unit D and E tuffs and obscure the ring faults. Elsewhere the debris flows are bounded by the ring fault and some overlap it, indicating they post-date its final movements. The debris flows have largely been sourced from Unit D, indicated by their abundant block content. They probably formed after erosion of Unit E exposed Unit D in the footwall of the ring fault. This erosional stripping of the rim deposits forms the reverse stratigraphy in the reworked deposits, Unit E-derived fluvial tuffs overlain by Unit D-derived debris flows.

3.3. Variation in Primary Products

The Medano tuff-ring provides information on the variations in eruptive products and mechanisms with time in a tuff-ring.

3.3.1 Tuff-ring products

Lithologically, the Units A to E are distinct, differences between them reflecting differences in eruptive style. Table 3.1 summarises some of the main features of the individual units and their proposed depositional mechanisms. It must be stressed that the variation in products is thought to be due to variation in the amount of water interacting with magma to form the phreatomagmatic explosions, and the depth of that interaction.

Units A and D are very similar, with large blocks of both accessory and cognate origin in a finer matrix of chilled sideromelane glass. The paucity of well-sorted, well-bedded finer material in the units and the upward fining of the coarse component indicates that the units were the airfall products of poorly-expanded, low eruption columns formed from powerful explosions. These explosions probably had a focus some distance below the ground surface, bringing up large lithic clasts. Minor surges were formed when magma:water interaction occurred near the surface, sourcing inclined eruption blasts, or when collapse of the unstable eruption column resulted in formation of surges.

Lithological Unit	Lithology	Thickness	bedding	Maximum clast size and composition	Sedimentary Structures	Depositional Mechanism
Deposits within central crater	Yellow-brown ash to lapilli tuff. Highly altered sideromelane tuff.	24m minimum	Thin well defined bedding with occasional massive units.	40cm. Mainly non-vesicular basalt.	Normal grading, flaser bedding, trough cross-bedding, clast imbrication, channels, very rare bomb sags at base.	Lacustrine, stream and debris flow reworking.
E	Yellow-brown to grey lapilli-tuff. Vesicular scoria and bombs. Sideromelane and tachylite.	30m . maximum	Thin to medium well bedded throughout.	15cm Juvenile and cognate/accessory basalt.	Normal and reverse grading. Rare sags. Large accretionary lapilli, plastered blocks, channels.	Air-fall and minor base surge.
D	Yellow lapilli-tuff with common blocks. Sideromelane tuff.	47m maximum	Massive at base, becoming better defined at top of unit.	150cm Mainly basalt, with trachyte, red scoria, bedded tuff, syenite and ignimbrite.	Overall fining upwards, rare sags, and lensoid coarser horizons at base.	Air-fall.
C	Creamy-yellow fine grained ash to lapilli-tuff. Rare isolated blocks, base rich in accretionary lapilli.	5m maximum	Thin well defined bedding throughout.	30cm Cognate/ accessory basalt	Graded bedding, dunes, channels, tabular cross-bedding, convolute bedding, slump folds, pronounced sags.	Base surge and air-fall.
B	Yellow-orange ash and lapilli-tuff. Occasional small bombs. Sideromelane tuff.	11.5m maximum	Well defined 2-30cm thick beds throughout.	20cm Mainly juvenile and cognate/ accessory basalt.	Normal and reverse grading. Rare sags. Thin clast rich horizon near top of unit.	Air-fall. Minor debris flow.
A	Yellow lapilli-tuff with common block-rich horizons. Sideromelane tuff.	17m minimum	Massive at base becoming thinner and better defined upwards.	2.5m at base 50cm at top. Mainly basalt with trachyte, bedded tuff, palaeosol , syenite and gastropod limestone.	Normal and reverse grading. Overall coarse-tail grading upwards. Lensoid block rich horizons, bedding sags. Massive basal layer	?Debris flow at base. Air-fall.

Table 3.1 Descriptions of the lithological units of the Medano tuff-ring.

The relative abundance of lithic clasts indicates that steam explosions due to high water:magma ratios were important, although nowhere near as important as in the mainly phreatic eruptions of maar volcanoes (Lorenz, 1973).

Units B and E are similar in that they contain only small amounts of accessory lithic clasts and a significant proportion of volcanic bombs, ejected whilst still molten. The units are medium-grained, well-bedded tuffs containing well-sorted thin beds of lapilli and ash. These units were formed by explosions with lower water:magma ratios which sourced small numbers of surges so probably occurred at shallower depths than the optimum for surge production. The low water content of the erupting tephra clouds allowed development of higher eruption columns due to less heat exchange between magma and water enhancing thermal convection processes in the column (Wilson et al., 1978). This in turn resulted in better sorting of particles in the column and thus better bedding in the deposits. The low lithic content is due to the shallow explosion focus level precluding extensive wall-rock spalling which is much more common in maars (Lorenz, 1973; 1974). Surges in Unit E are the product of more powerful eruptions with foci at the optimum depth, forming laterally-directed blasts containing highly fragmented material.

Unit C is different in that it is predominantly of surge origin and contains very high proportions of finely fragmented material as well as a few large ballistically emplaced blocks, The fine material is the result of highly efficient disruption of the magma and chilling by water. This is probably caused by high water:magma ratios and explosions at short distances below crater level.

Figure 3.17 is a schematic diagram illustrating the qualitative changes in water:magma ratios and depth of explosion foci. This shows that phreatomagmatic activity is essentially variable although at Medano it may have been cyclic with less water-influenced eruptions following more powerful eruptions in which more water was involved. Formation of surges was especially intermittent and this was probably because eruptions evolved through the optimum

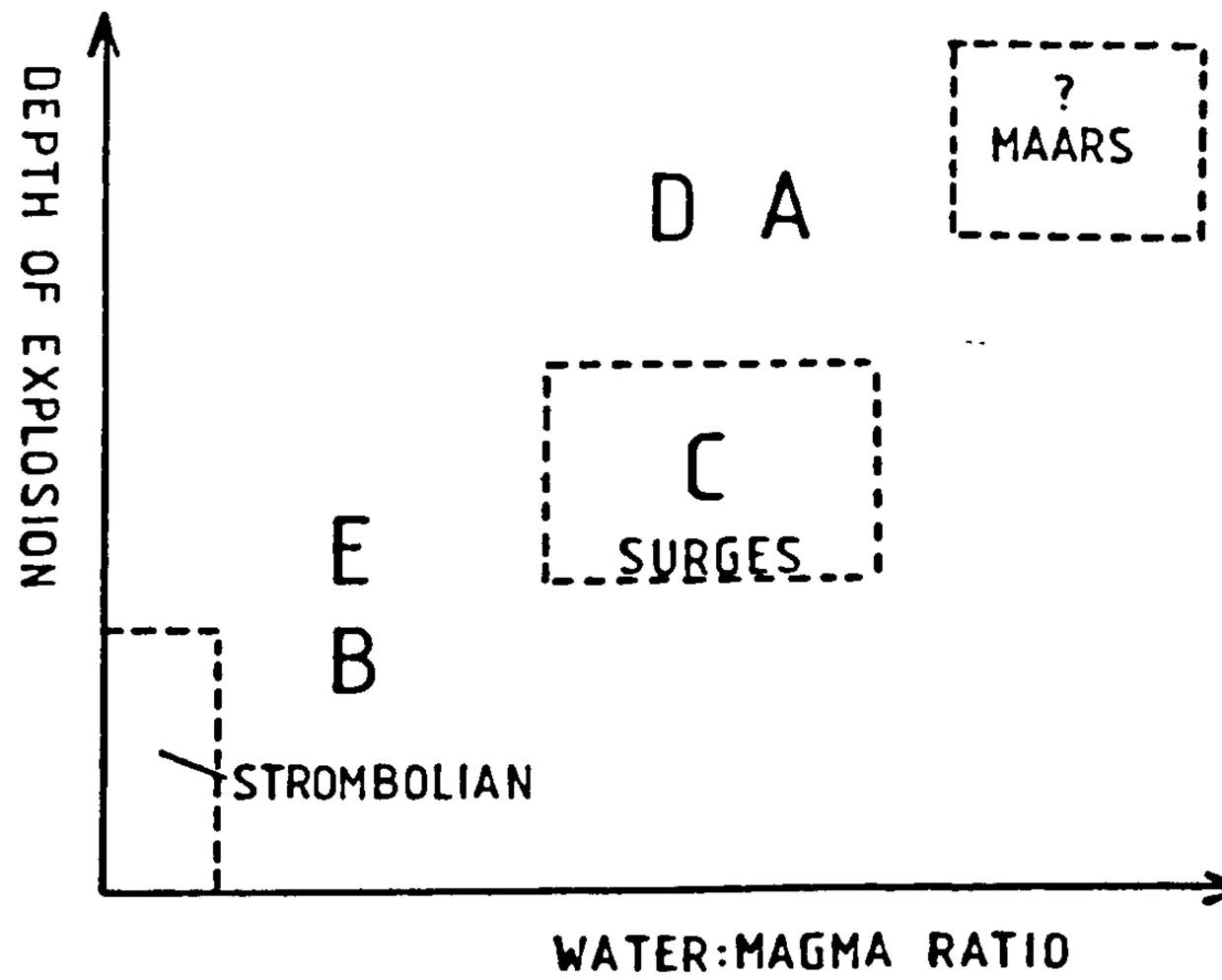

Fig. 3.17 Diagrammatic representation of dominant eruption conditions during formation of the Medano tuff units. Suggested conditions for the formation of maars are indicated.

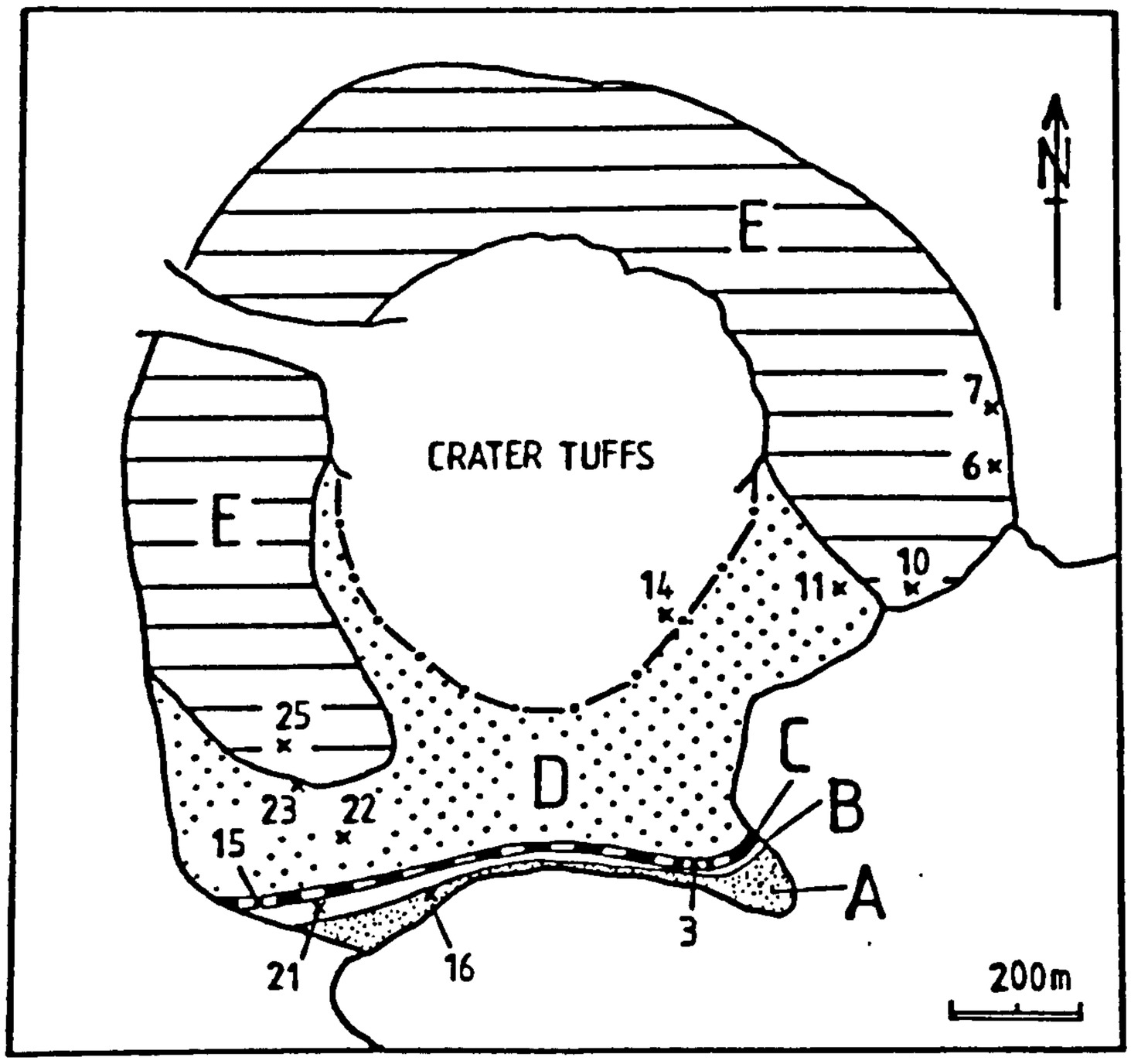

Fig. 3.18 Location of samples, numbered as they appear in the text.

surge-forming conditions often and rapidly, forming thin, poorly-developed surge horizons. Unit C was formed by eruptions which maintained these conditions for longer periods of time.

3.3.2 Base-surge mechanisms

The range of structures in Unit C has already been described (Section 3.2.1). Surge structures of different type are found in Unit E and were deposited by surges with different physical properties. Unit E surge deposits are thin, formed by numerous (at least eight) short-lived surge events. Large accretionary lapilli are common but bear little resemblance to the small, fine, concentrically rimmed types found in Unit C. The Unit E types are simply extreme examples of the abundant "rimmed lapilli" found throughout Units B and E. The thick-rimmed accretionary lapilli in Unit E probably began to accrete their poorly-sorted rims in the low eruption column. They were then incorporated into surges where they accreted more ash and were emplaced, usually at the base of surge deposits. Emplacement occurred before the lapilli reached a critical size of ca.5cm indicating that this was the maximum clast size which surges could transport.

The parabolic-shaped plaster coatings on many blocks indicate that moist ash was deposited by surges. The thin, often reversely-graded layering was formed by surges carrying material of fine grade in pulses, fine ash preceding coarser ash. Such structures indicate that at distances <500m from the crater centre the depositing surges carried only fine material, perhaps as a moist, expanded cloud ahead of the body of the surge. Coarser material which surrounds the plastered blocks was presumably emplaced as part of the body load of later surges. These did not adhere to the blocks because they were not strongly affected by water surface tension or interparticle adhesive electrostatic forces.

The surge channels commonly occur at the base of surge deposits, eroding underlying airfall beds. Often surges modify previously cut fluvial channels, as a result of

turbulence induced by topographic irregularities. Being like density flows (Fisher, 1977) surges are controlled by pre-existing topography and will thus tend to flow down such channels, especially as they are parallel to the radial motion of surges. The thin, fine, plaster layer which is deposited by surges at the margins of modified channels is significant. The layer is a surge deposit, whereas shortly before this surges have been purely erosive. This suggests that surge deposition is related to high moisture content and may signify that a hot, fast moving erosive stage is succeeded with time by a cool, expanded, moist depositional stage. The high moisture content of such surge deposits causes slumping and mass movement of channel infill material.

It is concluded that Unit E surge deposits, found only more than 500m from the crater centre, are not simply distal equivalents of the type of deposits found in Unit C. Due to the outcrop distribution, Unit C is exposed only on the S flank of the tuff-ring and Unit E mainly on the N and W flanks. It may be that Unit E surges were fundamentally different from Unit C types but this could simply be due to SW-directed surge blasts, with fewer, lower velocity surges reaching other parts of the tuff-ring. The large surge channels at the top of the Unit E sequence may indicate that in the final stages of activity this SW-directed activity ceased, allowing more powerful surges to reach the northern flanks. Supporting evidence for SW-directed eruptions is the increased thickness of Units A to D in the SW, where on average they are 50% thicker than in the E and SE.

3.4. Crater Deposits

The crater deposits are important in that they record the post-volcanic subsidence of the tuff-ring and the range of reworking processes which occurred.

The oldest crater deposits exposed are the thin lacustrine tuffs which presumably overlie older reworked crater tuffs. Fault collapse occurred before and to a small extent after their deposition. The crater lake formed during

a break in volcanic activity by ponding of rainwater into the central depression. The present topographic heights of the lacustrine tuffs (ca.50m a.s.l.) and lack of evidence of breaching of the tuff-ring rules out a marine origin for this lake. Renewed volcanic activity infilled the shallow lake and deposited airfall tuffs above.

Continued rainfall, probably derived mainly from steam-rich eruption clouds, sourced flash floods similar to present-day processes and reworked part of the airfall crater sequence. The cessation of volcanic activity allowed fluvial runoff to rework all but about 10m of the airfall tuffs and transport material into the crater centre. Continued subsidence in the centre due to magma withdrawal probably maintained it as a topographic depression and speeded-up the rate of erosion of the crater rim. Debris flows and braided stream processes occured at the crater rim due to high slope angles. As gradients decreased on the crater floor, fluvial action sorted and transported material into the centre.

Continued erosion of the crater rim stripped off Unit E and exposed Unit D. The latter, blocky tuffs sourced coarse debris flows which unconformably overlie subsided reworked crater tuffs. These debris flows dip at shallow angles into the crater and indicate that subsidence of the crater after their deposition has been of minor extent. Continued reworking and deposition of the products of other volcano's eruptions in the crater has occurred. This causes the crater sequence to be highly complex and here it bears little resemblence to the outer flank tuffs.

Crater subsidence occurred throughout the deposition of much of the infilling tuffs. Subsidence was slow, and greatest in the crater centre, tilting reworked tuffs and producing unconformities. Ring fault movements occurred purely as a response to central subsidence and thus lagged behind them. The ring fault formed along a major plane of weakness and allowed movement of crater deposits without affecting the outer flank tuffs in any way.

3.5. Volcanic History

Since the base of the tuff-ring is not exposed, the initial eruptive products are not seen and it is thus not known whether they were of subaerial, submarine or sublacustrine origin. However, the lack of tidal reworking in the distal tuffs indicates that sea-level was no higher at the time of formation of the tuff-ring than it is at present. If the tuff-ring formed during the cold phase of a glacial stage sea-level would have been appreciably lower and rainfall much higher than at present. In such a pluvial period standing water bodies would be abundant and it is suggested that the Medano tuff-ring was erupted into a shallow coastal lake of this type. The high rainfall during such a pluvial period would have sourced the streams which extensively reworked the crater tuffs and allowed a crater lake to form.

The origin of the water which interacted with magma to produce phreatomagmatic activity after the tuff-ring became completely subaerial is problematic. A break in the crater rim may have allowed easy access of coastal lake water during the early stages of volcanism. No trace of such a notch is now seen and thus final activity could not have resulted from such water. It is thought that Units A and D, which contain blocks from many levels of the country rocks, formed when water interacted with magma at some depth below the surface. The water may have percolated down from the surface lake, similar to the Eifel maars (Lorenz, 1973) or may have originated in a deep aquifer. The pressure reduction after a phase of eruption (Lorenz, op.cit.) spalls off sizeable blocks from the diatreme walls and these are transported upwards by the particle-charged gas jets of the eruption. Units B and E contain few xenolithic clasts and probably formed when magma rose to high levels before interacting with small amounts of surface, perhaps crater lake, water. This obviates the need for a crater wall breach, for which there is no direct evidence. Unit C is thought to have been formed when magma interacted with abundant surface-derived water at intermediate depths. Crater lake surface water would be

continuously replenished by rainfall from steam-rich eruption columns and the high climatic input. Aquifer water would need more time to be replenished. The cyclic nature of the Medano eruptions thus depended on the rate of replenishment of the surface water, its rate of downward percolation and the volume and rate of ascent of the magma (Section 3.6c).

The Medano activity may be summarised thus :-

a) Rising magma contacted groundwater within coastal deposits and built a tuff-ring which rapidly grew above the water surface. Downward percolation of water through the disrupted diatreme deposits underneath the crater led to magma:water interaction at depth. Largely vertically-directed eruptions produced Unit A airfall tuffs, containing country-rock derived blocks, and a few base-surge deposits.

b) Reduction in the amount of water and the depth of interaction led to the intermediate strombolian-phreatomagmatic activity of Unit B. SSW-directed eruptions caused thickening of the unit in the S and sourced base-surges.

c) Highly explosive surge-producing eruptions of Unit C occurred due to the interaction of large amounts of water with magma at intermediate depths. The SSW-directed eruptions caused lateral variations in the surge deposits, due to differences in the surge physical properties.

d) Renewed deep eruption foci sourced Unit D, mainly of airfall origin due to vertically-directed explosions. High water contents in the eruption column caused it to be poorly expanded and the airfall deposits are thus coarse and poorly sorted.

e) Unit E formed due to intermediate strombolian-phreatomagmatic activity as magma contacted moderate amounts of crater lake water at shallow depths. Crater lake tuffs were deposited above subsided primary and reworked tuffs. A reduced amount of water in the eruption column led to it being more expanded and more wind influenced, depositing well-sorted bedded tuffs. Abundant rimmed lapilli formed, some growing within base surge clouds which also eroded channels and deposited sticky ash layers over upstanding clasts.

f) Cessation of volcanic activity allowed complete reworking of the crater tuffs aided by high rainfall in a pluvial period. Transport of material into the crater centre occurred by fluvial and debris flow action aided by further collapse of the crater deposits. Erosional stripping of the crater rim sourced coarse debris flows which are the final main reworked deposit.
g) Lavas from a nearby scoria cone lapped onto the flanks of the tuff-ring. Later deposition of Granadilla pumice fall and associated ignimbrite followed over the whole of the area and is now preserved in the crater of the tuff-ring. Establishment of an arid climate reduced the rate of reworking and preserved the tuff-ring almost intact.

3.6. Petrography, Morphology and Alteration

3.6.1 Petrography

The Medano tuffs consist predominantly of juvenile sideromelane grains with rare tachylite. Variable proportions of cognate and accessory lithic clasts occur, as well as crystal fragments. Many sideromelane grains are altered to palagonite and authigenic minerals infill the pore spaces and vesicles of the altered tuffs. Figure 3.18 is a location map for all the samples studied in this section.

a) Sideromelane

The sideromelane grains are pale-brown in colour and are blocky or irregular in shape. The glass is in most respects similar to that in the Saefell tuffs with plagioclase microlites, opaque inclusions, vesicles of varying sizes and abundance and shattered margins. The Medano tuffs are generally more vesicular, especially in Units B and E, and many vesicles are elongate. Microlites are almost always flow-aligned although associated vesicles may be spherical or elongate parallel to the microlites. This indicates that magma was flowing just prior to quenching but was in places very fluid allowing spherical vesicles to develop. Elsewhere the magma was more viscous, the flow deforming the vesicles within it.

The change from fluid to viscous flow may often be seen within a single grain (Fig. 3.19). Grains containing stretched vesicles are often themselves elongate, indicating that the surface tension of the magma in part controlled particle shape (Lorenz, 1971). Other grains show flow-orientation structures unrelated to particle shape and were formed by quenching. In general, Units B and E contain elongate fragments with related stretched vesicles whereas Units A and D have mainly blocky grains containing spherical vesicles. Unit C is too fine-grained to determine the relationship between vesicle and juvenile particle shape.

Sideromelane grains reach a maximum of 1·5cm but are commonly much finer and contain inclusions of blocky opaques, probably magnetite. As well as the plagioclase microlites some rare laths of biotite up to 0·5mm long occur.

b) Scoria

Some black or dark brown lapilli consist of very vesicular fine-grained or tachylitic material, and may be termed scoriaceous. Most of the scoria occurs as volcanic bombs in Units B and E but rare scoriaceous lapilli occur in all the Medano tuffs except for Unit C. The volcanic bombs consist of >50% irregular vesicles in a matrix of tachylite containing many flow-aligned plagioclase microlites (Fig. 3.20). Larger crystals of magnetite and plagioclase up to 0·5mm occur as well as small clinopyroxene and biotite crystals. Vesicle density is so high in some bombs that bubbles coalesce and form composite vesicles up to 8mm diameter.

c) Vesicle size

In any single juvenile lapillus, vesicle radius varies by as much as 10times although most vesicles are between one third and a half of the average largest vesicle size. Most vesicles range from 0·02 to 0·2mm although sizes are much larger in scoriaceous grains. The average vesicle size of tephra from each Medano unit is different and indicates different depths at which vesicle growth was arrested by quenching.

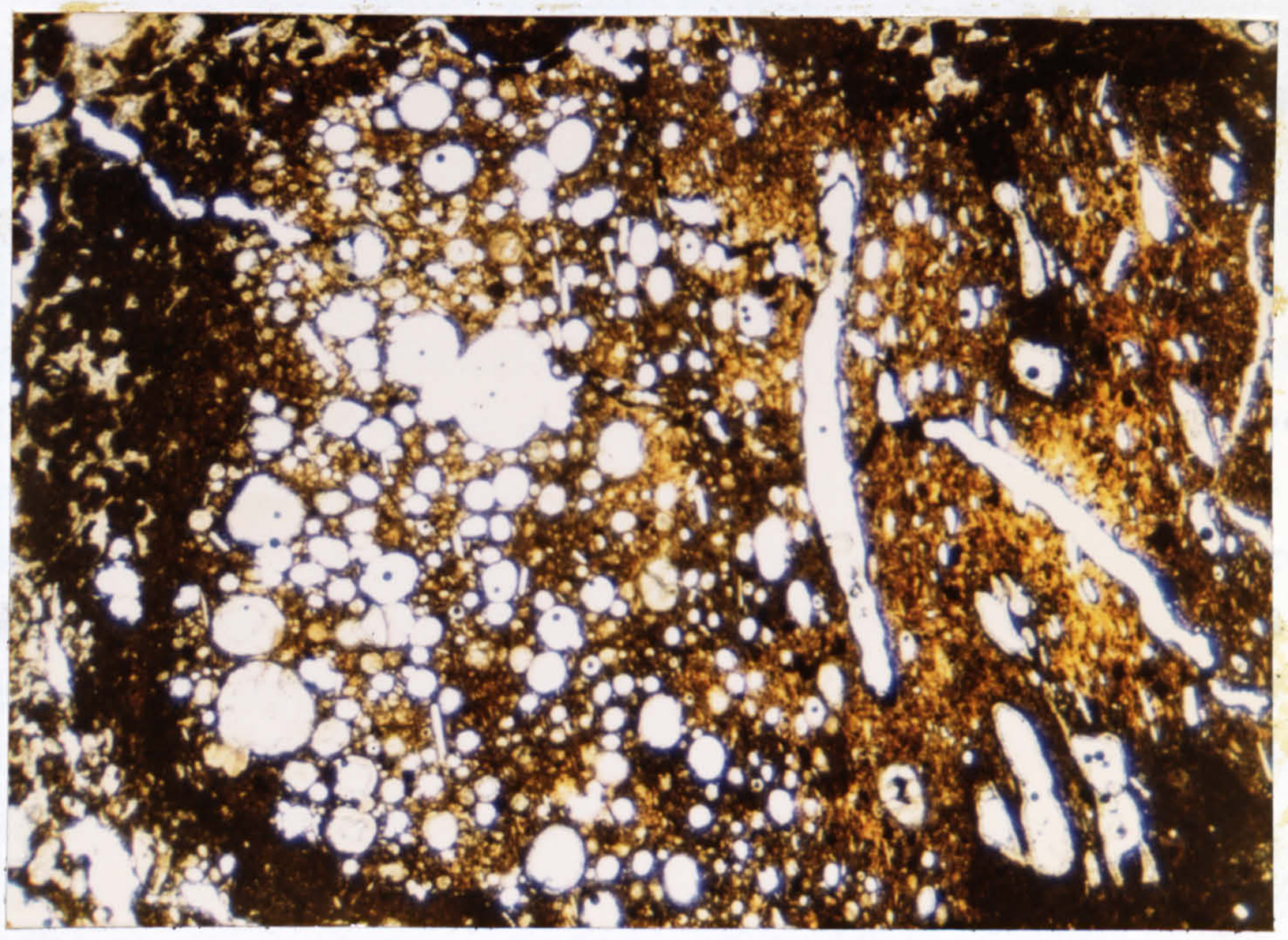

Fig. 3.19 Altered sideromelane lapillus containing spherical vesicles and aligned, stretched vesicles due to viscous flow. Plane polarised light. x4.

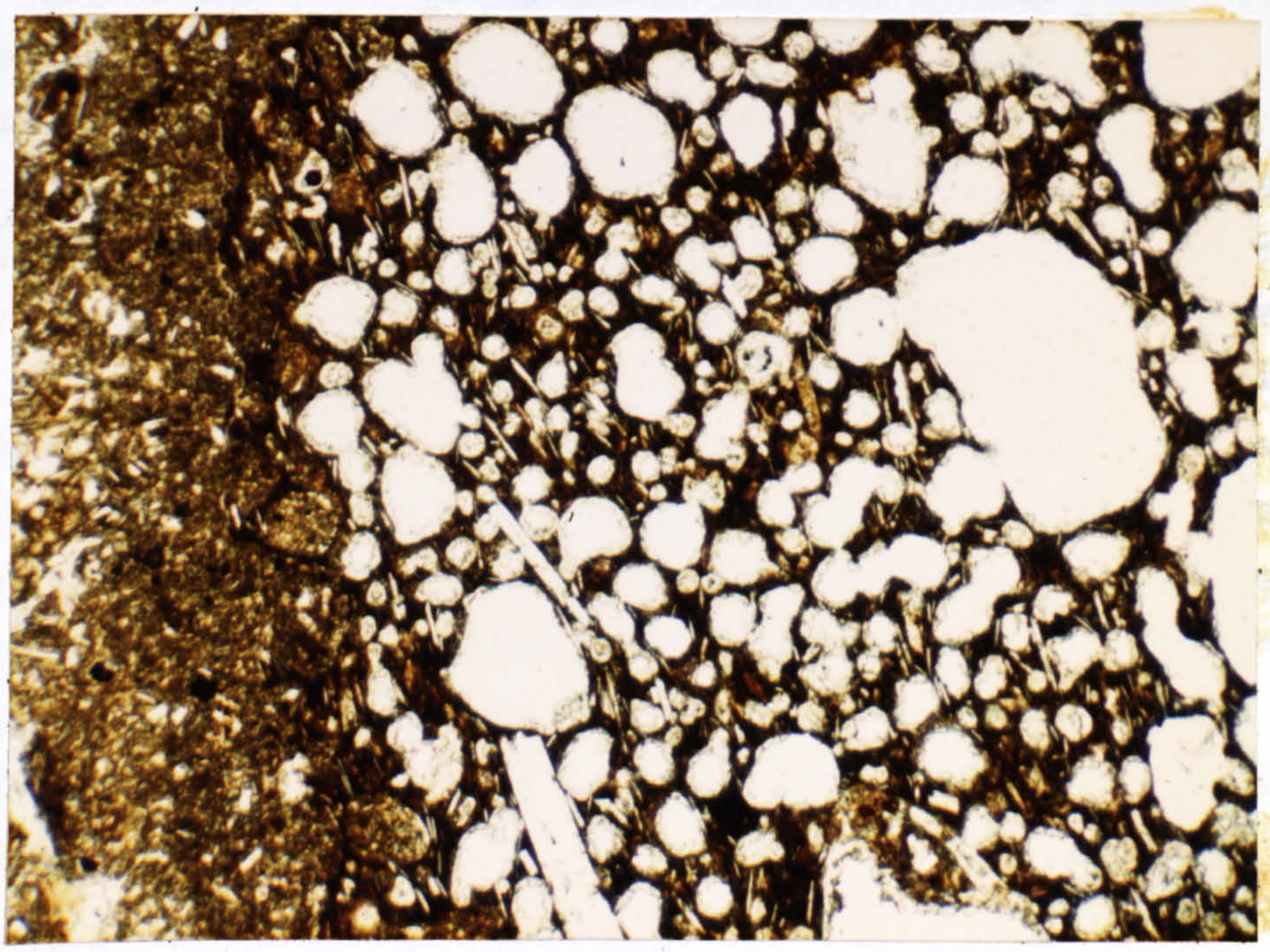

Fig. 3.20 Tachylitic scoria lapillus from Unit E. Note high proportion of vesicles, many of which are lined with zeolite fringes. Note also flow aligned microlites and the highly irregular margins of the lapillus. Plane polarised light. x10.

Units A and D have average maximum vesicle radii of 0·1-0·2mm whereas Units B and E contain sideromelane with vesicles of 0·3-0·8mm average maximum radius. This indicates that, all other factors remaining constant, the magma was quenched at greater depths during the eruption of Units A and D. Estimates of magma quench depth can be made assuming ascent rates of 5cm s^{-1}, H_2O content of 1·0wt.% and other parameters equal to Sparks' (1978, Fig. 8e) values. Such estimates indicate that Units A and D were formed by quenching of magma at 150-200m depth whereas quenching of Units B and E magma occurred at depths of about 100m. These estimates are useful only in comparing the relative depths of magma quenching. Quantitative results could only be obtained if average maximum vesicle radii were accurately obtained from large numbers of specimens. They would also depend on knowing the values for magma parameters such as ascent rate, water content, solubility constant and diffusion coefficient (Sparks, op.cit.).

Unit C is too fine-grained to allow many vesicle measurements but the few larger lapilli have vesicle sizes similar to Units A and D, indicating that quenching occurred at moderate depths. This result may be misleading however, since the extreme granulation of Unit C tephra would completely destroy all traces of larger vesicles.

If one assumes that the scoriaceous bombs in Units B and E cooled at or near the surface by contact with air then their maximum vesicle radii help to indicate the likely values of the various magma parameters. Values of 5mm average maximum radius are obtained indicating that magma conditions probably conformed closely to those of basalt with 1·0wt.% water in Fig. 8e of Sparks (op.cit.).

d) Fines

Similar to Saefell (Chapter 2) the Medano tuffs contain high proportions of fine ash (Table 3.2). Units B, C and E contain the highest fines content, which in most samples occurs largely in rims round larger grains. Units A and D contain less fines and these occur partly in thin accretionary rims and partly in the pore spaces between

TABLE 3.2 MODAL ANALYSES OF MEDANO TUFFS

Sample number	CLT5	6	7	10	11	14	15	16	21	22	23	25
Vesicular sideromelane	24·6	33·6	28·9	35·9	25·6	40·7	0·7	51·2	36·6	37·3	37·7	6·9
Non-vesicular sideromelane	3·4	7·5	11·0	5·9	8·8	9·1	0·4	2·2	4·4	5·6	5·7	29·4
Matrix	52·2	58·0	35·3	52·8	26·2	20·2	65·5	31·9	35·7	20·0	31·2	58·6
Crystals	0	0	0·2	-	0·4	0	2·6	0	0·2	1·0	0	0
Lithics	0	0·5	2·2	4·7	16·8	1·6	17·6	4·3	2·9	6·3	1·6	0
Tachylite	0·8	0	3·8	0	2·5	1·0	0·8	0·7	6·8	7·2	4·0	4·0
Opaques	0	0·1	1·7	0·1	0·4	5·4	0·7	1·9	0·3	0	0·6	0·1
Zeolite	16·8	0	16·6	0	18·3	19·8	1·0	6·6	12·8	20·2	15·3	0·8
Calcite	1·9	0	0	0	0·5	2·1	10·6	0·9	0·2	1·7	3·9	0
% Palagonite in rock	23·5	0·5	29·4	2·4	20·5	24·8	2·3	23·6	16·3	37·4	30·2	1·8

large clasts. The rims are identical to the Saefell examples (Section 2.6.1d) and reach 3mm thickness. Only in Unit C are the accretionary lapilli more like the type described by Moore & Peck (1962). Here, the rims are composed of fine ash (<0·02mm) which is faintly concentrically layered round larger nuclei (Fig. 3.21) but is poorly graded. The accretionary lapilli in the surge deposits of Section 1 (SSW of the crater) have slightly finer, better sorted rims than those of Section 2. This is thought to indicate that the Section 1 lapilli grew in a less moisture-rich eruption column or surge. Both lapilli types probably grew rapidly in the lower parts of the eruption column since their rims are poorly sorted.

The lack of well developed accretionary rims in Unit A and D tuffs probably indicates that they were deposited rapidly from low eruption columns. Fines in the column would be deposited at greater distances from the vent unless they were captured by accretion. In such proximal deposits this process did not have sufficient time to become established.

e) Crystal and lithic fragments

The main crystal phases occur either as megacrysts in juvenile lapilli or as loose crystals in the tuffs. These crystals are (in order of abundance) plagioclase, magnetite, clinopyroxene, olivine and biotite. Optically the plagioclase is labradorite-andesine (An_{46} -An_{58}) and this is confirmed by microprobe analyses of some microlites and loose crystals (Table 3.3). Analysis of the opaques indicates they are titano-magnetite (Table 3.3). Often plagioclase and magnetite form the only crystalline phases in the juvenile glass.

The clinopyroxene is purplish titanaugite and is found only as broken crystals in the tuffs or as a common phenocryst phase in non-vesicular basalt lithic clasts. Olivine, which has a composition Fo_{80} -Fo_{84} (determined optically), is likewise not found in association with juvenile glass. This does not imply, however, that these minerals are not of juvenile origin. If the pyroxene and olivine crystallised before magma quenching occurred it is

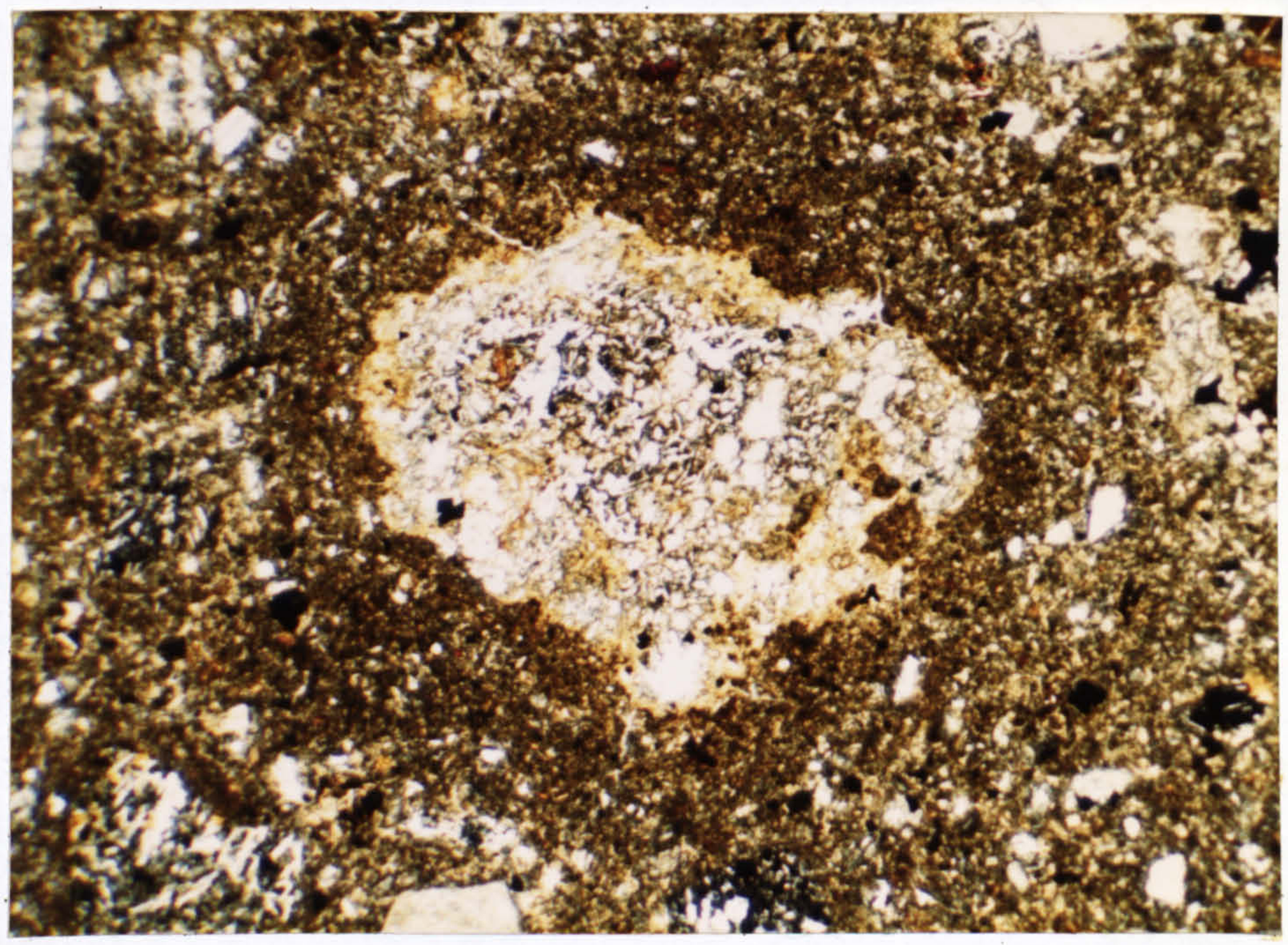

Fig. 3.21 Accretionary lapillus from Unit C Section (1) tuffs. Note the faint concentric layering in the accretionary rims and the high fines content of the tuff. Plane polarised light. x10.

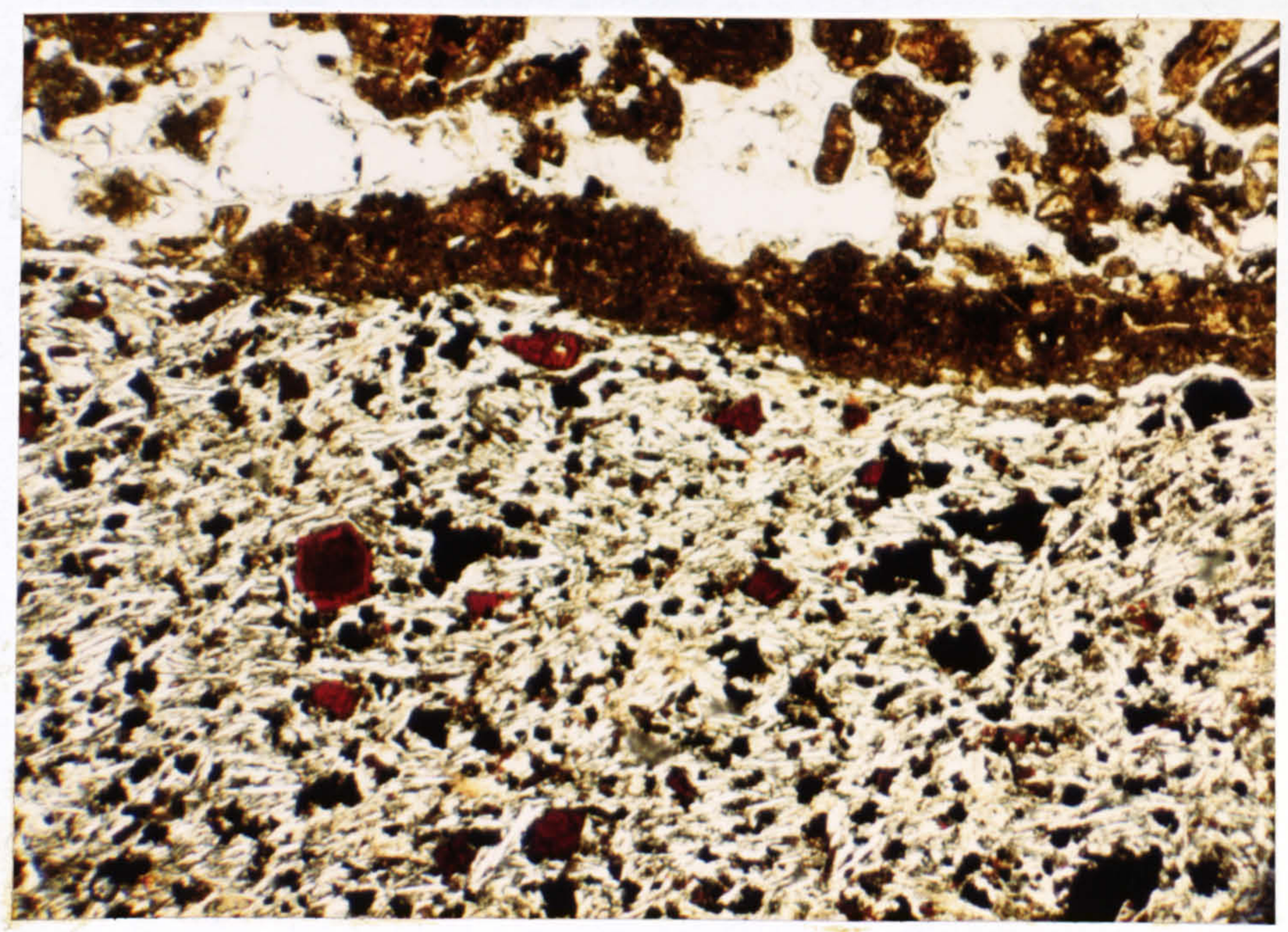

Fig. 3.22 Common basaltic lithic fragment in Medano tuffs consisting of clusters of augite and magnetite surrounded by flow-aligned laths of plagioclase. Reddish-brown hematite replaced crystals are common throughout the rock. Plane polarised light. x10.

TABLE 3.3 BASALT AND MINERAL ANALYSES

	(1)	(2)	(3)	(4)	(5)	(6)
SiO_2	49·8	49·5	53·1	51·8	0·48	0·46
TiO_2	2·12	2·22	0·09	0·19	14·4	14·2
Al_2O_3	17·0	16·9	27·3	27·1	4·56	4·71
Fe_2O_3	8·97	9·52	-	-	-	-
Feo	-	-	0·63	0·81	71·5	71·3
MnO	0·22	0·22	-	0·11	0·75	0·64
MgO	2·90	3·02	-	-	4·96	5·44
CaO	6·68	6·77	10·6	10·9	-	-
Na_2O	5·07	5·30	4·21	4·78	-	0·37
K_2O	2·49	2·50	0·35	0·37	-	-
P_2O_5	1·15	1·16	-	0·07	-	-
Total	96·40	97·11	96·28	96·13	96·65	97·12

(1) XRF analysis of scoriaceous bomb 15m above base of Unit E.

(2) XRF analysis of scoriaceous bomb within reworked crater tuffs.

All subsequent analyses are by electron microprobe :-

(3) Plagioclase microlite from CLT14 (reworked crater tuff).

(4) Plagioclase microlite from CLT14.

(5) Titaniferous magnetite from CLT21 (Unit B tuffs).

(6) Titaniferous magnetite from CLT21.

Total Fe as Fe_2O_3 in XRF analyses, as FeO in microprobe analyses.

quite likely that explosive granulation would break any glass surrounding them.

The biotite occurs as laths up to 2mm long in the tuffs and as smaller crystals in juvenile glass. Due to the lack of closely associated minerals little can be said about the crystallisation history of the magma. Magnetite probably crystallised first, followed by clinopyroxene, olivine, plagioclase and biotite (not in order) and lastly microlite plagioclase.

The lithic fragments are of many types, mostly derived from basaltic extrusive and intrusive bodies in the country rocks beneath the volcano. Augite and plagioclase-phyric as well as medium-grained aphyric basalt types occur. A common lithic type consists of glomeroporphyritic augite and magnetite with groundmass plagioclase and variable amounts of haematite crystals (Fig. 3.22). Analcite and calcite occur in veins or as vesicle infills.

Equigranular, coarse-grained syenite fragments occur, especially in Units A and D. Their mineralogy consists of orthoclase, oligoclase, nepheline, biotite and sphene. These blocks are considered to represent samples of the plutonic basement underlying the Tenerife volcanic pile (Fuster et al., 1968). Sedimentary clasts are rare and include limestone fragments with peloid and bryozoan structures.

f) Composition of the tuffs

Point count analyses of the tuffs (Fig. 3.23, Table 3.2) indicate that their composition is highly variable. The main points of note are :-

i) Extreme fines content of CLT 15 (Unit C surge deposit)

ii) Low lithic content of the Unit E samples

iii) Variable alteration of all samples.

The moderate lithic content of Units A and D is because most of the lithics are of lapilli grade or larger and cannot be counted in this section. Outcrop scale point counts indicate that both units contain 10-15% lithic clasts, most of which are thought to be of accessory origin.

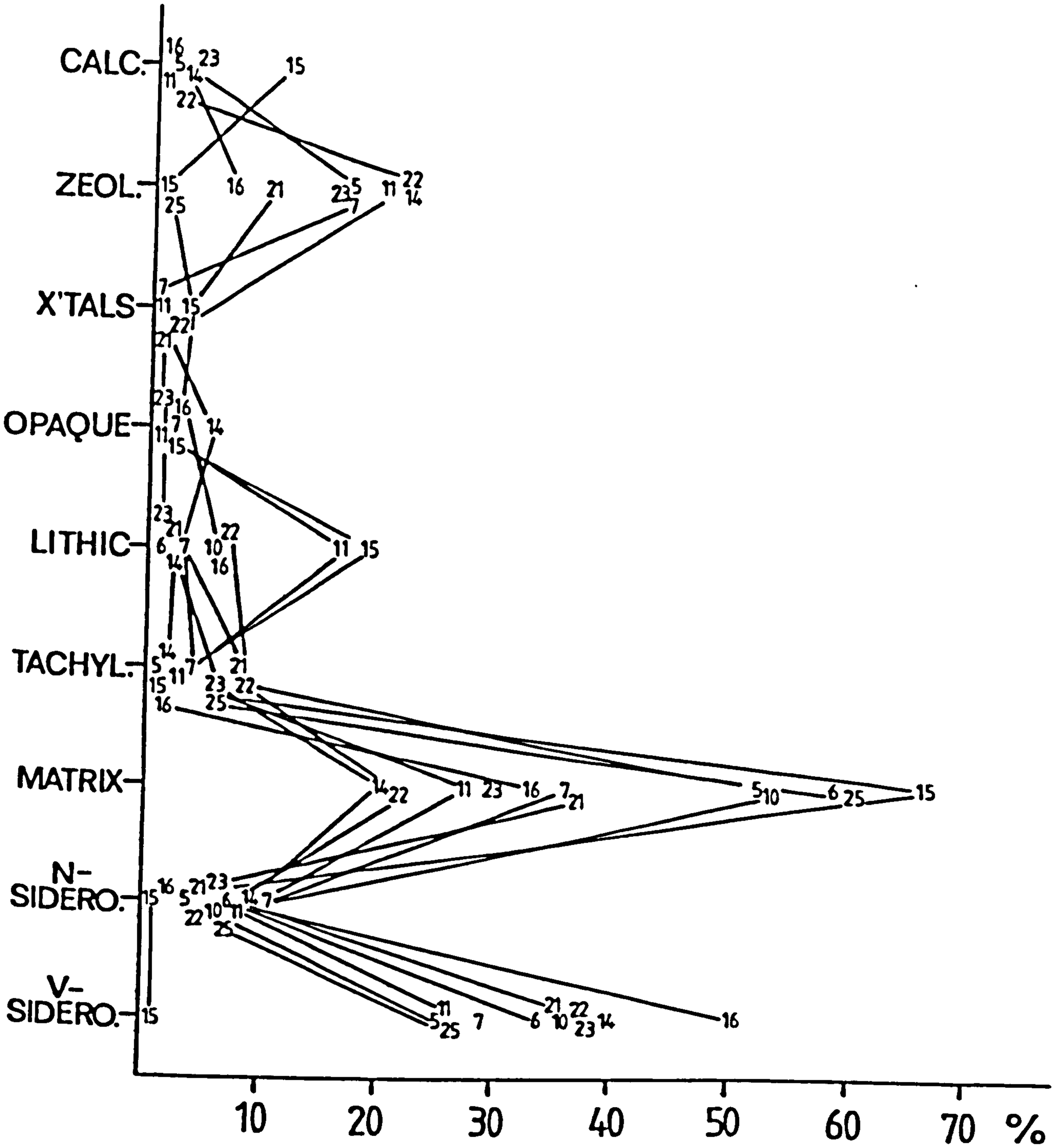

Fig. 3.23 Point count modal analyses of Medano tuffs.
N: non-vesicular, V: vesicular sideromelane

3.6.2 Grain size and morphology

a) Grain size studies

Thin section grain size values were obtained using point count methods as in Section 2.6.2. The altered matrix of some samples (CLT 11, 16, 23) made accurate determination of their fines content impossible and precluded measurements on more altered examples (Table 3.4).

On a Mdϕ/$\sigma\phi$ plot (Fig. 3.24a) the bulk of the samples are more poorly sorted than most surtseyan examples. This is thought to be due to their proximity to the vent and to the early fallout of fines by incorporation into accretionary lapilli. The Unit C samples (3 & 15) are strongly fine-skewed and moderately well-sorted, a characteristic base-surge feature (Crowe & Fisher, 1973).

When the samples are superimposed on Walker's (1971) plot (Fig. 3.24b) for differentiating mode of deposition, most of them plot within the flow field. The only samples which plot inside the field of fallout are the Unit C surge deposits. This diagram is not designed for use with surtseyan deposits and the moderate-to-low degree of sorting in these tuffs as a whole prevents using $\sigma\phi$ as a discriminant of transport mechanism. Most base-surge deposits plot in the overlap area between flow and fallout fields (Walker op.cit.) and the Unit C samples are thought to represent finer-grained deposits of this type.

The use of a C-M diagram (Sheridan, 1971) to discriminate between the tuffs is more instructive. Many of the samples cluster just above the field of dominant airfall modes (Fig. 3.24c). Their slightly coarser C values are probably due to their proximal location to the vent. Also, these samples generally have altered and replaced matrix material which could not be measured, thus making them less fine-skewed than the rest of the tuffs. The coarse fraction was estimated from photographs (Appendix 1) and was unaffected by alteration.

All the Unit E tuffs (Samples 6, 10, 25) plot within the rhyolitic ash flow field, towards the coarse C side. The reason for this is unknown, and may be because the deposits are generally fine-grained but contain sufficient

TABLE 3.4 THIN SECTION GRAIN SIZE ANALYSES

Sample number	CLT3	6	10	11	15	16	21	22	23	25
+6ø	52	33	28	16	54	22	19	14	18	29
+5	16	13	13	9	18	15	16	6	10	13
+4	7	5	3	7	5	5	3	5	4	4
+3	5	6	1	4	2	2	2	3	1	2
+2	6	9	6	7	7	4	6	6	6	10
+1	5	9	6	10	7	2	6	7	7	9
0	5	9	6	11	3	5	19	13	10	13
-1	2	5	15	12	4	12	18	22	18	7
-2*	0	0	16	11	-	6	4	5	12	5
-3	2	9	4	8	-	10	0	5	8	6
-4	-	2	2	5	-	12	1	4	6	2
-5	-	-	-	-	-	5	5	-	-	-

* Grain sizes coarser than -2ø (4mm) measured from slabs of tuff samples

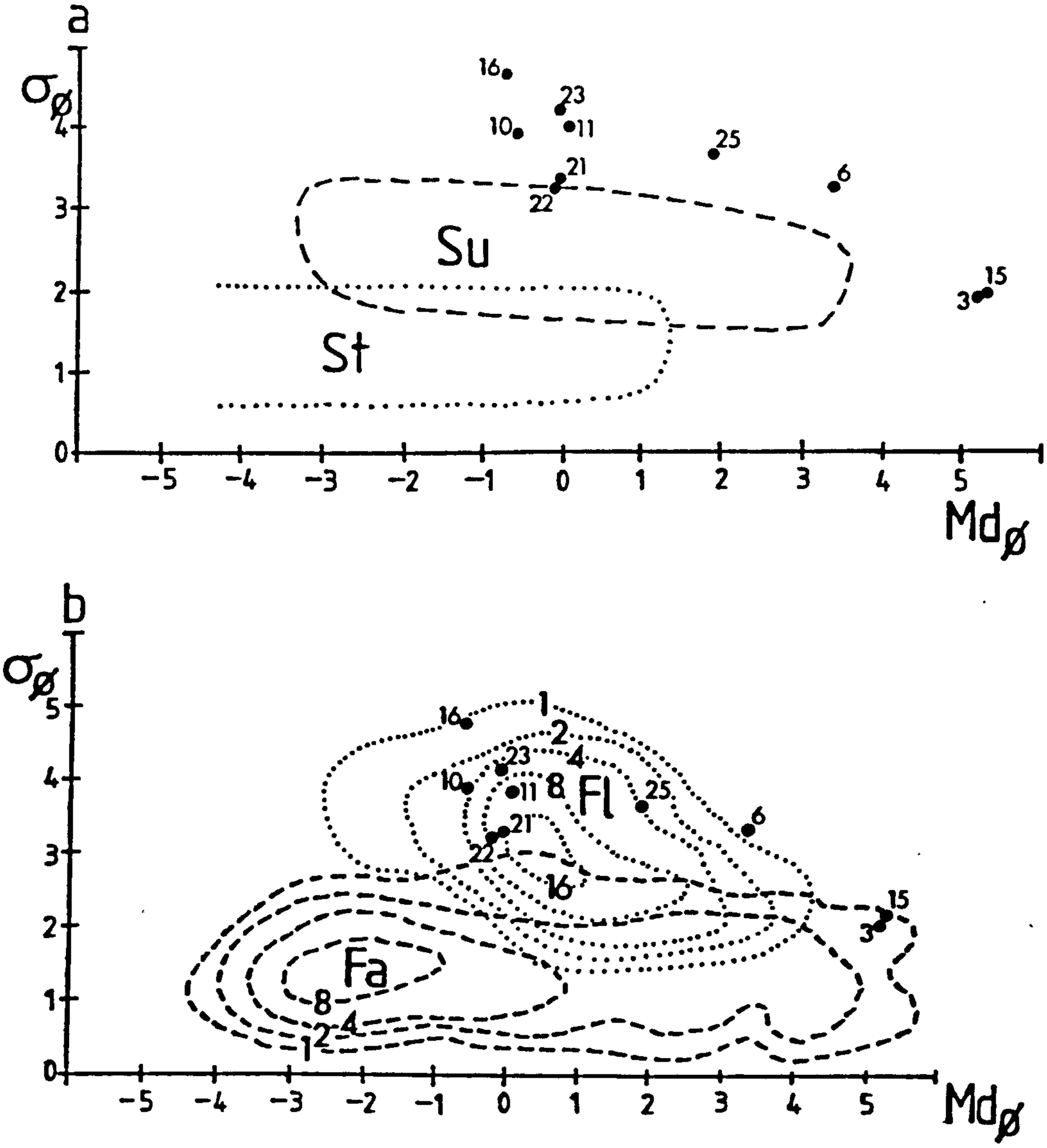

Fig. 3.24 Grain size plots of Medano tuffs. See text for description.

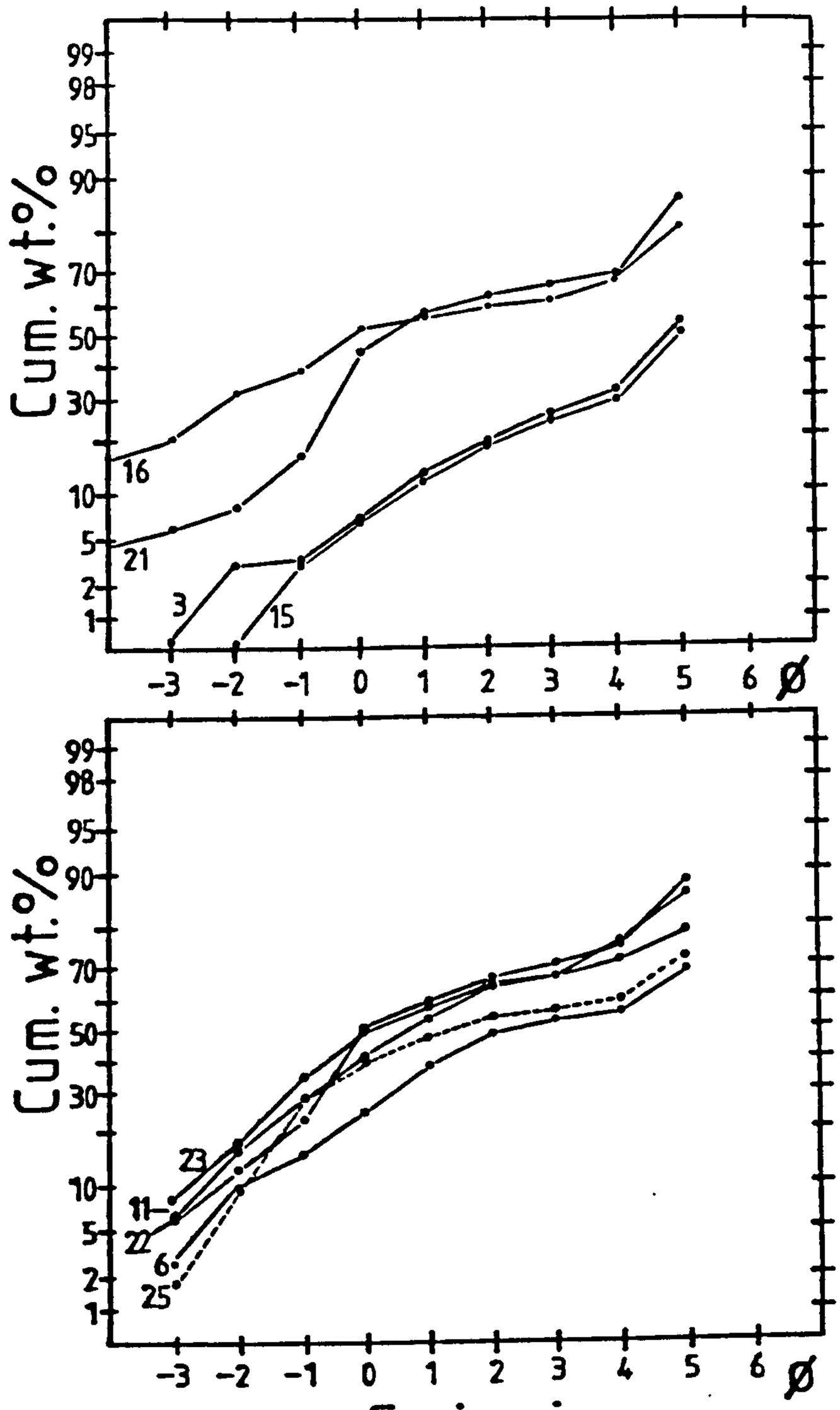

Fig. 3.25 Cumulative frequency curves of the Medano tuffs.

coarse material to give coarser C values. The Unit C deposits have very fine Mdø values which cause them to plot outside all Sheridan's fields.

Composite grain size frequency distributions (Fig. 3.25) indicate that most of the tuffs are similar to those of Surtsey (Sheridan, 1971). The exceptions to this are sample 16 (Unit A) and the Unit C tuffs. Unit A has a high coarse percentage and is very poorly sorted, almost bimodal. The sample is a coarse airfall deposit with its high fine content probably due to en masse fallout of moist ash from a low eruption column. The Unit C curves are the same shape as the other samples but are better sorted and much more fine-skewed. Surges carry the fine proportion of the erupted tephra away from the vent, turbulence within the surge sorting the material. The sorting values are very similar to proximal Surtsey deposits (Sheridan, op.cit.). With increasing distance from the vent surges sort material much better than airfall deposits (Crowe & Fisher, 1973).

The Medano samples plot largely outside, or are undifferentiated by most of the published plots. This is thought to reflect the lack of work done on tuff-ring deposits, whose tuffs are of mixed airfall and surge origin. The low dispersal of their products (Walker, 1973) and their fines-enriched nature are additional characteristics which add to the complexity of simple grain size discriminant plots.

b) Morphology of tephra

<u>SEM studies</u>

The Medano ash is typically blocky with fractured grain surfaces and moderate numbers of smooth-walled vesicles (Fig. 3.26a). The juvenile tephra is identical to Saefell, with ribbed impact fracture pits and etched surfaces. Spherical vesicle infilling structures are also present and are commonly cracked. These cracks resemble shrinkage cracks and may represent drying out of hydrous zeolite or palagonite (Fig. 3.26b).

Most grains are covered by fine ash and authigenic mineral growths, which obscure surface textures. Commonly

Fig. 3.26 a) SEM photograph of ash fragment with stretched smooth-walled vesicles. x400.

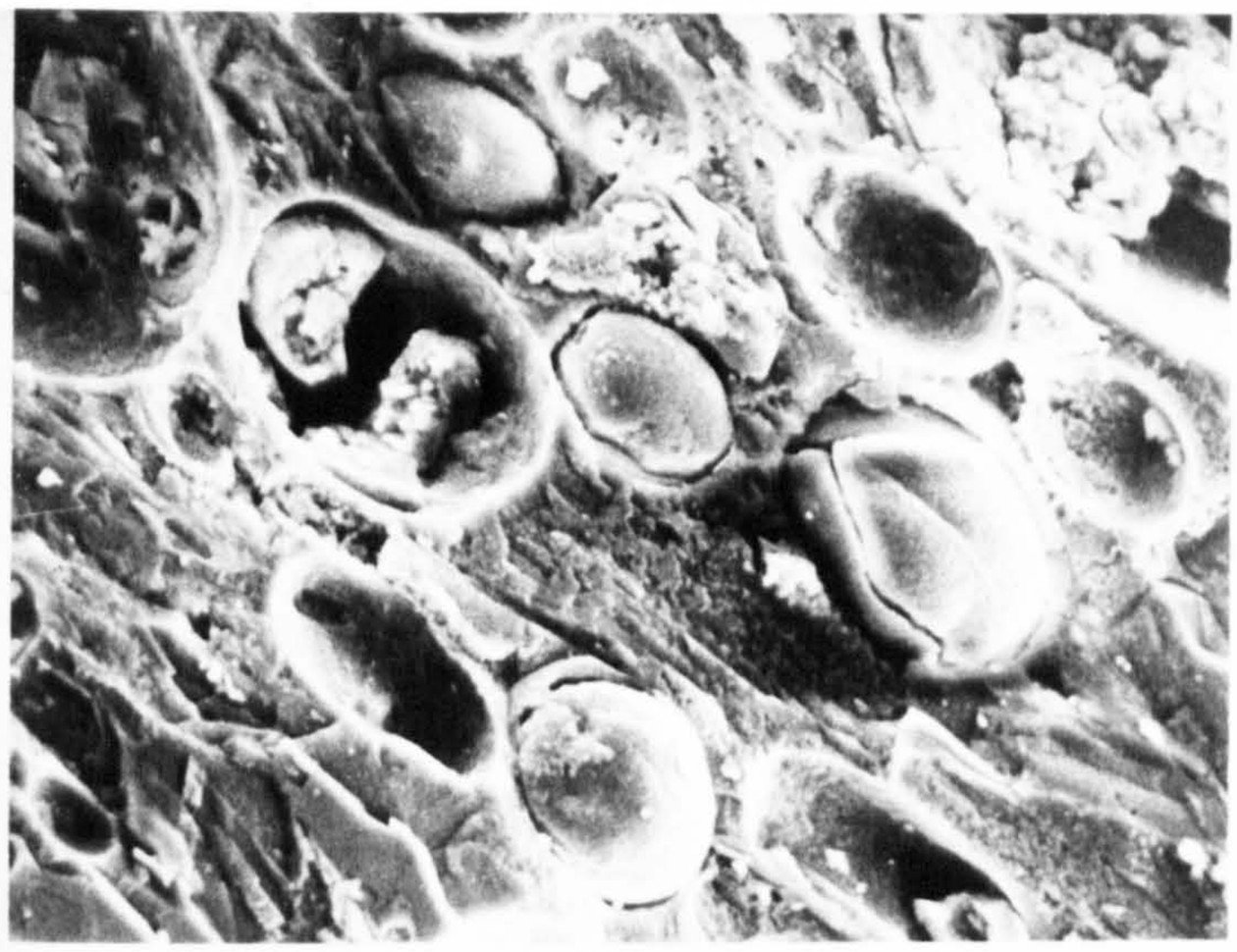

Fig. 3.26 b) SEM photograph of spherical vesicle infilling material. Cracks may be due to drying of hydrous zeolite minerals. x400.

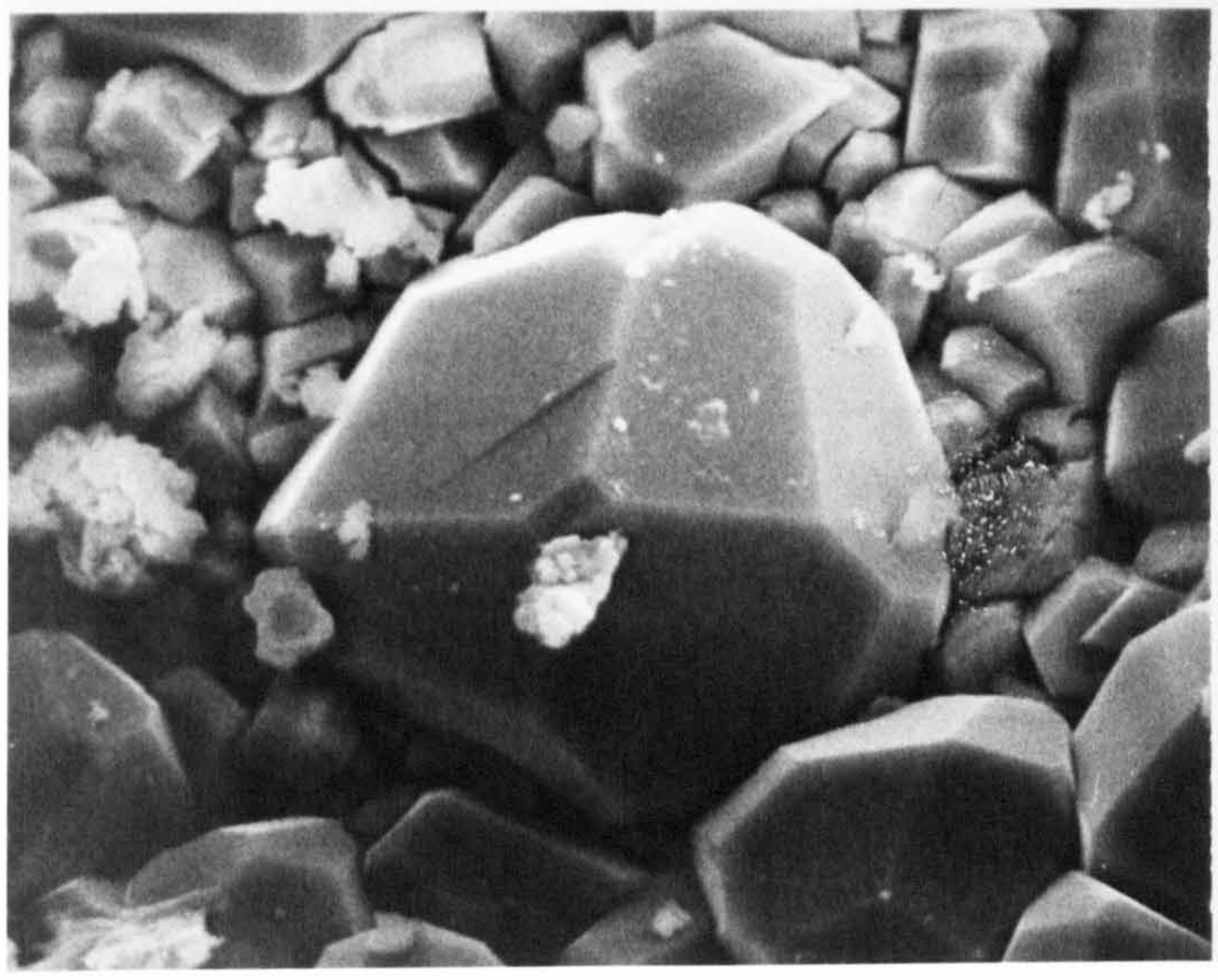

Fig. 3.26 c) SEM photograph of icositetrahedral analcite found as pore infilling in Medano tuffs. Free growth into these pores allowed well-formed crystals to develop. x1000.

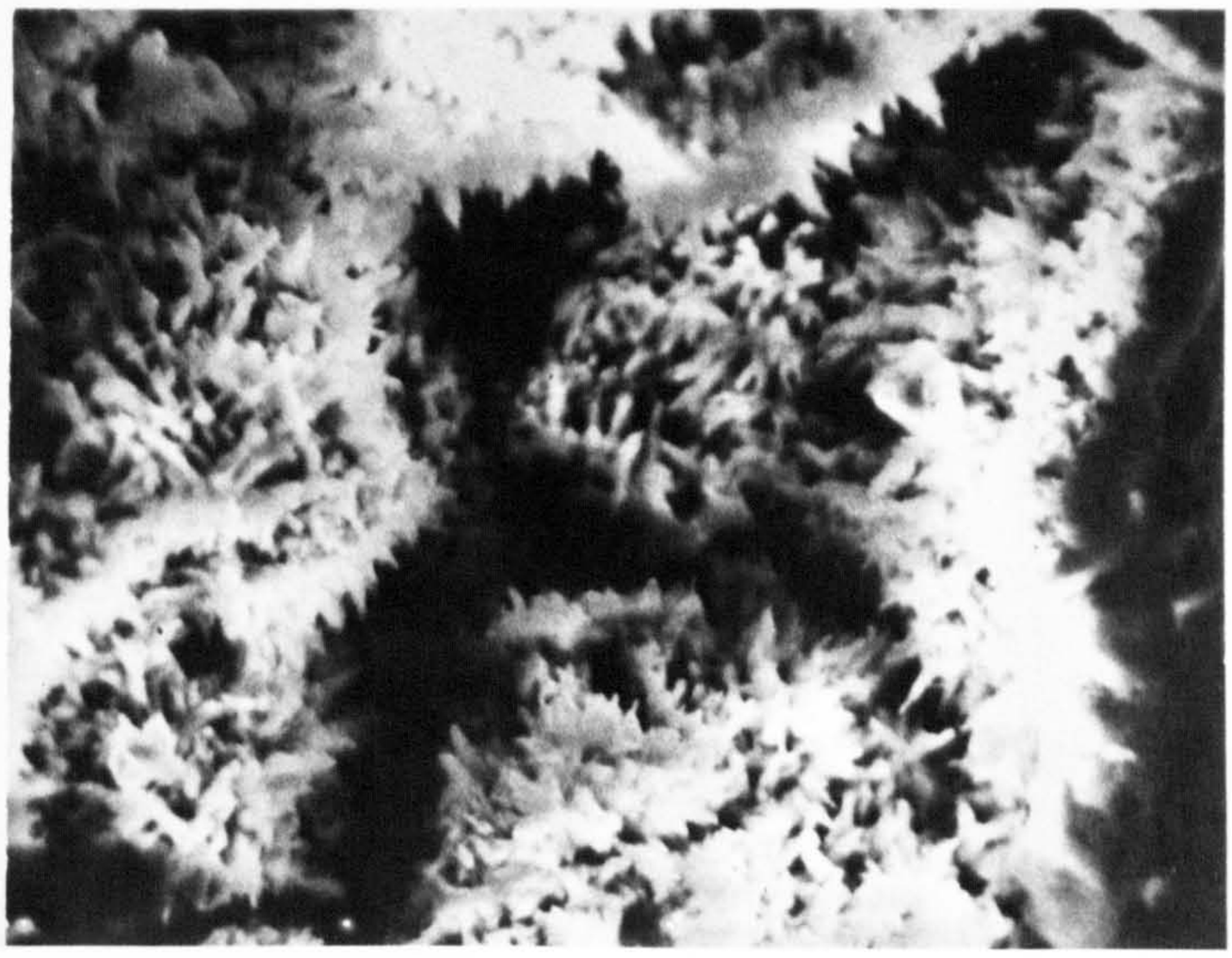

Fig. 3.26 d) SEM photograph of fibrous radiating zeolite found as fringes round altered grains. x600.

the authigenic minerals are fine-grained, amorphous and not easily identified. Occasionally however, the minerals are well formed and can be recognised from their form and by the use of energy dispersive semi-quantitative analyses.

Fig. 3.26(c,d) shows some of the typical authigenic minerals which occur within vesicles and pore spaces. Analcite, in icositetrahedral and acicular forms, has been recognised. Microprobe and EDS analyses in the SEM mode indicate that the analcite has a minor calcium and a significant potassium content (Section 3.6.3b).

SEM studies indicate that the tuffs have variable porosities due to variable amounts of matrix and the proportion of authigenic minerals. The permeability, which is also dependant on the above factors, is rapidly reduced in even slightly altered tuffs by authigenic bridging between matrix grains which are the first to be altered.

Quantitative grain morphology

PVC measurements on the Medano tephra were complicated by the alteration of much of the glass fragments. Palagonitization and corrosion of the grain margins by later cementing material made it impossible to measure many of the samples. The alteration is most marked in the older samples and thus only Units D and E were used in the analyses.

The PVC plots (Fig. 3.27a) show that most grains have low P values and only 17% plot above the P 20% line. This indicates that the majority of the Unit E tephra was derived by explosive fragmentation of the magma due to volatile exsolution. The Unit D samples are all altered and thus only 10grains were measured. It is not thought to be statistically meaningful to draw any conclusions from the Unit D PVC results in which 80% of the grains plot below the 20% line.

The data for three primary and one partly reworked Unit E samples agree with the petrographic information in suggesting that this unit was formed by eruptions of intermediate surtseyan-strombolian character. The eruptions were not wholly strombolian in type, since scoria tends to plot along the P 0% line on the ternary PVC

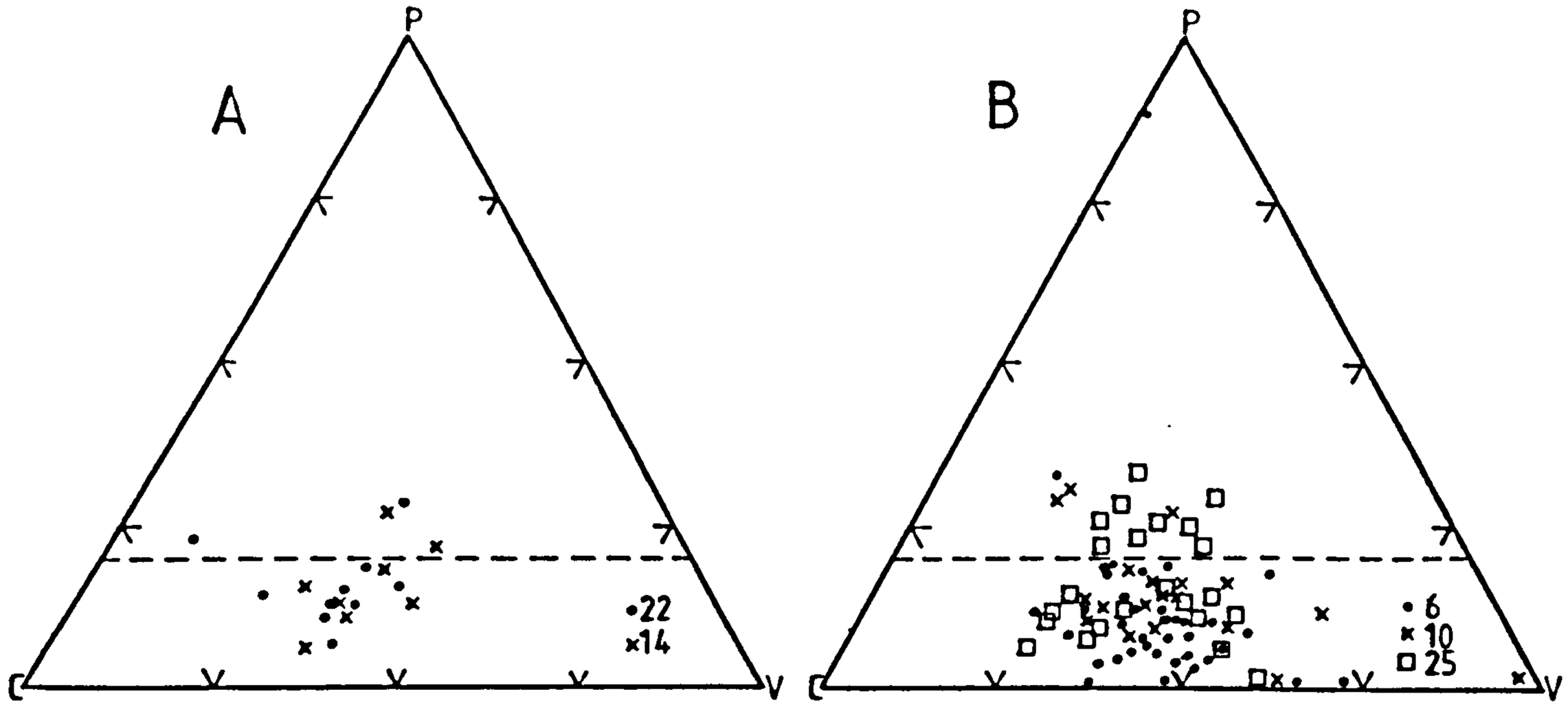

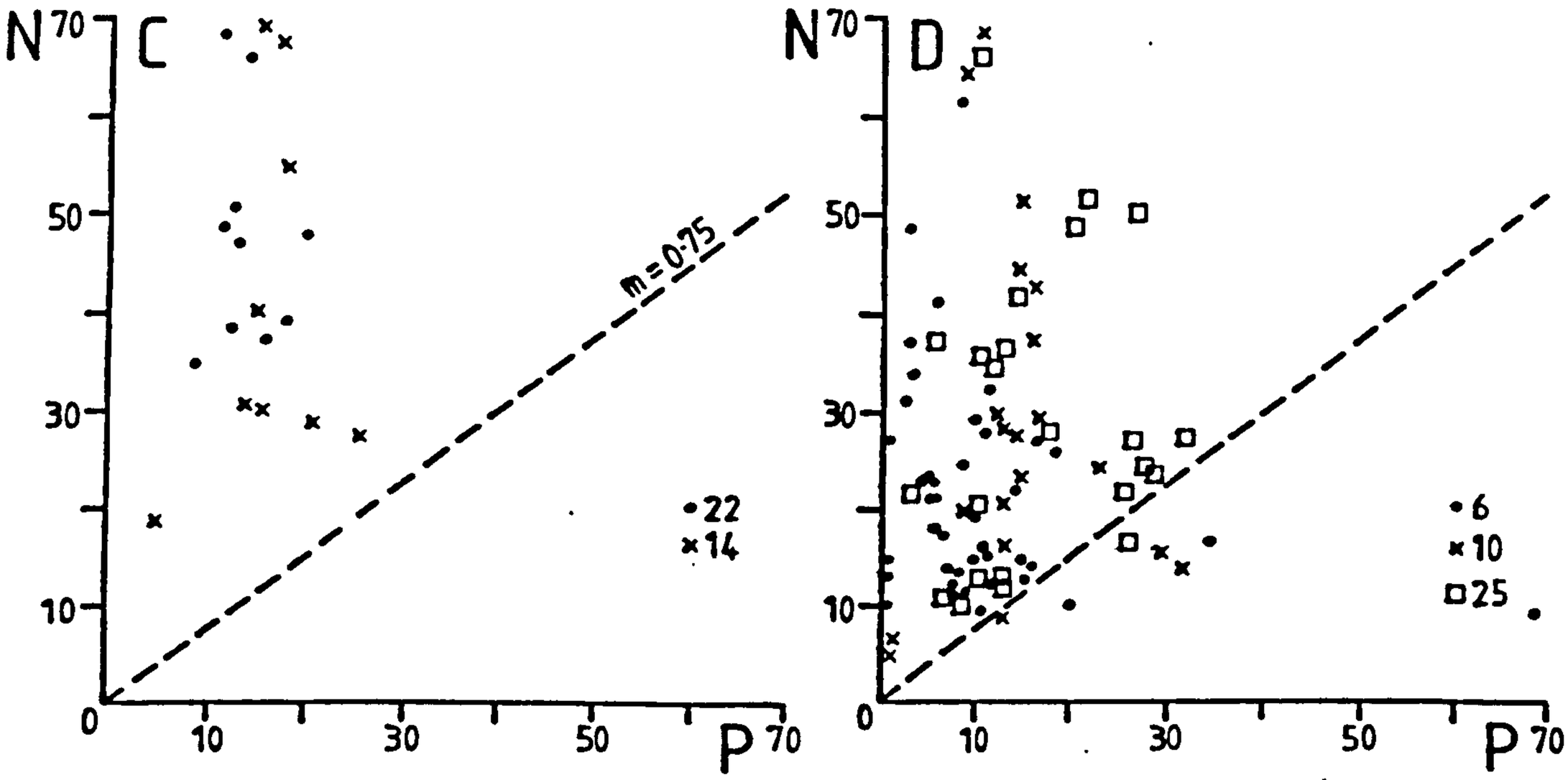

Fig. 3.27 PVC and P vs N plots for the Medano tuffs. See Chapter 2 for definitions of graph co-ordinates.

diagram (Honnorez & Kirst, 1975). The magma was therefore freely vesiculating at a high level when it came into contact with moderate amounts of probably surface-derived water and explosively erupted. The PVC plots of the Unit E tephra closely resemble those of Capelinhos and Surtsey (Honnorez & Kirst, op.cit.) when these volcanoes were well-established and water had restricted access to their vents.

The P vs N plots (Fig. 3.27b) support the above conclusions with over 90% of the samples plotting above the line with slope 0·75. On this diagram the Unit D tephra plot well within the hyalotuff field, perhaps indicating that they were derived by explosive quenching of vesiculating magma. The lack of samples in the hyaloclastic field, however, is in part due to the small number of fine ash grains measured. In all the Medano tuffs these grains are generally altered and could not be measured. This, and the lack of results from Units A, B, C and D means that comparisons with Saefell are difficult to make. In general the final stages of the Medano activity were more strombolian than any of the Saefell eruptions.

PVC and SEM studies indicate that deposits thought to be formed by eruptions transitional in character between strombolian and surtseyan consist of purely mechanical mixtures of both end member clasts. All lapilli studied are either strombolian scoria or phreatomagmatic tephra with no juvenile material of intermediate morphology. This agrees with studies of ejecta from mixed or transitional strombolian-phreatomagmatic activity (Francis & Thorpe, 1974; Self et al.,1980). The amount of water interacting with the magma determines the eruption characteristics and the proportions of strombolian and phreatomagmatic ejecta. It is probable therefore that in intermediate strombolian-phreatomagmatic eruptions all the available water is used up in reacting with some of the magma, chilling it completely. The remainder of the magma is not chilled and erupts as strombolian scoria.

3.6.3 Alteration of tuffs

a) Sequence of alteration

All the Medano tuffs are altered to some extent, the older tuffs generally more than the younger. The first noticable alteration occurs in the tuff matrix which becomes turbid whilst some grains alter to palagonite. In this initial stage isolated altered ash grains are sparsely scattered through the matrix whereas the rest of the ash appears completely fresh. Altered fragments are randomly distributed and their development must result from minute differences in the permeability of the tuffs around them and the micro-chemistry, pH and Eh of the solutions permeating through the tuffs at that point.

Progressive alteration continues with the development of palagonite rinds on larger lapilli and growth of authigenic minerals. Initial palagonite is orange-yellow, amorphous and isotropic and forms rinds of variable thickness (up to 0·2mm). Most of Unit E is presently at this stage of alteration except for one sample (CLT 7) which is highly altered and another whose matrix has been partly altered to clay.

The most extreme form of alteration consists of deep orange palagonite which forms rinds up to 0·6mm thick on larger lapilli and totally replaces smaller fragments. Rinds round grain margins tend to be structureless and isotropic to weakly birefringent, though the strong colour masks this. Rims of palagonite around vesicles consist of birefringent radiating fibres of length-fast material.

Authigenic mineral growth increases with increasing alteration (Fig. 3.28) in the bulk tuff as well as in individual vesicles. Movement of the solutions which precipitate the zeolites through the tuffs means that palagonite is more abundant in most samples. However, in one sample (CLT 5) of lacustrine tuff the zeolite minerals are slightly more abundant than the palagonite. This is thought to indicate that slightly alkaline lake waters directly precipitated additional zeolites and carbonate minerals in the tuffs (Hay, 1966). The sample studied may however have been a preferred precipitation site for

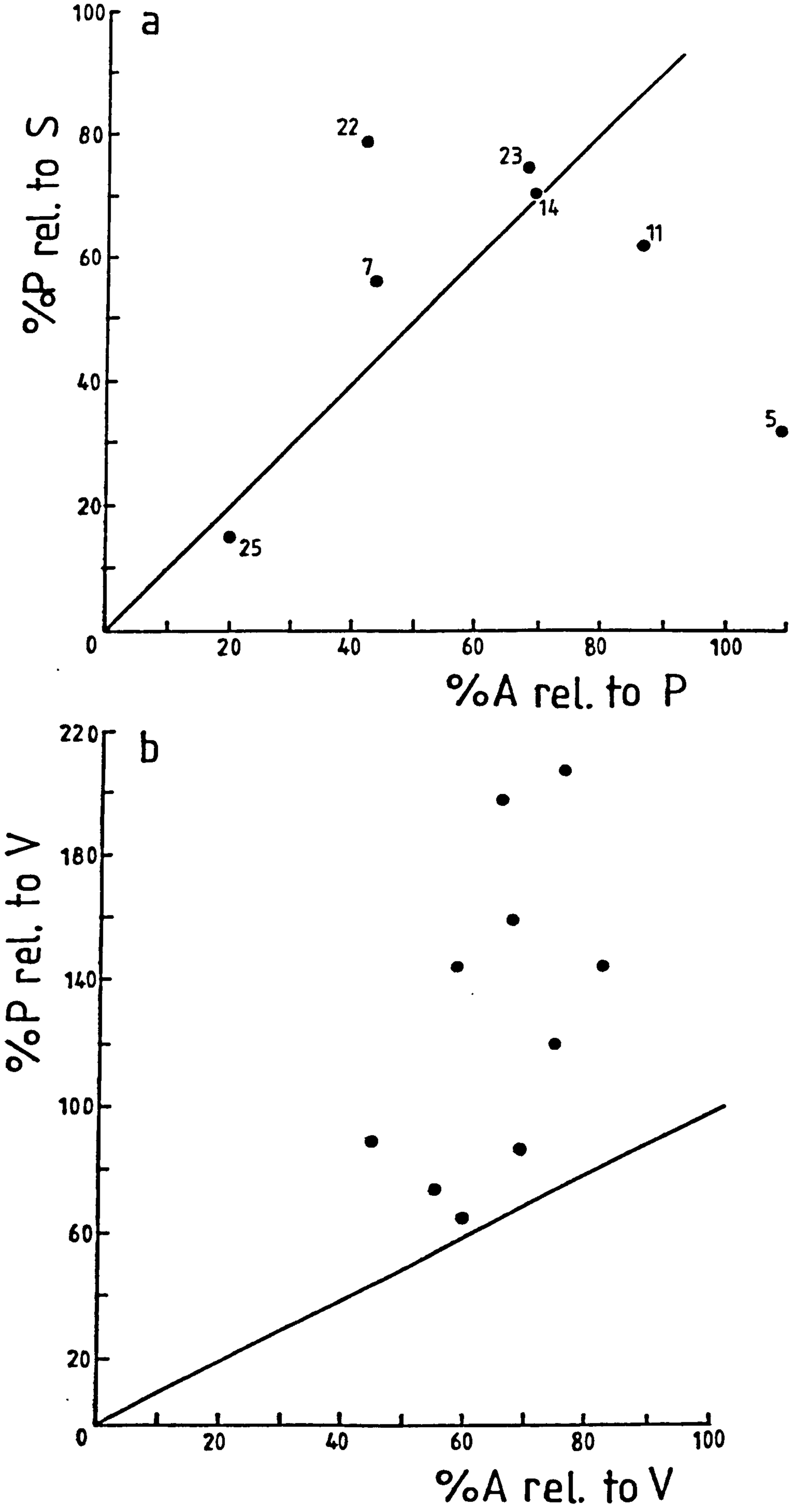

Fig. 3.28 Graphs of %A (authigenic material) vs %P (palagonite) relative to the volume of S (sideromelane) and V (vesicles) respectively.

palagonitization-derived zeolites from other areas of the tuffs.

The authigenic minerals in the tuffs are analcite, calcite and rare phosphatic material. In all cases the analcite formed first with calcite later filling up pores and vesicles. The analcite is white and massive or slightly fibrous in hand specimen. In thin section it is colourless, isotropic and has a blocky earlier form which is fringed with fibrous needles (Fig. 3.29). Analyses of the analcite indicate it is potassium bearing (Table 3.5) but both blocky and fibrous forms have similar compositions. The calcite is less abundant and formed after the analcite. Often, where an altered ash grain has zeolite in the vesicles within the palagonite rind, the fresh glass has calcite filled vesicles. This indicates that analcite was derived from the palagonitization process and precipitated close to the altered glass.

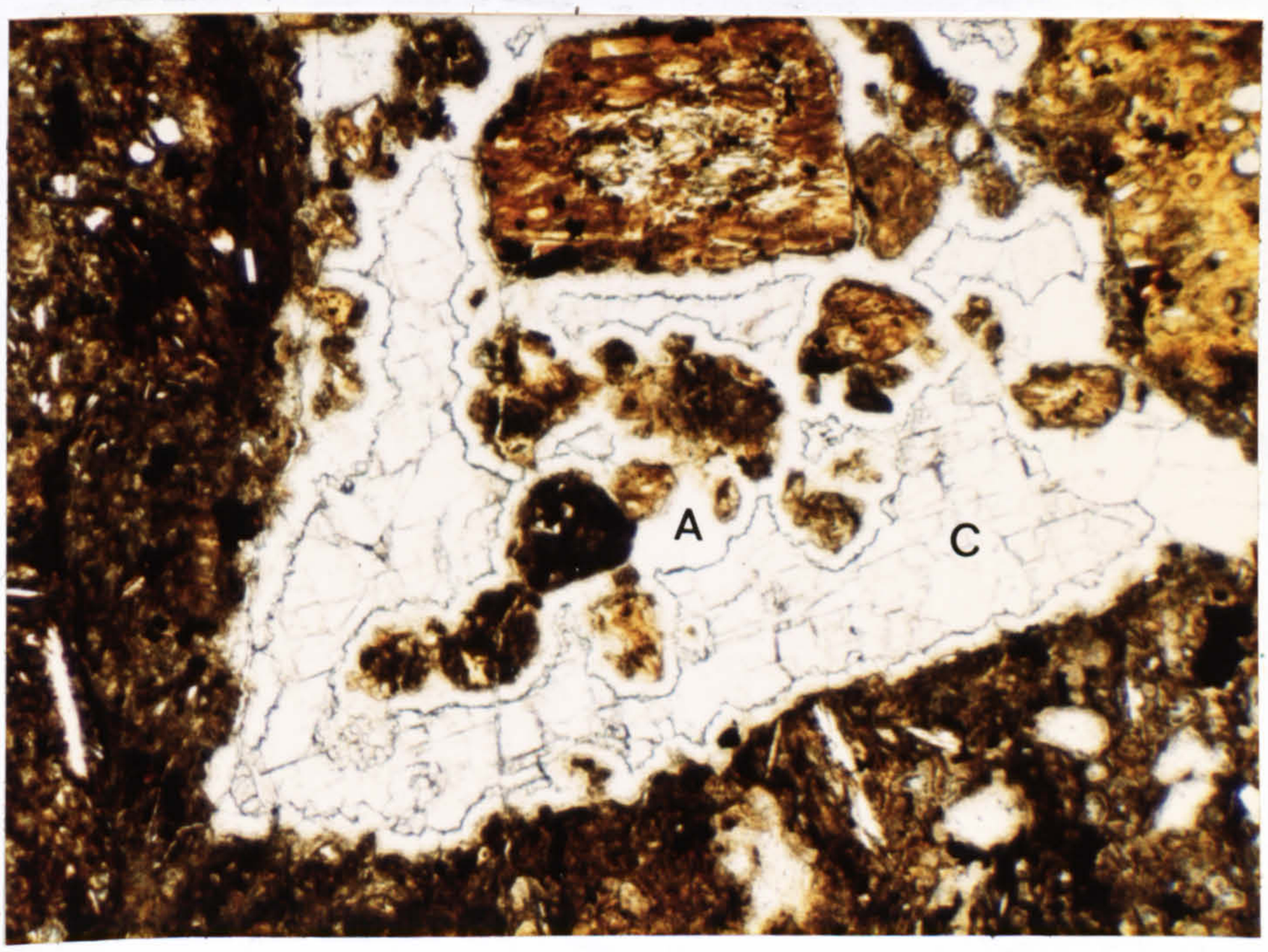

Fig. 3.29 Colourless, fibrous analcite (A) forming fringes around pore spaces with later calcite (C) infilling remaining voids. Plane polarised light. x10.

Calcite occurs in many of the tuffs but is not generally related to the amount of zeolite formed. The most altered tuffs contain the most calcite in general but its variable development suggests that carbonate solutions

TABLE 3.5 SIDEROMELANE, PALAGONITE AND AUTHIGENIC ANALYSES

	(1)	(2)	(3)	(4)	(5)	(6)	(7)	(8)
SiO_2	52·8	37·9	55·6	47·35	42·1	42·6	49·9	2·73
TiO_2	2·16	3·71	-	1·24	0·44	0·24	0·10	0·04
Al_2O_3	15·8	7·45	18·1	11·3	18·9	15·6	15·9	1·14
FeO	7·19	15·2	0·13	16·5	3·44	0·52	0·14	0·54
MnO	0·30	-	-	0·09	-	-	-	-
MgO	2·43	4·46	0·19	4·27	1·44	0·34	-	0·27
CaO	5·45	1·12	0·55	1·23	0·75	0·64	0·34	33·3
Na_2O	4·02	0·60	3·20	0·35	0·42	4·83	4·51	0·17
K_2O	3·02	1·80	4·97	3·57	1·21	5·14	5·85	0·13
P_2O_5	0·95	-	-	-	0·20	0·11	-	22·7
Total	94·12	72·24	82·74	85·90	68·90	70·02	76·74	61·02

(1) Sideromelane lapillus from CLT14 (reworked crater tuff).
(2) Palagonite rind around above lapillus.
(3) Zeolite pore infill near above lapillus.
(4) Slightly palagonitized glass lapillus from CLT21 (Unit B tuff).
(5) Palagonitized rind around vesicle in above lapillus (CLT21).
(6) Zeolite within vesicle in above lapillus (CLT21).
(7) Fibrous zeolite vesicle infill from CLT14.
(8) Vesicle infill of "apatitic" composition from CLT21.

have moved freely through the tuffs. Most of the calcite is thought to have formed directly from the palagonitization although some could have been brought in by groundwater percolation. Calcite fills many of the voids in the tuffs and greatly reduces permeability, preventing further leaching.

One sideromelane lapillus in sample CLT14 (reworked crater tuff) contains vesicles filled with colourless, radiating acicular crystals. Microprobe analyses (Table 3.5) indicate they contain Ca and P, suggestive of apatitic compositions. The minor amounts of phosphate found could be derived from alteration of the surrounding juvenile glass, which has a small P content.

b) Element distribution mapping

Microprobe element mapping (Appendix 2) was used to study the qualitative changes in glass chemistry during alteration. B.E.I. photographs clearly indicate that concentric zones of alteration occur as palagonite is formed (Fig. 3.30a). Computer maps (Fig. 3.30) display which elements have been mobile during alteration.

The mapped area comprises a partly-filled vesicle surrounded by well-bedded palagonite (Fig. 3.30). The palagonite occurs as a dark inner rind surrounded by a faintly-banded outer light-coloured rind. The vesicle infill consists of a layer of massive material around the vesicle wall with irregular, blocky crystals in the centre.

The palagonite outer rind is enriched in Mg, K and Fe relative to the fresh glass, and depleted in Al and Ti (Fig. 3.30b-e). Both the palagonite and the glass have similar Si contents. The inner palagonite rind is depleted in all of these elements except for Al, relative to the outer rind. The inner rind is probably a very hydrous phase formed by further leaching of initial palagonite.

The blocky inner vesicle infill is a Ca-phosphate containing traces of Mg, and is a form of apatite, possibly collophane. The rim of earlier authigenic material forming the initial vesicle infill is also predominantly composed of Ca and P. However, it also contains Mg, Al, Si and K. It is thought that this material formed under

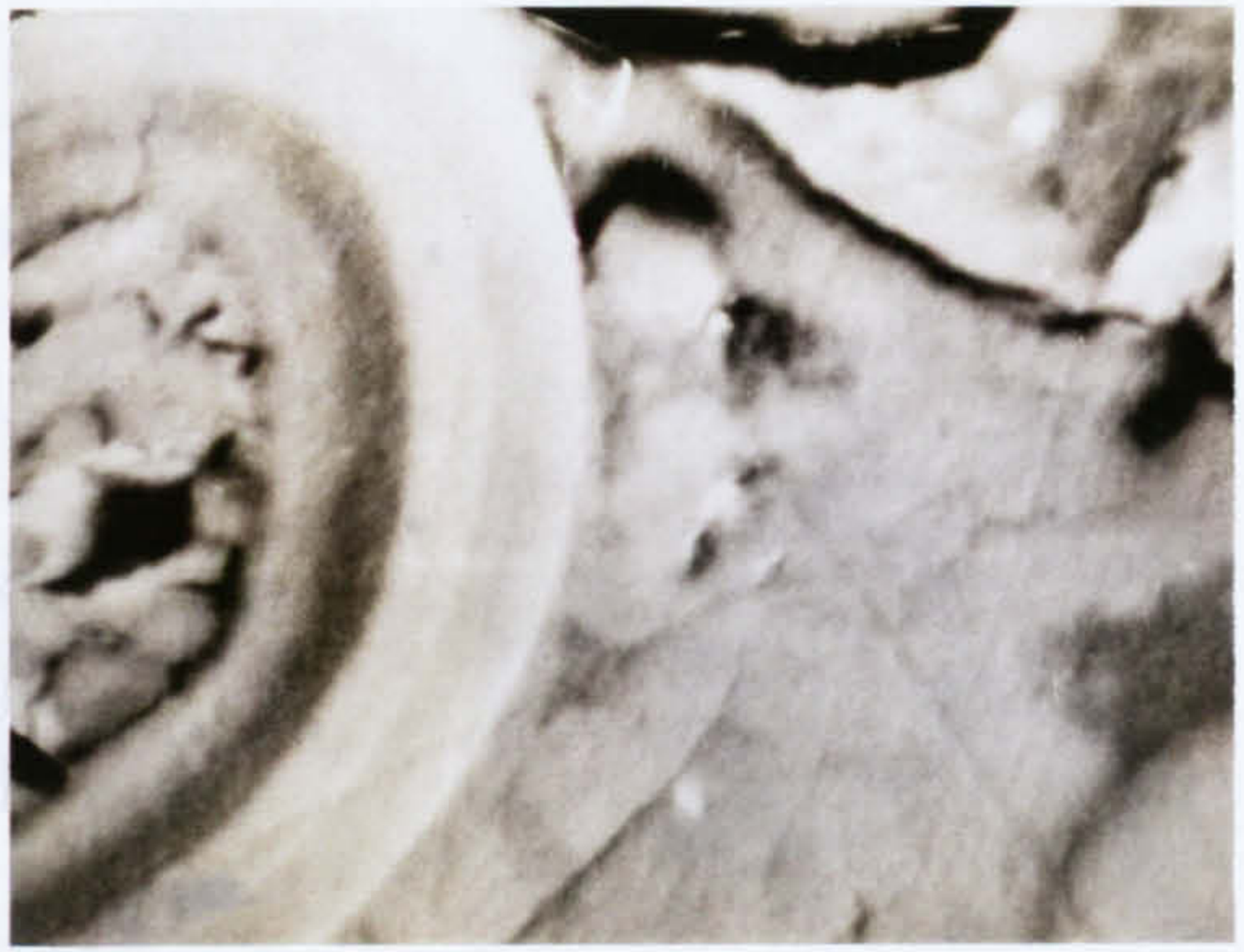

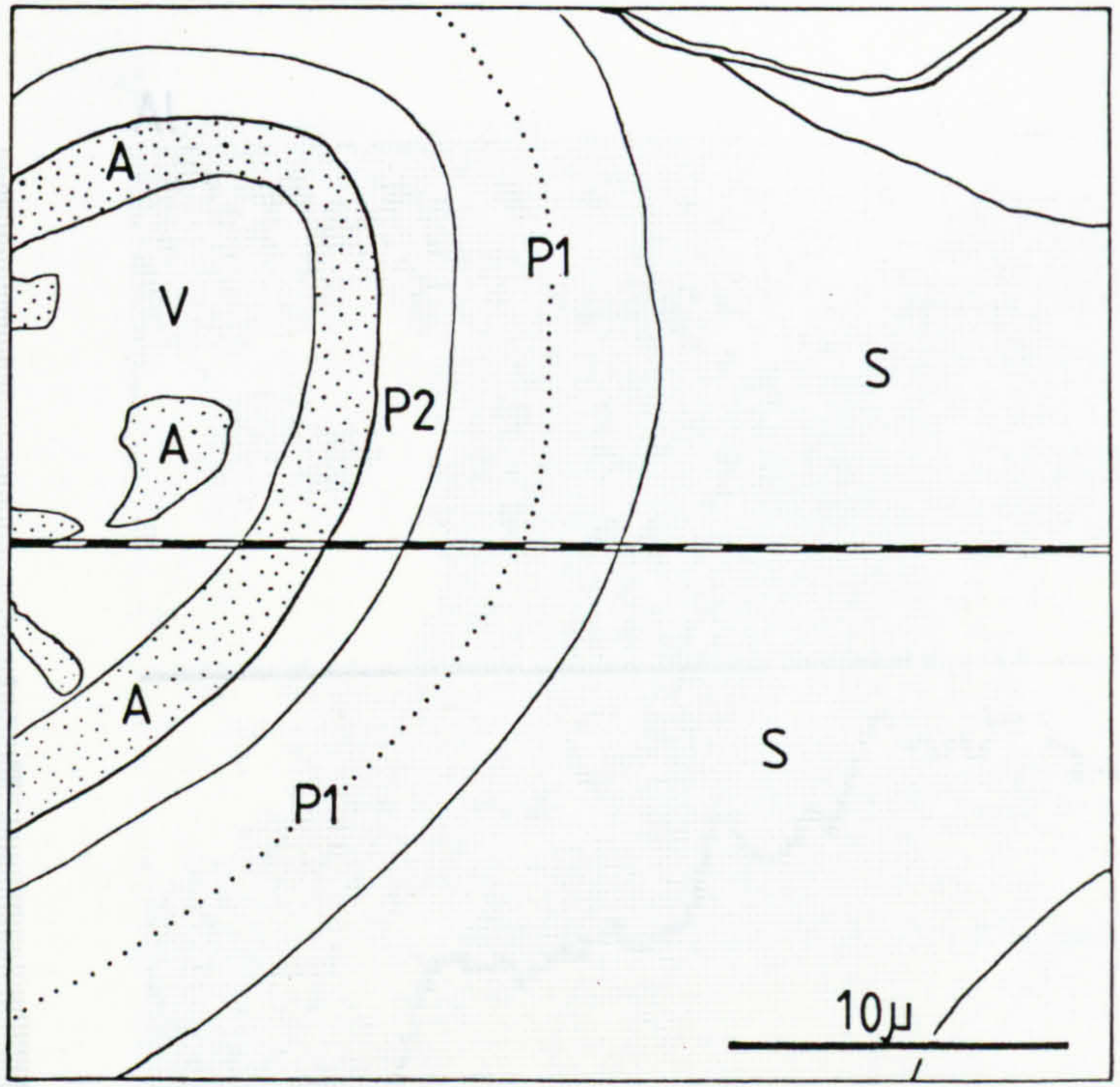

Fig. 3.30 a) BEI photograph and enlarged sketch of palagonitized lapillus used for element mapping.

A: authigenic material
P1/P2: palagonite bands
S: sideromelane
V: vesicle void space

Si

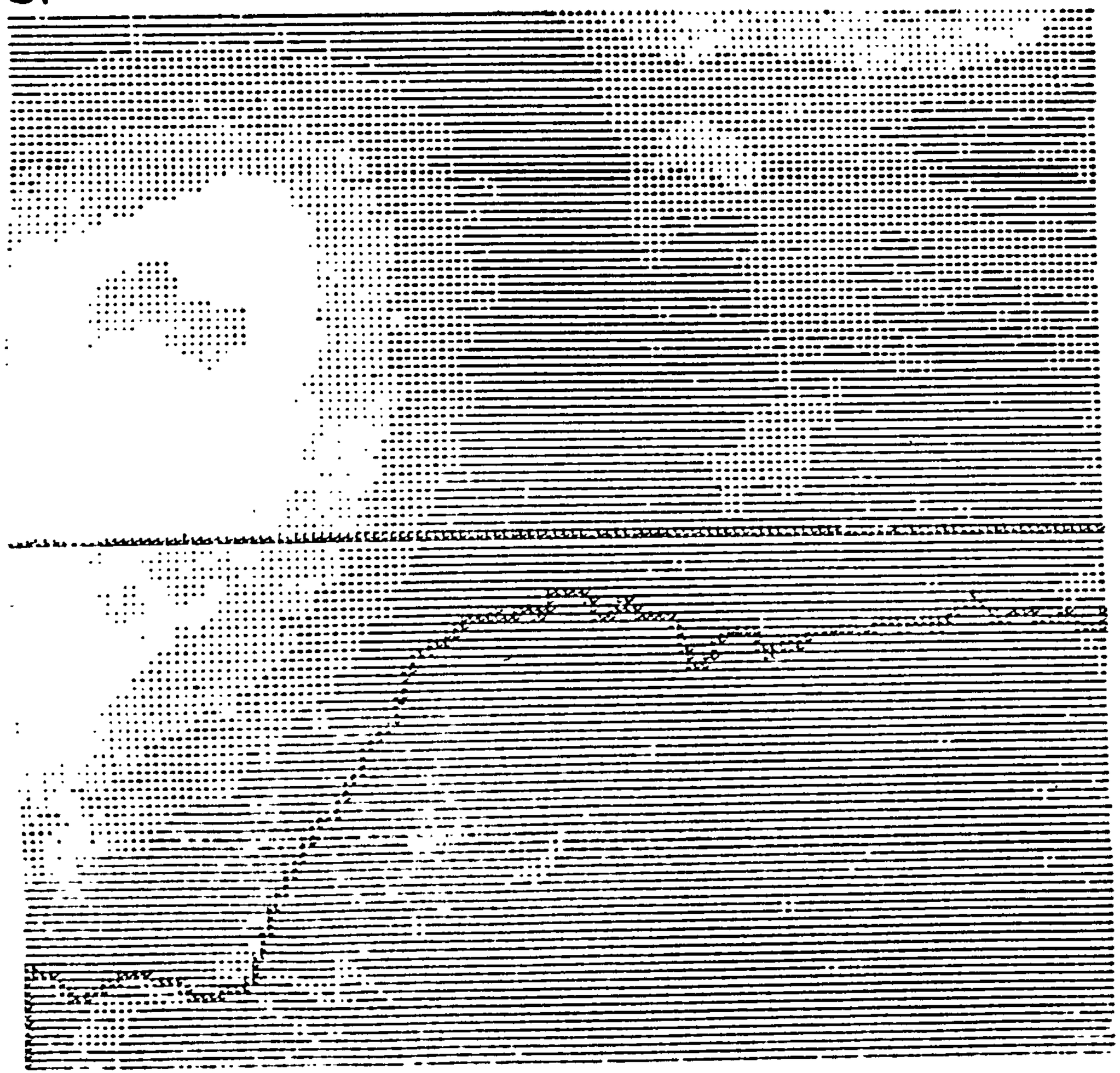

Al

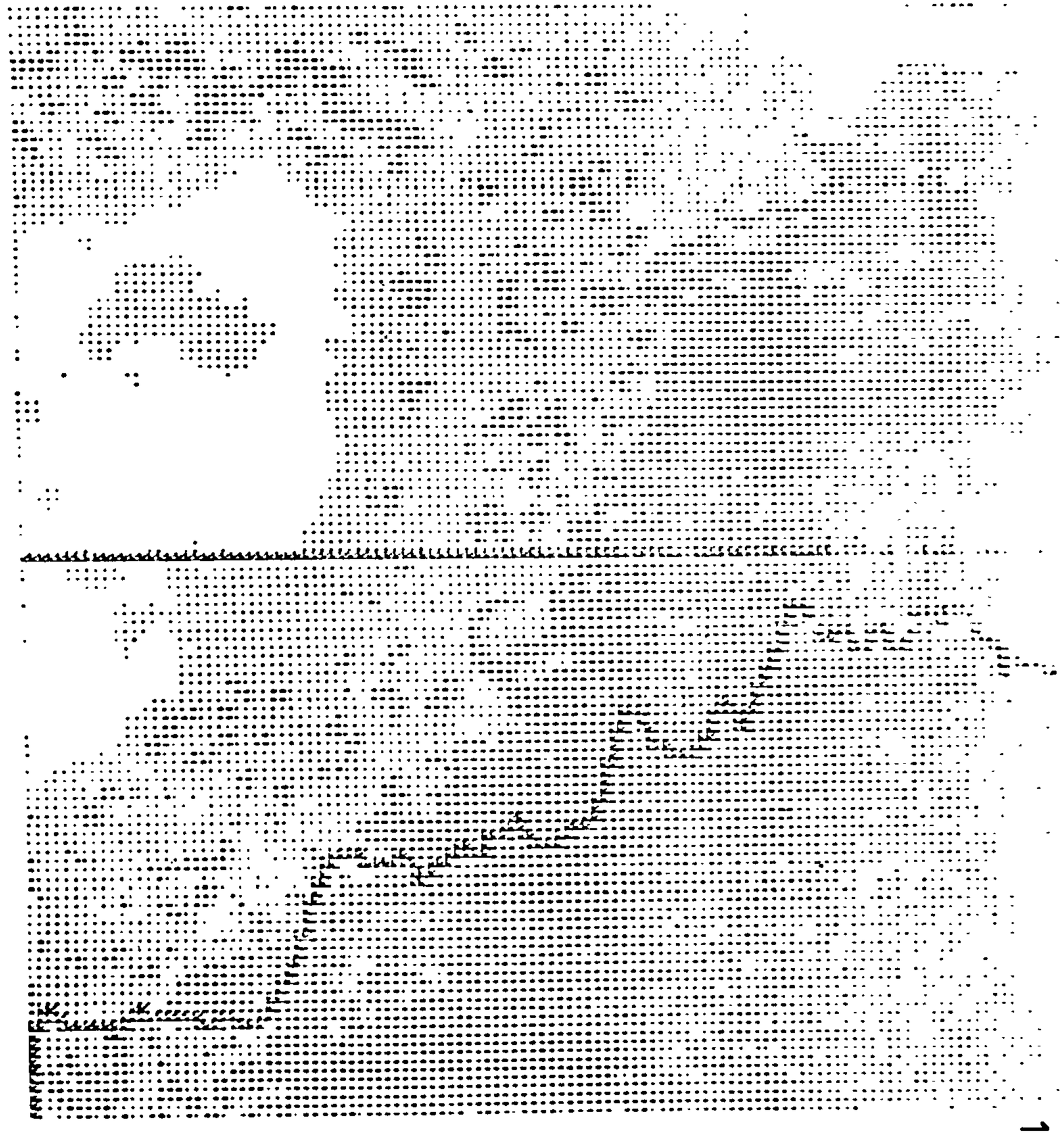

Fig. 3.30 b) Element distribution maps and linescans of Si and Al.

Mg

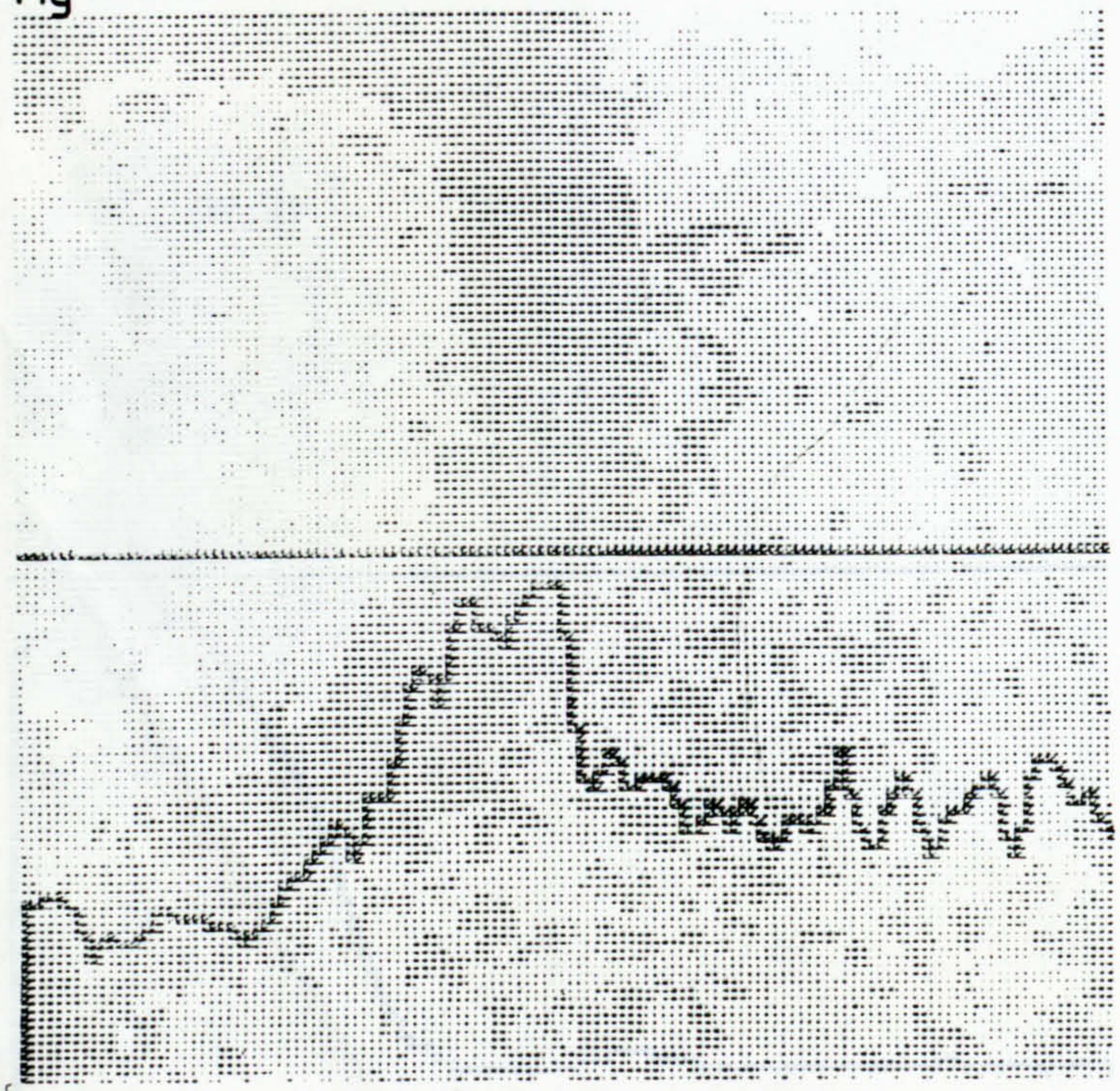

K

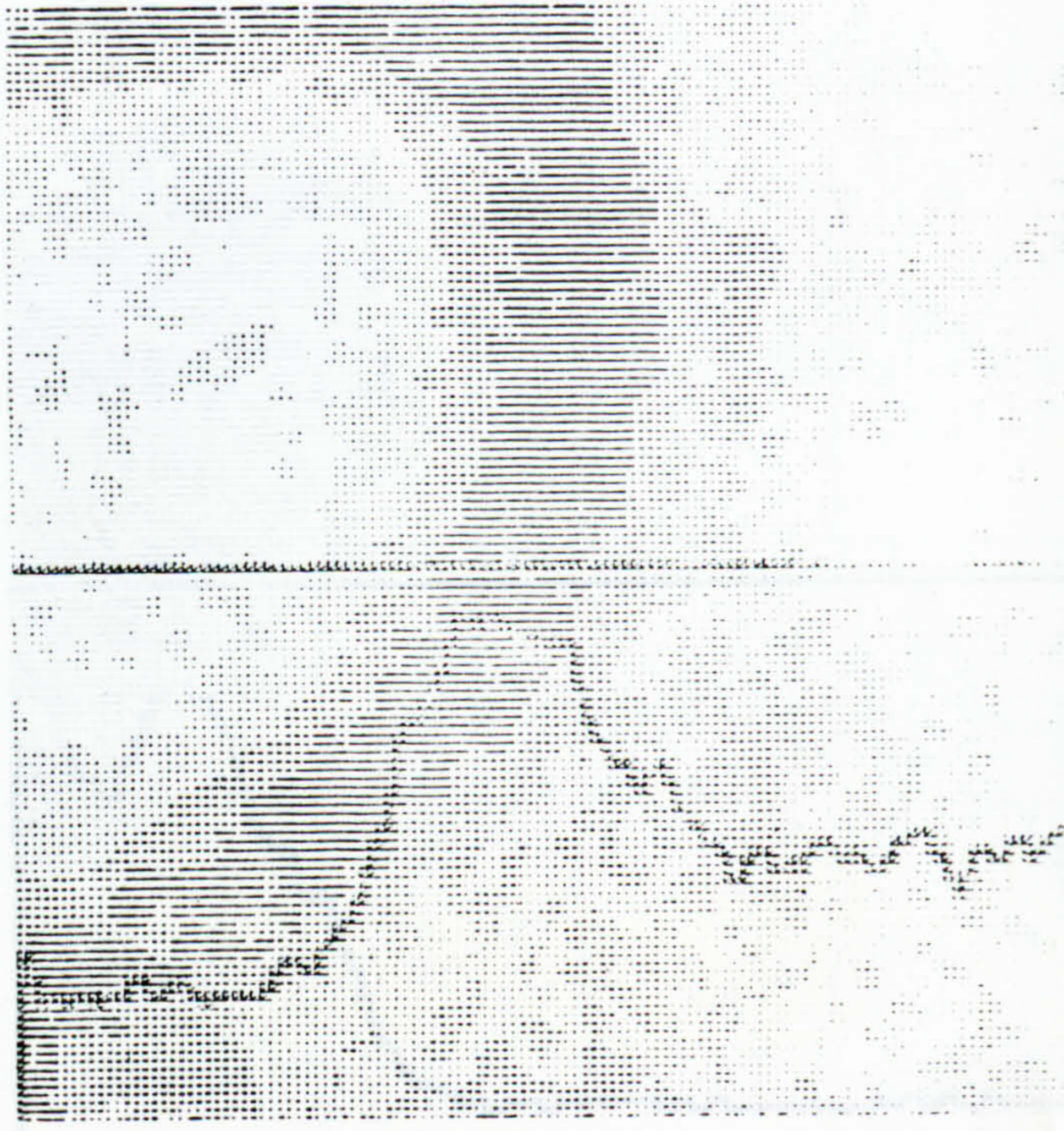

Fig. 3.30 c) Element distribution maps and linescans of Mg and K.

Ca

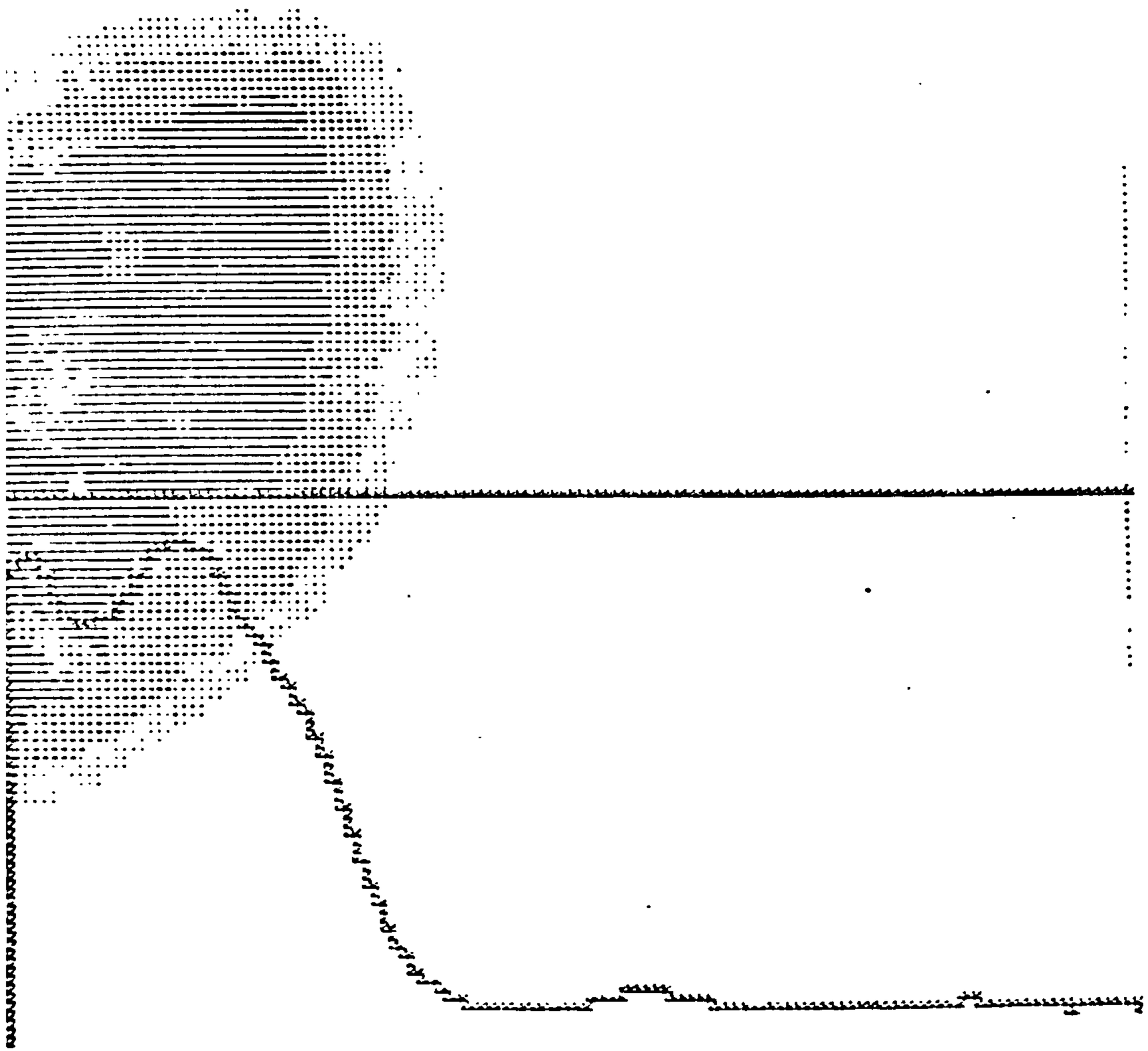

P

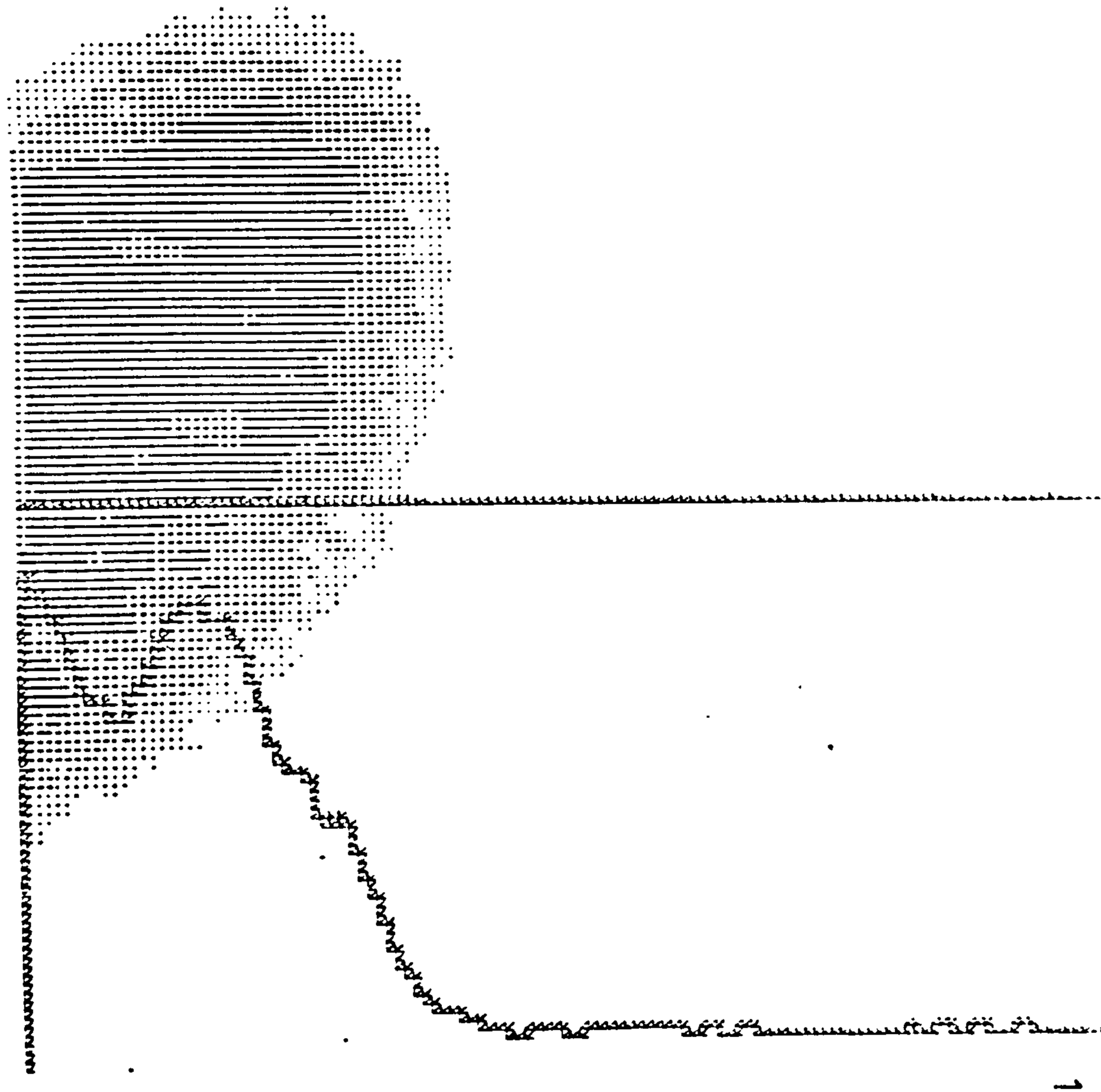

Fig. 3.30 d) Element distribution maps and linescans of Ca and P.

Ti

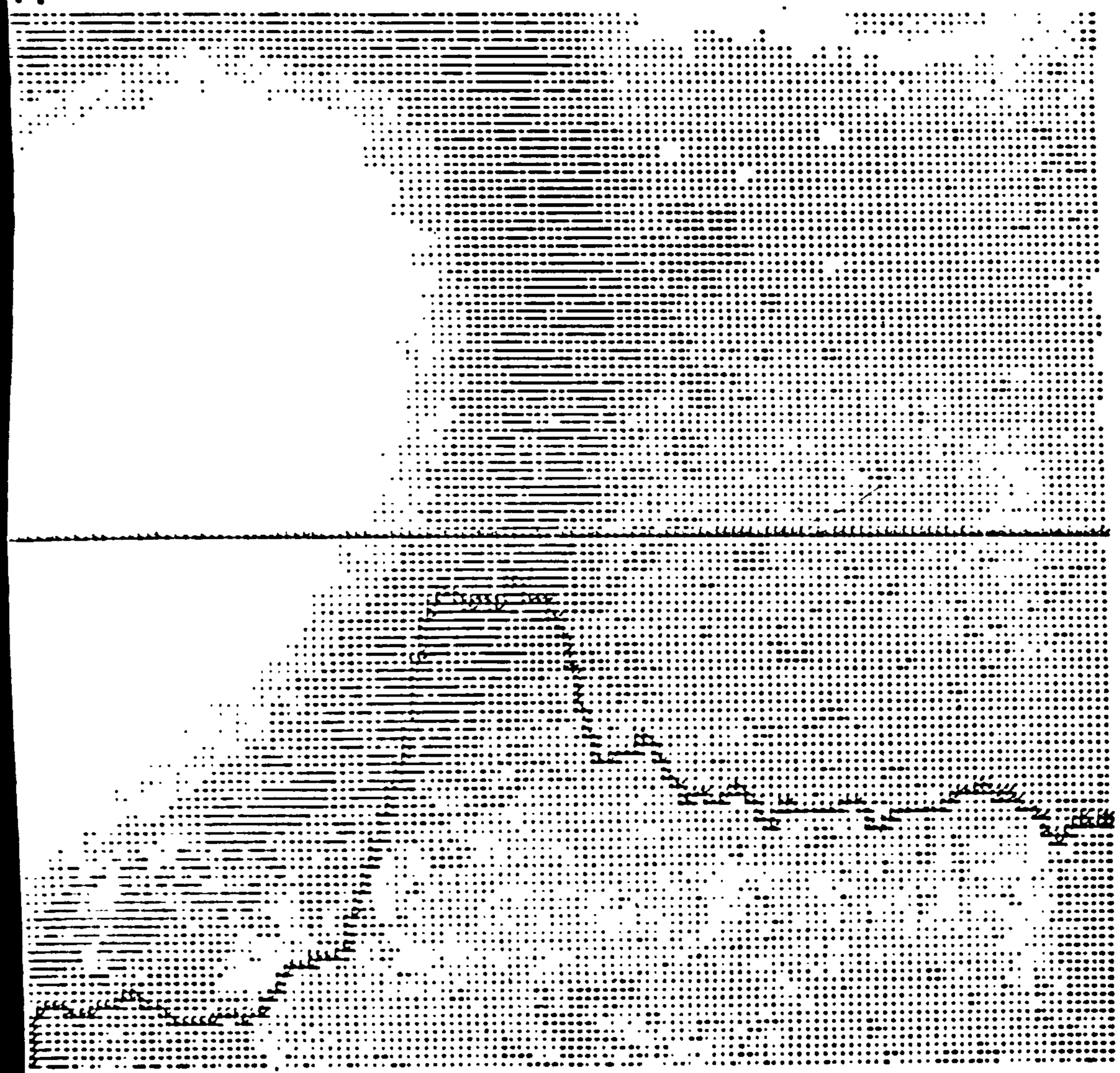

Fe

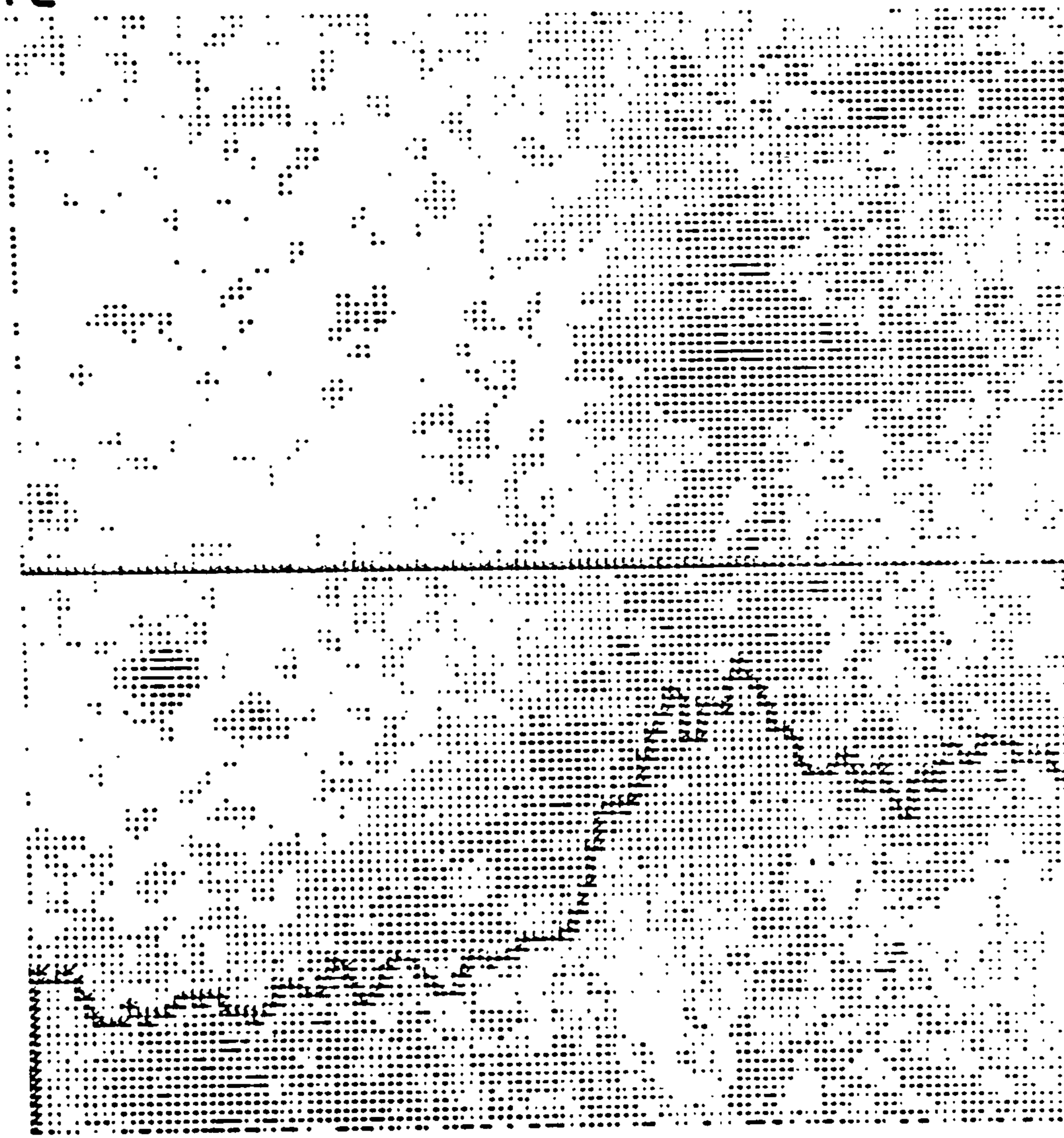

Fig. 3.30 e) Element distribution maps and linescans of Ti and Fe.

non-equilibrium conditions and is a hydrous gel, containing all the elements expelled from the juvenile glass during palagonitization. It may have taken in Ca and P during precipitation of the later apatitic phase. Although not shown on the computer maps, some movement of phosphorous and calcium in the glass towards the vesicle did occur.

The boundary between the palagonite and the glass is sharp, both optically and in terms of chemical gradients. This lack of a concentration gradient towards the palagonite has been explained by postulating rapid cation mobilisation (Harvey, 1974). The rapidity of the alteration process has been demonstrated by Furnes (1975) who studied the rate of palagonitization experimentally. Even at low temperatures (20°C), appreciable alteration took place within one year.

Even within the scale of a thin section, different thicknesses of palagonite occur around vesicles and lapilli margins. Concentrically banded palagonite rinds also occur, as do authigenic minerals with variable compositions. Element mapping indicates that the amount of cation depletion or enrichment in the palagonite also varies. All these changes are caused by variations in the micro-chemistry of the aqueous fluids surrounding each sideromelane fragment. Temperature and duration of alteration may also be important factors when considering changes in alteration on scales larger than hand specimen.

3.7. SUMMARY

1. The Nedano tuff-ring formed when trachybasalt magma ascended (along a fissure) and interacted with water derived from a shallow coastal lake.

2. Five lithologically distinct units were formed by phreatomagmatic eruptions. Variations between the products and structures of each unit are attributed to changes in the depth of eruption focus and the amount of water reaching the vent.

3. Surges are pulsatory density flows which eroded, or deposited different structures depending largely on their temperature (and thus moisture-content). Directed blasts caused marked variations in surge properties.

4. Ring-fault subsidence allowed a thick sequence of reworked tuffs to build up in the crater. Lacustrine, fluvial and debris flow deposits formed in the miniature basin and are presently being themselves reworked.

5. Vesicle size studies indicate that explosive magma quenching occurred at 150-200m during Units A and D eruptions and was shallower during Units B and E. Grain size distributions and petrography indicate that Units B and E eruptions were less water-influenced and thus less explosive.

6. Grain morphologies are similar to typical phreatomagmatic tephra. PVC results agree with this and also indicate the intermediate phreatomagmatic-strombolian nature of the Unit E eruptions. Such intermediate activity forms a mechanical mixture of phreatomagmatic and strombolian ash.

7. Palagonitization of the tuffs is variable in its development, due to variations in the micro-chemistry of pore fluids and tuff permeability. Cation mobility and

relative enrichment or depletion in palagonite is also variable, for similar reasons.

CHAPTER 4
RECENT PHREATOMAGMATIC ACTIVITY - A REVIEW

Before discussing ancient examples of phreatomagmatic volcanoes, a review of recent and observed types will be carried out. This will include comparisons with the Saefell and Medano tuff-rings and will establish a general model for activity of this type. Ancient examples may then be related to their original equivalents. The term phreatomagmatic is here used loosely to describe eruptions forming maars and tuff-rings.

4.1. Observed Phreatomagmatic Eruptions

Over the last thirty years many detailed accounts of observed phreatomagmatic eruptions have been published (Kienle et al.,1980; Machado et al.,1962; Moore et al., 1966; Muller & Veyl,1957; Nairn et al.,1979; Richards,1959; Thorarinsson et al.,1964). The 3-fold division of phreatomagmatic volcanoes proposed by Camus et al.(1981) provides a useful means of classifying eruption types, processes involved and products formed.

4.1.1 Initial activity

All three types of activity - phreatic, phreatomagmatic and surtseyan - begin by contact of magma with water. The mechanism and depth of this contact controls the type of volcano formed, as does the magma:water ratio and the rate of magma effusion. These factors will be discussed in the context of an overall model for phreatomagmatic activity (Chapter 7).

The initial activity of volcanoes formed by magma:water interactions consists of highly explosive blasts. These blasts occur at short intervals (1-30seconds on Surtsey) with smaller, more frequent explosions in between. Eruption clouds are highly charged with steam and punctured by tephra fingers which shoot out in all directions. These fingers have a bomb or block at their tips and draw out a trail of tephra behind them as they leave the central eruption column, forming the typical

"cocks tail" pattern (Fig. 4.1).

Base-surges form after large, especially directed explosions and leave the crater through notches in the rim. Most appear to be only partly related to column collapse processes. Such collapse processes are commonly observed and are theoretically predicted in the moisture-rich plumes of phreatomagmatic eruptions (Wilson et al., 1978). Surges move outwards as pulsatory density flows, being topographically channelled and transporting tephra down the volcano flanks (Fig. 4.1).

Scoriaceous tephra may be erupted at any time due to lesser amounts of water reaching the vent. During fissure-type eruptions, strombolian activity may occur at one point whilst phreatomagmatic activity occurs elsewhere. This mixed activity may sometimes occur within a single small eruptive crater (Ukinrek maars, Alaska; Kienle et al., 1980). The near-surface access of water to magma is periodic (Self et al., 1980) and controls the intensity and duration of phreatomagmatic explosions. Ollier (1974) discussed such a mechanism and termed a "tap model", where magma:water interaction is intermittant.

Constructive phases of volcano growth alternate with periods of repose. During activity considerable recycling of tephra which falls back into the crater occurs. This crater infill is supplemented by material which slumps off the crater walls. Also, explosions undermine the crater walls and break off large masses of more consolidated tuff. Some early formed concentric fissures (Thorarinsson et al., 1964) caused collapse of the crater walls of Surtsey during its early activity. Small nested cones built up by weak eruptions inside the crater are blasted away when powerful eruptions occur.

4.1.2 Syneruptive erosion

If the phreatomagmatic activity is surtseyan then wave action continually modifies the external shape of the tuff-ring. Breaching of the ring in various places occurred during the Capelinhos eruption (Machado et al., 1962), keeping the crater open to the sea. Tidal reworking

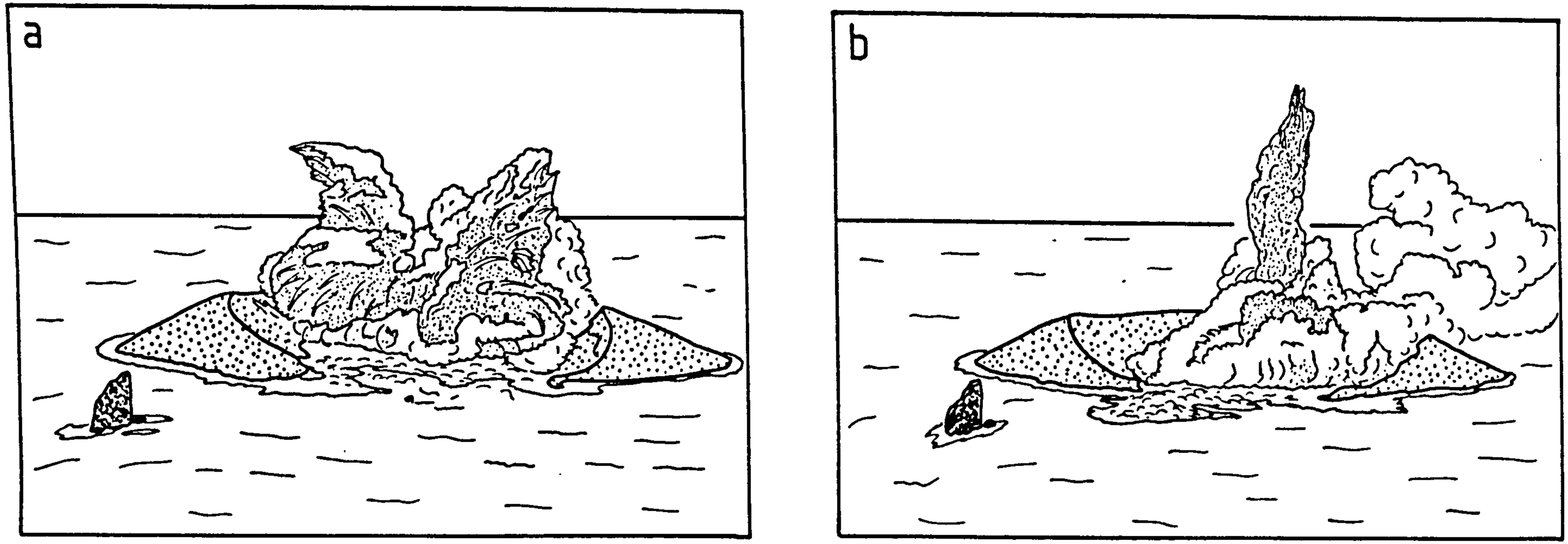

Fig. 4.1 Drawings from photographs of the Capelinhos eruption. a: cocks tail explosions b: vertically directed eruption c,d: base-surge formation from collapsing eruption columns.

affected the crater tuffs of both Capelinhos and Surtsey, removing large quantities of ash. When activity ceased, the tuff-rings were rapidly eroded, their survival prolonged by lava effusion in a later stage of activity.

Maars are not subject to syneruptive tidal reworking but are, along with tuff-rings, eroded by water runoff. This water may directly condense from the eruption column or be meteoric due to ash seeding rain clouds overhead. Nilahue maar (Muller & Veyl, 1957) was infilled largely by water from a small stream which flowed down the nearby hillside and breached the tephra rim. Rapid erosion of the unconsolidated tephra by debris flow and fluvial runoff results in the characteristic parasol ribbing seen on the outer flanks of many volcanoes (Fig. 4.2).

Maar craters rapidly become partly filled with a lake, often because the pit intersects the water table. These lakes often drain down fissures prior to renewed eruptions but are soon replenished afterwards. In this way phreatomagmatic eruptions maintain a water supply to fuel further magma:water explosions.

4.1.3 Late-stage activity

With time phreatomagmatic activity wanes as continued magma upwelling fails to contact copious amounts of water. Degassing of this magma prevents violent explosive activity even if water is present and lava ponds in the crater. These factors control whether a scoria cone or lava lake are formed although commonly both are present. Surtsey, Capelinhos, Taal and Ukinrek volcanoes developed late-stage strombolian activity with associated lava flows and more rarely domes. If activity continues the initial maar or tuff-ring may be buried beneath later scoria and lava such as on Surtsey and Capelinhos (Fig. 4.3). The change in eruptive style is solely due to the absence of water, either because of sealing of the crater from the sea (Surtsey), or because groundwater cannot be replenished rapidly enough (Ukinrek). Once the magma has degassed it forms lava flows and domes and will not explosively interact with any amount of water.

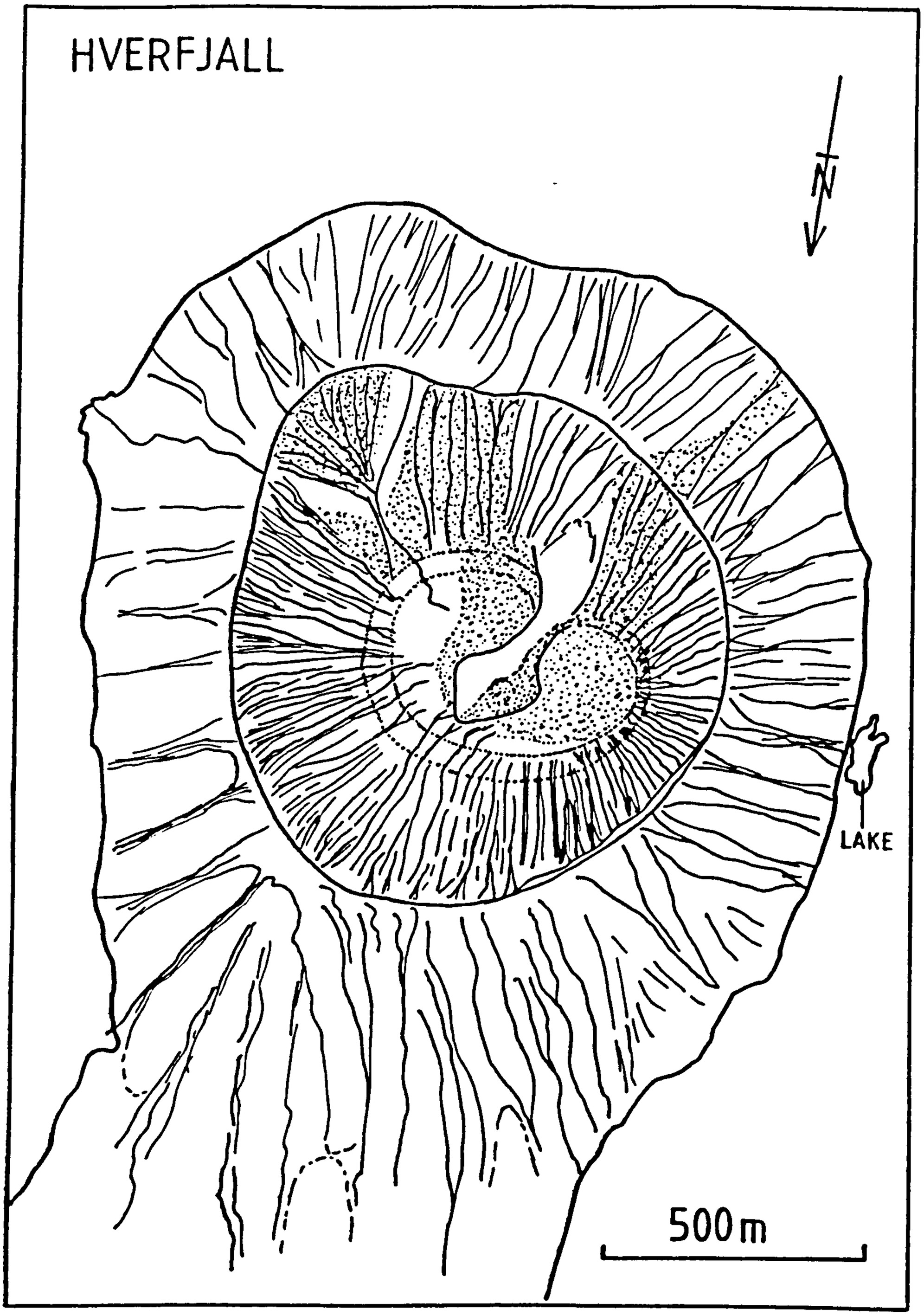

Fig. 4.2 Drawing from an aerial photograph of Hverfjall, Iceland, a Recent tuff-ring whose flanks have been extensively eroded by fluvial action. Note the mound of tephra within the crater, thought to represent a late-stage tuff cone.

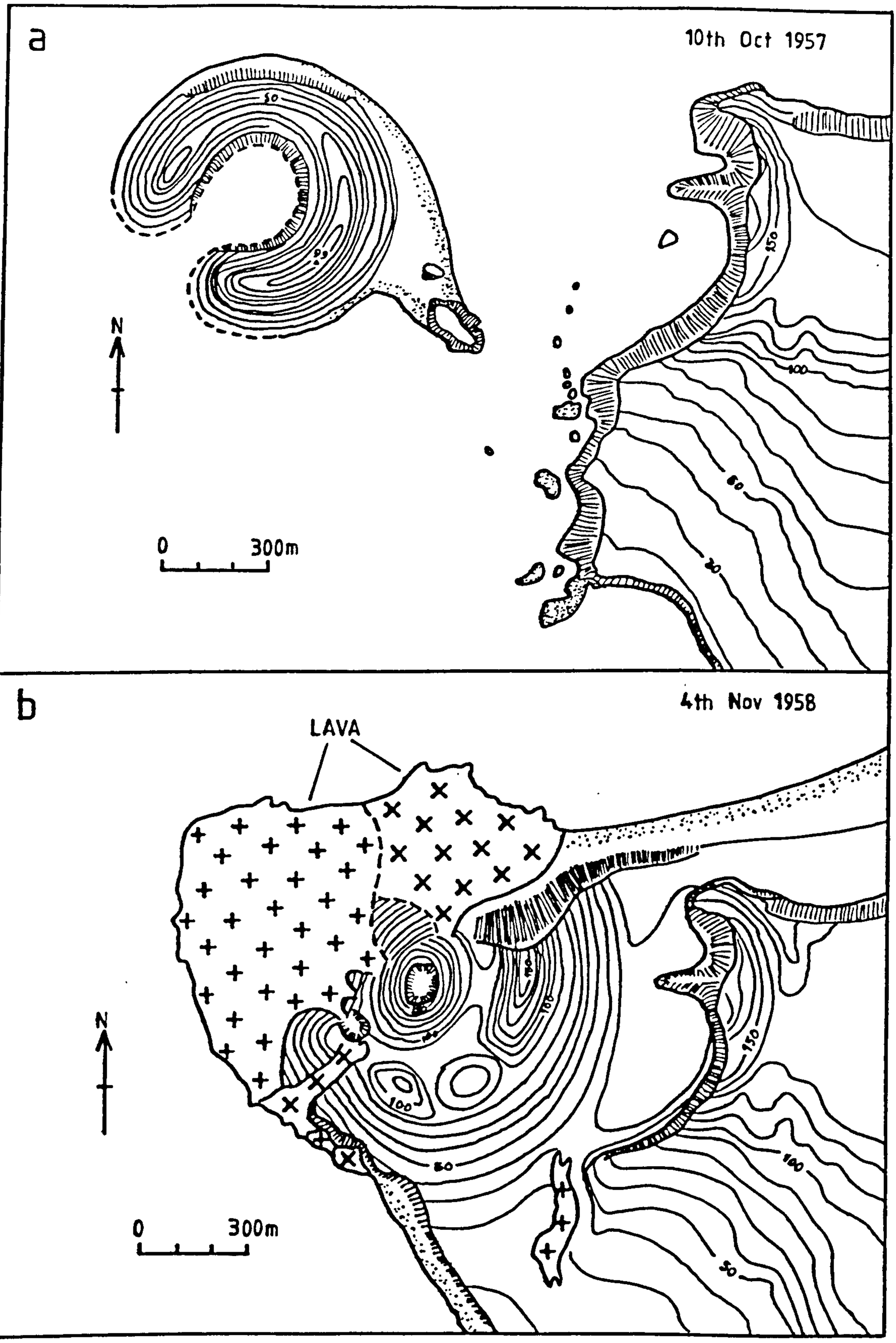

Fig. 4.3 a) Early stage in the growth of the Capelinhos tuff-ring, showing breached crater.

b) Final stage in the growth of the volcano, where lava flows have armoured the structure and protected it from erosion. Note alteration and addition to previous coastline.

Although the above descriptions apply to small, purely phreatomagmatic volcanoes many other composite, large volcanoes have phreatomagmatic phases. Examples of these include Vesuvius (Sheridan et al., 1981), Mount St. Helens (Moore & Sisson, 1982) and numerous examples in the I.A.V.C.E.I. Bulletin of Volcanic Eruptions. Data from such eruptions may be used to supplement the limited observations made on maar and tuff-ring activity.

4.2. Recent, Eroded Phreatomagmatic Volcanoes

Many descriptions of recent, though not historically active, phreatomagmatic volcanoes exist. Variable degrees of erosion allow the study of many products whose processes of formation could not be directly viewed during eruptions. In this study the main points of interest in the eroded samples are :-

1)Base-surge deposits
2)Collapse processes
3)Reworking and crater infill processes
4)Preservation potential.

A general review of maars, tuff-rings and diatremes is given by Lorenz et al. (1970). In the present study more attention will be paid to comparisons with the Saefell and Medano tuff-rings and information bearing on the origin, deposits and significance of diatremes.

4.2.1 Base-surge deposits

Base-surge channels are best developed near or on the crater rim (Barcena: Richards, 1959; Saefell). Surge dunes occur downslope from these on the outer flanks and are best developed in the sub-horizontal distal tuffs. This is thought to indicate that surges are highly chaotic particle:gas mixtures within and just outside the crater. On moving down the volcano flanks they become coherent pulse-like flows capable of depositing thin, well-sorted beds. Factors which favour deposition include loss of flow velocity (as surges move from steep to gentle slopes), decrease in temperature (causing condensation of steam and clumping of moist tephra) and expansion of surge clouds

(due to admixing of cool air at surge front causing dilution of the flow and collapse of turbulent grain support mechanisms). Admixing of cool air also lowers the surge temperature and thus increases particle loss.

Allen (1982) in a summary of the sedimentary features of pyroclastic surges and flows, mentions their similarity to turbidity currents. He classifies surge dunes (which he terms sand-waves) into progressive, stationary and regressive (Fig. 4.4a) types. These types are related to the temperature (and thus moisture content) and the sediment deposition rate relative to transport rate of surges. Using the direction and steepness of bedform climb one can get a rough idea of the temperature and relative deposition rate of a surge.

When the Saefell and Medano dunes are interpreted in these terms the results agree with Allen's (1982) conclusions. The first Saefell dune (Fig. 4.4b) is similar to his type A_1/A_2, a progressive bedform with preservation of complete sets and some erosional partings. The dune is a Unit 3 directed surge deposit with no associated accretionary lapilli. The block impact sag plastically deforms the dune laminae indicating they were slightly cohesive. The absence of accretionary lapilli, adhesion ripples and plastering structures indicates the surge was hot and relatively dry.

The slumped Saefell dune (Fig. 4.4b) passes from a regressive type C bedform upwards into a progressive type A_1 bedform. This change indicates the increasing temperature of the depositing surges with time, perhaps as the hot, dry head of a surge pulse overtook the cool, moist, expanded tail of a preceding pulse.

The Medano dune (Fig. 4.4b) is a type A_2 progressive bedform. The proximity of the dune to the crater and the lack of accretionary lapilli suggest that its depositing surge was hot and relatively dry. The presence of some moisture, however, is indicated by the ash plastered around the underlying block. It is thought that surges contain both hot, dry steam and cool, moist water vapour at all times. Thus even progressive bedforms contain some

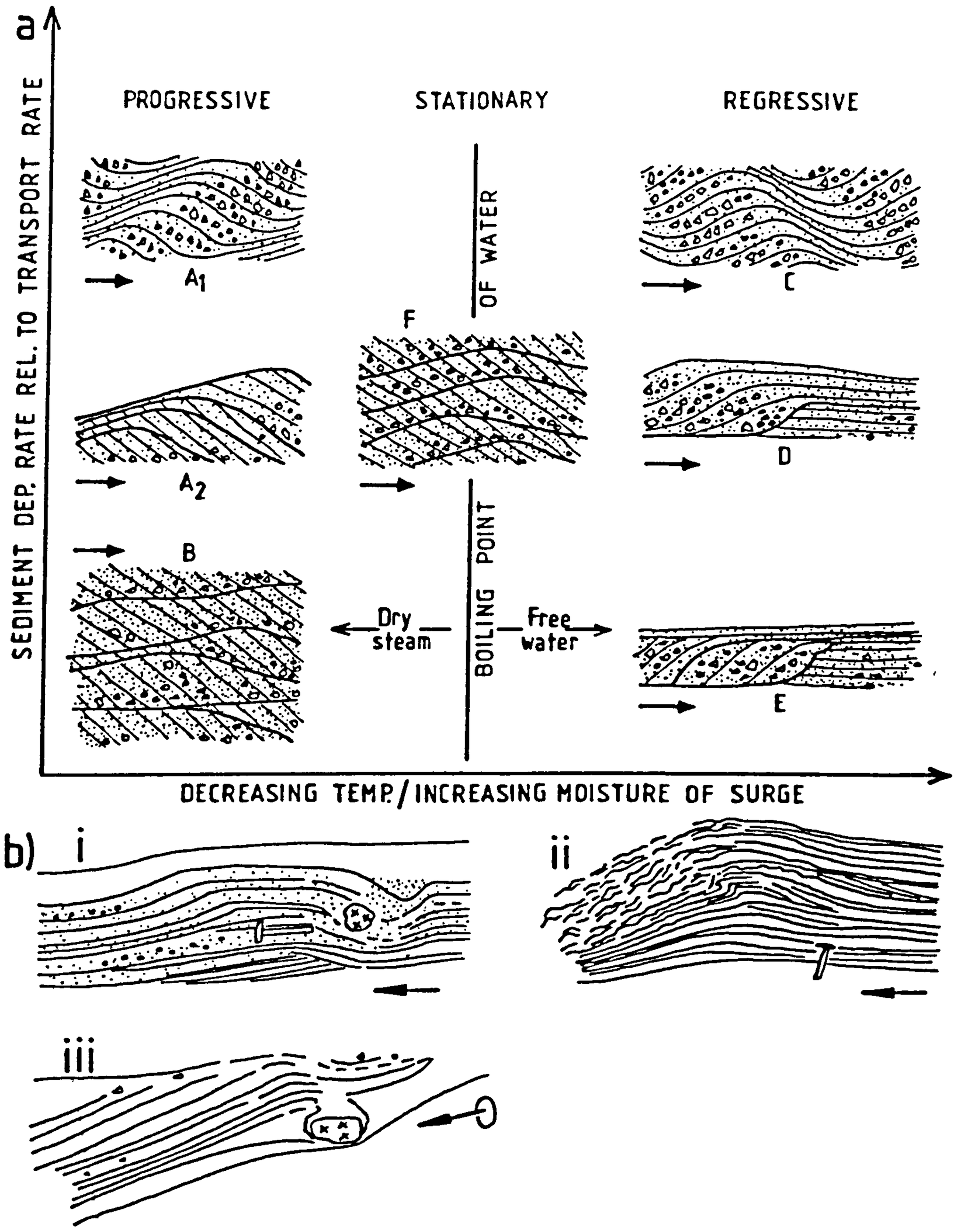

Fig. 4.4 a) Dune bedforms formed by surges, and their variation with steam temperature and deposition rate (Allen, 1982).

b) Dune forms from Saefell and Medano for comparison with theoretically predicted structures. Arrows indicate flow directions.
   i) Saefell Unit 3 dune, a progressive A1/A2 type bedform
   ii) Saefell Unit 1 dune, a regressive type C bedform which passes upwards into a progressive type A1
   iii) Medano Unit C dune, a progressive type A2 bedform.

moisture when deposited.

The Medano and Saefell surge deposits are broadly similar to the surge deposits of other volcanoes. The form, location, abundance and sequence of surge structures is variable even in a single volcano. These differences are dependant on the physical properties of the surges and the influence of external factors such as the volcano morphology. A general model for surge origin, motion and deposition will be presented in Chapter 7. For specific descriptions of base-surge deposits see Moore (1967), Fisher & Waters (1970), Waters & Fisher (1971), Crowe & Fisher (1973), Mattson & Alvarez (1973), Schmincke et al. (1973), Sheridan & Updike (1975) and Fisher (1977).

4.2.2 Collapse processes

a) Maars

Direct evidence for subsidence in phreatomagmatic volcanoes is common in maars but less obvious in tuff-rings. The Eifel maars (Lorenz, 1973) have smaller ejecta volumes than crater volumes due to collapse. Thick deposits of reworked pyroclastics (>175m) were found in a maar in the French Massif Central (Lorenz, op. cit.), separated from the surrounding country rock gneisses by a ring fault. This was interpreted to indicate prolonged subsidence of the crater infill after cessation of volcanic activity.

Syneruptive collapse processes were observed at Nilahue (Muller & Veyl, 1957) and Ukinrek maars (Self et al., 1980), with arcuate fractures and slumping. This slumping is thought to be the surface expression of subsidence along ring faults at depth (Lorenz, 1973). Excavation of an eruptive chamber at depth (Lorenz, op. cit.), due to wall-rock spalling as eruption pressure decreases, forms a diatreme beneath maars. Further subsidence in maars may occur after eruption, however, along ring fractures which develop outwith the eruptive crater. This subsidence is a type of caldera collapse, and results in en masse collapse of the diatreme deposits with remarkably little disruption (Gutmann, 1976).

b) Tuff-rings

As with maars, syneruptive subsidence in tuff-rings has been invoked to explain the occurrence of repeated slumping and collapse of the crater walls along arcuate planes (Capelinhos: Camus et al.,1981; Thorarinsson et al., 1964). In extinct tuff-rings it is frequently not possible to determine whether syneruptive collapse occurred. Rim beds which have slumped into the crater are often observed (Heiken, 1971) but may not represent crater collapse. Such slumped products could be reworked by subsequent eruptions and ejected from the crater, preventing its infilling.

Some subsidence does however occur along ring faults which leads to crater enlargement (Lorenz, 1970). Thick sequences of reworked tuffs such as at Medano (Chapter 3) indicate slow, posteruptive subsidence. The amount of subsidence in tuff-rings is likely to be less than in maars (Lorenz, 1973). This is because there is less disruption of the country rocks beneath tuff-rings, which have subsequently low proportions of accessory lithics. This has important consequences on the processes of diatreme formation and will be further discussed in the following chapters (Chapters 5, 6 & 7).

4.2.3 Reworking and crater infill processes

In one respect maars and tuff-rings may be treated as minature depositional basins with an abundant supply of uplifted, proximal, unconsolidated infilling material. Add to this the effects of volcanic explosions with associated ground tremor and copious supplies of water from eruption columns and its not surprising why a wide range of reworking processes are observed.

a) During eruption

As mentioned above (Section 4.2.2) syneruptive collapse of crater wall tuffs has been frequently observed in maars and tuff-rings. Slumping is facilitated by the high moisture content of the tuffs and explosions beneath the crater wall sequence (Thorarinsson et al., 1964). Much tephra falls directly back into the crater after eruption and probably contributes greatly to its infilling.

Fluidization of crater/vent material may occur in some phreatomagmatic volcanoes (Lorenz, 1970; McCallum et al., 1976) but in a brief review Wolfe (1980) concludes that this is unlikely. Other processes such as gas-streaming, ball milling and fines elutriation have been observed in volcanic conduits but are not strictly fluidization phenomena (Wolfe, op. cit.).

Active vents generally occupy small areas of the crater and thus eruptions do not totally disrupt crater tuffs. Lakes (or lagoons if surtseyan tuff-rings are breached) may occupy part of the crater whilst eruptions occur. On Surtsey (Thorarinsson et al., 1964) two main craters were formed. In one a shallow lake existed for some time whilst activity continued in the other. Renewed activity causes intercalation of reworked and primary tuffs many times during the life of phreatomagmatic volcanoes.

b) After eruption

As slow subsidence of the crater tuffs occurs, a thick pile of reworked tuffs builds up within the basin. Jahns (1959) illustrated that at Crater Elegante, Mexico, the infilling consists of talus breccia, deltaic and lacustrine sediments, alluvial fans and playa deposits (Fig. 4.5). The episodic nature of the subsidence is indicated by well-defined topset benches around the crater walls. In modern surtseyan tuff-rings such as Surtsey and Capelinhos there is little evidence of post-volcanic subsidence. It is thought unlikely that they will accumulate thick sequences of reworked deposits, for reasons which will be discussed in Chapter 7. In this respect the Medano tuff-ring is different to Saefell, which is like Surtsey in having suffered little post-volcanic subsidence.

Water runoff, on the inner and outer slopes of tuff-rings may occur at all times during and after eruption. Depending on the degree of consolidation of the tuffs, mudflow or fluvial channels are formed, producing the parasol ribbing seen on most pyroclastic volcanoes (Fig. 4.2). On the unstable submarine slopes of surtseyan

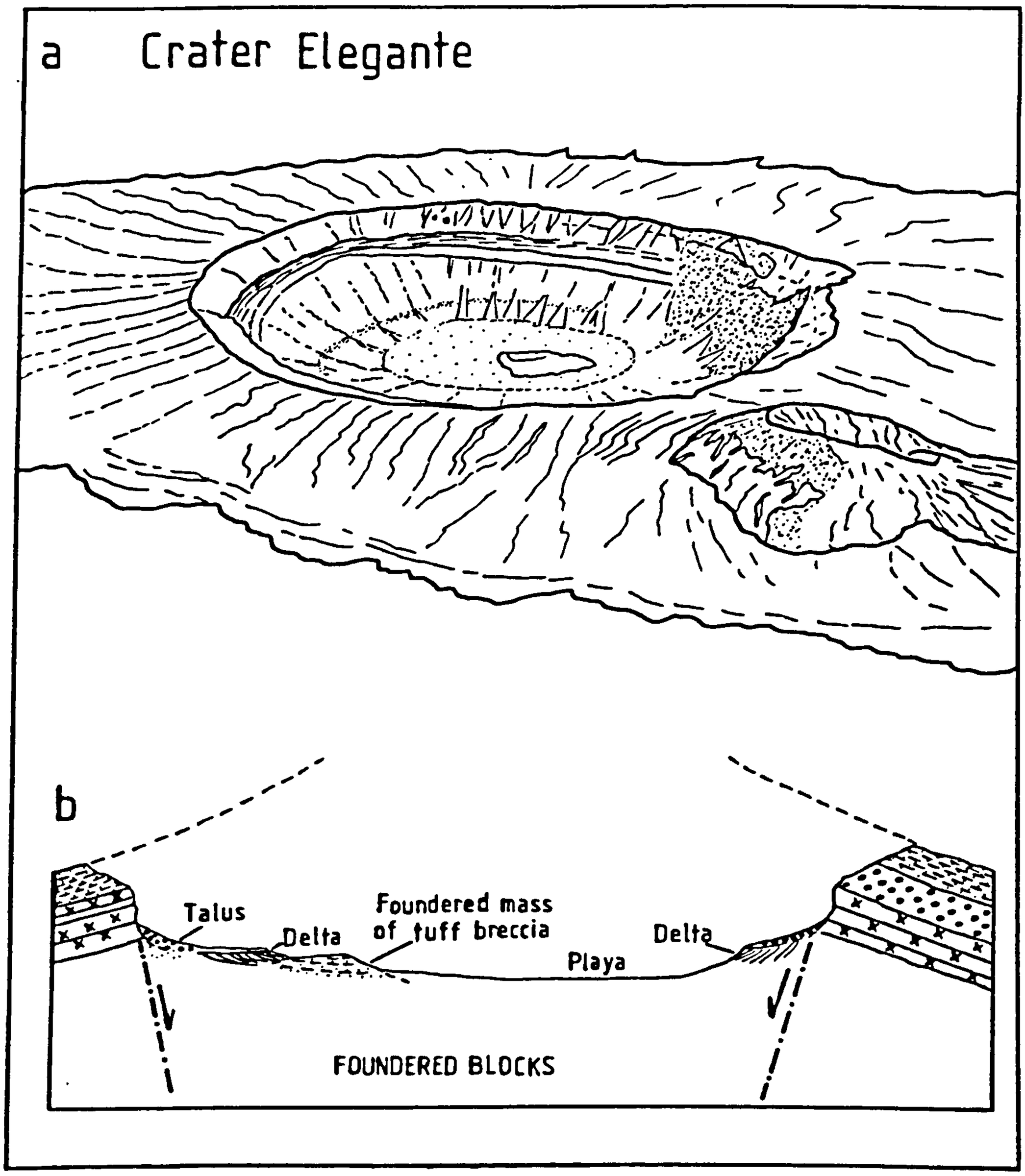

Fig. 4.5 a) Oblique view of Crater Elegante volcano showing low ejecta rim and deep crater (Jahns, 1959).

b) Diagrammatic section taken from Jahns (1959) showing reworking of the crater tuffs by various processes.

tuff-rings volcanic tremor and slumping initiates debris flows and turbidites(Alexandersson, 1972), although such processes are rarely recorded.

Wave action rapidly reworks surtseyan tuff-rings (Fig. 4.6), causing changes in shape and size as they grow. The parasitic vents of Surtsey (Thorarinsson, 1967) were eroded away in a matter of days. Wave erosion has also affected Capelinhos (Machado et al., 1959) and Saefell (Chapter 2) redistributing much of the flank tephra. Wind action may be locally important in removing fines and eroding loose tephra (Surtsey, Saefell).

4.2.4 Preservation potential

The reasons for the scarcity of phreatomagmatic deposits before the Tertiary are as follows :-

1) Small volcano sizes, low ejecta volumes and low dispersal aid rapid reworking.

2) They frequently occur in active sedimentary environments, since these often supply the water for explosive activity, e.g. Surtsey in shallow marine environment, Nilahue in stream valley, Menan Buttes (Hamilton & Myer, 1963) on river floodplain, Fort Rock (Heiken, 1971, 1972) in lake basin. These processes erode and redistribute tephra.

3) They are composed of unconsolidated tephra, aiding reworking. Alteration of tuffs occurs rapidly, improving their resistance to physical weathering but ultimately destroying most primary textures.

4) A large number of reworking processes affect phreatomagmatic volcanoes (Section 4.2.3). These processes are aided by the prolonged subsidence of the crater.

5) Phreatomagmatic volcanoes often erupt lavas at a late stage. These flows may breach the crater (Surtsey, Capelinhos) and obscure the previously formed tuffs. Often, however, such lavas prevent complete redistribution of the tuffs by "armouring" the structure against erosion.

Such reasons explain why few examples of ancient maar/tuff-ring products are documented in the literature, even though they are reported to be second only to scoria cones in abundance amongst volcanoes (Wood,in press).

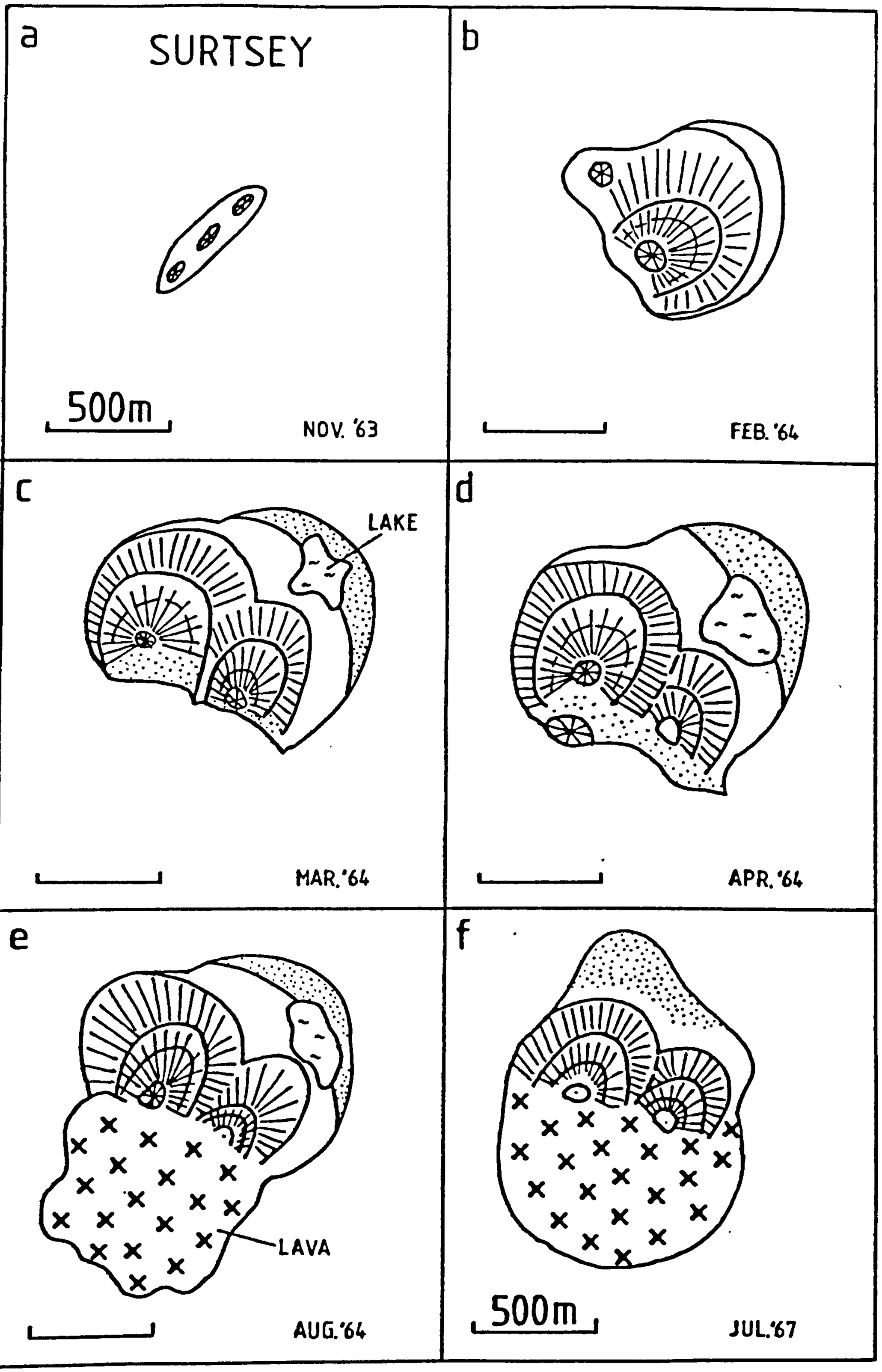

Fig. 4.6 Growth and change in shape of the Surtsey tuff-ring during the 4 years of its activity.

Another reason for this scarcity is probably lack of recognition in ancient rocks, because of alteration and similarities with sediments. Many maar beds contain < 20% juvenile material, the remainder consisting of comminuted sediment if phreatomagmatic activity was initiated by pore water from unconsolidated, newly-deposited sediments. In ancient rocks it is frequently sufficient that a volcaniclastic deposit is recognised, let alone an identification of the volcano type.

Factors which enhance the preservation of maar/tuff-ring products are as follows :-

1) Subsidence of tuffs into a diatreme. This preserves thick sequences of primary tuffs at depth below the erosion surface. Most ancient phreatomagmatic products are found in such structures (Lorenz et. al., 1971).

2) Deposition of tuffs along with sediments in a depositional basin. Rapid burial and consolidation of tuffs may occur, after which time they may be preserved depending on uplift and erosion.

3) Rapid alteration of primary glass fragments causes formation of authigenic minerals. Carbonate from alteration and precipitation from water bodies around or within the crater fill the pore spaces of the tuffs and stop the passage of solutions through them. This process of consolidation occurs within a short time under the right conditions, and improves the preservation potential.

It can be seen that preservation of phreatomagmatic material is dependant on many factors. Generalisations on these factors and the resultant deposits will be discussed in Chapter 7, with the formation of a facies model.

4.3. SUMMARY

1. Observed phreatomagmatic activity is highly explosive but periodic in nature. Access of water to the vent is the main factor controlling eruption style.

2. Airfall and base-surge processes deposit tephra but strombolian fire-fountaining may occur at any time if water is excluded from the vent.

3. Syndepositional slumping of loose tephra into the crater and concentric faults are the surface expression of syneruptive subsidence into a diatreme. Post-eruptive subsidence is common especially in maars and occurs along ring faults.

4. Late stage activity commonly consists of strombolian eruptions with associated lava flows, as water is used up or excluded from the vent.

5. Base-surge deposits in eroded maars/tuff-rings contain structures which largely reflect deposition from pulsatory density flows. Steam temperature (and thus moisture content) controls the type of structures formed by surges.

6. Reworking processes greatly modify deposits during and after eruption. The subsiding crater acts as a small depositional basin in which thick reworked sequences may accumulate.

7. Preservation potential of phreatomagmatic products is poor and depends on special conditions. Even though they are the second-most abundant volcano type, they are rarely found in pre-Tertiary sequences.

CHAPTER 5
EAST LOTHIAN DIATREMES

The following two chapters describe tuffs which have subsided to various depths in Scottish diatremes and are presently exposed at diverse structural levels. By comparing closely-spaced diatremes whose surface expressions were probably very similar a composite, idealised cross-section can be constructed. The East Lothian diatreme deposits are generally exposed at higher structural levels than those in Fife, and will be discussed first.

5.1. Introduction and Geological Setting

The East Lothian diatremes cut Upper Old Red Sandstone and Lower Carboniferous (Dinantian) sedimentary and volcanic strata exposed along the coast between North Berwick and Dunbar (Fig. 5.1). Those strata belong to the Garleton Hills Volcanic Rocks (McAdam, 1975) which thicken to the S and include both lavas and tuffs. Little previous work has been carried out on the diatremes although Martin (1955) briefly discussed the North Berwick examples and Francis (1962) described those around Dunbar. Graham & Upton (1978) reported gneissic clasts from tuffs to the W of Partan Craig diatreme which they interpreted as samples from a basement complex at 7-8km depth.

Although the present work is concerned mainly with the diatreme deposits the country rock sediments and tuffs are also mentioned briefly. They are significant because they represent the deposits accumulated around the flanks of those active volcanoes, fed by the diatremes, but themselves rarely and only fragmentarily preserved within the stratigraphical column (Francis, 1983, in press).

The regional dip of the country rocks is variable, but shallow, and results from gentle post-Carboniferous deformation which includes N-S trending open folding as well as normal faulting with a mainly NE-SW trend. These faults are sub-parallel to the Southern Uplands Fault which lies some 15km to the S.

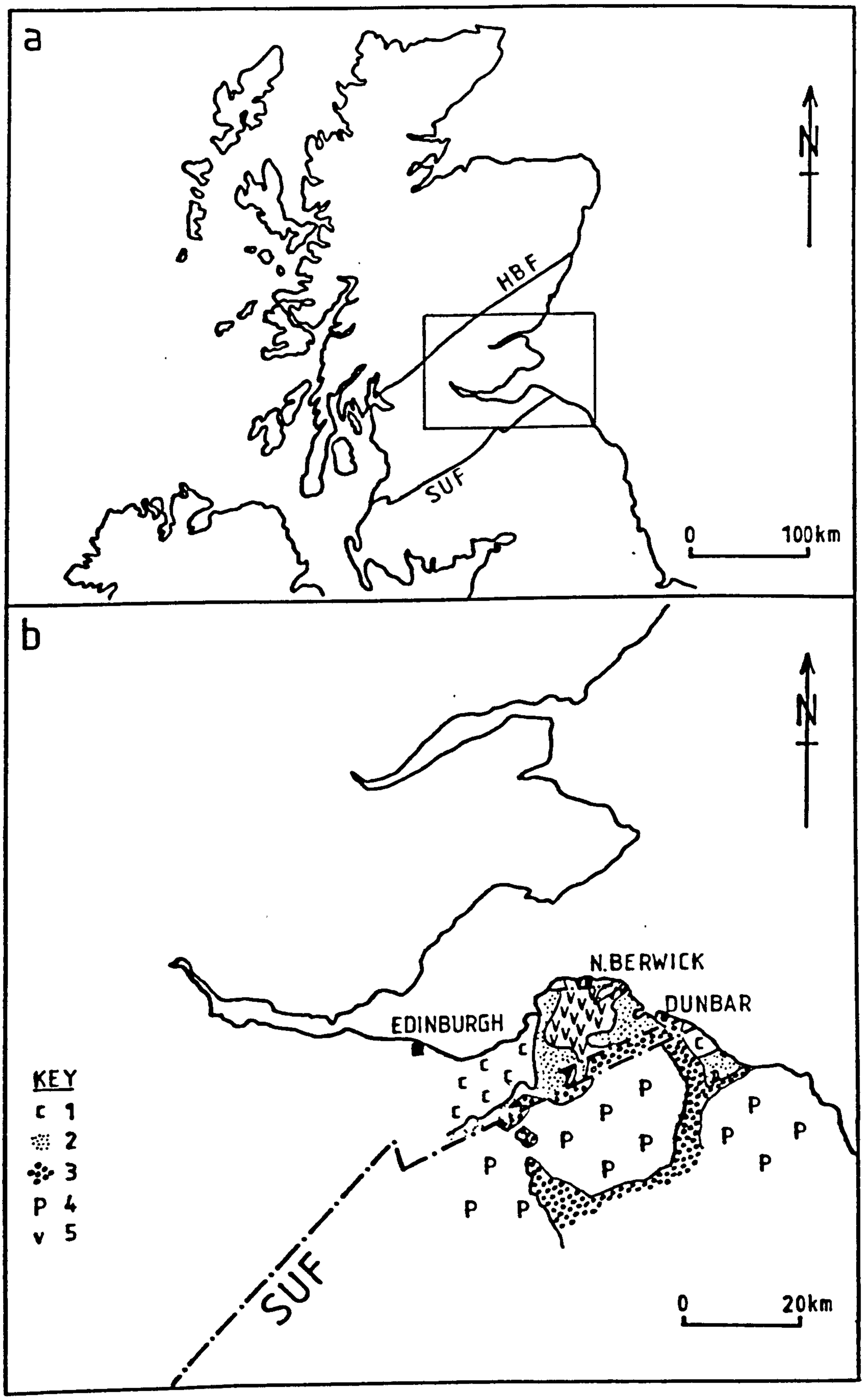

Fig. 5.1 a) Location of the East Lothian diatremes.

b) General geology.
1: Carboniferous Limestone Series
2: Calciferous Sandstone Series
3: Upper O.R.S. Series
4: Pre-Devonian rocks
5: Garleton Hills Volcanic Group

5.2. Country Rock Deposits

5.2.1 Dunbar area

At Dunbar, the country rock sediments and interbedded tuffs consist of >500m of sandstones and cornstones (carbonate palaeosols) of Upper Old Red Sandstone age overlain by >80m of Lower Carboniferous (Cementstone Group of the Calciferous Sandstone Measures) shales, sandstones and cementstones (Francis, 1962). The sediments are commonly red. The lower part of the Cementstone Group contains thin green interbedded tuffs within red marls. Although the sequence generally dips to the E, faulting causes the Carboniferous rocks to occupy the western, and Old Red Sandstone the eastern part of the coast (Fig. 5.2).

5.2.2 North Berwick area

Along the coastal strip from Seacliffe Tower to Milsey Bay, E of North Berwick (Fig. 5.3), the country rocks are all of Lower Carboniferous age and dip at shallow angles to the W. The general succession (after Grieves, 1981) is as follows :-

	Estimated thickness (metres)
Red Basaltic Tuff Formation	100
Limestone / cementstone	3
Green Basaltic Tuff Formation	100
Basaltic Lavas	8
----------Unconformity	
Canty Bay Sandstone Formation	250+

These thicknesses are approximate because lack of marker horizons makes it difficult to correlate across faults.

Canty Bay Sandstone Formation

The main outcrop of this formation is to the E of Seacliffe Beach, but due to faulting it also occurs in Canty Bay and to the S of Gin Head diatreme. The formation consists predominantly of red marls and mudstones with interbedded white sandstones and rare cementstones. Typical logs of the formation are shown in Fig. 5.4. Much of the

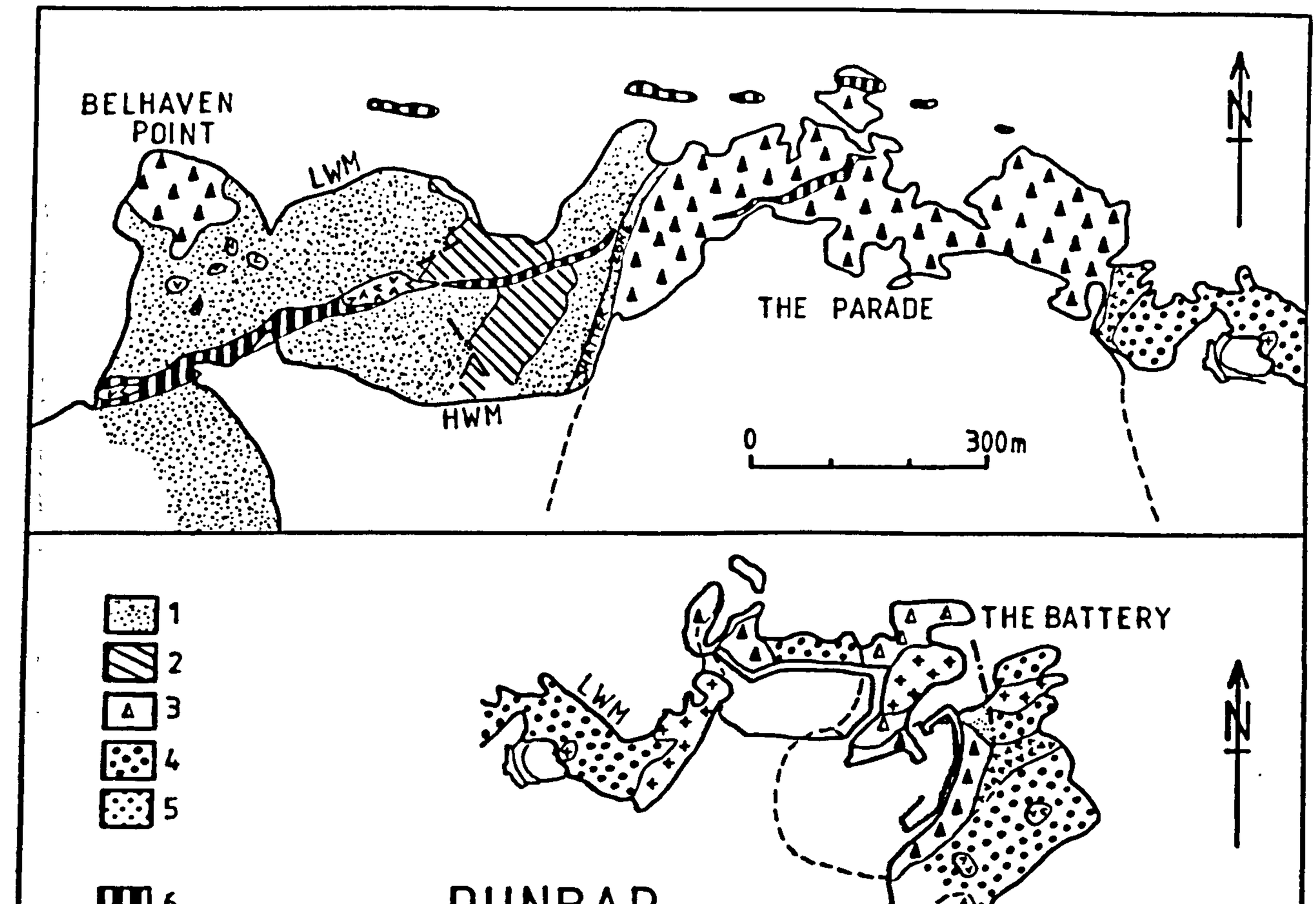

Fig. 5.2 Geological map of the Dunbar area after Francis (1962).
1: Lower Carboniferous cementstones and mudstones
2: Lower Carboniferous sandstones
3: Bedded country rock tuffs
4: Upper ORS sandstones and cornstones
5: Upper ORS flags
6: Quartz dolerite
7: Basalt
8: Diatreme tuffs
9: Tuffisitic breccia

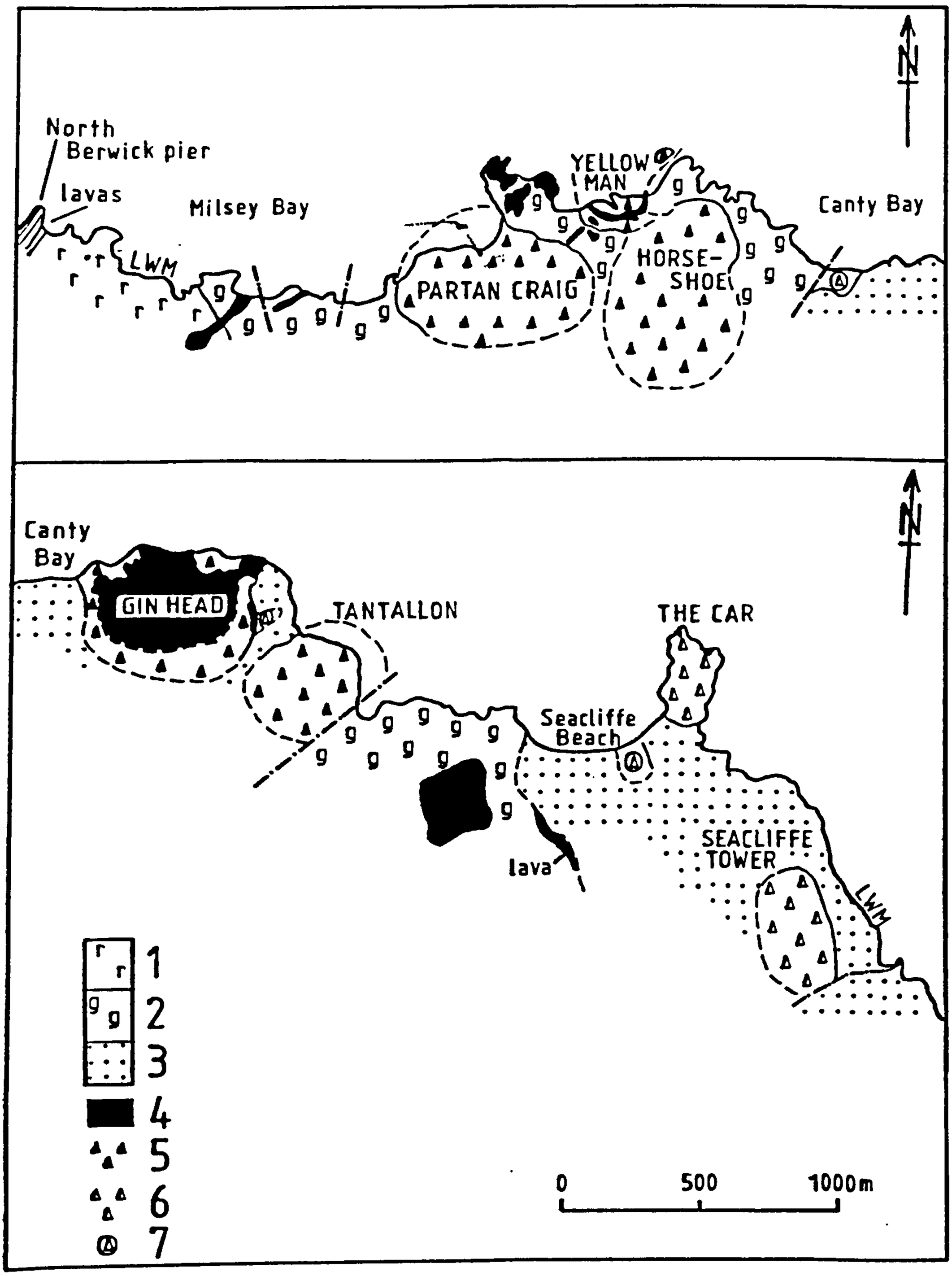

Fig. 5.3 General geology of the North Berwick diatremes.
1: Red Basaltic Tuff Formation
2: Green Basaltic Tuff Formation
3: Canty Bay Sandstone Formation
4: Basaltic lavas and intrusions
5: Tuffs in Green Group diatremes
6: Tuffs in Red Group diatremes
7: Crypto-volcanic structures

following description is taken from Clough et al.(1910) and Grieves (1981).

The red marls and mudstones are well laminated and contain thin siltstone lenses. Low-angle trough cross-bedding is occasionally present, with small intraclasts lying along the bases of the troughs. Some climbing ripples occur, associated with thin silt bands.

Within and generally towards the base of the red marls are more calcareous units. These units are up to 1·5m thick and consist of red cementstone beds individually 5-20cm thick. Some horizons of poorly stratified calcareous siltstone contain abundant sub-spherical, randomly scattered calcrete nodules up to 5cm diameter.

The sandstones are generally white to pink although green patches occur due to reduction of hematite. They are calcareous, medium to fine-grained and up to 3·5m thick. All the sandstone units have erosive bases (Fig. 5.4) which often contain marl and mudstone rip-up clasts, in places so numerous as to form mud clast breccias up to 40cm thick.

At their base the sandstone horizons are trough cross-bedded with foresets up to 1·5m long. Some units contain climbing ripples toward their tops but most fine upwards into plane-bedded siltstones. Laterally discontinuous, thin, structureless horizons with erosive bases are common. These often have planar top-surfaces and are succeeded by trough cross-bedded layers. Cross-laminae are in places disturbed forming soft sediment deformation and dewatering structures (Fig. 5.5).

Towards the top of the Canty Bay Sandstone Formation the marly beds become progressively tuffaceous. The tuffaceous material consists of poorly-sorted red and green ash and fine lapilli in beds up to 5cm thick. Often the ash layers pick out low-angle trough cross-bedding structures in the tuffaceous marls. Only fine volcanic material occurs in the sediments; no blocks or coarse lapilli are found.

The depositional environment of the Canty Bay Sandstone Formation was probably an alluvial plain with meandering rivers. The climate was arid or semi-arid, forming the calcrete horizons associated with soil

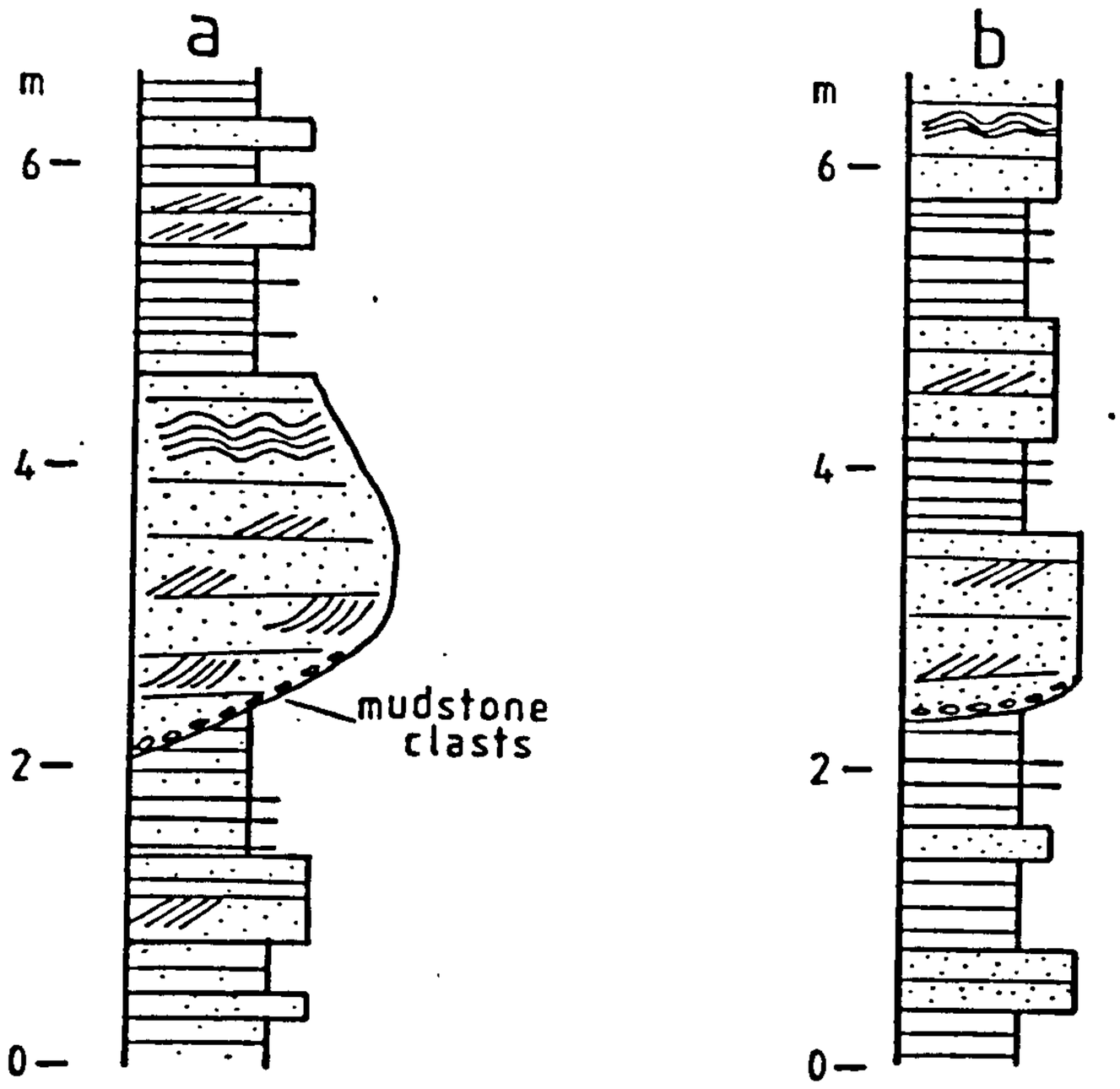

Fig. 5.4 Logs of the Canty Bay Sandstone Formation.
a) Channel sandstone body near Seacliffe Tower
b) Interbedded mudstones and sandstones near the Car diatreme

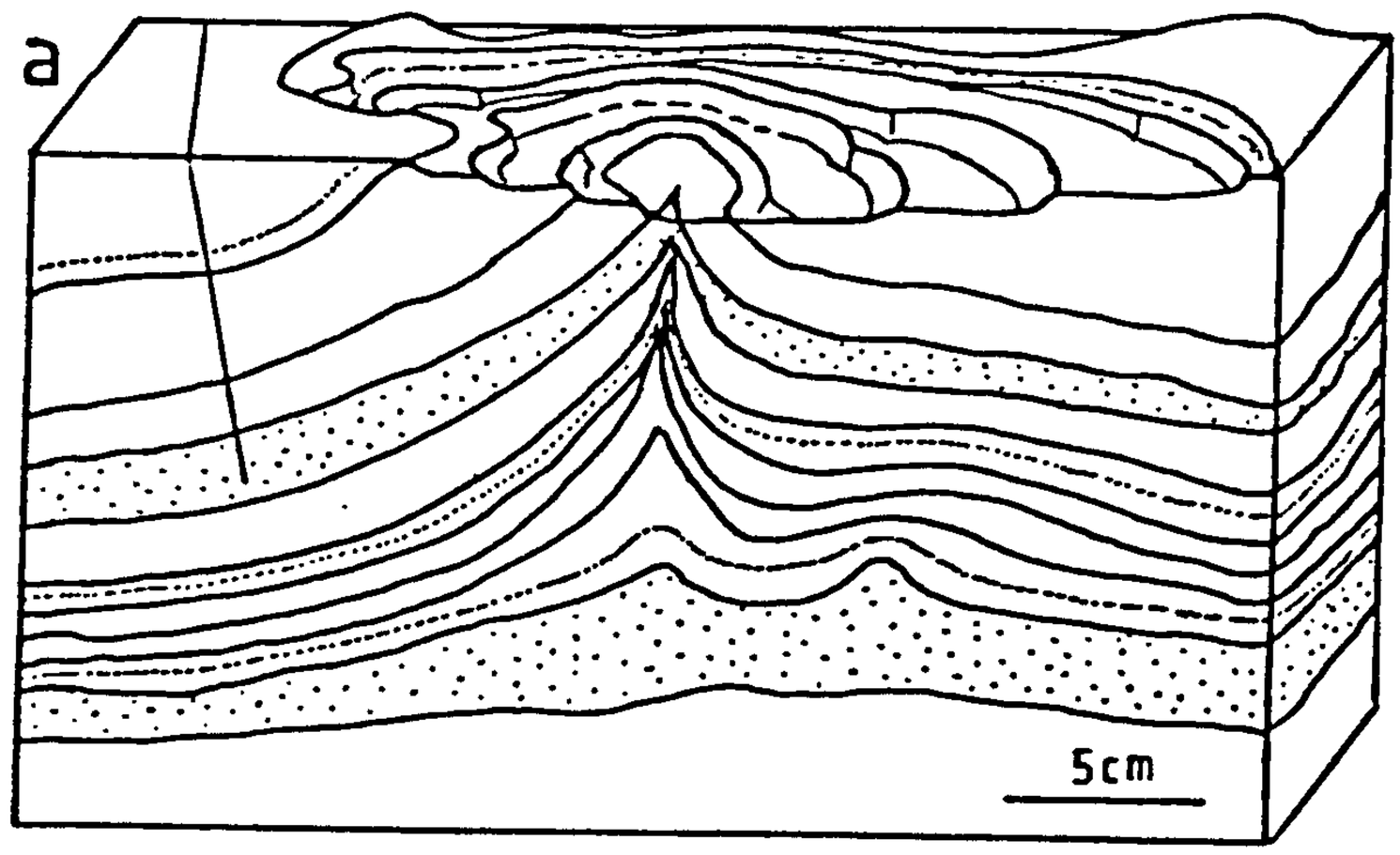

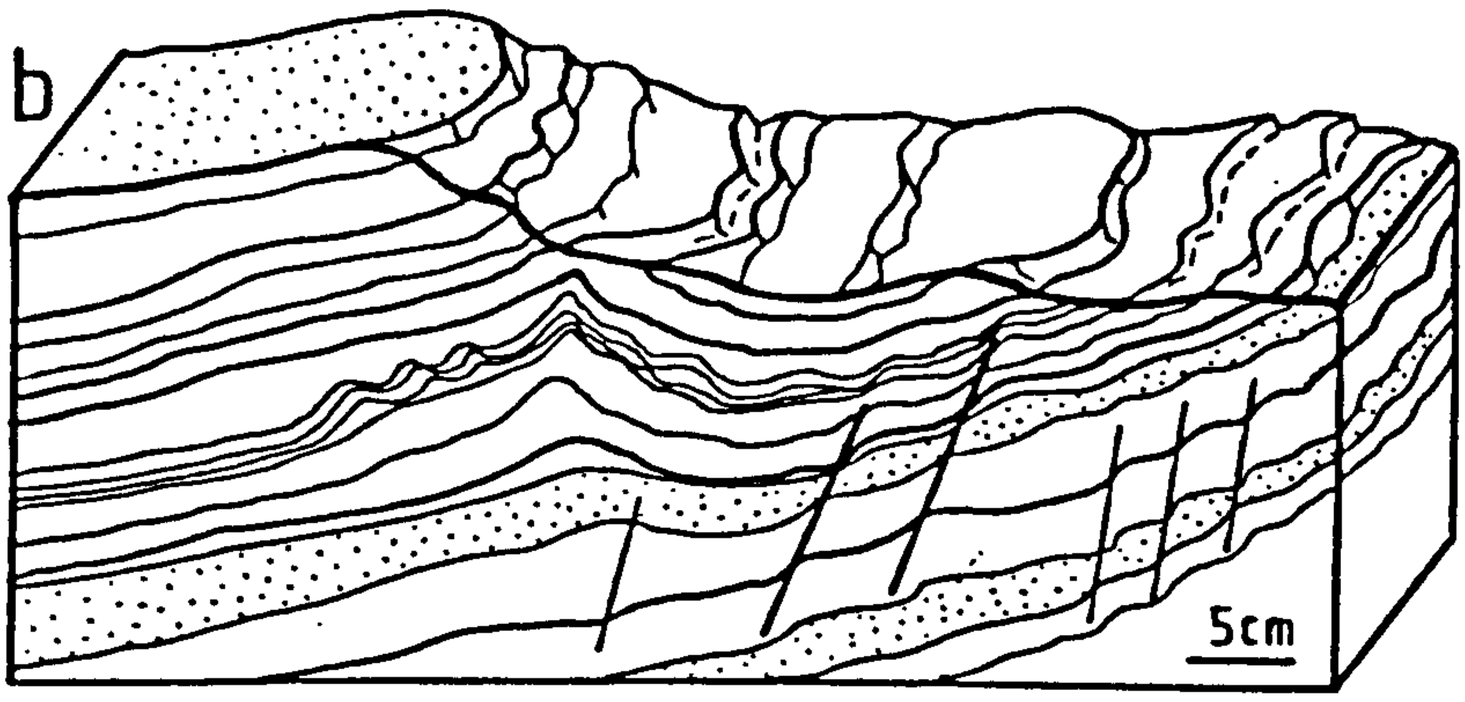

Fig. 5.5 Soft sediment deformation structures in the Canty Bay Sandstone Fm.
a) Sand volcano
b) Slumped bedded sandstones

development on alluvial plains during breaks in deposition. Eruption of Green Basaltic Formation tuffs began nearby and increased in magnitude during deposition of the Canty Bay Sandstone Formation. Reworking of distal tuffs led to their incorporation within the marly overbank deposits.

Green Basaltic Tuff Formation (G.B.T.F.)

This formation crops out a few metres W of Canty Bay Sandstone Formation sediments at the western side of Seacliffe Bay (Fig. 5.3). It appears to overlie them with slight, probably local, angular unconformity. In the cliffs to the S the unconformity is marked by 8m of lavas which have irregular inclusions of sediment within them. The top of the lavas is eroded and G.B.T.F. deposits overlie them. Here the tuffs are red but become locally green to the W due to reduction of hematite.

Near their base the tuffs are red to orange, well laminated and contain variable but generally high proportions of sediment (Fig. 5.6). Typically, fine tuffs are interbedded with tuffaceous siltstones up to 40cm thick, although rare coarse tuffs with basaltic blocks occur near the base. Lenticular blocky units, rich in rounded marl and siltstone clasts up to 20cm, have channel-like erosive bases. Many of these clasts originated by erosion of the underlying deposits. Other blocky units formed by slumping of the tuffs consist largely of bedded tuffs and tuffites. Upwards the proportion of blocky units decreases and the tuffs become finer. Moderately-sorted gravels and lenticular sandstones predominate over blocky deposits. Rare large blocks (up to 70cm) of sediment with asymmetric sags indicate that volcanic activity occurred to the S or SE of the area.

Clast imbrication and rare cross-laminations in the finer units indicate local current directions from the E. Three angular unconformities occur in the lower parts of the G.B.T.F. To the W of this the tuffs lose their red colouration, become bleached and are cut by small faults infilled with hematite and calcite. An E-W normal fault exposed in the cliffs separates red tuffs to the S from green tuffs on the foreshore SW of Seacliffe Harbour.

This fault has a downthrow of 3-4m and is presumed to have acted as a barrier to solutions which caused the local colouration of the tuffs. To the W and and up-sequence the red tuffs merge into green tuffs over a zone 50m wide.

The green tuffs are generally finer, more calcareous and contain fewer sediment clasts than the red tuffs (Fig. 5.6). Lapilli-rich tuffs are commonly interbedded with marls, with rare blocky units formed by slumping and debris flows (Fig. 5.7). Many of the lapilli-rich tuffs are normally graded and all are well sorted. The marls and cementstones are most abundant towards the exposed top of the unit, where they contain much carbonaceous plant debris.

Sedimentary structures (Fig. 5.8) in the green tuffs include small-scale cross-bedding, mud lenses, soft sediment deformation by impact of basaltic bombs, wave ripples and channels. One large channel (Fig. 5.9) occurs in the cliffs SE of Oxroad Bay. The channel is a largely constructional feature perhaps related to infilling of a depression. Some of the marly tuffs are fossiliferous and contain worm-burrows. In places tuffaceous sandstone dykes have been injected into the tuffs. They may be either tuffistic, gas-fluidized intrusions or sediment injections.

The G.B.T.F. also forms the country rocks around the Partan Craig, Yellow Man and Horseshoe diatremes (Fig. 5.3). Here the formation consists of well-bedded tuffs with interbedded siltstones, mudstones and marls. Low-angle trough cross-bedding, channels and blocky debris flows occur as well as many normally graded units. Cementstone beds occur in small basins NE of Partan Craig and also at the top of the formation in Milsey Bay (Fig. 5.3). Towards the top of the formation thin tuffaceous sandstones are interbedded with the tuffs. These have asymmetric, sinuous-crested ripples and small rhomboid ripples on their top surfaces (Fig. 5.10). Rare basaltic blocks within the tuffs sometimes have small sags beneath them, indicating fallout onto tuffs accumulating subaqueously. One example of a deep impact crater is seen beneath a small block in the country rock tuffs N of Horseshoe diatreme (Fig. 5.11). The tuffs above the block are coarse and poorly-bedded and probably

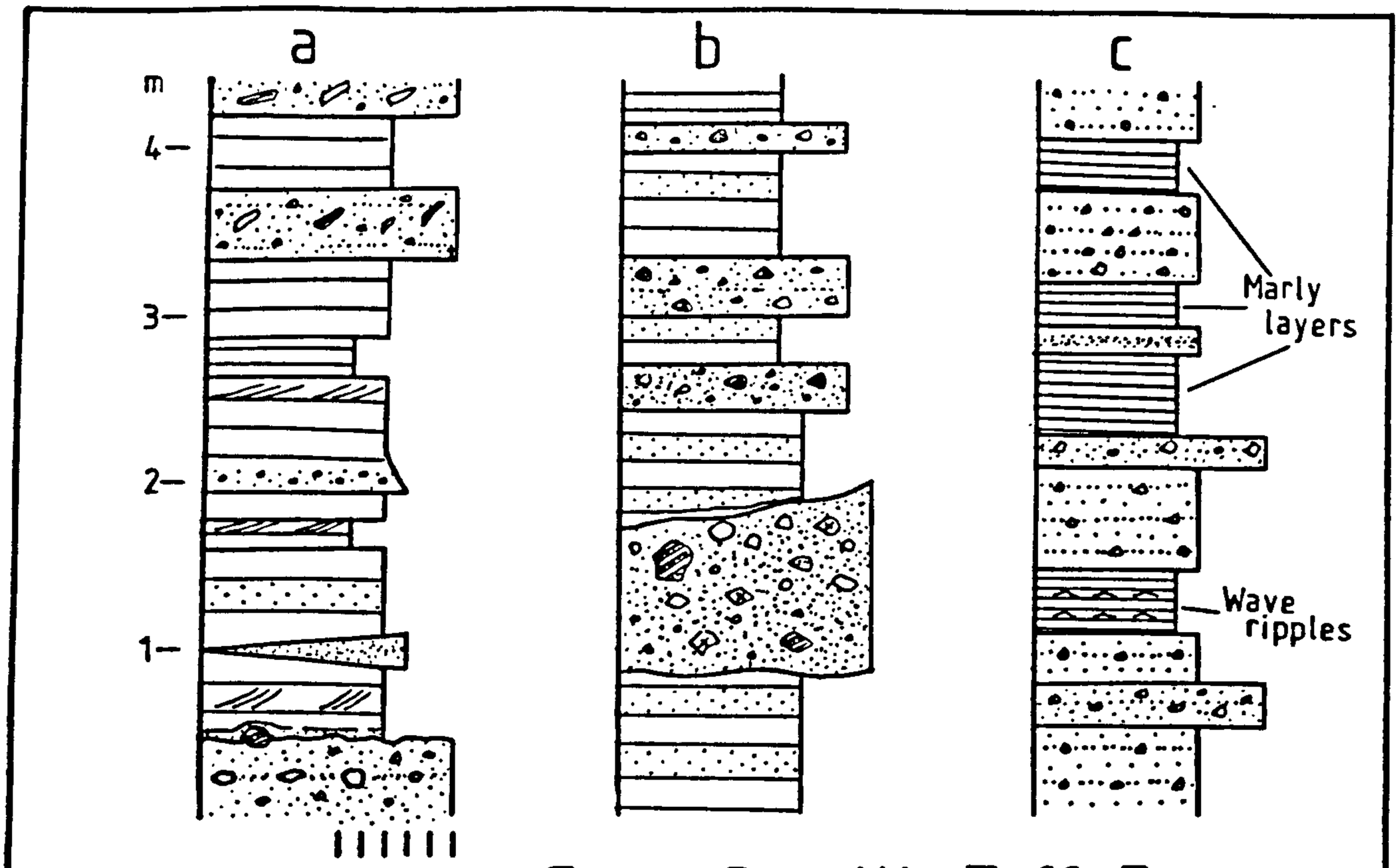

Fig. 5.6 Green Basaltic Tuff Fm.

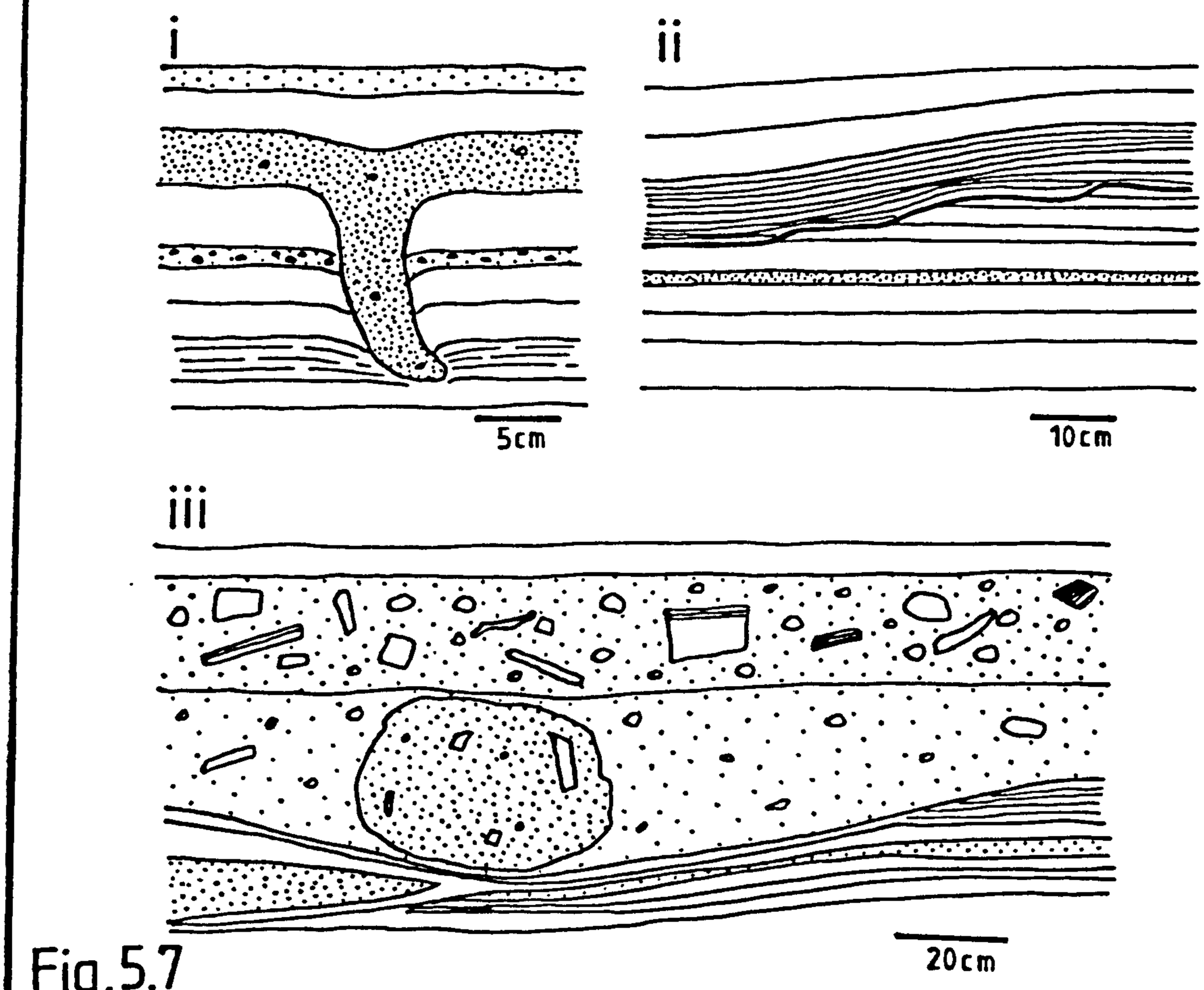

Fig. 5.7

Fig. 5.6 Logs of the Green Basaltic Tuff Fm.
a) W of Seacliffe Beach
b) Between the Car and Tantallon diatremes
c) Near the SE margin of Tantallon diatreme

Fig. 5.7 Structures in the G.B.T.F. W of the Car diatreme.
i) Downward-cutting injection structure
ii) Small erosional unconformity
iii) Load structure at base of coarse debris flow.

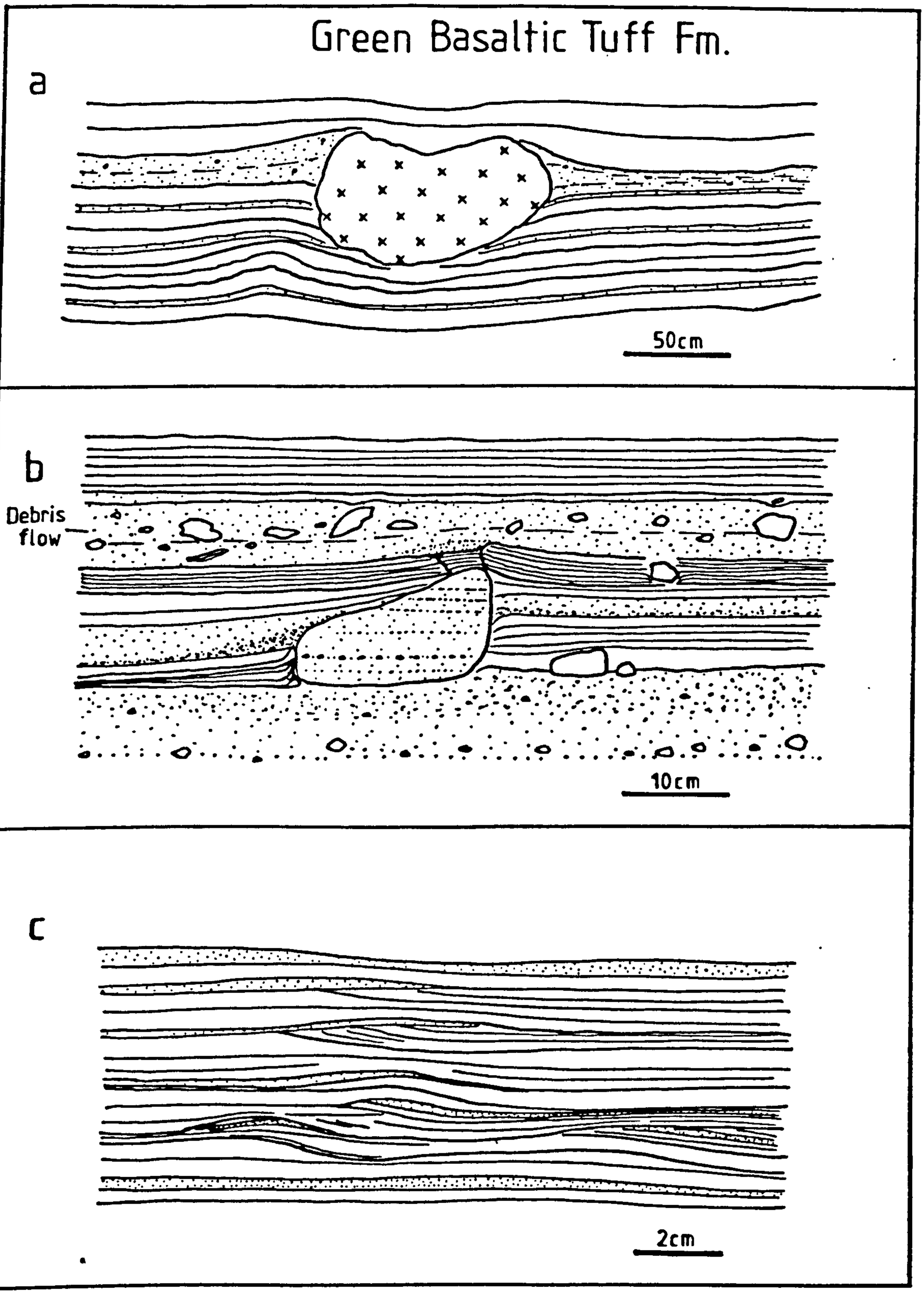

Fig. 5.8 Structures in the G.B.T.F. E of the Tantallon diatreme.
a) Basalt block which probably fell into shallow water in which the tuffs were deposited.
b) Blocky debris flows which moved into shallow water. Projecting blocks were mantled by fine waterlain ash.
c) Small ripples in marly tuffs indicative of weak currents in shallow lakes.

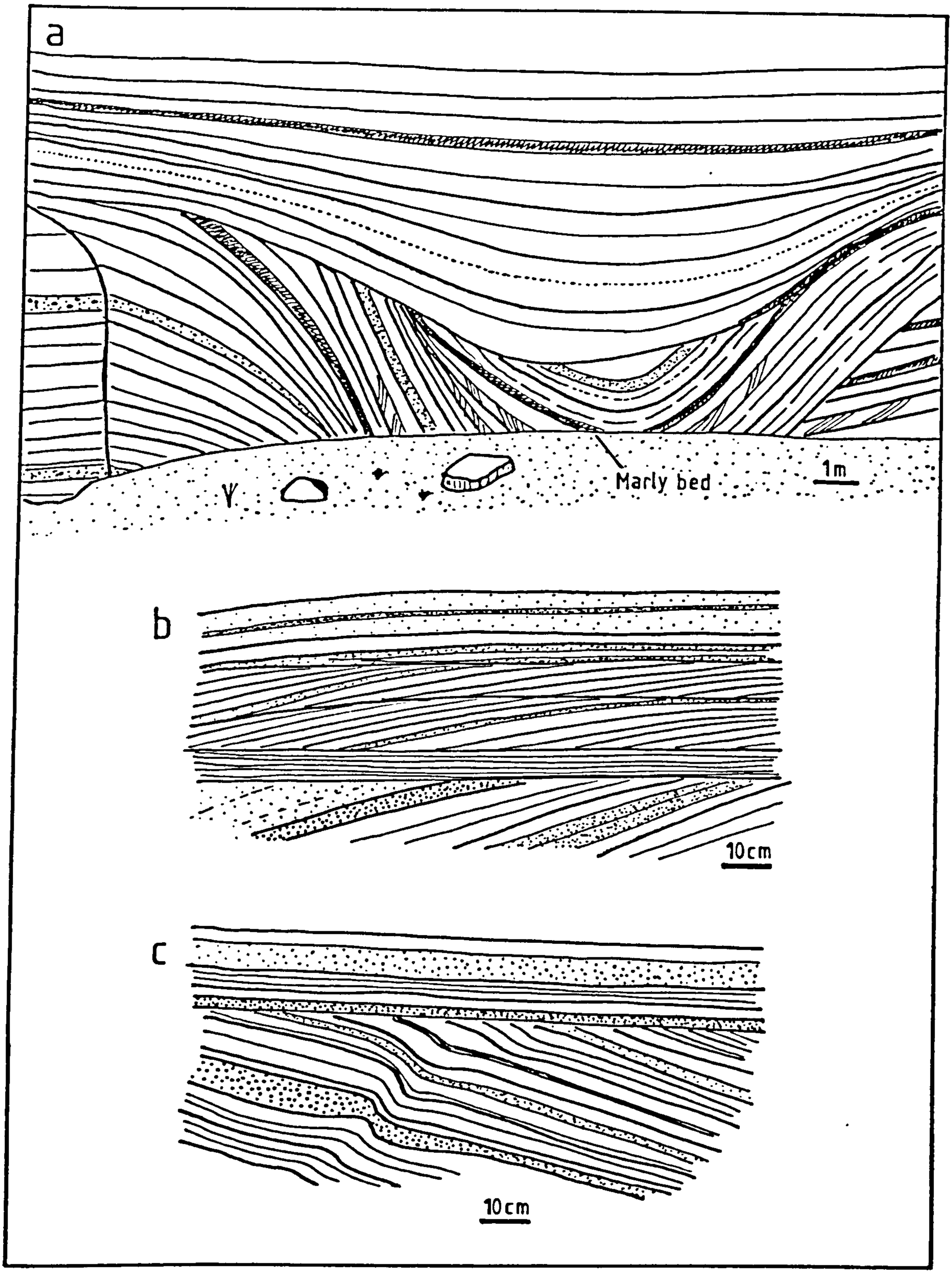

Fig. 5.9 a) Large channel in the G.B.T.F. E of Tantallon diatreme. Note oversteepened bedding due to subsidence, and erosive partings in the infilling sequence.
b) Convex-upward cross-bedding in the channel fill tuffs, perhaps due to dune faces being eroded during migration.
c) Slightly slumped cross-beds in the channel fill deposits.

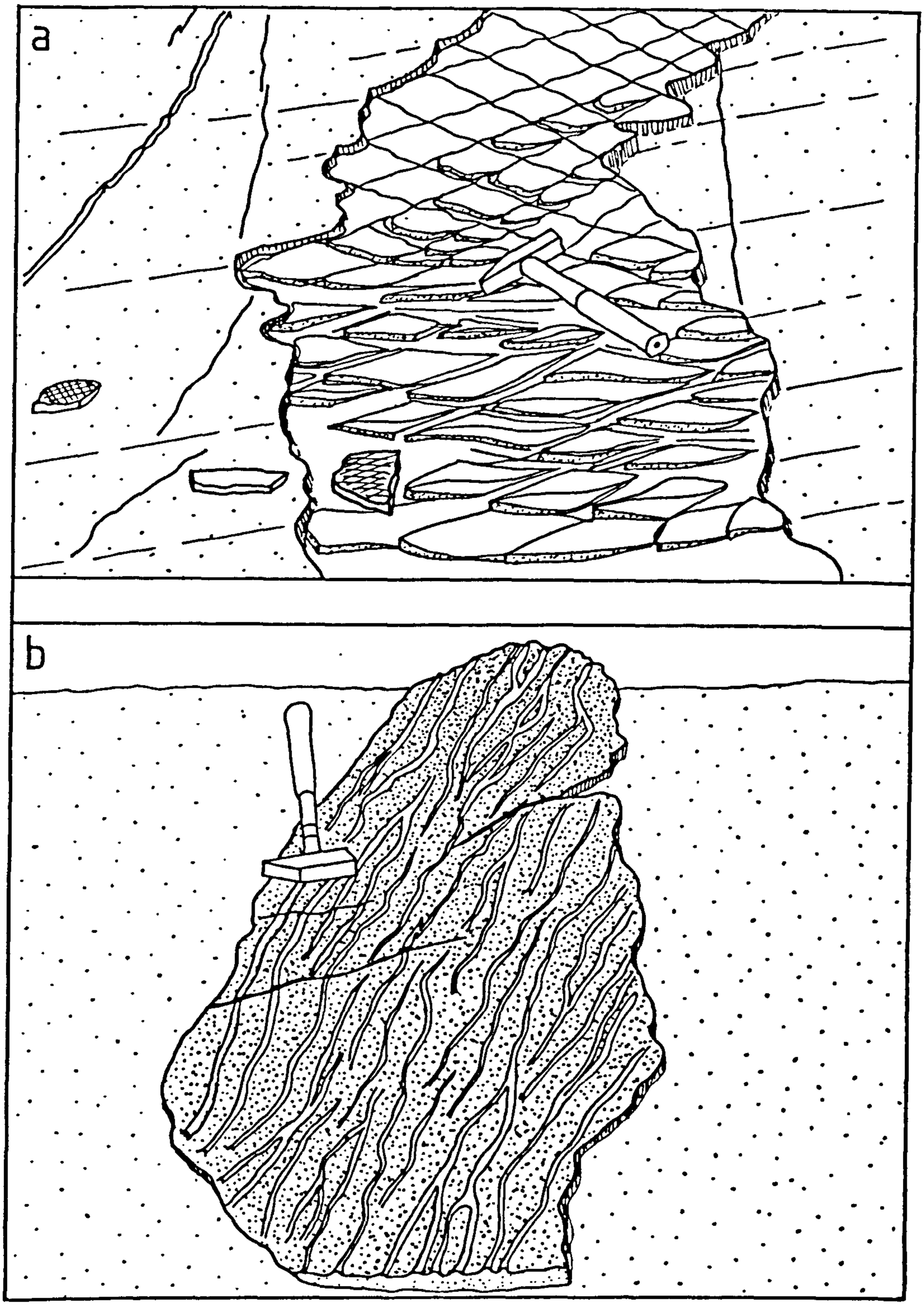

Fig. 5.10 G.B.T.F. deposits W of the Partan Craig diatreme.
a) Rhomboid ripples in reworked tuffs
b) Rippled tuffaceous sandstone, probably reworked by tidal action

represent airfall material deposited on reworked water-saturated tuffs exposed at the surface or beneath shallow water.

The G.B.T.F. contains a number of units laid down in spatially associated environments. The lowermost unit consists largely of proximal-to-mid alluvial fan red deposits with interbedded debris flow, sheetflood and channel layers. The red colour is due to the incorporation of large amounts of red sediment, although further breakdown of ferromagnesian minerals may have occurred after deposition.

The succeeding unit consists mainly of lacustrine reworked tuffs into which debris flows occasionally brought coarser clasts. Volcanism was more active, though distal, and contributed mainly fine ash. This calcareous facies might be interpreted as playa deposits or floodplain silts which encroached on to the alluvial fan as relief subsided (Collinson, 1978).

The uppermost unit consists of playa deposits on an alluvial plain across which meandering channels migrated. Some of the lakes were large enough to have generated wave ripples. Algal limestones (Turner, 1980) in the tuffs W of North Berwick indicate shallow water lagoonal conditions. Locally, volcanic activity reached a peak during deposition of the G.B.T.F. in the W and declined towards the top of the formation.

Red Basaltic Tuff Formation (R.B.T.F.)

The top of the Green Basaltic Tuff Formation is separated from the base of the R.B.T.F. by 3m of green calcareous mudstone. In Milsey Bay (Fig. 5.3) this bed marks the transition between green calcareous tuffs of the upper G.B.T.F. and red tuffaceous marls of the lower R.B.T.F. The remainder of the R.B.T.F. consists of red tuffs with interbedded cementstones and tuffaceous marls. Both red and green lapilli occur in a red fine-grained, tuffaceous matrix which also contains basalt blocks up to 15cm across. Normally graded units are abundant, as are low-angle cross-laminations.

A conglomeratic unit occurs to the W of a 80m wide disturbed zone in which large bedded blocks have rotated

almost in place due to syndepositional slumping (Martin, 1955). This unit contains rounded blocks of both red and green tuffite as well as basalt and cementstone. The coarse unit has an erosive, channelled base and fines upwards into tuffaceous marls and siltstones. At the top of the formation four lavas conformably overlie the red tuffs. The lowest lava is overlain by 5m of red tuffaceous sediments and contains irregular sediment inclusions at its base.

The R.B.T.F. was deposited in shallow, probably lacustrine, water into which ash was falling. Slumping of consolidated tuffs was perhaps initiated by volcanic tremor which might also have been associated with local uplift, thereby providing a source area for the fluvial conglomerate (Turner, 1980). A reversion to lacustrine sedimentation afterwards was followed by flow of lavas into the shallow water with incorporation of some of the wet sediments at the bases of flows.

A schematic diagram illustrating the sedimentary environment into which the East Lothian volcanoes erupted is shown in Fig. 5.11.

5.3. Diatreme Deposits

The diatremes in East Lothian have been divided into a Red Group and a Green Group (on the basis of their different infilling deposits) by Martin (1955) who believed the Green Group diatremes to be the younger because they cut younger sediments than the Red Group. This evidence is not conclusive and the likely ages of the diatremes will be discussed later. In addition to the diatremes, smaller areas of brecciated country rock occur along the coastal section. As these crypto-volcanic structures represent initial, arrested stages in the formation of diatremes (and their surface volcanoes) it is convenient to treat them first (Fig. 5.4).

5.3.1 Crypto-volcanic structures

Numerous small circular or oval areas (10-50m diameter) of brecciated country rock occur at Dunbar (Fig. 5.2). These structures were described by Francis (1962) as

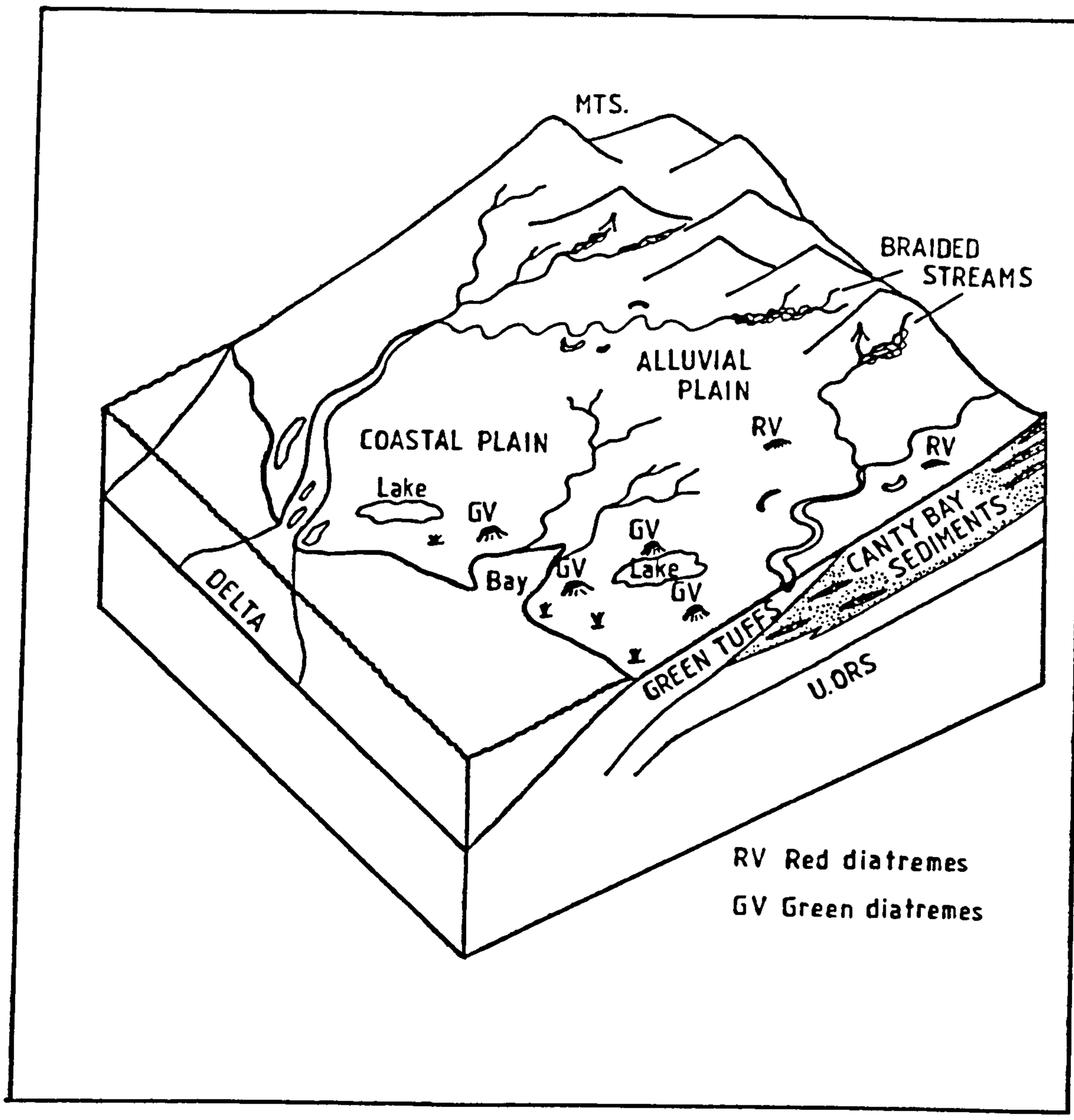

Fig. 5.11 Depositional environment during formation of the East Lothian diatremes. Green diatremes formed in more marginal environment than the Red diatremes.

"incipient necks which never reached the surface". Doming of the country rocks occurred with intrusion of tuff and brecciation of the central beds of the dome. Flow-alignment of elongate blocks forms narrow concentric zones at the margins of these ring structures, which are often defined by inwardly inclined fractures. Collapse of brecciated material into the centre of the rings caused basin-like structures to be developed (Fig. 5.12). Some ring structures contain much comminuted sediment and fragments from various adjacent levels in the country rocks. These represent deeper erosional levels than structures whose breccia blocks are larger and may be directly correlated with the surrounding strata. Elongation of some of the structures along a NE-SW trend occurs, and activity may have been fault-controlled.

The crypto-volcanic structures E of North Berwick are generally larger than those at Dunbar, but formed in the same way. The best example occurs on Seacliffe Beach S of the Car (Fig. 5.2). Here, the disturbed zone measures at least 150x300m and its well-exposed eastern margin cuts red mudstones, sandstones and marly tuffs of the Canty Bay Formation. The margin is sharp and rotated blocks of country rock strata dip into the structure at up to 70°. Blocks reach lengths of 12m and are embedded in a matrix of occasionally flow-banded red tuffaceous mudstone. Many blocks of tuffaceous mudstone and marl have rounded margins whereas the sandstone blocks are angular and irregularly shaped.

Some of the blocks are veined by tuffisite which penetrates along bedding planes or stopes small fragments from the block margins. The sandstone blocks often contain deformed laminae and areas of "swirled stratification" suggesting plastic deformation of poorly-consolidated sediment. The margins of the sandstones are covered with small irregular pits and hollows (Fig. 5.12). These formed by weathering out of small stringers of intrusive tuff which infiltrated the blocks.

Blocks of red tuff, unlike any lithology found in the adjacent country rock sequence, are also found. These

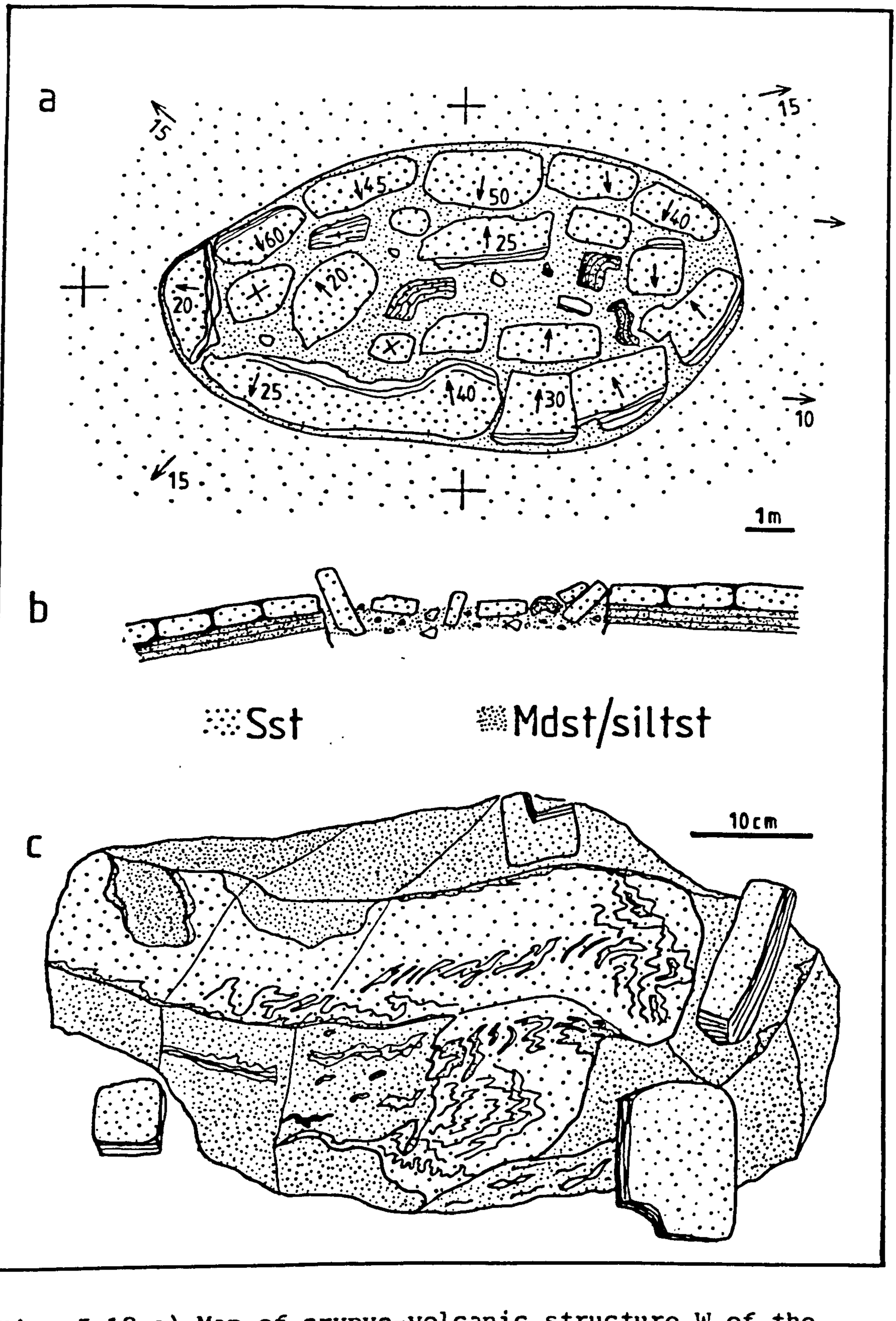

Fig. 5.12 a) Map of crypyo-volcanic structure W of the Parade diatreme.
b) Section of the structure showing doming of country rocks.
c) Block of sandstone with irregular margins cut by tuffisite and invaded by mudstone stringers.

contain base-surge cross-bedding and accretionary lapilli and will be described in the following section on diatreme deposits. It is suggested that the tuffs were incorporated by subsidence of material from higher levels in the Canty Bay Sandstone Formation, which has since been removed by erosion.

5.3.2 Red Group diatremes

The best exposed members of this group are the Seacliffe Tower and the Car diatremes E of North Berwick, and the Parade diatreme at Dunbar.

Seacliffe Tower

This diatreme (Fig. 5.13) cuts lower Canty Bay sediments 6km E of North Berwick (Fig. 5.3). Its NW margin consists of a step-like wall of poorly-bedded tuffs against which country rock sediments are turned down (Fig. 5.14). The margin is irregular and faulted; the shallowly NW-dipping country rocks outside are turned-over so as to dip SE into the neck at up to 50° within 10m of the contact. In the SW the margin is a curved normal fault. Detached blocks (up to 20m across) of country rock frequently occur within the diatreme near the margin, along with collapsed bedded tuffs.

The diatreme infill consists of red, bedded tuffs and unbedded tuffs containing large blocks of sediment and older tuff. The bedded tuffs are predominantly of lapilli and ash grade but agglomeratic layers occur in places. All the "tuffs" have a sedimentary component which may vary between 10 and 90%, and many would be better described as tuffites.

The bedding is defined by moderately-sorted lapilli layers up to 30cm thick, interspersed with fine red ash. In places the lapilli layers have pinch-and-swell structures or wedge out. Most beds are ungraded although clast-rich layers sometimes exhibit coarse-tail grading. Clasts include mudstone, siltstone, marl, bedded tuff, tuffaceous sediments, basalt (blocks and bombs) and rare sandstone. Coarse layers are laterally discontinuous and some consist largely of bedded tuff clasts in a fine tuff matrix.

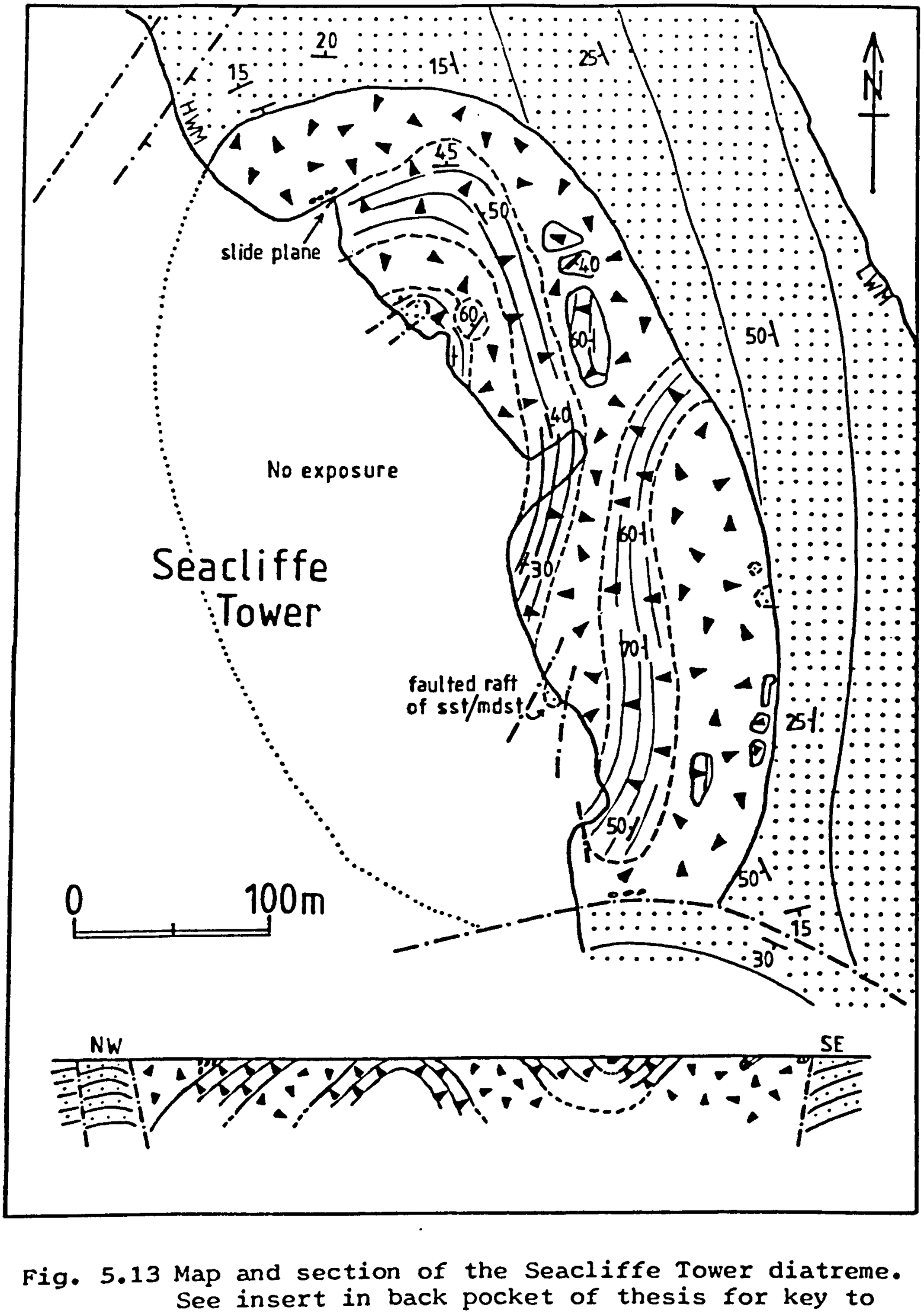

Fig. 5.13 Map and section of the Seacliffe Tower diatreme. See insert in back pocket of thesis for key to diatreme maps.

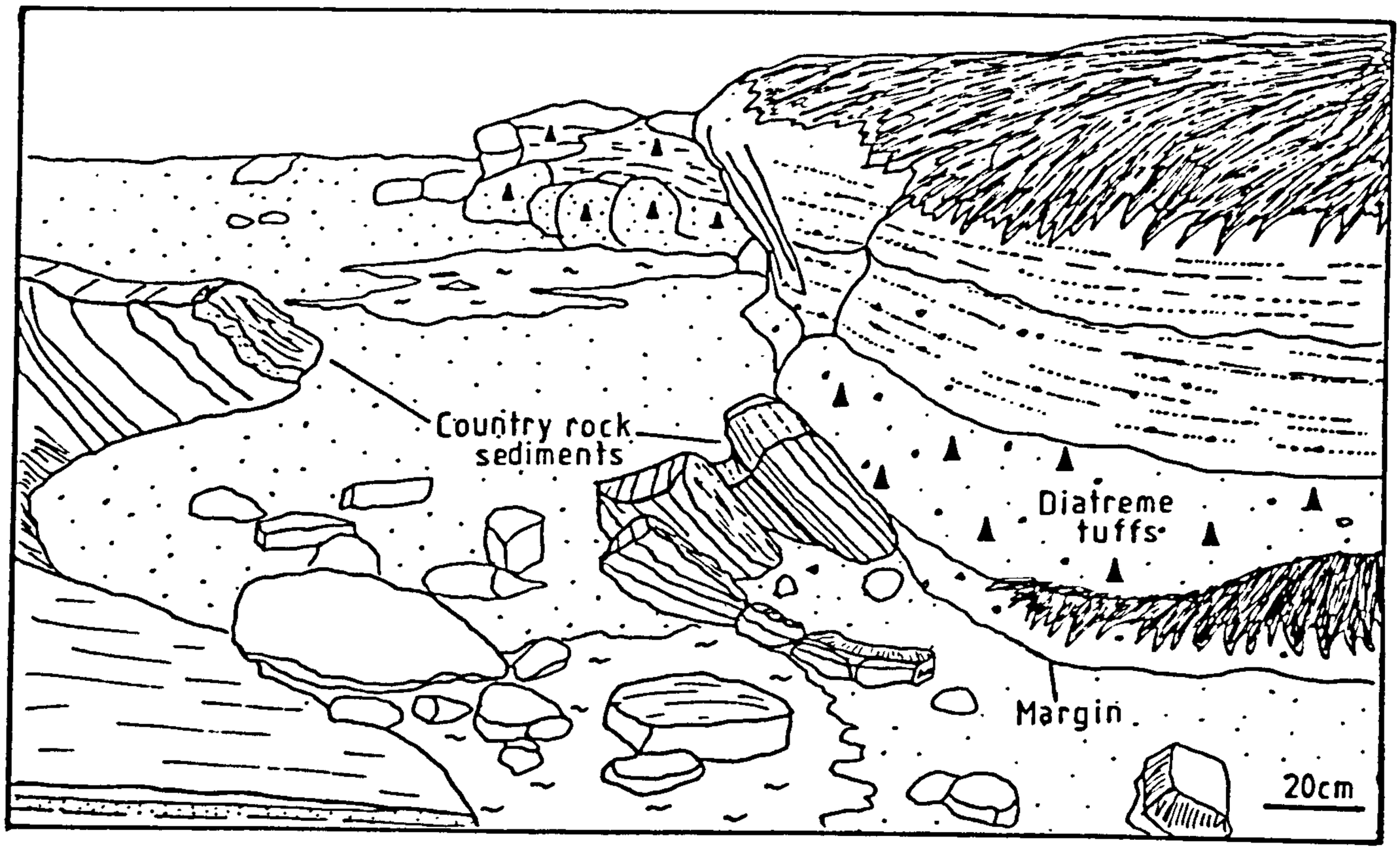

Fig. 5.14 Western margin of the Seacliffe diatreme. Note country rocks dipping into the margin.

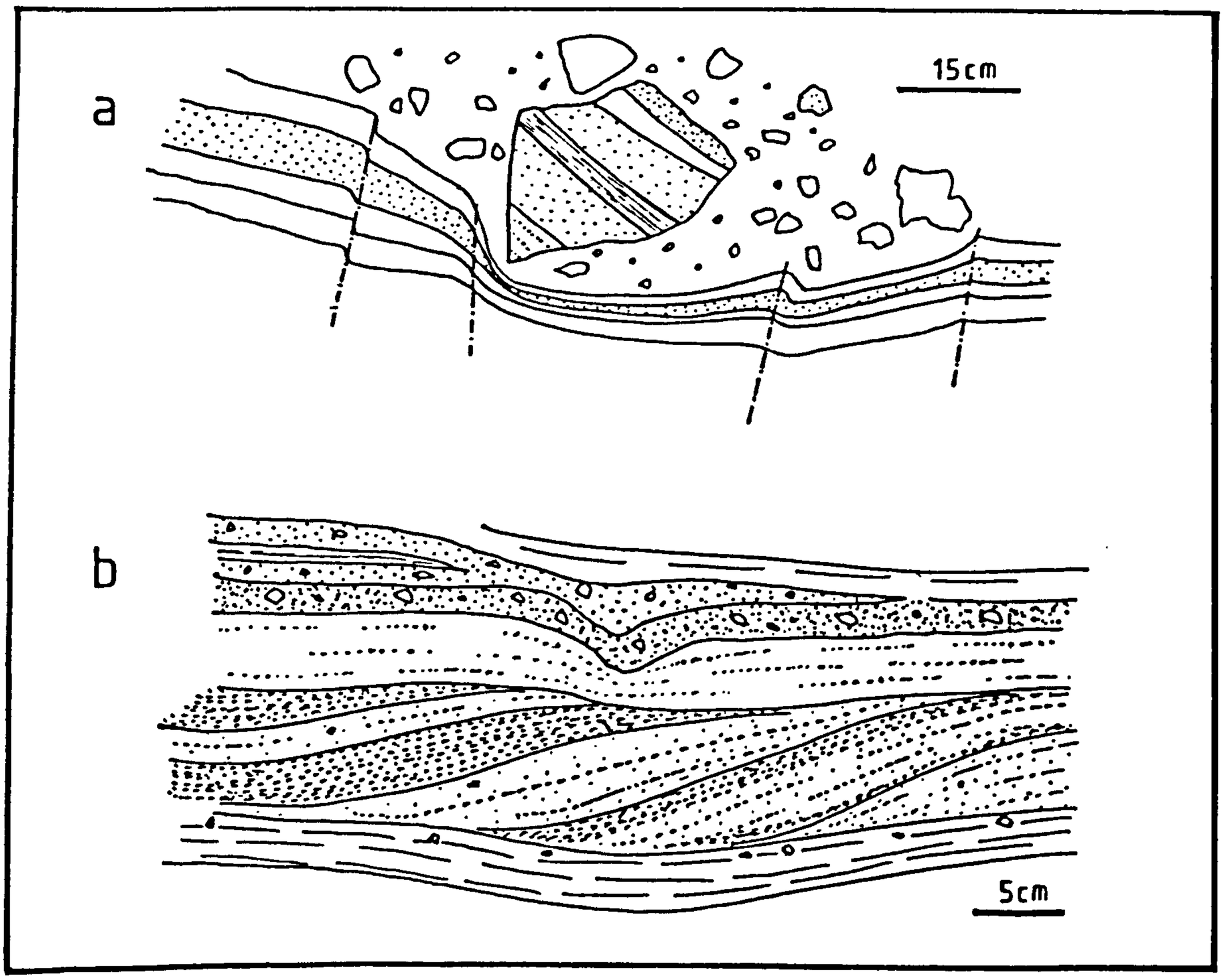

Fig. 5.15 a) Block sag in the Seacliffe diatreme tuffs, showing deformation of tuffs by plastic flow and by microfaulting.
b) Surge trough cross-bedding in the Seacliffe diatreme tuffs. Note the sigmoidal shape of some of the sets.

In places these layers have slightly erosive bases and are interpreted as debris flows.

Block sags are rare, largely because clasts tend to occur in discrete coarse layers (Fig. 5.15a). Blocks impacting onto such layers would cause much less deformation than if isolated blocks fell onto fine, bedded ash. Where blocks do occur in well-bedded tuffs they often plastically deform the underlying layers (Fig. 5.14), indicating that the tuffs were moist and cohesive. Some blocks are mantled by layers which thin over, or are thicker on one side of the block.

Cross-bedding is not readily distinguished in the tuffs but small-scale examples are recognised throughout the diatreme. In the finer tuffs, cross-laminations are trough shaped and dip at 10-15° (Fig. 5.15). In coarser tuffs, cross-bedding is sigmoidal, low-angle and defined by trails of lapilli. All the cross-bedding is small-scale and sets rarely exceed 50cm long and 20cm high. The low-angle form of the cross-bedding and its common association with pinch-and-swell bedding, shallow channels 1-2m wide and beds which thin over the top of projecting blocks indicate that deposition was by base-surges. The 3-D exposures are too poor for making directional readings on such structures. Typical logs of the Seacliffe tuffs are shown in Fig. 5.16.

Structurally the diatreme consists of discrete zones of bedded and massive tuffs separated by sharp or gradational contacts. The bedded zones are roughly concentric to the neck margin and their dips define basin and domal structures separated by unbedded tuffs (Fig. 5.13). The margins of some parts of the bedded zones are diffuse, marked by breakdown of bedding into blocks which are rotated and separated by unbedded tuffs. Slide planes parallel to bedding (Fig. 5.17) form sharp boundaries above which blocky unbedded tuffs occur. In places, the slide planes slightly cross-cut the bedding, but are remarkably parallel over ten's of metres. One slide plane separates a raft containing steeply dipping tuffs from gently dipping tuffs below. The contact dips NE at 25° and is represented by a 10cm brecciated zone full of irregular sediment clasts.

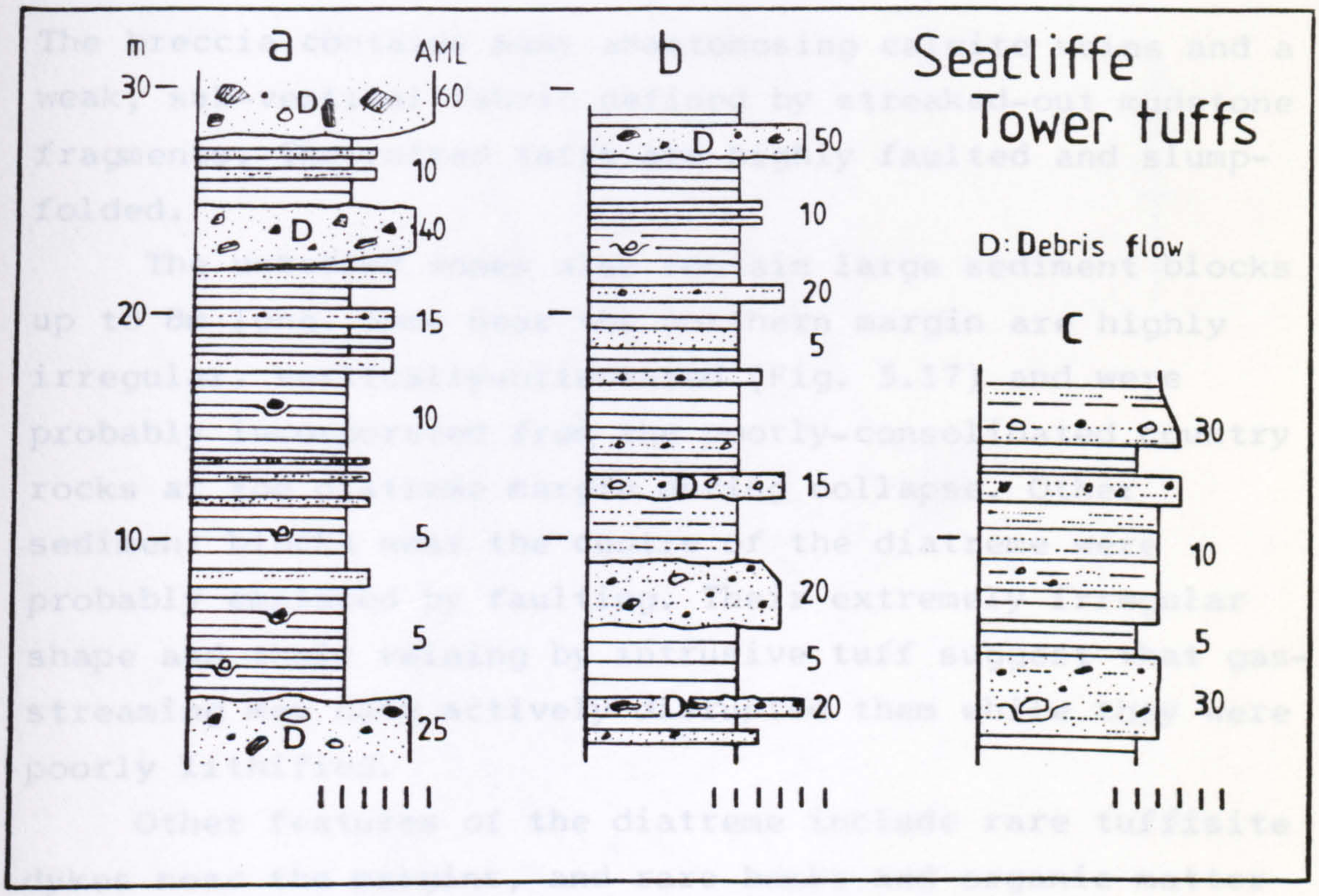

Fig. 5.16 Typical logs of the Seacliffe Tower diatreme tuffs
a: near northern margin b: centre of diatreme
c: near southern margin

Fig. 5.17 Slide plane separating bedded Seacliffe tuffs from massive tuffs containing white mudstone clasts. Hammer measures 30cm.

The breccia contains many anastomosing calcite veins and a weak, sub-vertical fabric defined by streaked-out mudstone fragments. The rafted tuffs are highly faulted and slump-folded.

The unbedded zones also contain large sediment blocks up to 8m long. Some near the northern margin are highly irregular, vertically-orientated (Fig. 5.17) and were probably incorporated from the poorly-consolidated country rocks at the diatreme margin during collapse. Other sediment blocks near the centre of the diatreme were probably emplaced by faulting. Their extremely irregular shape and their veining by intrusive tuff suggest that gas-streaming may have actively disrupted them while they were poorly lithified.

Other features of the diatreme include rare tuffisite dykes near the margins, and rare bombs and organic matter in the tuffs. The bombs have a cracked, slightly vesicular outer surface and may be of cauliflower type (Lorenz, 1973), although similar structures could have been formed by shattering of an intrusive plug at depth. The organic matter consists of calcite-replaced twigs or plant stems up to 2cm diameter. The tuffs around the twigs are green due to local reducing conditions around the decaying vegetation.

The internal deformation of the diatreme tuffs is thought to be due to compression on collapse. Grieves (1981) interpreted the structure as being due to the subsidence of crater deposits which contained a small parasitic tuff-cone. No evidence for such a structure is present other than domed tuffs. The slide planes and the large areas of unbedded tuff suggest that subsidence of tuffs largely occurred whilst they were poorly consolidated.

<u>The Car</u>

This diatreme (Fig. 5.18) cuts Cànty Bay Formation sediments at the E side of Seacliffe Beach (Fig. 5.3) and forms a peninsula exposed only at low tide. The southern margin is similar to the Seacliffe diatreme with country rock sandstones and marls dipping into the structure at 30° to 50°. An embayment in the eastern margin contains disrupted sediments and may be a faulted raft incorporated

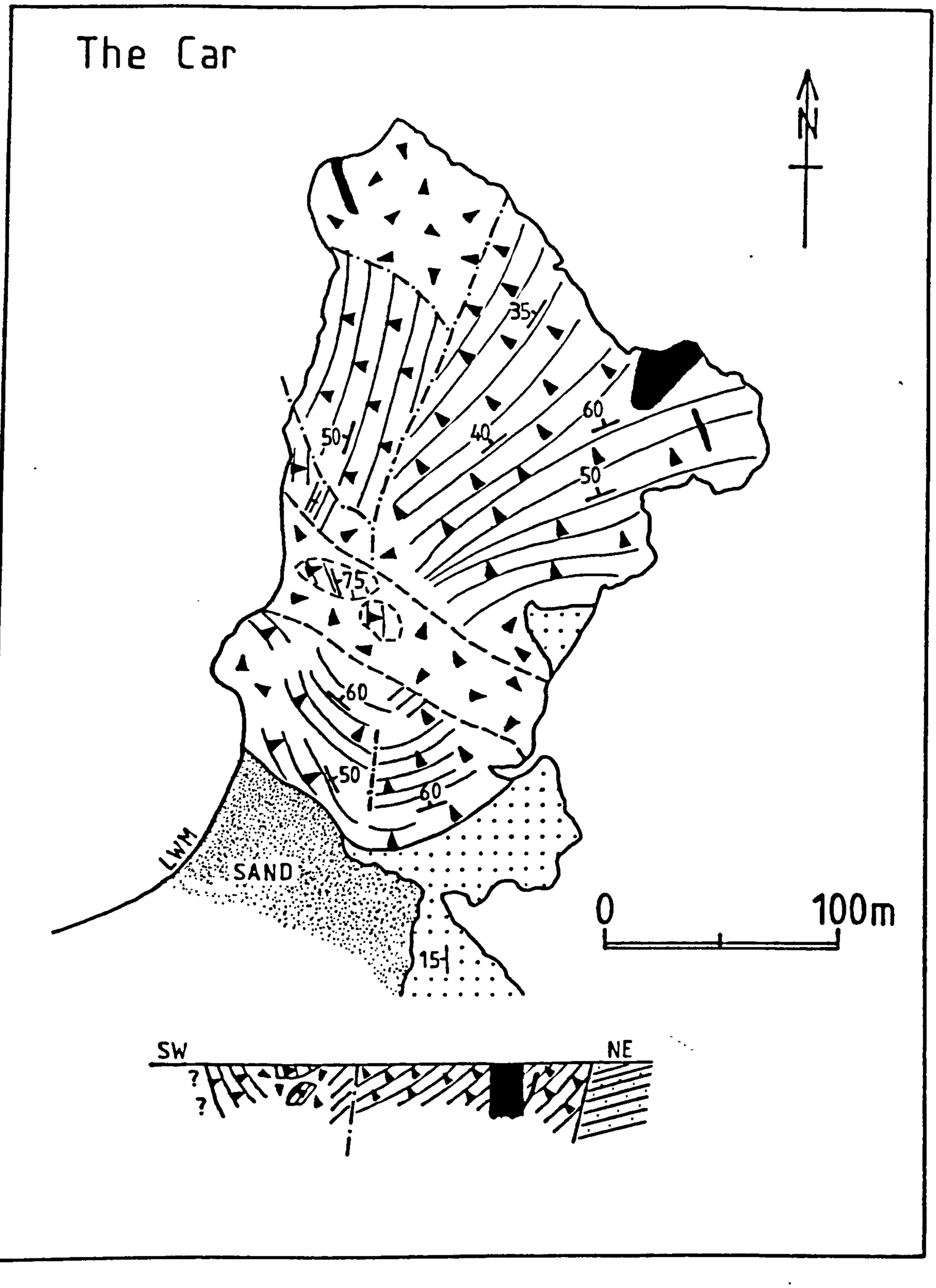

Fig. 5.18 Map and section of the Car diatreme. See insert in back pocket of thesis for key to diatreme maps.

during subsidence. Immediately inside the southern margin the diatreme infill consists of randomly-oriented blocks of bedded tuff.

The diatreme tuffs are red, fine-grained and generally contain less sediment than the Seacliffe tuffs. The most common clasts are basalt (some rare vesicular bombs occur) and bedded tuff. One unbedded area in the northwestern part of the diatreme is particularly rich in basaltic blocks, and is associated with a dyke suggesting break up of an intrusive body. A basalt plug cuts the bedded tuffs in the northeastern part of the diatreme and was probably intruded at a late stage in the subsidence.

Generally, the bedded tuffs consist of monotonous alterations of ash and lapilli tuff. Many blocks lie within prominent impact sags and in places blocky units dominate the succession. Rare lensoid and cross-bedded horizons occur throughout the tuffs, indicating periodic surge activity.

Two sequences of surge deposits are seen in the southern part of the diatreme. The first, near the S margin, consists of fine, well-bedded tuffs containing well-sorted lapilli layers up to 4cm thick (Fig. 5.19).

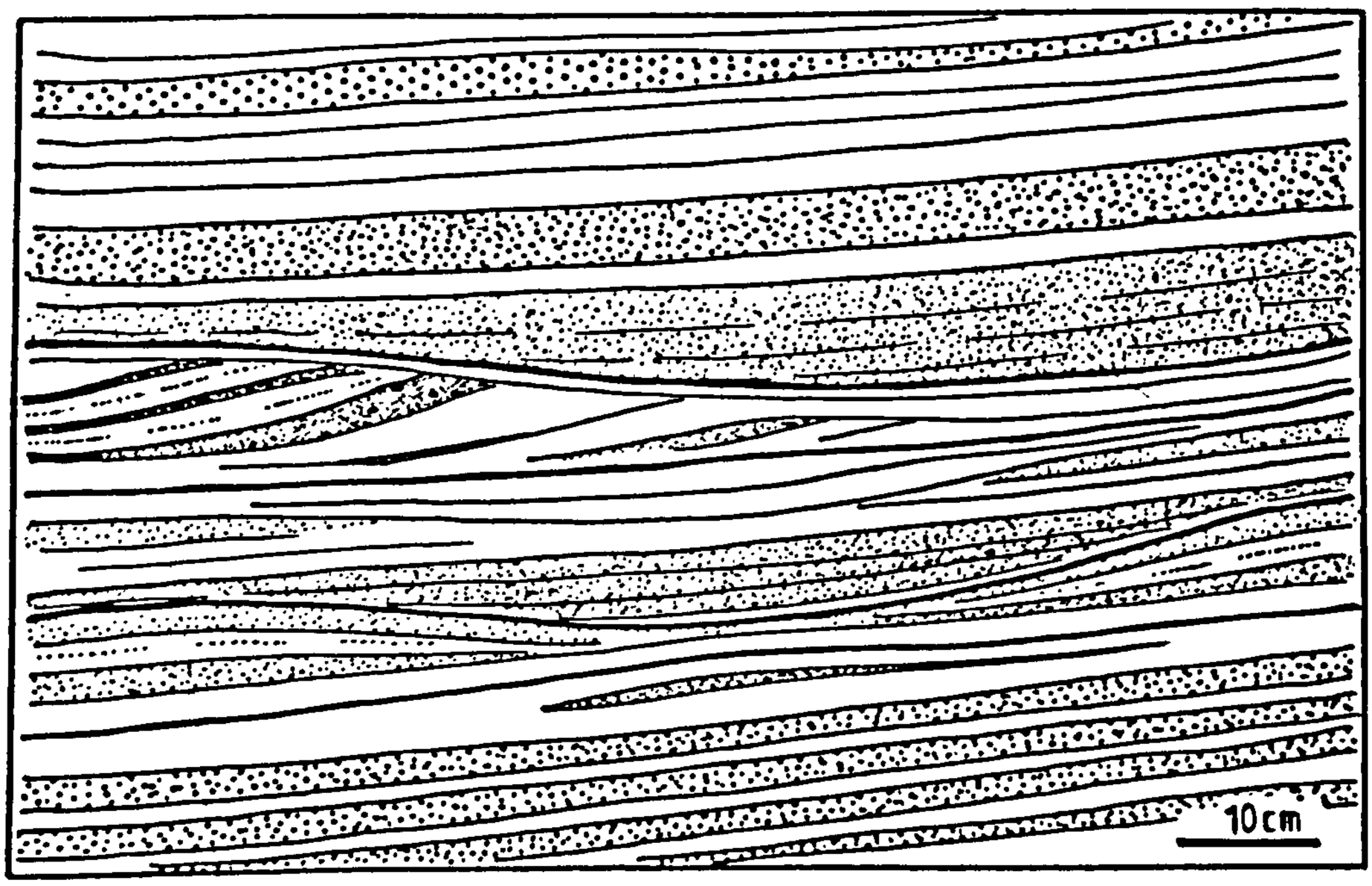

Fig. 5.19 Low-angle surge trough cross-bedding in the Car diatreme tuffs. Note preservation of some low-profile dunes.

These lapilli layers pinch-and-swell and thin over the top of clasts which project from the underlying beds. They are associated with small-scale, low-angle trough cross-bedding which often develops in hollows cut into underlying lapilli beds. Low profile dunes have wave-heights of 3-7cm and wavelengths of 80-140cm with cross-laminae dipping at 4-6°.

Separated from these deposits by faults is a second sequence of similar low profile dunes, some with climbing cross-lamination, and pinch-and-swell features (Fig. 5.20). In addition, they include thin,blocky layers up to 10cm thick which thin and fine over dune crests. Small blocks 2 to 8cm across have sags up to three times that diameter beneath them (Fig. 5.20). The small size of the cross-bedding and the generally fine-grained nature of the tuffs perhaps indicate deposition by low-velocity, expanded surges. The inferred high moisture content of such surges is reinforced by the deep impact sags beneath even the smallest clasts.

Structurally, the diatreme is composed of a number of bedded areas, separated by faults (Fig. 5.19). A linear unbedded zone in the centre of the diatreme contains numerous blocks of bedded tuff and basalt. Many of the faults are curved and are assumed to have formed when the tuffs were poorly consolidated. In a large sector of the northeastern part of the diatreme the strike of the bedding curves as though centroclinal to a centre in the NW.

The crypto-volcanic structure (Section 5.2.1) exposed 250m SW of the diatreme contains tuffs which may represent the distal outer flank deposits from the Car. Some of the disrupted blocks comprise well-bedded lapilli tuffs with accretionary lapilli and low-angle trough cross-bedding (Fig. 5.21). The accretionary lapilli are small (<5cm diameter) and generally spherical though some are more irregular. They are further discussed in the petrography section (Section 5.4).

The trough cross-bedding typically forms sets 15cm high and 120cm long with tangential bottom contacts and truncated tops. Low-angle climbing cross-bedding also occurs, though whether migration is up- or downstream is

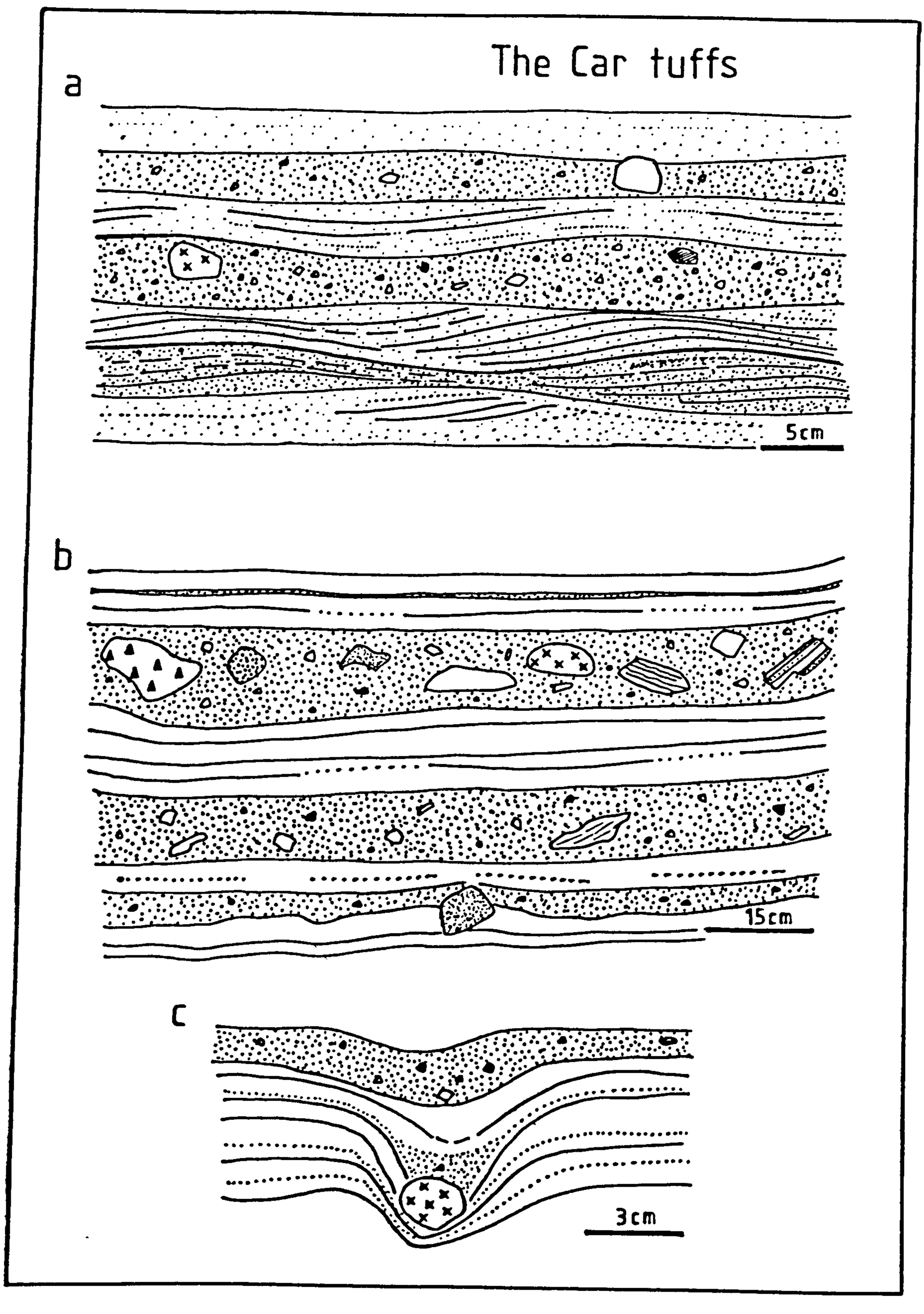

Fig. 5.20 a) Climbing cross-laminated tuffs interbedded with coarse units which pinch and swell.
b) Blocky debris flows interbedded with well-bedded tuffs.
c) Deep sag beneath small basalt clast, indicating moist, cohesive tuffs on impact.

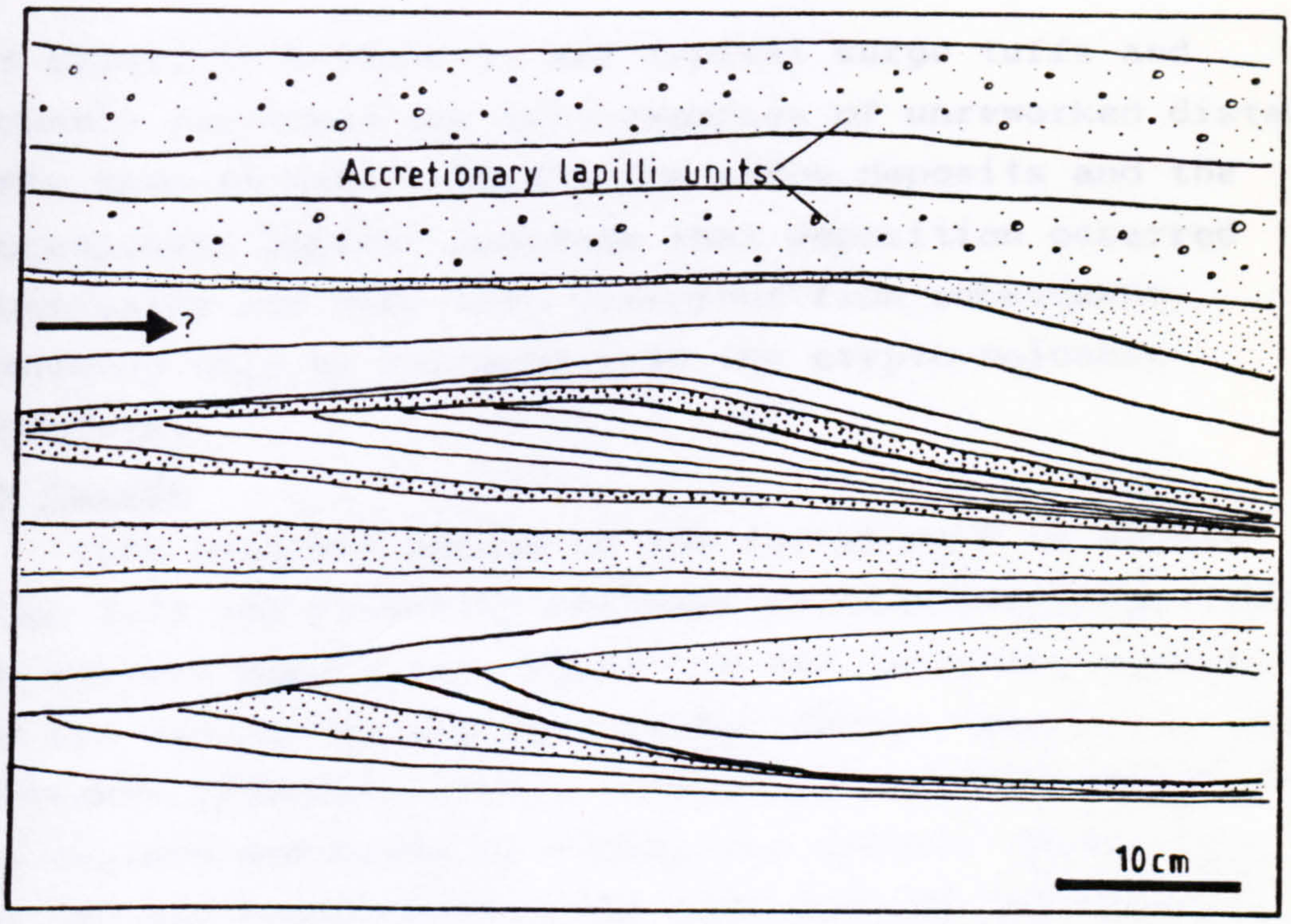

Fig. 5.21 a) Low-angle trough and dune cross-bedding from crypto-volcanic tuffs S of the Car diatreme, showing location of accretionary lapilli units.

Fig. 5.21 b) Accretionary lapilli in crypto-volcanic tuffs S of the Car diatreme. Note the fine rims around cores composed of ash aggregates. Coin measures 17mm across.

not clear. Such deposits are typical surge tuffs and probably represent the only examples of unreworked distal tuffs seen in East Lothian. The surge deposits and the accretionary lapilli indicate that deposition occurred subaerially and they were preserved from subsequent reworking only by collapse into the crypto-volcanic structure.

The Parade

This diatreme occurs on the foreshore N of Dunbar (Fig. 5.2) and presently measures ca.800x500m (Fig. 5.22). Its eastern margin cuts Upper Old Red Sandstone sediments and its western margin cuts Carboniferous Cementstone Group sediments (Francis, 1962), indicating relative downthrow of the western sediments by >300m. The eastern margin is faulted and consists of a 40m wide zone of brecciated country rock siltstones. The brecciated zone is separated from the diatreme by a 1m band of fault gouge. The sediment blocks in the brecciated zone generally dip into the diatreme at high angles, and are often intruded by tuffisite.

Towards the western margin the country rock cementstones dip into the diatreme at up to 50° and pass into a 15m wide disrupted zone. This zone contains steeply dipping, shattered sediments which pass into unbedded tuffs containing sediment blocks. Within the diatreme the tuffs dip E or NE at moderate angles, becoming steeply inclined near the western margin. The eastern margin obliquely truncates the gently eastward dipping sequence of bedded tuffs.

Although the diatreme is cut by many small faults, joints and dykes the tuffs, younging to the E, form an almost continuous bedded succession equivalent to a stratigraphic thickness of >300m (see Fig. 5.27 for representative sections). The red-brown tuffs are similar to those of the Car and Seacliffe diatremes. Their volcanic component consists of crystalline basalt and altered glass with their sedimentary component comprising clasts of similar lithology to the country rocks along with their constituent minerals (quartz, feldspar, mica). The proportion of these two components varies between

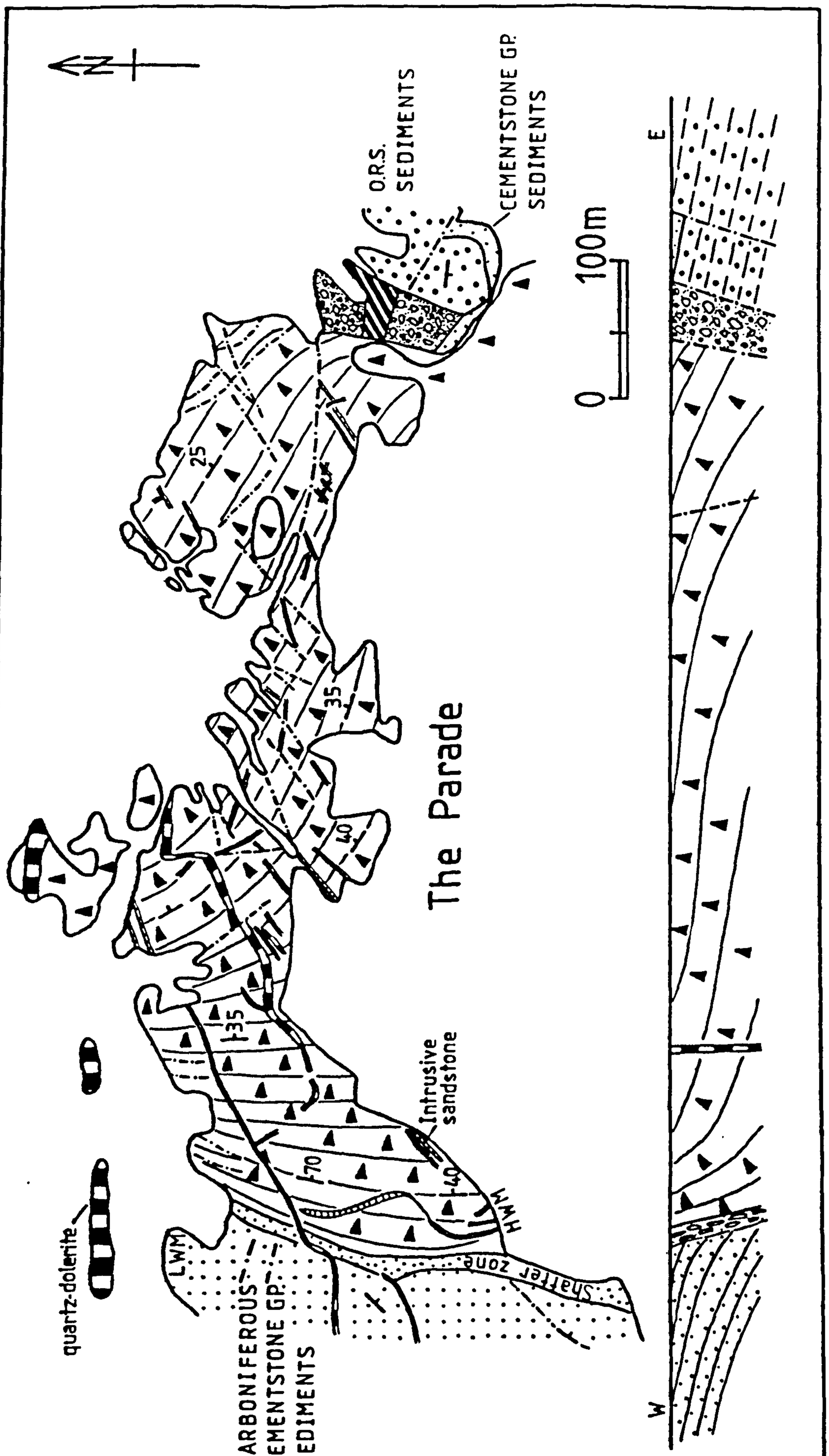

Fig. 5.22 Map and section of the Parade diatreme, after Francis (1962).

successive beds, giving rise to alterations, a few metres thick, of tuff and tuffite. The bedded tuffs are mainly of lapilli-ash grade but contain block-rich layers up to 1·5m thick. At the base of the sequence, near the western margin, they are predominantly of airfall origin with only rare low-angle cross-bedding attributable to surges. Throughout the diatreme these cross-bedded layers are rich in sediment, suggesting that their depositing surges resulted from phreatic steam explosions. Coarse beds are laterally discontinuous along strike, and most wedge out over a few metres. Successive coarse beds are often separated by thin, fine tuff laminae which are cut out by the overlying units. Block sags are common in the lowest 10m of the succession, but are rare above. Many of the sags are asymmetric and indicate block derivation from the E to the NE. Localised breakdown of bedding is interpreted to have been formed by slumping of poorly-consolidated material, often associated with slip along bedding planes.

Low-angle trough cross-bedded tuffs first occur 25m up the succession and subsequently form a variable, but often substantial proportion of the diatreme infilling. Typically, the trough sets are defined by moderately-sorted ash and lapilli layers up to 5cm thick. These layers dip at up to 12° (more commonly <6°) and have tangential or concave shapes (Fig. 5.23). Cross-set amplitudes reach 35cm and dune wavelengths in excess of 2m are indicated. Isolated clasts up to 6cm lie along the cross-sets and do not deform them, indicating emplacement by flow. Cross-bedding is commonly truncated by erosion surfaces, although in places complete preservation of dune forms occurs. Rare U-shaped channels which trend normal to the bedding strike are associated with cross-beds. The size, shape and sorting of the cross-bedding indicates deposition by base-surges.

The dune forms (Fig. 5.24) are generally symmetrical, although internally they often consist of cross-lamination dipping predominantly in one direction with minor oppositely dipping sets. No definite conclusions as to the current direction can be made, but by analogy with most other surge dunes the main cross-laminae are fore-set /

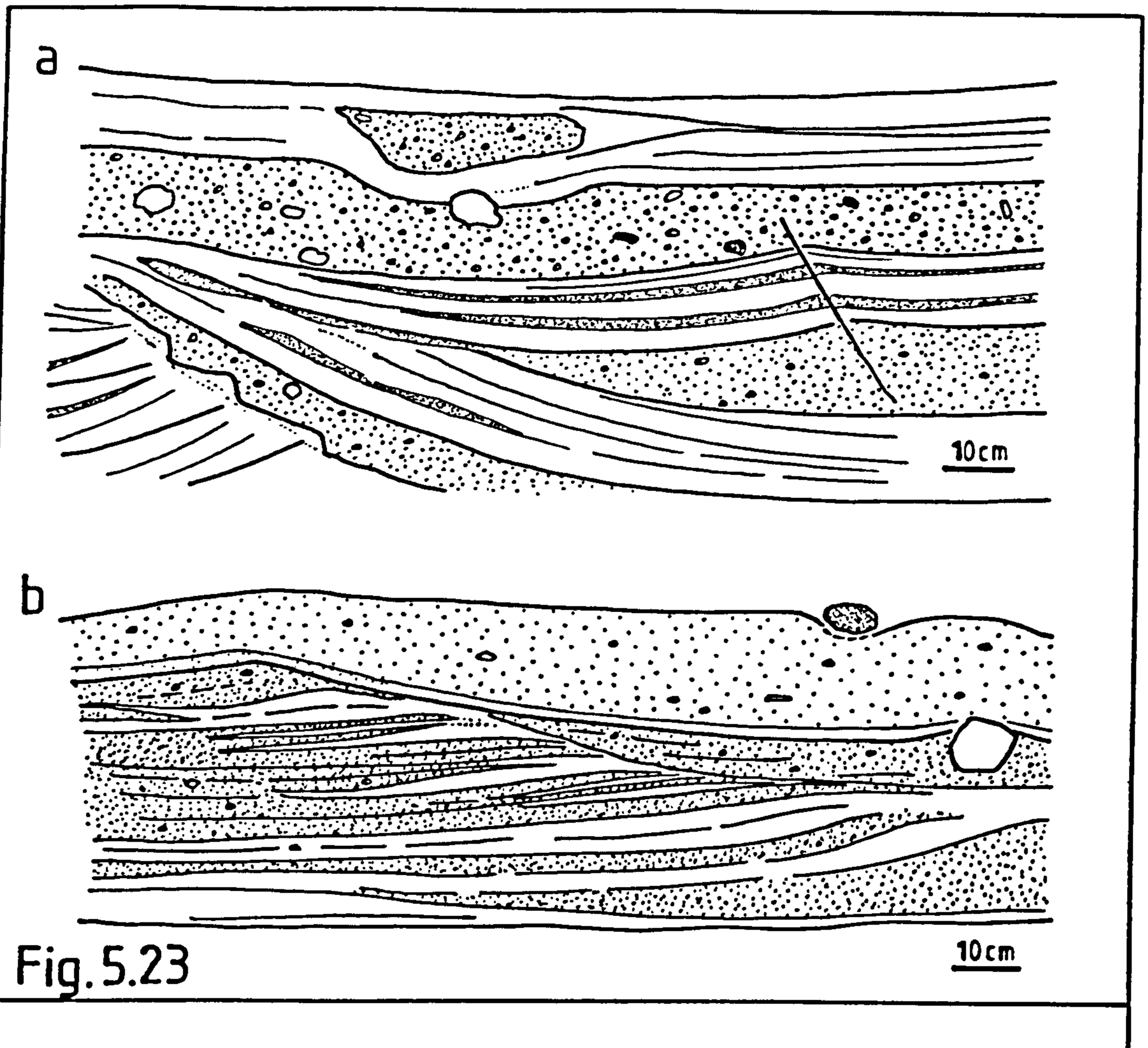

Fig.5.23

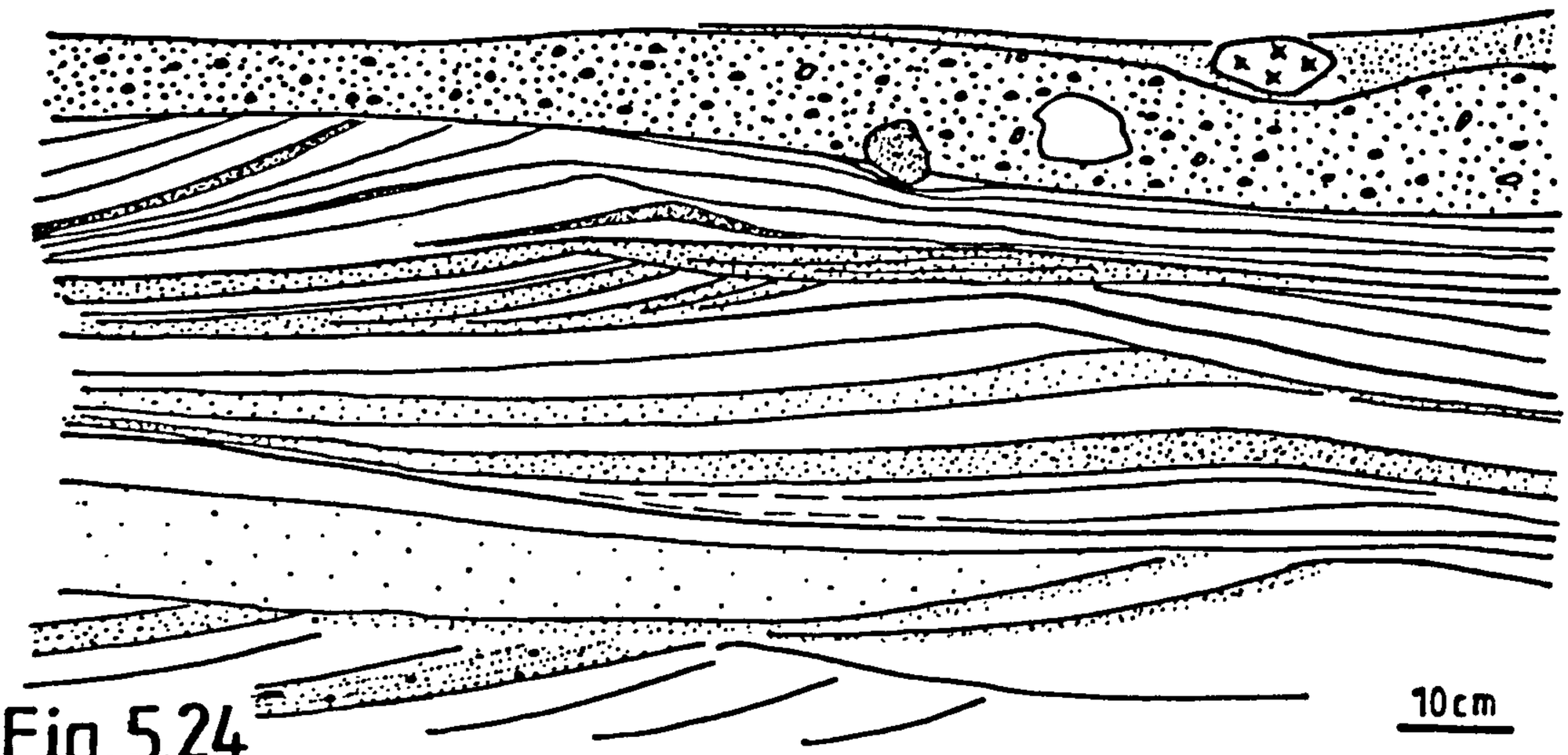

Fig.5.24

Fig. 5.23 Surge cross-bedding in the Parade diatreme tuffs.
a) Large-scale trough sets formed above eroded tuffs. Note interbedded massive units.
b) Large dune containing low-angle cross-sets.

Fig. 5.24 Well-developed surge dunes in the Parade diatreme. Note increasingly peaked dune crests upwards and climbing cross-laminations. Dune mantled by massive layer which is block-sagged in places.

lee-side accumulations. The rare stoss-side sets were deposited during the final stages of dune migration, perhaps as flow power diminished in surges.

A good cross-section of a surge dune occurs in the northeastern part of the diatreme, about 15m from the top of the exposed bedded sequence (Fig. 5.25).

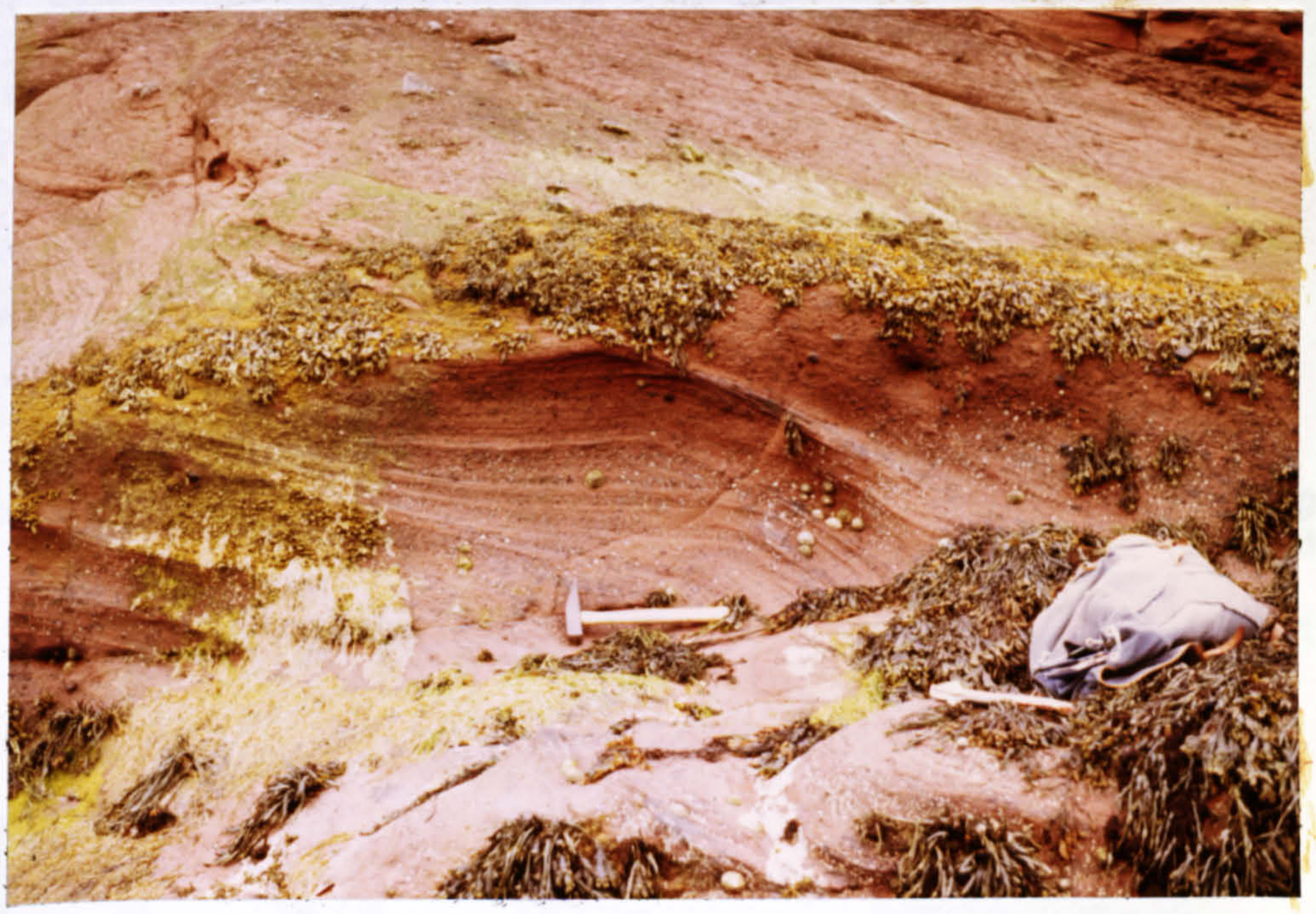

Fig. 5.25 Surge dune developed in NE-dipping tuffs. Flow from right to left. Concave lee-side laminae thin and fine away from the dune crest, which is rounded initially but becomes sharper upwards. Stoss-side laminae are planar and dip at lower angles than the lee-side if correction is made for regional dip. Downstream climbing cross-lamination at increasing climb angles occurred as the dune built up. Crestal erosion forms many internal unconformities. Hammer handle measures 30cm.

The estimated current direction is from the NE which is updip relative to the present orientation of the tuffs. Directional data are difficult to estimate from cross-bedding which is seen only on strike faces, but most examples suggest currents from the NE, E or SE.

The layers within the cross-bedded units are arranged so commonly as to suggest that they can be used as an indicator of surge depositional processes. In idealised

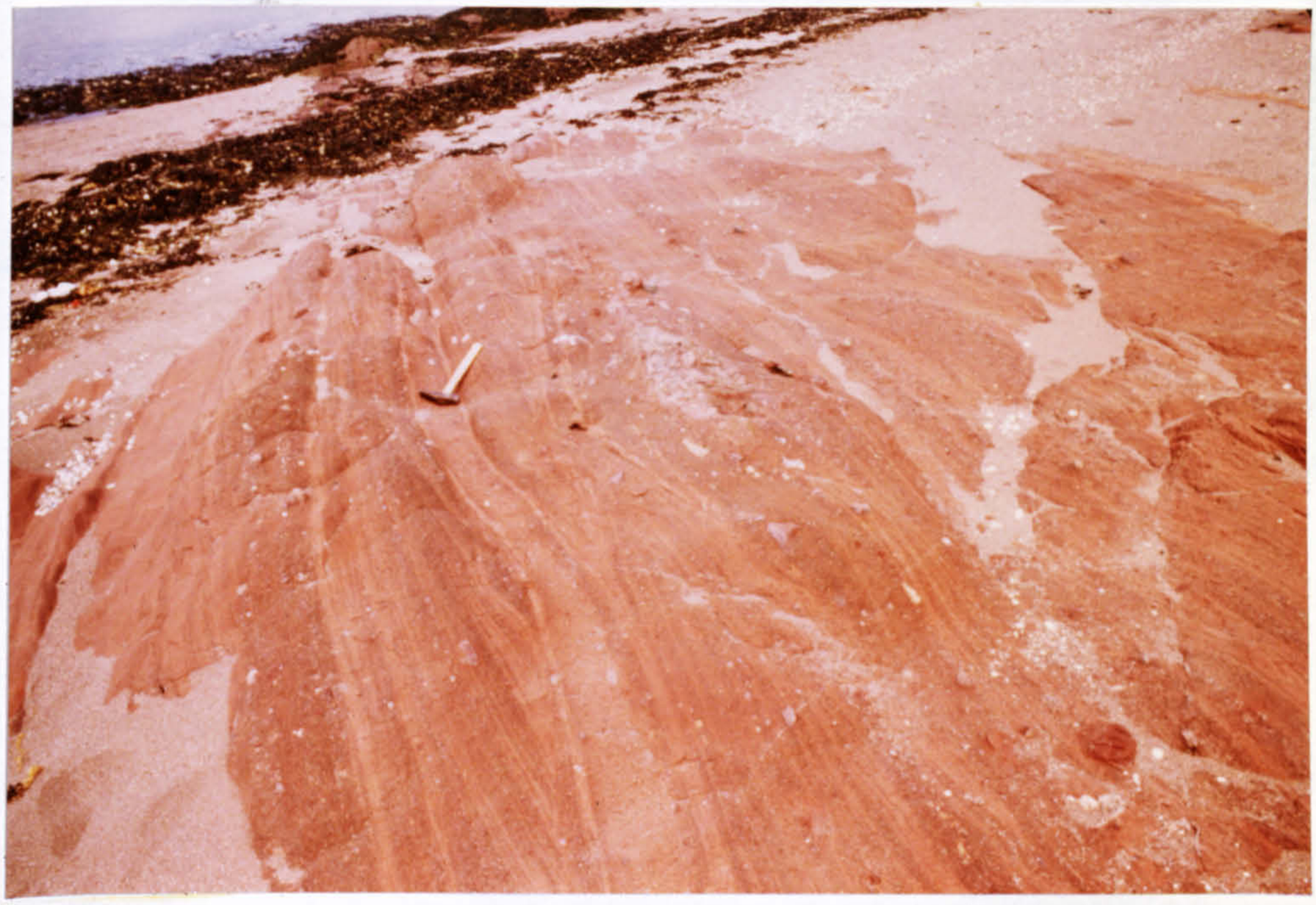

Fig. 5.26 a) Oblique view of surge dunes and cross-bedding in the Parade tuffs. Hammer measures 30cm and lies on division 3 of the idealised surge sequence with divisions 2 and 1 underlying it to the left.

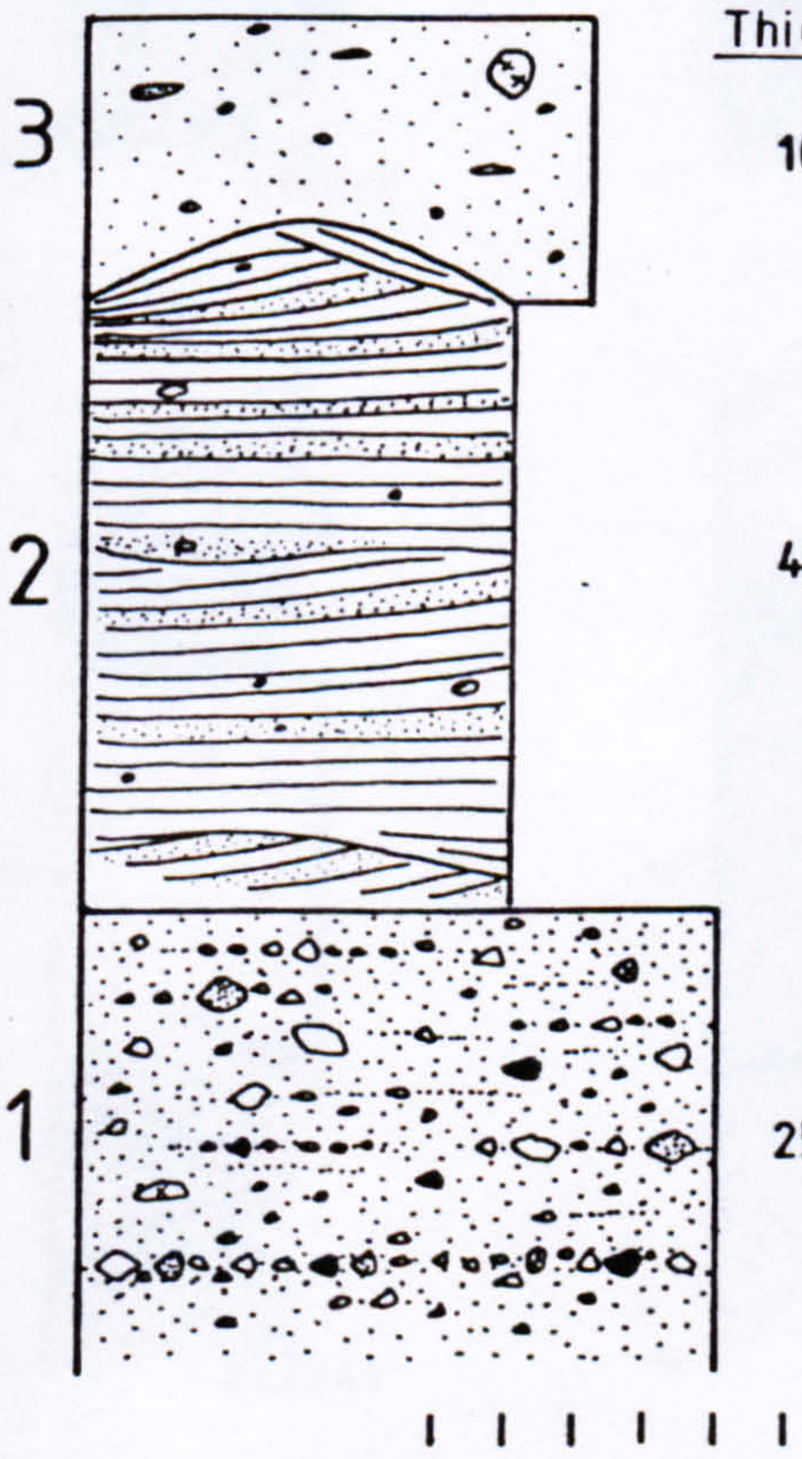

Idealised surge sequence: Dunbar

Fig. 5.26 b) Idealised surge sequence from the Parade tuffs.

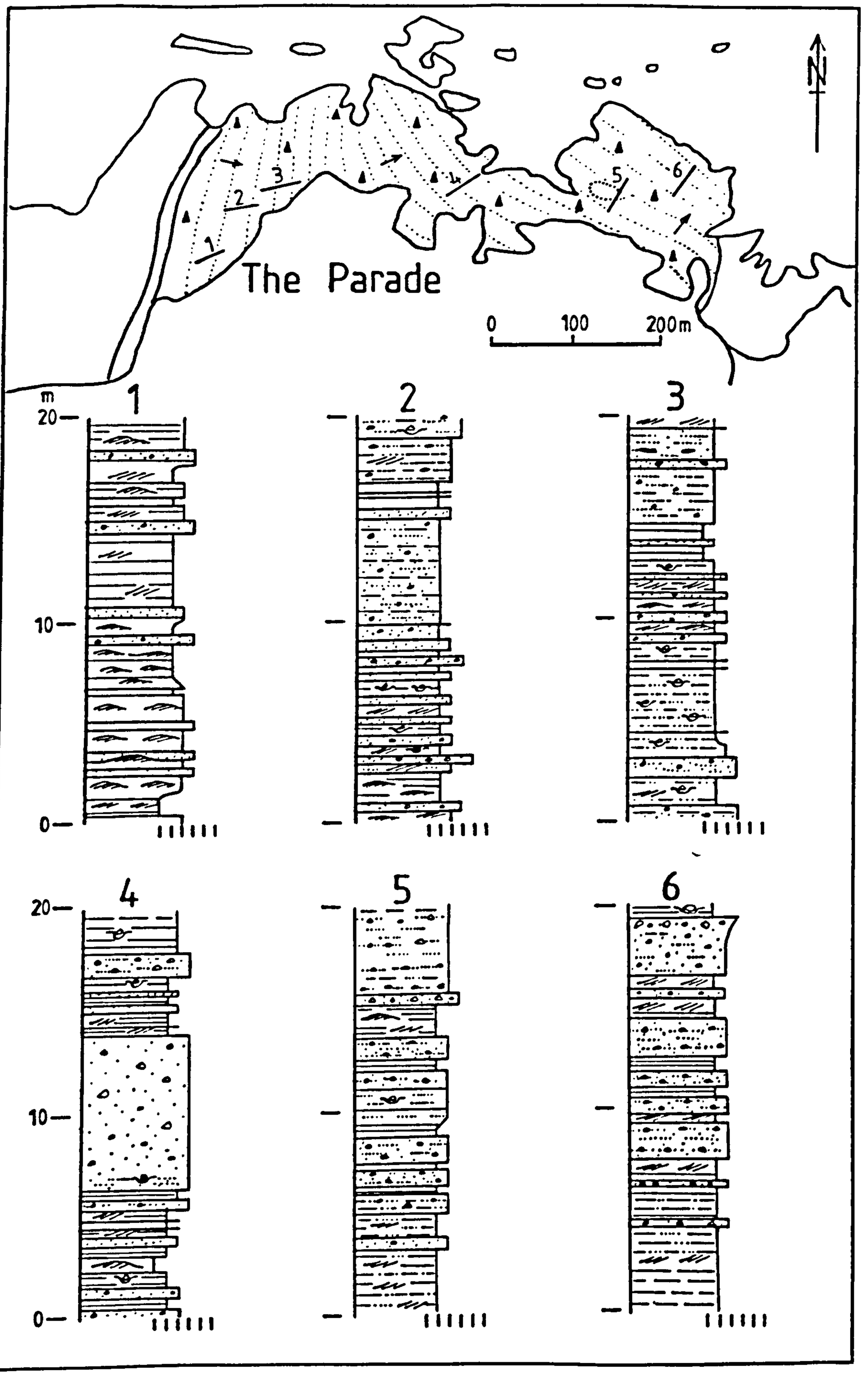

Fig. 5.27 Logs of the Parade tuffs with their locations indicated. Note the abundance of surge cross-bedding and dunes throughout the tuffs.

form, this sequence consists of a coarse, poorly-bedded base 20-40cm thick, dune cross-bedding for 40 to 70cm at the centre and 10 to 25cm of massive tuff which thins over the dune crests at the top. This topmost layer is often missing and the dunes are then overlain by coarse, poorly-bedded tuffs of the succeeding sequence.

Each layer is thought to represent the deposit of a different region within the surge cloud, namely a basal traction carpet, a turbulent suspension in the main body of the surge and an end-phase laminar flow due to en masse collapse of the eruption column. Surge models are further discussed in Chapter 7.

Blocks of sediment, mainly siltstone and mudstone, are found throughout the tuffs. Some of the finer grained clasts have very irregular margins, suggesting they were moist and plastic when ejected. As sandstone blocks are angular, they must have been indurated before ejection; indeed poorly-consolidated coarser sediments would have been readily comminuted by eruptions, Finer, clay-rich sediments would have been more cohesive and thus survive. Often, irregular sediment clasts occur within coarse surge beds, indicating the resistance of cohesive, plastic sediment to attrition. One mudstone clast in a surge bed appears to have been plastically deformed over an underlying basalt block during post-emplacement compaction. Some of the plastic, tuffaceous sediments might represent crater lake deposits disrupted during renewed activity. Blocks of bedded tuff, unlike any lithology outside the diatreme, probably represent crater tuffs reworked by explosions.

The moist nature of many of the tuffs on deposition is indicated by load structures, soft sediment faults and rare flame structures. Block impact sags plastically deform well-laminated tuffs and in places small clasts have sags deeper than twice the clast diameter.

NE-trending joints and small faults, and joints parallel to the strike of the bedding cut the tuffs. Many of these fissures are filled with intrusive sandstones which commonly exhibit flow banding. These dykes contain almost entirely sediment-derived material (Francis, 1962)

and field as well as petrographic evidence suggests at least two successive intrusive phases. Later NE-trending quartz-dolerite dykes cut the diatreme tuffs but are in places deflected along or cut by small faults.

The lack of internal bedding disruption and the wide-marginal fault zones are features exhibited by few other diatremes in Scotland. Other features of difference include the large size, the high proportion of surge deposits and the abundant intrusive sandstone bodies. The relevance of these differences is discussed in Section 5.5.

5.3.3 Green Group diatremes

The diatremes of this group are situated E of North Berwick and include Tantallon, Gin Head, Horseshoe, Yellow Man and Partan Craig (Fig. 5.3). Their green colour is largely due to chloritic replacement of their abundant juvenile glass component.

Tantallon Diatreme

This diatreme measures ca.400m across and cuts the Green Basaltic Tuff Formation to the S and the Canty Bay Sandstone Formation to the N (Fig. 5.28). The northern margin is a vertical fault defined by a 1m zone of brecciated tuff and sediment. The country rock beds are turned down within 5m of the contact and are locally brecciated. The marginal diatreme tuffs, which form a raised platform on the foreshore, initially consist of rotated blocks of green, bedded tuff which have steep or vertical dips. Within 10m of the contact the blocky tuffs merge into massive, unbedded lapilli tuffs.

The southern margin is more irregular and is defined by a number of NE-trending faults, which bound large upthrown rafts of Canty Bay Formation sediments. A series of basaltic dykes are intruded along the margin at HWM and cut a 3 to 5m zone of brecciated tuffs and sediments. The diatreme tuffs near the southern margin are unbedded and massive or contain blocks of bedded tuff and tuffite.

The diatreme infilling consists of green-to-brown lapilli tuffs with abundant blocks of basalt, and less numerous clasts of green tuff, red tuffaceous mudstone and

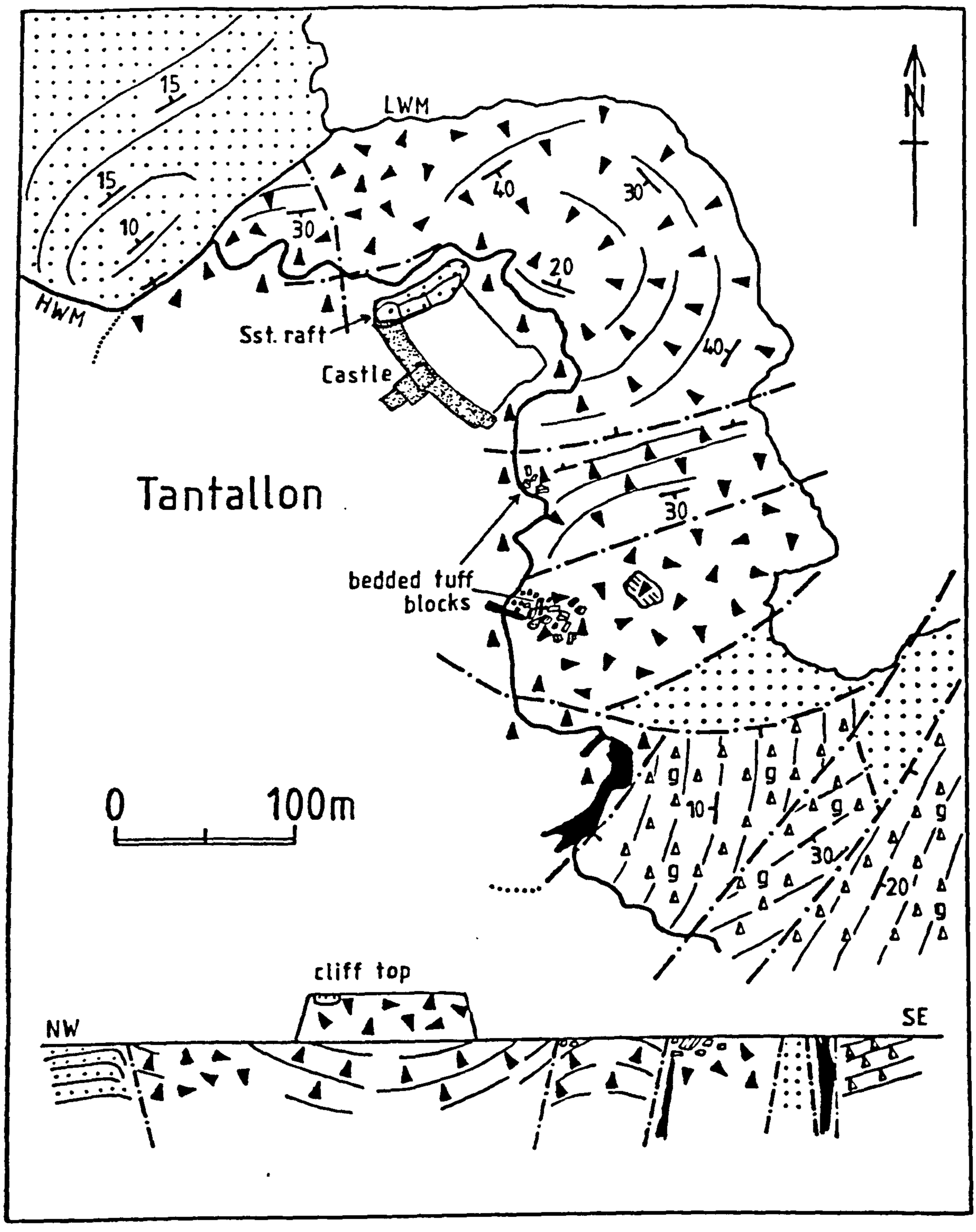

Fig. 5.28 Map and section of the Tantallon diatreme.

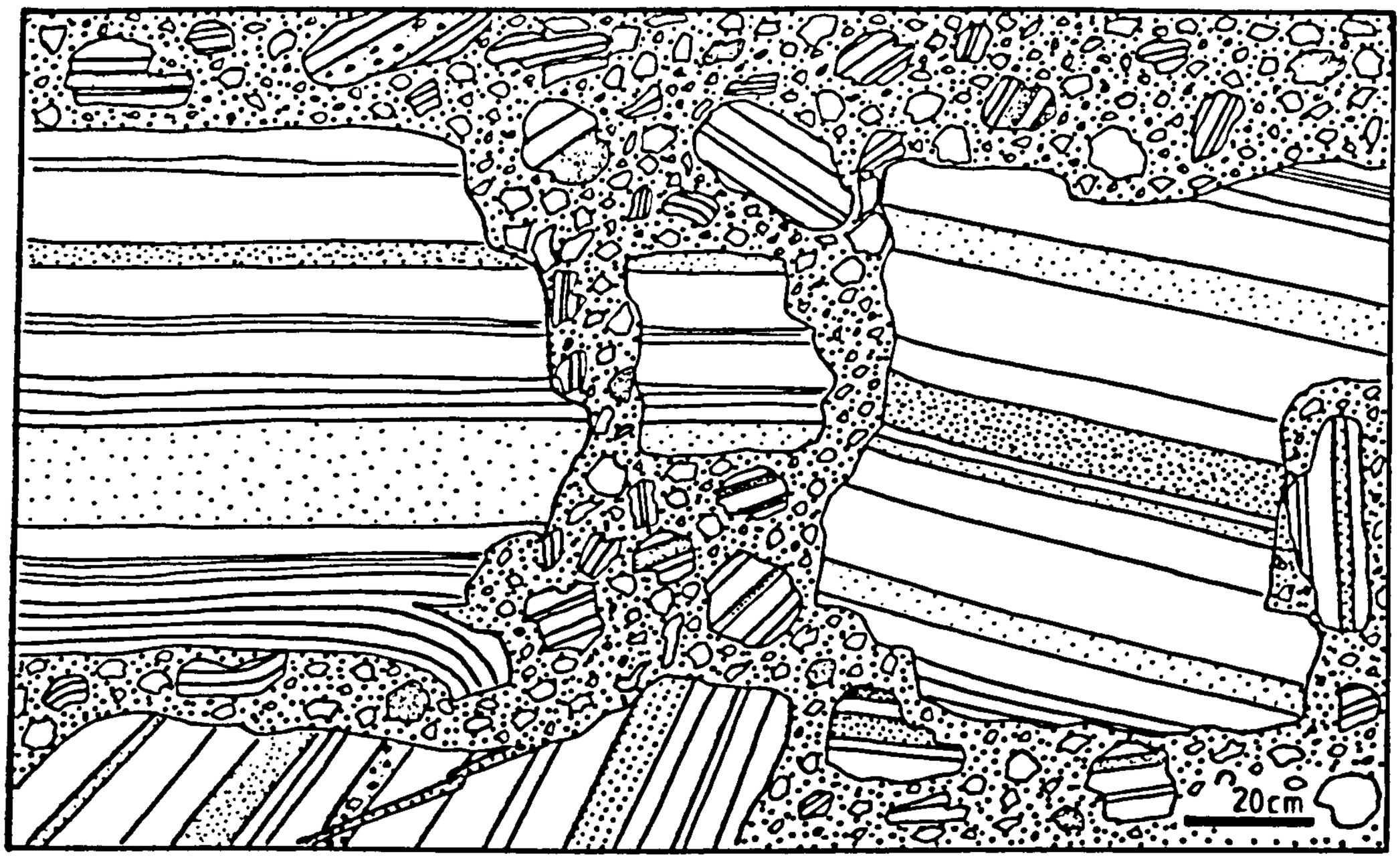

Fig. 5.29 Collapse-bedded tuffs in the SW of the Tantallon diatreme.

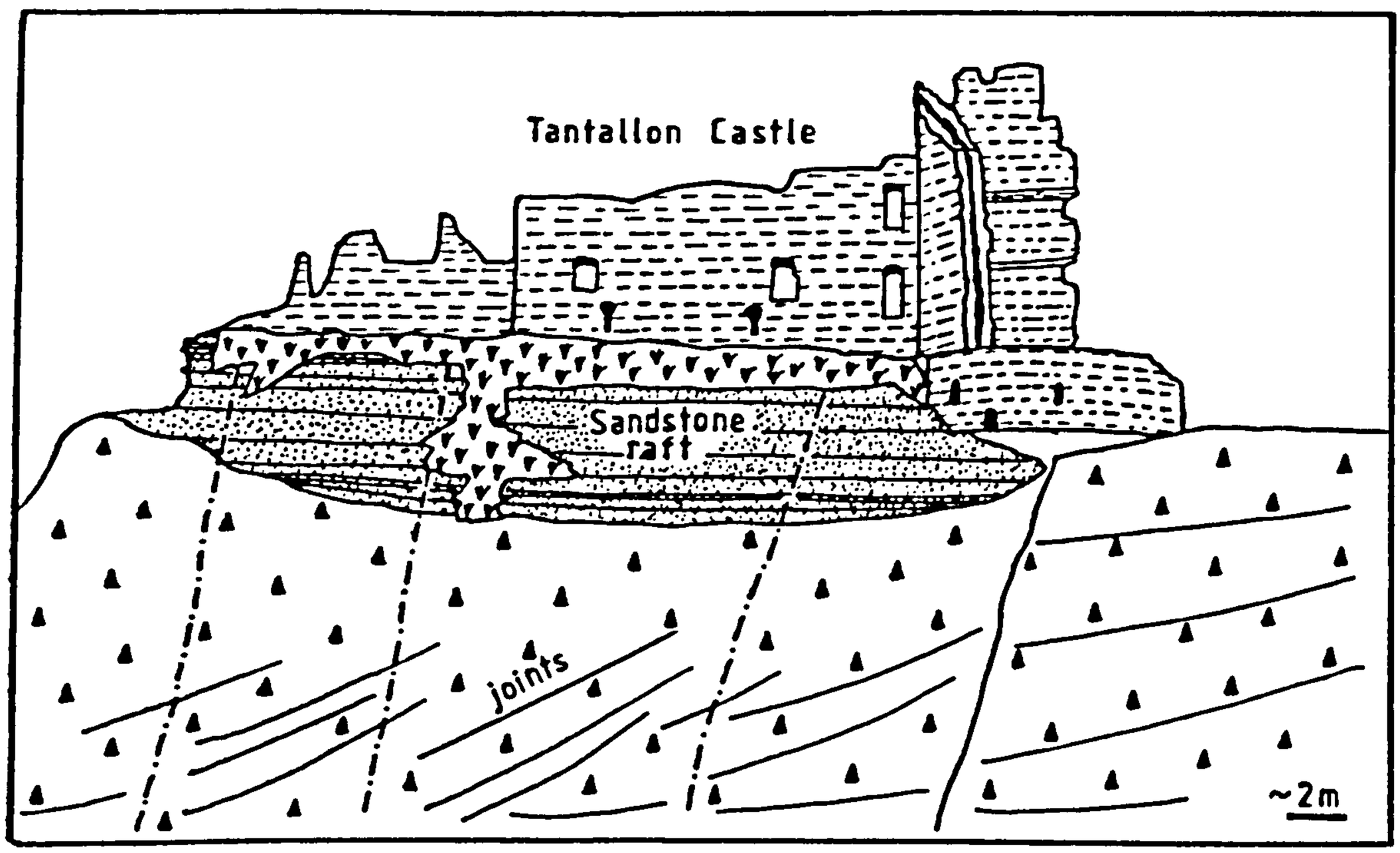

Fig. 5.30 Sandstone raft lying above tuffs in cliffs beneath Tantallon Castle.

sediment. Rounded vesicular basaltic bombs up to 1m diameter are also rarely found. Where bedding is well developed in the centre of the diatreme the tuffs are moderately well sorted and contain few coarse beds. A central basinal structure is formed by tuffs which are cut by shallow, wide channels infilled by coarser tuffs. Rare cross-bedding and U-shaped channels occur in the bedded tuffs to the S of the centre.

The southern half of the diatreme consists largely of agglomerate containing blocks of bedded tuff and tuffite. In places those blocks are so numerous that they indicate break-up almost in situ, perhaps by slumping. One area consists of a clast supported deposit containing blocks up to 2m across of bedded tuffs (Fig. 5.29).The tuffs are well sorted and finely laminated, with occasional low-angle trough cross-bedding. Nearby blocky deposits contain abundant red tuffaceous mudstone and were perhaps incorporated from the country rocks by collapse. Large rafts containing brecciated siltstone and mudstone are surrounded by blocky tuffs. The rafts have sharp, irregular margins, and appear to represent brecciated sedimentary sequences which have collapsed into the diatreme fill. Whether these sediments were derived from the poorly-consolidated country rocks or represent collapsed post-eruption crater infilling material is not known. A further raft is exposed in the cliffs beneath Tantallon Castle (Fig. 5.30) and measures 20x12x5m. It consists of medium-grained, horizontally-bedded white sandstone and is surrounded by massive tuffs. It probably represents a block detached from the wall rocks during collapse.

Gin Head Diatreme

This diatreme measures ca.700m across and cuts Canty Bay Sandstone Formation sediments (Fig. 5.31). The western margin is sharp and irregular, with country rock mudstones turned down against it. The mudstones are folded in some places, broken up into blocks in others, and are cut by red intrusive marl dykes. Inside the diatreme, bedded blocky tuffs at first dip at up to 40° into the centre although bedding can no longer be discerned beyond 2m from the

margin. The eastern margin is similar except that it cuts across a poorly-exposed crypto-volcanic structure which disrupts the country rock mudstones.

The bulk of the diatreme is occupied by intrusive basalt which has vertical jointing in places, indicating a sill-like form. The remaining fill consists mainly of unbedded agglomerate with blocks of tuff, basalt, mudstone, siltstone, limestone and tuffaceous sediment. Bedded areas contain rare basaltic bombs with impact sags. Agglomerates near the eastern margin are blocky, poorly bedded and interbedded with sandstone.

These marginal beds are cut by a shallow channel 15m wide with a base dipping at 15° towards 310° (Fig. 5.32). The channel is filled by massive tuffaceous siltstone with clasts up to 15cm long derived by erosion from the underlying units. Migration of the channel is indicated by lateral accretion surfaces. The upper part of the channel is filled with well-laminated tuffs overlain by massive blocky agglomerate. A 1·5m sill intrudes the beds 3m above the channel.

The channel is interpreted as having been cut by streams flowing into a tuff-ring crater during an early phase in the history of the Gin Head structure. Sediment was perhaps derived from breaching of the tuff-ring by rivers. Debris flows, which probably originated from the crater wall, reworked the tuffs. Marginal faulting brought the reworked tuffs down to their present position, and was accompanied by intrusive activity at depth.

Two rafts of sandstone occur within the diatreme, near the eastern margin. One measures ca.20x6x10m and is exposed in the cliffs at HWM where it is surrounded by green, blocky unbedded tuffs. The raft is irregularly shaped and consists of well-bedded, often trough cross-bedded micaceous sandstone. The tuffs beneath the base are highly jointed and laced by calcite veins. Some copper carbonate staining occurs locally along the contact. The base of the raft dips into the diatreme at 40° and is cut by a few steep, normal faults with downthrows of 3-4m to the S.

The other raft is smaller (12x3x5m) and overlies a

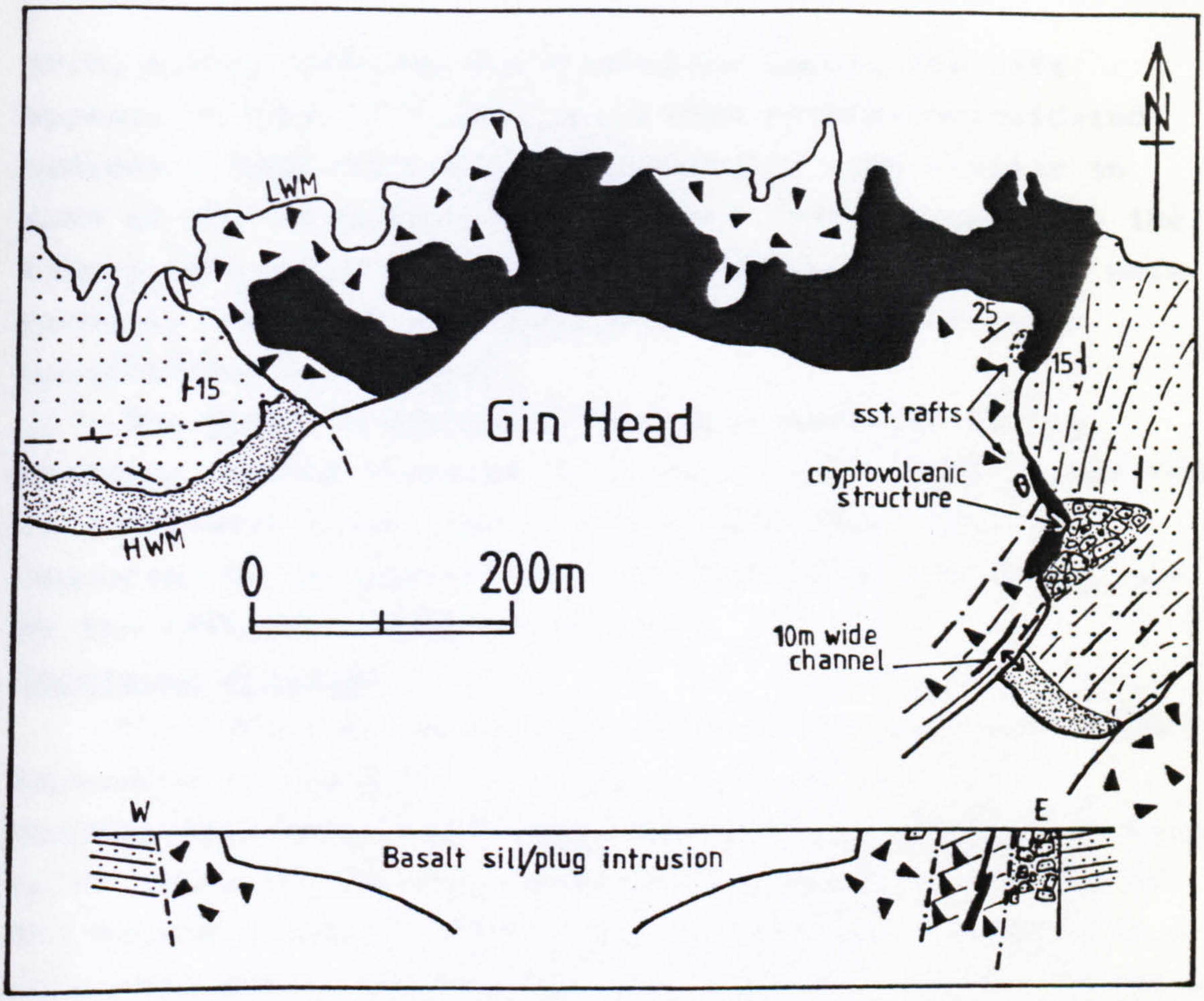

Fig. 5.31 Map and section of Gin Head diatreme.

Fig. 5.32 Fluvial channel cutting tuffs at southeastern margin of Gin Head diatreme. Hammer measures 30cm and lies in the centre of channel. Note lateral accretion surfaces at left side of channel and truncation of beds to the right.

thin, highly sheared, green mudstone layer. The raft appears to have slid into place over poorly-consolidated sediment. Both rafts are lithologically very similar to some of the Canty Bay Formation sandstones, especially the larger raft which contains slumped bedding. The rafts were probably incorporated during collapse, from the well-consolidated wall rocks.

The high proportion of intrusive material in the diatreme perhaps suggests that the erosion level in Gin Head is relatively lower than in other diatremes. This is supported by the general lack of bedding in the tuffs, and by the collapse-incorporated rafts.

Horseshoe diatreme

This diatreme measures ca.350m across and cuts tuffs belonging to the G.B.T.F. (Fig. 5.33). At HWM the southeastern margin is poorly exposed but at LWM it is seen to be sharp and faulted, with little change in the dip of the adjacent country rocks. The northwestern margin cuts obliquely across the country rock tuffs and is defined by a steep, 1 to 2m zone of unbedded tuffs. This marginal zone is cut by many anastomosing calcite veins and a few intrusive sandstone dykes. The dykes may be tuffisitic or are perhaps due to liquefaction of wet sediment by volcanic tremor. The country rock tuffs dip into the margin at 30°.

The tuffs of the diatreme are distinguished from those of the country rocks by their coarser grain size, poorer sorting and block content. In the diatreme they are generally of lapilli grade with blocks of basalt, sediment and tuffaceous sediment (Fig. 5.34). In the southern part of the diatreme they contain large blocks of mudstone and siltstone, which are cut by dykes of intrusive sediment. Flow banding in the tuffs surrounding some of the sediment blocks suggests they were emplaced along fractures which acted as pathways for gas-streaming. The very irregular shapes of some of the mudstone blocks indicate they were emplaced in a plastic condition.

One tuffaceous sandstone body in the southern sector of the diatreme appears to represent collapsed channel infill material. The body (Fig. 5.35) has an erosive base

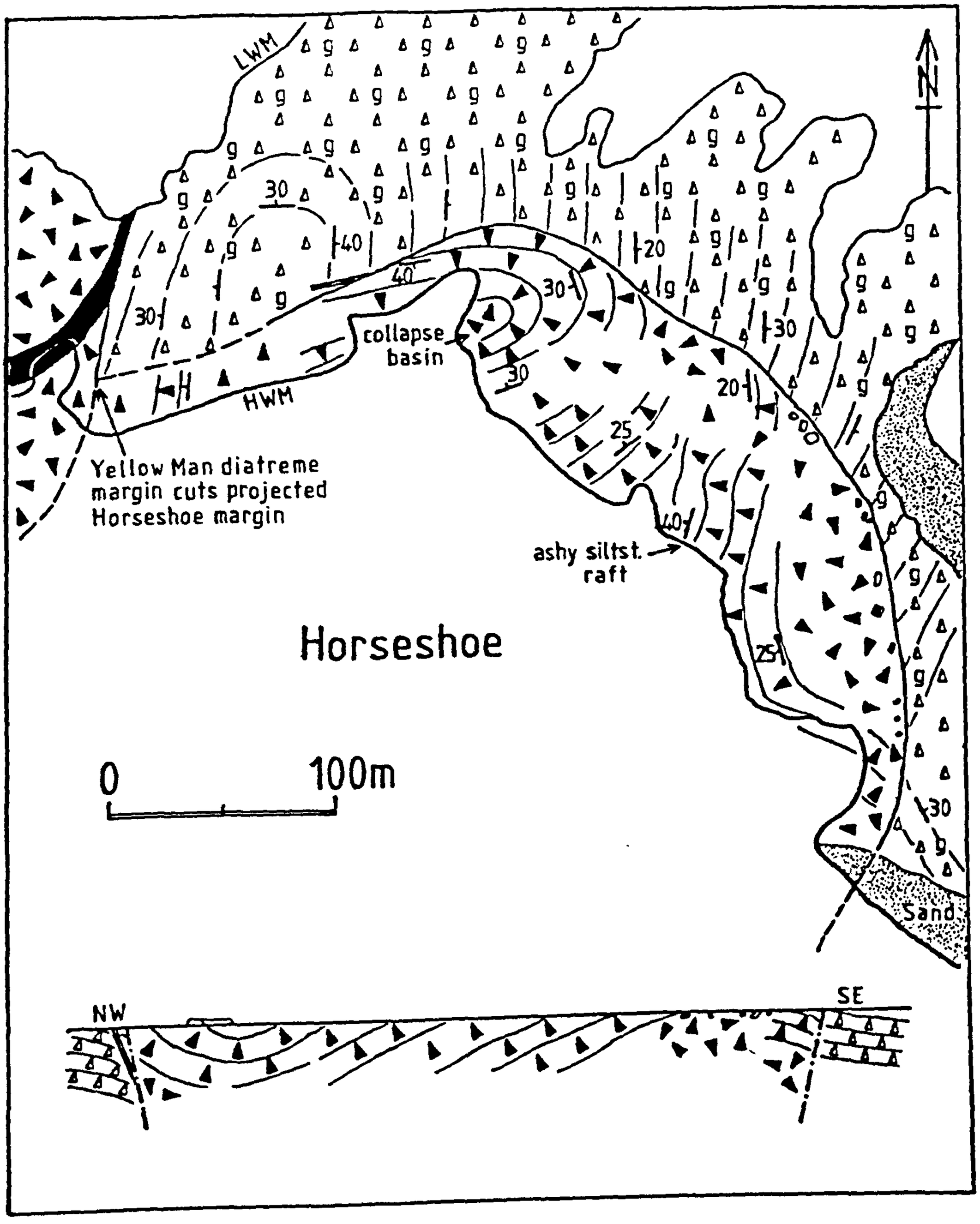

Fig. 5.33 Map and section of the Horseshoe diatreme.

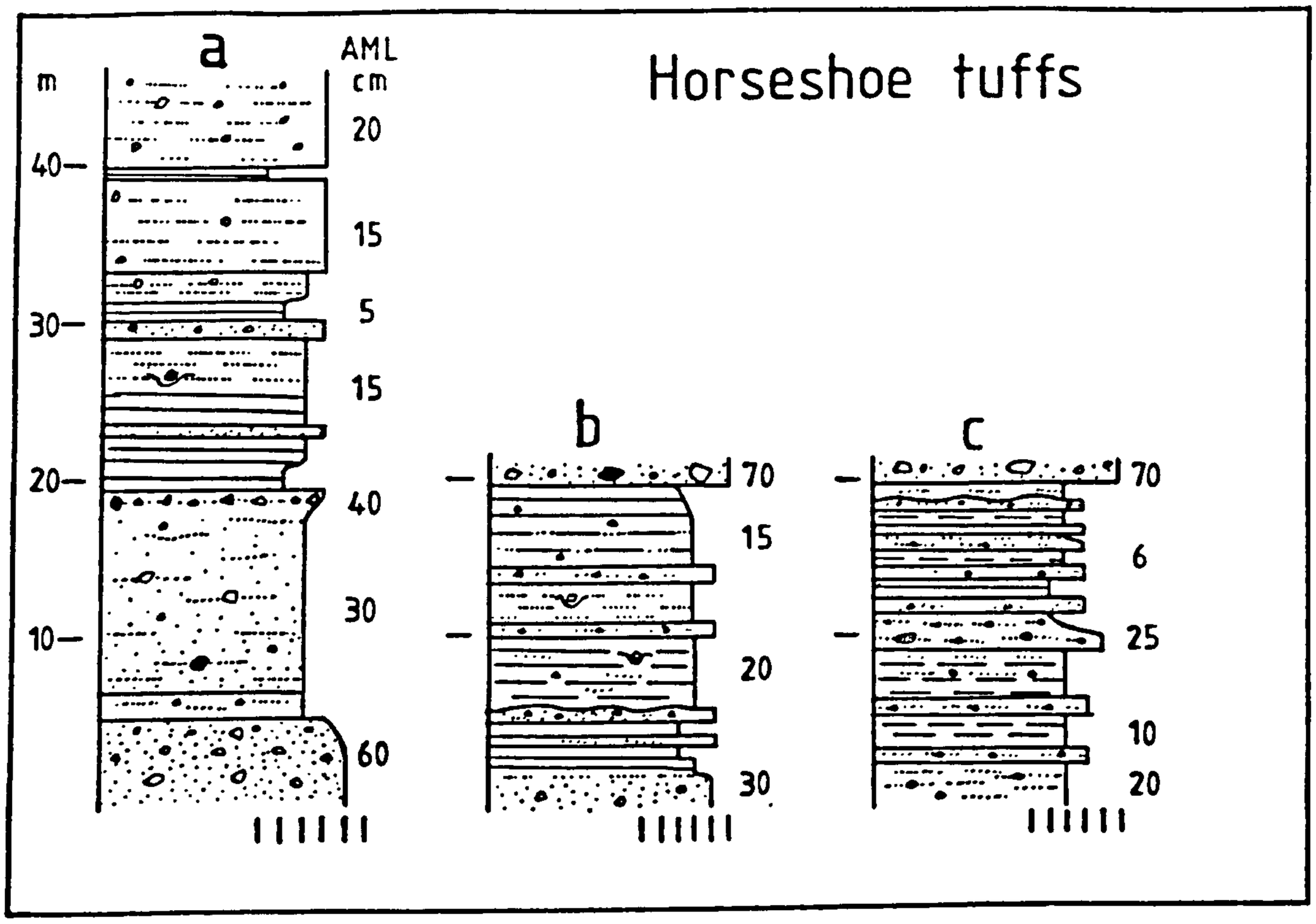

Fig. 5.34 Representative logs of the Horseshoe tuffs.
a) Near southern margin
b) Near centre of diatreme
c) Near northern margin

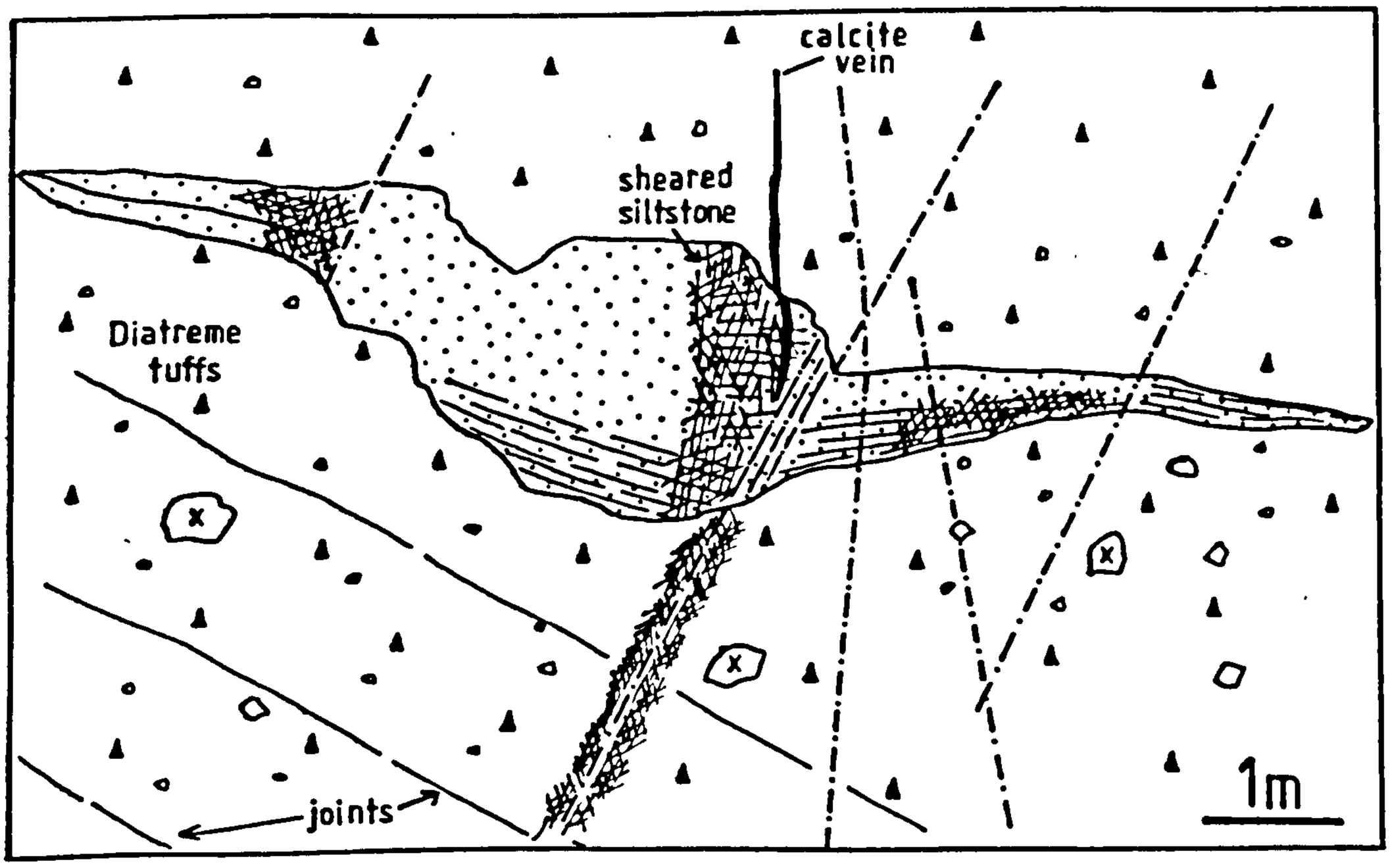

Fig. 5.35 Tuffaceous siltstone block within the Horseshoe diatreme which may represent a reworked channel body included in the tuffs by collapse.

and contains sediment bedded parallel to its base. Some of the surrounding poorly-bedded tuffs have slumped into the sandstone. A vertical normal fault cuts the northern margin of the sandstone. The body is interpreted as a channel infill which formed during a late-stage in the eruptive activity and was incorporated in the diatreme by collapse.

Well-preserved wood fragments occur sparsely in the tuffs. These, and carbonised material in some of the intrusive sediment dykes, are thought to have been derived from the poorly-consolidated country rock sediments.

Structurally, the diatreme tuffs consist of a number of poorly to well-bedded areas, along with massive, often blocky, agglomerate. The blocky zones occur mainly around the margins of the diatreme. The bedded tuffs are folded into a basin-like structure in the NW and to the SE are gently flexed, dipping generally into the centre of the diatreme.

Yellow Man diatreme

This diatreme measures ca.200m across and, like the Horseshoe diatreme, cuts the G.B.T.F. tuffs (Fig. 5.3, 5.36). The western margin is defined by a 1 to 2m faulted zone containing structureless blocky tuffs. The country rock tuffaceous mudstones are brecciated up to 5m outside this zone, or are abruptly truncated by it. Vertical faults and joints parallel to the margin contain calcite with vertical growth fibres. Intrusive sediment dykes cut the country rocks and trend at 90° to the margin.

The eastern margin is partly defined by a basalt dyke and is also faulted. The country rocks dip into the margin at 30°, and are intruded by sediment dykes. According to Martin (1955) the margin cuts the western margin of the Horseshoe diatreme at HWM. Current exposures of the tuffs outside the diatreme here are poor, and the material (poorly-bedded lapilli tuff cut by small faults and intrusive sandstone dykes) could represent either the Horseshoe tuffs or the country rock tuffs.

The bulk of the diatreme infill consists of unbedded, often blocky, tuffs. In the W, however, poorly-bedded coarse tuffs define a small basin structure. The lowest

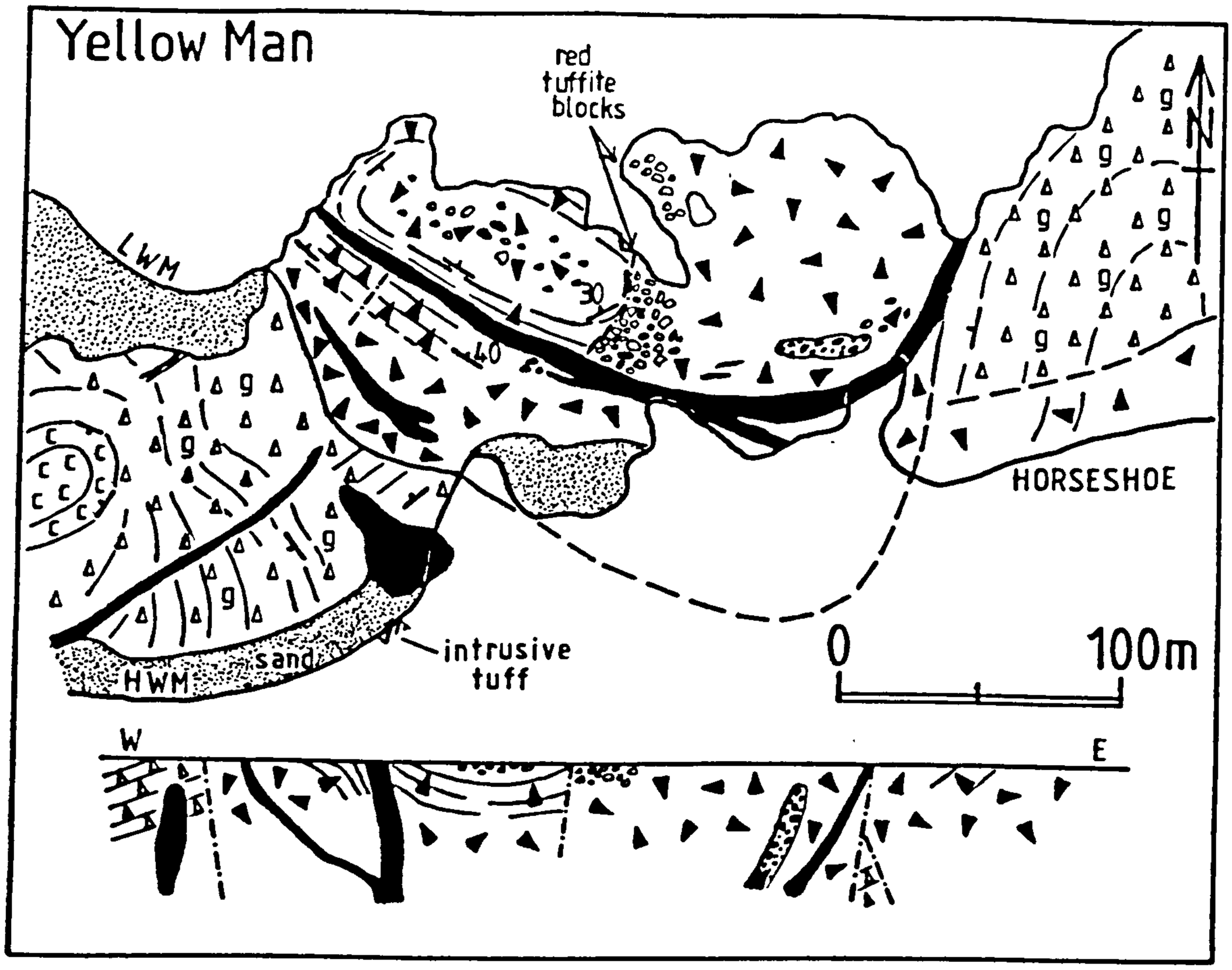

Fig. 5.36 Map and section of the Yellow Man diatreme.

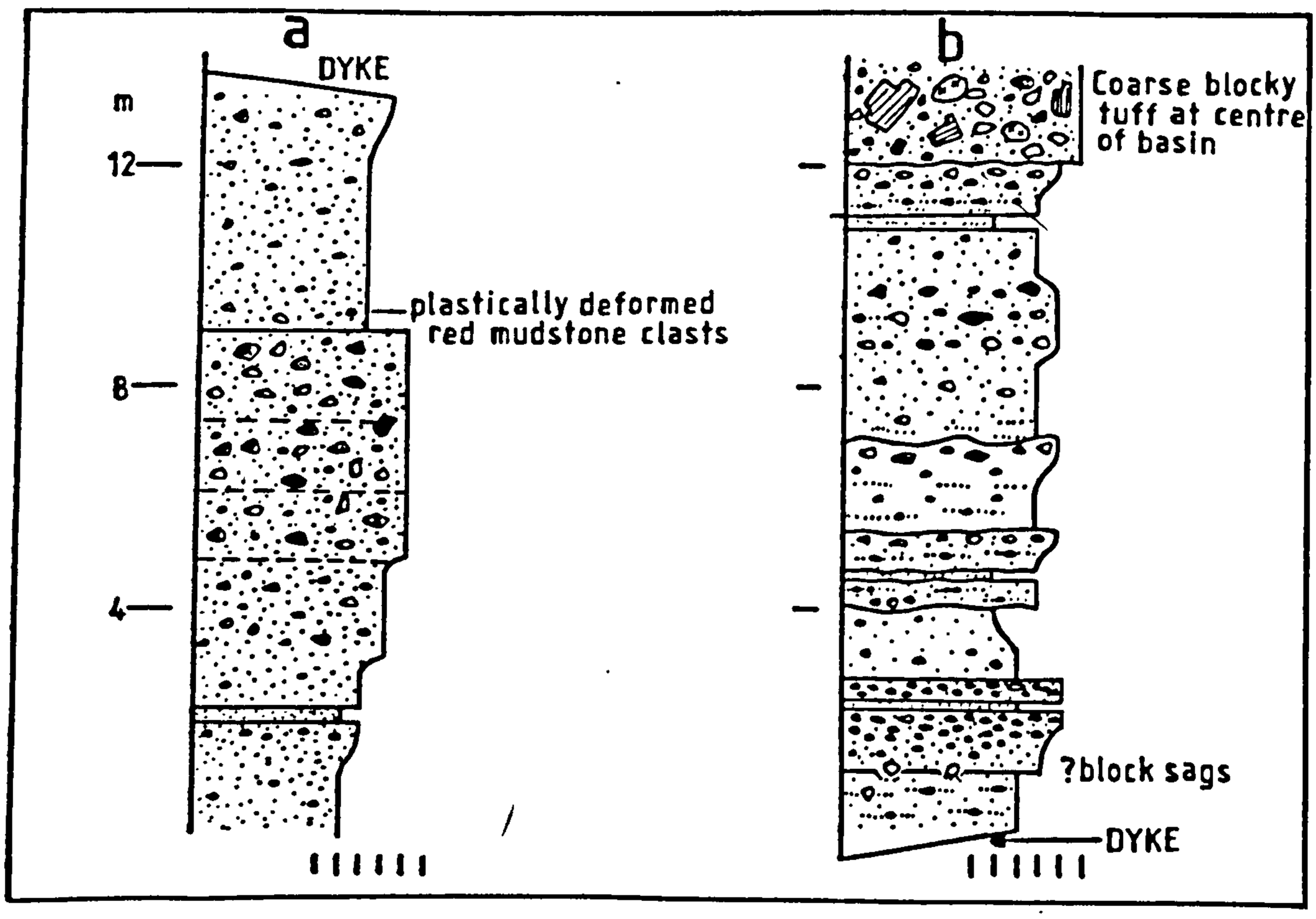

Fig. 5.37 Logs of the Yellow Man tuffs on either side of the NW-SE dyke.

bedded tuffs occur ca.50m within the margin and contain aligned blocks in poorly sorted layers. Upwards the beds become even coarser (Fig. 5.37) and contain blocks up to 1·5m across. The blocks consist of basalt, bedded red tuffaceous siltstone and some streaked-out mudstone clasts. Some of the layers are almost clast-supported, but become finer upwards and dip at progressively steeper angles. A dyke slightly cross-cuts the poorly-bedded sequence and N of it the bedding dip decreases into the centre of the basin.

The centre of the basin is filled by very coarse, unbedded material including blocks of basalt (up to 2·3m), red tuffaceous siltstone, bedded green tuff, red marl and grey cementstone. Most of the blocky layers which form the basin structure have probably been emplaced as debris flows, perhaps initiated by collapse.

The remainder of the diatreme contains unbedded agglomerate tuffs, cut by dykes. East of the faulted margin of the basin is a breccia crowded with blocks of red, bedded, tuffaceous mudstone in a matrix of similar material finely comminuted. Breccia zones rich in these blocks occur throughout the diatreme, with blocks reaching 3m diameter. Many of the tuffite blocks near the margins of the zones are veined and broken up by intrusive tuff. The tuffites in the blocks are well-sorted, well-laminated and often contain small-scale trough or planar cross-bedding. These characteristics as well as the fine grain size and the lack of impact sag structures indicate that the tuffites were originally deposited in a quiescent, subaqueous environment. Perhaps they represent collapsed remnants of deposits originally laid down within the breached crater of the Yellow Man volcano. Conversely, the diatreme, which contains few recognisable airfall tuffs, may represent an advanced crypto-volcanic structure. On that interpretation the red tuffites may be country rock deposits disrupted by the cryptovent. Collapse back into the diatreme, which perhaps never fed a fully developed subaerial volcano, resulted in brecciation and intrusion of dykes into the tuffites.

Areas near the main E-W dyke contain abundant rounded

blocks of basalt, some of which have lobate margins. These pillow-like surface structures are thought to be due to intrusion into fluidized, wet unconsolidated tuffs. Similar lobate structures were reported by Kokelaar (1982) at the bases of sills intruded into wet sediment. The blocks commonly occur in elongate zones parallel to the major dyke and probably represent broken up dykes. Intrusive tuffisite dykes and pods are associated with the dykes at the eastern margin. They formed by gas-streaming, perhaps largely due to the production of steam after intrusion of basalt into wet tuffs and sediment.

Whether or not the Yellow Man diatreme had a subaerial volcanic expression, the high block content, the lack of airfall tuffs, the abundance of brecciated reworked tuffs and the intrusions all suggest that present exposures represent a comparatively deep-level section through a collapsed diatreme.

Partan Craig diatreme

This diatreme (Fig. 5.38) measures ca.600m across and cuts the Green Basaltic Tuff Formation about 1·5km E of North Berwick (Fig. 5.3). The eastern margin cross-cuts the undisturbed country rock marly tuffs, and is defined by a 1m zone of unbedded tuff. This zone is sheared in places and is cut by anastomosing calcite veins trending both parallel and normal to the margin. Within the diatreme, bedded lapilli tuffs are cut by a coarse brecciated zone, containing blocks up to 3.5m across of basalt, tuff, marl, sandstone and tuffite. Bedding within some of the blocks is crumpled and faulted. Near the margin the country rocks are folded into a small elongate basin structure whose long axis trends NE-SW, normal to the diatreme margin. A thin, similarly-trending dyke cuts the country rocks SE of the basin and abruptly terminates against the diatreme margin. It thickens towards the Yellow Man diatreme and probably had its source there.

At LWM, the western margin appears to consist of a low-angle sheared zone, separating blocky diatreme tuffs from underlying green mudstones. Outside the diatreme a large raft of bedded tuffs has been emplaced by sliding

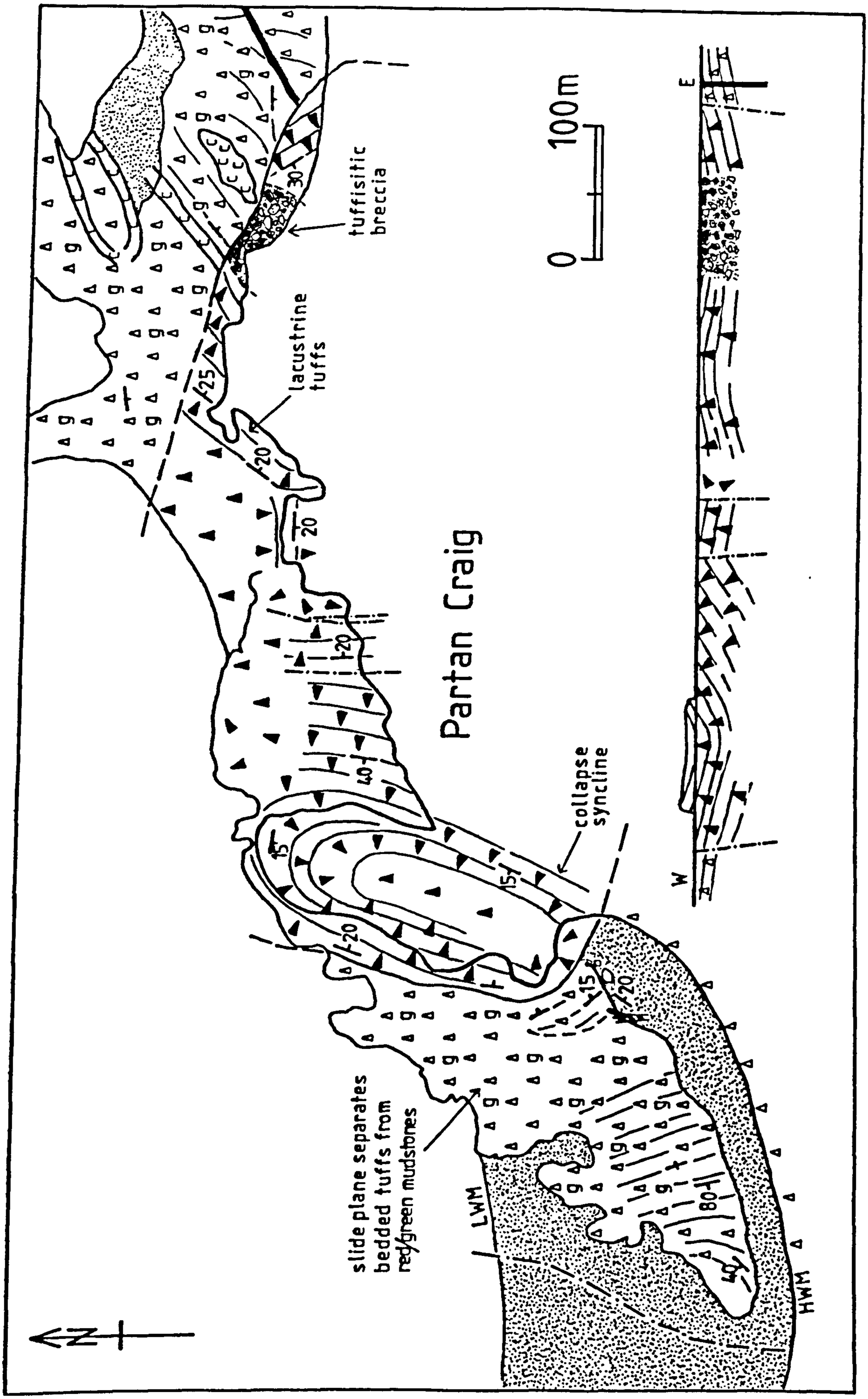

Fig. 5.38 Map and section of the Partan Craig diatreme and the surrounding G.B.T.F. tuffs.

over green and red mudstones (Martin, 1955), now visible in erosional "windows" through the raft. At HWM smaller blocks of mudstone, tuff and tuffite form a poorly exposed breccia, cut by intrusive sandstone dykes. Here, the diatreme margin is steep and faulted, truncating coarse diatreme tuffs which occupy the southwestern limb of an elongate basin.

The lowest exposed part of the basin is formed of poorly-bedded, blocky agglomerate and breccia. The beds (Fig. 5.39) contain blocks of basalt, tuff and bedded red-green tuffaceous mudstone.

Fig. 5.39 Blocky units at the western margin of the Partan Craig diatreme which broke up and formed debris flows. Bag measures 30cm and lies at base of unit comprising tuffaceous sandstone blocks.

One particular unit, 2m thick, consists almost entirely of blocks of tuffaceous sandstone. Above the blocky units, some of which have slightly erosive bases, the bedding becomes better-defined and lapilli grade beds alternate with more blocky horizons (Fig. 5.40). Upwards, basaltic blocks predominate and the beds resemble airfall tuffs. The blocky lower units are mainly thick debris flows which contain plastically deformed mudstone clasts and block trails. Some of the blocky units are oligomict, almost

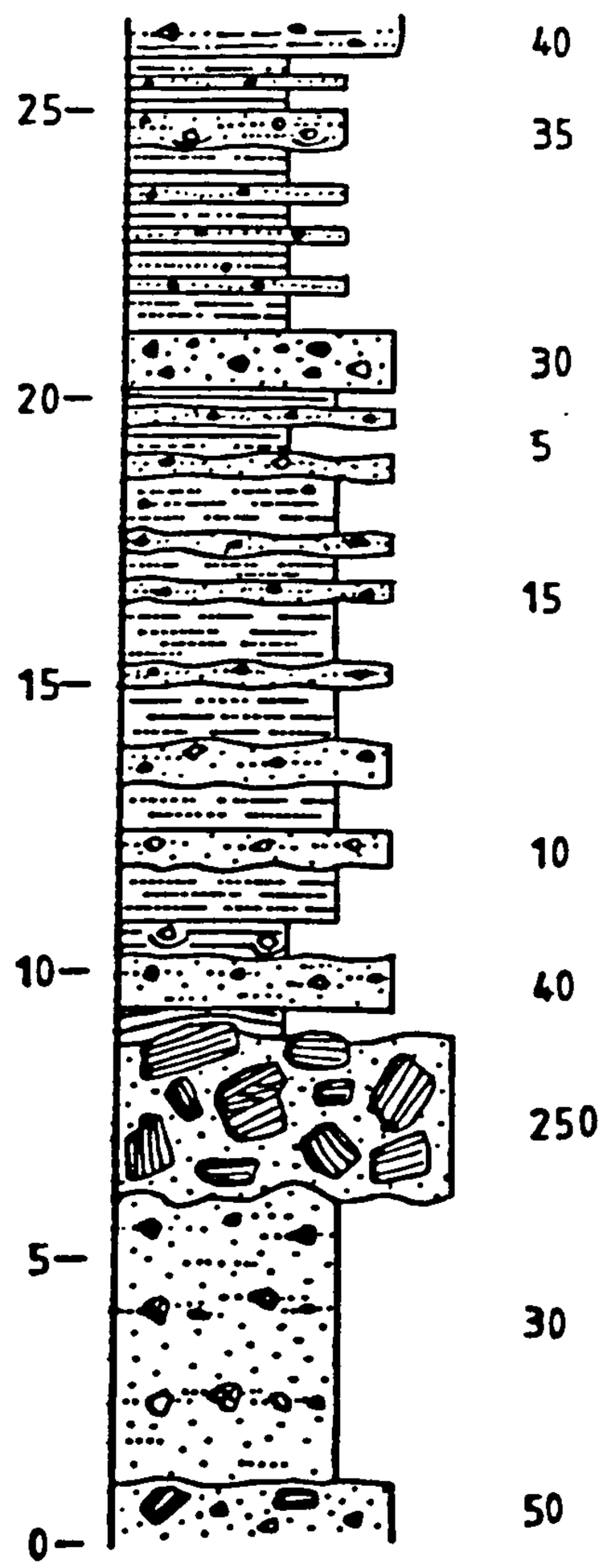

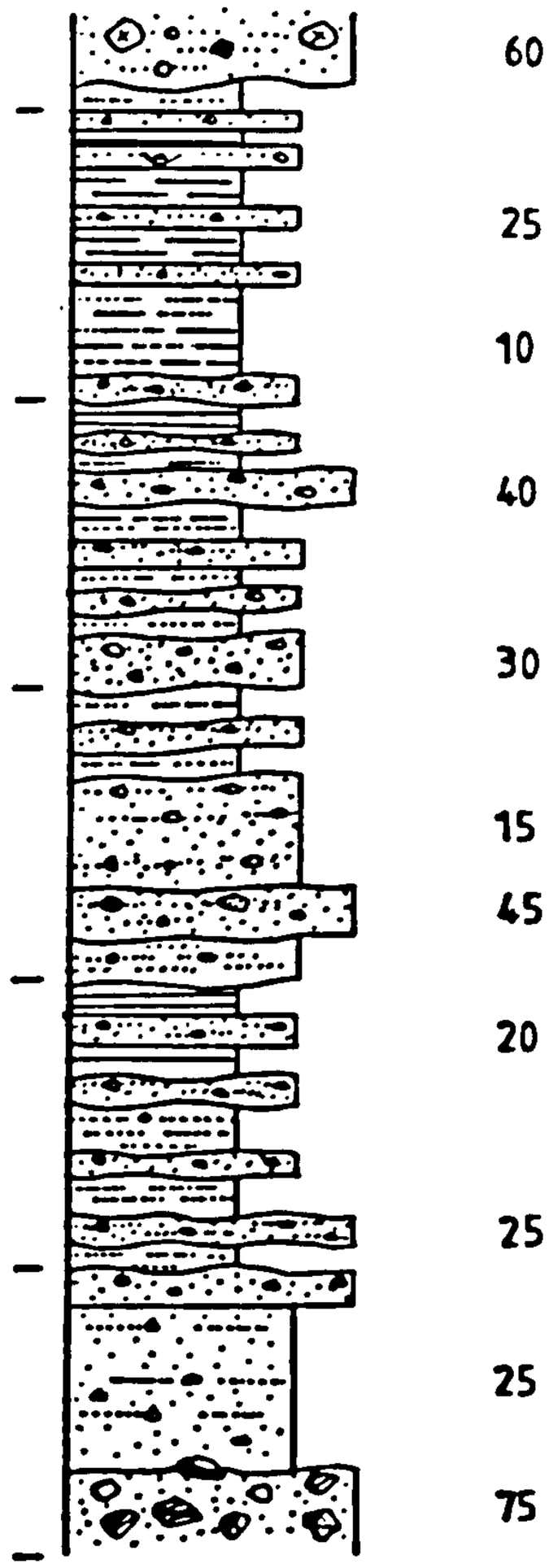

Fig. 5.40 Logs of the Partan Craig diatreme tuffs.
a) Western margin basin sequence
b) Eastern side of western marginal basin

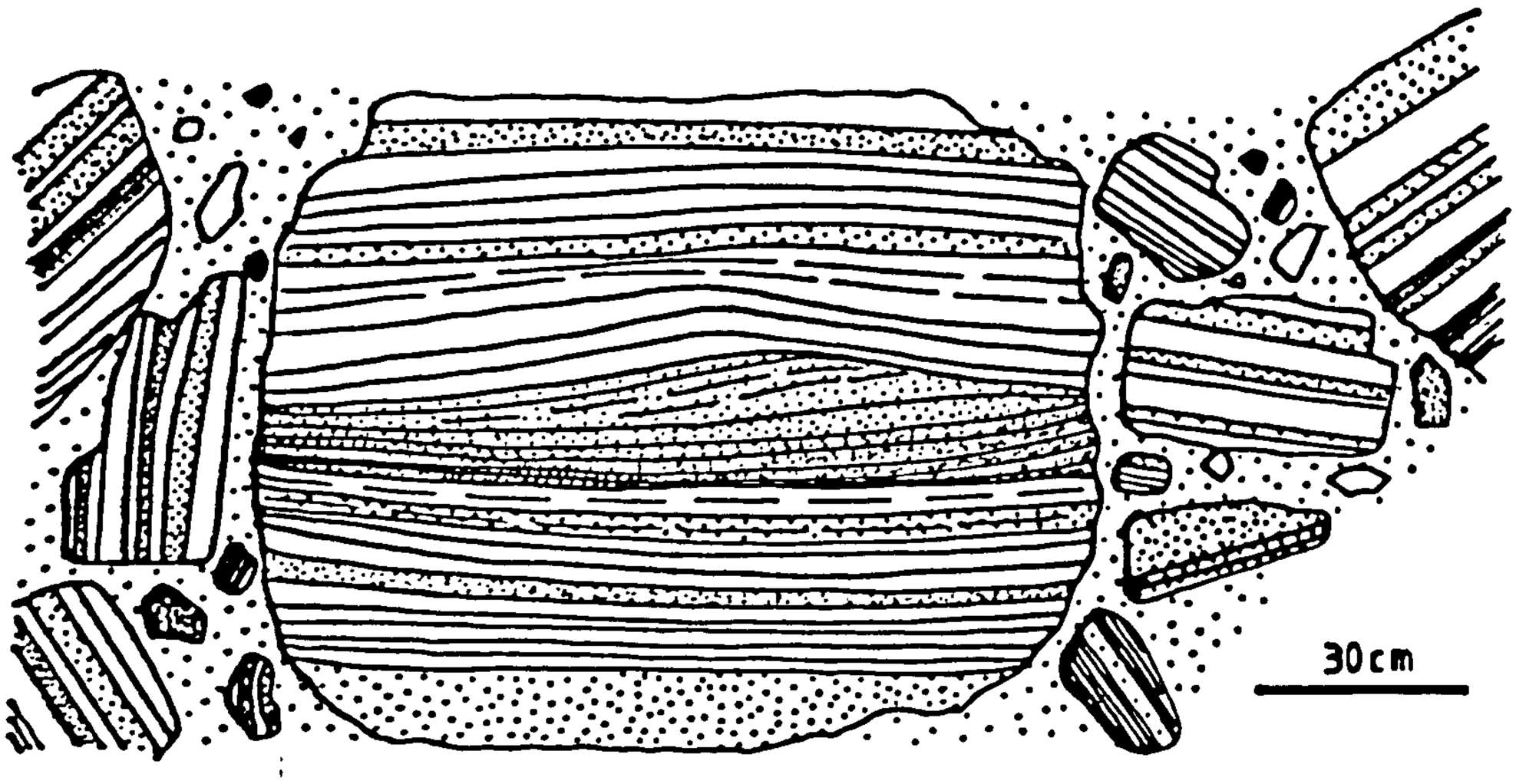

Fig. 5.41 Block of red tuffaceous siltstone in debris flows at western margin of the Partan Craig diatreme. Note low-profile dune containing climbing crestal cross-laminae, indicating surge deposition.

clast-supported, conglomerates and cannot have travelled very far. Breakdown of bedding along strike into the basin suggests that subsidence may have initiated debris flows by oversteepening.

The blocks of tuffaceous mudstone which are common in the Partan Craig debris flows are found in many of the North Berwick diatremes. The mudstones contain 20-70% of tuff and are well-sorted, well-bedded, often cross-bedded deposits. The cross-bedding in the Partan Craig blocks is commonly low-angle, trough-shaped and of moderate scale. One block contains an asymmetric dune with climbing cross-laminations (Fig. 5.41). This structure is similar to surge dunes at Saefell (Chapter 2), but is smaller, possibly because the Partan Craig dune is a distal surge structure.

The remainder of the deposits within the diatreme are largely poorly-bedded green lapilli tuffs. They contain blocky layers, some of the blocks with impact sags, and small channels. The channels contain coarse lapilli and are in places associated with faintly cross-bedded tuffs. Many of the structureless units appear to have formed by flow, since they have irregular bases, block trains, and lack internal sorting. Some of the better bedded units are affected by slumping, which has in places resulted in movement along shear surfaces. Block impact sags are rarely seen, because of debris flow reworking and because larger clasts seldom overlie bedded finer units. Rare gneissic clasts occur in the western part of the diatreme. They are similar to clasts described by Graham & Upton (1978) except that none were seen to be mantled by basaltic material.

The youngest deposits in the northeastern part of the diatreme comprise green tuffaceous sediments thought to have been deposited in a crater lake. The deposits - well-laminated tuffaceous marls and siltstones - overlie coarse debris flow material (Fig. 5.42) and consist of thin (up to 40cm), laterally discontinuous units. Further description of these deposits is given in Section 5.4. In places, blocky layers cut into the tuffaceous marls and incorporate rip-up clasts at their base. One such clast (Fig. 5.43) has been folded by being sandwiched between two bedded tuff

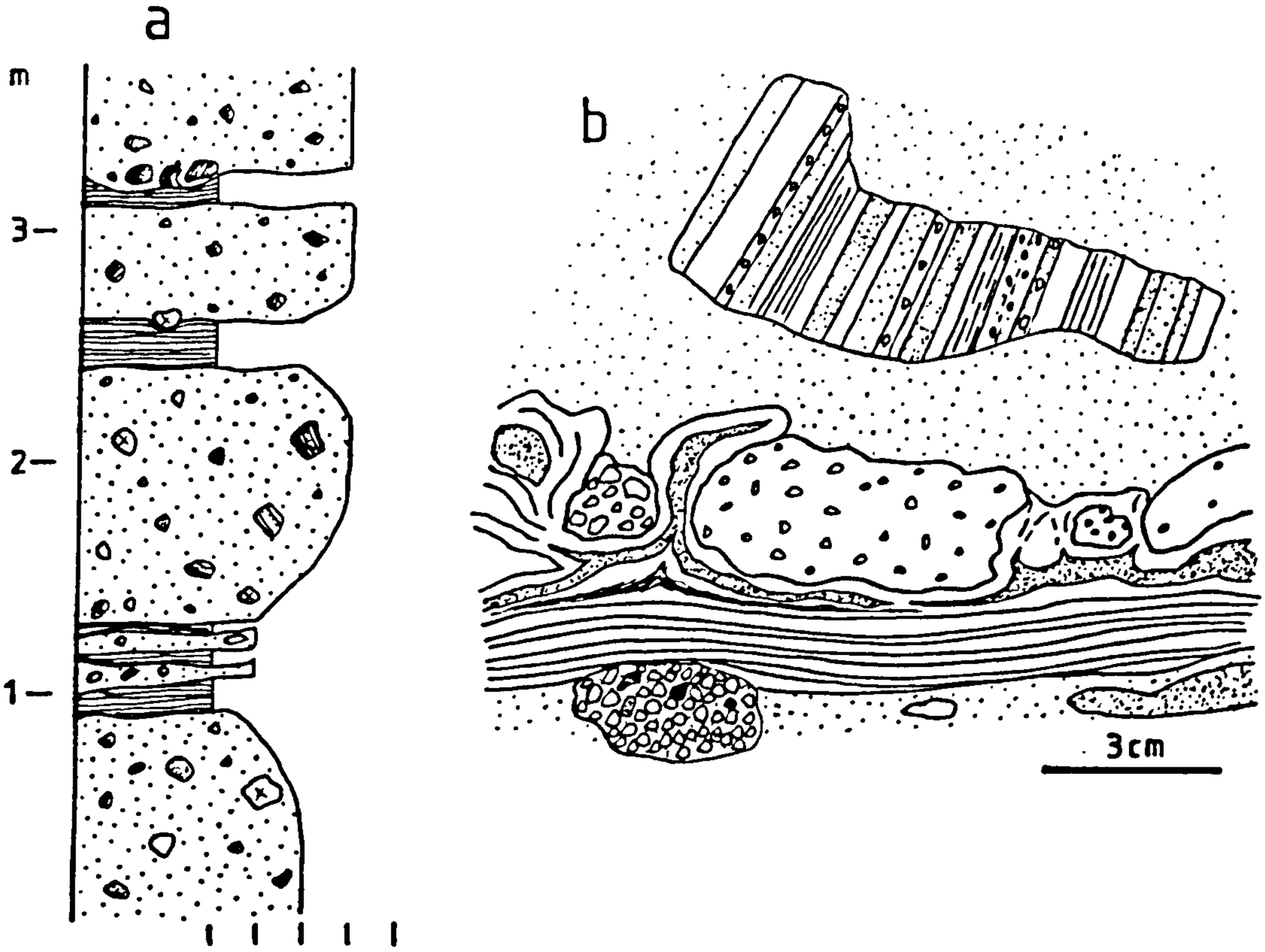

Fig. 5.42 a) Logs of Partan Craig marly tuffs.
b) Debris flow blocks deforming marly tuffs.

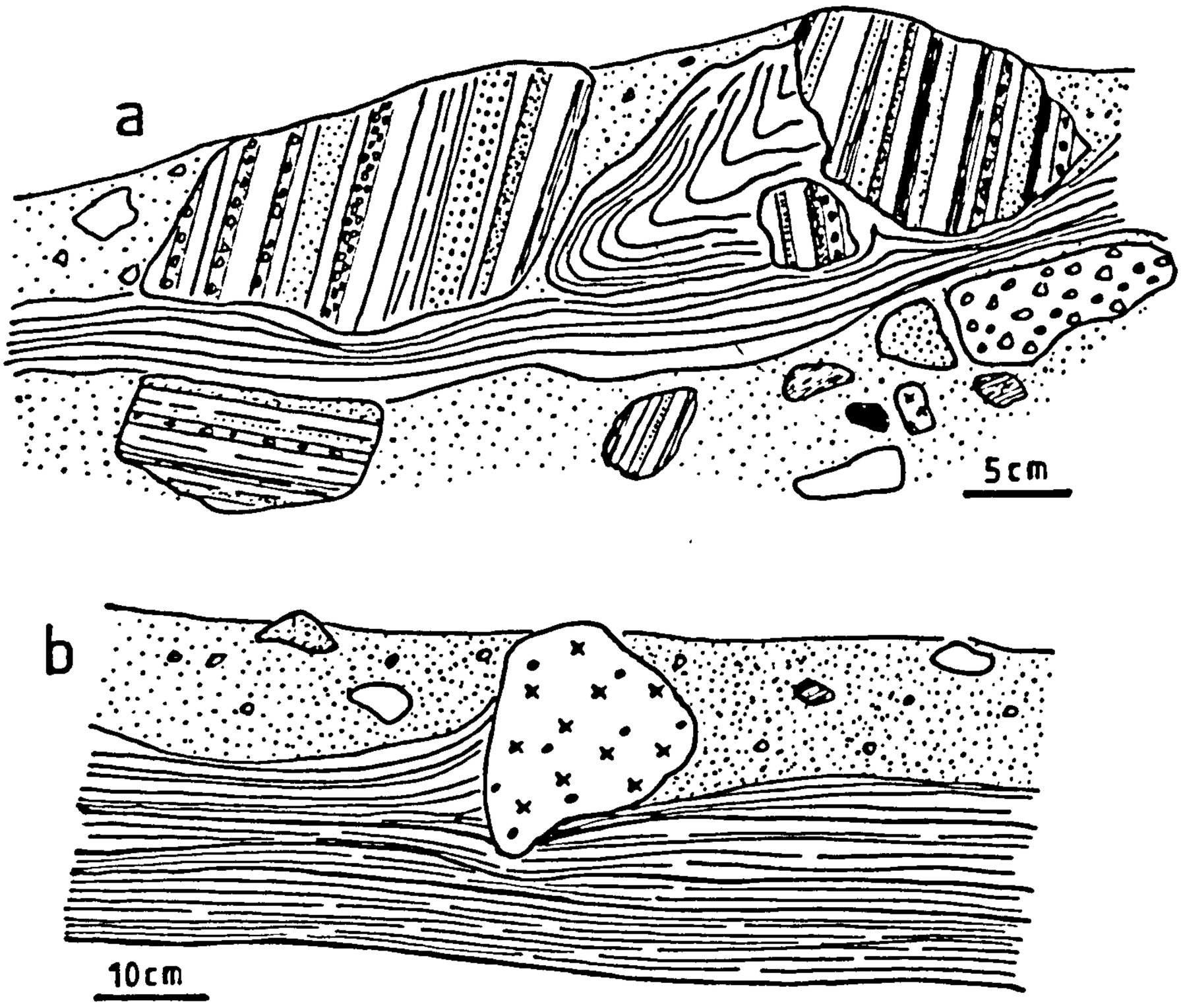

Fig. 5.43 a) Folding of marly tuffs due to debris flows moving into shallow lake and rucking-up sediments.
b) Rucking-up of marly tuffs by block protruding from overlying debris flow.

blocks. Other features of the marly layers include loadcasts, flame structures, desiccation cracks and small sags, apparently of impact origin.

The tuffaceous marls represent lacustrine deposits formed at a late stage in the volcanism, presumably within the crater of the Partan Craig volcano. Weak eruptions are thought to have ejected only fine ash, but triggered debris flows which moved into the shallow lake and disrupted the sediments accumulating there. The lack of current-formed structures in the lacustrine tuffs suggests that the crater walls were not breached at this time. It is possible that the lake formed after cessation of the Partan Craig activity, and that nearby volcanoes supplied the fine ash which now forms the thin, normally graded laminae within the lacustrine deposits.

Structurally, the diatreme consists of gently folded tuffs cut by steep faults of unknown displacement. The folding is on NNE axes, similar to the fault trend. The large size of the diatreme, its comparatively minor internal deformation and the abundance of reworked tuffs suggest that relatively little collapse has occurred. This is supported by the presence of rafts of bedded tuff outside the western margin, which are thought to be Partan Craig outer flank deposits. Sliding and downfaulting preserved these largely unreworked tuffs close to their collapsed crater equivalents in the diatreme.

5.4. Petrography, Morphology and Alteration

5.4.1 Petrography

The red and green diatreme tuffs contain different proportions of juvenile and non-juvenile material, as well as having been altered and replaced by different minerals. The country rock tuffs and tuffaceous sediments are similar, though generally more altered than their presumed diatreme equivalents and will be discussed along with the latter.

a) Juvenile fragments

Although the tuffs are highly altered (Section 5.4.4), vesicular and non-vesicular fragments of originally

juvenile glass can be recognised in many samples of both red and green tuffs. Generally, the particles are blocky and subangular with irregular, often corroded margins. In the country rock tuffs the juvenile fragments are more rounded and equant, due to reworking.

The lapilli reach 5mm diameter but most are 1-2mm. In the largely indeterminate matrix grains <0·3mm are common. The smaller ash grains tend to be less vesicular than the larger lapilli and, where preserved, their margins are more angular.

Some of the fragments consist of what appears to be unaltered sideromelane. This is especially true of the Parade tuffs, many of which comprise yellow-orange, almost isotropic, structureless material containing opaque inclusions (Fig. 5.44). However, on closer examination the material is seen to consist of small, yellow, isotropic areas within fragments largely replaced by chlorite and clay. In the green tuffs, similar patches, apparently of original sideromelane, survive within the centres of lapilli.

In general, the juvenile material in the green tuffs (Fig. 5.45) is more vesicular than that from the red tuffs. Both types of lapilli sometimes contain elongate vesicles, largely unrelated to the shape of the enclosing fragment. Flow structures have partly controlled the irregular shapes of some fragments. Inclusions in the juvenile fragments are largely replaced by chlorite and calcite, apart from sediment xenocrysts, such as quartz and feldspar. Opaque spots are scattered throughout the fragments, which in the red tuffs are often oxidised to hematite. Pseudomorphs after olivine, pyroxene and feldspar also occur, especially in the red tuff lapilli.

Vesicles in the grains reach a maximum of 0·4mm, with the larger vesicles occurring singly in large lapilli. Smaller vesicles often occur in clusters although only rarely do bubbles coalesce. A general increase in vesicle size into lapilli centres indicates that grain interiors cooled less rapidly than their margins.

Some grains are full of disseminated iron oxide crystals and may represent original tachylite. These grains

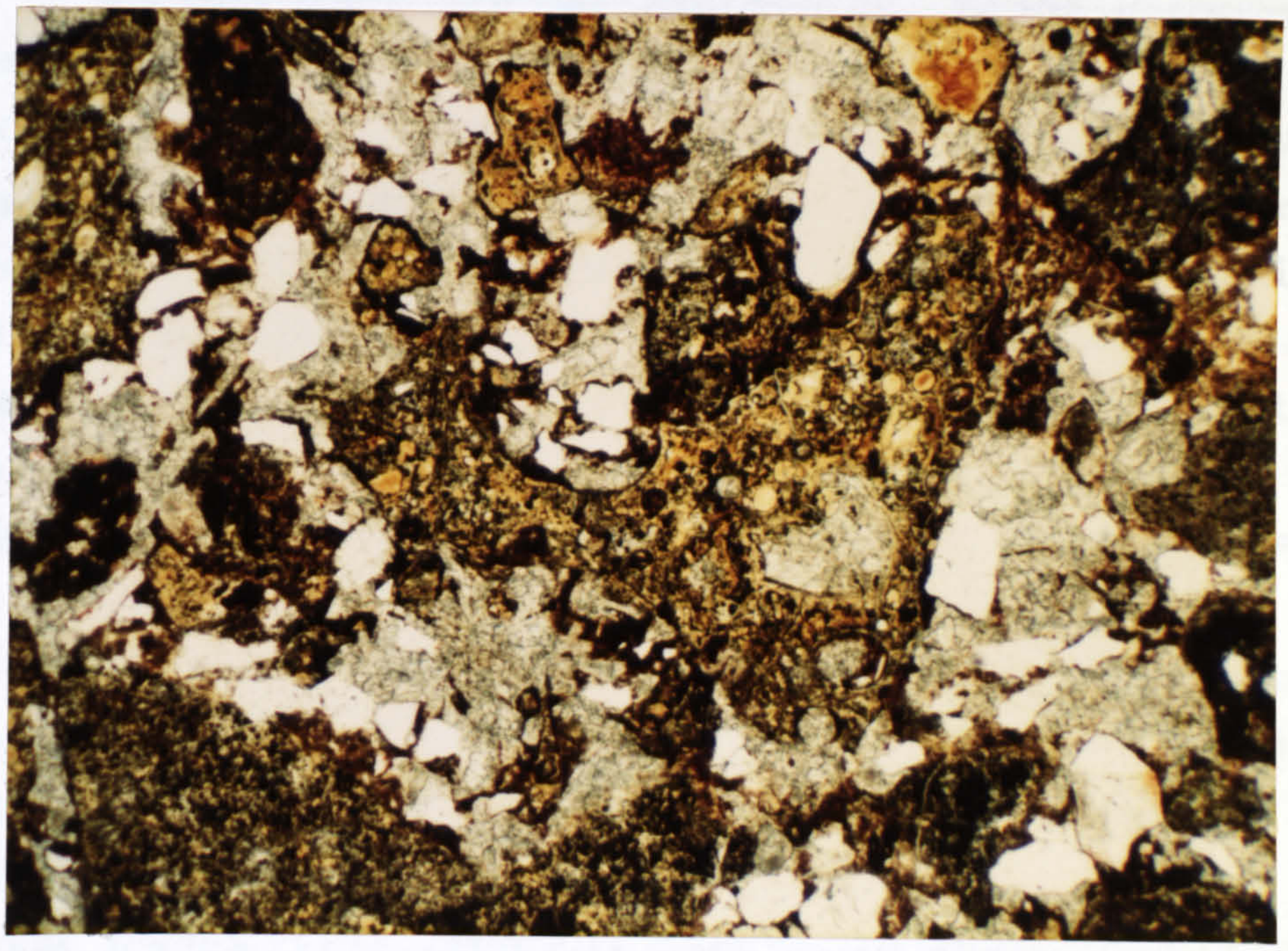

Fig. 5.44 Vesicular ash grain from the Parade tuffs, now replaced by vermiculite and chlorite. Much of the matrix is chlorite replaced and surrounds relict ash and quartz grains. Plane polarised light. x10.

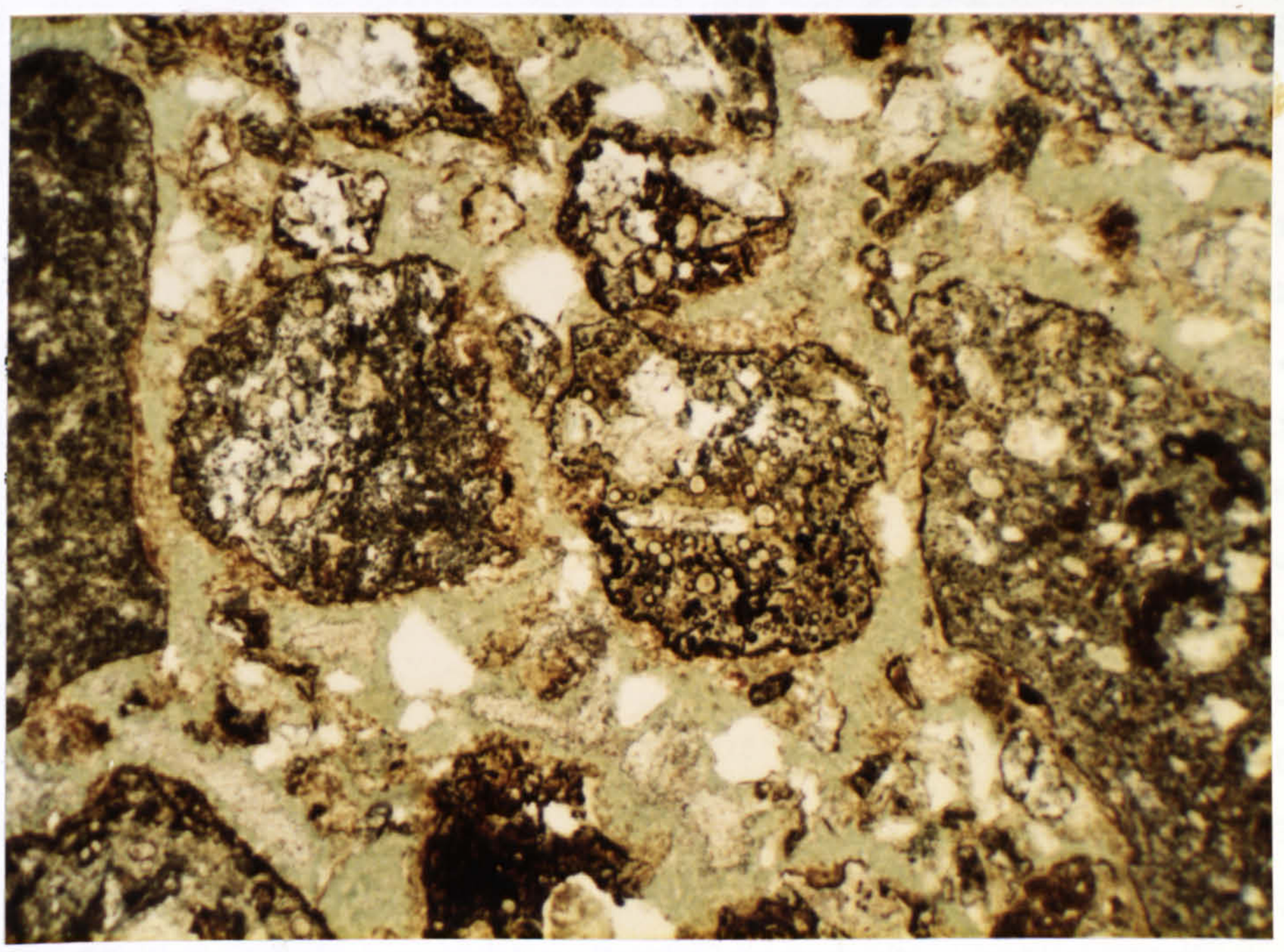

Fig. 5.45 Vesicular ash from the Partan Craig diatreme tuffs, now replaced by chlorite and calcite. Matrix is largely chlorite replaced and contains corroded ash and quartz grains. Plane polarised light. x10.

tend to contain more irregularly-shaped, often elongated vesicles. Such fragments also contain small laths of plagioclase feldspar which are aligned parallel to vesicle elongation. The microlites are up to 0·1mm long and are often the only unaltered phase in the juvenile tachylite lapilli. They are seldom found within altered grains thought to have been originally sideromelane - probably because they were only able to crystallize during the slower cooling of the tachylite. Further evidence for this is indicated by grains which have interiors rich in iron oxide with some microlites, and margins which contain little iron oxide and no microlites. Differential cooling rates allowed tachylite to form within quenched sideromelane rims.

b) Phenocrysts

The phenocrysts commonly occurring within the juvenile lapilli can now be recognised only by their shapes, since the original minerals have generally been pseudomorphed by alteration products. Most pseudomorphs appear to be after olivine, pyroxene and feldspar. The type and proportion of the different crystals present varies between diatremes, reflecting either source magmas of different composition or the time at which a fractioning common source magma was tapped.

The green diatreme tuffs contain mainly pseudomorphs after partially resorbed olivine, which commonly occur as crystal aggregates in the centres of juvenile lapilli. The red diatreme tuffs have a different crystal content with both the Seacliffe Tower and the Car diatremes containing mainly pyroxenes. The Car pyroxenes are moderately abundant and are generally fresh, often concentrically-zoned augites. The pyroxenes are generally partially corroded and enclosed by thin rims of altered glass. The Parade diatreme tuffs contain some feldspar, pyroxene and olivine pseudomorphs as well as a few large, altered, subhedral crystals up to 3mm across. These often have rounded outlines but a few better-formed examples have typical olivine shapes.

As well as the previously mentioned crystals, some rare biotite laths occur in the red diatreme tuffs. In one instance a partly-resorbed biotite crystal is rimmed by

altered glass, indicating it may be of juvenile origin.

c) Vesicle sizes

Due to the small number of samples collected from each diatreme, only generalisations about vesicle size ranges can be made. More detailed conclusions can be made on the Parade diatreme, which has been comprehensively sampled and studied.

The average maximum vesicle radius varies with stratigraphic levels in the Parade. In general, the average vesicle size increases from ca.0·02 to 0·05mm going up sequence from the western margin and decreases upwards in a logged section near the youngest exposed tuffs. Within this general trend abrupt variations in average vesicle size indicate rapid fluctuations in magma vesicularity on eruption, due to changing eruption characteristics. Such fluctuations are observed over short periods of time in recent eruptions (Chapter 4).

In general, the North Berwick diatreme tuffs contain larger vesicles than the Parade tuffs. The smallest maximum vesicle radius is found in the Seacliffe Tower diatreme tuffs. Although the green diatreme tuffs have similar maximum vesicle radii to the red diatreme tuffs, their vesicles are more abundant. The average size of vesicles is slightly larger in the green diatreme tuffs, ranging between 0·05 and 0·07mm. It is thought that the green diatreme volcanoes had shallower eruption foci, or their magma had different physical properties, to the red diatreme volcanoes.

The rapid fluctuations in vesicle size in the Parade tuffs suggest that external factors influenced bubble growth. However, only tentative conclusions may be drawn from such evidence because it is based on thin section data, which represent statistically very small samples.

d) Accessory lithic fragments

The lithic fragments in the East Lothian diatremes consist of two types, volcanic and sedimentary. The volcanic component comprises lava fragments and clasts of tuff from previous eruptions. The lava fragments are generally of fine-grained basalt containing calcite and

chlorite pseudomorphs after pyroxene and olivine. The tuff clasts are more highly altered than their host tuffs, as are recycled juvenile grains from previous eruptions. The volcanic lithic clasts are often highly angular and reach much larger sizes than juvenile grains. Many poorly vesicular basaltic clasts may be cognate rather than accessory lithic fragments, but no means of distinguishing these has been found.

The sedimentary component is usually more abundant than the volcanic, especially in the red tuffs, and consists of both single grains and rock fragments. The single grains comprise quartz, orthoclase, microcline, plagioclase and mica, as well as accessory sphene and tourmaline. The grains range in size from 0·01 to 0·3mm, are poorly sorted and have angular to sub-rounded shapes. Some of the grains in the red tuffs have hematitic rims. The quartz generally has strained extinction and occasionally occurs as granular aggregates of small sub-grains derived by mechanical breakdown of large particles. In one of the Parade tuffites, many of which are tuffaceous siltstones, a rounded quartz grain has a syntaxial quartz rim (Fig. 5.46). This rim is corroded by the clay matrix of the rock however, and may have formed before the quartz grain was incorporated in the tuffite, or at least before the growth of the authigenic matrix.

The sedimentary rock fragments are often sub-rounded in shape and include siltstone, mudstone, shale, cementstone and limestone. The coarser sediment clasts all have carbonate cements or a clay matrix and are less abundant than the finer sediment clasts. This suggests that the more cohesive fine sediment was better able to survive disruption by volcanic explosions. Coarse sediment would be broken down more easily, especially as the sediments were poorly consolidated. Numerous sediment grains occur as inclusions within juvenile fragments, indicating that the bulk of the sediment in the tuffs was derived from the country rock succession. Rounding of many smaller sedimentary rock clasts probably occurred during transport within the volcanic conduit.

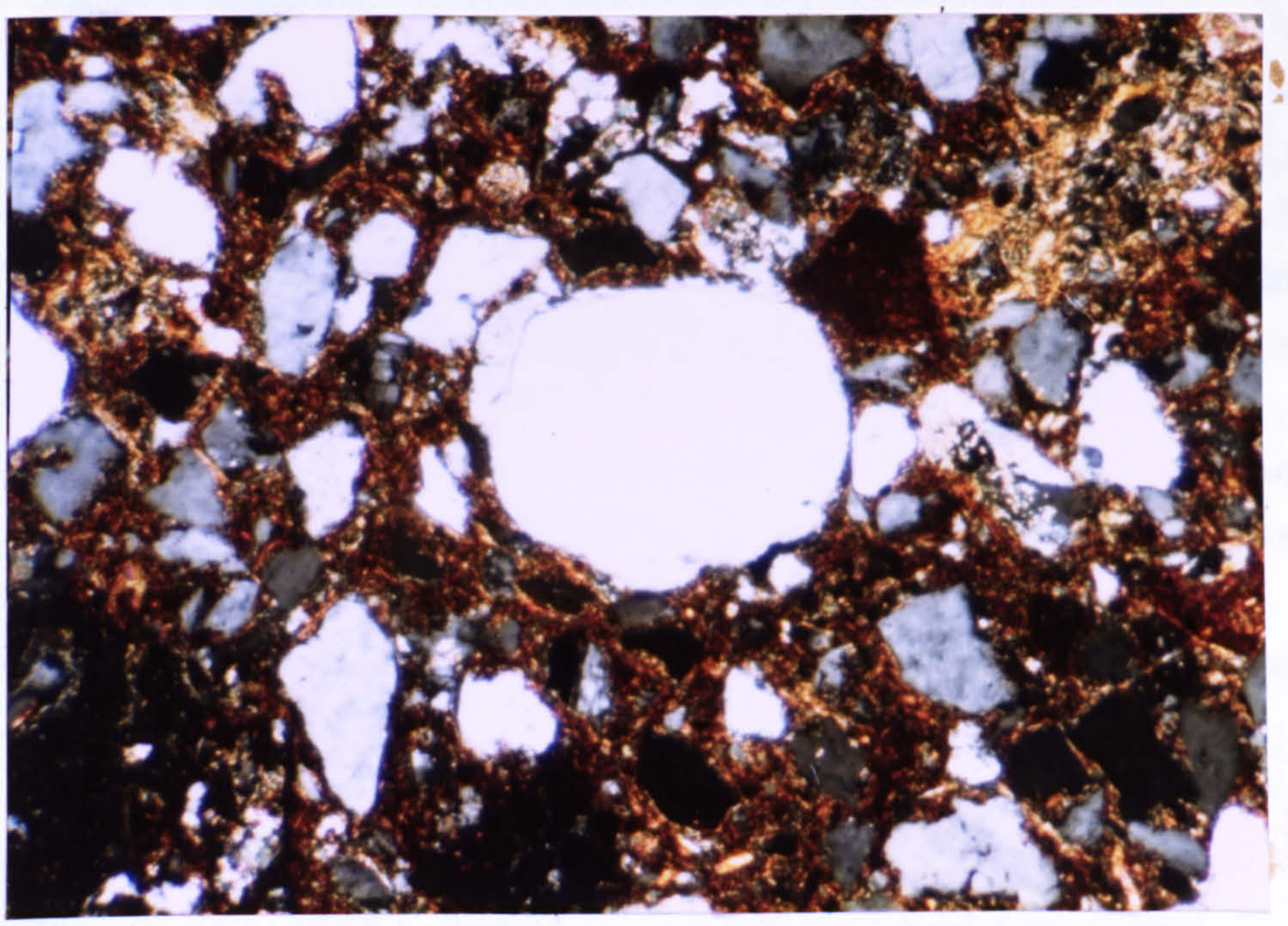

Fig. 5.46 Syntaxial quartz rim around quartz grain in the Parade tuffs. Matrix is rich in clay which corrodes the quartz rim and other sedimentary lithics. Note hematite staining of much of the matrix. Crossed polars. x25.

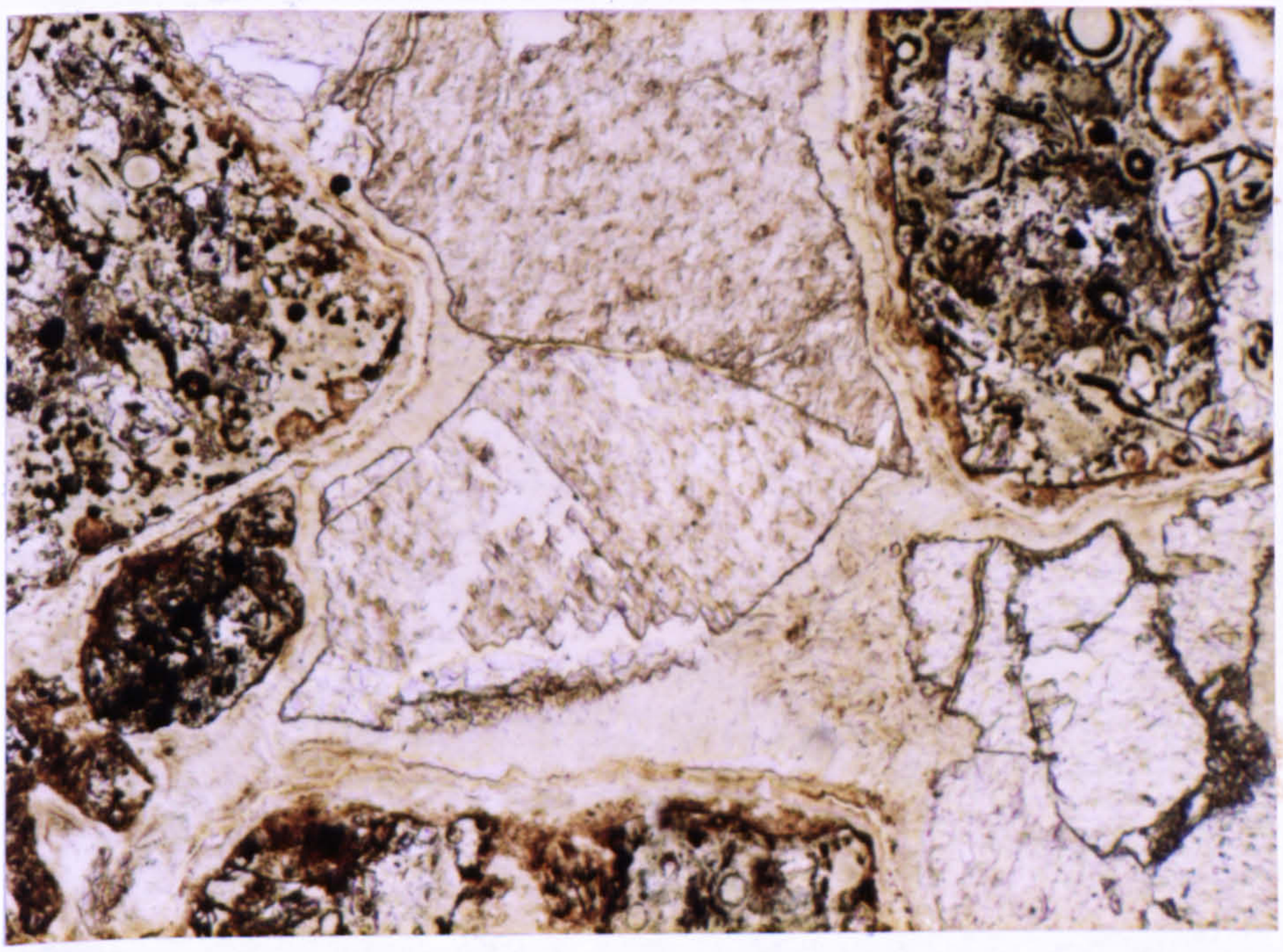

Fig. 5.47 Pore spaces in Horseshoe diatreme tuffs infilled with chlorite and later sparry calcite. Plane polarised light. x25.

e) Matrix / Cement

A variety of matrix types occur in the tuffs along with cements, which may occasionally replace the matrix and occupy all the pore spaces between larger grains. In the red tuffs much of the matrix consists of hematite-stained clay minerals (Fig. 5.46). Optically, the clay minerals appear to be montmorillonite and kaolinite which are associated with sericite flakes in places. Small sediment grains as well as altered juvenile ash occur throughout the matrix, which often wraps around them. Sparry calcite cement fills voids and occasionally replaces some of the matrix, where it is associated with micrite. Corrosion of both juvenile and lithic clasts by matrix or cement is common.

The green tuffs generally lack matrix material and have pore spaces infilled with calcite and chlorite cements (Fig. 5.47). Often, juvenile lapilli occur in a sparry calcite cement. A few samples have a matrix of fine ash and lithic grains but this is always replaced by chlorite and calcite to some extent.

The accretionary lapilli in the disturbed country rocks SW of the Car consist of matrix-grade material and merit

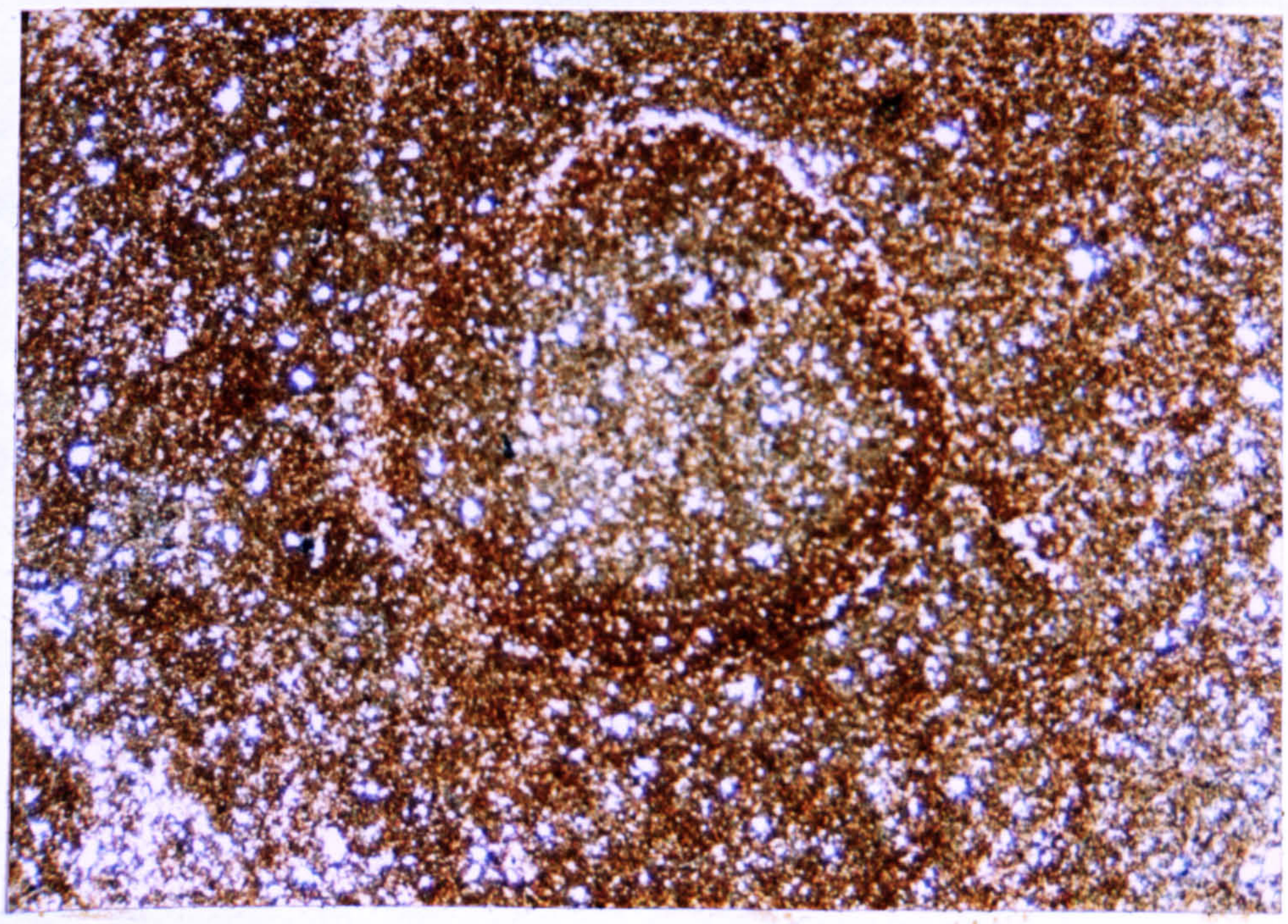

Fig. 5.48 Accretionary lapillus from crypto-volcanic structure SW of the Car diatreme. Core consists of a structureless aggregate of ash surrounded by faintly concentric bands of fine ash. Plane polarised light. x4.

further description. Typically, they are 2 to 5mm in diameter, sub-spherical and contain well-sorted cores of silt-grade material with thin, finer rims (Fig. 5.48). The lapilli cores are largely structureless, though faint concentric layering is occasionally defined by thin clay laminae. The rims are concentrically banded, up to 0·5mm thick and decrease in grain size outwards. The material in the lapilli is identical to the hematite-stained, tuffaceous siltstone of the matrix and both are similarly highly calcite replaced. Some of the lapilli adhered together during growth and accreted a common rim. Others broke on impact with the ground, rupturing their outer rims. No post-emplacement deformation of the lapilli has occurred.

The lapilli are identical to those described by Moore & Peck (1962) and were formed in the upper regions of phreatomagmatic eruption columns. The accretionary lapilli were subsequently deposited some distance from their source vent. Similar, though less obvious, accretionary rims around larger grains in some of the diatreme tuffs are more like the armoured lapilli in proximal tuffs described previously from Saefell (Chapter 2).

f) Origin of tuff colouration.

The origin of the different colours of the diatreme tuffs is of interest because it reflects differences in their diagenetic histories. The green tuffs contain abundant green chloritic replacement of juvenile lapilli. Locally, however, the matrix of the green tuffs is reddened. This is most common in narrow zones around blocks of red sediment. In places, thin sediment-rich layers are interbedded with the green lapilli tuffs, and these layers are often hematite-stained.

The red tuffs contain a hematite-rich clay matrix with many sediment and volcanic grains having hematite rims. In extreme cases, volcanic grains may be completely replaced by hematite and the clay matrix by calcite. Some chlorite is often present in pore linings or as a replacement of volcanic grains.

Lorenz (1972) ascribed the reddening of Permian diatreme tuffs in West Germany to circulation of oxidising

groundwaters from country rock red sediments. He noted that red tuffs were always found adjacent to red sedimentary horizons outside the diatreme. Drab-coloured tuffs in the diatremes are associated with drab sediments and both must have been simultaneously affected by reducing groundwaters. At the present erosion level all the East Lothian green diatremes are surrounded by green tuffs and all the red diatremes by red tuffs, suggesting a similar origin.

It is thought that the colour in the red diatreme tuffs is partly due to passage of oxidising solutions. However, since red tuffs contain a high proportion of sediment material derived from the country rocks, it is likely that they underwent similar diagenetic changes to these sediments. Features of these changes include :-

1) the alteration and replacement of ferromagnesian minerals, and the survival of heavy minerals such as sphene and tourmaline
2) the distribution of hematite as grain coatings and in the interstitial matrix
3) the alteration of feldspar by sericitization
4) the replacement and dissolution of quartz and juvenile lapilli
5) the presence of authigenic clay, chlorite and calcite.

These features are similar to those noted by Turner (1980) in Triassic sediments thought to have had a similar diagenetic history to sandy alluvium described by Walker (1976). Here, unstable ferromagnesian grains were altered intrastratally to produce reddening. In the case of the East Lothian red tuffs the alteration of volcanic glass may have contributed to this reddening process. The colour of the red tuffs is thus largely due to in situ alteration.

A further contribution to reddening may have been provided by ageing of the ferric hydroxide precursor (Turner, 1980). Such material may well have been deposited in large amounts along with the clay-rich suspended load in floodplain environments. Oxidising conditions prevailed here due to periodic drying and lowering of the water table, and iron hydroxides changed to hematite with time. The Canty Bay Sandstone Formation floodplain deposits are red

suggesting that such a reddening process may have occurred. The drab channel sandstones and the Green Basaltic Tuff Formation lagoonal and lacustrine tuffs were deposited in reducing conditions. Here, ferric hydroxides were unstable and were removed in solution. No estimate of the importance of deposition and ageing of hematite precursor to the intrastratal alteration of ferromagnesian minerals and volcanic glass can be made. However, it is thought that both processes were more important than secondary (post-diagenetic) reddening in forming the country rock red beds.

The red diatreme tuffs, with their high sediment content, were affected by the same processes which reddened the country rocks. The green diatreme tuffs, which contain few accessory clasts, are green because no primary or secondary reddening processes affected them.

g) Modal composition

Point count modal analyses (Fig. 5.49, Table 5.1) indicate the essential differences between the red and green diatreme tuffs. In many of the red tuffs the matrix is finely comminuted sediment and clay, which increase the accessory lithic content of these deposits to 90% in some cases. More juvenile-rich red tuffs do occur, indicating that activity occasionally became phreatomagmatic rather than phreatic.

The green tuffs are generally highly calcite-cemented whereas the red tuffs contain abundant matrix. Where altered fragments could be recognised, they were counted as though original fresh material. This explains the low chlorite and calcite content of many of the tuffs whose juvenile fragments are completely replaced, but are still recognisable.

5.4.2 Grain size studies

The high sediment content of many of the tuffs increases the difficulties in quantitatively comparing thin section grain size analyses with published sieve analyses of modern pyroclastics (Appendix 1). This is because the varied fragment composition increases density contrasts between grains. Thus, especially in lithic-rich tuffs

TABLE 5.1 MODAL ANALYSES OF THE NORTH BERWICK TUFFS

Sample number	NB8	NB13	NBY2	NBY5	NBP3	NBH1	NBH4	NBC1	NBC2	NBS1	NBS6
Vesicular glass	35	19	32	37	38	34	36	30	10	24	25
Non-vesicular glass	11	13	20	13	3	10	8	14	6	9	12
Matrix (+clay)	-	21	10	3	-	22	-	16	31	33	22
Crystals	2	-	2	2	1	1	1	9	3	1	-
Sedimentary lithics	12	22	6	8	9	12	12	13	43	23	22
Igneous lithics	6	4	7	8	8	2	5	4	6	3	7
Opaques	2	-	-	-	-	-	1	-	-	-	-
Calcite	22	17	23	24	24	15	27	14	1	6	3
Chlorite	10	4	-	5	17	5	10	1	-	1	3

TABLE 5.1 MODAL ANALYSES OF THE PARADE TUFFS, DUNBAR

Sample number	D1	D2	D3	D4	D5	D6	D7	D9	D12	D13
Vesicular glass	7	42	49	2	12	36	1	2	37	23
Non-vesicular glass	3	4	11	5	12	3	9	5	3	4
Matrix (+clay)	44	24	5	36	34	22	41	45	31	34
Crystals	-	1	5	-	-	1	-	-	-	-
Sedimentary lithics	42	22	8	53	32	22	45	46	26	25
Igneous lithics	-	1	2	1	3	10	1	-	-	9
Opaques	1	-	-	1	1	1	-	1	-	1
Calcite	3	5	2	1	-	3	3	1	3	1
Chlorite	-	1	16	-	6	2	-	-	-	3

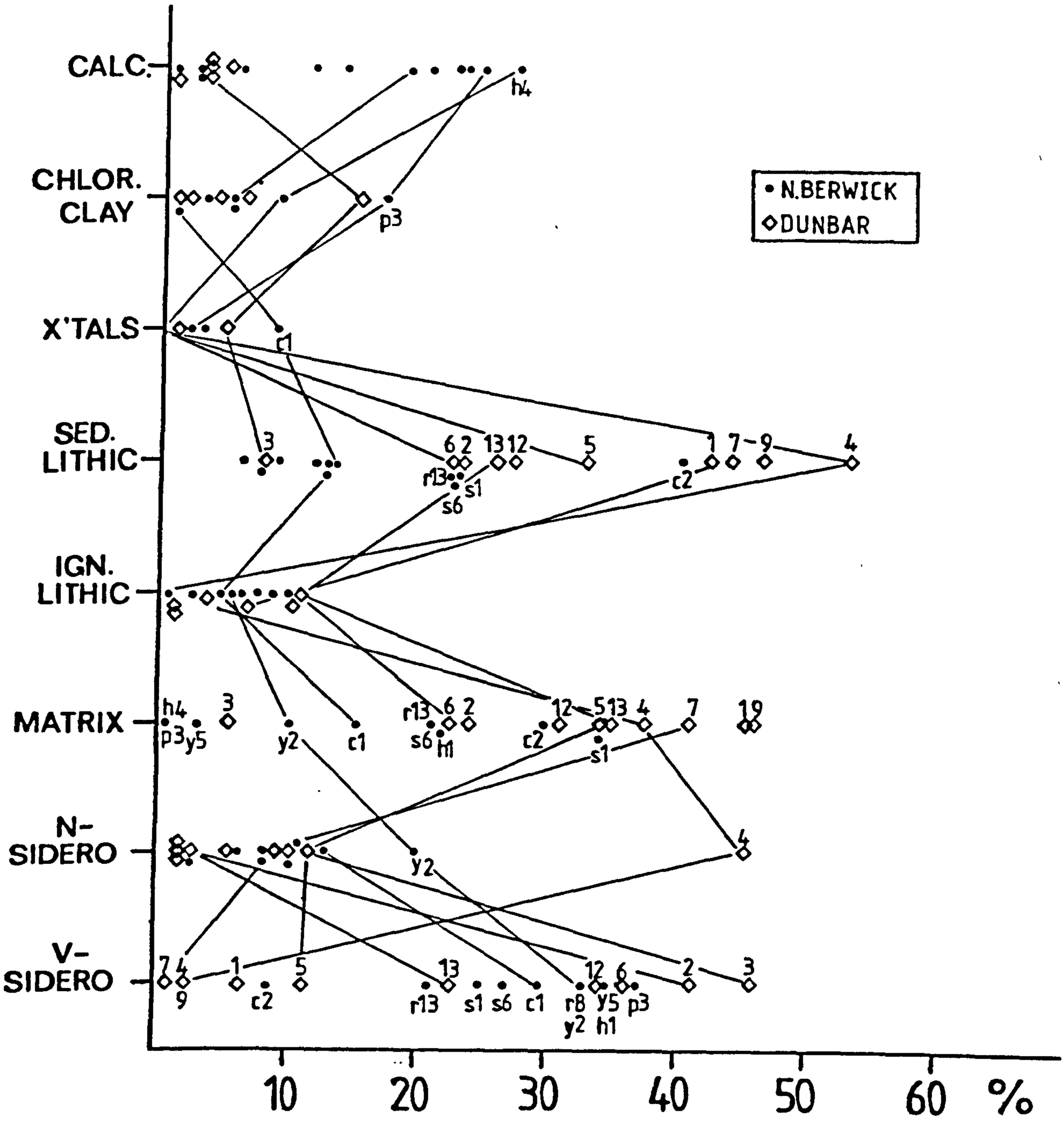

Fig. 5.49 Modal analyses of the East Lothian tuffs.
c: Car h: Horseshoe p: Partan Craig
r: G.B.T.F. s: Seacliffe y: Yellow Man

grain size results determined in thin section may only be qualitatively compared with published sieve analyses.

On Mdϕ/$\sigma\phi$ diagrams the East Lothian tuffs generally plot within the surtseyan field of Walker & Croasdale (1971), or are skewed to the finer Mdϕ side of the field (Fig. 5.50a). Most samples plot within or close to the area of overlap between the flow and fall fields of Walker (1971). This is thought to be partly due to deposition by base-surges, although proximal airfall deposits also plot in the high $\sigma\phi$ region of the airfall field. Some of the Parade tuffs plot towards the fine Mdϕ side of the airfall field, and would thus appear to be either distal airfall tuffs or the proximal products of weak explosions. The poorly sorted Parade tuffs, which plot in the flow field (Fig. 5.50b) may be proximal airfall tuffs, or proximal surge tuffs. Close to the vent such a distinction may be meaningless since both laterally and vertically direcred tephra are simultaneously ejected. The almost continuous fallout of ejecta would mix airfall material into any proximal surge deposit. Finer material would be entrained by surges but coarser fragments would fall through the surge clouds and be incorporated into their proximal tuffs, forming poorly-sorted deposits.

The East Lothian tuffs are widely scattered on Sheridan's (1971) C-M diagram (Fig. 5.50c). Some of the deposits plot in the airfall field, and since they also plot in the fall field on Mdϕ/$\sigma\phi$ diagrams may be safely assumed to have this origin. Samples 4, 5, 7 and 9 are from surge cross-bedded tuffs in the Parade diatreme, and plot within or close to the rhyolitic base-surge dune field. Their fine-skewness compared to basaltic base-surge deposits (Sheridan, 1971) is perhaps due to more violently explosive fragmentation of the magma. Distal basaltic surge tuffs would be finer and better sorted than Sheridan's Surtsey deposits, and may thus be what the Parade tuffs represent. It is interesting to note that the Parade surge deposits have much higher sediment contents than airfall tuffs from the same diatreme (Fig. 5.49, Table 5.1). This suggests that violent, dominantly phreatic explosions

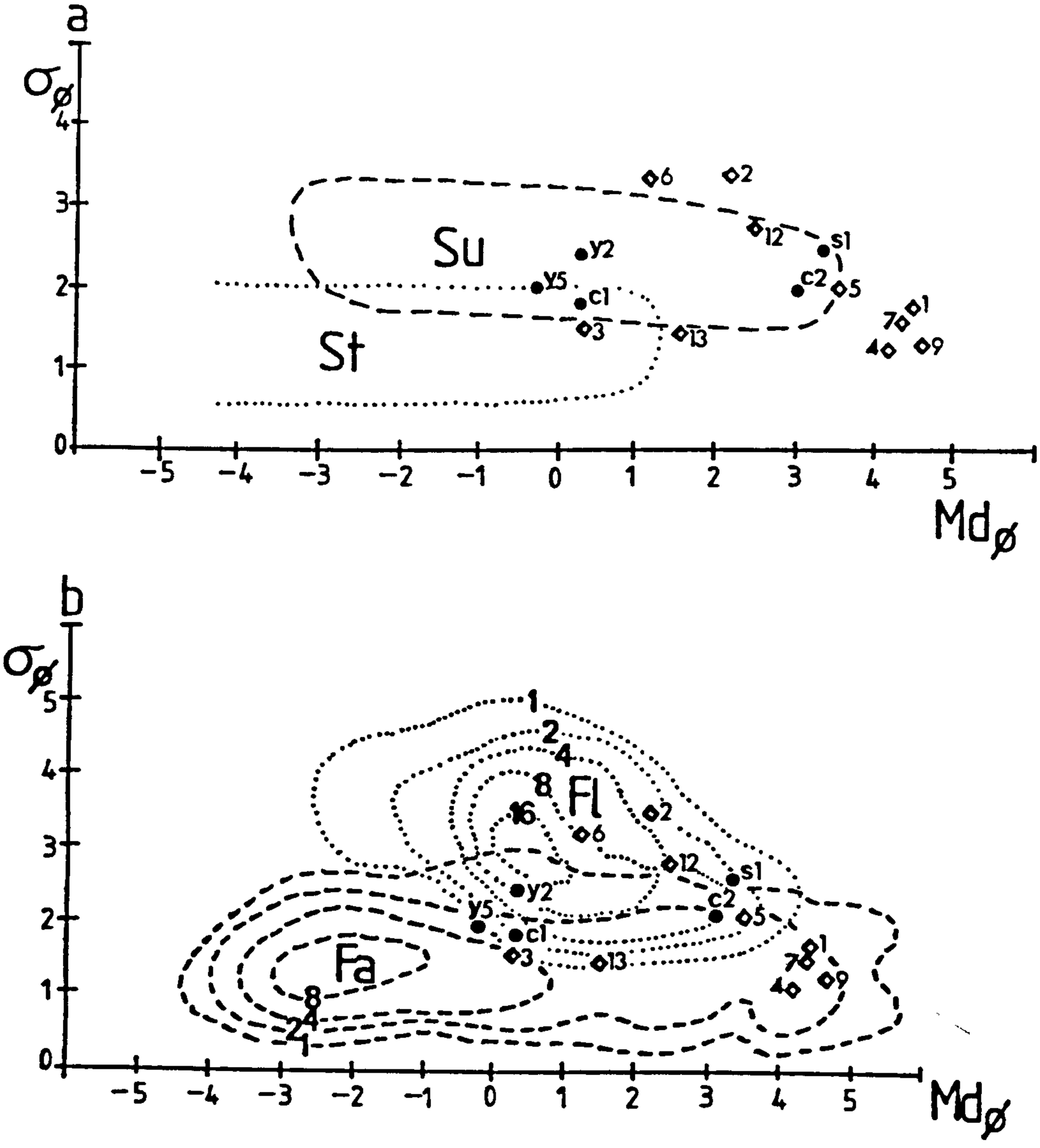

Fig. 5.50 Grain size plots of the East Lothian tuffs. Symbols as in Fig. 5.49.

fragmented the country rock sediments and fed base-surges. Eruptions more phreatomagmatic in type ejected greater amounts of juvenile material and sourced airfall deposits. The same relationship holds for the North Berwick diatremes, where samples s1 and c2 are possible surge deposits which contain much sediment.

The massive tuffs associated with surge cross-bedding generally plot in the rhyolitic ash flow field. These tuffs are typically more poorly sorted than the surge cross-beds which they are associated with, but are finer than airfall deposits. The massive beds may be the base-surge equivalent of massive ash flow deposits which have associated ground surge deposits. The limited data suggest the massive beds have grain size distributions intermediate between those of surge cross-beds and airfall deposits.

Cummulative grain size frequency distributions help to discriminate between the various tuffs (Fig. 5.51). The North Berwick tuffs all have parabolic fine-skewed curves similar to Surtsey tuffs (Sheridan, 1971). One sample (Y5) is much less fine-skewed than the others and is also apparently better sorted. However, this sample has a matrix partly replaced by calcite, which reduces the number of fines and accounts for the shape of its cumulative curve.

The Parade tuffs are likewise broadly similar to surtseyan deposits in their cumulative distribution curves. The airfall samples (D3 and D13) have similar distributions to the basalt airfall curves of Sheridan (1971). The proposed massive surge deposits (D2, D6 and D12) have similar distributions to those of Surtsey (Sheridan, op.cit.) and partly similar to the massive surge beds of Sheridan & Updike (1975). The proposed surge cross-bedded tuffs (D1, D4, D5, D7 and D9) are more fine-skewed than the Surtsey tuffs but are similar to the sand wave size-distribution curves of Sheridan & Updike (op.cit.), who analysed rhyolitic surge deposits in Sugarloaf Mt., Arizona.

Comparisons between the basaltic Parade tuffs and the rhyolitic Sugarloaf Mt. tuffs suggest that massive and cross-bedded surge tuffs from each volcano have similar

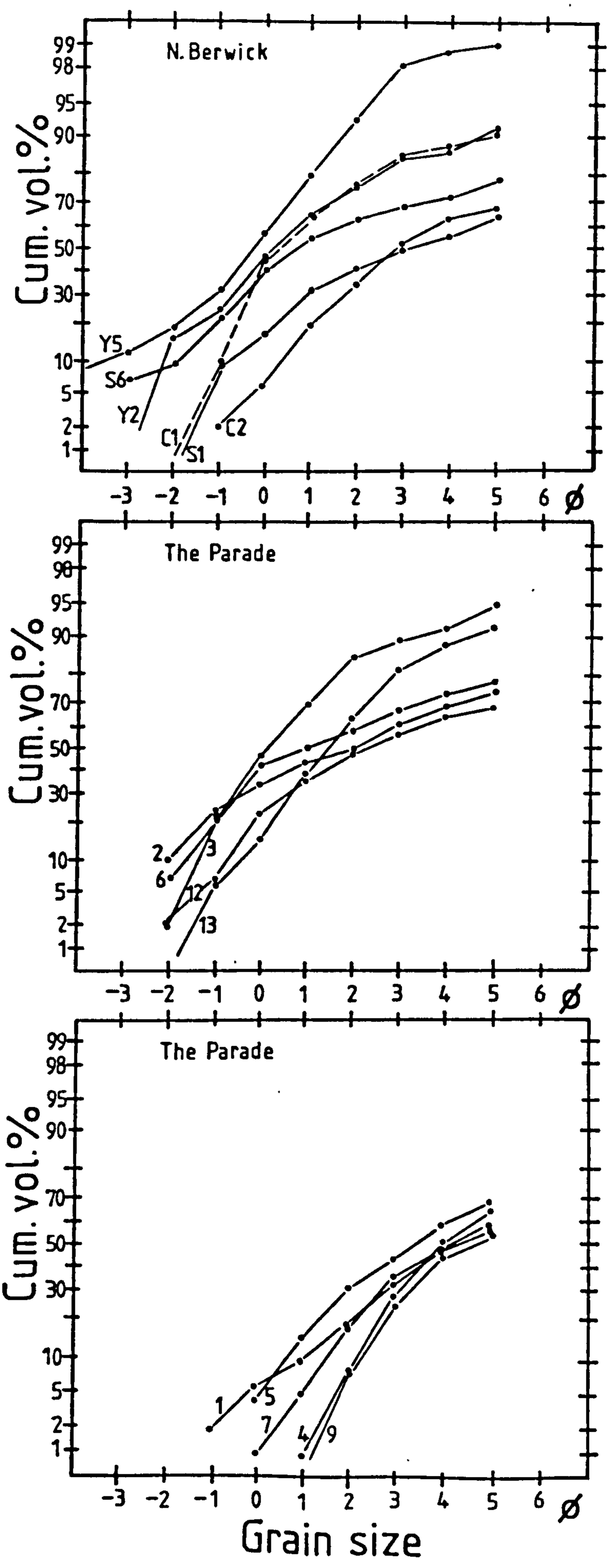

Fig. 5.51 Cumulative grain-size frequency curves of the East Lothian tuffs.

size-distribution curves. The Parade massive bed curves are, however, more poorly sorted than those of Sugarloaf Mt., and the Parade cross-beds slightly more poorly sorted. This probably reflects the proximal position of the Parade tuffs whereas the Sugarloaf Mt. tephra are more distal. The composition of the magma appears to have had little effect on the surge size-distribution curves of both centres. The fine-skewed distribution of the Parade airfall tuffs compared to those of the Sugarloaf Mt. is due to thin section grain-size techniques which are not applicable to coarser lithologies. Consequently, only the finer Parade airfall layers could be measured (Table 5.2).

5.4.3 Morphology of particles

a) SEM studies

Alteration and replacement of the juvenile fragments has obscured most of the details of their morphology. However, where visible they are seen to be typical blocky phreatomagmatic ash bounded by planar fracture surfaces. Small vesicles are commonly present but do not control grain shape.

Sediment grains, especially quartz, are the only unaltered easily studied particles in many of the deposits. Both highly angular and sub-rounded quartz grains occur. The more rounded grains have frosted surfaces and lack conchoidal breakage patterns. One such grain (Fig. 5.52) has a rather smooth surface perhaps due to diagenesis (Krinsley & Donahue, 1968). Small V-shaped and irregular pits occur in clusters on its surface (Fig. 5.53). These are thought to be abrasion features of quartz grains in subaqueous environments (Krinsley & Doornkamp, 1973) although recently Al-Saleh & Khalaf (1982) have described similar features in aeolian dune sands. Such aeolian grains also contained dish-shaped depressions, similar to some of the Parade grains. Transport of these grains into or from marine environments would explain their presence in the East Lothian diatremes.

No textures uniquely attributable to the transport of grains by volcanic processes were noted. In any event,

TABLE 5.2 THIN SECTION GRAIN SIZE ANALYSES

Sample number	NBC1	NBC2	NBS1	NBY2	NBY5	D1	D2	D3	D4	D5	D6	D7	D9	D12	D13
+6o	11	33	38	8	1	43	26	6	35	34	22	41	45	32	11
+5	5	5	8	5	-	9	5	2	14	7	5	9	10	4	2
+4	3	11	5	2	-	15	8	4	22	16	6	12	20	7	8
+3	9	18	9	9	6	14	11	5	7	12	9	20	17	9	18
+2	11	14	9	11	13	9	8	15	1	16	8	13	8	12	23
+1	19	13	15	18	23	4	9	23	1	11	9	4	-	14	22
0	32	4	8	23	25	4	10	25	-	4	20	1	-	15	10
-1	10	2	8	8	14	2	13	18	-	-	14	-	-	5	6
-2	-	-	-	16	6	-	10	2	-	-	7	-	-	2	-
-3	-	-	-	-	-	-	-	-	-	-	-	-	-	-	-
-4	-	-	-	-	12	-	-	-	-	-	-	-	-	-	-

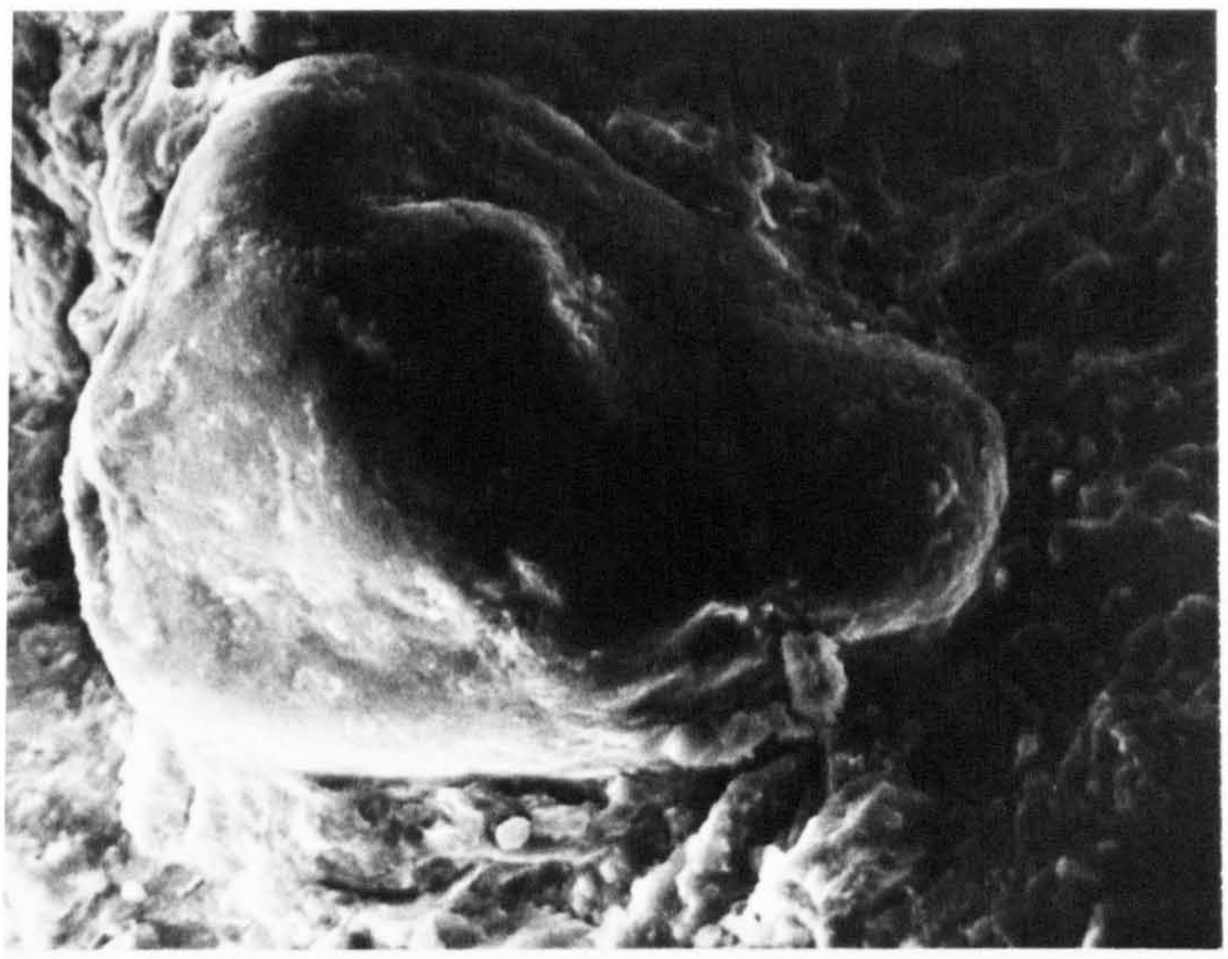

Fig. 5.52 SEM photograph of quartz grain from the Parade tuffs. Note overall rounded shape and abundant pits on surface. x350.

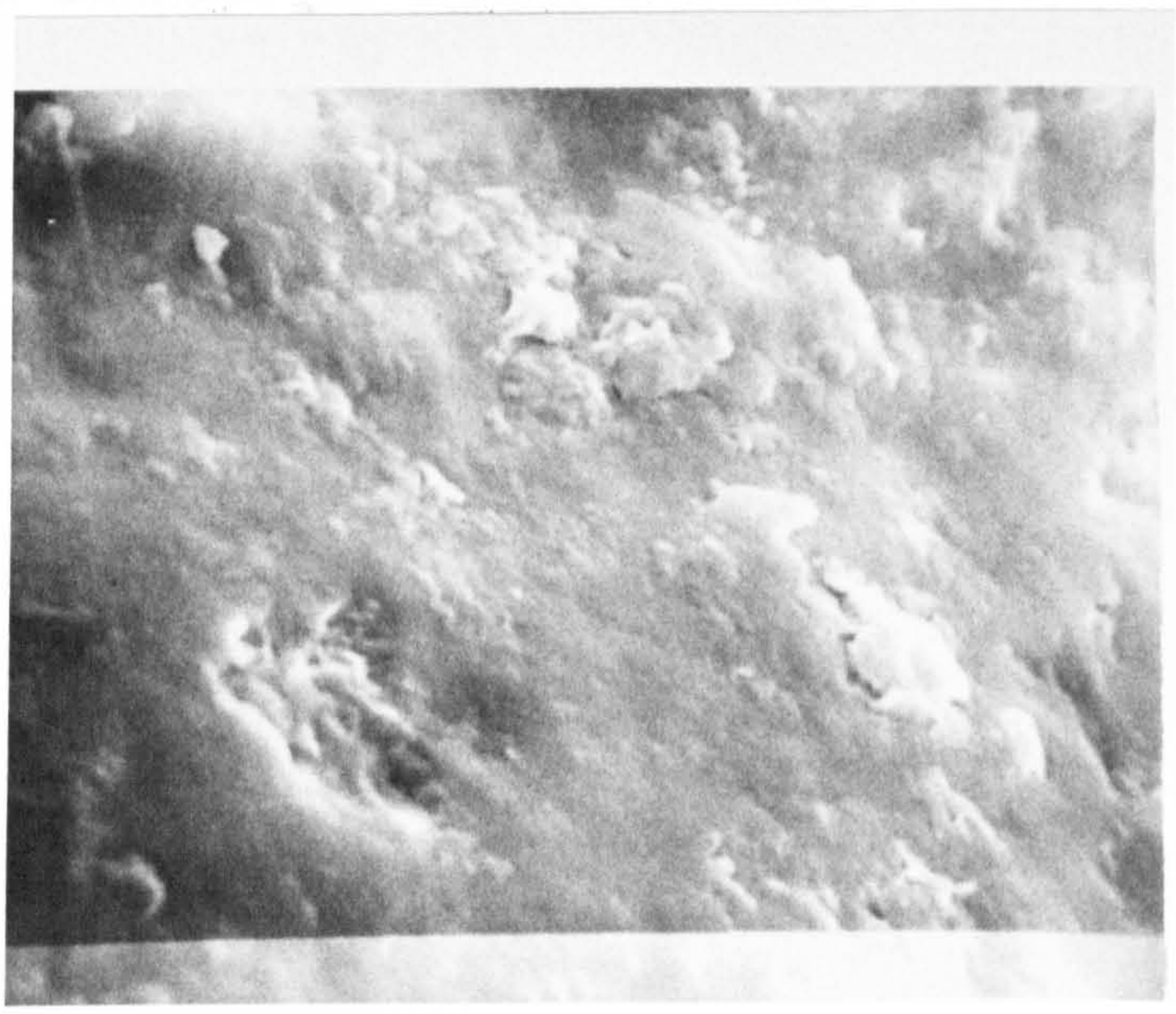

Fig. 5.53 SEM photograph of small pits on surface of quartz grain shown in Fig. 5.52. Note smooth surface and upturned plates which may be diagenetic features. x3000.

such features would probably be indistinguishable from aeolian grain surface textures.

b) Quantitative grain morphology

Only fragments which were not highly altered or corroded were measured. This resulted in mainly the larger granules being studied, since fines are generally replaced, although in some cases even their grain shapes are well-preserved.

On a PVC diagram (Fig. 5.54a) the North Berwick and the Dunbar diatreme tuffs plot in similar fields. The plot distributions are slightly skewed towards the C apex, indicating the preponderance of concave boundaries. Both shattering of glass and intersection of grain margins with vesicles form such embayments. The plots are not successful in distinguishing green diatreme tuffs from red diatreme tuffs and often ash from the same diatreme has a wide spread of PVC values. The one country rock tuff sample measured has a similar spread of values to the diatreme tuffs, indicating it was probably derived from them. Reworking in a lagoonal environment has had little effect on the grain shapes. No samples of tuffs reworked in more active environments were studied because of alteration, but where visible, juvenile grains do appear to have been slightly rounded.

On a P vs N diagram (Fig. 5.54b) the bulk of the grains plot above the line with slope 0·75. This indicates that explosive vesiculation, rather than granulation, formed the lapilli (Honnorez & Kirst, 1975). However, since finer ash could not be measured it is not surprising that the samples all plot in the high-N field. Comparison with Saefell (Chapter 2) and Medano (Chapter 3) suggests that the fines would probably have plotted in the high-P, hyaloclastic field. The spread of results in the East Lothian diatreme tuffs is thus very similar to the modern examples studied; all must have formed by similar processes.

5.4.4 Alteration of tuffs

a) Green tuffs

The green tuffs are all similar in having chlorite-

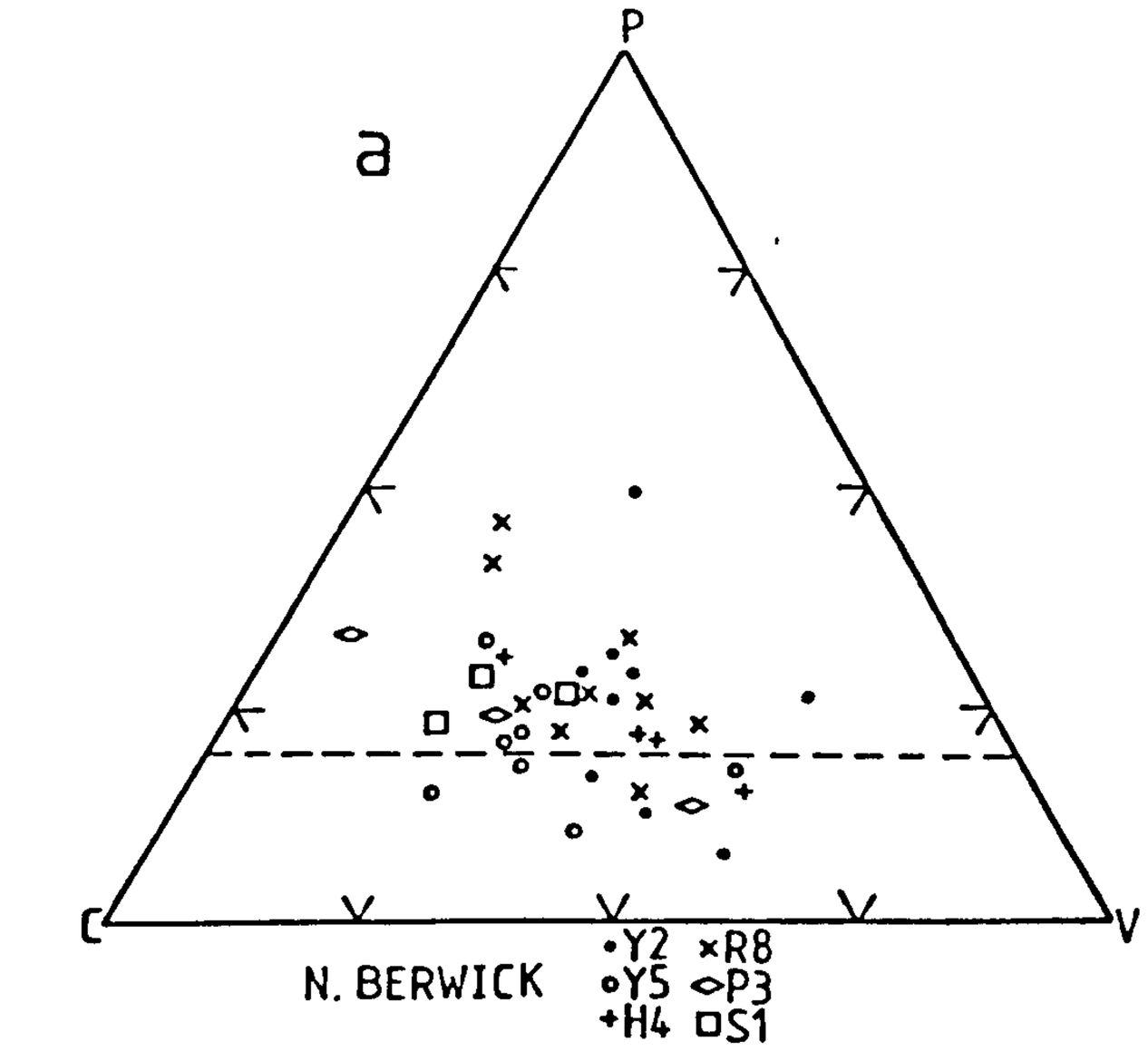

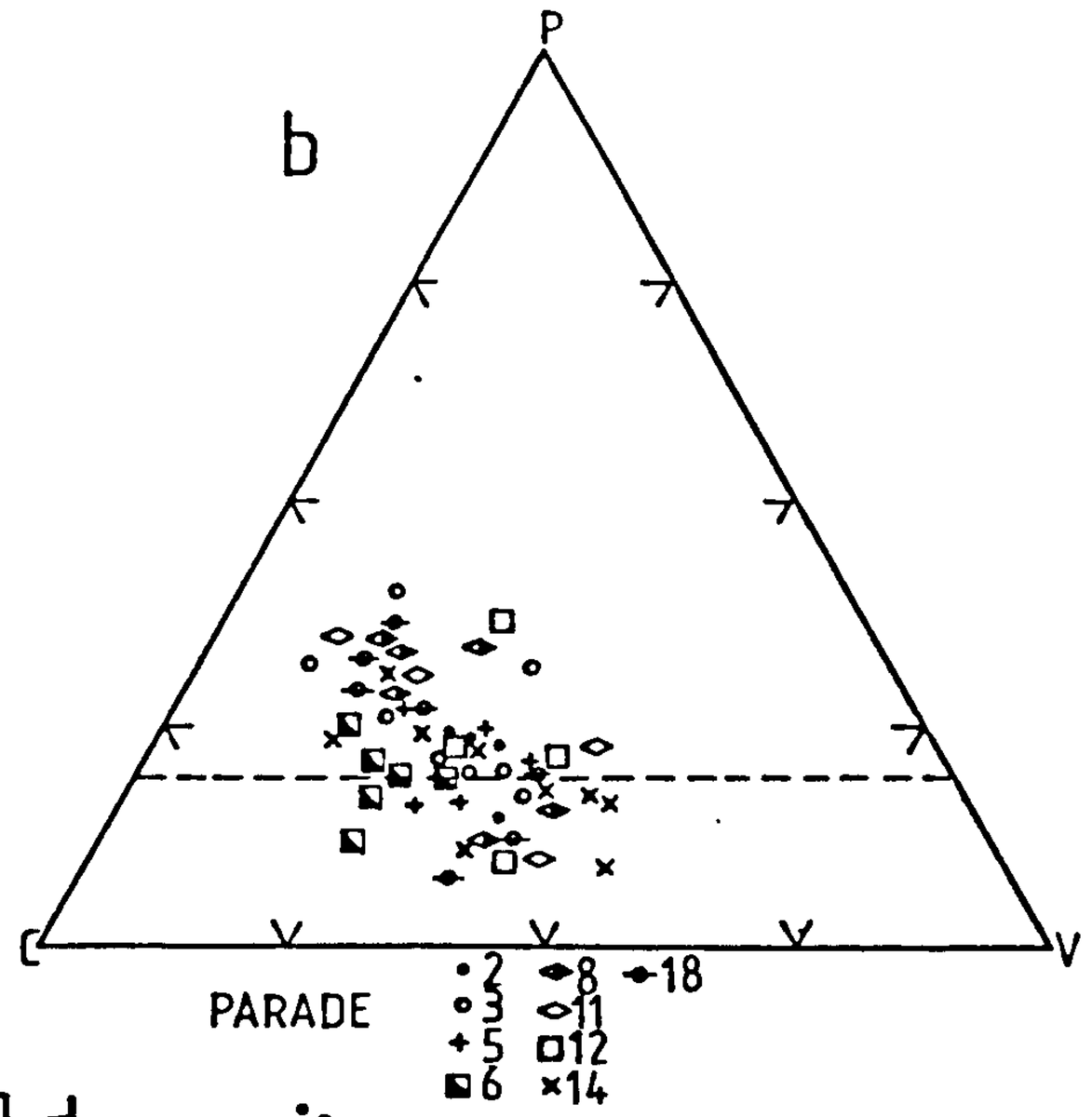

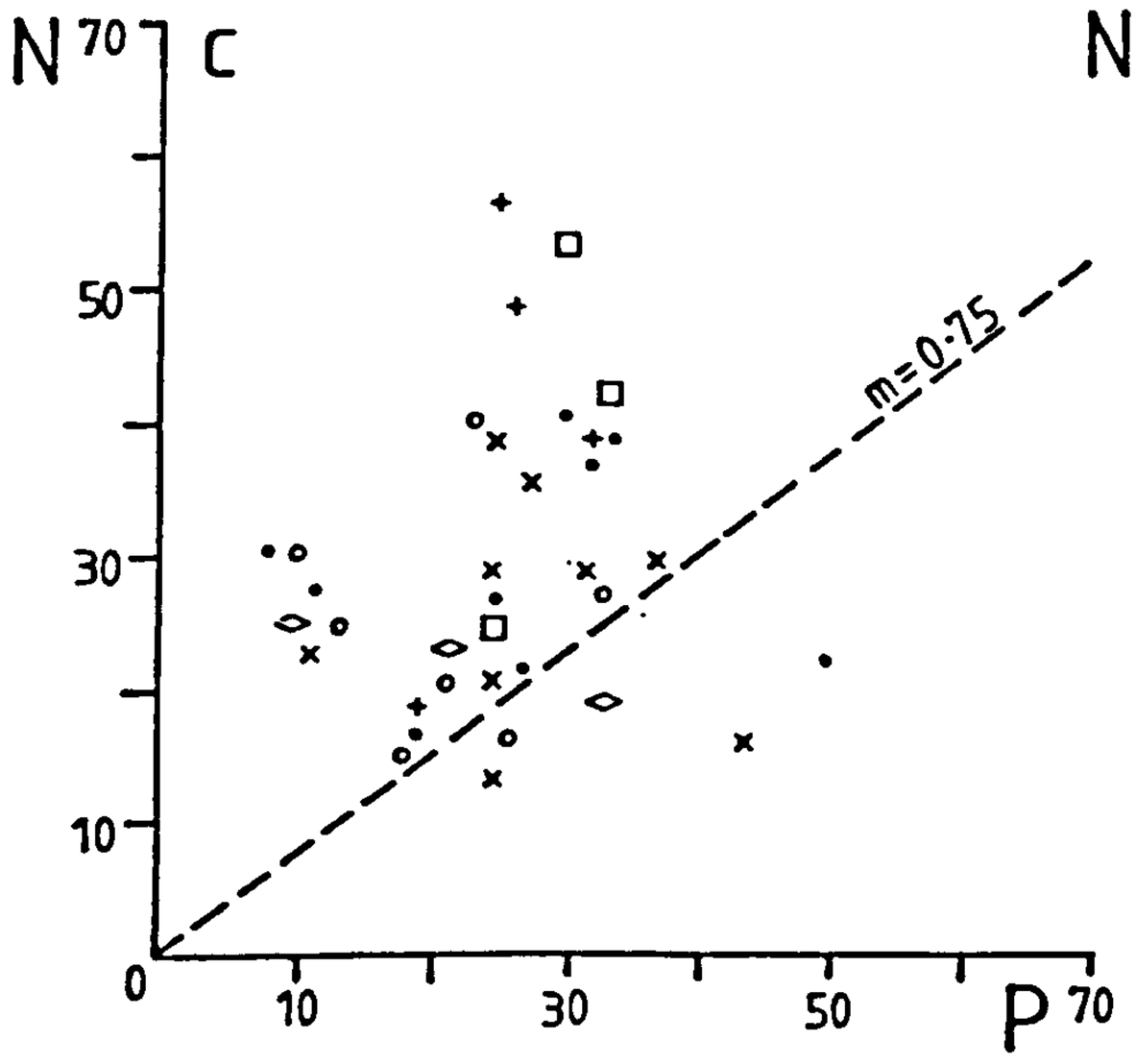

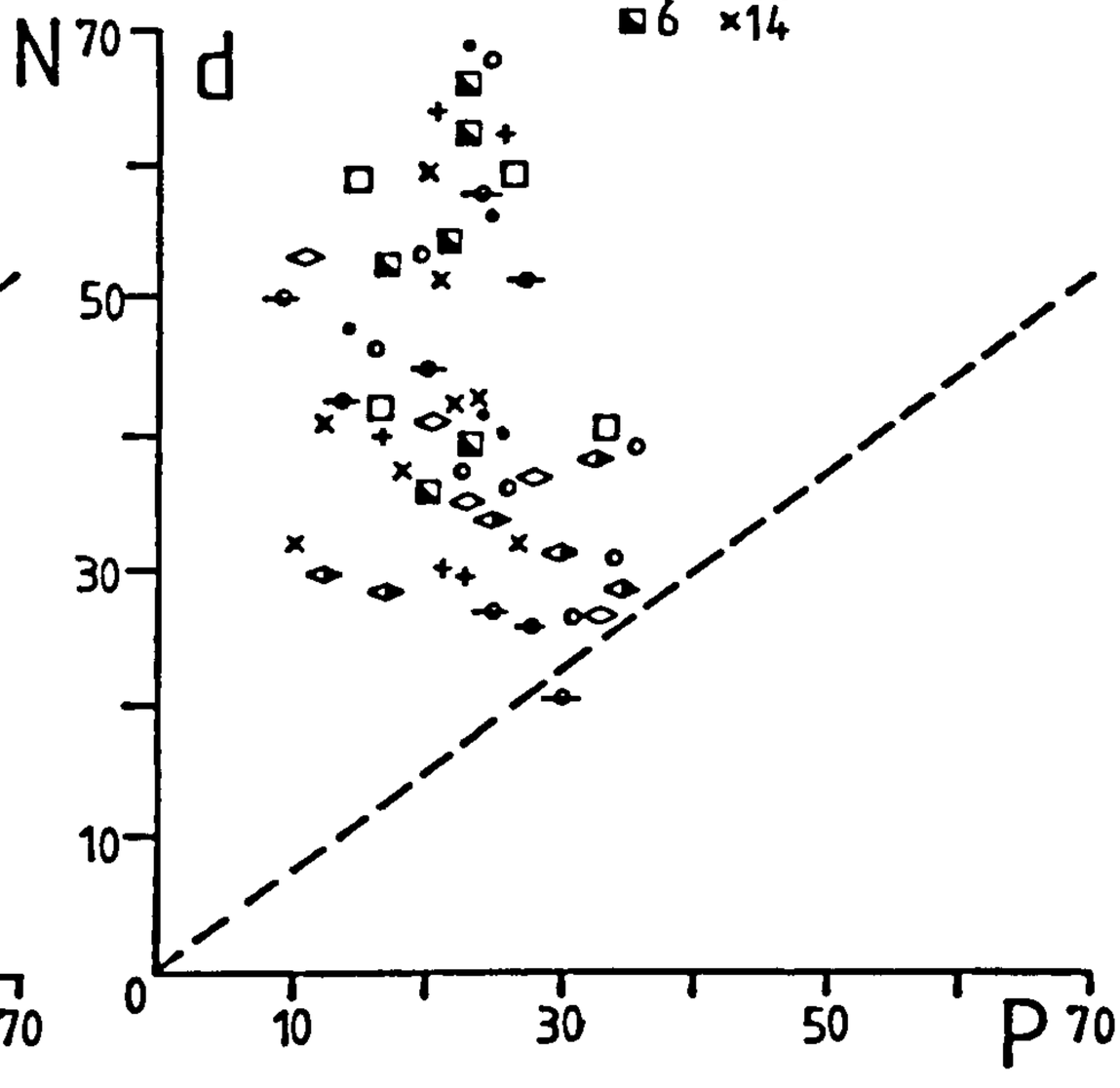

Fig. 5.54 Quantitative grain morphology of the East Lothian tuffs.
a) PVC diagram of the North Berwick tuffs.
b) PVC diagram of the Parade tuffs.
c) P vs N diagram of the North Berwick tuffs.
d) P vs N diagram of the Parade tuffs.

replaced juvenile lapilli in a generally sparry calcite cement which has replaced most traces of the original tuff matrix. A few relatively fresh glass fragments have survived the alteration (Fig. 5.55) and consist of pale to dark brown isotropic glass. Some of the relict glass grains have concentrically-banded rinds around both vesicles and the grain margins. These bands probably represent palagonite rinds developed soon after formation of the glass. The vesicles are filled with concentrically-banded chlorite which is partly replaced by calcite. At least three stages of chlorite growth are represented in the bands. Presumably alteration of these relict grains was prevented because surrounding pore spaces were rapidly filled by authigenic minerals which formed a barrier to alteration solutions.

Most of the chlorite is apple-green in colour, weakly pleochroic and has low birefringence. Under crossed polars it is seen to form radiating or flakey aggregates which may occur in radial layers around grain boundaries (Fig. 5.56). Optically it appears to be prochlorite. Chlorite often only partially replaces volcanic grains, and is associated with calcite which is generally later. Many grains have chlorite replaced rims spotted with opaques and calcite replaced cores. In extreme cases, calcite has totally replaced grains with vesicles containing concentrically-banded chlorite.

Rinds around many vesicles, thought to represent replaced palagonite, are often full of small rounded high relief crystals and dusty opaques (Fig. 5.56). The disseminated grains often form trails parallel to the concentric banding in the rinds, which reach 0·05mm in thickness.

Calcite occurs as both a replacive and a pore-infilling mineral. In places relict grain shapes can be distinguished in sparry calcite which has replaced and pseudomorphed the matrix (Fig. 5.57). A common pore infilling sequence is :-

iron oxide rim around grains
chlorite
banded radial calcite
vuggy calcite with interpenetrant large crystals.

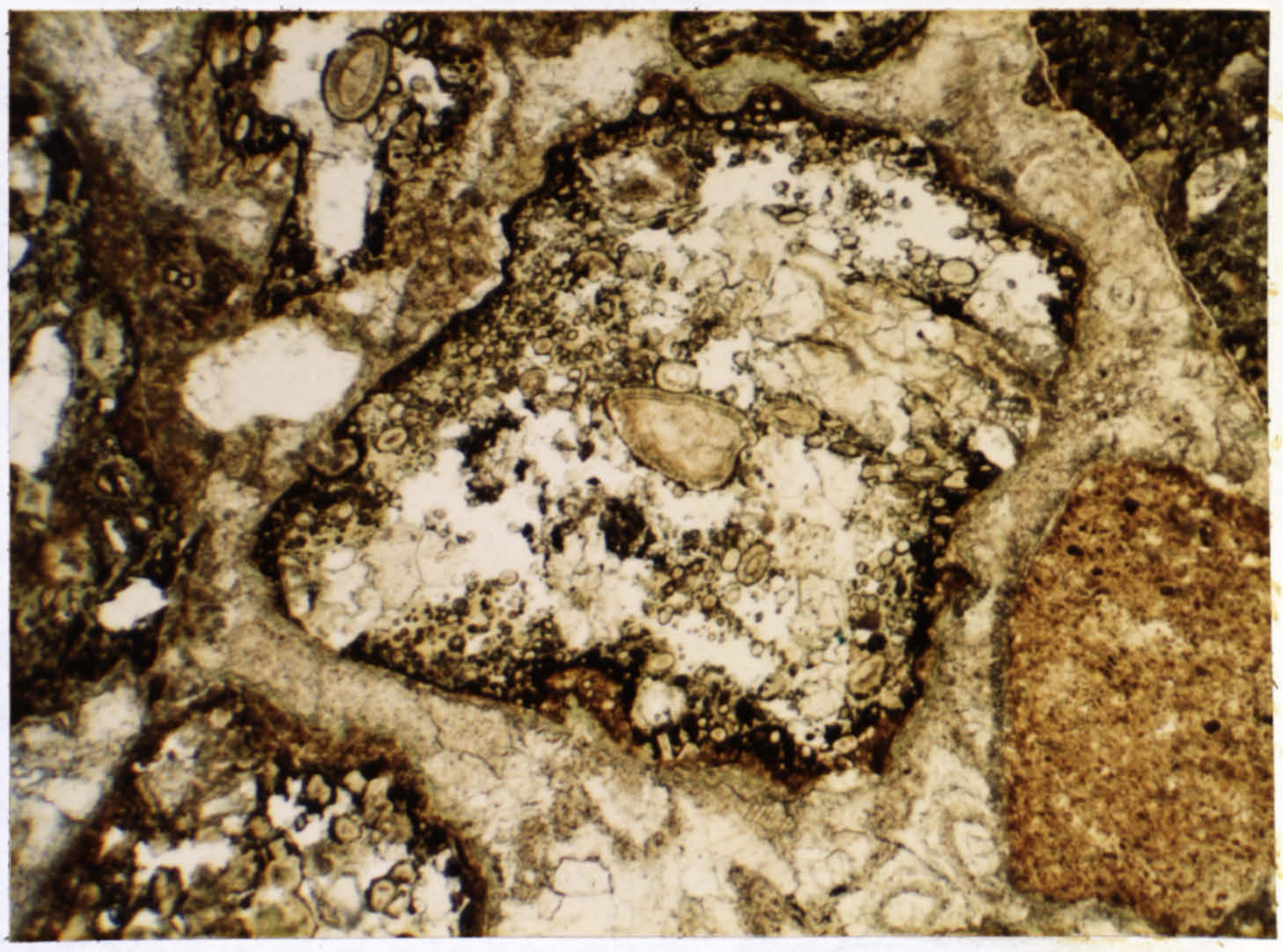

Fig. 5.55 Vesicular lapillus from the Partan Craig diatreme tuffs. Note preservation of vesicles and grain shape even though the fragment is chlorite and calcite replaced. Concentric structures around vesicles probably represent replaced palagonite rinds. Plane polarised light. x10.

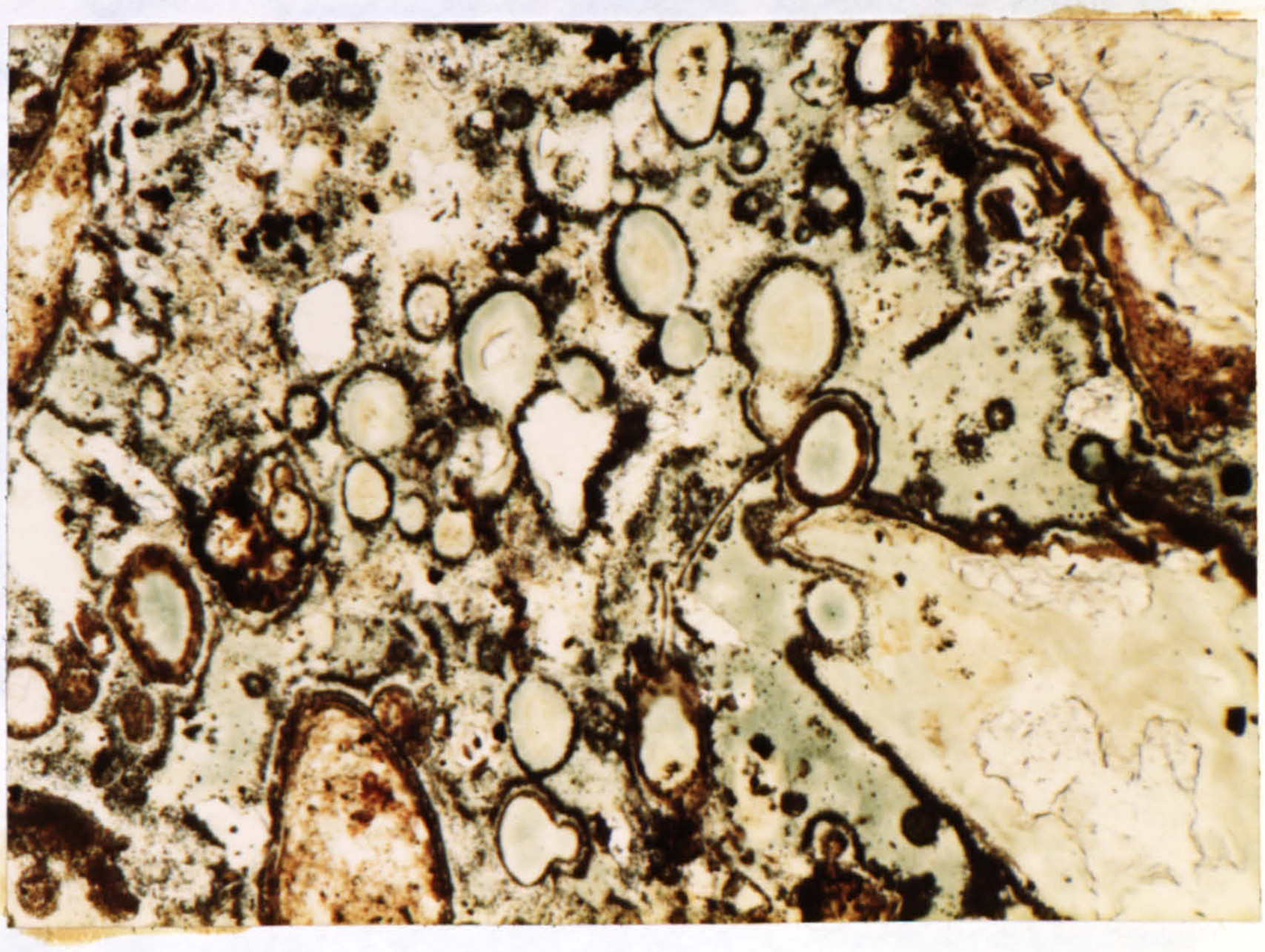

Fig. 5.56 Prochlorite-replaced vesicular lapillus from the Horseshoe diatreme tuffs. Rinds around vesicles contain dusty opaques, which also occur around the grain perimeter. Plane polarised light. x40.

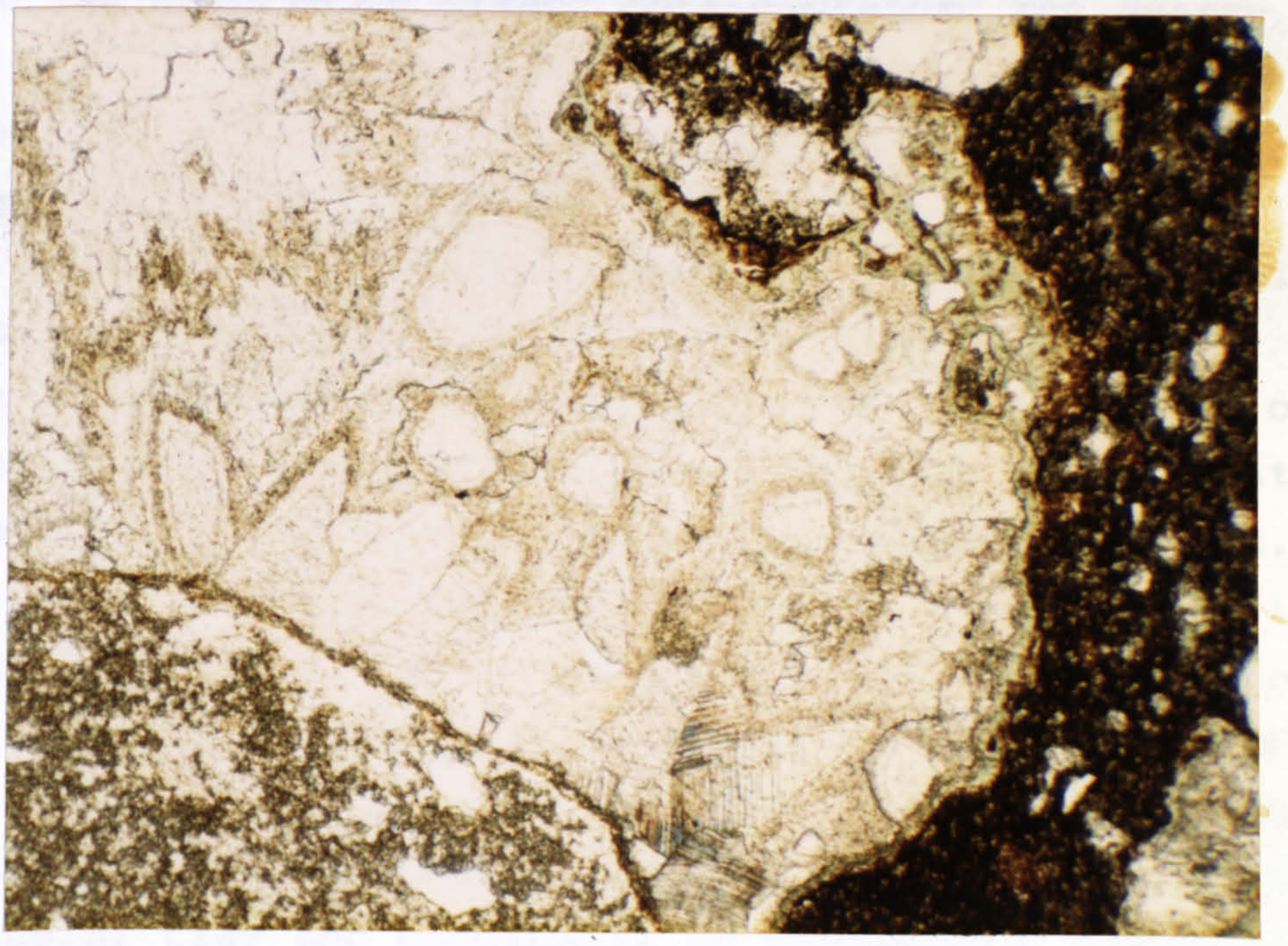

Fig. 5.57 Relict grain shapes visible in calcite replaced matrix of the Partan Craig diatreme tuffs. Plane polarised light. x10.

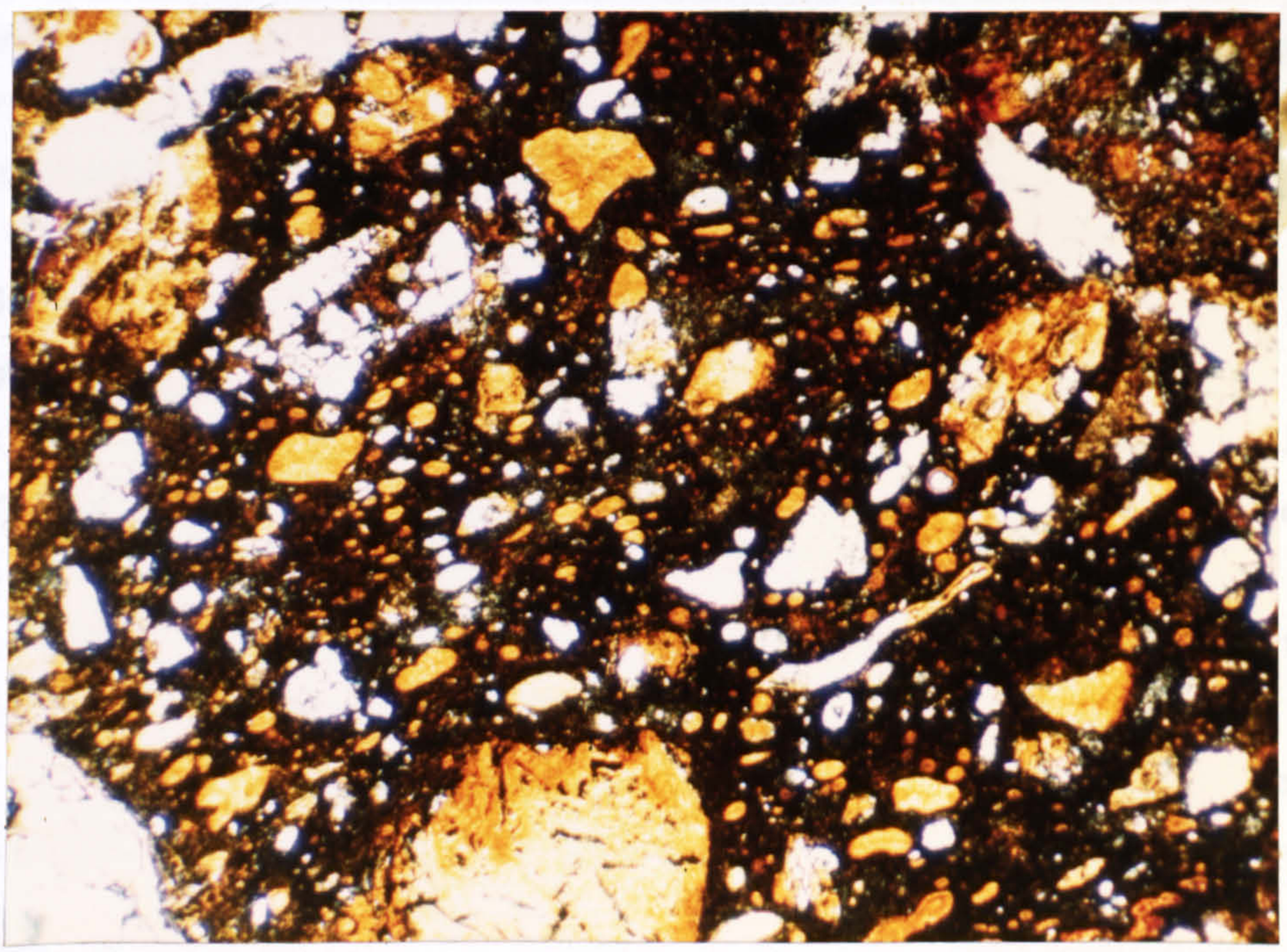

Fig. 5.58 Vesicular lapillus from the Parade diatreme tuffs. Vesicles infilled by orange, fibrous vermiculite which, along with hematite replaces most of the fragment. Plane polarised light. x10.

Replacive calcite is either coarse-grained and sparry or more micritic in type, with opaque spots and other impurities often giving it a turbid appearance.

b) Red tuffs

The red tuffs contain a wider variety of alteration products than the green tuffs and in addition are extensively hematite-stained. The sediment component of the tuffs is largely unaltered, apart from the sericitization of feldspar and the hematitization of the clay matrix.

The most common alteration product of the juvenile and lithic fragments is an orange-brown, slightly pleochroic mineral with low relief and low-to-moderate birefringence (Fig. 5.58). It forms radial fibrous layers, radiating "booklets" or aggregates of small crystals. It resembles vermicular clay and chemically is similar to vermiculite, or some forms of chlorite (Table 5.3). There appears in places to be a gradation between pale yellow chlorite, with low relief and low birefringence, and orange-brown vermiculite, with slightly higher relief and higher birefringence. In other samples chlorite is enclosed and corroded by the vermiculite, or vice-versa. Often, the chlorite is full of opaques and the contact with the clay is defined by a layer of hematite.

Chlorite and clay replace most volcanic grains, pseudomorph phenocrysts and infill vesicles. Variable, though generally small amounts of calcite are often associated with the above minerals. The calcite usually occurs as the final phase of vesicle infill or replaces the cores of volcanic fragments. Often, the outer rims of a grain are replaced by orange vermiculite, with chlorite inside this and calcite at the grain centre. Numerous spots of disseminated hematite are scattered through many grains, and are often concentrated around grain and vesicle margins. Common vesicle infill / alteration sequences are :-

Chlorite-banded vermiculite-fibrous vermiculite-calcite

Chlorite-hematite-vermiculite-calcite

Banded vermiculite-calcite-banded vermiculite.

Most of the primary structures have been preserved even in highly altered volcanic grains. The most obvious

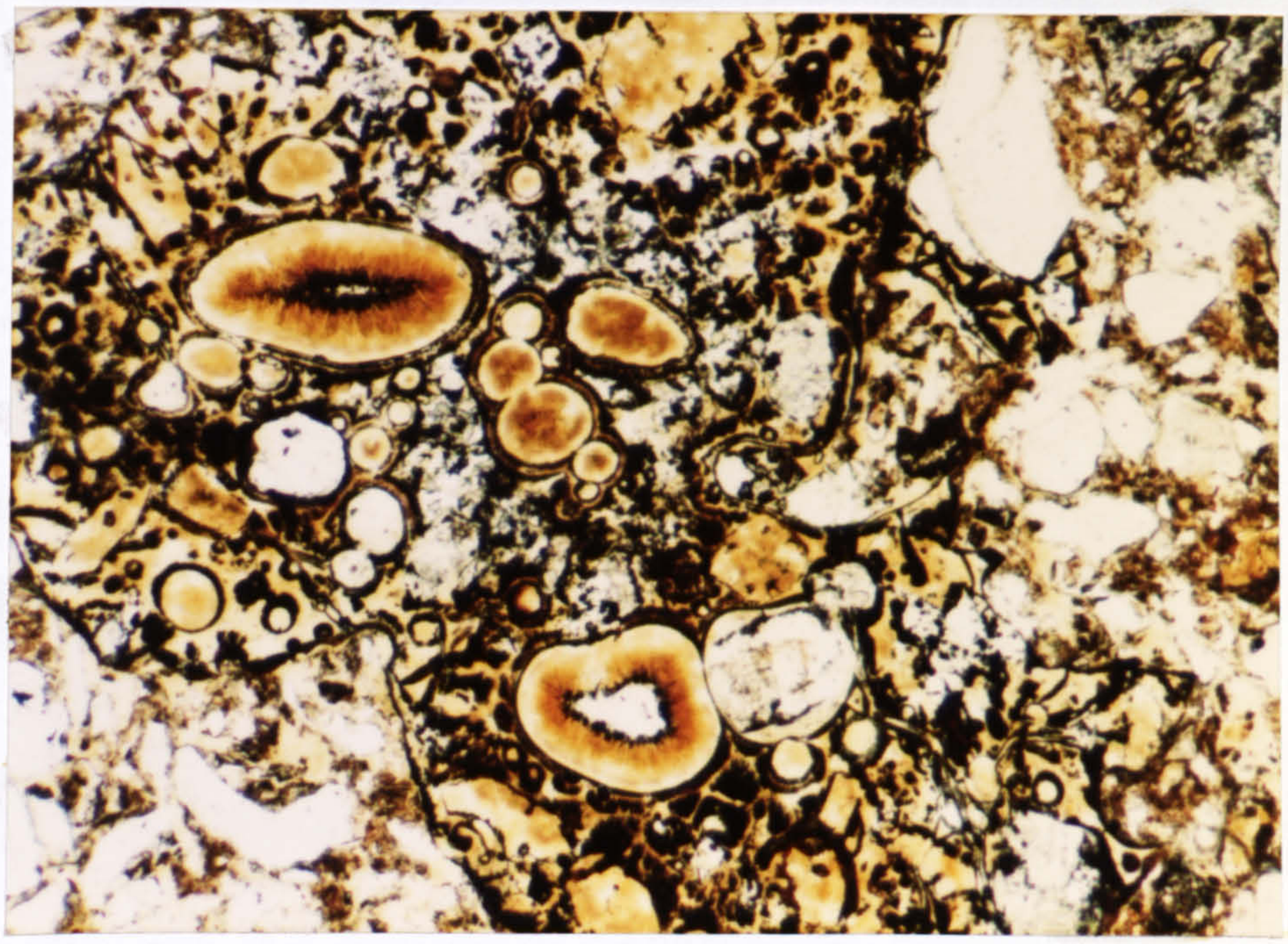

Fig. 5.59 Vermiculite and chlorite replacement of vesicular lapillus from the Parade diatreme tuffs. Concentric bands around vesicles represent vermiculite replacement of palagonite rinds. Within vesicles, zoning of vermiculite may represent replacement of composite authigenic phases. Plane polarised light. x25.

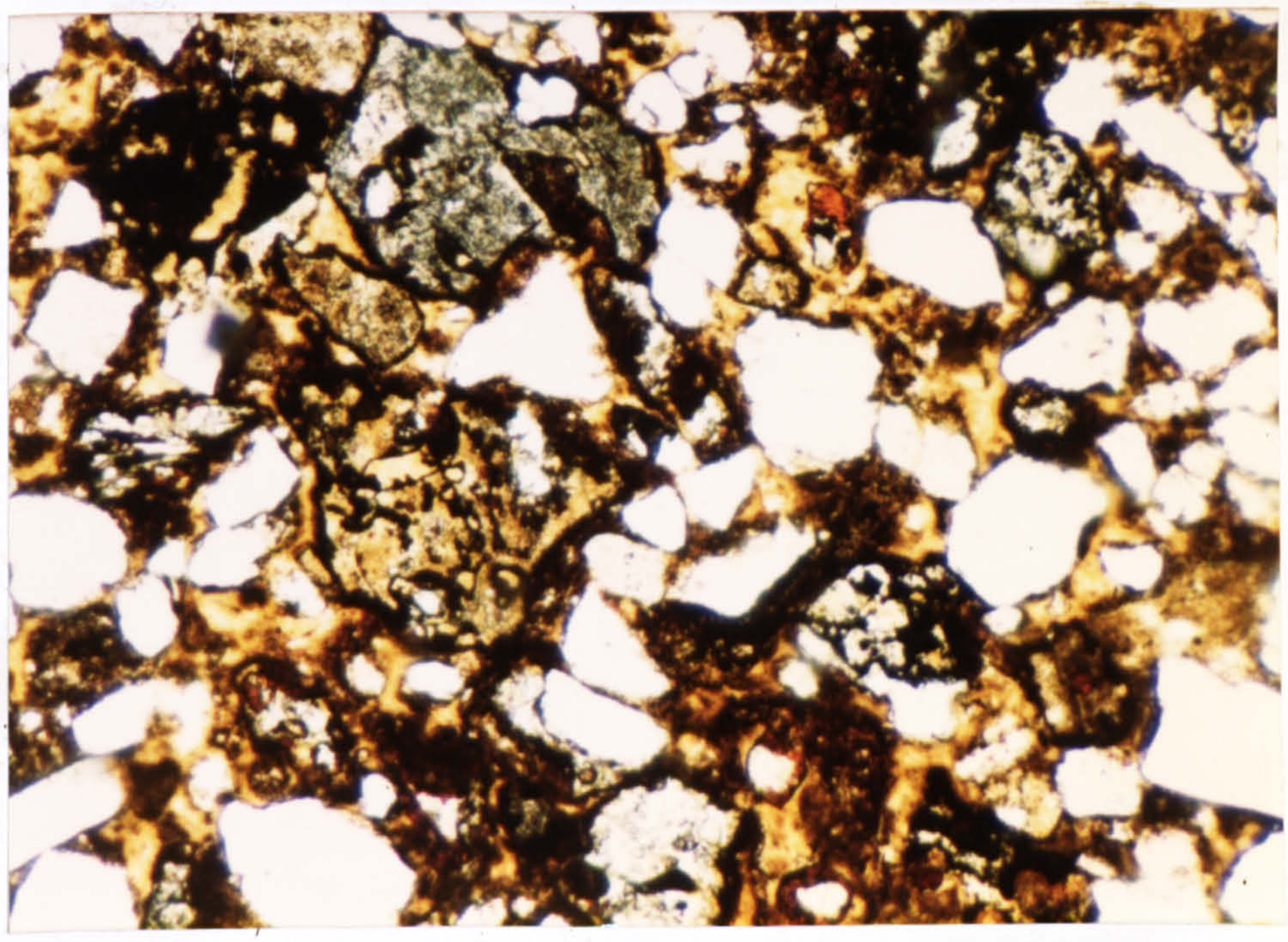

Fig. 5.60 Tuffaceous siltstone from the Parade diatreme, showing clay replacement of the fine matrix. Much of the matrix and the ash grains are replaced by hematite, which also forms rims around some of the quartz grains. Plane polarised light. x25.

TABLE 5.3 MICROPROBE ANALYSES OF SAMPLE D6

	(1)	(2)	(3)	(4)	(5)	(6)
SiO_2	35·3	34·3	33·8	34·0	65·7	4·51
TiO_2	0·10	0·79	0·19	-	-	0·89
Al_2O_3	15·5	15·2	15·1	15·4	19·9	1·84
FeO	11·8	15·2	18·4	*8·01	0·26	75·6
MnO	0·14	0·21	0·26	-	0·10	1·13
MgO	24·3	23·1	17·4	22·6	1.55	0·25
CaO	0·19	0·40	0·41	-	10·4	0·42
Na_2O	0·49	1·01	-	-	0·19	-
K_2O	0·07	0·26	0·15	-	-	0·34
Total	87·89	90·47	85·71	80·01	98·10	84·98

(1) Chlorite/vermiculite vesicle infill.
(2) Chlorite/vermiculite in altered lapillus.
(3) Chlorite/vermiculite in altered lapillus·
(4) Vermiculite analysis (Deer et al., 1975)
*(Fe as Fe_2O_3).
(5) Zeolite (?analcite) vesicle infill.
(6) Hematite replacement of vesicular lapillus.

are the vesicles which have been infilled, but still retain their original shapes. Some of the banding in the chlorite and vermiculite around the vesicles is similar to that seen in the green tuffs and is thought to be replacive after palagonite (Fig. 5.59). The hematite rims around vesicles and grain margins may be partly due to alteration of earlier iron-rich palagonite rinds. Within vesicles, zoning in the alteration minerals may represent replacement of earlier composite or partly-filled vesicles (Fig. 5.59). Alternatively, slight changes in the composition of the altering fluids may have precipitated slightly different replacement minerals with time.

The matrix of the red tuffs is largely composed of hematite-stained clay, probably kaolinite or montmorillonite (Fig. 5.60). Most of the clay is colourless or turbid, extremely fine-grained, and has low relief and low-to-moderate birefringence. The fine-grained matrix is sometimes replaced by orange vermiculite cement, especially around highly altered volcanic grains. In places, calcite cements fill pore spaces or replace the matrix. Veins filled with sparry calcite cut many of the tuffs and are a post-compaction feature.

Vermiculite is reputedly often found as an alteration product of biotite (Deer et al., 1975), but such a paragenesis is hard to envisage in the red tuffs, even though they do contain small amounts of generally fresh biotite. In K-rich marine waters vermiculites are said to be derived from volcanic material and chlorite (Deer et al., op.cit.). In the red tuffs vermiculite commonly replaces chlorite, similar to vermiculites formed by weathering of chlorite in soils. Saline groundwaters might well have affected the tuffs since the volcanoes are thought to have formed near a palaeo-shoreline, on a coastal alluvial plain. Why the green tuffs never developed vermiculite is unclear. The reason may be related to the sediment which was incorporated in the red tuffs. If biotite was present in the newly-deposited continental alluvium of the Canty Bay Formation it would have rapidly decomposed under oxidizing conditions, forming mixed-layer clays and hematite (Turner,

1980). Perhaps the colour of the tuffs and the origin of the vermiculite is in part due to an originally high biotite content in the sediments, now removed by alteration. In addition to the sedimentary biotite, clasts of biotitite (or glimmerite) are known in some of the Dunbar tuffs (Upton, 1982). Alteration of this cumulate igneous biotite may have added to the reddening process at the Parade diatreme.

5.5. Discussion

The red and green diatremes differ in many ways, the most important of which are :-

a) Sediment content; the red tuffs contain abundant country rock material, the green tuffs mainly juvenile fragments.

b) Colour; this is related to sediment content and the Eh of groundwaters.

c) Age; the green diatremes are slightly younger (Martin, 1955).

d) Alteration; this is largely dependant on sediment content and groundwater composition.

e) Internal structure; the red diatremes contain generally well-bedded sequences of tuffs, the green diatremes largely poorly-bedded, often blocky tuffs.

f) Location; the red diatremes lie to the S and E, the green diatremes to the N and W of the area studied.

g) Depositional environment of the country rocks around the diatremes; the red diatremes are surrounded by alluvial plain sediments, the green diatremes by lagoonal or lacustrine deposits.

These differences are thought to represent fundamentally different styles of volcanic activity. The red diatremes erupted into unconsolidated, water-rich alluvial plain sediments and explosively comminuted them. The green diatremes erupted into shallow lake water and ejected mainly chilled magma fragments. The red diatremes are thus thought to be eroded maars, whereas the green diatremes are eroded tuff-rings.

The reasons for the different styles of activity may be related to the source and abundance of the water which

contacted the magma. Perhaps convective heating of pore waters in the alluvial sediments led to mainly steam explosions above the slowly ascending red diatreme magma. periodic upwelling of magma may have initiated retrograde boiling in the superheated water column above it and geyser-like jets sprayed out a mixture of chilled glass and sediment.

The green diatremes were probably formed when magma first contacted pore water and then rose to near surface depths where shallow lakes provided an abundant water source. The main explosions were triggered by the direct contact of magma with abundant water, and took place within the upper part of the intrusion, ejecting mainly chilled glass. Rapid ascent rates probably allowed magma to reach very high levels before disruption by phreatomagmatic explosions. The depth of interaction of magma and water was thus important in determining whether tuff-rings or maars were formed (Lorenz, 1973). The actual products and structures forming the red and green tuffs are similar, reflecting similar depositional processes.

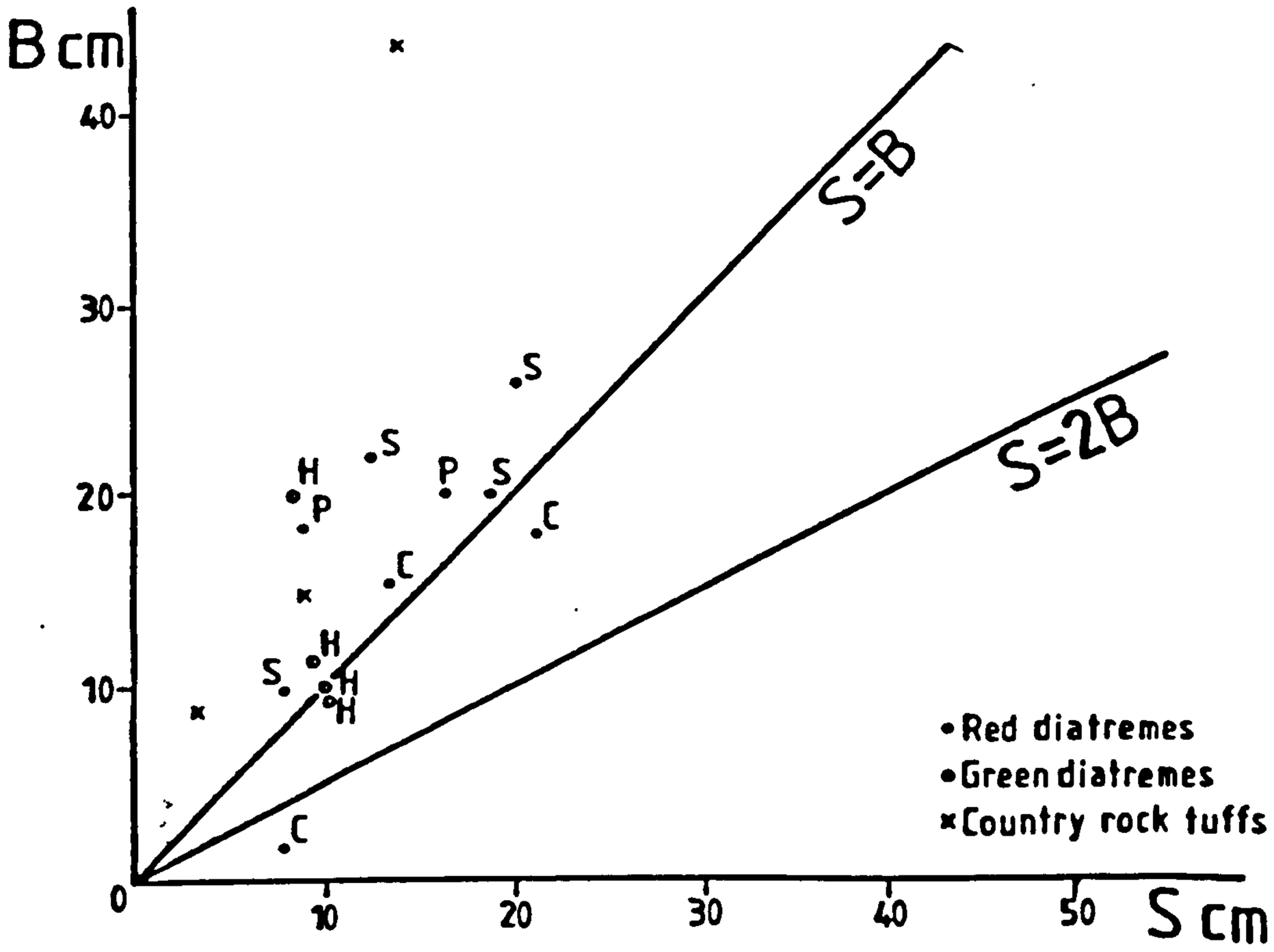

Fig. 5.61 Block impact sag measurements. Symbols as in Fig. 5.49.

An example of this is given by the block impact data (Fig. 5.61) which indicate that the tuffs had generally similar cohesive properties. Unfortunately, the lack of data prevents detailed comparison between deposits. The range of products and the type of volcano formed by water:magma interactions is further discussed in Chapter 7.

The Parade diatreme is rather different from the North Berwick red diatremes, the main differences being as follows :-

a) Marginal features: The Parade margins are wide shear zones which extensively disrupt the country rocks whereas the North Berwick red diatreme margins are narrow and sharply truncate the country rocks.

b) Internal structure: The Parade tuffs are relatively undisturbed and form a >300m thick E or NE-dipping sequence within the diatreme. The North Berwick red diatreme tuffs are often disturbed by sliding and slumping with bedding largely centroclinal, forming sequences up to 100m thick.

c) Sedimentary structures: The Parade tuffs contain a high proportion of base-surge cross-bedded tuffs whereas the North Berwick examples contain few such structures.

It is thought that the Parade diatreme contains a fault bounded block of bedded crater tuffs which subsided en masse after cessation of volcanism. The maar which erupted these tuffs must have been large, because of the thickness of the deposits. Subsidence occurred mainly after lithification of the tuffs, which are remarkably little disturbed. The North Berwick red diatremes represent maar crater tuffs which subsided whilst poorly consolidated into narrow diatremes, causing buckling of the bedded tuffs. The Parade tuffs subsided, probably along concentric ring faults outside the original diatreme margins, with no associated space problems. These faults offset the country rock sediments such that those in the W are downthrown by at least 300m relative to those E of the diatreme (Francis, 1962).

The abundance of base-surge deposits in the Parade diatreme and their scarcity in all of the other East Lothian diatremes is hard to explain. The outer flank tuffs

of maars in Germany often contain a high proportion of base-surge deposits, but their crater tuffs are generally poorly exposed. Perhaps the eruptions of the Parade volcano were completely dominated by surge activity because magma: water explosions occurred at the optimum depth for the production of base-surges (Moore, 1967).

5.6. SUMMARY

1. Newly-deposited Lower Carboniferous alluvial plain and lagoonal sediments were intruded by basaltic magma, initiating phreatomagmatic and phreatic activity.

2. Maars formed when sediment pore waters were heated by slowly ascending magma. Tuff-rings formed when more rapidly ascending magma directly contacted water in standing water bodies.

3. Crypto-volcanic structures formed by short-lived gas-streaming as steam and magmatic gases were injected into country rocks at depth. Similar fault-controlled activity formed intrusive tuffisite dykes.

4. Tuffs deposited around the volcanoes were reworked forming thick tuffite sequences. Minor reworking within volcanoes resulted from water runnoff and crater breaching.

5. Primary volcanic tuffs were deposited by airfall and base-surge processes. The proportion of each type of deposit depended on the depth of magma:water interaction.

6. Both massive and cross-bedded surge tuffs occur and are thought to be the deposits of different regions of surge clouds. Different depositional mechanisms formed tuffs with distinctive grain-size characteristics.

7. Subsidence during or just after volcanism brought mainly crater tuffs down into the diatreme. Slumping of poorly-consolidated tuffs and compression during collapse into an increasingly narrow conduit deformed the tuffs. Rafts of country rock were incorporated in many diatremes by marginal collapse.

8. Reddening of maar diatreme tuffs occurred due to in situ oxidative weathering of country rock-derived ferromagnesian minerals and alteration of glass. Some

groundwater exchange with the country rock red beds may also have occurred. Green diatreme tuffs altered to chlorite, surrounded by green sediments which accumulated in reducing environments.

9. The Parade diatreme tuffs are the product of ring fault collapse of a large thickness of maar crater tuffs. Base-surge deposits are abundant and contain more sediment than associated airfall deposits. Optimum conditions for surge formation were often fulfilled by the Parade volcano and involved explosions at depth, entraining abundant sediment.

10. All the features of the East Lothian diatreme tuffs are consistent with a phreatomagmatic origin. Collapse into diatremes, reworking and alteration have obscured, but not destroyed many of the primary features of maars and tuff-rings which once existed.

CHAPTER 6
EAST FIFE AND AYR DIATREMES

Numerous diatremes are well exposed along the coastline of East Fife and provide excellent exposures for the study of various structural levels in collapsed diatreme tuffs. The Heads of Ayr diatreme, a large structure exposed on the W coast of Scotland, is briefly described and compared with the Fife examples.

6.1. Introduction and Geological Setting

The diatremes (Fig. 6.1) cut Carboniferous sediments which range from Calciferous Sandstone Measures to Coal Measures in age (Forsyth et al., 1977). Over a hundred diatremes have been located throughout East Fife but only a small number of these are sufficiently well-exposed to permit detailed examination. The diatremes have long been the subject of scientific interest but only comparatively recently have attempts been made to compare them with modern volcanoes (Francis, 1970).

The diatreme tuffs are composed of altered alkali-basalt fragments along with sediment derived from the surrounding country rocks. The age of the diatremes has, in general, been difficult to assess and cross-cutting relationships have proved the only reliable method for determining their minimum ages (Francis, in Forsyth et al., 1977). Great difficulties in correlating bedded tuffs in the surrounding Carboniferous strata with specific diatremes have largely prevented the use of this method of dating. The identification of distinctive blocks in the diatreme tuffs has also proved of little use in determining the minimum age of diatremes. Potassium-argon dating (Francis, op.cit.) has established a minimum age of 289±10my for intrusions and lavas in some of the diatremes. However, these ages conflict with the lack of evidence for basanitic volcanism at this time in the Carboniferous succession of East Fife. Palynological evidence suggests an early Westphalian age for one diatreme but those diatremes lacking intrusions or fossil spores cannot be accurately

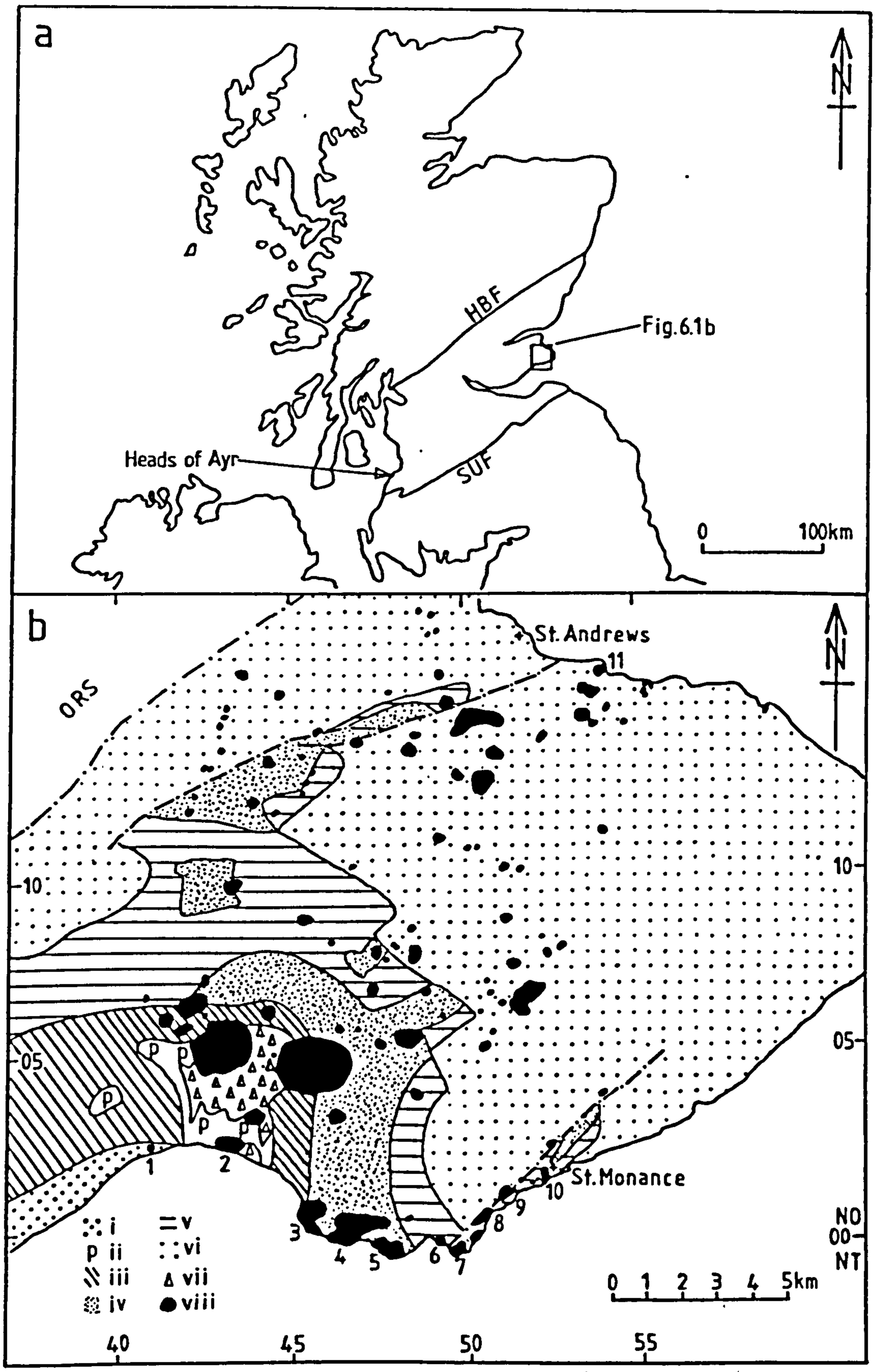

Fig. 6.1 a) Location of the East Fife and Ayr diatremes.
b) General geology of East Fife.

i) Coal Measures
ii) Passage Gp.
iii) Upper Limestone Gp.
iv) Limestone Coal Gp.
v) Lower Limestone Gp.
vi) Calciferous Sandstone Measures
vii) Country Rock tuffs
viii) Diatremes

Diatremes 1: Lundin Links 2: Viewforth 3: Ruddons Point
4: Kincraig 5: Craigforth 6: Elie Harbour
7: Elie Ness 8: Ardross 9: Coalyard Hill
10: St. Monance 11: Kinkell Ness

dated. Figure 6.2 summarises the current information on the diatreme ages.

During the Lower Carboniferous, deposition in East Fife was fluvio-deltaic or shallow marine in character, building up a thick sequence of sediments in this part of the subsiding Midland Valley Trough. With time, marine incursions became more frequent and limestones were formed, but towards the end of the Carboniferous the development of on-delta swamp conditions led to the formation of thick coal seams. Throughout the Carboniferous, a cyclic pattern of deposition occurred in East Fife, due to subsidence and delta migration.

Structurally, the area has been affected by gentle folding and major faulting (Forsyth et al., 1977). Many of the diatremes post-date the folding but pre-date the faulting, the age of which is thought to be Upper Carboniferous. Some of the diatremes appear to have formed along linear zones which may represent the early expression of faults.

In the following account, only the diatreme features relevent to the present study will be mentioned. Brief descriptions of all the East Fife diatremes have recently been published in a Geological Survey Memoir (Forsyth et al., 1977) and the reader is referred to these for discussions of diatreme features outside the scope of this report.

The diatremes range from small crypto-volcanic structures which had little (if any) surface expression, through approximately circular features filled with varying proportions of bedded, collapsed or unbedded tuffs, to large, irregularly-shaped structures containing much intrusive or brecciated material. The diatremes filled mainly with bedded tuffs are most relevant to this study and will be described first.

6.2. Diatremes containing Mainly Bedded Tuffs

6.2.1 Elie Ness diatreme

This diatreme (Fig. 6.3) cuts Calciferous Sandstone Measures sediments SE of the town of Elie and measures

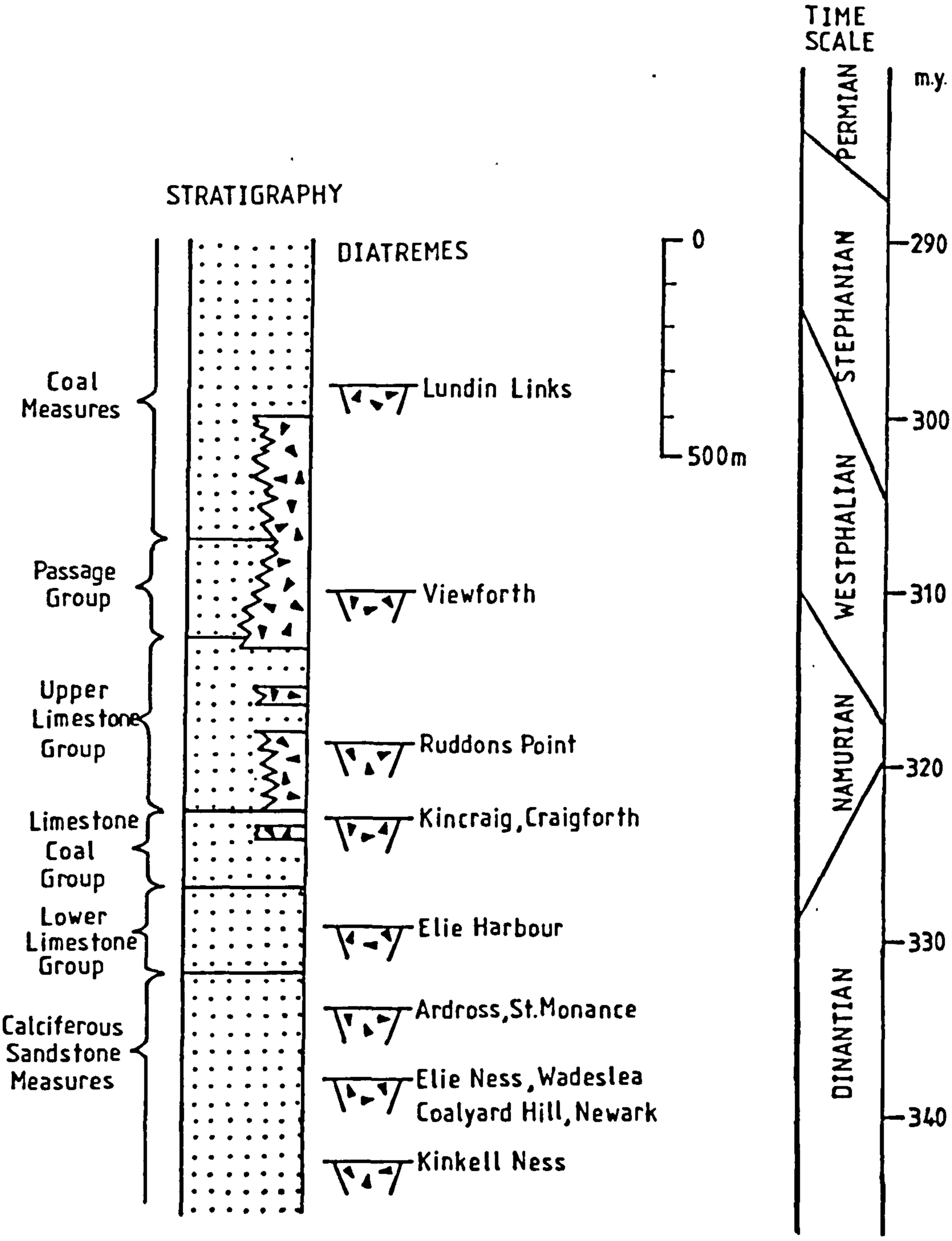

Fig. 6.2 Stratigraphic positions of the East Fife diatremes showing the ages of the country rocks which they cut. Adapted from Forsyth et al. (1977) and Francis (1970).

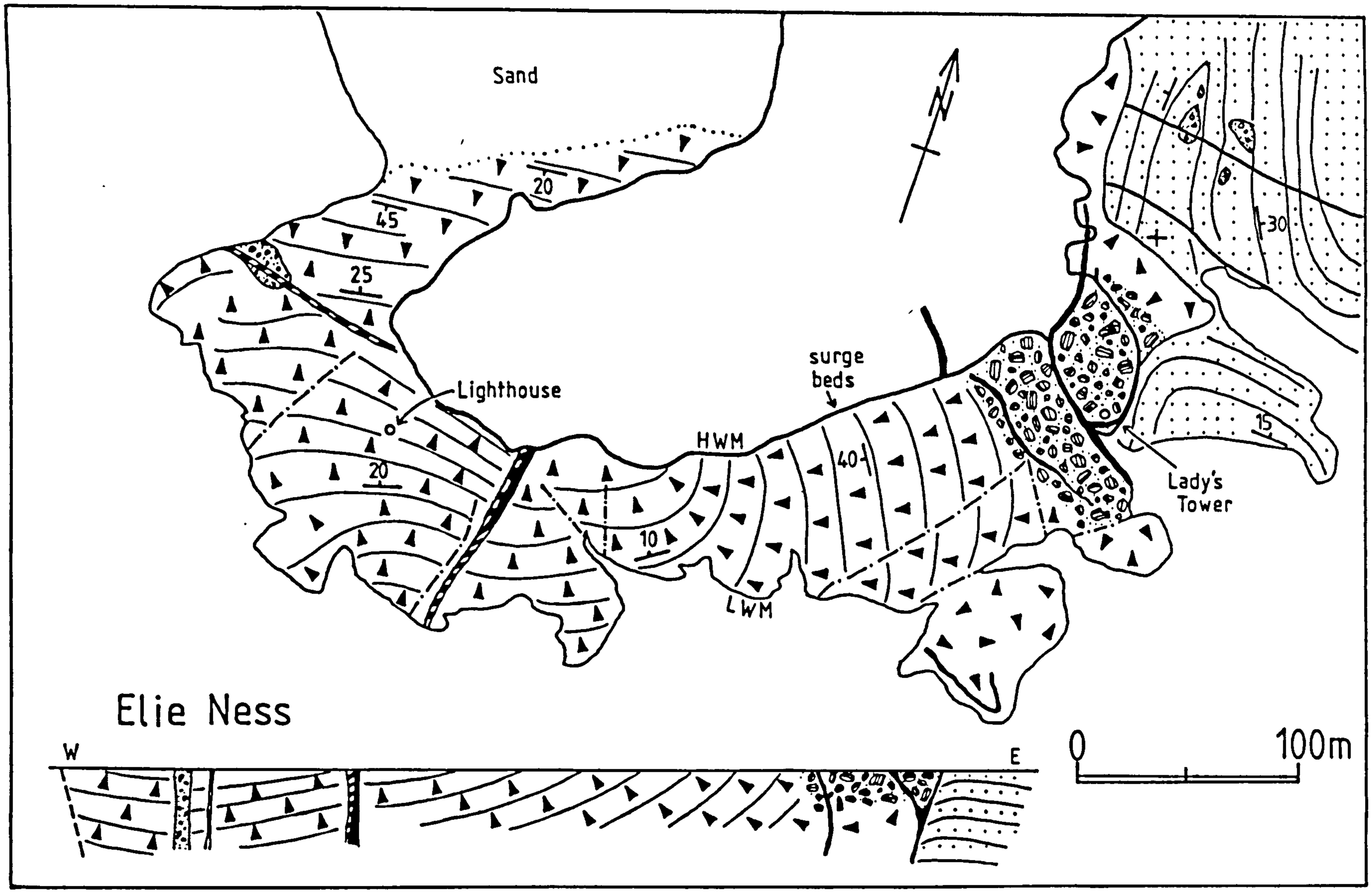

Fig. 6.3 Geological map and section of the Elie Ness diatreme.
See insert in back pocket of thesis for key to diatreme maps.

ca.500x300m.

Eastern margin

The eastern margin is sinuous and separates agglomeratic, unbedded tuffs from brecciated sediments which are turned down against it. The tuffs at the eastern diatreme margin consist of a ca.100m wide zone of generally unbedded, lapilli-grade material with irregular agglomeratic areas. The blocks in these areas reach 5m in size and comprise alkali basalt, bedded and massive tuff, limestone, sandstone and red mudstone. Some of the tuff blocks are highly rounded (Fig. 6.4) and may have been abraded by gas-streaming processes thought to occur at diatreme margins (Francis, 1970).

The marginal zone is intruded by NW-trending basanite dykes which are emplaced en echelon. The dykes often have irregular, lobate margins which in places break down and pass into basanitic breccia. The dyke margins are commonly unchilled and are flanked by intrusive tuff which often contains flow-banded lapilli trails parallel to the contact. These features indicate that magma was injected into poorly-consolidated, perhaps fluidized tuffs during collapse of material into the diatreme. Further evidence of gas-streaming is indicated by irregular sandstone blocks which occur in the marginal diatreme tuffs near the Lady's Tower (Fig. 6.3). These blocks contain crumpled bedding which is often intruded by small stringers of sediment-rich tuffisite. The surfaces of the blocks are pitted and embayed in a manner resembling carious weathering, but this texture has only been found in sandstones intruded by tuffisite. It is thought to be a characteristic feature of gas-streaming processes which have abraded poorly-consolidated coarser sediment clasts. The texture has been found in many blocks within diatremes and crypto-volcanic structures.

A basalt-rimmed, rounded tuff-block occurs in unbedded agglomerate near the above sediment blocks (Fig. 6.5). This rimming by magma is only seen around a few, isolated large clasts in the diatreme. The reason for the scarcity of such blocks is probably connected with their size, since many juvenile lapilli contain quartz grains and other small

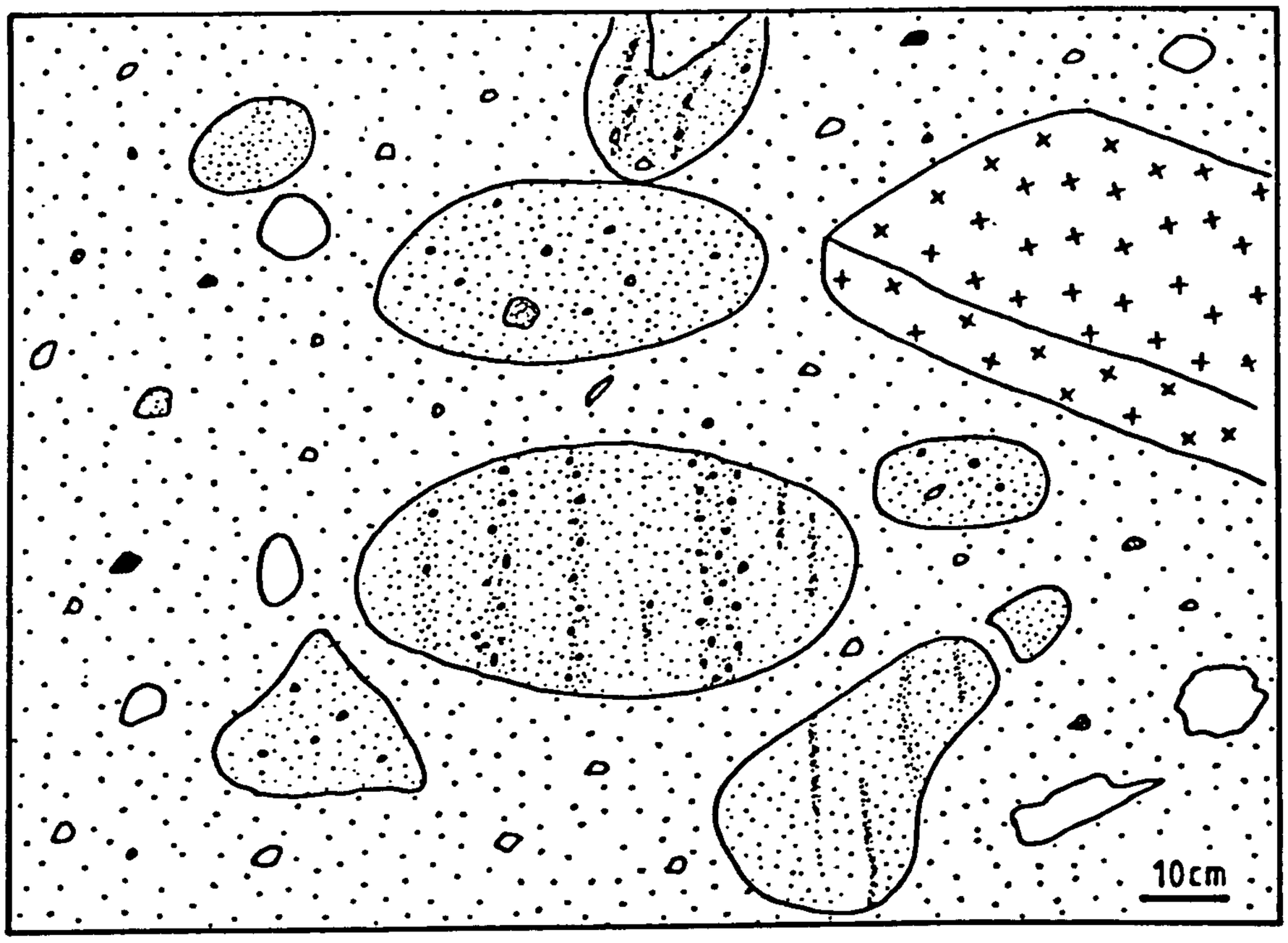

Fig. 6.4 "Ball-milled" rounded autolithic blocks from the eastern margin tuffs in the Elie Ness diatreme.

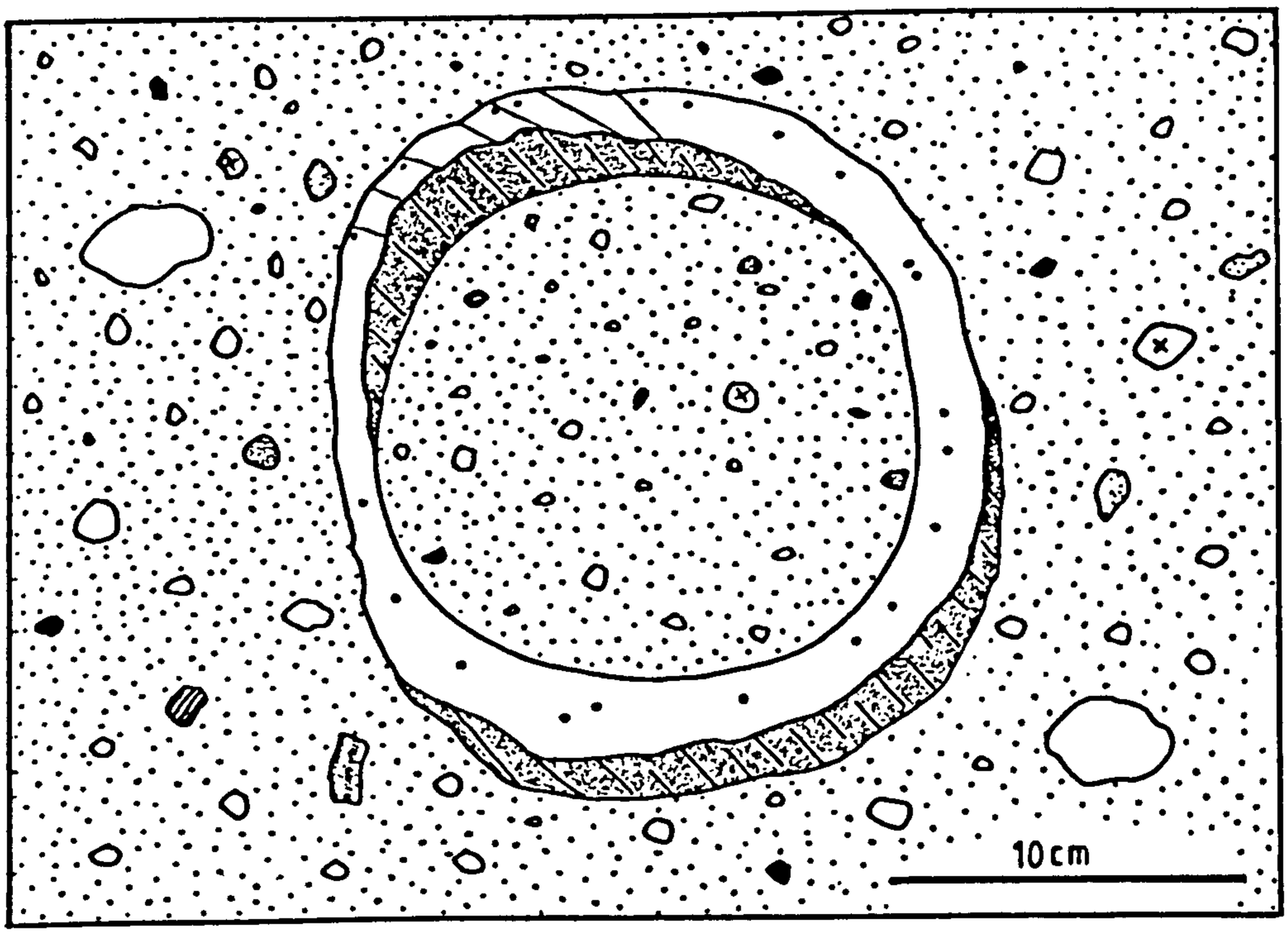

Fig. 6.5 Tuff block with a vesicular juvenile basalt rim. Eastern margin tuffs in the Elie Ness diatreme.

xenocrysts and lithics. Presumably, any large block which does manage to directly contact the magma may accrete a rim. This rim, however, is likely to be destroyed in the explosive chilling following contact of the magma with water. Only fragments smaller than the optimum stable size of juvenile lapilli produced in the eruptions (generally <1cm) are thus rimmed by glass. The presence of large rimmed clasts indicates less explosive chilling of the magma, perhaps due to a relative lack of water.

Collapsed-bedded tuffs

Moving W into the diatreme the unbedded marginal zone passes into a zone of collapsed-bedded tuffs (Fig. 6.3). This zone is ca.40m wide and is bounded on both E and W sides by NW-trending dykes. The zone contains rotated blocks of well-bedded tuff up to 3m long, many of which have rounded shapes, in a structureless lapilli tuff matrix.

Internally, the blocks are moderately to well-bedded lapilli tuffs with rare clasts up to 10cm across, mainly of basanite. Some of the blocks contain fine laminae of well-sorted, often graded, ash with small-scale trough and planar, sometimes climbing, cross-lamination structures. These blocks contain very sediment-rich layers, in places contorted by loading and injection structures. These tuffs are thought to represent water-reworked deposits formed during the initial build up of volcanic detritus in a shallow subaqueous environment. Other bedded tuff blocks are less well sorted, and contain block sags and are probably of airfall origin.

The collapsed bedded area passes to the S into largely structureless, occasionally blocky tuffs which also form the small island to the SW (Fig. 6.3). Here, structureless lapilli tuffs are cut by sub-vertical, sediment-rich dykes. similar, horizontal bands appear to have acted as planes of movement for large structureless tuff rafts. These may be either tuffisite dykes intruded along faults or slide planes, containing either flow or shear-aligned lapilli. Basanitic dykes cut coarse tuff breccias containing angular tuff blocks in the S part of the island, and contain pink anorthoclase crystals up to 10cm across.

Eastern bedded tuffs

The collapsed-bedded area is separated from well-bedded tuffs to the W by a NW-trending linear zone of unbedded tuffs cut by tuffisite dykes and a later, bifurcating basanite dyke. Near the dyke the bedded tuffs grade into a 1m zone of flow-banded lapilli tuff, banded parallel to the dyke. West of the dyke, N and NW-trending faults cut the tuffs, which locally contain blocks and rare, possibly breadcrust bombs of basalt.

The bedded tuffs to the W of the dyke dip NW at between 30° and 75° and are initially coarse, with blocks up to 70cm in diameter. The bedded sequence is summarised in log form in Fig. 6.6 and only its more important features will be discussed.

Initially, the tuffs are poorly-bedded with lapilli and block trails and rare finer horizons, which are often impact deformed. Upwards, the bedding becomes better defined as more fine units occur and coarse units become better sorted. Traced to the SW along strike many of the blocky beds coarsen, perhaps due to directed eruption blasts. Within some of the coarser units, lapilli and blocks are occasionally rimmed with coats of fine ash, similar to armoured lapilli described previously from Saefell (Chapter 2). Larger, ovoid or spherical aggregates of lapilli and ash may be armoured mud balls formed by fluvial erosion of partly consolidated tephra slopes. Similar structures have been found by the author in a tuff-ring on Procida, an island off Naples, Italy.

Discrete layers rich in sediment clasts occur throughout the bedded sequence and become more abundant upwards, suggesting that explosions periodically enlarged the vent by disruption of the country rocks around the conduit. The most common clast types are red mudstone and grey, often shelly limestone. Some of the clasts are plastically deformed, indicating their poor consolidation on ejection.

The finer layers are generally sandwiched between blocky units which often have loaded bases. Many of the fine units contain trough cross-bedding, which is low-

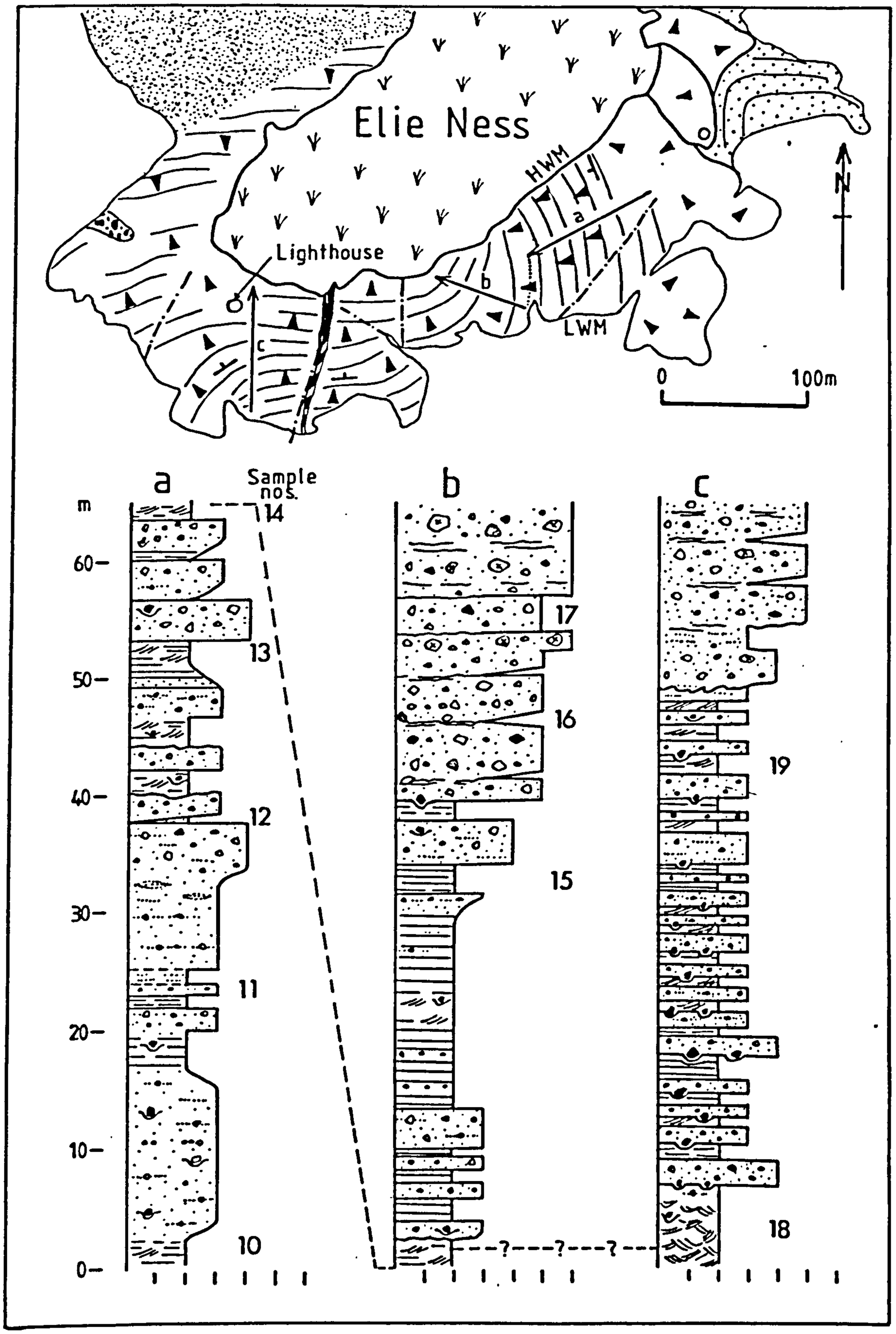

Fig. 6.6 Logs of the Elie Ness diatreme tuffs with their locations marked. Possible correlation of surge cross-bedded tuffs at the base of logs b) and c) is indicated. See insert in back pocket of thesis for key to diatreme logs.

angle and of long wavelength (Fig. 6.7). Pinch-and-swell bedding, thinning of units over the tops of projecting blocks and beds at steep repose angles suggestive of plastering indicate that these fine tuffs are of surge origin (Fig. 6.8). Because of their extremely low profiles and the lack of 3-D exposure, directional data are hard to collect. However, some troughs indicate derivation from the SW or S, as do the asymmetric block sags.

There is a commonly developed sequence of tuffs within the surge units, which may represent deposits from different parts of the surges. Generally, trough and planar-bedded fine-grained layers are overlain by massive, structureless tuffs which may be inversely graded (Fig. 6.9). The cross-bedded layers sometimes overlie coarse, blocky, poorly-bedded units but the latter are not abundant. Some of the surge units are deformed by block impact sags, which generally affect their upper layers. In places the cross-bedded units are partly eroded and loaded by overlying coarser tuffs, some of which appear to have flowed slightly.

The contacts between the sub-units in any surge deposit are generally gradational but are in places abrupt, especially above cross-bedded tuffs. Most of the abrupt contacts are erosive. Although the most common sequence has been described above and in Fig. 6.9, the constituent sub-units may overlie one another in any order, separated by abrupt contacts. In these instances the sub-units are generally thinner than 30cm individually, whereas they reach up to 1·5m thick in the best-developed sequences.

To the W and upwards in the bedded tuff succession the surge units die out and coarse, blocky beds become abundant (Fig. 6.10). These beds are 0·5-3m thick and contain blocks of crystalline basalt up to 1·5m across, though more commonly 10-30cm. Internally, they contain trails of blocks which define a crude bedding, and some laterally discontinuous layers of bedded tuff. The latter bedded layers are often eroded and cut out by the coarser tuffs above. These layers contain some blocks with impact sags though large blocks in the massive tuffs above often directly overlie them without deforming them. In places,

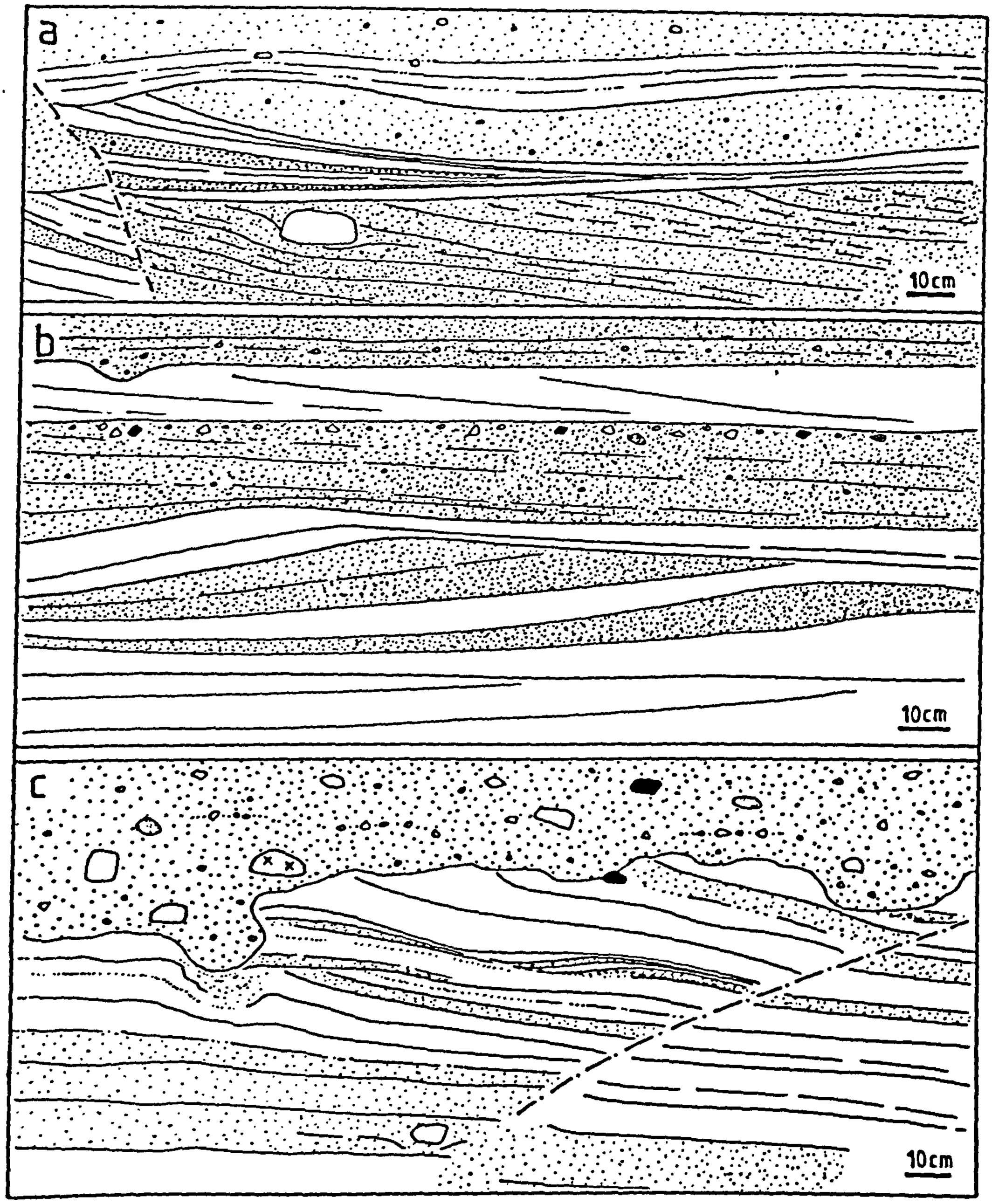

Fig. 6.7 Surge cross-bedded tuffs from the east-central tuffs in the Elie Ness diatreme.
a) Low-angle trough sets with pinch-and-swell bedding, deformed by a block impact sag.
b) Dune with climbing cross-lamination structure. Note low profile and almost horizontal bedding sets on the right side of the dune. Flow direction uncertain but thought to be from right to left.
c) Cross-bedded tuffs overlain by massive bed which cuts down into them and has load structures at its base.

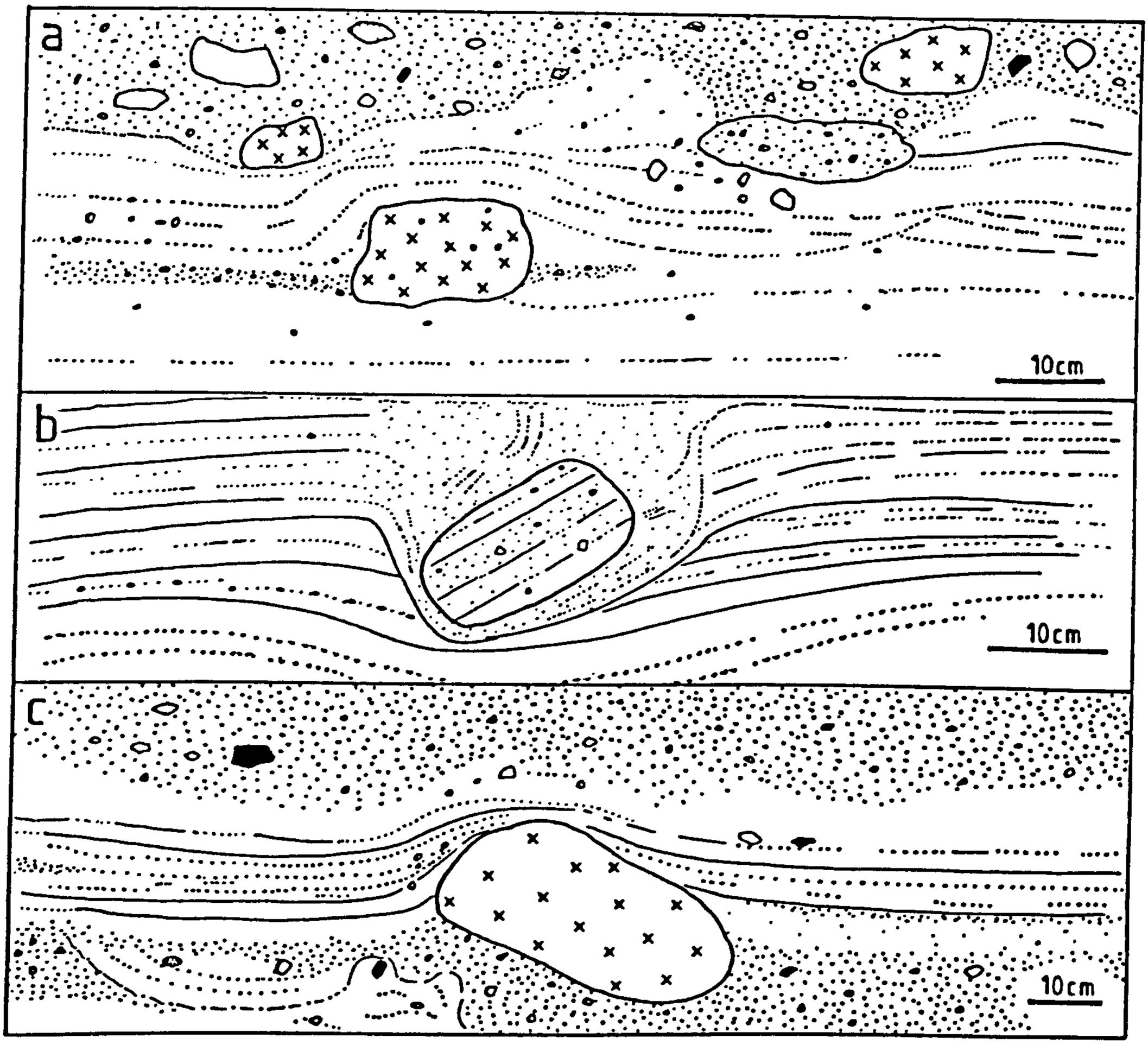

Fig. 6.8 Structures in the eastern Elie Ness surge tuffs.
a) Mantling of an upstanding block by surge beds
b) Deep impact sag of block in surge tuffs
c) Surge mantling of a projecting block. Note thinning over top of block and steep angle of repose, suggestive of surge plastering.

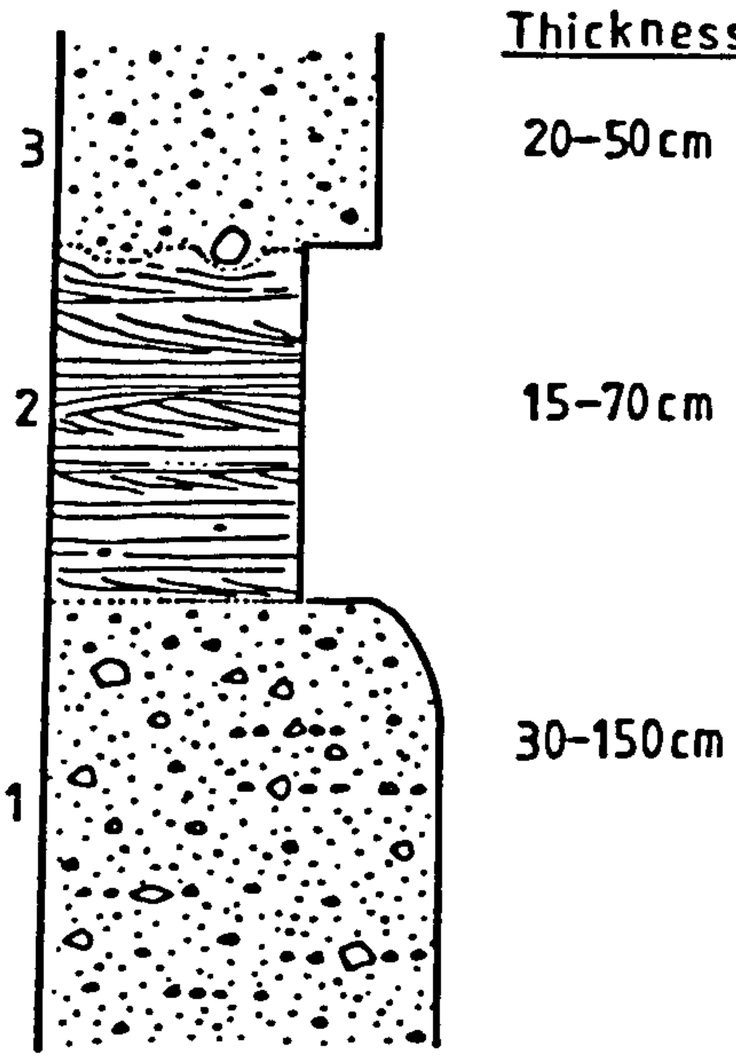

Fig. 6.9 Idealised surge sequence from the Elie Ness diatreme. Note thickness variations of each unit.

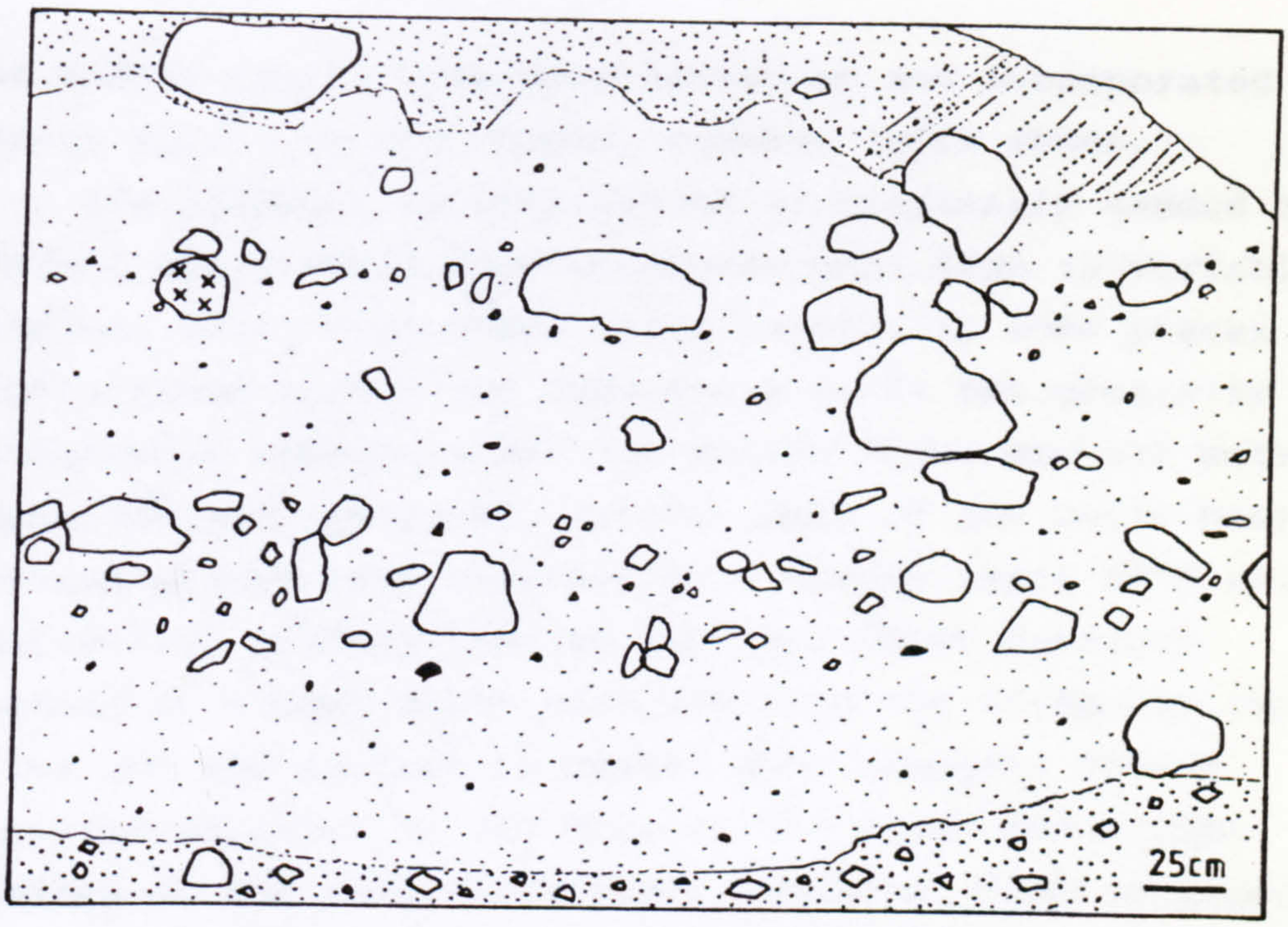

Fig. 6.10 a) Debris flow tuffs from the centre of Elie Ness diatreme. Note block trails and fine structureless matrix.

Fig. 6.10 b) NW-dipping debris flows in the Elie Ness diatreme. Note variations in block size between successive units and their overall poor sorting. Large block at top of low cliff measures 40cm across.

the bedded layers have been broken up and incorporated as rip-up blocks in the coarse, massive tuffs above.

The sequence is interpreted as originally bedded coarse airfall tuffs which have undergone mass flow to variable extents, with interbedded finer layers. In some places the debris flows eroded the underlying tuffs but generally they conformably overlie them. The debris flows are all matrix-supported and are poorly sorted. Some of the units have a reverse-graded base overlain by a blocky layer with slight coarse-tail grading towards the top. Other features include :- blocks which protrude from the irregular top of flows and are mantled by bedded ash, elongate blocks oriented parallel to the base of the flows and slight loading of the underlying finer deposits. Flow occurred immediately after deposition of the coarse units, which are generally conformably overlain by finer well-bedded tuffs. These debris flow tuffs are probably the youngest exposed deposits in the diatreme and may have been initiated by tremors associated with the ejection of the coarse blocks. There is a general increase in block size upwards in the succession, indicating that explosions became more violent with time.

West-central bedded tuffs

The bedded tuffs in the SE part of the diatreme are separated from those to the W by a major composite dyke of basalt and tuffisite (Fig. 6.3). The dyke is 5m thick at HWM and comprises mainly basalt flanked by thin, grey flow-banded tuffisite. Towards LWM the central basalt dyke becomes brecciated and mixed with the tuffisite. Further to the S the dyke becomes completely tuffisitic and contains blocks of basalt, folded sandstone and tuff in a flow-banded matrix which resembles vertically-bedded shale or siltstone (Francis, in Forsyth et al., 1977). A steep normal fault of unknown displacement, 5m W of and parallel to the dyke has a downthrow to the E.

West of the fault the tuffs consist of N-dipping, well-bedded lapilli and ash. The features of these tuffs are summarised in log form in Fig. 6.6. At LWM, the lowest exposed deposits are trough cross-bedded tuffs exposed

approximately normal to the current direction, forming a complex festoon pattern (Fig. 6.11). Individual troughs reach depths of 50cm and widths of 2m, and are strongly curved. The festoon-bedded tuffs occur mainly within a N-S trending gully cut in the surrounding bedded tuffs. This gully appears fault-bounded and measures 6m deep by at least 8m across, and is poorly exposed at LWM. The festoon bedding is probably due to repeated surge deposition and erosive channelling within this gully, forming nearly symmetrical troughs with erosive margins. Rare block sags deform the cross-bedding, especially towards the top of the festooned unit. The sequence is cut by small soft sediment faults with offsets of <10cm, which may be related to compaction of the cohesive tuffs.

Above the festoon-bedded unit there is a >30m thick sequence of well-bedded tuffs alternating with coarser, sometimes blocky, poorly-bedded layers. The finer tuffs are often cross-bedded, with low-angle planar and trough sets. One example of climbing cross-lamination in a surge dune occurs towards the top of the unit, with downflow crest migration at climb angles of 10° to 15° (Fig. 6.7). Although current directions are hard to obtain, some foresets indicate a source to the S or SE.

The cross-bedded layers reach up to 1m thick and are commonly overlain by coarser, poorly-bedded tuffs up to 2·5m thick. These tuffs may be coarse tail reverse-graded or contain a blocky layer overlain by lapilli tuff. Many of these blocks penetrate deeply into the underlying bedded tuffs and plastically deform them. This alternating fine-coarse sequence is repeated at least 15 times throughout the tuffs in this part of the diatreme.

Above the alternating sequence, near the lighthouse, the tuffs become coarser and poorly bedded. Some beds are completely structureless and may be debris flows whereas others are poorly bedded and represent coarse airfall deposits. Some finer, bedded layers occur, but these are broken up by block impact sags or wedge out due to erosion by debris flows.

The tuffs in this part of the diatreme thus comprise

Fig. 6.11 a) Trough cross-bedded tuffs in the SW part of the Elie Ness diatreme with sets forming a complex festoon pattern. Surge motion normal to plane of photograph. Hammer measures 30cm.

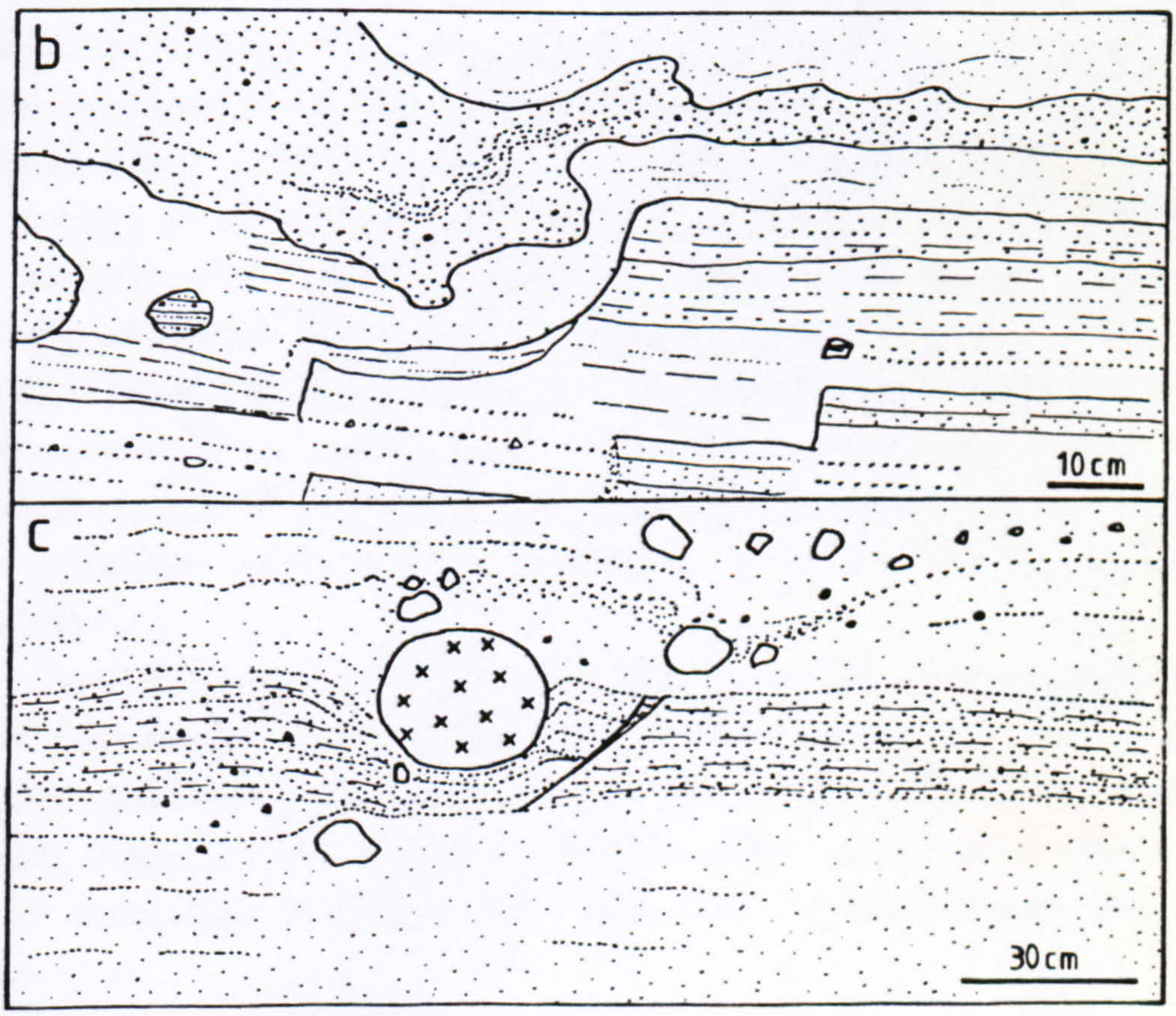

Fig. 6.11 b) Slumped, contorted bedding in tuffs near the Elie Ness lighthouse. Note small step-faults some of which deformed poorly consolidated tuffs.

c) Block impact sag in the Elie Ness tuffs near locality b) above. Note plastic deformation beneath the block and the asymmetric sag above it to the right.

a thick sequence of cross-bedded tuffs alternating with coarser, poorly-bedded tuffs and overlain by mixed debris flows and coarse airfall tuffs. This sequence correlates with a similar succession to the W (Fig. 6.6). Downthrow of at least 10m of the eastern tuffs relative to those in the W has occurred, along faults, one of which is now followed by the major composite dyke.

Western bedded tuffs

The deposits in the W of the diatreme are moderately to well-bedded lapilli tuffs with occasional layers rich in basalt blocks (Fig. 6.6). Some cross-bedded tuffs occur and indicate surge derivations from the E. Coarser horizons commonly have loaded bases which project down into the finer tuffs below. A basaltic breccia plug cuts the bedded tuffs, which dip into it, in the extreme W of the diatreme. The breccia appears to rest irregularly on the bedded tuffs to the S (Francis, in Forsyth et al., 1977) and may be partly extrusive. The plug is cut by both tuffisite and carbonate veins. Francis (op.cit.) suggested that the breccia marked the centre of the neck because of the surrounding inward dips of the tuffs. Late-stage intrusion of a plug into subsiding tuffs could occur at any location in the diatreme, and may merely indicate the final position of the volcanic centre, or be unconnected with it. The centroclinal bedding in the tuffs is a more convincing indication of a former volcanic centre but collapse processes may form basin structures totally unrelated to the original attitude of the beds, and obscure the site of the vent.

The coarser tuffs in the W of the diatreme contain wood fragments and crystals of pyrope garnet, zircon and alkali-feldspar, as well as amphibole and pyroxene nodules. Often, lapilli of juvenile basalt have small crystals at their centres, although no large clasts are rimmed in this way.

Summary and conclusions

1. The Elie Ness diatreme consists of a fault-bounded marginal zone along which subsidence movements occurred, with collapsed bedded tuffs further into the diatreme which

were only partly affected by such movements. The major part of the diatreme consists of bedded tuffs which subsided en masse and are only slightly folded, although cut by faults of small displacement.

2. The sequence of tuffs begins with water-reworked ash deposits at the base. Above, airfall tuffs with minor surge deposits give way to a surge dominated sequence. The overlying tuffs are coarse airfall tuffs partly reworked by debris flows which may have been triggered by violent late-stage eruptions and by collapse into the diatreme. Some of the youngest tuffs are cut by basaltic breccia and later tuffisite dykes, indicating a final intrusive phase of gas-poor followed by gas-rich magma.

3. The surge tuffs occur in a characteristic sequence thought to represent the deposits of different parts of the surge clouds. Commonly, cross-bedded tuffs are overlain by coarser, often reverse-graded, blocky tuffs which are poorly bedded. A massive, unbedded lapilli tuff bed may in places occur between the cross-bedded and the blocky tuffs. The significance of this sequence will be discussed further in Chapter 7.

4. Collapse of bedded tuffs into the diatreme, and incomplete exposures have made conclusions about the probable vent position hard to make. However, the evidence from most of the surge deposits indicates derivation from S of the presently exposed tuffs. Asymmetric block impact data support this, as does the southward coarsening of blocks along strike in airfall layers. The centroclinal attitude of the beds may thus be related to a later vent, or more probably is a feature of differential subsidence within the diatreme.

6.2.2 Elie Harbour diatreme

The Elie Harbour diatreme (Fig. 6.12) measures ca.130 x230m and cuts Lower Limestone Group sediments at the S side of the Elie pier. The diatreme contains well-bedded lapilli tuffs intruded by basaltic dykes and a plug of basaltic breccia. A raft of sandstone lies in the central part of the diatreme and is highly tuffisitized in places.

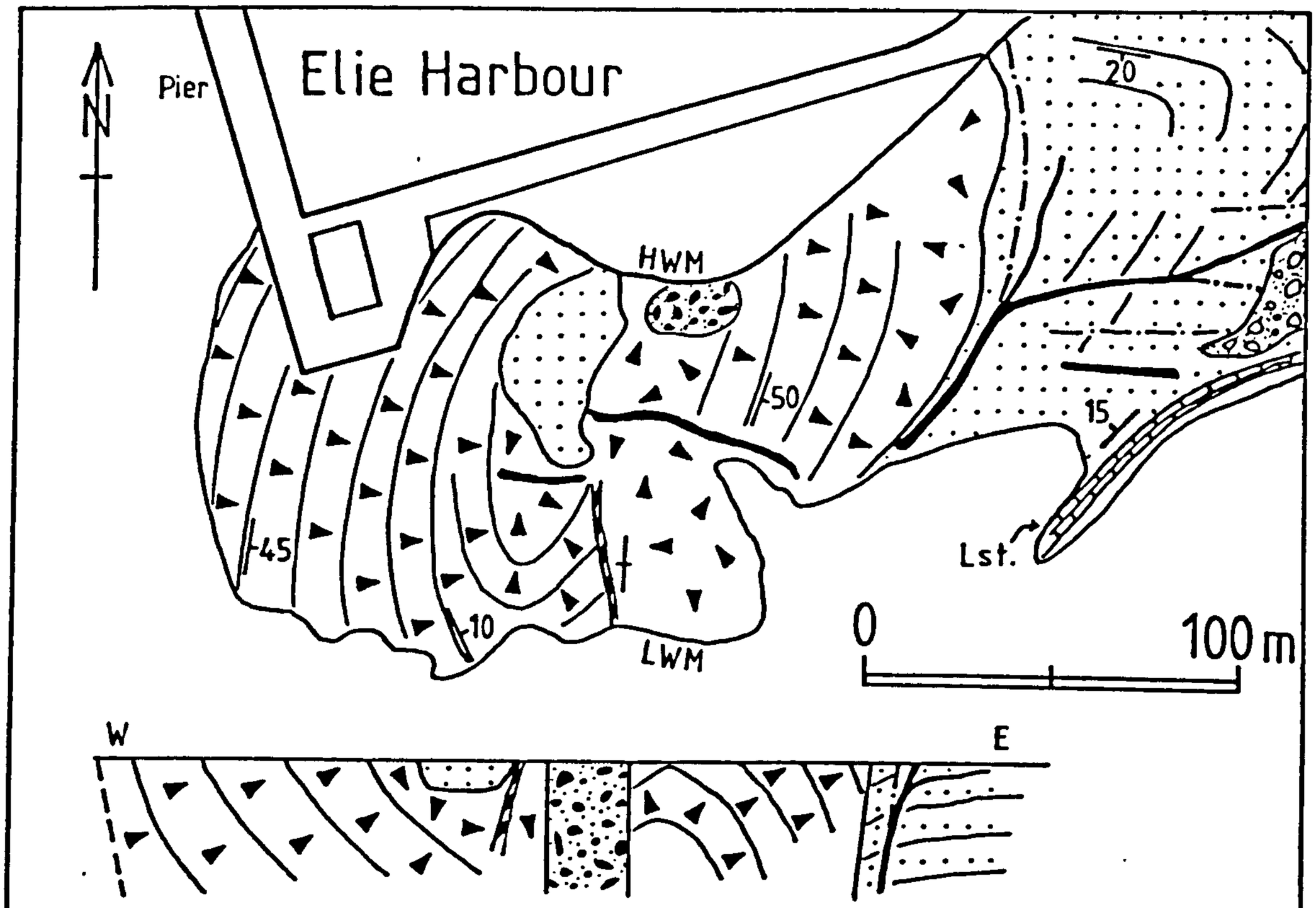

Fig.6.12

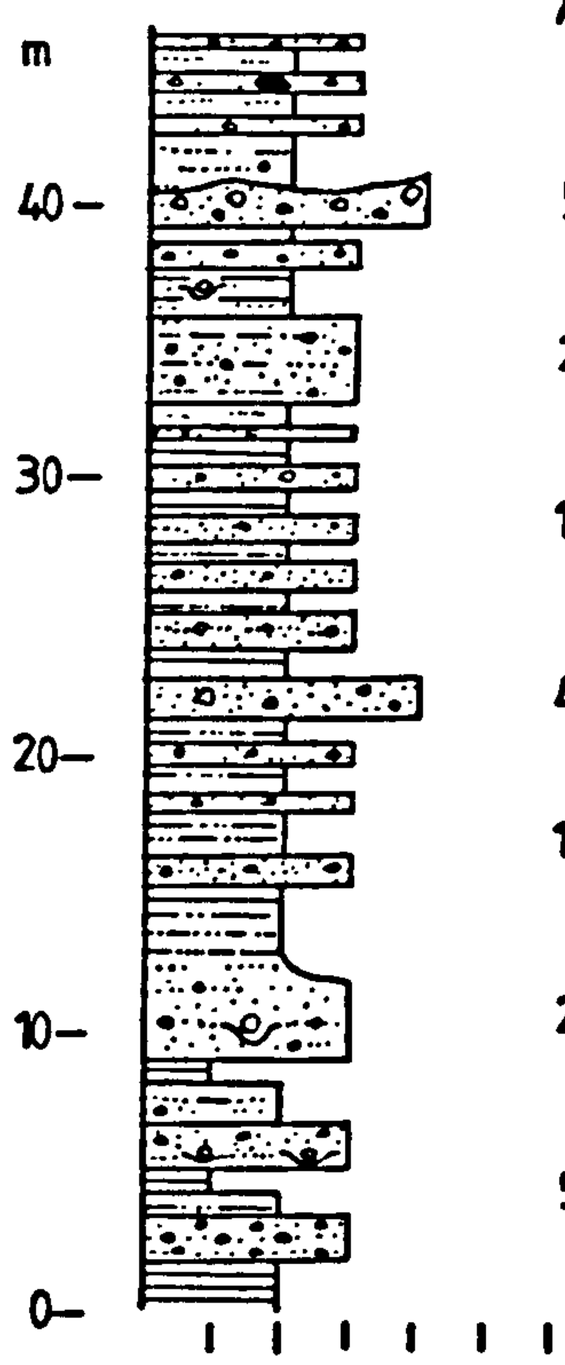

AML(cm)	Features
50	Lapilli lenses
20	
15	Monotonous lapilli/ash interbeds
40	
10	Airfall mantling of protruding blocks
25	
5	Limestone clasts

Fig.6.13

Fig. 6.12 Geological map and section of the Elie Harbour diatreme.

Fig. 6.13 Log of western bedded tuffs showing internal features. Note increase in block size upwards in the sequence.
AML: average maximum lithic size

Only the eastern margin of the diatreme is exposed, on the wave-cut platform.

Eastern margin

The margin consists of a trough feature some 1-2m wide containing tuffs highly veined with calcite. Outside this ring fault the country rock sediments are turned down against the margin, forming vertically banded blocks in a zone 4-6m wide. Outside this, a curved fault parallel to the margin separates the zone from less disturbed country rocks which dip into the diatreme at up to 60°. Basalt dykes follow the disturbed zone and continue eastwards, with radial orientation to the diatreme.

Bedded tuffs

The bedded tuffs are best exposed in the W side of the diatreme, where a 55m thick sequence occurs in the W-dipping beds (Fig. 6.13). At the base of the exposed sequence are well-bedded lapilli tuffs with interbedded poorly-bedded coarse, blocky layers. Thin, well-laminated ash layers are laterally very continuous and mantle blocks from underlying beds. Impact sags are rare, mainly because of a scarcity of blocks immediately overlying well-bedded layers. Blocks are mainly of basalt but some rare limestone, sandstone and coal clasts are found.

Upwards, the blocky layers become scarcer and overall the sequence becomes finer and better bedded. Some of the finer units pinch-and-swell along the strike. In one place near LWM the tuffs are cut by a curved shear surface along which movement occurred whilst the tuffs were moist. Coarse units become more common by 30m up the sequence and some isolated blocks up to 1·5m occur. Francis (in Forsyth et al., 1977) noted the presence of scoriaceous basalt bombs but only vesicular, sometimes rounded, blocks of basalt have been found. None of the blocks contain structures indicating they were molten on ejection (Fig. 6.14).

Towards the top of the bedded sequence blocks become more abundant and reach 1·8m diameter, though are on average 20-30cm. Along strike to the S the block component of the tuffs becomes coarser (Table 6.1) perhaps indicative of directed eruption blasts.

N part of diatreme A.M.L. size (cm)	Height in log (m)	S part of diatreme A.M.L. size (cm)
5	20	8
3		10
5	16	30
12		35
10	12	5
10		10
5	8	20
20		30
15	4	25
2		30
5	0	2

Table 6.1 Comparative block sizes in the Elie Harbour tuffs

Some of the finer layers in the upper part of the sequence are occasionally loaded, with flame injection structures. Very small-scale cross-bedding occurs in places, the origin of which is uncertain.

At the top of the bedded sequence a coarse, blocky deposit occurs, in the centre of the centroclinally bedded tuffs (Fig. 6.15). This deposit is largely unbedded, although it contains low-angle irregular partings. The blocks are mainly of basalt, which reach 75cm and these are scattered through a poorly-sorted lapilli tuff matrix. The coarse tuffs form an upstanding mass above the wave cut platform to the W and may be bounded by a fault. The tuffs themselves may thus be a collapse breccia or a debris flow. The distinction may be semantic since flow could well have occurred during collapse.

The unbedded tuffs abut against a large (50x20m) raft of coarse sandstone. The raft is heavily tuffisitized, especially at its margins with mixed sediment and tuff cut by grey tuffisite dykes. Gritty bands in the sandstone often contain muscovite, feldspar and garnet. Another sediment raft is found within a tuffisite dyke in the SE part of the diatreme. The raft is of similar, through finer, lithology to the major raft and is more highly broken up and intimately penetrated by grey intrusive tuff.

The major raft has a faulted contact with the tuffs in the W but in the E its margin is obscured. An E-W basalt dyke cuts the tuffs E of the raft and terminates against it. The eastern tuffs are poorly exposed but are generally finer than those in the W and dip to the E at 40-60°. The tuffs are cut by an oval basaltic breccia plug near HWM.

Fig. 6.14 Large basaltic blocks in the Elie Harbour diatreme tuffs. Note shattered margins and the lack of fluidal structures. Hammer measures 30cm.

Fig. 6.15 Unbedded, blocky deposit at centre of the Elie Harbour centroclinally bedded tuffs. Note low-angle, irregular partings. Hammer measures 30cm.

Summary and conclusions

1. The small, ring fault bounded diatreme consists of centroclinally-bedded tuffs in the W with a large, faulted sediment raft sitting in its centre. To the E, the tuffs dip at high angles and are cut by basaltic intrusions. The structure is quite simple, and appears to be the result of collapse along ring faults.

2. The tuffs are all of airfall origin, with an apparent lack of surge deposits. The central tuffs are unbedded and may be debris flows triggered by collapse. Directed eruptions caused the tuffs in the W to become coarser along strike to the S.

3. The small size of the diatreme perhaps indicates that its surface expression was also relatively small, since the general lack of bedding disruption and intrusive material indicates that the tuffs have not apparently subsided to great depths. Collapse occurred en masse with some differential movements along a ring fault in the E. The sediment raft was probably included by collapse, and it subsided whilst being intruded by tuffisite. A basalt breccia plug may be situated at, or close to the original vent position.

6.2.3 Craigforth diatreme

The Craigforth diatreme (Fig. 6.16) cuts Limestone Coal Group sediments W of Elie, and is one of the few diatremes which is almost completely exposed.

Margins

The easterm margin is well exposed near HWM and is defined by a tuffisite dyke which separates bedded tuffites within the diatreme from tuffisitic breccia outside it. The dyke contains flow-aligned coal and sediment clasts and is in places cut by irregular, polygonal joints. The bedded diatreme tuffites are sharply and obliquely cut by the dyke but towards HWM the bedding becomes folded and oriented sub-parallel to the contact.

The western margin is a fault which dips into the diatreme at a high angle, with the surrounding country rocks folded and dipping into the magma. To the S the

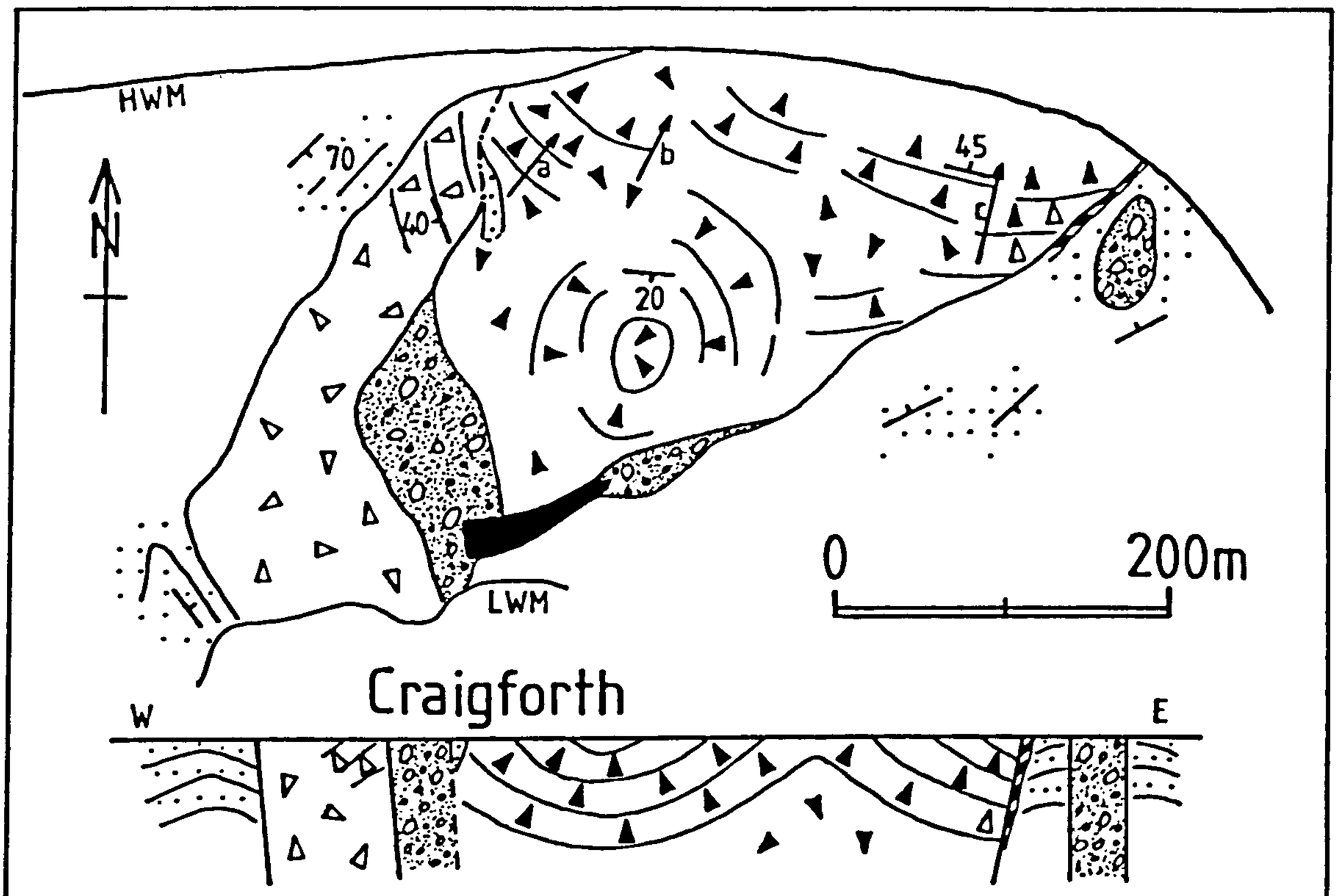

Fig.6.16

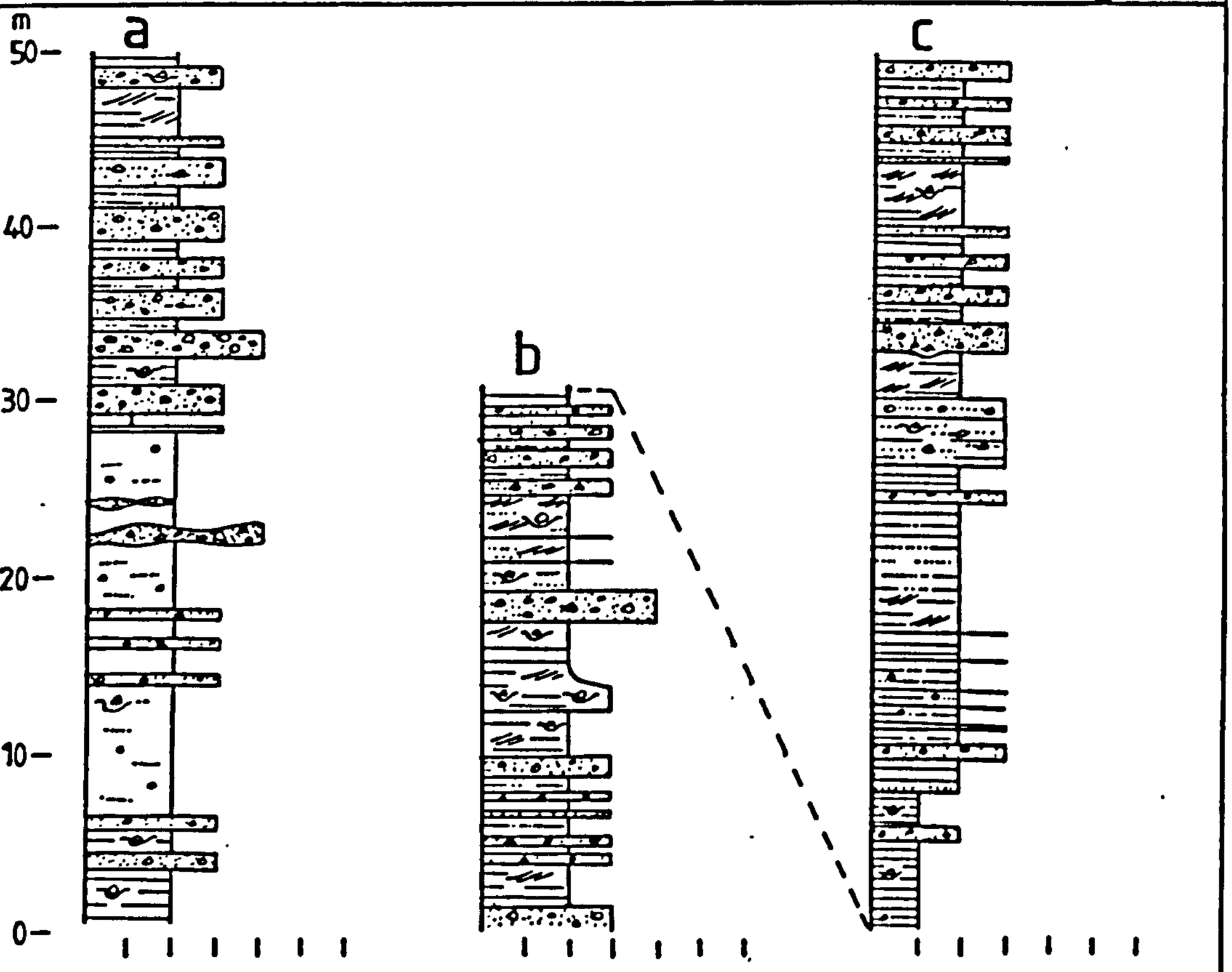

Fig.6.17

Fig. 6.16 Geological map and section of the Craigforth diatreme.

Fig. 6.17 Logs of the Craigforth tuffs with locations marked in Fig. 6.16. No correlation of log a) with log b) because of blocky unbedded tuffs between.

margin is defined by a basaltic dyke, a linear pod of tuffisitic breccia or a fault.

Eastern tuffs

The first 9m of the exposed tuffites at the eastern side of the diatreme consists of tuffaceous shale and siltstone with thin beds of carbonate-cemented tuffaceous sandstone (Fig. 6.17). Blocks of sediment up to 50cm occur, many with deep, plastic impact sags beneath them. Calcite veins are abundant, either sub-parallel to bedding or filling tension gashes oriented at 070-110°.

Towards the top of the 9m sequence the tuffites become well-sorted, well-laminated ashy siltstones which in places contain low-angle trough cross-bedding. The laminae are sometimes reverse-graded and are often erosively cut-out by overlying coarser layers. These deposits are interpreted as fine base-surge tuffites formed at an early stage in the evolution of the volcano, when ejecta were rich in sediment derived from the country rocks adjacent to the conduit.

Immediately above the fine surge deposits, a 15cm thick lapilli tuff horizon with a slightly irregular base occurs (Fig. 6.18). In contrast to the underlying tuffites the lapilli horizon is completely composed of juvenile volcanic fragments, set in a calcite replaced matrix. Above this, the diatreme tuffs contain low proportions of accessory lithics and resemble the green tuffs found in most East Fife diatremes.

The main features of the bedded sequence are summarised in the logs (Fig. 6.17), but some merit further description. The tuffs contain many soft-sediment deformation structures, including flame structures and diapiric injection structures. Often, coarser horizons have loaded bases and in one place they contain pseudonodule structures. The moist nature of the tuffs is confirmed by the many deep impact sags beneath even small clasts. Small soft-sediment faults are also common, as are tuffisite dykes.

Cross-bedded tuffs become common towards the exposed top of the sequence, the features of which indicate they are of surge origin. Trough cross-bedded units are often

erosive on one another, and are generally overlain by coarse, poorly-bedded lapilli tuffs (Fig. 6.19). Dunes up to 2·5 wavelength and 50cm wave height occur, some containing climbing-ripple lamination. Directional data are difficult to interpret but the best-exposed examples indicate currents from the S or SE.

Western tuffs

The tuffs in the W of the diatreme dip out towards the margin at 25-35°. The tuffs are generally sediment-rich and are separated from the main diatreme tuffs by a fault. The marginal tuffites are very similar to those in the E, and comprise tuffaceous shales and siltstones interbedded with more tuffaceous lapilli beds (Fig. 6.17). Block sags occur in the highly disturbed tuffites, and many tuffisite dykes and sills cut the deposits near the margin. At the margin the tuffites become better bedded and more sediment-rich.

Across the fault which bounds the marginal tuffites the tuffs become rich in volcanic material. Up the sequence into the diatreme centre, the tuffs become better bedded and towards the top contain cross-bedded tuffs (Fig. 6.17). A large raft of red mudstone occurs near the fault and is intruded by tuffisite at its margins (Fig. 6.16).

Central tuffs

The central tuffs correlate beneath sand cover with those in the E and are of similar lithology (Fig. 6.17). The deposits are green, juvenile-rich tuffs with many trough cross-beds. Other surge features include pinch-and-swell bedding and piling up of coarse material on one side of upstanding blocks. Cross-bedding indicates currents from the S or SW, roughly from the present geometrical centre of the diatreme.

Structure

The tuffs in the centre and northern part of the diatreme are centroclinally bedded around poorly exposed unbedded tuffs, although they are folded in the N so that the tuffs dip outwards. The sediment-derived tuffs are symmetrically disposed around the margins, apart from in the S where tuffisitic breccia occurs . Generally, bedding becomes poorly-defined to the S, towards the breccia.

Fig. 6.18 Lapilli tuffs overlying fine, sediment-rich surge cross-bedded tuffs near the E margin of the Craigforth diatreme. Tape measures 30cm.

Fig. 6.19 Surge trough cross-bedded tuffs overlain by poorly-bedded tuffs above an erosion surface. Pen measures 14cm.

The diatreme is elongated NE-SW and contains much internal evidence of collapse, much of which occurred whilst the tuffs were poorly consolidated. Post-consolidation collapse occurred along faults, which were intruded by tuffisite along the margins.

Summary and conclusions

1. The oldest exposed tuffs are sediment-rich and contain some surge structures. These are probably the initial volcanic products, formed as poorly-consolidated sediments were explosively disrupted. The lack of juvenile material indicates that the initial activity was dominated by steam explosions, which perhaps formed an initial maar.
2. The incoming of juvenile magma occurred abruptly and continued throughout the life of the volcano. The maar was thus rapidly transformed into a tuff-ring as the conduit became largely isolated from the country rocks.
3. Surges were very common throughout the volcanism and were probably sourced from the direction of the present centre of the diatreme, although directional data are hard to collect and folding of the tuffs has confused the interpretation of the results.
4. Collapse occurred throughout the volcanic activity and the late-stage movements were accompanied by gas-streaming. Disturbance and rotation of the tuffs was limited, perhaps because collapse was "lubricated" by the gas-streaming. A later, minor phase of intrusive activity emplaced a basalt dyke along the southern margin.

6.2.4 St. Monance diatreme

This diatreme (Fig. 6.20) cuts Calciferous Sandstone Measures sediments S of the Town of St. Monance.

Margins

The western margin is faulted with the tuffs and sediments highly penetrated by tuffisite. Many sandstone blocks are incorporated in the structureless diatreme tuffs near the margin. A basalt dyke cuts the margin and passes out into the country rocks, where it becomes bleached and carbonated. The eastern margin is sharp and the diatreme tuffs contain many irregular rafts of red mudstone, The

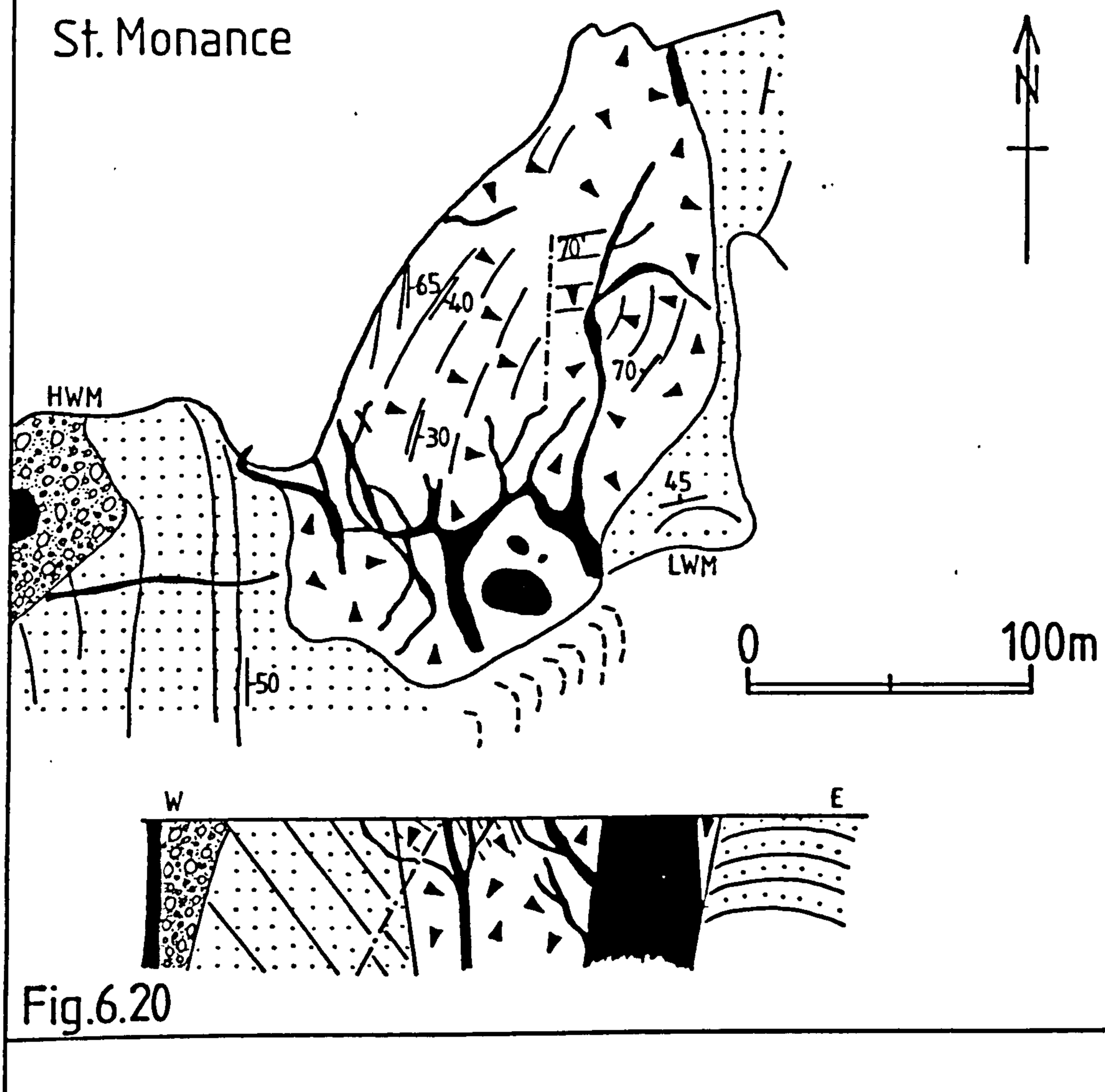

Fig.6.20

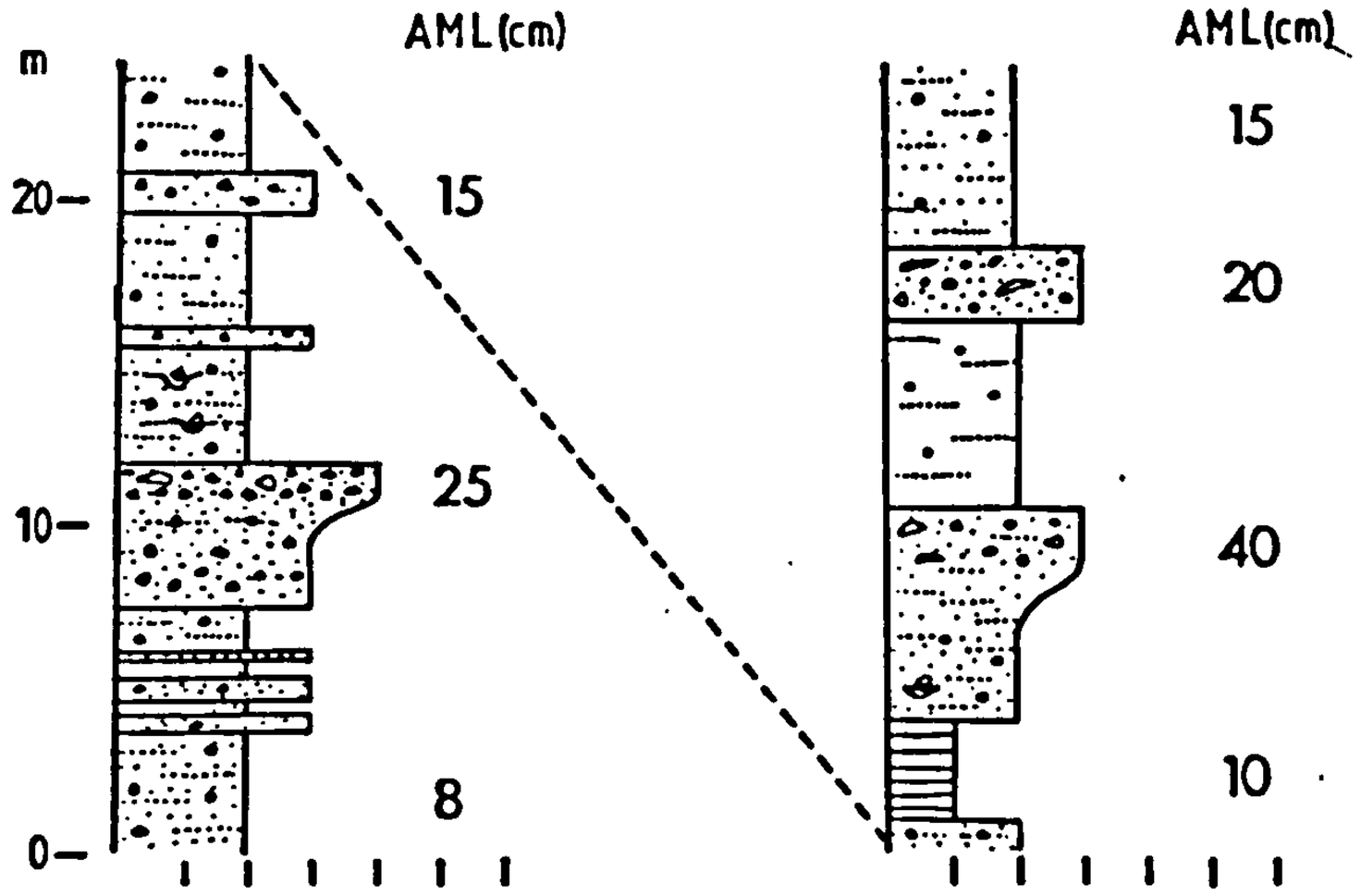

Fig.6.21

Fig. 6.20 Geological map and section of the St. Monance diatreme.

Fig. 6.21 Logs of bedded tuffs in western side of the diatreme.

country rocks surrounding the diatreme are steeply turned down against the margins, and in the S their bedding traces are deflected.

Diatreme tuffs

Although bedding in the diatreme is not easily detected, it is best seen from the low cliffs at HWM. At HWM the bedded tuffs in the W are broken up, folded and dip at steep to vertical angles. The tuffs comprise well-bedded alternations of lapilli and ash which are in places deformed by impact sags from small blocks.

To the E the collapsed tuffs pass into structureless tuffs which form a zone approximately parallel to the cliff-line at HWM. East of this the tuffs are faintly bedded and dip E at 30-50°. The tuffs form a 50m thick sequence which is cut off to the E by faults and multiple dykes (Fig. 6.20). The deposits are summarised in log form (Fig. 6.21) and comprise bedded lapilli tuffs with occasional block-rich horizons. Block sags are common, especially near the base of the unit but become rare upwards where bedding becomes poorly defined.

The most common blocks are basalt and red mudstone, which reach up to 1.5m. The red mudstone clasts are often plastically deformed, and elongated parallel to bedding. Some of this deformation may be due to compaction of the tuffs but in some cases deformation occurred at the time of impact of the blocks. One elongate mudstone clast is deformed over the top of a block which protruded from an underlying unit (Fig. 6.22). Another elongate clast is itself deformed by a basaltic ?bomb which impacted onto it (Fig. 6.23). Some large mudstone blocks are more angular, and were more consolidated on ejection, perhaps because they were derived from deeper levels in the country rock sequence.

The lack of well-defined bedding may indicate that many of the tuffs have flowed to some extent. Much of the bedding is defined by blocky trails or lenses of coarser material in a largely structureless matrix. Sorting is poor or absent, especially towards the centre of the diatreme, and the tuffs generally coarsen upwards. Collapse led to

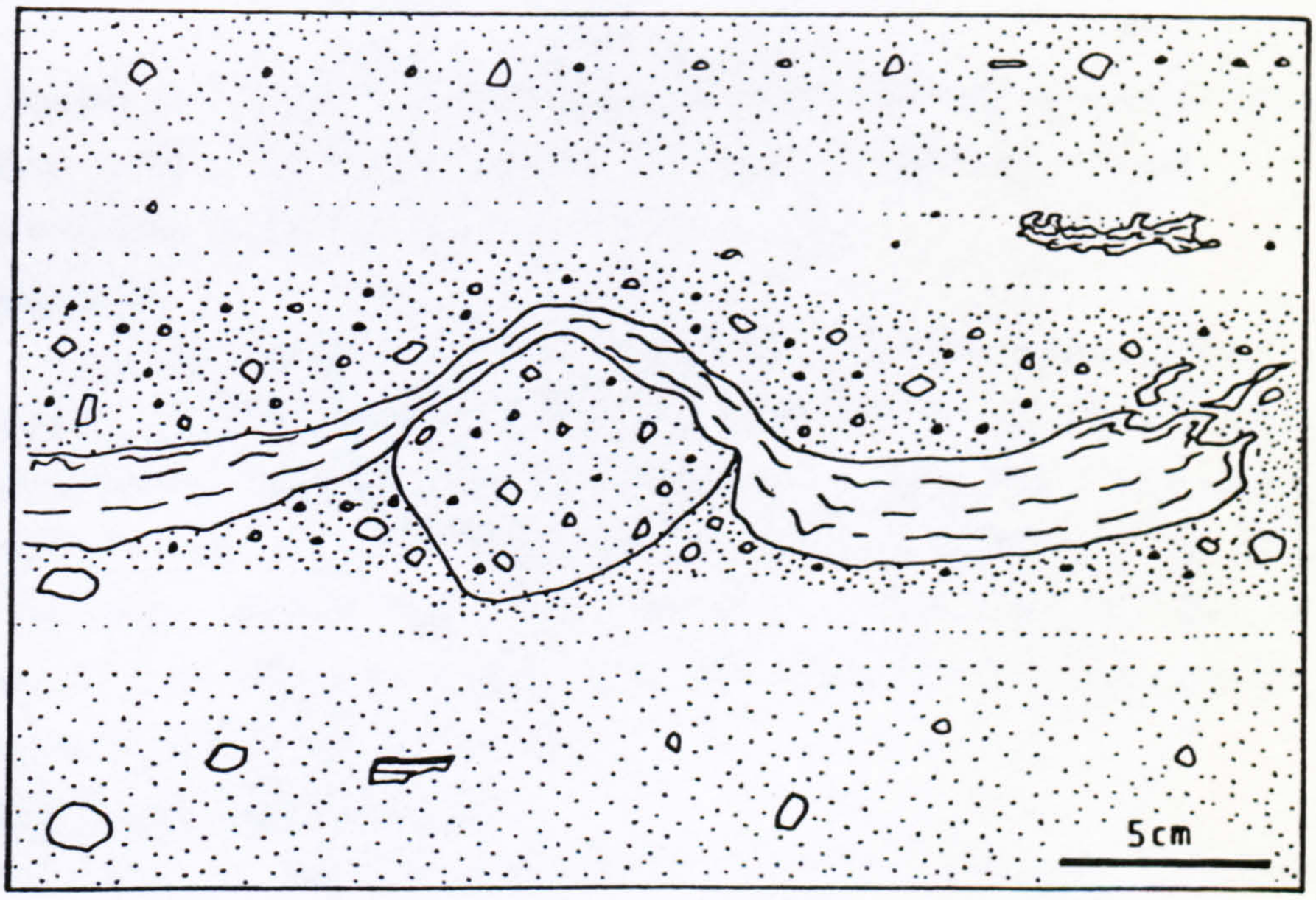

Fig. 6.22 Elongate mudstone clast which is deformed over a tuff block which protruded from the underlying bed. Western bedded tuffs in the St. Monance diatreme.

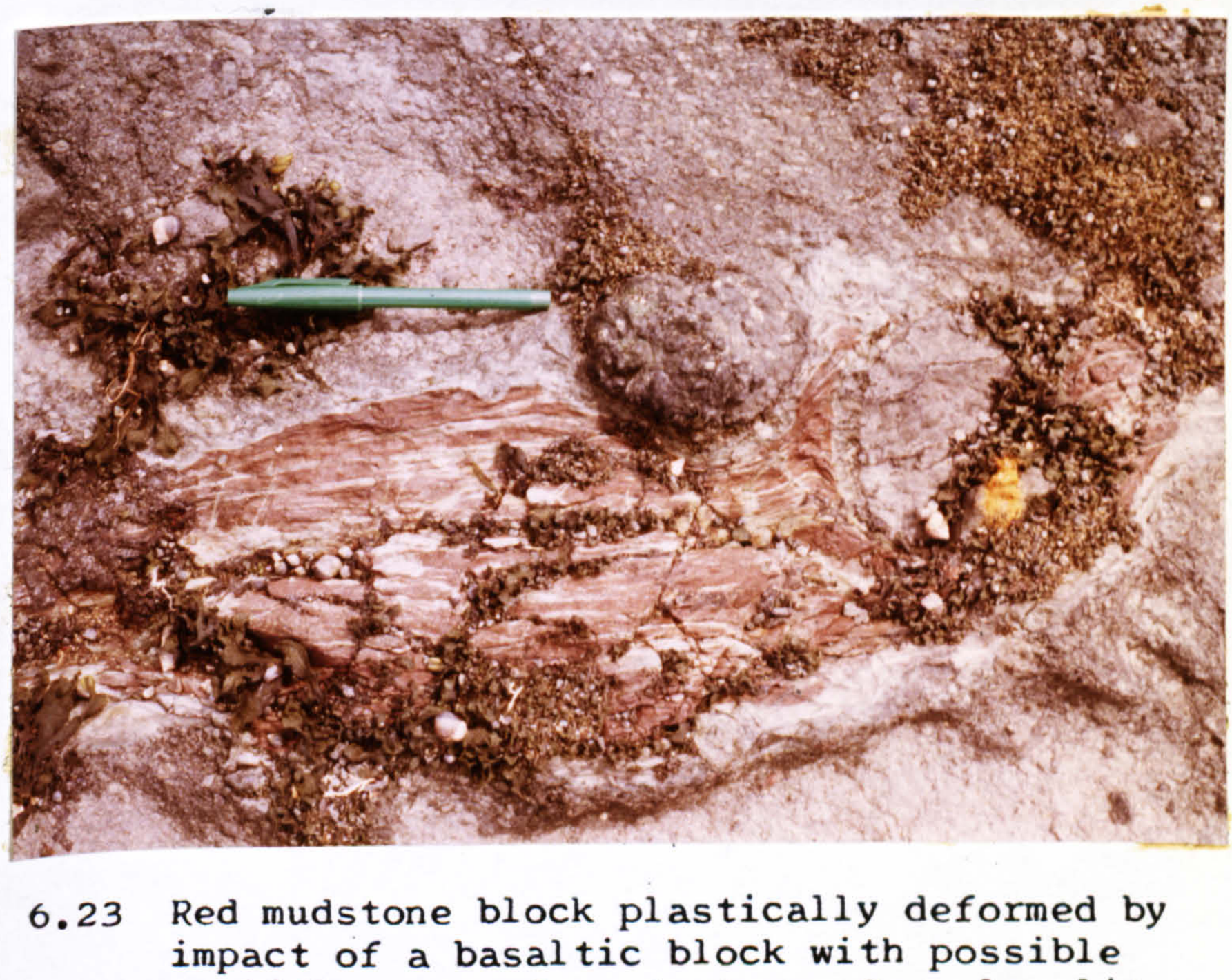

Fig. 6.23 Red mudstone block plastically deformed by impact of a basaltic block with possible cauliflower surface texture. Same locality as Fig. 6.22. Pen measures 14cm.

the mass movement of newly-deposited tuffs, whereas older bedded tuffs were better consolidated and survived oversteepening.

Structure

Various bedded areas occur in the diatreme and, although now bounded by faults, the tuffs in these areas appear to be bedded centroclinally to the mass of intrusive basalt in the S. The diatreme is cut by many dykes, trending N-S or E-W, which emanate from the large plug to the S. The dykes follow faults which cut the tuffs and bound large rotated bedded tuff rafts.

Summary and conclusions

1. Bedding in the younger tuffs in the diatreme has been largely obscured by debris flow reworking. Older, more consolidated tuffs were affected by faulting and folding. The present attitude of the bedded tuffs suggests collapse about a centre now intruded by basalt plugs and dykes.
2. Large amounts of red mudstone clasts were erupted along with the juvenile volcanic ejecta. Less consolidated clasts were deformed by loading on compaction of the tuffs, or by impact processes at the time of fallout. Larger, angular blocks were more consolidated and behaved in a brittle manner on eruption.

6.2.5 Kinkell Ness diatreme

This diatreme cuts Calciferous Sandstone Measures sediments on the coast SE of St. Andrews (Fig. 6.24). The diatreme margins are sharp, and are generally defined by tuffisitic breccia, and in the SE a fault separates tuffs, basanite and tuffisitic breccia from the country rocks. The margin is irregular and cuts across the strike of the country rocks, although their bedding traces are deflected by it in the SE. Within the diatreme the bedded tuffs dip centroclinally towards a centre now concealed beneath drift at HWM.

Bedded tuffs

An 80m thick, continuous sequence of W-dipping tuffs is exposed in the S of the diatreme (Fig. 6.25). The deposits comprise interbedded ash and lapilli tuffs with

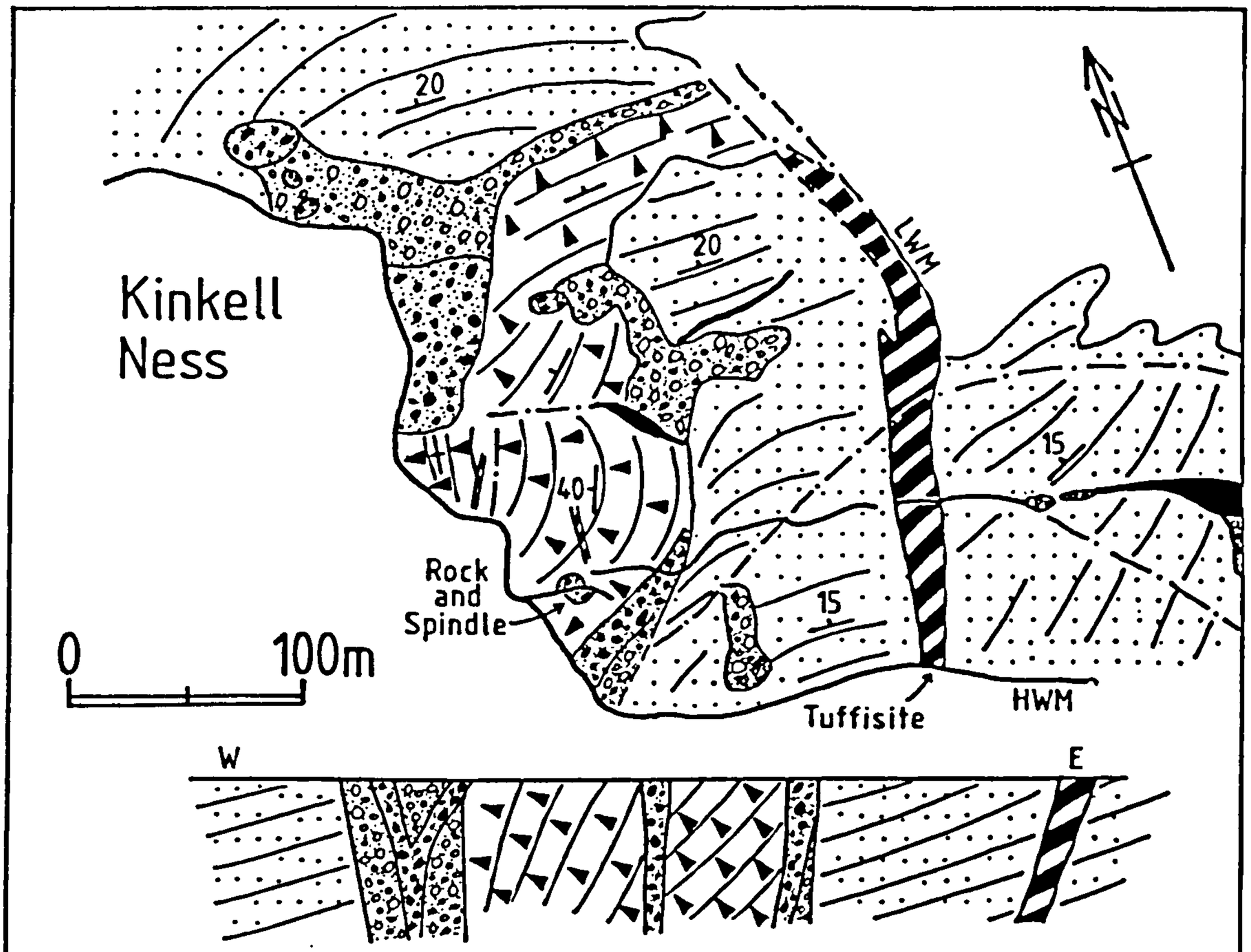

Fig.6.24

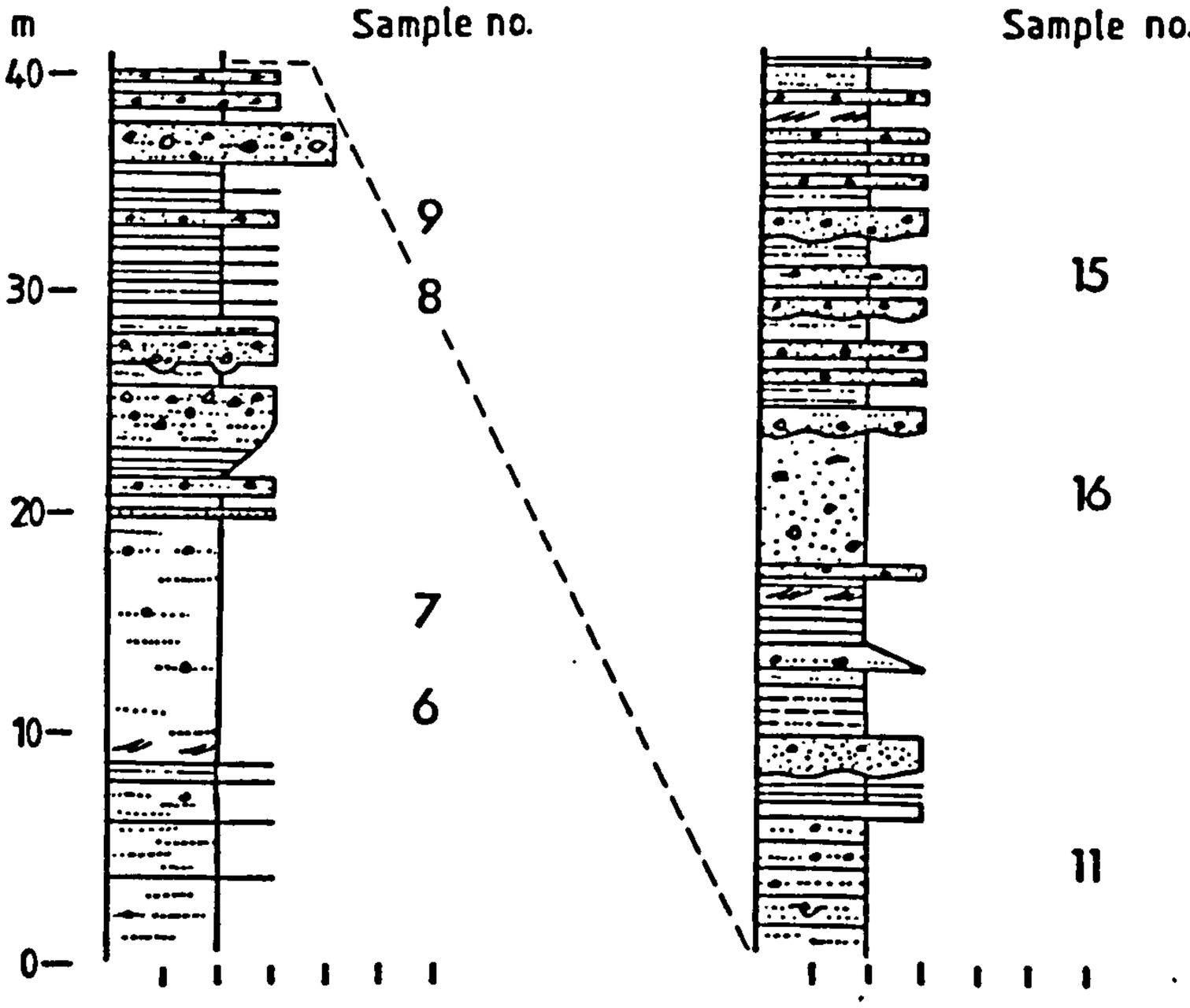

Fig.6.25

Fig. 6.24 Geological map and section of the Kinkell Ness diatreme.

Fig. 6.25 Logs of the bedded tuffs in the southern part of the diatreme, showing sample locations.

occasional poorly-bedded blocky layers. Block sags occur throughout the tuffs and, together with the poor-to-moderate sorting, rapid alterations in grain size between beds and rapid lateral thickness variations indicate their largely proximal airfall origin. Some of the finer tuffs contain low-angle cross-bedding which is thought to be of surge origin.

The cross-bedding (Fig. 6.26) is trough-shaped or sometimes sigmoidal and individual laminae dip at $<10^{\circ}$. Some examples of climbing cross-lamination occur but little can be said about the direction of climb relative to current direction. This is because the current direction cannot be calculated, due to the lack of suitable 3-D exposures. In some places small dunes are preserved, probably because of their rapid deposition and burial beneath overlying surge or airfall tuffs. Cross-bedded tuffs are often overlain by poorly-bedded, poorly-sorted lapilli tuffs. These overlying coarse tuffs, like their equivalents in other diatreme surge deposits, infill the irregularities in the tops of the cross-bedded units.

Upwards in the bedded sequence the tuffs become coarser, with many blocky, poorly-bedded layers. Cross-bedded units also become more abundant upwards, and are interbedded with coarser, lapilli-rich beds up to 40cm thick. These beds are rich in pyroxenite xenoliths which are elsewhere only rarely found. Perhaps the magma pulse which carried these xenoliths was more gas-charged, and formed more surge blasts on interacting with water near the surface than other pulses which erupted mainly airfall tuffs.

The tuffs exhibit many penecontemporaneous deformation structures, indicating their moist, plastic nature on deposition. Examples include load structures, flame structures, gravity slump structures and rare contorted bedding. Towards HWM the tuffs are cut by tuffisite dykes which are very sediment-rich in places. One dyke contains lens-shaped pods of gritty sandstone which are bedded parallel to the dyke margins. The dyke also contains elongate, angular bedded blocks of sandstone which are cut

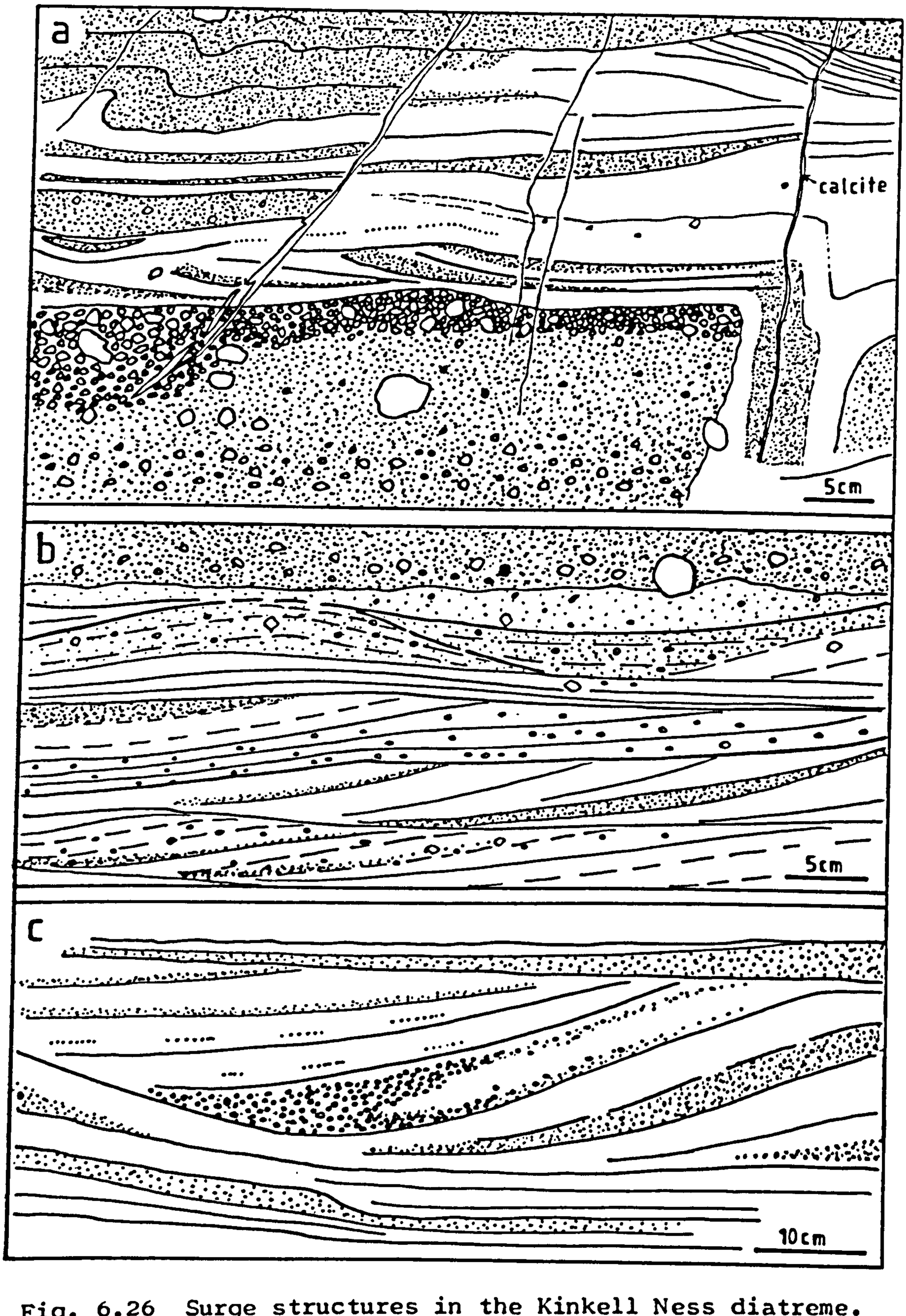

Fig. 6.26 Surge structures in the Kinkell Ness diatreme.
a) Cross-bedded tuffs containing convolute bedding and cut by numerous calcite-filled faults.
b) Low-angle trough cross-beds, showing many erosive partings between sets.
c) Probable surge foreset beds showing coarsening and thickening of lapilli horizons towards the base of the troughs. Flow direction from right to left.

by grey tuffisite. The blocks are partly incorporated into the tuffisite and probably represent country rock fragments emplaced along faults which also served as pathways for gas-streaming. Other tuffisite intrusions contain bedded tuff blocks derived from earlier, collapsed tuffs in the diatreme.

The diatreme contains many crinoidal and some coral-bearing limestone clasts which Forsyth et al. (1977) indicate were derived from Carboniferous strata at least 600m above those which the diatreme is now seen to cut. Collapse of at least this amount must therefore have occurred to bring these blocks to their present position. The diatreme is famous for containing the Rock and Spindle, a stack consisting of intrusive and brecciated basanite. Many other intrusions cut the diatreme tuffs as well as the surrounding country rocks (Fig. 6.24). A linear tuffisite intrusion cuts the sediments E of the diatreme, and is approximately parallel to the diatreme margin. It was probably emplaced along a concentric, outer ring fracture, similar to marginal fractures described by Francis (1962) from Dunbar which were formed during the initial "drilling" of the diatreme.

Summary and conclusions

1. The Kinkell Ness diatreme contains interbedded airfall and surge tuffs, the proportion of surge tuffs increasing upwards along with an increase in the number of blocky units. Surge deposits are associated with coarse units containing pyroxenite xenoliths, suggesting that magma pulses had different physical properties at this time.
2. Collapse by at least 600m caused the centroclinal attitude of the bedded tuffs, and their internal deformation by faulting. Syndepositional deformation of the water-rich tuffs previously affected the tuffs on a small scale. Collapse was accompanied by intrusion of magma, some so highly gas-charged that it comminuted and incorporated fragments of the country rock sediments and older, collapsed, bedded tuffs. Intrusion of tuffisite also occurred along an outer ring fracture probably initiated during the formation of the diatreme.

6.3. Other Diatremes

Many of the other diatremes in East Fife contain features which are relevant to the present discussion. More complete descriptions of the general features are given in the relevant Geological Survey Memoir (Forsyth et al., 1977).

6.3.1 Coalyard Hill diatreme

This diatreme consists of an outer zone composed of sediment-rich tuffs which is cut by an inner zone composed of green basaltic tuffs (Fig. 6.27). The outer diatreme contains many rafts of sandstone, together with sediment-rich tuffs which are cut by numerous tuffisite dykes and breccia. The inner diatreme contains bedded and structureless basaltic tuffs, cut by basaltic dykes and plugs, one of which is locally sill-like. The basaltic intrusions are often surrounded by basaltic breccia, due to break-up on intrusion into poorly-consolidated, perhaps moist tuffs. The bedded tuffs are of airfall origin and generally occur within rafts up to 8m across.

At HWM, poorly-bedded and structureless tuffs are cut by low-angle planes, some of which consist of a 2-5cm thick band of sheared fine-grained tuff. Whether movement occurred whilst the tuffs were poorly-consolidated by soft sediment sliding, or after consolidation by a low-angle fault is often uncertain. The sense of displacement seen on some of the planes and the occasional break-down of bedding above the toe of some curved planes suggest they are mainly slump features.

The outer diatreme is elongated NE-SW and its southeastern margin is defined by the Ardross Fault (Fig. 6.27). The inner diatreme is approximately circular and contains basaltic tuffs which have subsided from their original depositional level. As Forsyth et al. (1977) point out, the Coalyard Hill diatreme began as fissure-controlled eruptions which changed to a single-centre volcano with time. The initial activity was essentially maar-like and formed sediment-derived tuffs by gas-streaming whereas later a tuff-ring formed within this as the input of juvenile magma increased. In this respect the volcano may

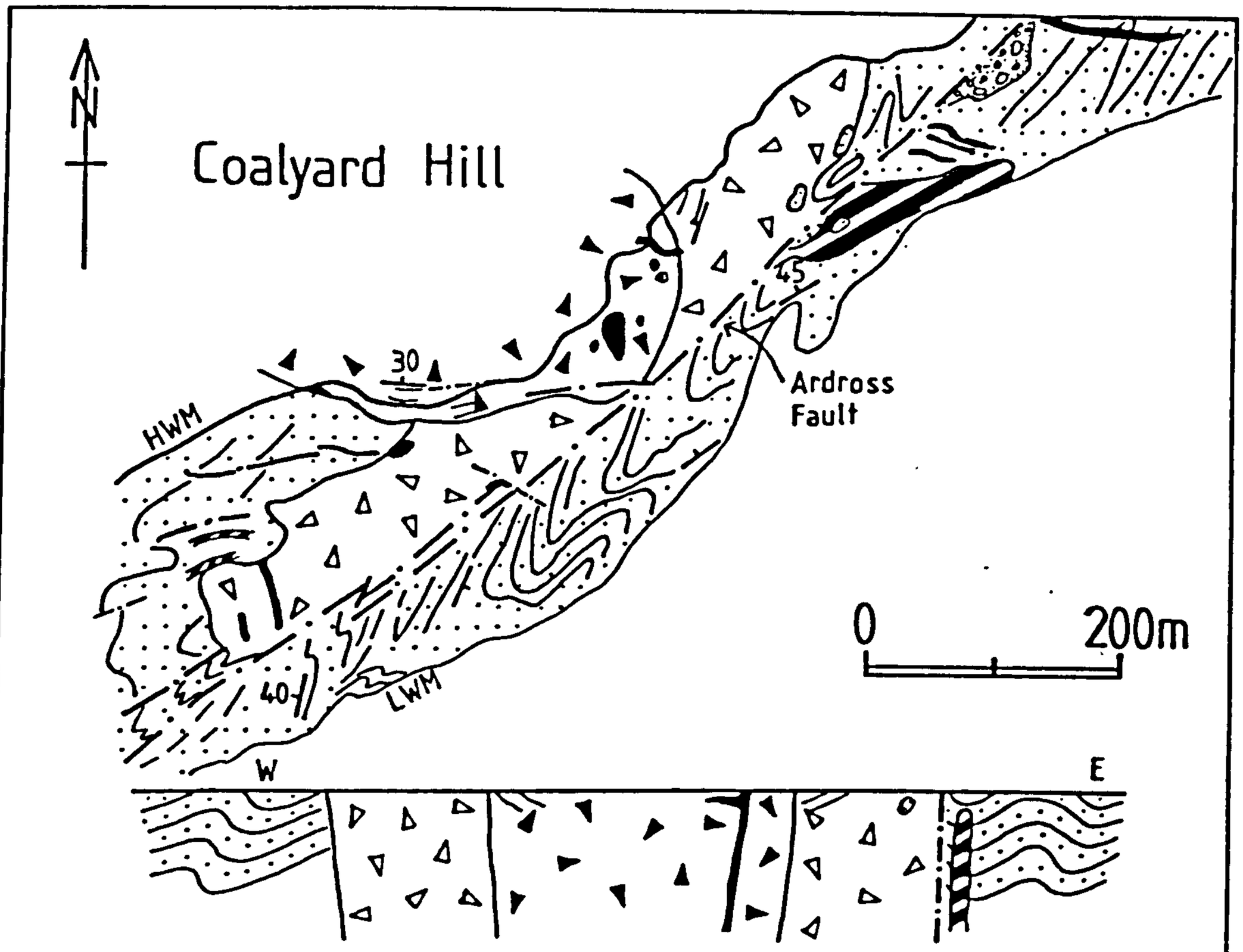

Fig.6.27

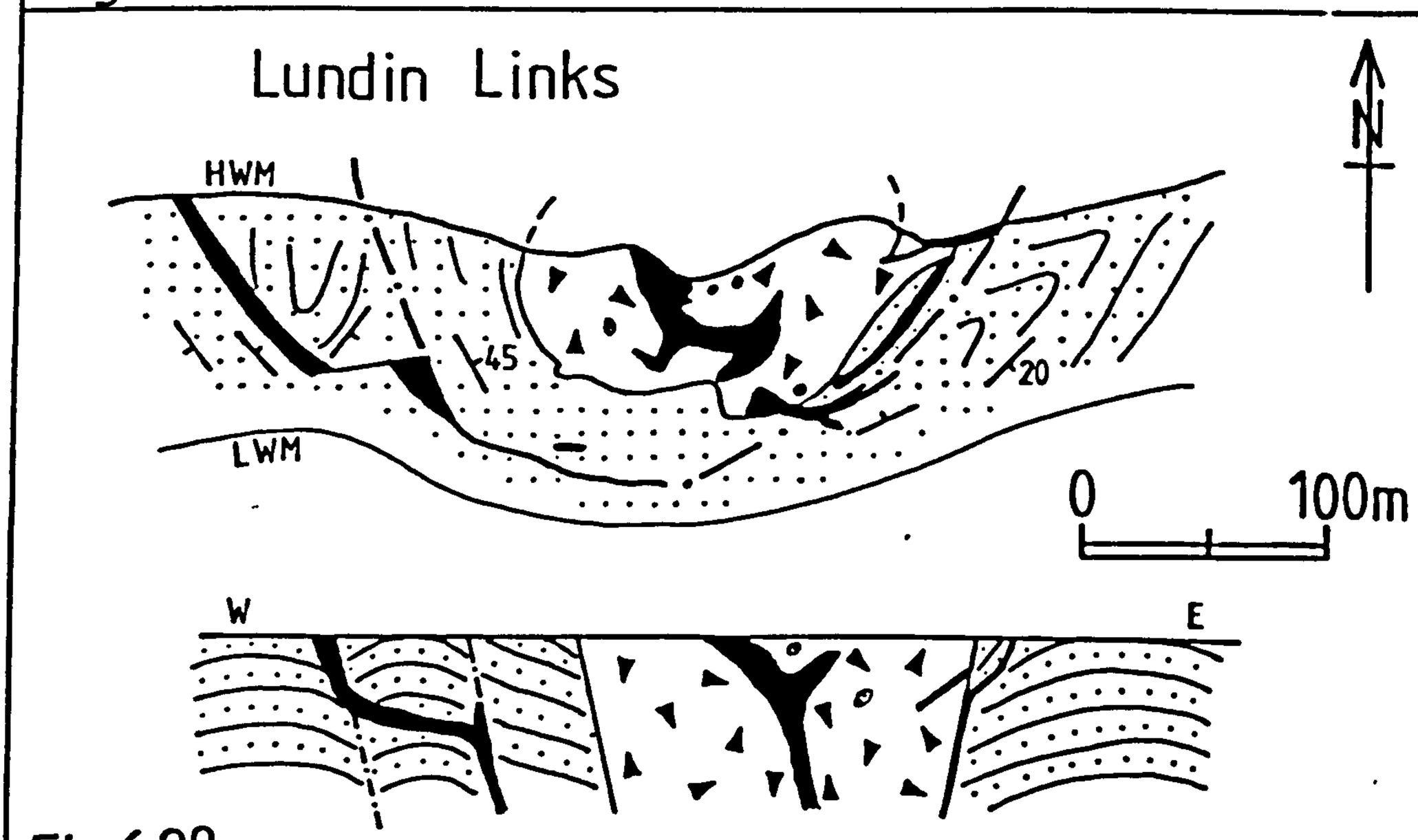

Fig.6.28

Fig. 6.27 Geological map and section of the Coalyard Hill diatreme. Note outer sediment-rich tuff and inner basaltic tuff.

Fig. 6.28 Geological map and section of the Lundin Links diatreme. Note outer ring fracture partly occupied by basalt dykes.

have resembled Surtsey in some ways, since the latter began as a fissure eruption and reverted to a single- centred tuff-ring with time. The Ardross Fault thus formed a major tectonic feature which influenced the volcanism (Francis & Hopgood, 1970).

6.3.2 Lundin Links diatreme

This small diatreme (Fig. 6.28) is of interest because it probably represents a structure which had little surface expression, or a very deep level in one which did source a surface volcano. It contains unbedded basaltic tuffs which are cut by irregular basaltic intrusions. The individual lapilli are often very angular or ragged and are well-mixed with their ash matrix. The completeness of this mixing suggests they were emplaced by turbulent flow, perhaps by gas-streaming.

Country rock blocks up to 10m across occur within the tuffs, but only become abundant at the diatreme margins, where sandstone, coal and shale fragments are common. Outside the eastern margin the country rock sediments are deformed and were intruded by tuffisite whilst poorly consolidated, resulting in soft-sediment folding and slumping. Within the diatreme the marginal tuffs are locally flow-banded around large clasts, and have been reddened by groundwater exchange with the red country rock sediments.

The lack of any blocks of subaerially-deposited bedded tuff, the small size of the diatreme and the abundance of basalt suggest that the present erosion level is some considerable distance below the original eruption surface, or that the diatreme is a well-developed crypto-volcanic structure.

6.3.3 Viewforth diatreme

This diatreme is significant because it contains presumed crater lake post-volcanic tuffaceous sediments and may have sourced reworked tuffs associated with the Passage Group sediments to the E. The tuffites overlie bedded tuffs in the centre of the diatreme (Fig. 6.29)

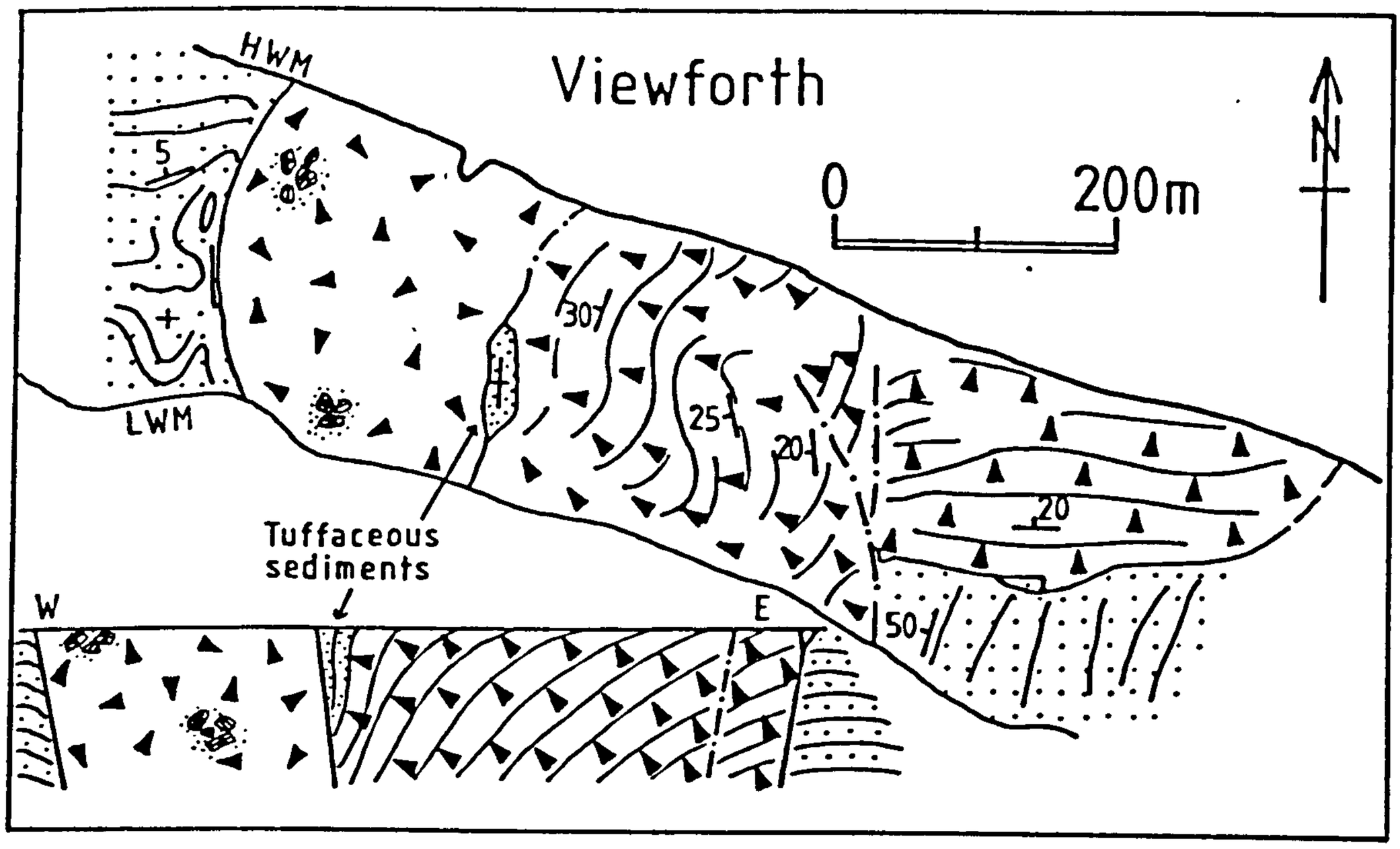

Fig. 6.29 Geological map and section of the Viewforth diatreme.

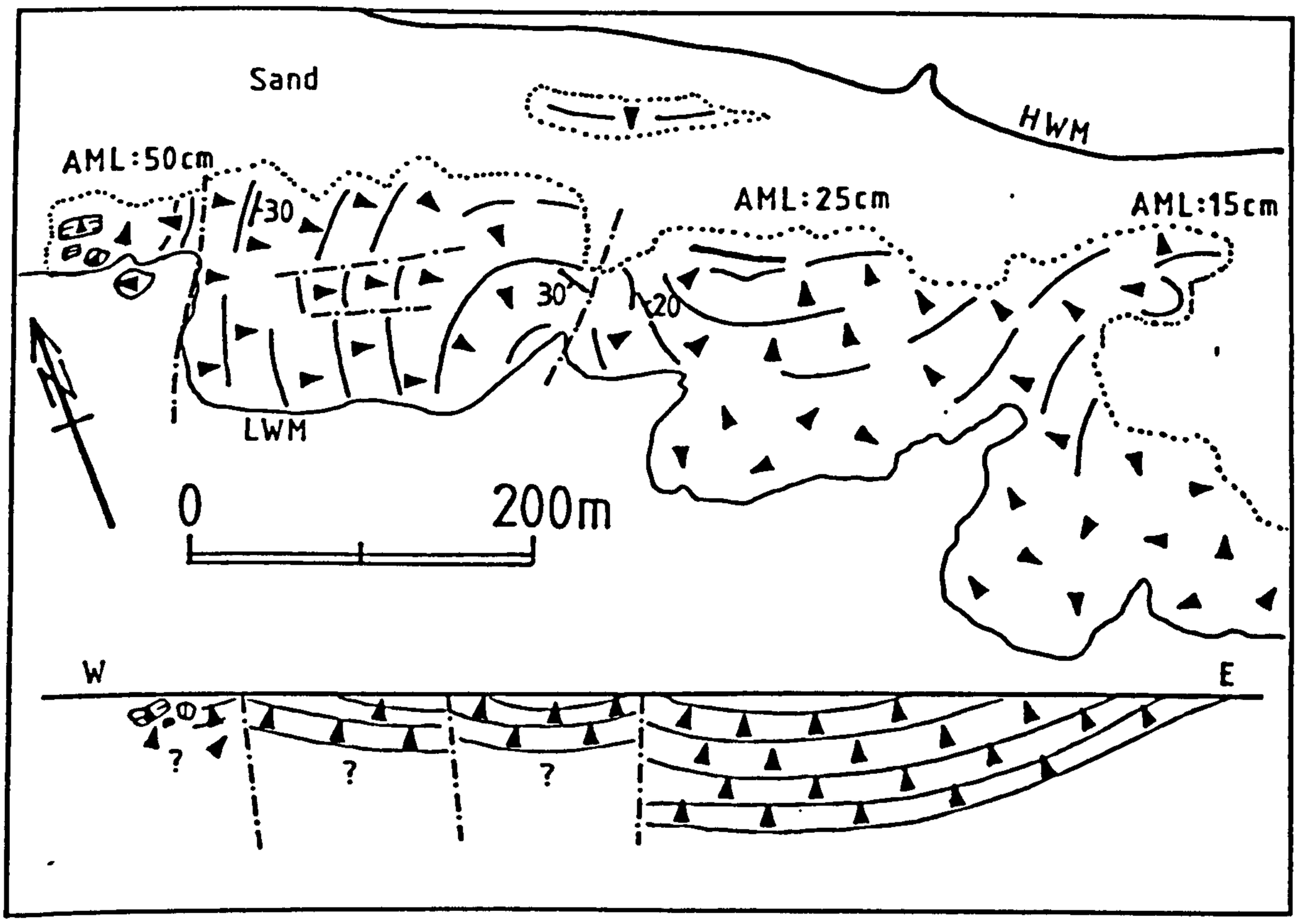

Fig. 6.30 Geological map and section of the country rock tuffs 500m E of the Viewforth diatreme. Note decrease in lithic size (AML) to the E.

and comprise tuffaceous siltstones and marls with a thin coal. The sediments contain miospores which indicate an age of early Westphalian (Forsyth et al., 1977). Since the country rocks outside the diatreme belong to the Passage Group, the deposition of the tuffaceous sediments is assumed to have occurred before a final phase of subsidence into the diatreme.

A large area of tuffs is found 250m to the E of the diatreme (Fig. 6.30). The deposits consist of interbedded lapilli and ash tuffs with many block-rich units. Although faulted and folded, a continuous sequence at least 75m thick is exposed. Towards the apparent top of the sequence in the E the tuffs become fine-grained and very well laminated. The excellent sorting of the tuffs indicates they have been at least partially reworked. Thin, coarse, blocky units which occur in the sequence are interpreted as debris flows. Other features which indicate reworking are small washout channels filled with tuffaceous sandstone and small-scale cross-bedding, thought to be of fluvial origin.

The sequence is thought to represent the distal deposits of a phreatomagmatic volcano whose younger products have been reworked. Because of faulting these tuffs are not seen in conformable contact with the country rock sediments and may have been sourced from the Viewforth diatreme. The fact that the tuffs fine away from the diatreme might support this suggestion. The faults which separate the tuffs from the Passage Group sediments do not resemble diatreme margins, suggesting that the tuffs do not lie within a large previously unrecognised diatreme structure.

6.3.4 Kincraig diatreme

This diatreme is the largest coastally-exposed example in East Fife and is internally very complex (Fig. 6.31). Structurally the diatreme consists of bedded tuffs which dip towards two centres, now marked by basalt and basaltic breccia intrusions. The bedded tuffs consist of mixed airfall and surge deposits, which contain blocks of basalt up to 1·5m across and numerous red mudstone clasts.

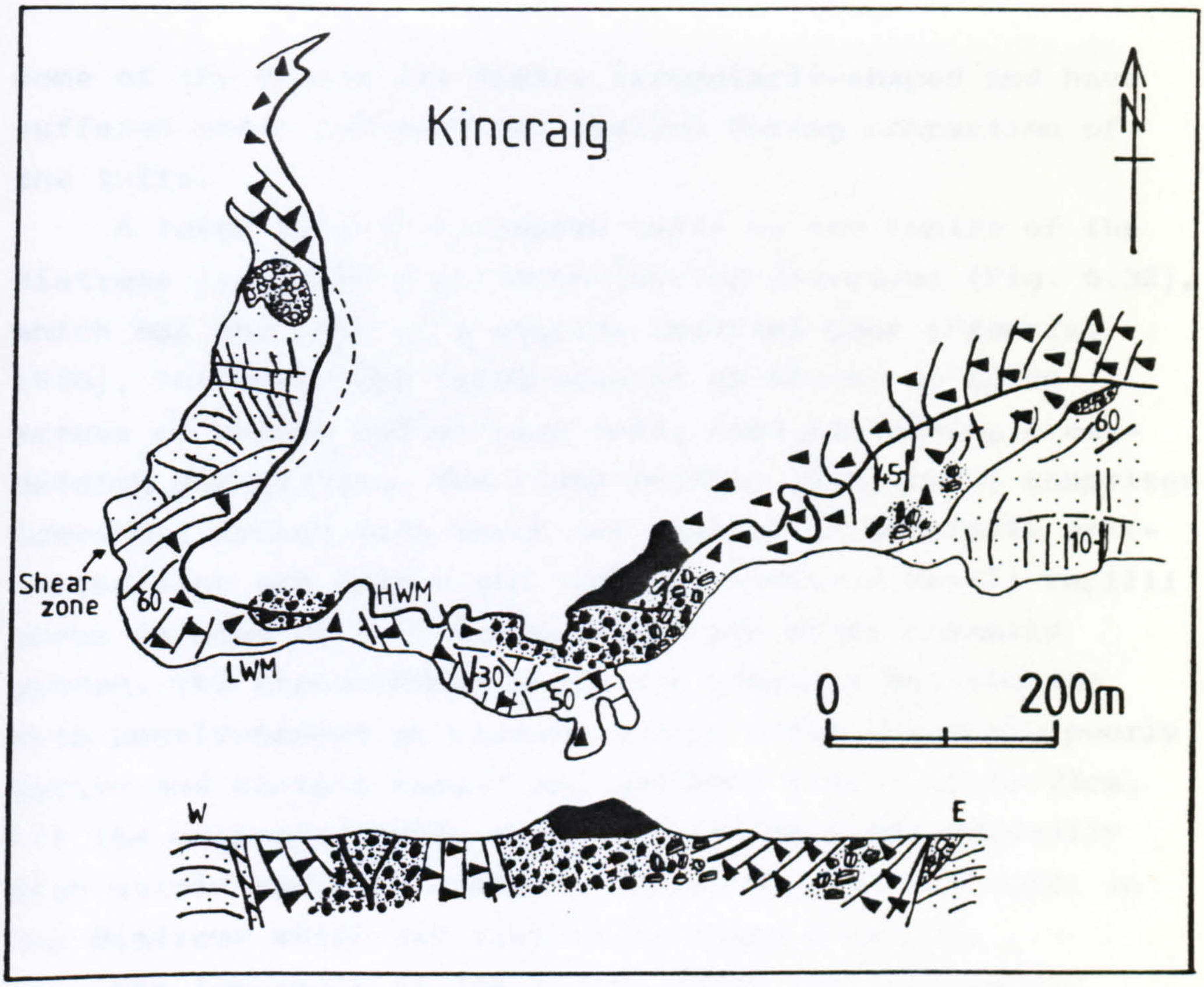

Fig. 6.31 Map and section of the Kincraig diatreme.

Fig. 6.32 Columnar-jointed basaltic intrusion at the centre of the Kincraig diatreme. Jointing indicates that the plug is shaped like an inverted cone.

Some of the clasts are highly irregularly-shaped and have suffered soft- sediment deformation during compaction of the tuffs.

A large area of collapsed tuffs in the centre of the diatreme is cut by a columnar-jointed intrusion (Fig. 6.32), which has the form of a shallow inverted cone (Francis, 1970). The collapsed tuffs consist of blocks up to 2m across of bedded and massive tuff, some containing cross-bedding and grading. The cross-bedding (Fig. 6.33) comprises low-angle trough sets which are made up of generally well-sorted fine and coarse ash laminae. Isolated basalt lapilli occur in some of the layers, which are often normally graded. The cross-bedded units are commonly interbedded with poorly-bedded or massive coarse tuffs which are poorly sorted and contain basalt and sediment clasts up to 25cm. All the collapsed tuffs contain a variable but generally high matrix sediment content, unlike most of the tuffs in the diatreme which are rich in juvenile material.

The low-angle of the trough sets, the interbedded massive tuffs and the occurrence of occasionally poorly-sorted cross-beds suggest that they are of surge origin. The trough cross-beds perhaps represent the deposits of low-power surges which deposited only fine material. The massive beds may represent coarse airfall tuffs partly reworked by debris flows. Intrusion of the large plug during collapse of the tuffs subsequently broke up the bedding.

The occurrence of two apparent centres in the diatreme may be due to the presence of vents of different ages in the same, large diatreme. A modern analogue of this situation is Surtsey, which developed two large vents with time. Later collapse of tuffs into the centres and intrusion by magma would probably lead to a Kincraig-like structure being formed. En masse subsidence of the entire diatreme material would explain the shear zone at the western margin and the disturbance of the surrounding country rocks.

A block of the tuffaceous siltstone occurs in tuffisitic breccia near the eastern margin of the diatreme, and contains structures indicating deposition by turbidity

Fig. 6.33 a) Surge cross-beds in the collapsed bedded tuffs at the centre of the Kincraig diatreme. Coin measures 2·5cm.

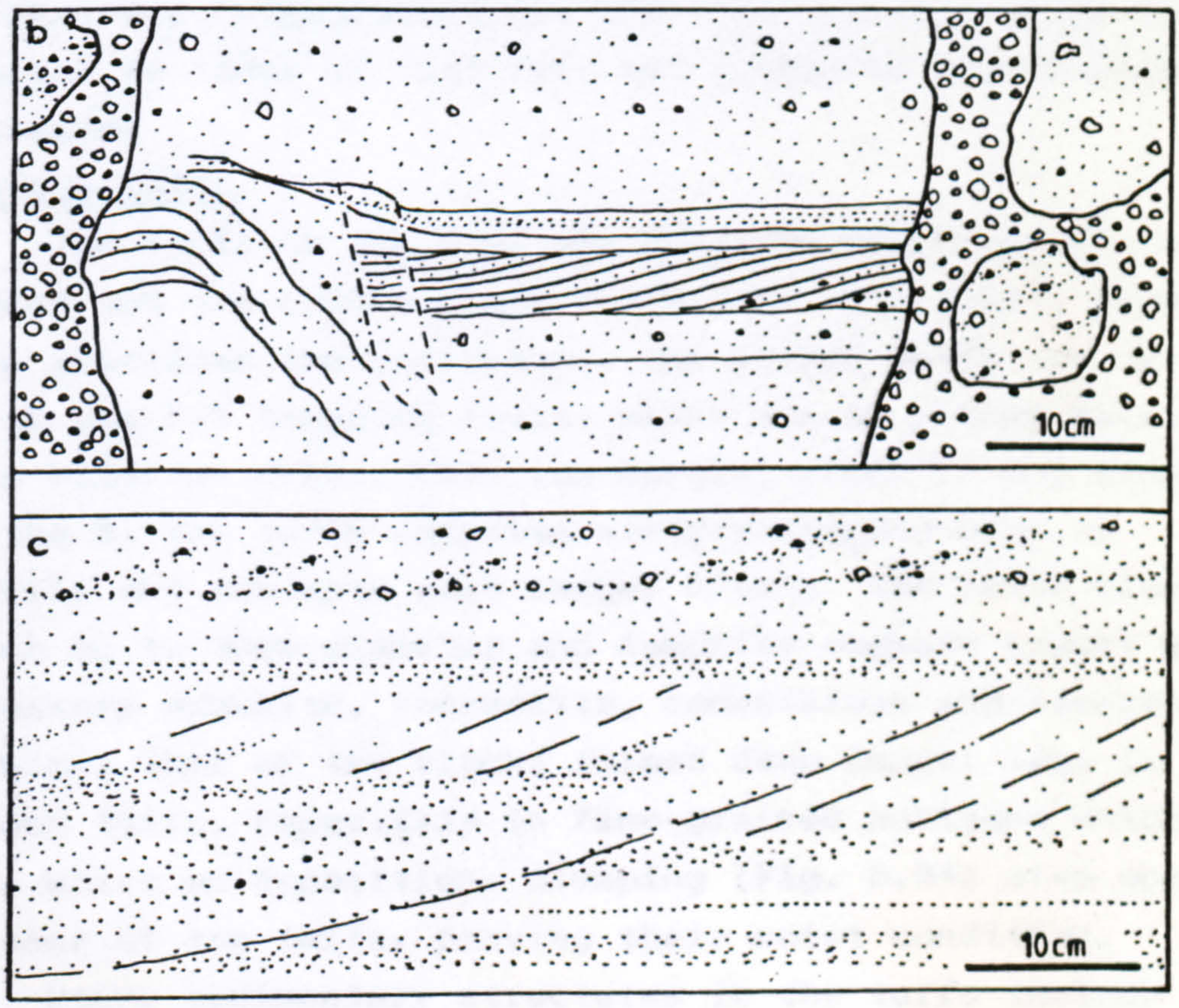

Fig. 6.33 b) Block in Kincraig collapsed bedded tuffs, containing fine-scale cross-bedding which is partly slumped and faulted.

c) Trough cross-bedding in collapsed block at same locality as b) above. Note thickening and coarsening of tuffs towards the base of the troughs.

currents. Such structures include well-laminated, graded horizons with small-scale cross-bedding and load structures. The origin of the deposit is problematic though it may represent early volcanic products reworked in marginal lakes or lagoons.

6.4. Heads of Ayr Diatreme

This diatreme occurs on the SW coast of Scotland (Fig. 6.34) but has many comparable features to those in East Fife and merits further description. The diatreme was comprehensively studied by Whyte (1964) and his descriptions and maps provided a basis for the present study.

The diatreme cuts Lower Carboniferous Cementstone Group sediments SW of Ayr and contains green tuffs which are well-bedded in the W and massive towards the E. The central part of the exposed diatreme is occupied by a large area of country rock sediments which is cut by basaltic intrusions. Petrographically (Section 6.5) the tuffs are similar to those of East Fife and formed by phreatomagmatic processes.

Western tuffs

The tuffs in the W of the diatreme are generally well bedded and are folded along NE-SW axes into gently plunging open synclines and anticlines. The folded tuffs are cut by NW-SE and E-W trending faults which are in places marked by thin basaltic dykes. Near the margin, which is not exposed in the W, the tuffs comprise steeply-dipping beds of lapilli and ash with rare larger clasts. The large clasts reach up to 30cm diameter and comprise cognate basalt and accessory andesite, lherzolite, cementstone and limestone lithics. Some of the blocks formed deep impact sags in the bedded tuffs, especially in fine-grained horizons which were moist on deposition. Slumping (Fig. 6.35) also occurs in some of the tuffs, proving their moist condition.

Other sedimentary structures in the tuffs include grading and cross-bedding. Both normal, and more commonly, reverse-grading occurs, especially in the finer tuffs where coarse material comes in gradually. The cross-bedding (Fig. 6.36) is small-scale and consists of low-angle planar and

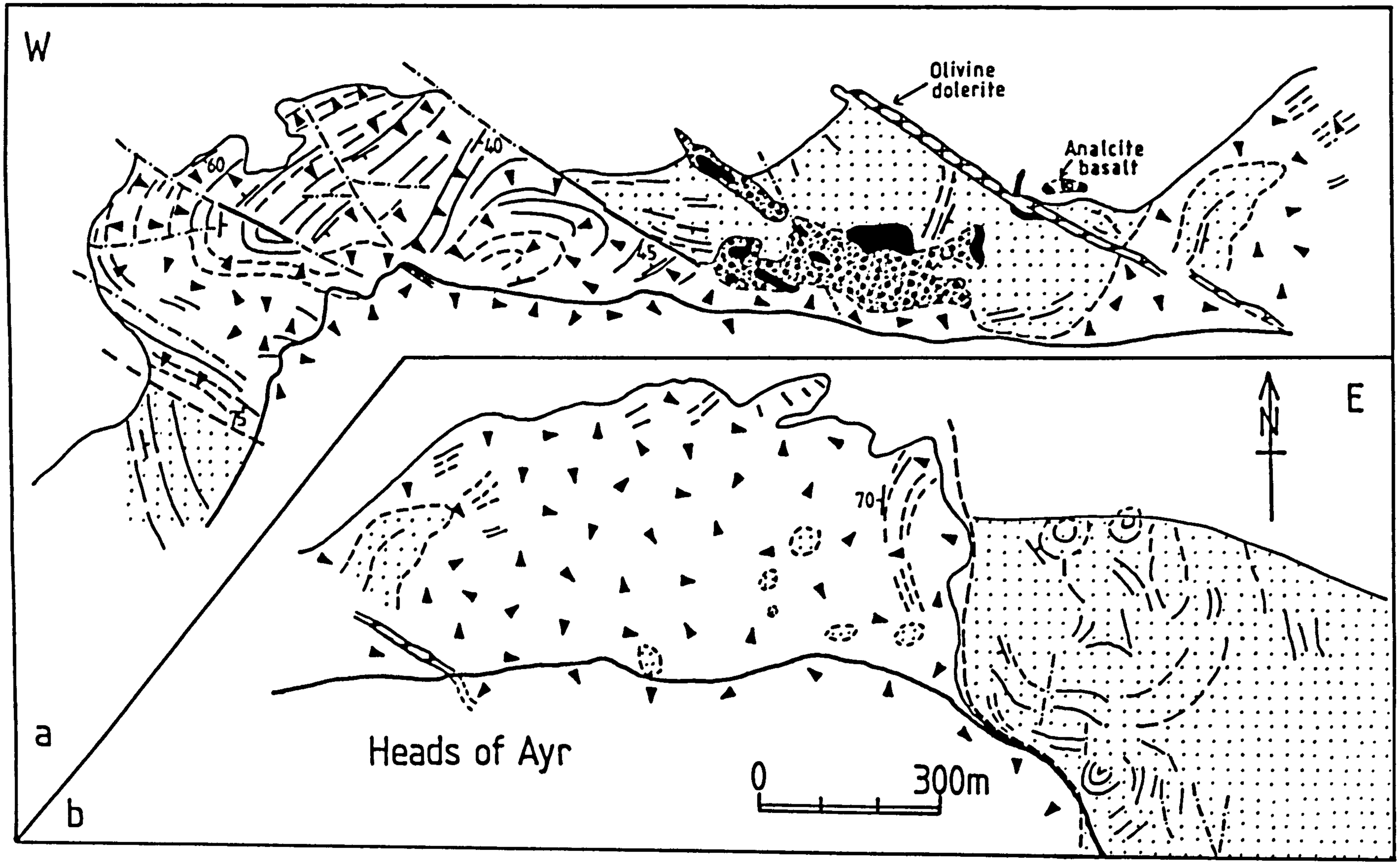

Fig. 6.34 Geological map and section of the Heads of Ayr diatreme, after Whyte (1964). Map b) is the eastern continuation of map a).

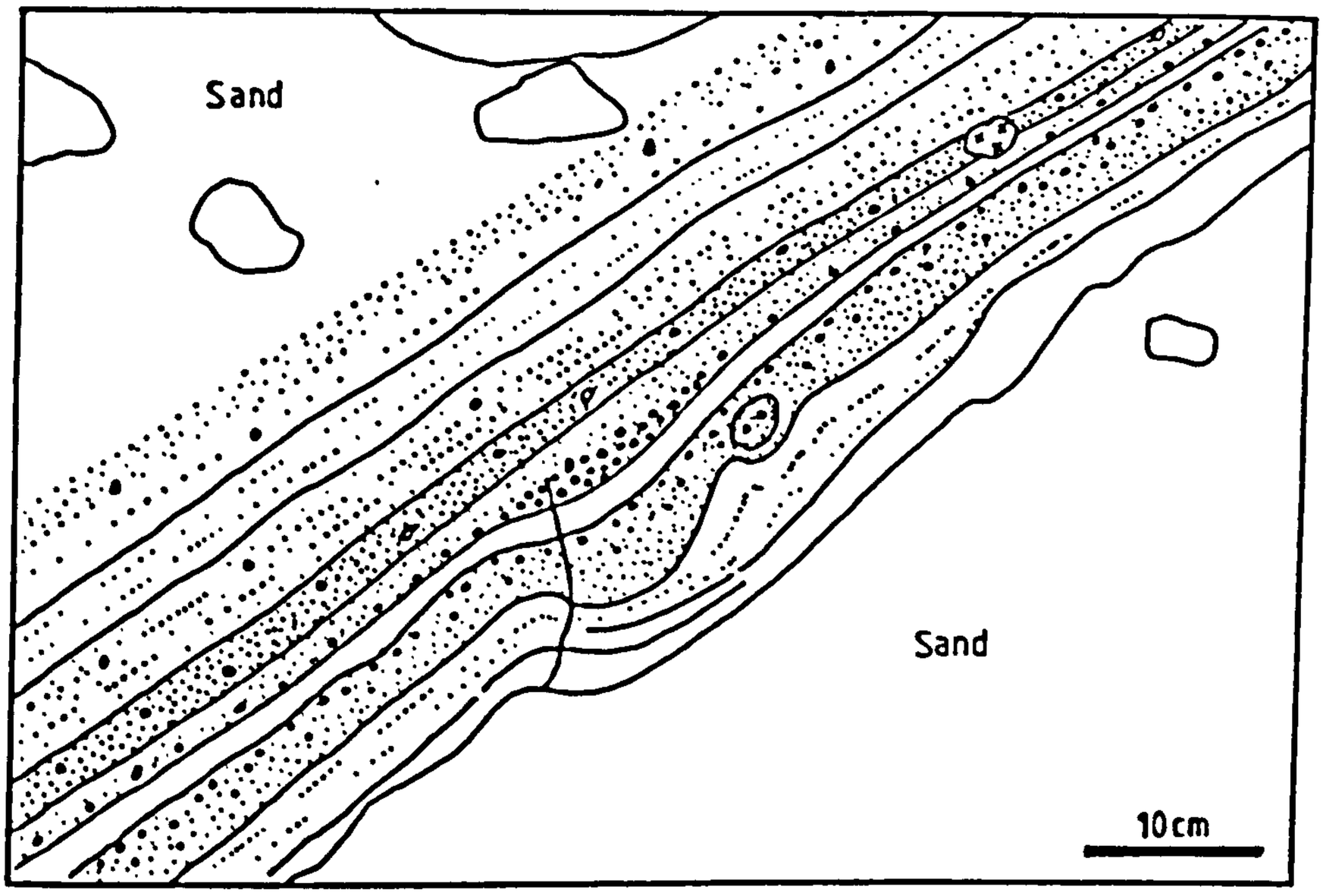

Fig. 6.35 Block impact sag and slumping in the western tuffs of the Heads of Ayr diatreme.

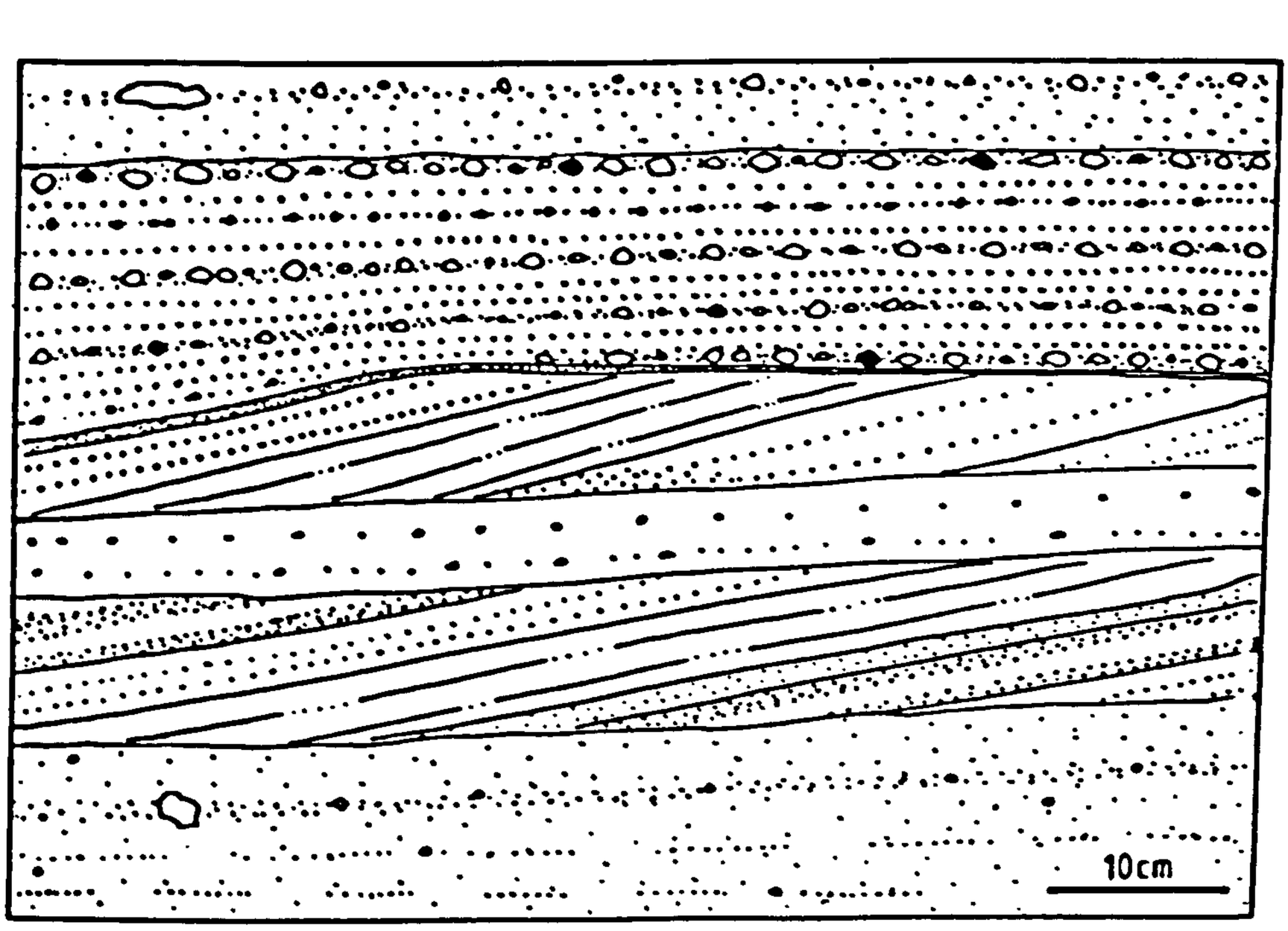

Fig. 6.36 Low-angle planar cross-sets in the western Ayr diatreme tuffs. These beds may be water-reworked or of surge origin.

trough cross-sets. The individual cross-beds are fine-grained, well-sorted and occur in sets of up to 15cm height. Cross-bedded units reach maximum thicknesses of 20cm and are commonly interbedded with well-sorted, graded tuffs. The small scale of the structures, their association with well-sorted fine tuffs and the lack of distinctive surge features suggest they are water-reworked tuffs.

The tuffs near the western margin contain large amounts of carbonate in their pore spaces which Whyte (1964) thought to be primary. This would suggest that much of the western tuffs accumulated in lakes from which carbonates were being precipitated. The lakes were probably only shallow, allowing periodic emergence of the tuffs and subsequent subaerial deposition. Such lakes were common in this area during Cementstone Group times, with the country rock sediments containing abundant evidence of lacustrine sedimentation, in the form of mud-cracks, rare evaporites and non-marine fossils (Belt et al., 1967).

The features of the tuffs in the W of the diatreme indicate that they were deposited initially in a shallow subaqueous environment with wave-reworking, slumping and debris flows. As volcanic activity continued, rapid deposition of the tuffs infilled the lakes and later tuffs were laid down subaerially.

The oldest western diatreme tuffs are very similar to the Greenan Castle Ash (Whyte, 1964), which is an approximately 30m thick bedded tuff deposit interbedded with the country rocks at the top of the Cementstone Group, some 2km E of the diatreme. These country rock tuffs are well-bedded, often well-sorted fine tuffs which are locally cross-bedded or slumped. They contain large amounts of carbonate cement, which replaces much of their fine ash matrix. The tuffs are the distal, reworked deposits from the diatreme, the remainder having been removed by erosion.

Eastern tuffs

The eastern tuffs are composed of similar material to those in the W, but are largely unbedded and massive. The eastern margin is similar to those in the East Fife diatremes, and consists of a sharp fault separating

collapsed bedded tuffs from country rock sediments which dip into the margin at up to 50°. Some of the diatreme tuffs are flow-banded and contain a variety of sedimentary and igneous clasts. The eastern tuffs also contain many rafts of Cementstone Group sediments, which reach 100m in size. The rafts consist of broken-up blocks of sandstone, which are often contorted and cut into by tuffisite. One of the smaller rafts contains cementstone conglomerate which has been displaced upwards by 40-70m from its stratigraphic position at the base of the Ayrshire Cementstone Group outside the diatreme (Whyte, 1964).

Where present, bedded tuffs comprise poorly sorted lapilli and ash beds with rare block-rich horizons. Poor exposures obscure much of the detail, but bedding appears to break-down gradually into the surrounding massive tuffs as though deformation occurred whilst the tuffs were poorly consolidated. Near the eastern margin, bedded tuffs dip into the diatreme at steep angles and are cut by small joints and faults with little displacement which trend normal to the bedding.

Fig. 6.37 Carbonated ultrabasic block with juvenile basalt rim. See text for description. Penknife measures 8cm.

Both the eastern and western tuffs contain blocks of carbonated ultrabasic material and calcified wood fragments. The ultrabasic blocks are altered lherzolite, reach 35cm diameter and are often coated with an irregular rim of juvenile basalt (Fig. 6.37). This coating reaches a thickness of 3cm and consists of pale-green basalt with flow-aligned, concentric vesicles. Many smaller, angular lithic clasts are also coated by such rims, which in these cases tend to smooth out the irregularities in the clast shapes and form near-spherical lapilli. Such rims were accreted during the rise of the gas-charged magma, and resemble those described from the Hegau diatremes, SW Germany (Lorenz et al., 1970).

The Hegau lapilli are highly spherical and smooth-surfaced and reach maximum sizes of 12mm, with larger lapilli having less regular shapes. The Ayr lapilli and block rims are thought to have been shaped by surface tension and rotation whilst fluid, larger fragments having less regular rims due to less rapid rotation and impacts with other clasts. Such structures are present in Ayr, but not in other Scottish diatreme tuffs, perhaps because the viscosity and surface tension of the Heads of Ayr magma favoured their formation.

Calcified wood fragments are generally less than 5cm, but a large fragment occurs in the eastern tuffs at HWM. Whyte (1964) suggested that such material was derived from vegetation growing on the active volcano flanks but this is thought to be unlikely. Such fragments could have been derived from the poorly-consolidated country rocks which the diatreme intruded, or have been washed in by rivers or tides which reworked the flank tuffs. In the latter case the wood fragments would be included in the diatreme by collapse.

Central area

The central part of the diatreme is occupied by Cementstone Group shales and cementstones which are bounded by NW-trending dykes (Fig. 6.34). Both dykes obliquely cut the bedding in the sediments and probably mark fault-zones. The eastern, olivine dolerite dyke post-dates the diatreme

and has been assigned to the Tertiary by previous workers (Whyte, 1964).

The sediments are cut by numerous plugs of monchiquite basalt up to 40m across, which are irregular or elongated NW. All the plugs are surrounded by intrusive breccias which contain high proportions of poorly-baked sedimentary clasts, some of them showing evidence of partial-melting (Alexander, 1980). The breccias formed by break-up of the plugs on intrusion into consolidated sediments. Although the sediments in the central area are largely unexposed, they do not appear to be highly deformed. Exceptions to this occur around the intrusive breccias where the sediments dip inwards towards them, and at the margins of the central area where the sediments become broken-up and their bedding traces deflected into parallelism with the dykes.

Country rocks

The Cementstone Group sediments to the E of the diatreme are highly faulted and contorted (Fig. 6.34). Within 250m of the diatreme the country rock mudstones and sandstones are deformed into a number of circular basins, one of which is cut by a monchiquite breccia plug. The depressions are crypto-volcanic collapse structures similar to those seen in East Fife and East Lothian, where rising gas and magma streams intruded and domed the country rocks which then collapsed as the magma withdrew.

Diatreme formation

Whyte (1964) proposed that the Heads of Ayr volcano reached a height of 600-1000m, based on the outcrop extent of the eastern tuffs. The volcano is thought by the present author to have been a tuff-ring, based on field and petrographic evidence, and as such would have had a low, wide profile. This tuff-ring, by analogy with similar volcanoes, was formed above a diatreme into which tuffs and wall rocks periodically collapsed.

The western, well-bedded tuffs in the diatreme probably represent partly-reworked flank deposits. The eastern tuffs may represent collapsed crater tuffs, since they lack well-defined bedding and contain flow-banded tuffs. Collapse into the diatreme along ring faults, and

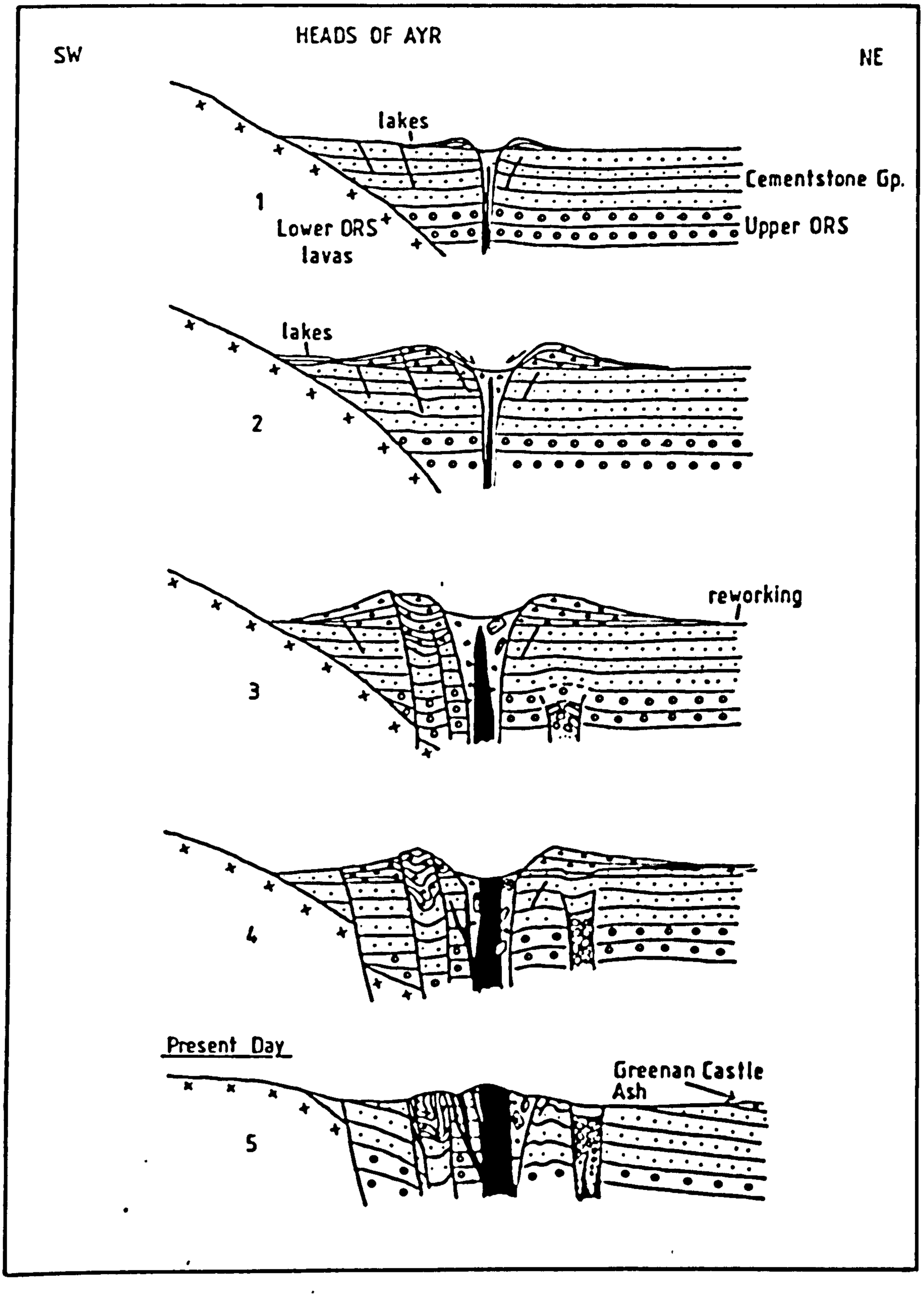

Fig. 6.38 Evolution of the Heads of Ayr volcano showing growth of tuff-ring, fault subsidence and erosion to present level. Note crypto-volcanic structures E of the main volcano.

movements on NW-SE faults controlled by regional stresses, resulted in the present, complex outcrop distribution (Fig. 6.38). The folding of the western tuffs appears to be purely the result of compression during subsidence.

The central area of Cementstone Group sediments probably pre-dates the volcanism and may represent a relatively stable block about which the tuffs subsided. The central area may itself have subsided, but to a lesser extent than the surrounding tuffs. The area was intruded by vesiculating monchiquitic basalt, which brecciated the sediments. A dyke of similar material cuts the western tuffs (Whyte, 1964) suggesting that the intrusions were emplaced at a late stage in the volcanism.

The eastern tuffs resemble well-mixed diatreme deposits described by Cloos (1941) in S. Germany, which contain subsided country rock rafts and moderately-sorted, often flow-banded tuffs. Slumping, gas-streaming processes and explosions destroyed much of the bedding in these subsided crater tuffs, which collapsed whilst many of them were probably poorly consolidated.

Summary and conclusions

1. The Heads of Ayr diatreme contains tuffs formed by phreatomagmatic eruptions, probably when magma contacted groundwater within late Cementsyone Group lacustrine / marginal marine deposits. A wide, low tuff-ring built up whose outer flanks were partly reworked by fluvial and lacustrine processes.
2. Subsidence occurred along ring faults and on faults initiated by regional stresses in the tectonically active Midland Valley. The western flank tuffs subsided slowly after compaction and were deformed by compression, whereas the eastern tuffs represent crater deposits which subsided and were broken-down by gas-streaming and other processes whilst poorly consolidated. The central sediments represent subsided material from the pre-eruption country rocks which was intruded by late-stage magma injections.

6.5. Petrography, Morphology and Alteration

Two of the East Fife diatremes, Elie Ness and Kinkell

Ness were selected for petrographic study and extensively sampled. Samples from many of the other diatremes were studied, and this confirmed their broad similarity to the above two examples which may be taken as representative. The Heads of Ayr diatreme tuffs differ in some respects from those of East Fife, and comparisons between them help to identify the factors responsible for these differences. Sample localities are marked on the geological maps of the diatremes or their position in bedded sequences is shown on the relevant logs.

6.5.1 Petrography

All the tuffs consist of varying proportions of juvenile, crystal and lithic fragments in a fine-grained matrix which is often partly or completely replaced. Minor amounts of primary carbonate and zeolite cement occur, but these are often indistinguishable from replacive, secondary cements.

a) Juvenile fragments

All the juvenile fragments consist of altered, often vesicular ash and lapilli up to 1·5cm diameter. The fragments are generally angular, with small-scale irregularities in their outlines due to breakage across vesicles or flowage of magma prior to quenching. In general the Elie Ness tuffs contain the most angular lapilli with the largely equant fragments containing planar or slightly curved boundaries cut by concave vesicle embayments (Fig. 6.39). The Kinkell Ness and Heads of Ayr lapilli are much more irregularly-shaped with some very ragged margins. All the diatreme tuffs, however, contain variable proportions of fragments with blocky through to fluidal shapes, the proportions varying even within one bed. No systematic variations in grain shape occur throughout any of the studied sequences of bedded tuffs.

The Elie Ness juvenile lapilli contain variable, though generally small numbers of vesicles which are usually spherical and reach a maximum of 0·5mm diameter. The fragments contain small microlites up to 0·03mm, which are probably plagioclase. These microlites are flow-aligned

around crystals and parallel to the rare examples of elongate vesicles. Many of the lapilli contain fragments of country rock quartz as well as altered crystals of clinopyroxene, biotite and olivine. Spots or clumps of iron ore, probably magnetite, occur throughout most lapilli, occasionally becoming so abundant that the lapilli resemble tachylite. Some of the more tachylitic fragments have hematite-stained rims, giving the host tuffs a dull red colouration. The Kinkell Ness juvenile fragments are mostly similar to the Elie Ness lapilli, except that they are generally more vesicular and contain fewer microlites.

The Heads of Ayr juvenile lapilli are on average more vesicular than their East Fife equivalents and contain many more plagioclase microlites, which are of oligoclase-andesine composition. The microlites are often aligned parallel to elongate vesicles which are in turn sometimes parallel to fragment elongation (Fig. 6.40). Other examples of flow include rounded lapilli with concentrically-aligned microlites, probably formed by spinning of magma droplets during cooling. Tachylitic and hematite-stained lapilli are locally abundant, some of these fragments having a thin marginal zone containing less iron oxide and fewer vesicles than their cores. Such a zone is due to chilling of the margins, whilst the cores cooled less rapidly and exsolved more magnetite and volatiles. The juvenile Ayr lapilli also contain rare crystals of quartz, clinopyroxene and plagioclase, as well as pseudomorphs possibly after olivine.

Although now largely altered and replaced, the juvenile lapilli in all the diatremes represent original sideromelane and tachylite glass, as well as more crystalline types. Most of the primary textures have been preserved by pseudomorphing of crystalline phases, although smaller grains are often highly corroded and replaced.

b) Matrix / Cement

Where present, the matrix of the tuffs consists of a mixture of juvenile ash grains and igneous and sedimentary lithic fragments along with minor crystal and opaque grains. These fragments are generally enclosed within largely unresolved fine dust-grade material which contains

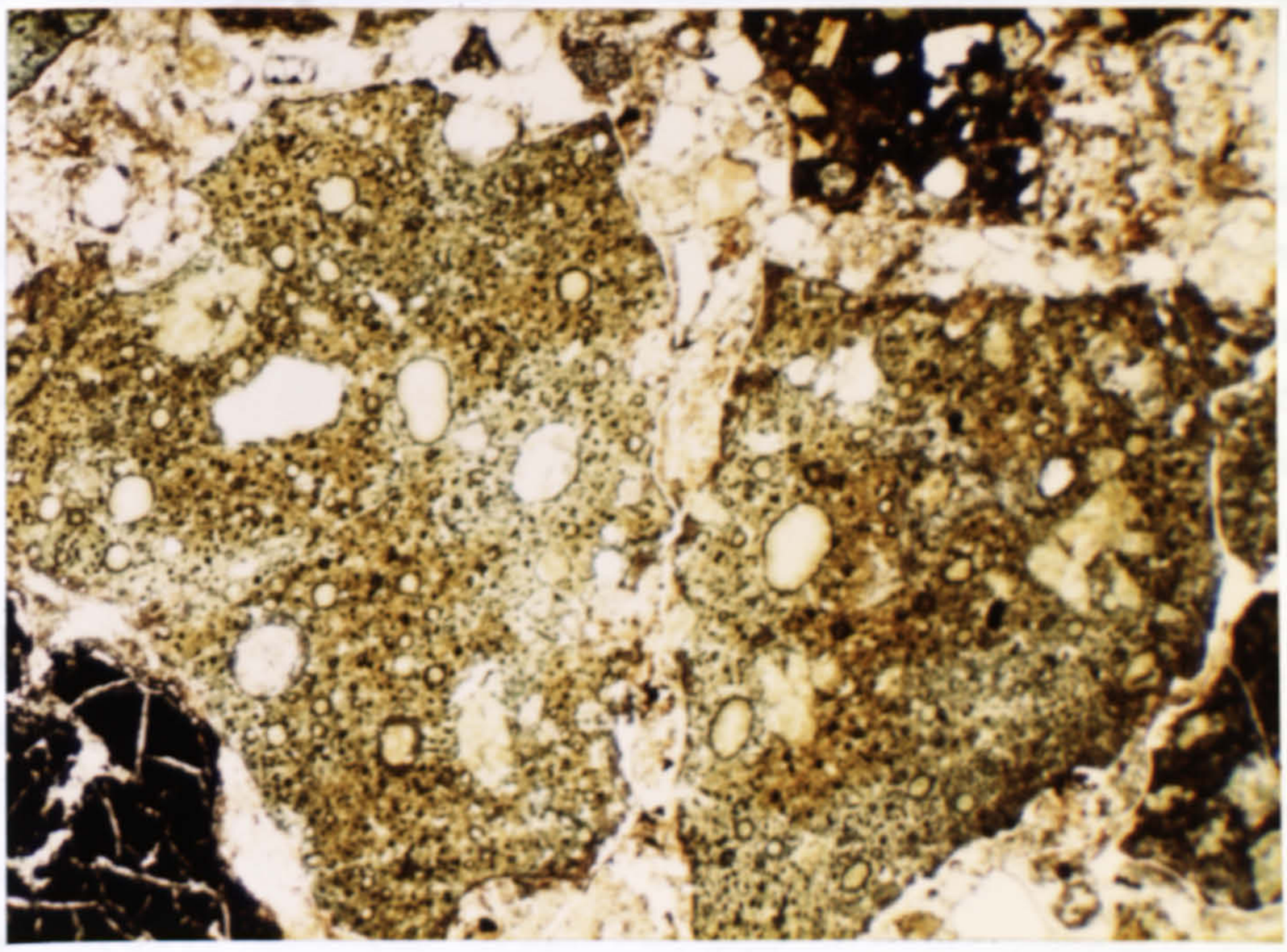

Fig. 6.39 Typical blocky, juvenile lapilli from the Elie Ness tuffs. Note preservation of grain shapes and internal structure, even though totally replaced by chlorite. Plane polarised light. x10.

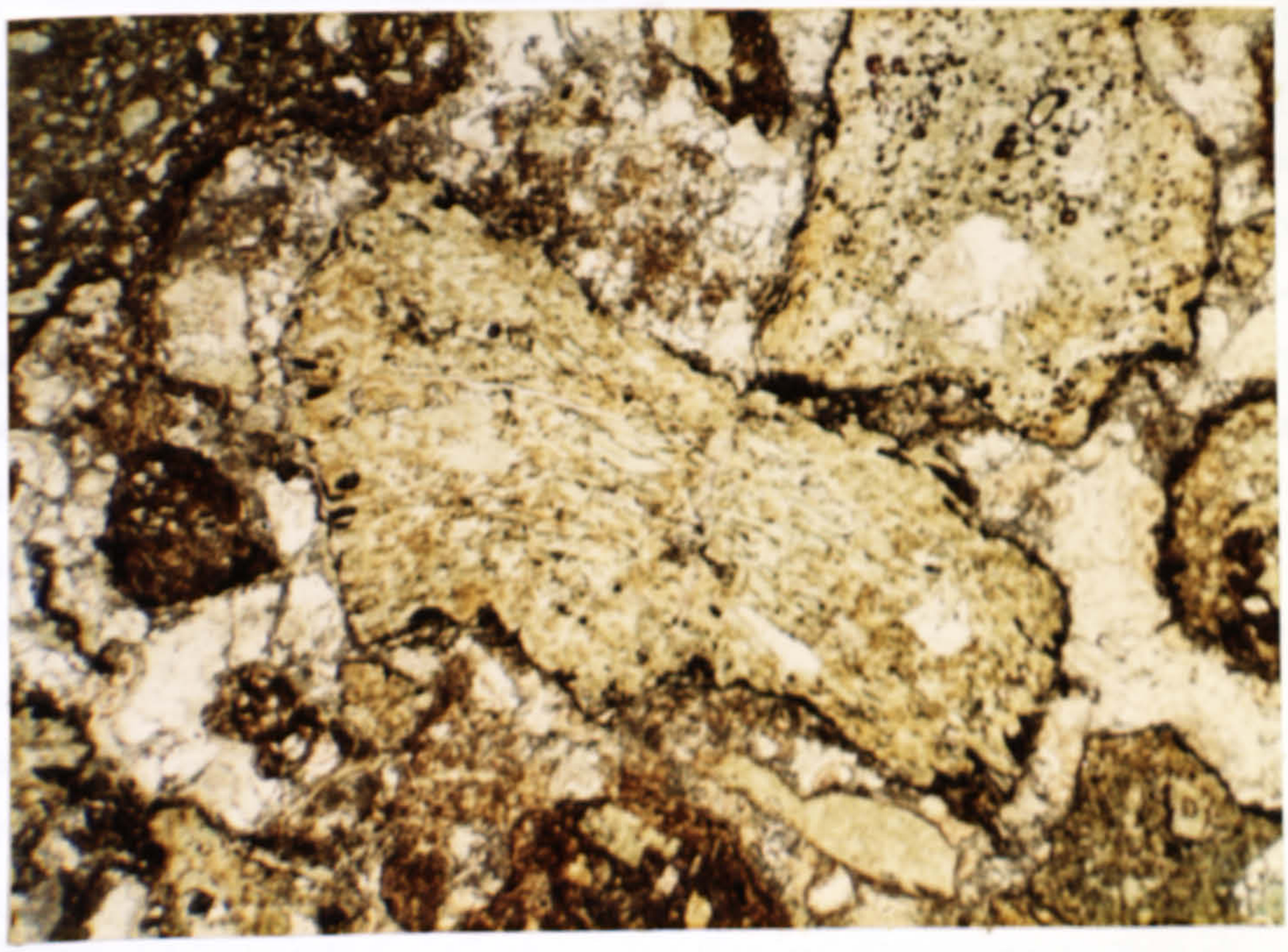

Fig. 6.40 Heads of Ayr juvenile lapillus with stretched vesicles parallel to the fragment elongation. Note ragged grain edges and other more fluidal textures than the Fife lapilli. Plane polarised light. x10.

turbid clay minerals. Most of the tuffs have a high matrix content (Section 6.5.1e) and few clast-supported deposits occur.

Different types of cement, which may be primary or replacive, occur in the tuffs of East Fife and Ayr. The most common is a calcite cement, which is particularly abundant in the tuffs in the western Heads of Ayr tuffs. Here, coarse recrystallised calcite forms up to 30% of the tuffs and commonly penetrates the lapilli and sediment grain margins. Some grains have been totally replaced by calcite, and only their iron oxide rims can now be recognised.

In many instances, the larger fragments in the tuffs are surrounded by thin turbid rims of fine matrix, with sparry calcite between (Fig. 6.40). In such cases calcite is replacive after the matrix and the thin, often iron-stained coatings protect the fragments from corrosion. Whyte (1964) thought that the calcite was a primary phase precipitated from shallow water in which the tuffs were accumulating. This may be the case for some of the calcite but some is undoubtedly replacive.

Calcite is generally less abundant in the East Fife diatreme deposits, but coarse tuffs contain some replacive calcite. It appears that the lack of connected pore spaces in fine tuffs prevented free percolation of carbonate-bearing solutions through the rock. The poor sorting of the coarse tuffs facilitated the movement of solutions. Some of the tuffs are cut by hairline fractures, which are commonly calcite filled, and these allowed access of solutions even into well-sorted, compacted fine tuffs. Such fractures probably formed by displacive calcite crystallization.

Another common cementing material is analcite, which occurs either as fringes round pore spaces or as complete pore infillings (Fig. 6.41). The analcite is colourless, has weak-to-nil birefringence and occurs as blocky aggregates. Individual crystals are often euhedral, with rounded or octagonal cross-section. The analcite is generally corroded by calcite, which often forms the final

pore-infilling.

The zeolite is not itself replacive of any other material but grew freely in pore spaces within the tuffs. In places, the matrix which previously filled the pores was removed before analcite growth occurred. It is thought that the analcite grew authigenically as a result of alteration of the tuffs which liberated Na, Al and Si to solution. The most analcite-rich sample is from the Greenan Castle Ash, Ayr, which contains up to 20% of the zeolite. The abundance of analcite is perhaps due to alteration of volcanic glass plus an input from lake brines. Both analcite and calcite replace and pseudomorph small, fibrous, radiating crystal aggregates found as pore linings. The fibrous minerals are thought to represent earlier authigenic zeolites.

A further cement found in the East Fife and Ayr tuffs is chlorite, which generally occurs in small patches but may locally be widespread. The chlorite occurs as authigenic fringes round altered grains or as a massive replacement, pseudomorphing larger fragments but completely obliterating all traces of matrix-grade material. Relict juvenile and lithic fragments are often preserved floating in a chlorite cement. Quartz grains generally survived corrosion and are often rimmed by fibrous chlorite.

The order of formation of the various cements is similar in many of the tuffs and typical sequences consist of :-

chlorite(authigenic)-analcite-sparry calcite (Fig. 6.42)
analcite-chlorite-calcite

The diagenetic history of the tuffs is complex, and dependant on many factors which vary over short distances. However, common features of many tuffs include an early phase of dissolution, forming voids where matrix was once present, and hematite-staining, resulting from in situ alteration of ferromagnesian minerals (Turner, 1980).

c) Lithic fragments

The lithic fragments in the tuffs consist of both igneous and sedimentary material. It is largely impossible to convincingly identify cognate lithics, and only rarely

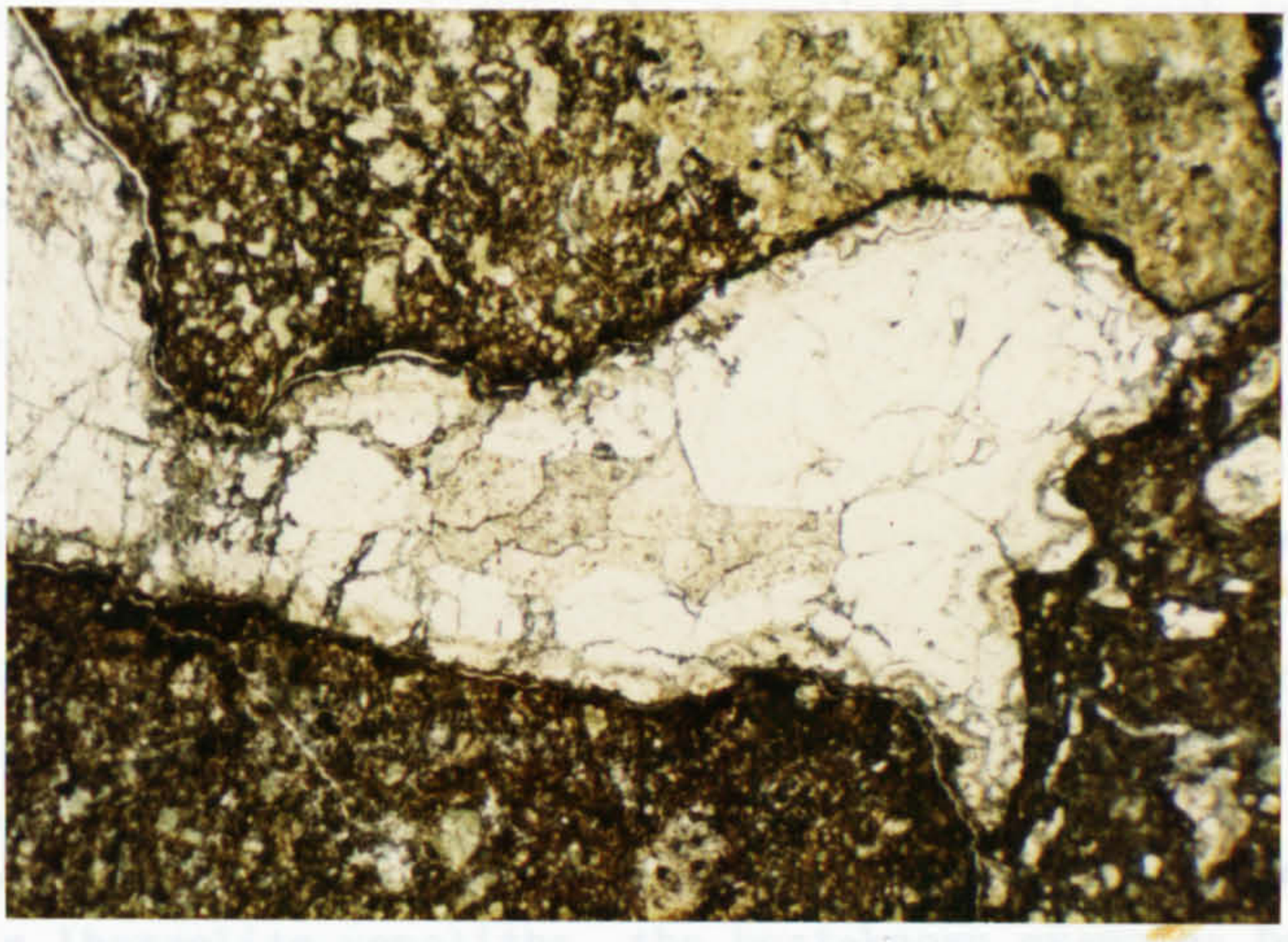

Fig. 6.41 Colourless analcite infilling voids in the Ayr diatreme tuffs. Slightly turbid sparry calcite forms the last stage of pore infilling. Note relict spherulitic texture around the pore walls, which represents replaced fibrous authigenic phases. Plane polarised light. x10.

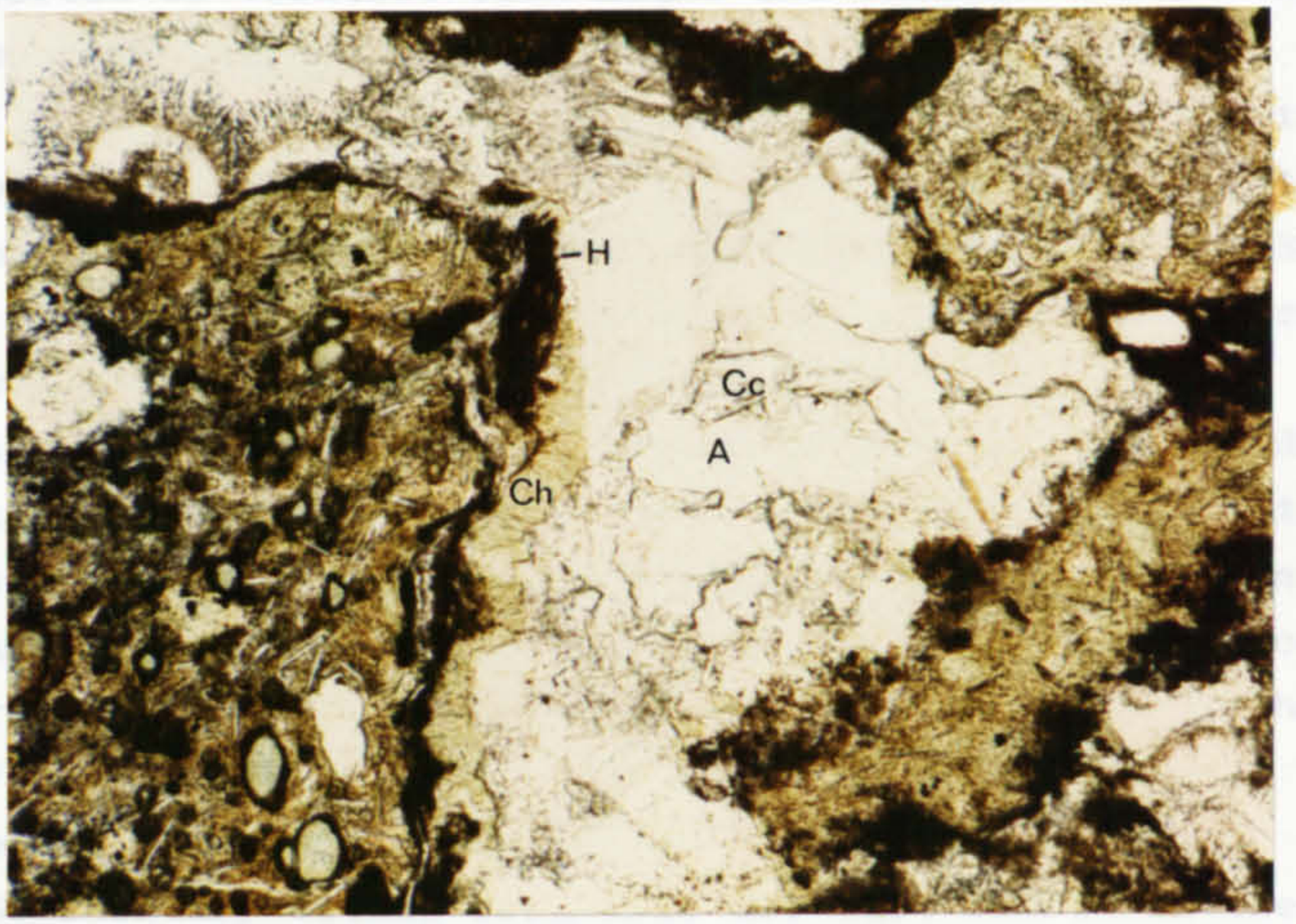

Fig. 6.42 Pore infilling sequence in the Ayr diatreme tuffs. Sequence comprises :- hematite(H)-chlorite(Ch)-analcite(A)-calcite(Cc). Plane polarised light. x40.

can accessory igneous lithics be correlated with rock-types known to form part of the country rocks beneath the volcanoes.

The East Fife igneous lithics consist of both hypabyssal and deep-seated types (Forsyth et al., 1977). The hypabyssal types (Fig. 6.43) consist of basanites, nepheline-basalts and monchiquites with analcite-bearing varieties reported by the Survey (Forsyth et al., op.cit.). More deep-seated xenoliths include hornblende-clinopyroxene rocks, clinopyroxenites and biotite-clinopyroxene rocks. Often such aggregates are highly carbonated and one from Elie Ness consists of euhedral augites and anhedral biotite plates surrounded by calcite-replaced tabular crystals, possibly feldspar. Some of the other diatremes and intrusions contain lherzolite xenoliths, the best-known examples being from the Coalyard Hill diatreme (Chapman, 1974). One of the pyroxenite xenoliths from Elie Ness has a thin rim of basalt containing concentrically-aligned elongate vesicles which are now calcite filled. The rim has a chilled outer margin and all the evidence indicates that the xenolith was transported by volatile-rich magma and chilled whilst the rimmed clast was spinning.

Igneous lithic fragments from the Heads of Ayr diatreme have been well described by Whyte (1964). He concluded that the common andesite clasts were derived from Lower O.R.S. lavas which probably extend beneath the volcano. Conspicuous grey-white fragments in the tuffs consist of highly carbonated lherzolites which Alexander (1980) considered to be picritic. The xenoliths contain clinopyroxene, enstatite, olivine, plagioclase and spinel of pleonaste composition (Alexander, op.cit.). All the minerals are highly replaced by serpentine, chlorite and abundant calcite. As with the East Fife xenoliths, some of the lherzolite blocks are mantled by highly irregular rims of vesicular basalt.

Sedimentary lithic fragments are most common in the Kinkell Ness diatreme, although sediment-rich layers occur in most of the diatreme tuffs studied. Some of the Kinkell Ness tuffs would be better termed tuffites since their sediment proportions often exceed 30%. Most of the

sedimentary fragments consist of single quartz grains but siltstone, mudstone and limestone clasts are also common. Most of the coarser-grained clastic fragments have a calcareous cement or a clay matrix which prevented their being completely comminuted during eruption. The lack of sandstone fragments suggests they were derived by disruption of poorly-consolidated, newly-deposited sediments around the vent.

As well as these fragments, single grains of orthoclase, microcline biotite, muscovite and rare plagioclase occur, most of which probably represent originally detrital sedimentary grains derived from the country rocks. Small wood fragments are found in many tuffs, and are generally replaced by calcite or more rarely opaques, possibly pyrite.

Large sedimentary clasts are never seen rimmed by juvenile basalt, although many juvenile lapilli contain individual quartz grains. Sediment clasts found in the diatreme intrusions of East Fife are often slightly baked, with patchy development of chlorite, augite and occasional cordierite (Forsyth et al., 1977). Individual quartz grains found within intrusions are often surrounded by augite prisms, which represent reaction rims. Nests of augite with a core of glass or augite are thought to represent completely resorbed quartz grains (Forsyth et al., op.cit.). Such reaction rims are not seen around quartz grains within juvenile lapilli, presumably because the magma droplets were chilled before reaction could take place. The only effects on the quartz xenocrysts appear to be mechanical breakage, infiltration of now chloritised glass and the development of chlorite rims (Fig. 6.44).

d) Crystal fragments

Single crystal fragments are relatively common in all the tuffs studied, especially those in the Elie Ness diatreme. This diatreme is famous for its varied suite of xenocrysts, which include garnet, zircon, augite, amphibole, biotite, olivine and alkali feldspar. Many of the xenocrysts are probably derived from disintegration of igneous xenoliths although garnet has not been reported in any

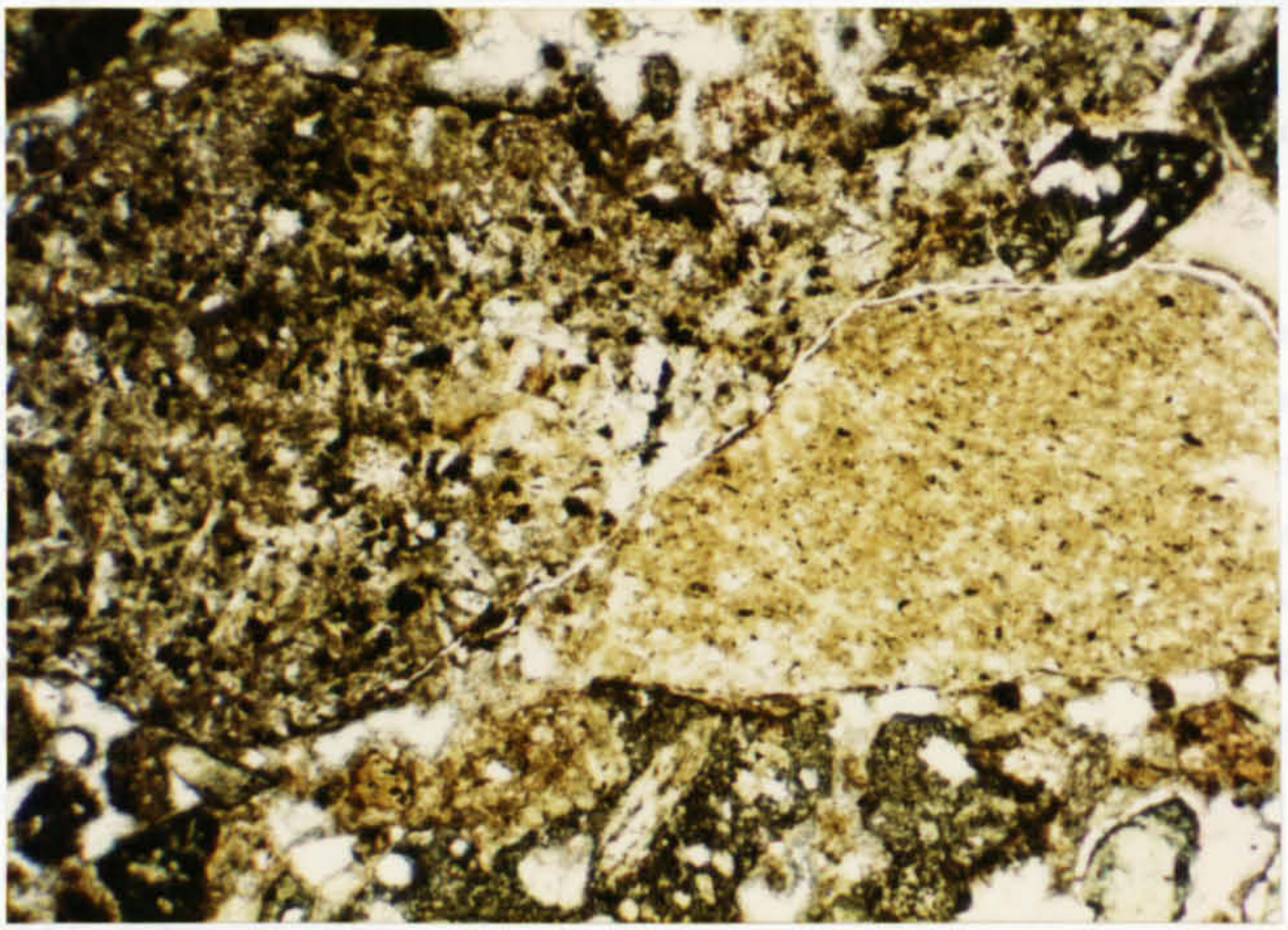

Fig. 6.43 Typical lithic clasts in the Elie Ness tuffs. Fragment on left is altered basalt and on the right is a mudstone clast. Plane polarised light. x10.

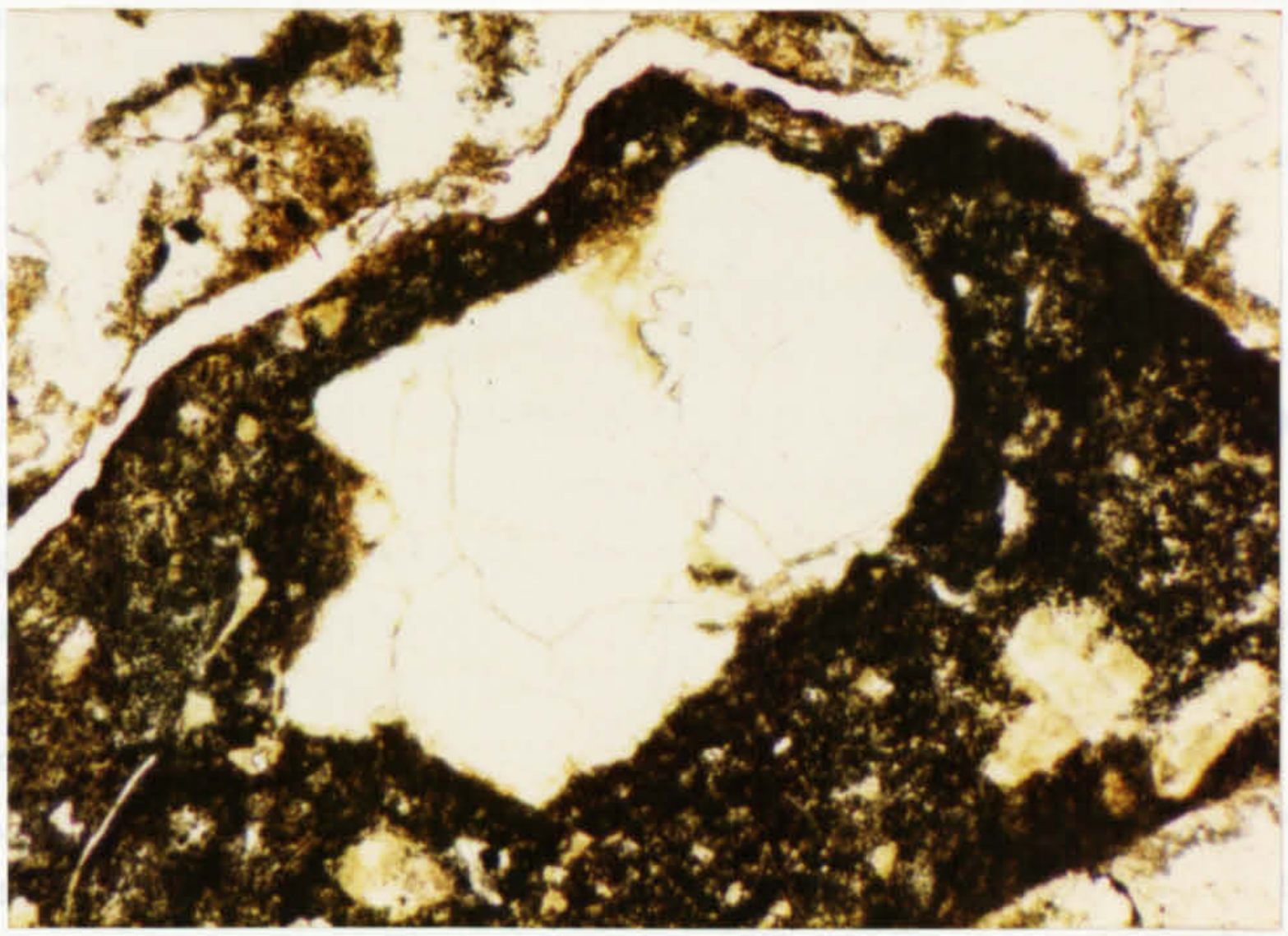

Fig. 6.44 Fracturing and infiltration of chlorite into quartz xenocryst within Elie Ness juvenile lapillus. Note corroded grain margins and irregular, embayed shape. Plane polarised light. x25.

xenolith. This, along with its pyrope composition prompted Colvine (1968) to suggest that it crystallized from a suitable magma at depth and was carried rapidly upwards before resorption occurred.

Chapman (1974) proposed that the Elie Ness magma crystallized garnet at over 70km depth, followed by augite and biotite near the mantle/crust boundary. The presence of zircon, biotite and anorthoclase xenocrysts, along with large apatites suggests that the source magmas for the Elie Ness and other Fife diatremes were rich in K, P, Zr and presumably other large lithophile cations (Upton, 1982). The high CO_2 content of these magmas is indicated by the common occurrence of partly carbonated xenocrysts and xenoliths.

e) Modal composition

Modal analyses of the Fife and Ayr diatreme tuffs (Fig. 6.45, Table 6.2) indicate their highly variable composition. Apart from alteration and replacement of the matrix by authigenic cement, the greatest variation occurs in the lithic and juvenile basalt components. In general, as the lithic component increases, the juvenile basalt component decreases, with other components remaining roughly constant. This reflects eruption types ranging from phreatic, with little juvenile magmatic input and mainly steam blasts, to phreatomagmatic, with greatly increased magmatic input.

Looking at one bedded diatreme sequence in particular (Fig. 6.45), little systematic variation in tuff composition occurred with time. However, there appears to be an antipathetic relationship between vesicular juvenile lapilli and sediment fragments, for the reasons outlined above. The matrix content, which is an indicator of the violence of the explosions (Self & Sparks, 1978) fluctuates widely throughout the sequence, indicating the essentially variable nature of the explosions. However, there is a broad trend, on which these fluctuations are imposed, of gradual decrease and increase in eruption strength with time.

f) Grain size

Thin section grain size analyses were carried out by point counting methods on samples which have not been badly

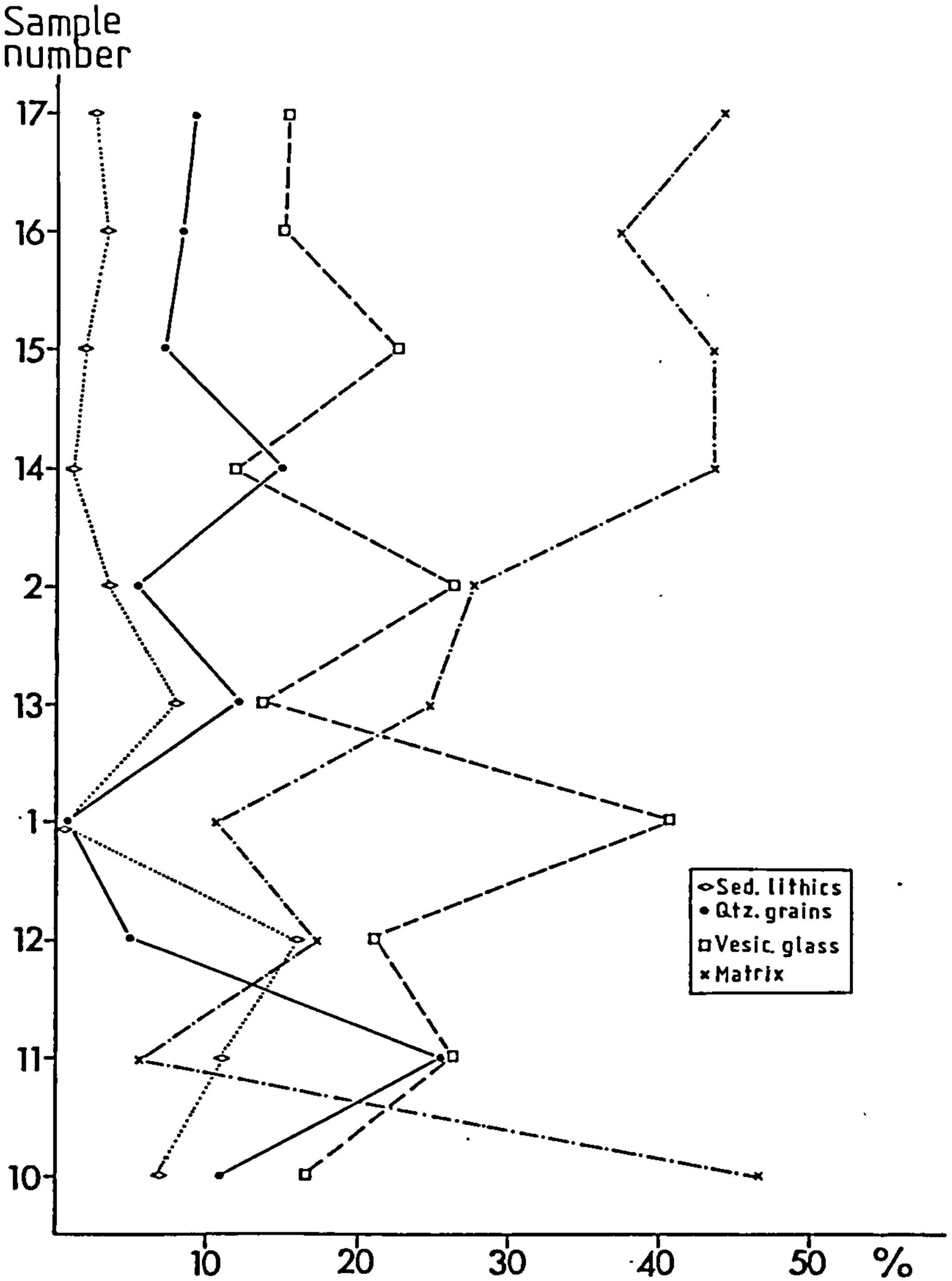

Fig. 6.45 Modal analyses of the east-central, bedded Elie Ness diatreme tuffs showing variations in component proportions up the stratigraphic sequence. Note antipathetic relationship between quartz grains and vesicular juvenile glass as eruptions change from phreatic to phreatomagmatic.

TABLE 6.2 MODAL ANALYSES OF ELIE NESS TUFFS

Sample number	FEN1	2	3	9	10	11	12	13	14	15	16	17	18	19	20
Vesicular glass	41·4	24·5	41·2	10·6	16·5	27·1	21·4	13·7	11·7	22·6	15·1	15·6	8·3	10·0	30·7
Non-vesicular glass	7·9	10·6	2·8	1·1	1·0	1·0	1·2	0·5	0·8	3·8	1·5	2·8	1·2	2·0	2·9
Matrix	10·7	25·9	12·5	46·7	46·8	5·5	17·1	25·5	44·2	44·2	38·2	44·9	45·7	46·5	34·4
Crystals	-	3·6	1·1	3·9	0·4	1·0	-	0·5	0·4	0·7	1·9	0·2	0·4	0·5	0·8
Quartz grains	0·6	5·7	1·7	13·0	10·7	25·8	5·2	12·1	15·1	7·3	8·4	9·7	18·5	16·9	10·1
Sedimentary lithics	0·8	3·8	7·2	5·9	7·1	11·2	14·9	9·2	1·2	2·0	3·7	2·6	3·3	8·8	3·1
Igneous lithics	11·3	14·7	21·1	13·4	8·7	14·3	21·5	7·3	15·8	11·3	22·5	8·6	8·7	9·1	11·1
Calcite	18·9	2·1	2·4	1·4	2·1	13·2	8·3	11·7	7·2	3·4	4·2	1·6	6·8	5·6	5·6
Chlorite/ zeolite	8·0	8·5	9·8	3·1	6·4	1·3	10·1	19·4	3·4	4·5	4·0	13·7	6·8	0·7	1·0
Opaques	-	0·7	-	0·3	-	0·2	0·4	0·2	0·2	0·1	0·2	0·2	-	-	0·1

TABLE 6.2 MODAL ANALYSES OF FIFE AND AYR TUFFS

Sample number	FRS4	6	7	8	9	15	A1	2	3	4	6	7	8	10	11	12
Vesicular glass	30·4	29·6	14·1	34·8	37·5	26·4	55·0	23·3	31·3	41·0	52·0	46·0	54·6	41·7	44·3	54·7
Non-vesicular glass	0·8	4·9	2·0	1·4	5·1	3·5	8·7	9·0	23·0	17·3	9·0	16·0	19·3	9·0	9·0	10·0
Matrix	39·5	42·8	23·8	35·2	32·3	34·1	0·1	8·0	2·3	20·0	11·6	19·7	2·7	26·7	34·7	1·0
Crystals	0·5	0·6	-	0·1	-	-	-	0·7	-	-	1·0	-	-	1·7	-	0·7
Quartz grains	16·8	20·2	53·5	3·5	14·9	21·7	0·1	6·3	7·7	8·7	6·0	3·3	2·7	4·7	4·0	6·7
Sedimentary lithics	0·9	1·1	3·3	3·2	5·2	3·1										
Igneous lithics	1·4	0·6	1·2	8·1	1·3	2·3	6·6	22·7	4·3	3·0	1·6	2·0	2·7	4·0	4·7	3·7
Calcite	8·8	0·1	2·0	12·2	2·4	10·4	12·3	7·3	21·7	9·3	4·0	11·3	13·3	6·7	2·3	3·7
Chlorite/ zeolite	0·4	-	-	1·4	-	-	15·0	6·6	6·7	-	14·7	1·7	4·7	8·3	1·0	19·7
Opaques	0·4	-	-	0·1	-	-	-	-	-	-	-	-	-	-	-	-

affected by alteration. Tuffs which have had their matrix replaced by cement have been analysed to allow at least partial comparisons with less altered samples. Grain size arrays were converted to sieve equivalents and are listed in Table 6.3.

East Fife tuffs

The Elie Ness tuffs (Fig. 6.46a) plot well within the surtseyan field of Walker & Croasdale (1971) on an Mdϕ/$\sigma\phi$ diagram, with the exception of sample FEN 13 which is a very poorly-sorted surge tuff. The Kinkell Ness tuffs lie below this field and are consistently better sorted than the Elie Ness samples. On a similar diagram (Fig. 6.46b) marked with flow and fallout fields (Walker, 1971) most of the Elie Ness tuffs plot in the area of overlap whereas the Kinkell Ness tuffs plot well within the fallout field.

On Sheridan's (1971) C-M diagram (Fig. 6.46c) the Elie Ness tuffs plot in his areas 2 and 3. Those samples from surge cross-bedded units (FEN2, 13, 14, 18 and 19) generally plot in area 2, which is Sheridan's rhyolitic ash flow field. Other samples, presumed to be of airfall origin plot in area 3, the airfall field. The Kinkell Ness tuffs plot between or close to the area between the three fields. FRS7, from faintly-bedded fine tuffs near the margin of the Kinkell Ness diatreme is the only sample to plot in area 1, the field of rhyolitic base-surge dunes.

The cumulative volume % curves for the East Fife tuffs (Fig. 6.47) show how poorly sorted and fine-skewed the base-surge tuffs are. Overall the cumulative curves for the Kinkell Ness tuffs are more fine-skewed but most of the curves have similar shapes. This perhaps indicates that during the formation of these proximal deposits, airfall and surge deposition occurred simultaneously and resulted in much mixing of products.

Ayr tuffs

The Ayr tuffs (Fig. 6.48a) plot in two distinct areas on a Mdϕ/$\sigma\phi$ diagram. One group is very poorly sorted and plots around the high $\sigma\phi$ side of the surtseyan field of Walker & Croasdale (1971), but well within the flow field of Walker (1971) (Fig. 6.48b). The other group is only

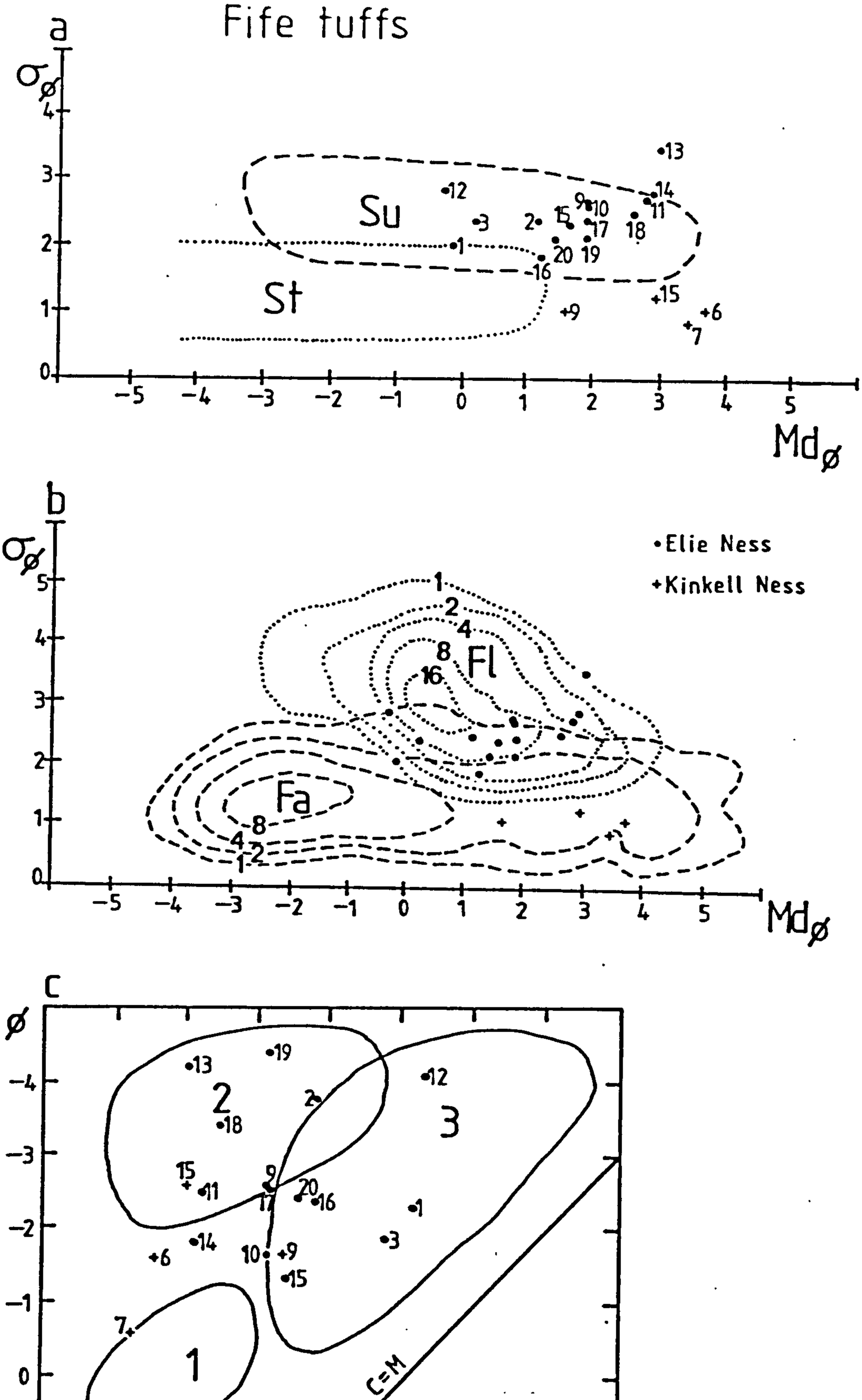

Fig. 6.46 Grain size plots of the Elie Ness and Kinkell Ness diatreme tuffs.

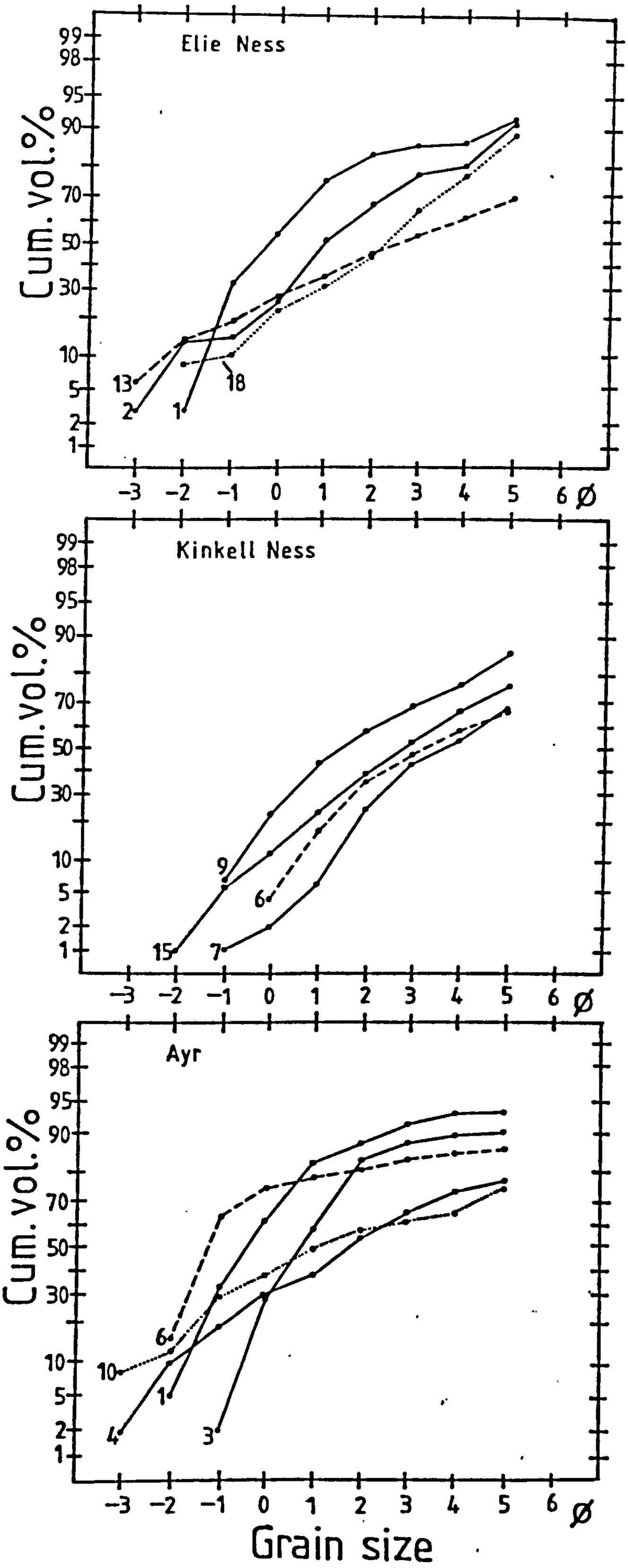

Fig. 6.47 Cumulative grain size curves of the Elie Ness, Kinkell Ness and Heads of Ayr diatreme tuffs.

moderately poorly sorted and plots around the strombolian/ surtseyan overlap zone but within the fallout field of Walker (op.cit.). The latter group has suffered calcite replacement of the matrix, causing a spurious increase in sorting. These samples would plot alongside the remainder of the tuffs if alteration had not occurred.

On Sheridan's (1971) C-M diagram the tuffs all plot in the airfall field, except for samples A4 and A10, which plot in the rhyolitic ash flow field. These two samples are bedded and unbedded lapilli tuffs from the western and eastern areas of the Heads of Ayr diatreme respectively, and are thought to represent coarse airfall tuffs.

Cumulative volume % curves (Fig. 6.47) indicate the general coarse-skewed nature of the Ayr tuffs, with samples A4 and A10 having the coarsest tails. The smooth curves of many of the samples closely resemble cumulative plots of Surtsey tephra (Sheridan, 1971). These tephra are thought by Sheridan to have had two modes of transport, the coarse fraction resembling airfall material and the fine fraction resembling suspended load material. It seems reasonable to assume that near the vent, coarse material continually falls out of the eruption column and mixes with fine material transported horizontally by surges.

Compared to the Fife tuffs the Ayr samples are similar but generally less well sorted. The Ayr cumulative curves show more evidence of two sub-populations than the Fife tuffs, indicative of mixing of airfall and surge deposits. Both differences could be explained if the Ayr tuffs were more proximal than their Fife equivalents. However, since the deposits occur within diatremes they are all assumed to be very proximal. A more reasonable explanation might be that the Heads of Ayr volcano was larger and built by more powerful eruptions than the Fife examples. The size of the diatreme and the thickness of the Greenan Castle Ash - 25m thick at 2·5km from the diatreme - suggest the volcano was of considerable size. More powerful eruption blasts would have deposited more coarse-skewed, poorly-sorted tuffs near the vent than weaker eruptions.

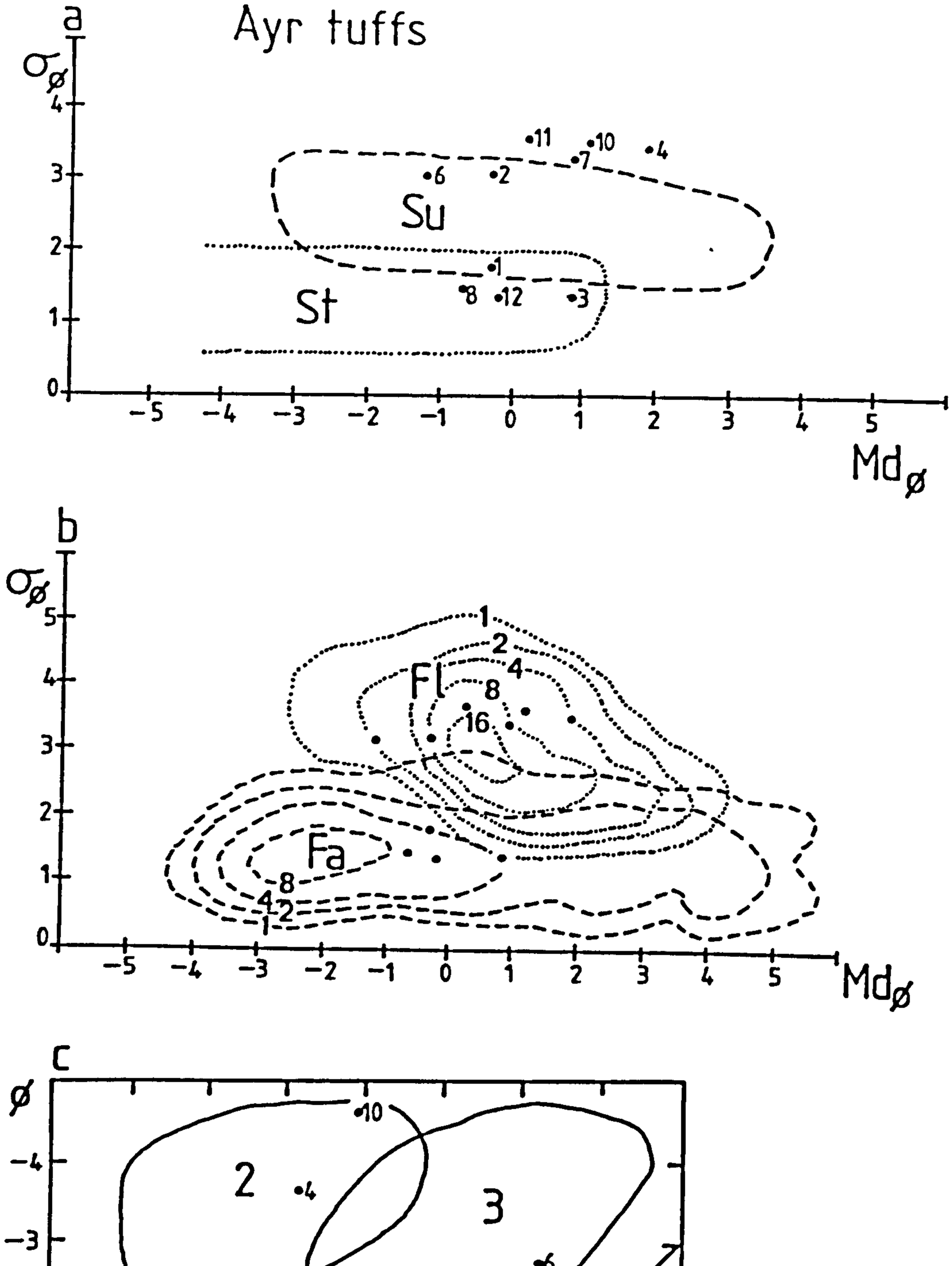

Fig. 6.48 Grain size plots of the Heads of Ayr diatreme tuffs.

TABLE 6.3 THIN SECTION GRAIN SIZE ANALYSES : ELIE NESS

Sample number	FEN1	2	3	9	10	11	12	13	14	15	16	17	18	19	20
+6o	8	12	8	14	20	22	9	30	25	11	6	17	13	7	12
+5	5	11	6	9	13	15	7	9	9	10	7	11	12	11	12
+4	1	4	2	12	8	10	4	9	12	7	9	9	13	12	8
+3	3	11	4	11	7	9	4	8	11	12	12	12	19	14	8
+2	8	15	12	12	13	6	5	9	11	20	20	15	13	18	14
+1	21	23	19	13	14	8	13	7	13	19	26	10	9	18	19
0	22	10	29	14	15	13	26	9	11	20	9	15	11	8	14
-1	28	1	19	12	10	13	22	5	8	-	10	6	2	3	13
-2	3	10	-	3	-	4	5	7	-	-	1	3	8	9	-
-3	-	3	-	-	-	-	4	6	-	-	-	-	-	-	-

TABLE 6.3 THIN SECTION GRAIN SIZE ANALYSES : FIFE AND AYR

Sample number	FRS6	FRS7	FRS9	FRS15	A1	2	3	4	6	7	8	10	11	12
+6o	32	30	25	17	-	10	9	21	14	24	3	25	37	1
+5	9	14	8	9	3	2	2	3	1	1	-	9	2	-
+4	11	11	15	8	2	2	2	8	1	4	1	4	2	1
+3	11	19	13	10	4	4	5	12	2	7	3	3	2	3
+2	18	19	16	16	7	7	24	16	2	11	10	8	5	13
+1	14	4	12	18	21	15	29	11	4	15	15	11	7	23
0	4	1	5	16	28	24	27	10	12	20	24	10	21	27
-1	-	1	5	6	28	28	2	9	46	16	37	17	20	32
-2	-	-	1	-	6	6	-	8	17	3	7	5	4	-
-3	-	-	-	-	-	-	-	2	-	-	-	8	-	-

6.5.2 Morphology

Due to the highly altered nature of the tuffs, SEM techniques were found to be of little use in studying ash morphology. However, in thin section grain shapes are often well preserved and quantitative PVC measurements can be made.

In general, the Fife tuffs plot in an area of the triangular diagram with low P and moderate to high V and C values (Fig. 6.49). Some of the Elie Ness samples (FEN12, 19) are more closely grouped than the others, possibly indicating that one mechanism of tephra formation was dominant at those times. The Kinkell samples plot within a similar area to the Elie Ness tuffs, indicating similar tephra-forming processes and magma vesicularity.

The Ayr tuffs (Fig. 6.49) plot in a similar area to the Fife samples and are assumed to have formed under similar conditions. The finer ash grains were plotted separately from the coarse lapilli but were not found to occupy significantly different areas of the triangular diagram.

On a P vs N plot, the Fife tuffs plot above or close to the line with gradient 0·75 (Fig. 6.50). The spread of points generally parallels the N-axis, indicating that both small and large grains have similar P values which generally lie between 10% and 30%. As with the PVC plots, some of the grains from the same sample tend to plot in closely-spaced groups. The Kinkell Ness tuffs best display this feature with sample FRS6 plotting about the dividing line and samples FRS8 and FRS11 plotting above it.

The Ayr tuffs have very similar distributions on a P vs N diagram (Fig. 6.50), and these are almost identical to the Fife samples. Grains from the same sample occasionally plot in loosely defined groups within the overall field of points.

In conclusion, the Fife and Ayr tuffs generally plot in the field of hyalotuffs (Honnorez & Kirst, 1975). The samples plot well within the hyalotuff field on P vs N diagrams but are more skattered on PVC diagrams. The similarity of all the sample distributions on PVC diagrams suggests either that Honnorez & Kirst's P = 20% line does

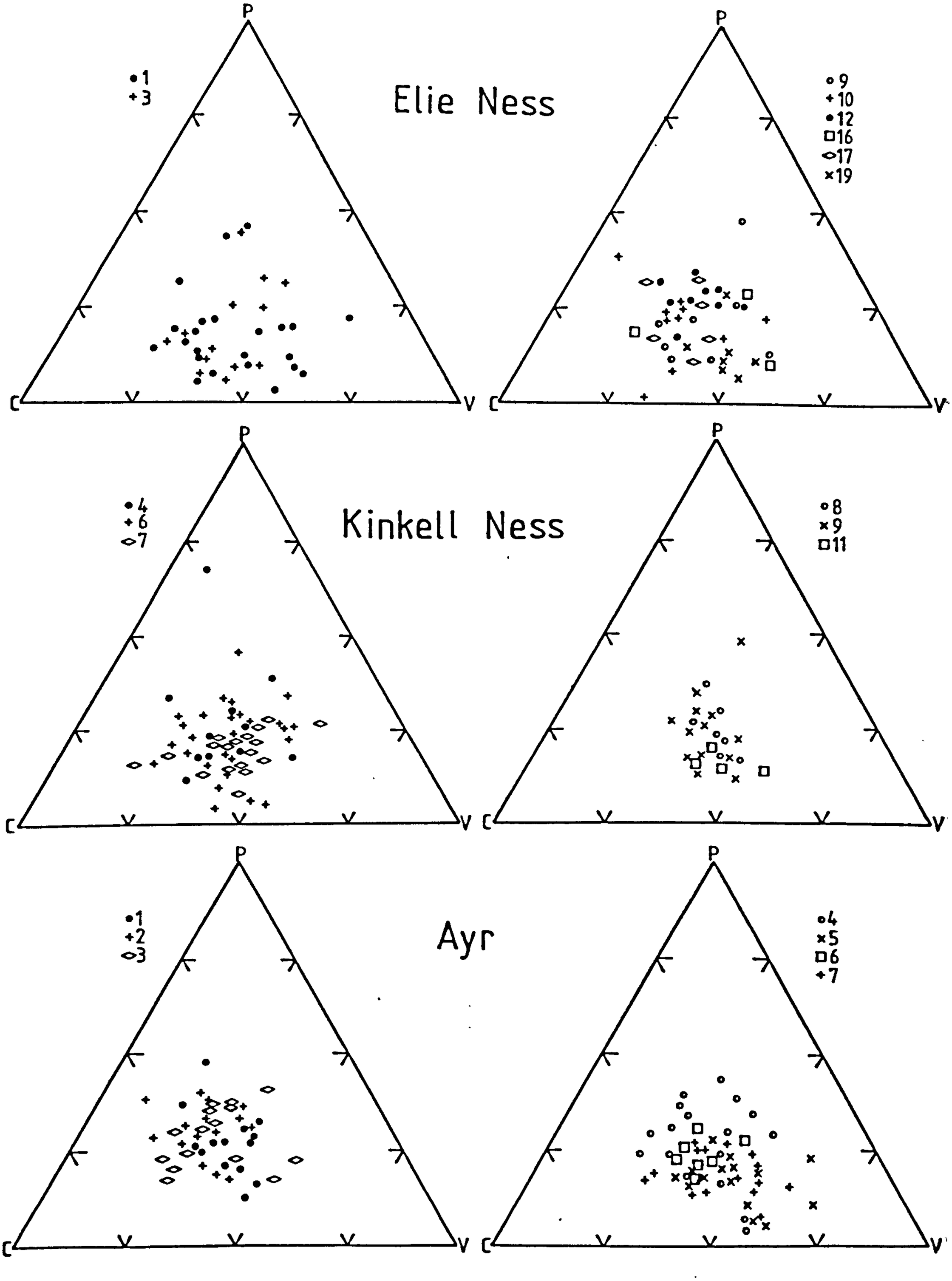

Fig. 6.49 PVC triangular diagrams of the Elie Ness, Kinkell Ness and Heads of Ayr diatreme tuffs.

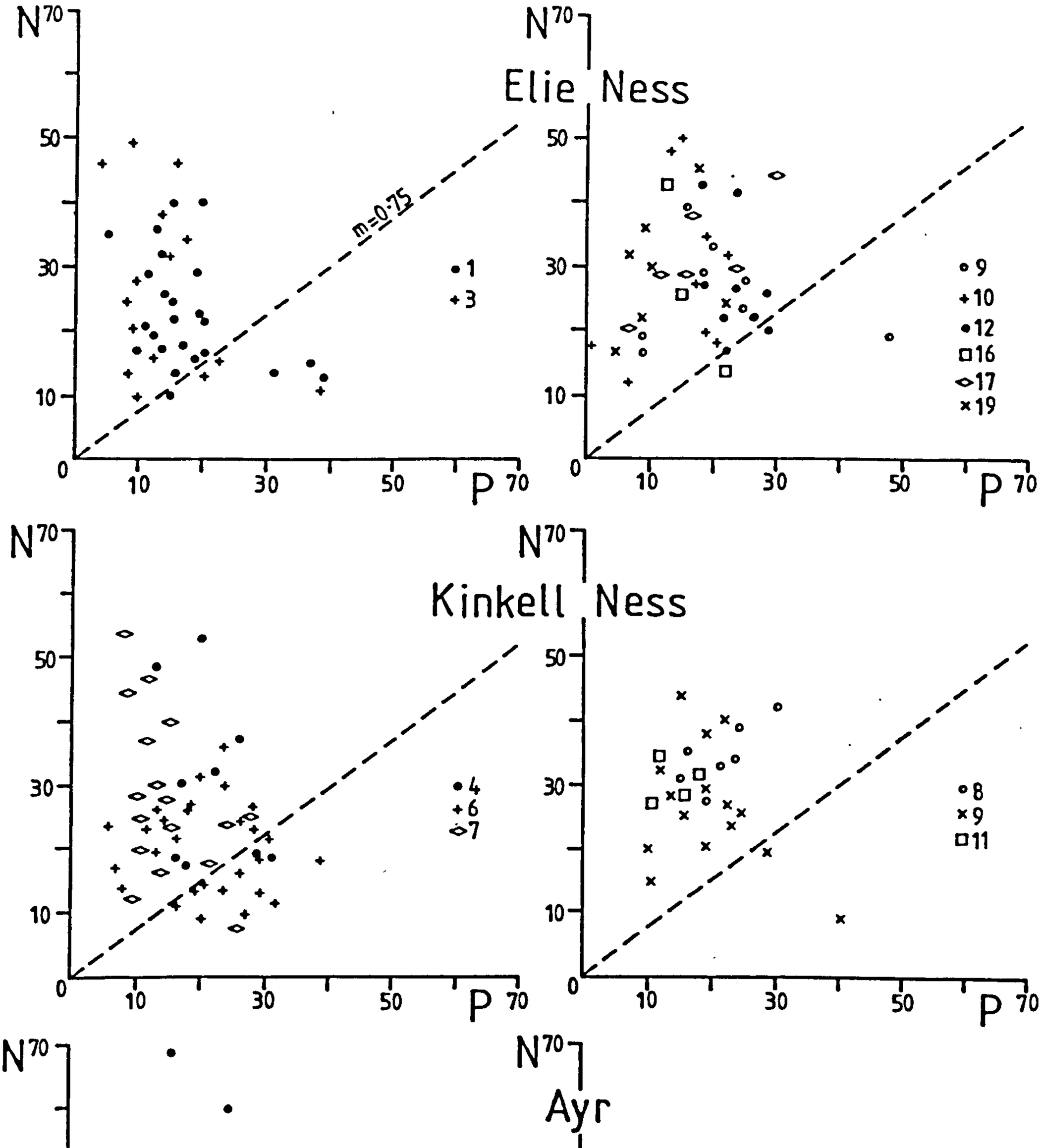

Fig. 6.50 P vs N plots for the Elie Ness, Kinkell Ness and heads of Ayr diatreme tuffs.

not fully define hyalotuffs or that the Fife and Ayr tephra was formed by a mixture of processes. This latter explanation is thought to be more likely, especially since phreatomagmatic eruptions are known to vary from highly water-influenced to almost strombolian.

6.5.3 Alteration of tuffs

The juvenile lapilli and igneous lithics from all the tuffs are mostly replaced by chlorite, calcite or hematite. In sediment-rich tuffs the chlorite tends to be colourless or pale-yellow but elsewhere it is pale-green and pleochroic. Chlorite analyses from Elie Ness and Ayr (Table 6.4) indicate that both types have similar compositions and are most similar to ripidolite.

Calcite is often replacive after chlorite, resulting in many juvenile lapilli having chlorite-filled vesicles surrounded by sparry calcite (Fig. 6.51). Where lapilli are not calcite replaced their margins are often corroded by calcite cement which commonly replaces the tuff matrix. Many sedimentary fragments are partly corroded by calcite but this does not occur in sediment-rich tuffs where only the volcanic fragments are altered.

Hematite replacement occurs most commonly in the tuffites, where the clay-rich matrix becomes full of opaque or brown oxide dust. The hematite never becomes abundant enough to give the rocks a red colouration but locally, patches of red-brown tuffs do occur. The hematite is partly derived from red sediment clasts derived from the country rocks beneath the volcanoes. Some hematite is sourced from the in situ breakdown of silicate minerals. In some of the tuffites, hematite-replaced fragments are seen squeezed-out between quartz grains (Fig. 6.52). It is thought that silicate (?ferromagnesian) minerals were altered to clay which was then squeezed between framework grains due to compaction of the rock. If the silicate had been a ferromagnesian mineral, alteration to clay would have released Fe to solution, which then precipitates as authigenic hematite. Such a process is common in the formation of red-bed deposits (Turner, 1980).

TABLE 6.4 MICROPROBE ANALYSES

	(1)	(2)	(3)	(4)	(5)	(6)
SiO_2	31·2	31·9	35·3	25·6	50·3	52·7
TiO_2	0·15	0·14	-	0·90	0·62	0·07
Al_2O_3	14·0	14·9	14·9	21·2	1·52	27·1
FeO	21·3	22·5	16·2	21·6	12·8	0·72
MnO	0·12	0·14	0·10	0·40	0·47	0·02
MgO	16·5	17·1	16·9	15·3	9·55	-
CaO	0·31	0·28	0·21	0·16	21·1	11·2
Na_2O	-	-	0·63	-	1·41	4·58
K_2O	0·10	0·12	0·73	-	-	0·37
				*(3·88)		
Total	83·68	87·08	84·97	89·04	97·77	96·76

(1) Chlorite vesicle infill from sample FEN1.
(2) Chlorite replacement of lapillus from sample FEN1.
(3) Chlorite replacement of lapillus from sample A12.
(4) Ripidolite (prochlorite) comparative analyses (Deer et al., 1975) (*=Fe_2O_3).
(5) Altered pyroxene from sample FEN1.
(6) Plagioclase crystal from sample A12.

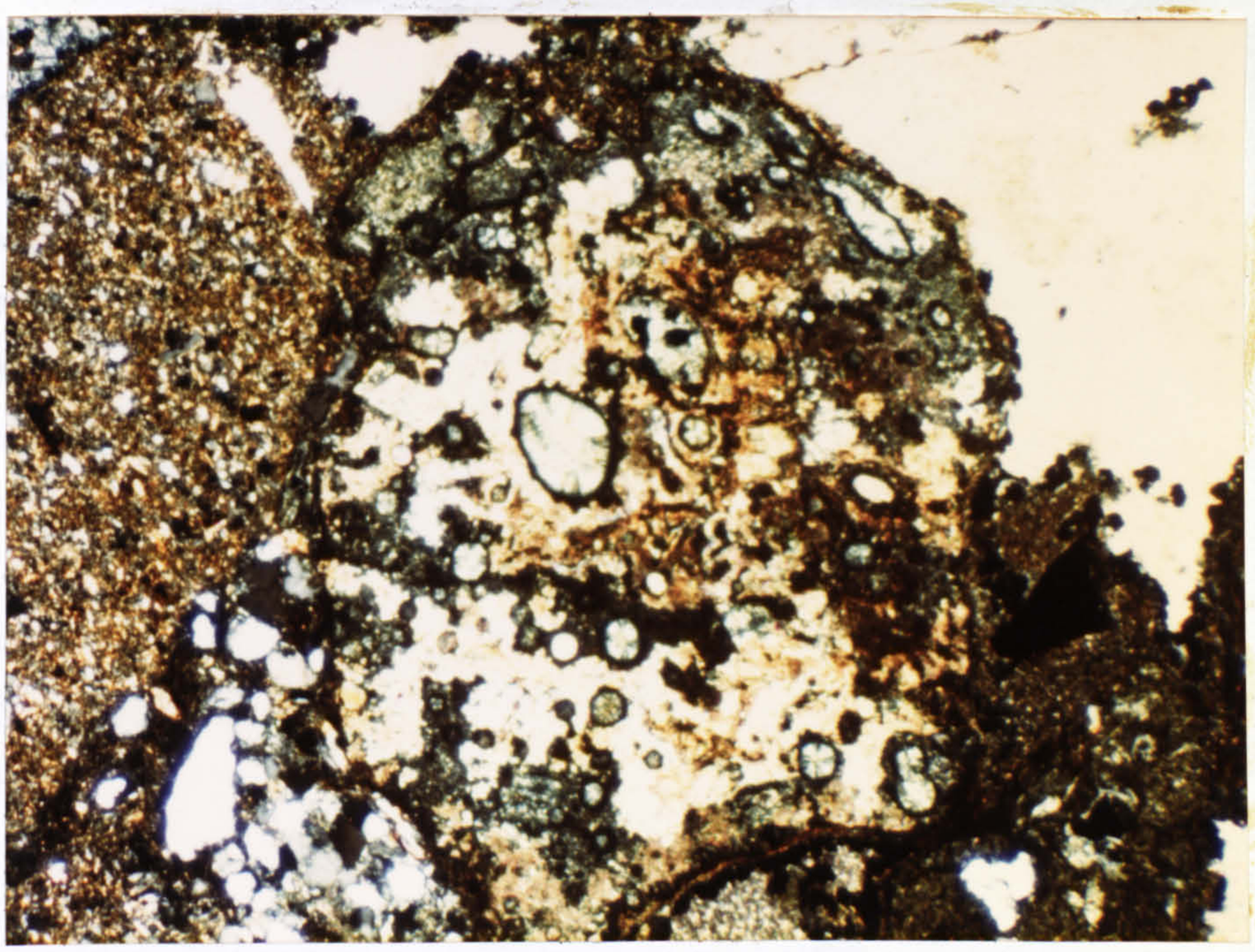

Fig. 6.51 Juvenile Elie Ness lapillus containing vesicles which are chlorite filled whereas the core of the fragment is replaced by calcite. Note calcite replacement of matrix in upper right area of photograph. Plane polarised light. x10.

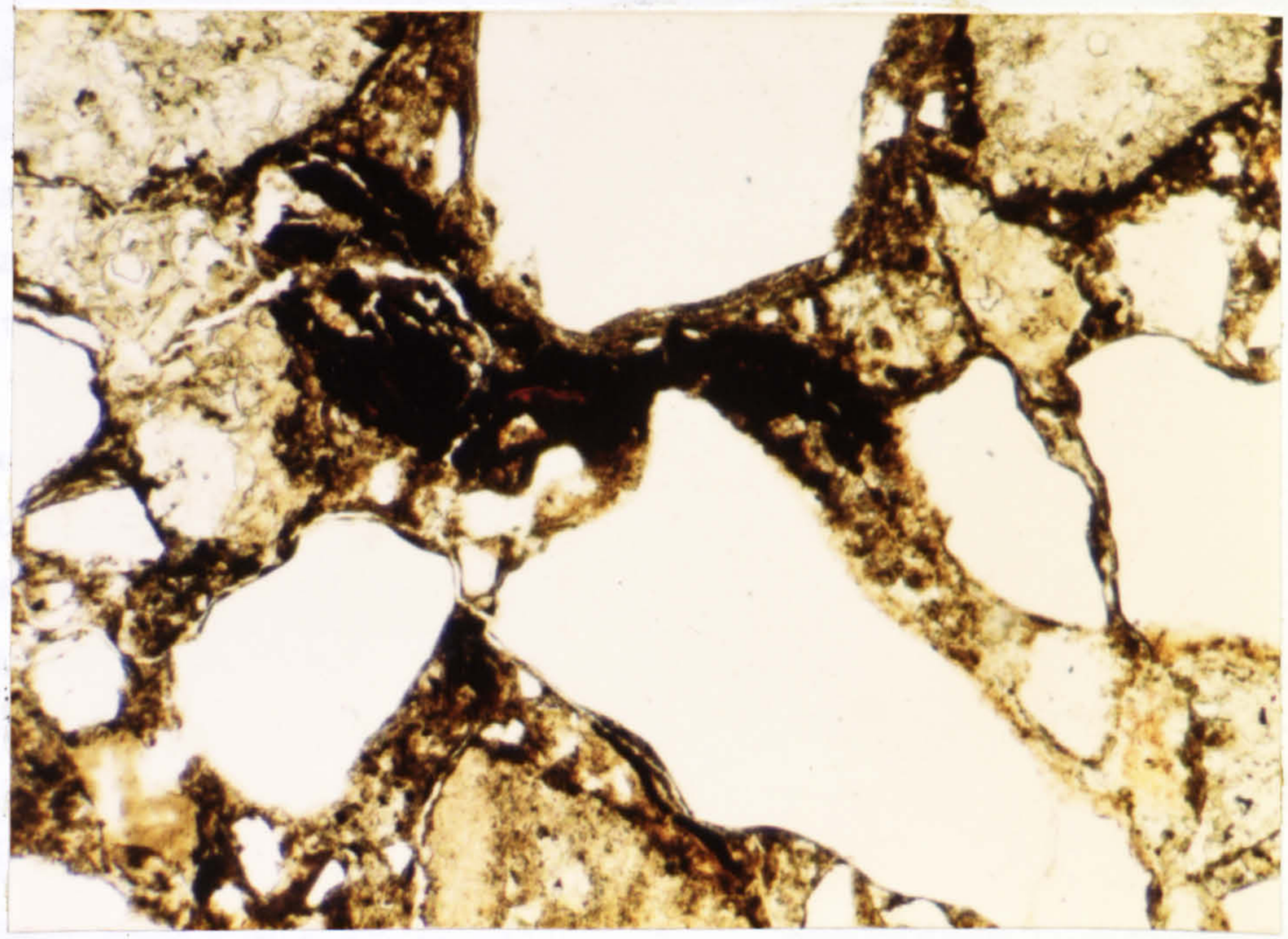

Fig. 6.52 Squeezed-out fragment of now hematite-replaced material. Alteration of an initial ferromagnesian mineral to clay was followed by compaction of the rock and reduction of pore space. Kinkell Ness diatreme tuffs. Plane polarised light. x25.

As might be expected, all the juvenile lapilli, which were originally unstable basaltic glass, have now been completely altered. The tuffs have not, however, been extensively leached or hydrothermally altered, since many igneous lithic fragments are almost completely fresh. Only olivine, which is rather susceptible to alteration, has been almost completely replaced.

It is thought that devitrification and alteration of basaltic glass occurred in a mild hydrothermal system associated with sub-volcanic intrusions. Precipitation of authigenic minerals resulted from this alteration and from groundwater exchange with the country rocks. This effectively closed most of the pore spaces in the tuffs and greatly reduced subsequent solution percolation. Alteration continued slowly, essentially as a diagenetic/weathering process, there being no evidence of metamorphic reactions in the rocks. The definition of the onset of very low-grade metamorphism is taken to be the reaction :

analcite+quartz = albite+water (Winkler, 1979).

6.6. Discussion

The East Fife and Ayr diatremes contain the deposits of phreatomagmatic volcanoes which formed when ascending, vesiculating magma contacted water-rich unconsolidated sediments deposited in the subsiding Midland Valley Basin. Surface water bodies known to have reworked distal tuffs from these volcanoes also provided an abundant source of water to maintain explosive activity.

Some of the diatremes are known to have been sourced from the tops of alkaline sills injected into poorly-consolidated wet sediments (Francis, 1968). However, as Upton (1982) pointed out, the presence of megacrysts and xenoliths of deep-seated origin indicates rapid transport velocities from depths below which sills or wet sediments could exist. Some of the explosive volcanism was thus initiated at deep levels, by exsolution of CO_2 and other volatiles, and the diatreme was rapidly drilled out when the ascending gas-fluid mixture contacted abundant pore-waters. Some of the carbonated material in the diatremes may

thus have been formed by reaction with magmatic CO_2, although much is thought to be due to decarbonation of organic-rich sediments.

Major deep-seated faults and other surface lineaments probably underlain by faults provided lines-of-weakness exploited by the ascending magmas (Upton, 1982). Alkali-basalt volcanism was characterised throughout the Midland Valley by highly explosive activity, which was predominantly phreatomagmatic. The major faults which controlled the volcanism also controlled the position of the many smaller subsiding basins within the Midland Valley. The faults thus brought together magma and wet sediment, and near the surface the faults would have acted as local sinks for ground water, increasing the likelihood of phreatomagmatic activity.

Injection of degassed magma into diatremes at a late stage in the volcanism did not source explosive eruptions. Rather, intrusion into wet tuffs and sediments led to minor fluidization and brecciation of the plug or dyke. The late-stage gas-streaming often concentrated at the diatreme margins is the result of final degassing of magma at depth along with steam-fluidized jets formed by heating of pore-water. Afterwards, intrusive activity ceased due to the high viscosity of the volatile-depleted, cooled magma. Presumably, many of the plugs which cut the tuffs were intruded at depth as a result of collapse of material into the diatreme, forcing magma to be injected along planes of weakness.

The absence of lavas may be due to their not being formed, or to subsequent erosion. The presence of major basalt intrusions in some diatremes indicates that there was no lack of magma to source extrusive flows. Upton (1982) suggested that fine-grained fragments of volcanic rock found in diatremes but not in the surrounding country rock succession represent now eroded lava flows from the volcano. No lava flow-structures have been found in any of these blocks and it is suggested they originated by disintegration of shallow intrusive bodies. Since there appears to be no reason why lava flows should not have formed after the

cessation of explosive activity, it is possible that such volcanoes sourced some of the lavas in the Midland Valley Carboniferous succession.

6.7. SUMMARY

1. The East Fife and Ayr diatremes represent the collapsed equivalents of phreatomagmatic volcanoes which erupted in in the Midland Valley Basin during the Carboniferous. Abundant pore-water in thick successions of newly-deposited sediments and surface water bodies initiated explosive volcanism. Although some diatremes were sourced from the tops of sills others represent pipes formed by magmas which ascended rapidly from deep levels in the crust.

2. Initial volcanism was sometimes of fissure-type, with the ejection of large amounts of derived sedimentary material. Subsequent activity was highly variable, ejecting predominantly juvenile or lithic material and depositing it by surge of airfall processes.

3. Outer flank tuffs were reworked in fluvial or lacustrine environments and all tuffs were affected by slumping and mass flow processes. Debris flows often occurred at a late stage in the volcanism, perhaps triggered by violent eruptions which deposited blocky tuffs. Some evidence of crater breaching exists, with the formation of post-volcanic crater lake sediments.

4. Collapse occurred during and after volcanic activity, along marginal faults and by slow subsidence due to the withdrawal of magma at depth. Centroclinally bedded tuffs often define collapse basins, the position of which does not necessarily correspond to the site of the vent. Collapse is accompanied by magmatic and tuffisitic intrusive activity, which further disrupts already subsided tuffs.

CHAPTER 7
A MODEL FOR PHREATOMAGMATIC VOLCANOES

The diatreme deposits extensively described in the previous chapters are so similar to modern phreatomagmatic volcanoes (s.l.) in terms of depositional structures, lithology, petrography, grain size and grain morphology that their origin cannot be doubted. The information from the modern and ancient examples in this report may thus be used, along with published work, to produce an idealised model for the formation, growth and subsequent collapse of phreatomagmatic volcanoes. Each volcano is inherently a unique structure, so the model approach is most useful in indicating the possible range of processes and their deposits, and the factors which affect these.

7.1. Initiation of Phreatomagmatic Activity

The type of initial activity to a great extent controls the subsequent evolution of the volcano and its ultimate collapse history. It must be stressed that maars and tuff-rings are the product of different mechanisms which account for their differences in structure and products (summarised in Chapter 4). However, these terms apply to end members of a continuum, each of which may evolve into one another (Lorenz, 1973). At any given time, therefore, a tuff-ring may eject products more characteristic of maars or even scoria cones depending on the amount, rate and duration of supply of external water as well as other factors. The most important factors, and those which have been used to classify explosive magma:water eruptions into three types, are 1)the amount of water reaching the magma, 2)the intimacy of the contact and 3)the environment in which this occurs. The three types defined by Camus et al. (1981) are phreatic, phreatomagmatic (s.s.) and surtseyan, used strictly to define types of volcano which are morphologically distinct and formed under different conditions.

7.1.1 Surtseyan eruptions

Surtseyan eruptions will be described first, since

the Surtsey eruption of 1963-67 is one of the best-documented of all eruptions. Any model for this type of activity has to explain the following characteristic features (see Chapter 4) :-

a) Submarine fissure eruption rapidly evolving to single vent activity

b) Very low proportions of accessory lithic material in the ejecta

c) Activity becomes strombolian only when crater becomes sealed off from the sea

d) Abundant evidence of slumping of material into crater and subsequent reworking by explosions

e) Variation from steam explosions to tephra-laden jets with some periodicy in the timing of major blasts

f) Inclined eruption blasts and base-surges often observed

g) Little evidence of post-volcanic subsidence at the surface.

The low accessory lithic content and the lack of appreciable post-volcanic subsidence strongly suggest that this type of volcano is not underlain by a diatreme which cuts deep into the rocks beneath the sea-floor. Instead, a fissure opens and allows rising magma to directly contact seawater, forming a pile of hyaloclastite debris. The following model for this type of activity is summarised in Fig. 7.1 and will be described in detail in the text.

Stage 1

In the initial stages (Fig. 7.1a), water flashes to steam and forms a carapace around the granulated pile, insulating it from the rest of the water. Small steam explosions trigger more widespread explosions by slightly raising ambient pressures in the pore-waters of the pile (Nelson & Duda, 1982). The continued extrusion of magma sets up instabilities in the pile, which becomes slumped and forms fluxoturbidites.

No truly explosive, pyroclastic activity has yet occurred, because steam can freely expand outwards away from the magma. As well as collapsing outwards, the unconsolidated pile continually subsides onto the underlying fissure. Irregular fragments of wet ash are engulfed by the magma as it is extruded, These fragments

are rapidly heated and steam expands outwards, disrupting the partly chilled outer skin of the magma and allowing further incorporation of wet ash. The overburden of the pile of shattered debris suppresses steam explosions and may direct them inwards into the magma, causing further disruption and mixing of magma and wet sediment.

Colgate & Sigurgeirsson (1973) suggested various ways in which magma and water may be thoroughly mixed. Industrial analogues of this process, when a hot fluid mixes with a cold, vapourisable fluid, have sometimes occurred with disastrous results. Here, mixing becomes self-sustained as each explosion increases the interaction between hot and cold fluids. The process rapidly leads to all the heat of the hot fluid being used up in vapourising the cool fluid. The interaction causes fuel-coolant explosions which are exceptionally violent and have strengths comparable to nuclear bomb detonations. Colgate & Sigurgeirsson (op.cit.) speculated that some of the most violent volcanic eruptions, such as Krakatoa, may have been the result of fuel-coolant explosions.

Self & Sparks (1978) describe plinian analogues of basaltic phreatomagmatic volcanoes which result from the interaction of silicic magma with water. They propose that such highly explosive eruptions result from magma/water interaction, superimposed on fragmentation imparted by earlier vesiculation. This leads to a large surface area of fragmented magma contacting water, initiating fuel-coolant interactions. In silicic magmas which source plinian eruptions, volatile exsolution becomes increasingly marked as the magma nears the surface, and disrupts it into a dispersion of released gas and liquid/plastic fragments (Wilson, 1980). The exit velocity through the vent is commonly above $100ms^{-1}$ and discharge rates are also very high. Thus, if erupted subaqueously, a well-dispersed mixture of magma fragments would interact very fully with the surrounding water. Basaltic magmas which source strombolian eruptions are disrupted by coalescence and bursting of large bubbles which occurs very near the magma surface, ejecting spatter (Wilson, op.cit.). Magma rises at only a

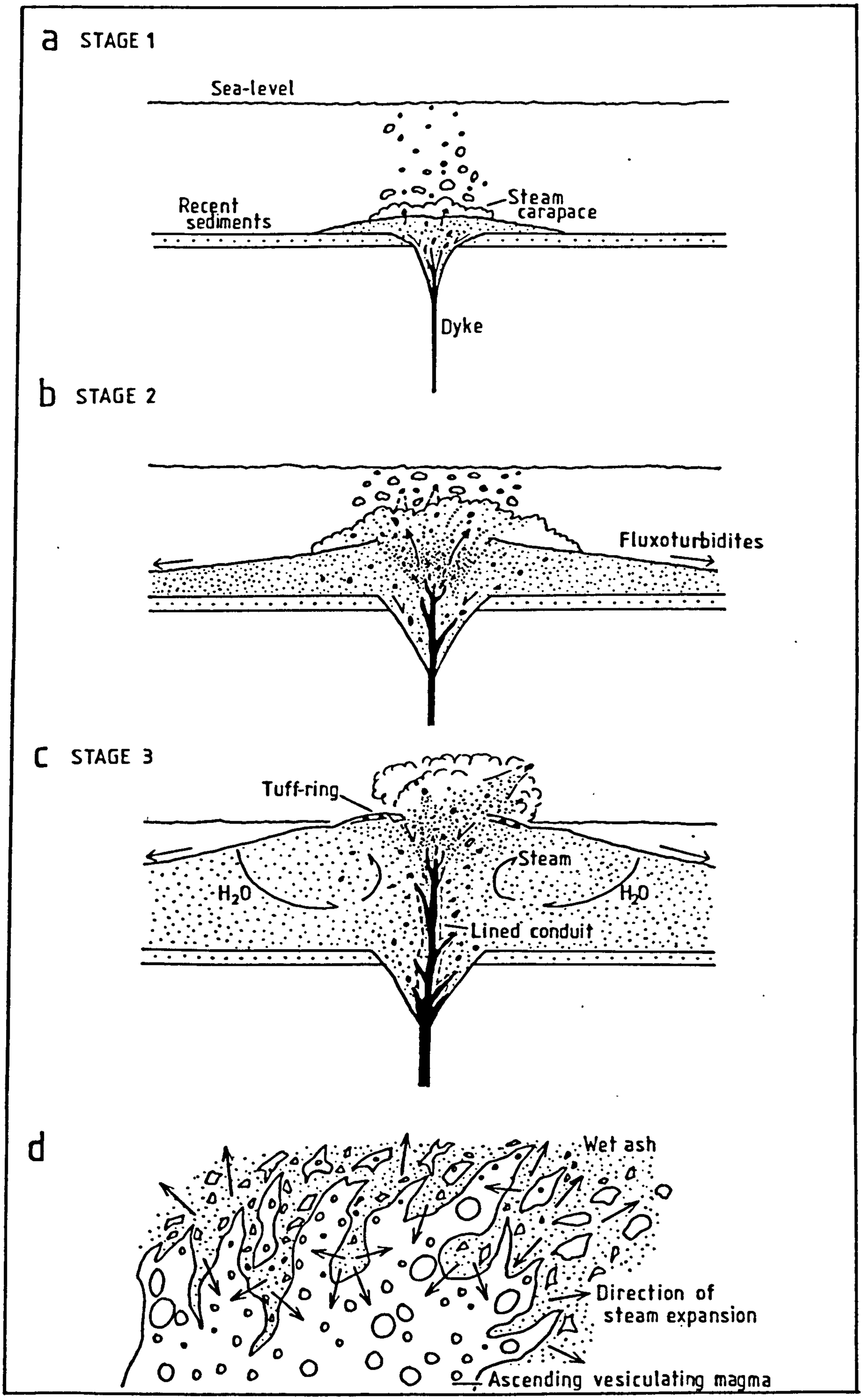

Fig. 7.1 a)-c) Evolution of a surtseyan tuff-ring. See text for description.
d) Contact of magma with wet ash. Note direction of steam expansion jets which further disrupt the magma.

few metres per second in the conduit and ejection velocities are low compared with plinian activity. The magma is thus vesiculating when it is erupted subaqueously, but the degree of disruption and rate of mixing of magma and water is many times less than in plinian eruptions. This explains why intensively explosive fuel-coolant interactions do not occur in basaltic phreatomagmatic activity, and why low dispersal tuff-rings rather than extensive plinian ash sheets are formed.

Phreatomagmatic explosions (s.l.) may become self-sustaining for a short time but never culminate in exceptionally violent explosions. The fact that at Surtsey the explosions were almost silent (Thorarinsson et al., 1964) strongly suggests that fuel-coolent explosions, which result in loud detonations, did not occur. The reasons for the lack of self-sustaining reactions are as follows :-

i) Magma effusion rate is too slow to cause rapid extrusion of large volumes of hot fluid. As soon as small amounts of extruded magma come into contact with water they are chilled and explosively granulated. Explosions disrupt only the outer skin of the magma, preventing whole-scale mixing. Volatile exsolution has only slightly fragmented the magma before contact with water, and this also reduces effective heat transfer and thus explosivity.

ii) Escape of steam jets outwards through the unconsolidated hyaloclastite pile continually removes hot ash particles. The pile is thus cooled and its pore-water only locally approaches boiling temperatures. This prevents explosive spontaneous vapourisation of the pore-waters.

iii) The surrounding water is too abundant to allow vapourisation of more than a small proportion of it by explosive mixing. Input of water rapidly damps down any explosion before it can become fully self-sustaining.

Stage 2

The pile of granulated debris grows upwards and outwards although much material is transported away by slumping (Fig. 7.1b). As the pile grows, the pore-water in the material around the fissure is vapourised, and thus magma can rise further into the pile since it is insulated

by a steam carapace. Only at the upper margins of the pile is this insulation destroyed by explosions and collapse of overlying material. The magma also lines its conduit with chilled basalt as the pile grows upwards.

The explosions in the upper part of the pile form an unstable, expanded dome filled with steam which sits above the magma. Such a steam-dome was observed at Surtsey as the pile neared the surface (Thorarinsson, 1967). Explosions eject shattered magma droplets into this cavity, allowing some material to cool slowly enough to form tachylite. Surtla, a subaqueous vent near Surtsey which never had a subaerial expression, contains tachylite and lapilli with fluidal shapes thought to have formed in this way (Kokelaar, in press).

Stage 3

Once the pile builds up above the water surface (Fig. 7.1c) the amount of water reaching the magma is reduced. However, large amounts of water can still percolate through the subaqueous pile. The lack of water overburden means that steam jets can expand much more readily, and a wide tephra-ring is constructed. This lack of overburden, however, means that water is not continually forced into the magma. Any water which does percolate down through the pile is vapourised as it nears the magma and does not explosively interact with it.

The continuing phreatomagmatic activity is due to incorporation of masses of wet ash which subside into the magma as it is intruded. The magma has a low viscosity, because of its high temperature and high volatile content. Camus et al., (1981) suggest that steam dissolves in magma involved in phreatomagmatic eruptions and lowers its viscosity still further. This mobile magma is able to thoroughly mix with the wet ash, which is itself highly disrupted by steam expansion. After mixing, explosive steam expansion results in truly phreatomagmatic eruptions.

The periodicity in the explosions may be a function of the rate of magma extrusion and the time needed for water to percolate into slumped tephra and be vapourised. Major periodic blasts may be due to the explosive release of

overpressures generated by slumped tephra masses overlying the magma conduit. Such blasts remove the blockages in the vent and are followed by quiet steaming as water percolates down and directly contacts the magma. Only when slumping has again blocked the vent do pressures begin to build up, culminating in another major blast.

Magma sometimes contacts water at very shallow depths resulting in an abundance of inclined eruption blasts. The blasts excavate a funnel-shaped crater in the tephra, which is continually filled by slumping. Water generally has access to the crater because of breaches in the tephra-ring but when it is temporarily sealed-off the activity changes (Thorarinsson et al., 1964). Whereas previously the explosions were intermittent, now the eruptions change to a continuous uprush of tephra and steam which may continue for many hours. Fully molten lava bombs are ejected and the eruption column may reach 2km in height. This type of activity is caused by rapid exsolution of dissolved volatiles in the magma, along with some chilling due to contact with water. The activity might be termed phreato-strombolian, since true fire-fountaining does not occur. Some strombolian activity only occurs once the vent is completely isolated from the sea.

The negligible amount of observed post-volcanic collapse (Tryggvason, 1968) on Surtsey is due to the absence of a deep diatreme beneath the volcano. Subsidence of crater tuffs is limited by the size of the funnel-shaped crater which is itself rather small. The lack of a diatreme also explains the lack of accessory lithics in the tuffs, since few country rock fragments were entrained by the magma as it rose up its source fissures. Only seafloor sediment material is found as lithic fragments, indicating that only on intruding these wet sediments did explosive activity begin. Other examples of surtseyan volcanoes include Capelinhos, Azores (Camus et al., 1981); Myojin Reef, Japan (Moore, 1967) and some of the tuff-rings at Fort Rock, U.S.A. (Heiken, 1972).

7.1.2 Phreatomagmatic eruptions (s.s.)

This type of eruption is very similar to surtseyan, except that magma contacts water at greater depths below the contemporaneous ground surface. This can occur when magma intrudes a thick sequence of newly-deposited, water-laden sediments or contacts groundwater in a thick aquifer. Water may also gain access along pre-existing fault planes up which magma is ascending or fissures which open up ahead of rising magma (Lorenz, 1973).

Lorenz et al., (1970) state that vapourisation of water occurs only adjacent to the intrusion, and unless this lies at a very shallow level no breakthrough to the surface can occur. In the case of poorly-consolidated sediments, intrusions are likely to take the form of sills. Convection causes circulation of a rising current of heated water above the intrusion. The final result is that a column of pore-water in the sediments is brought to boiling temperature appropriate to the corresponding depth from the surface. The column finally reaches the complete distance from the intrusion to the surface. An explosive, purely phreatic eruption due to vapourisation of heated groundwater at the surface then propagates downwards as a decompressional wave (Lorenz et al., op.cit.). This wave taps the magma which then rises into the pipe, carrying fragments of country rock upwards.

Downward migration of the eruption focus causes explosions at progressively deeper levels and brings up fragments of the underlying country rocks. A diatreme is thus excavated, which is filled with juvenile and lithic material, and tuffs subsided from the tuff-ring. Surface processes are the same as surtseyan activity since magma: water interactions are the driving mechanism, except that subsidence into a diatreme occurs. Often, surface water is present in addition to groundwater at depth and it may be difficult to distinguish tuff-rings underlain by diatremes to those lacking such features.

This type of activity commences with phreatic explosions, which disrupt the country rocks and form a diatreme. As magma rises up the diatreme and sources

phreatomagmatic eruptions it gradually transforms the initial maar into a tuff-ring (Lorenz, 1973). Such tuff-rings may be characterised by wide craters which lie only slightly above the level of the surrounding region, which represent infilled maars. The oldest ejecta of such volcanoes are often rich in accessory lithics, although later products tend to mask them. Their subsidence history is often indicated by thick successions of reworked pyroclastics deposited from post-volcanic crater lakes.

Once a diatreme has been formed it is enlarged by spalling of the wall rocks. Small blocks are commonly carried upwards and rounded by gas streams whereas large rafts subside, sometimes without suffering breakdown or abrasion (Cloos, 1941). Thus, at any given time a tuff-ring of this type may erupt substantial amounts of comminuted wall rock material. Keller (1974) describes one composite volcano in Anatolia which began with the formation of a tuff-ring in a shallow lake. Later explosions had a deeper focus and formed a maar crater which dissected the tuff-ring. Subsidence was accompanied by scoria fire-fountaining presumably as the magma became isolated from the surrounding groundwater. Other examples of phreatomagmatic tuff-rings include Hverfjall, Iceland (Lorenz et al., 1970); Velay, France (Camus et al., 1981) and Split Butte, U.S.A. (Womer et al., 1980).

7.1.3 Phreatic eruptions

This type of eruption is initiated in the same way as the phreatomagmatic eruptions previously described. Essentially, heated groundwater is vapourised above a moderately shallow intrusion and drills a diatreme to the surface. The main difference is that magma does not intimately mix with the water but merely heats it, sourcing purely steam-blast explosions. This activity forms maars which, because they eject many wall-rock clasts but little juvenile material, develop deep craters.

Lorenz et al. (1970) note that maars may also form by subsidence as a result of withdrawal of magmatic support and that high proportions of accessory lithic material need

not be present. Depending on the amount of subsidence maars may be formed by both phreatic and phreatomagmatic activity. By definition, therefore, maars possess deep diatremes into which material subsides. When only eroded diatreme deposits are present in an area, it is difficult to determine whether their surface expression was a maar or phreatomagmatic tuff-ring. Only when the diatreme tuffs contain substantial amounts of accessory lithic clasts can a maar origin be proposed. Other features which favour a maar origin include evidence for collapse of surface-deposited material to substantial depths, diatremes with large diameters and evidence of widespread gas-streaming (thought to be a more common process in the larger diatremes of maars).

Since maars and phreatomagmatic tuff-rings are formed by a similar range of processes the determination of the surface expression of diatremes is probably of doubtful validity. More important is to determine whether phreatic or phreatomagmatic processes formed the now collapsed diatreme deposits, since this indicates the degree of wall rock disruption.

7.1.4 Deep diatremes

Some diatremes, such as kimberlite pipes were, until recently, thought to have originated at great depths and penetrated upwards by mechanisms unrelated to shallow phreatic or phreatomagmatic explosions (Lorenz et al., 1970). However, even these diatremes terminate downwards in dykes at depths of 3km or less below their supposed eruption surface (Hawthorne, 1975). Lorenz (1975) has proposed that formation of the diatremes resulted from contact of kimberlitic magma with groundwater, initiating phreatomagmatic eruptions. The evidence he presents is convincing and leads to the conclusion that most, if not all diatremes, formed in various structural settings and from magmas of varying composition, are the result of near-surface magma:water interaction.

The role of explosively exsolved magmatic CO_2 in forming diatremes cannot be ruled out (Coe, 1966). Kennedy & Nordlie (1968) suggest that this process aids sampling of

deep-seated levels in the crust and upper mantle by detonating into short-lived fractures, carrying fragmented wall rocks. However, as Lorenz (1980) points out, ascent of volatile-charged magmas often occurs along planes of crustal weakness. The rising magma reacts with groundwater which accumulates in the upper levels of the fractures. Since the amount of water which reaches the surface is small, diatremes are formed. Larger quantities of melt reaching the surface will rapidly use up the available groundwater and initial phreatomagmatic deposits are buried beneath scoria and lava flows (Fig. 7.2).

It must be emphasised yet again that diatreme formation by phreatomagmatic processes is purely a high-level phenomenon. These processes merely require that ascending magma contacts water at depths shallow enough to allow vapourisation to occur, generally resulting in diatreme breakthrough to the surface. Diatreme formation thus indicates nothing about the origin, physical properties or ascent mechanisms of magmas from deep levels, nor does it say anything about the sampling and transport of mantle or other deep-seated xenoliths.

7.2. Diatreme Processes

Once a diatreme has been formed beneath a surface volcano numerous processes occur which result in features now observed in eroded examples. Such processes have been summarised by many authors (references in Lorenz et al., 1970) and will merely be listed here :-

a) Flow-banding
b) Ball-milling
c) Fluidization
d) Explosive fragment comminution
e) Wall rock bursting and spalling
f) Subsidence along faults, by slumping and during defluidization
g) Magmatic intrusion

Lorenz et al. (op.cit.) used the term fluidization to describe all processes in which dense particles are distributed within a rising liquid or gas phase.

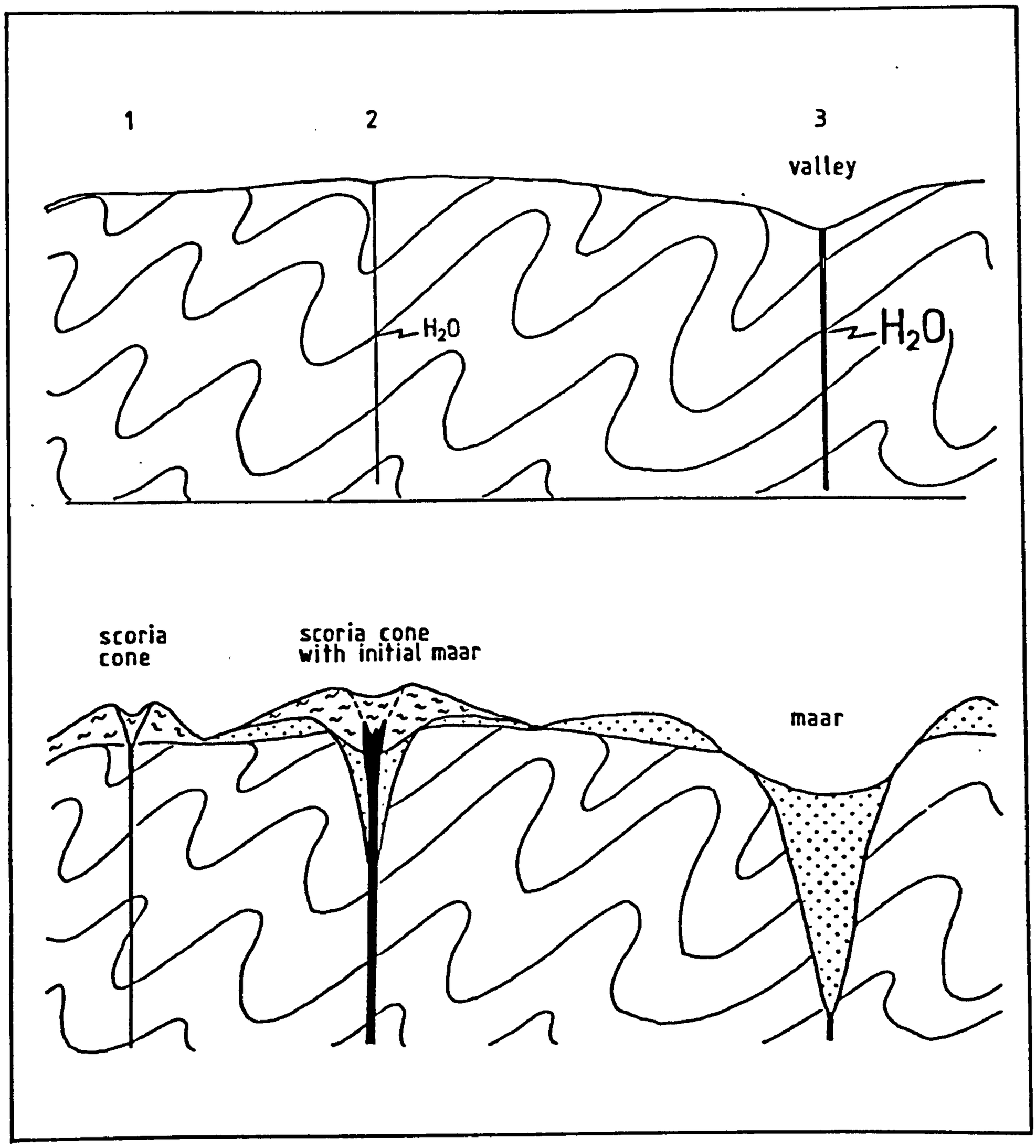

Fig. 7.2 Influence of hydrogeology on the formation of maars, after Lorenz (1980).
1: Ascending magma reaches the surface without contacting water and forms a scoria cone.
2: Ascending magma rises up a healed fracture which contains small amounts of water. An initial maar forms which is buried beneath a later scoria cone after the water is used up.
3: Ascending magma rises up an "open" fracture which underlies a surface valley and thus contains abundant water. A large maar is formed.

Wolfe (1980) criticised their definition of fluidization as applied to diatremes and noted that only very high velocity gas-streaming or explosions could support or raise dense lithic fragments within such breccia pipes. He concluded that true fluidization is only involved in pyroclastic flows and flow-banded tuffisitic intrusions.

Nevertheless, many examples of large blocks in diatremes are found to have subsided, or more rarely risen, without suffering the intense comminution expected if explosions had emplaced them. It is thought that explosions at the base of the diatreme momentarily fluidize the surrounding particles and might, by a series of bursts, allow large blocks to gently subside over great distances. Smaller blocks would be thrown upwards by the blast, and channels filled with high velocity particle streams would dissect the diatreme material. Ejection and reworking of a large part of the diatreme infill would only occur if explosions were very powerful or had a shallow focus.

The role of continuous, smaller explosions is thought to be most important in sorting and milling the materials within the diatreme. Large blocks subside and are broken down into smaller fragments which are then able to ascend in the diatreme as explosions continue. As a general rule, the deeper the source of the clasts, the smaller their maximum diameter, indicating an emplacement mechanism able to produce size-sorting with time (McGetchin, 1966). Some maars contain deep-seated xenoliths which occur as discrete, well-rounded fragments that increase in abundance and size with upward stratigraphic position in the ejecta, and therefore with time in the eruptive sequence (McGetchin & Ullrich, 1973). Migration of explosion foci downwards as decompression waves tap the magma is thought to account for this phenomenon.

7.3. Surface Volcanic Processes

At the surface the processes which occur in phreatic, phreatomagmatic and surtseyan volcanoes are very similar and consist essentially of airfall and base-surge deposition.

7.3.1 Airfall processes

Airfall processes are well understood and the main differences between airfall deposition from phreatomagmatic volcanoes and those where water played no part in the eruption are in the size, density and stability of the eruption column. Phreatomagmatic eruption columns tend to be lower, less expanded and more liable to collapse (Wilson et al., 1978). Most of the tephra formed in phreatomagmatic eruptions is thus deposited near the vent. Even fine particles, which in other eruption-types are widely dispersed by convection currents and winds, are proximally deposited. This is due to the formation of accretionary lapilli, principally at low levels in the column, and by flocculation of ash into clumps (Self & Sparks, 1978). Such clumps form in the steam-rich column and often do not develop into accretionary lapilli, and are thus difficult to detect in ash deposits.

7.3.2 Base-surge processes

The origin of base-surges has been briefly discussed in Chapter 4 (Section 4.1.), as have some of their observed features and deposits. In this section some attempt will be made to review the origin of surges and to relate sequences in their deposits to the different regions of surge clouds thought to have deposited them.

Eruption characteristics

Surges can be formed at any time during volcanic activity but are most common at the beginning of powerful eruptions. Surges may be associated with shallow blasts which eject tephra in all directions, or may occur during strongly vertically-directed eruptions. Although column collapse need not always directly feed horizontal surge clouds, the vast mass of falling tephra may force subsequent eruption blasts sideways with the same effect.

Nuclear explosion tests have shown that there is an optimum explosion depth for surge production, which varies according to the strength of the blast and the type of overburden (Moore, 1967). For poorly-consolidated tephra this is probably quite shallow but it must be stressed that

surges of lesser range do form from explosions of depths other than the optimum.

An interesting natural analogue of this situation is cited by Schmincke et al. (1974), who describe maars on Gran Canaria, Canary Islands. Here, they state that increasing diameter and depth of the three craters correlates with the increasing size of ejected blocks and the greater volume of pyroclastic deposits, ratio of accessory to juvenile fragments and the degree of base-surge transport. Assuming that the contact of magma with groundwater was at the same level for each maar, the most powerful eruptions sourced more base-surges. This factor controls the formation of surges and it may be proposed that to form surges of optimum range, maars must be fed by more powerful explosions than tuff-rings, since the latter volcanoes generally have deeper explosion foci. The effects of variation in explosion depth and power explain why some maars, such as Pulvermaar, W. Germany have high proportions of surge deposits and other maars, such as Tazenat, France have low proportions of surge deposits.

Surge models

Fisher (1979) developed a model for surge formation which he ascribed to progressive collapse of eruption columns. Flow-differentiation within the conduit concentrates larger clasts towards the centre of the column as it is erupted. Fisher's (1979) model requires that a finer-grained sheath around the column becomes partly mixed with air as collapse continues. A relatively small-volume, low-concentration surge thus precedes the main pyroclastic flow which results from collapse of the coarser interior of the eruption column.

This model adequately explains ground surge deposits which commonly underlie voluminous pyroclastic flows, but fails to account for many of the features of base-surges. Base-surges may emanate directly from the vent (primary base-surges) or form as a result of column collapse (secondary base-surges) (Moore, 1967). They are not succeeded by voluminous pyroclastic flows but thin, coarse, poorly-sorted deposits associated with cross-bedded tuffs

may represent the phreatomagmatic analogue of such flows. It is proposed that shallow explosions source primary base-surges whereas deeper explosions form ascending eruption columns which collpase to form secondary surges. If column collapse occurs rapidly, secondary surge pulses feed the primary surge which is often more steam-enriched (Moore, 1967). Sometimes, as at the Ukinrek Maars, Alaska (Kienle et al., 1980) small phreatomagmatic explosions form primary surges after the cessation of a major column-forming eruption. This indicates upward migration of magma after the end of the major eruption, forming surges which in this case were strongly directionally controlled by notches in the maar rim and by shallow valleys around the vent.

Wohletz & Sheridan (1979) proposed a model based on observations of surge deposits, which they divided into three facies - massive, planar and sandwave - on the basis of their dominant bedforms. They maintained that pyroclastic surges are initially fluidized systems which deflate with time outwards from the vent. During transport the cloud passes from a proximal viscous mode of flow, characterised by deposition of the sandwave facies, to a distal inertial mode of flow represented by deposition of the planar facies. The gradual transition from viscous to inertial is coincident with deposition of the massive facies. Their model, however, refers to pyroclastic surges which, unlike base-surges, contain minor amounts of steam. This steam content accounts for many of the characteristic features of base-surge deposits (see below).

Although it is agreed that surges will decrease in thickness with time as particles settle towards the bed, the present author considers that fluidization is not a correct term to apply to their transport mechanism. Fluidization requires that an externally supplied fluid be forced upwards through a mass of grains such that their weight is balanced by the fluid drag. The only external source of fluid in base-surges is that ingested at the flow head, resulting in a mechanism known as bulk self-fluidization (Allen, 1982). As will be discussed later this ingestion is too limited to result in more than short-lived

fluidization within the head of the surge. Grain self-fluidization, in which the fluid phase comes from gases exsolved from the fluidized particles themselves, has been considered an important process in pyroclastic flows (Sparks, 1976). However, this process is thought to be unimportant in base-surges, which contain rapidly quenched tephra.

The surge model proposed by the present author draws analogies with turbidity currents, which are better understood and have been the subject of much research. Both base-surges and turbidity currents are dissipative gravity-current surges which derive their excess of density from the presence of internally-dispersed particles (Allen, 1982). Near the vent surges contain both fine and coarse tephra, with hot steam as the enveloping fluid. Outwards, the coarse tephra falls out and the steam cools, leaving fine, moist, suspended tephra which may clump together and be deposited on cohesive particle-capturing beds. Thus, the surge cloud density decreases outwards, as does its effective thickness due to settling of particles.

Three main regions in surges are thought to be responsible for depositing material by different mechanisms :-

a) The head region

Lobes-and-clefts seen on the head of surges (Fisher, 1977) form as a gravitational instability effect and are related to the continuous engulfment of the ambient fluid (air in base-surge clouds). This mixing dilutes the concentration of material in the head and causes increased turbulence (Fig. 7.3), maintaining at least fine tephra in suspension. The amount of air admixed at the head decreases as its overhang height decreases. Overhang height and the thickness of the head are a function of the Reynolds number of the surge (Simpson, 1972). Measurements by the present author from photographs of surge clouds indicate that the ratio of their overhang height to head height varies from 0·03 to 0·1, agreeing well with the predicted values for such high Reynolds number flows. The low value of this ratio in surges indicates that the effect of air ingestion at the head is of limited importance, as is also the case in many turbidity currents (Middleton & Hampton, 1976).

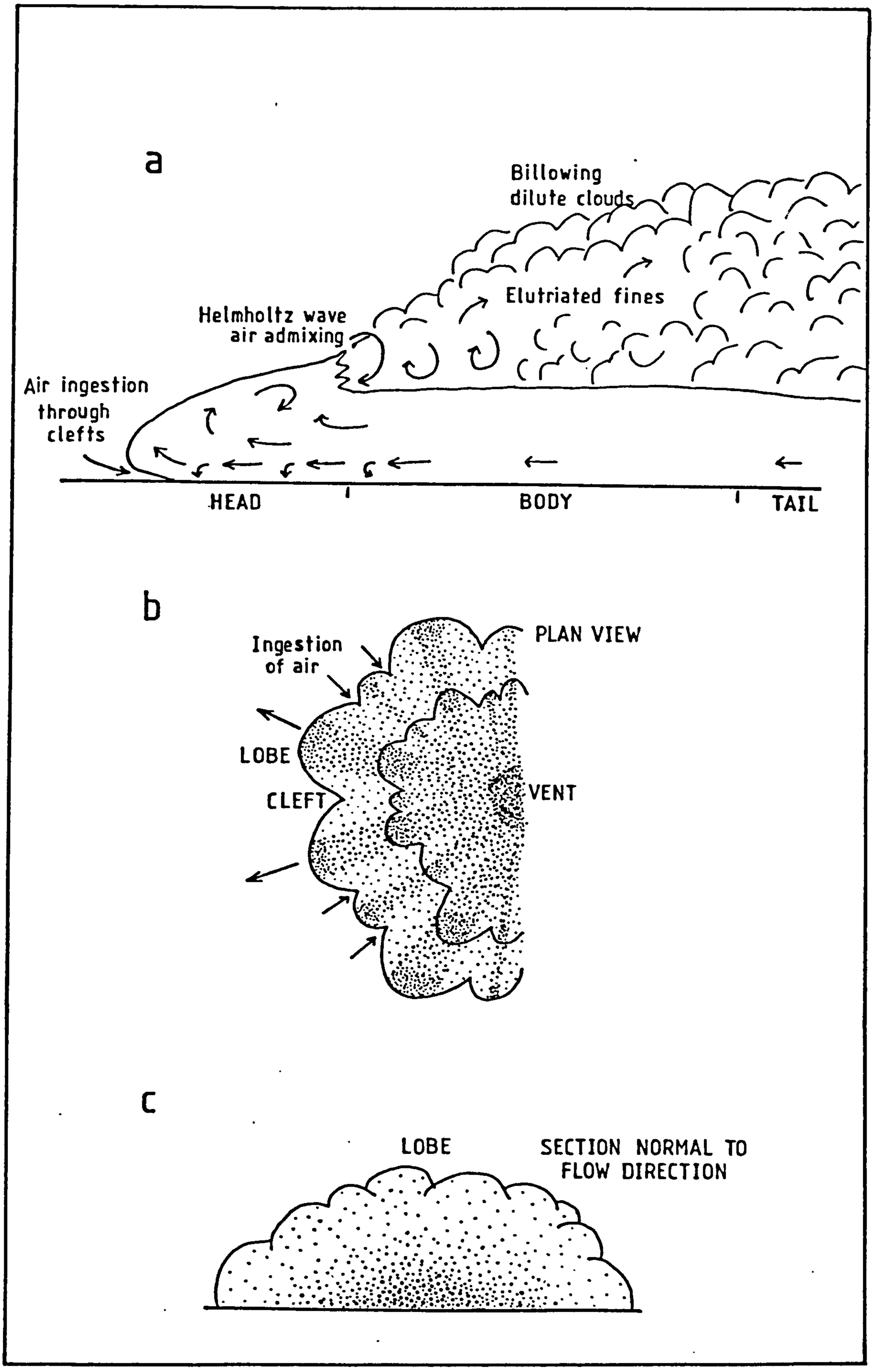

Fig. 7.3 Structure and features of base-surges.
a) Section showing flow directions and air ingestion mechanisms.
b) Plan view showing lobe-and-cleft structures and successive surge pulses.
c) Section of surge lobe showing particle concentrations within it.

The lobate nature of the head may be important in forming both erosional and accretionary grooves. Fisher (1977) attributed surge channels to erosion by the lobes on the front of surges. Allen (1982) suggested that lobes and clefts imply the existance of transverse variations in shear stress and therefore sediment transfer rate. Where these rates are positive, radial ash waves form but grooves form between these where the rates are negative. The different rates of sediment transfer are independant of the occurrence of lobes or clefts.

b) The body region

The body of a turbidity current has an approximately constant thickness and, if the current surge is large, flow in the body approximates a steady, uniform state (Middleton & Hampton, 1976). Since the body constitutes most of the surge, it follows that most sediment is carried and deposited from this region. Mixing with the ambient fluid does occur along the upper surface of the body (as Helmholtz-type waves), but is likely to be of minor importance (Allen, 1982).

c) The tail region

The tails of turbidity currents and pyroclastic surges are thin and more dilute than the other regions, and carry mainly fine sediment, much of it in suspension.

Mixing due to billows on the top of the head region (Allen, 1982) leads to marked dissipation of gravity-current surges. Fine material and steam is constantly lost from the base-surge by this mechanism, forming voluminous clouds which expand slowly due to turbulence and mixing with air. The lower parts of these expanding clouds are dragged along by the moving surge below and may deposit thin layers of fine ash after the surge has passed (Fig. 7.3). Such clouds of elutriated fines are the surge equivalent of co-ignimbrite ash clouds (Sparks & Walker, 1977). In base-surges such clouds are liable to be poorly expanded due to condensation of steam preventing turbulent convection, and are probably the source of much of the accretionary lapilli found in proximal surge deposits (Hoblitt et al., 1981). Thin airfall layers from such clouds are only liable to be

found above the last surge deposit from a particular eruptive phase, since the clouds will be ingested and reworked by succeeding surges during pulsatory surge activity.

Surge depositional mechanisms

A characteristic vertical sequence of sedimentary features is found in the surge deposits of East Lothian (Chapter 5), Fife (Chapter 6) and examples from the literature. The Saefell (Chapter 2) and Medano (Chapter 3) surge deposits contain similar but less complete sequences.

The idealised sequence has been described in detail previously (Section 5.3.2) and its deposits subdivided into three divisions, here named 1, 2 and 3 to distinguish them from the Bouma divisions of turbidities. The sequence comprises a basal poorly-stratified, blocky unit (Division 1) overlain by well-bedded, often cross-bedded tuffs (Division 2) with an overlying massive unit (Division 3) which often exhibits marked lateral thickness variations.

Division 1

These coarse tuffs are thought to be basal lag breccias transported as a traction carpet beneath the head region of surges (Fig. 7.4). Particle segregation by size or density is prevented by rapid deposition rate relative to transport rate. High particle concentrations in this basal region inhibit turbulence, which also prevents sorting. The block trails which define a crude stratification probably represent the deposits from pulsatory surges whose bed-load fluctuates rapidly in thickness and grain size. Poorly-developed normal grading is a result of an upward and backward decrease in particle size and concentration in the head.

Division 2

This division is thought to represent the deposits from the body behind the surge head (Fig. 7.4). Here, particle concentration, size and deposition rate are low enough to allow turbulent sorting and grain-by-grain deposition to occur. Plane beds and dune cross-bedding are formed, rare normal grading being developed due to more rapid deposition of coarser particles.

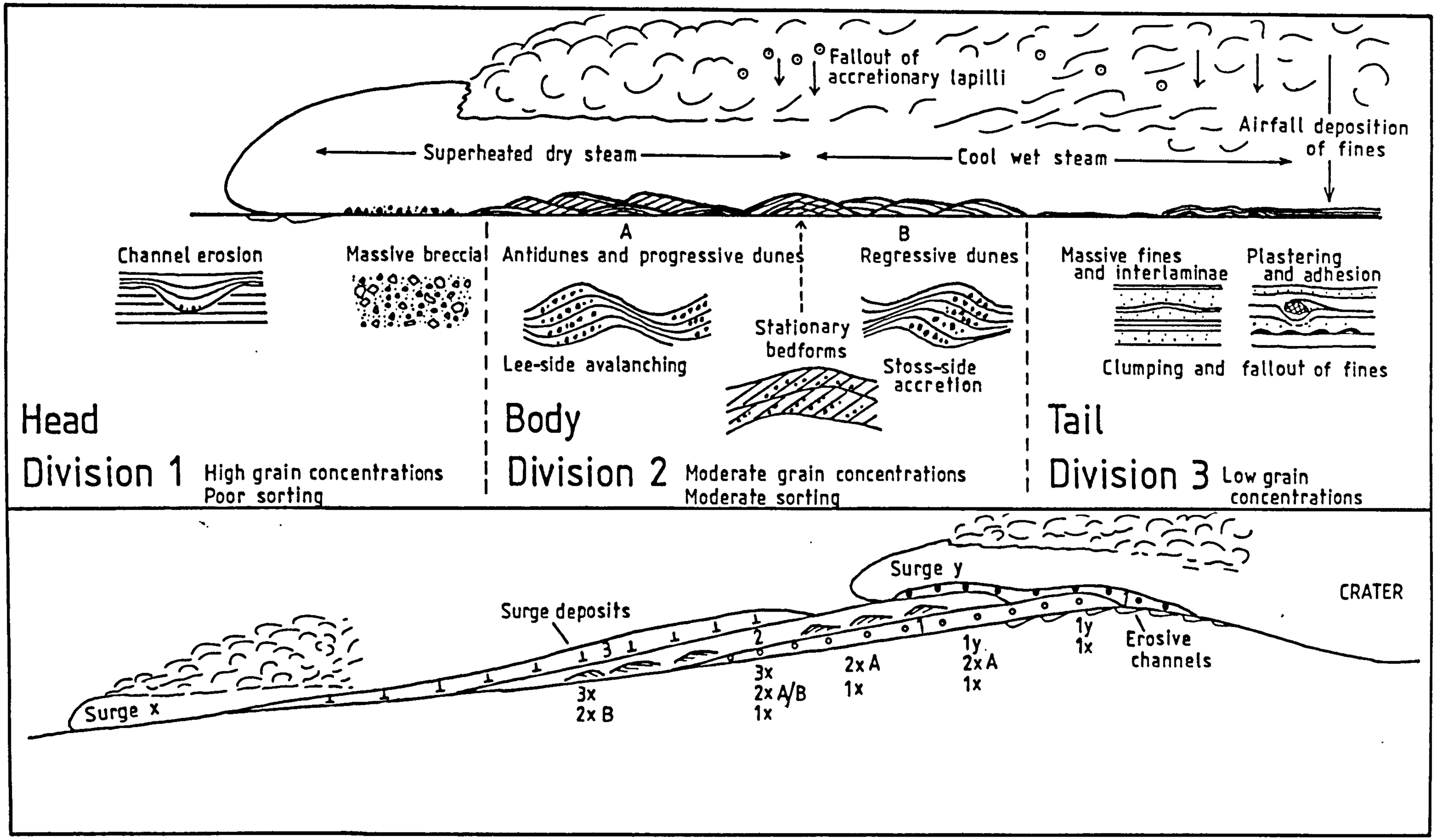

Fig. 7.4 Base-surge depositional mechanisms and structures. Note the effects of successive surge pulses on proximal surge sequences.

Erosion of previously deposited layers is indicated by the occurrence of truncated cross-sets although often complete bedforms are fully preserved, probably because of rapid deposition rates.

Division 3

This division is thought to represent the deposits from the rear of the body and the tail of the surge (Fig. 7.4). Its lack of well-defined bedding or grading suggests that particle deposition rates were too high to allow size-sorting. Such rapid deposition rates are probably due to clumping and fallout of cohesive tephra in a part of the surge where steam is cooling and condensing. The deposits of this division resemble thinner, finer analogues of those from pyroclastic flows, in which sorting is also poor (Walker, 1971). The lateral thickness variations in Division 3 are the result of preferential deposition in even small topographic depressions. Pyroclastic flows behave like other fluids and do not adhere to slopes, causing them to pond in hollows. Division 3 is often thinly developed, partly because surges carry most material in the head regions and because the next surge pulse will "consume" the tail and body of the preceding pulse. Even within one discrete surge, the head decelerates more rapidly than the body and the surge eventually consumes itself (Allen, 1982).

Comparison with turbidite divisions

Turbidites have been divided into five main divisions based on characteristic internal features, and these have been interpreted as the deposits of decelerating flows. The structures within the divisions indicate decreasing flow power with time as turbidite deposition continues. Division 1 of base-surge deposits is approximately analagous to Division A of turbidites since both are coarse, massive and normally graded. Division 2 is analagous to turbidite divisions B and C, since all contain plane and cross-bedded layers.

Division 3 has no analogue in turbidites, perhaps because the much more rapid particle fall velocities in base-surges cause their body tephra to be deposited en masse. The much slower particle fall velocities in turbidites

allows grains carried in the body to be sorted before deposition, forming bedded layers. The moisture in surge clouds probably prevents their becoming as well expanded as turbidity currents, which also inhibits sorting within them. The E division of turbidities corresponds to the airfall deposit from the ash cloud above base-surges, rarely seen because of the frequency of subsequent surge pulses.

The decreasing flow power of surges has previously been discussed using the concept of flow regime (Section 2.3.4). As Allen (1982) states, the use of flow power or bed shear stress is more meaningful when applied to turbidite and surge structures. Decreasing flow power outwards from the vent and the outward cooling of super-heated steam lead to proximal surge deposits containing Divisions 1, 2 and 3, and more distal surge deposits containing only Divisions 2 and 3 (Fig. 7.4). This is observed at Saefell (Chapter 2) where distal surge deposits contain cross-bedded and massive tuffs but lack a basal coarse division. Associated thin airfall tuffs at Saefell may represent deposits from the ash cloud above surges. The presumed proximal deposits from the East Lothian (Chapter 5) and Fife (Chapter 6) diatremes contain all the surge divisions. Similar sequences of deposits were recorded from the 1980 Mt. St. Helens directed blasts, where proximal, coarse, basal tuffs are overlain and gradually outwardly replaced by surge deposits and finally fine airfall tuffs (Hoblitt et al., 1981), and from the Laacher See surge tuffs (Schmincke et al., 1973).

Wohletz and Sheridan's (1979) study of pyroclastic surge deposits indicates there are three main types, sandwave, massive and planar. Some of their figured sections show transitions similar to those seen in base-surge deposits studied by the present author. Differing transitions and surge sequences from those presented above may be partly explicable because Wohletz & Sheridan studied mainly distal, pyroclastic surge deposits from major eruptions, whereas in the present study only more proximal, base-surge deposits of rather small eruptions have been examined. The transition from hot, dry steam to cool, wet

steam is not discussed by Wohletz & Sheridan and may explain many of the features of base-surge deposits.

Steam condensation

The effect of cooling of hot, dry steam to cool, wet vapour in base-surges with time has been discussed previously (Sections 2.3.2, 4.2.1). This process does not occur in turbidity currents and accounts for many of the different structures in surge deposits compared to turbidites. Allen (1982) suggested that as steam cools, progressive (i.e. downstream migrating) bedforms change to regressive (i.e. upstream migrating) types due to increased stoss-side particle capture by cohesion. He states that this important difference between surge and subaqueous bedforms means that dunes, antidunes and chute-and-pool bedding do not occur in a hydrodynamic sense in base-surge deposits.

The present author agrees with this conclusion but, since dunes and antidunes may be used as purely descriptive terms (cf aeolian versus subaqueous "dunes"), this means that it can still be, and has here been used to describe the broadly sinusoidal shape and structure of certain bedforms. This is acceptable as long as attempts are not made to apply formulae determined for subaqueous systems to surge deposits to derive estimates of the flow speed or other properties. Only in progressive dunes, where evidence for steam condensation is lacking, might such formulae be applied.

So, as well as thinning and fining away from the vent, and becoming dominated by cross-bedded, planar and massive tuffs, surge structures will increasingly reflect the increased "wetness" of the surge clouds. Thus, distal surge deposits will contain vesiculated tuffs, plastering structures, adhesion ripples, regressive dune structures and armoured and accretionary lapilli. The lack of such structures in most of the diatreme surge tuffs studied suggests that they represent proximal, hot, dry surge deposits.

7.3.3 Collapse processes

The processes which allow great thicknesses of

subaerially-accumulated deposits to subside into diatremes have been well summarised by Lorenz et al. (1970). Syn-eruptive subsidence has been proposed for phreatomagmatic volcanoes, in which periodic eruptions fracture and eject wall rock material and subsidence occurs during the periods of repose. The deeper levels of diatremes contain broken-down remnants of bedded tuffs formed at an early stage in the volcanism. Progressively higher levels contain large rafts of country rock or bedded tuff which have subsided by as much as 2km.

Post-eruptive subsidence largely occurs along ring faults which may be the subsurface equivalents of the crater rim unconformities present in maars and tuff-rings. Some ring faults occur outside and concentric to the diatreme margins, and cause subsidence of arcuate slices of wall rocks. Sometimes the inner slices of rock have subsided more than the outer ones, due to frictional drag against the marginal ring faults (Hearn, 1968).

An important fact to note is that the now subsided subaerial tuffs largely represent the deposits from the surface crater of the maar or tuff-ring. That so many of the diatremes studied in this report contain thick successions of well-bedded tuffs indicates that the final phase of subsidence was accompanied by only weak eruptions. Strongly explosive activity would have broken up these thick sequences and ejected many blocks of bedded tuff. The marginal breccias and tuffisitic intrusions in many of the diatremes indicate that late-stage activity was often localised along ring faults. This marginal gas-streaming lubricated the subsidence of the central block which continued to subside slowly after the cessation of volcanic activity.

A qualitative estimate of the relative amount of subsidence of diatreme materials may be achieved by noting the type of diatreme infill now exposed. Deep levels contain mainly intrusive material, higher levels contain more subaerially-deposited tuffs and at the highest levels diatremes are completely occupied by undisturbed tuffs which may contain post-eruptive deposits.

7.4. Comparison of Volcanoes Studied

Detailed descriptions have been given of all the volcanoes in the present study and a model for this type of activity has been erected. The final part of the study is to fit the volcanoes into the model, allowing comparison between examples at a variety of erosion levels.

7.4.1 Recent volcanoes

Saefell (Chapter 2) is wholly analogous to Surtsey, and thus represents a surtseyan tuff-ring. Magma contacted water in a shallow submarine environment, initiating phreatomagmatic explosions which built up a subaqueous pile of hyaloclastite and hyalotuff. Access of water to the magma was maintained by crater breaching after growth of a subaerial tuff-ring. Phreatomagmatic explosions continued by incorporation of collapsed wet tuffs into the magma and by direct contact of water with fragmented vesiculating magma. No major diatreme underlies the tuff-ring, since wall rock incorporation and ejection was of minor extent. The limited subsidence which occurred was a result of compaction of loose tuff in the subaqueous pile and magma withdrawal.

Medano (Chapter 5) is more analogous to a phreatomagmatic, rather than a surtseyan tuff-ring. Its deposits contain many accessory lithic clasts derived from the country rock sequence, and it has a crater filled with subsided reworked tuffs. This indicates that the tuff-ring is underlain by a diatreme into which syn- and post-eruptive subsidence has occurred. Activity was initiated at depth by the contact of magma with groundwater which may have preferentially collected in the fissure which the magma utilised for its ascent. Due to the variations in the water supply, phreatic explosions resulting from low magma:water ratios sometimes brought up mainly lithic clasts. At other times, especially towards the end of volcanic activity, mixed phreatomagmatic/strombolian eruptions resulting from high magma:water ratios ejected scoria, lava bombs and chilled ash.

7.4.2 Ancient volcanoes

The East Lothian diatremes (Chapter 4) are subdivided into two groups, red and green, on the basis of colour, lithic content and internal structure. The red diatremes appear to be exposed at lower structural levels than the green diatremes, since they presently cut thick sedimentary sequences whereas the latter cut green tuffs thought to represent their reworked distal equivalents. The red diatremes were predominantly formed by phreatic explosions which disrupted the unconsolidated country rock sediments. They apparently contain more surge deposits than the green diatremes, which may reflect more explosions at the optimum depth for surge formation. The red diatremes are bounded by major ring faults or shear zones, suggesting that post-eruptive collapse has played an important role in their formation. It is suggested from all the above evidence that the red diatremes contain subsided maar tuffs. Phreatic explosions were initiated by magma contacting abundant pore and ground water held in poorly-consolidated, newly-deposited sediments.

The green diatreme deposits are close to their original eruption surface and have subsided only by a small amount. They generally contain low proportions of lithic material, although some tuffs are rich in quartz grains. The margins of the green diatremes are commonly faulted, but these faults are sharp and probably represent only slight movements compared to the shear zones around some of the red diatremes. It is suggested that the green diatremes contain collapsed tuff-ring deposits. Whether the tuff-rings were surtseyan or phreatomagmatic is unknown, but the lack of evidence of major collapse perhaps indicates they are of surtseyan type, or represent a type of phreatomagmatic tuff-ring with only a small diatreme. Eruptions were initiated by the contact of magma with shallow lacustrine or lagoonal water, plus an input from pore and groundwaters in high level sediments. Perhaps the initial eruptions were phreatic forming a small maar which was transformed into a tuff-ring as more magma ascended to high levels.

The Fife diatremes (Chapter 6) all contain tuffs which

have high proportions of juvenile material. Evidence for initial phreatic eruptions occurs in at least two diatremes, Craigforth and Coalyard Hill, and such activity may have preceded the formation of tuff-rings throughout the area. It is thought that most of the Fife diatremes contain collapsed phreatomagmatic tuff-ring deposits, since up to at least 500m subsidence is thought to have occurred in some cases. One diatreme, Viewforth, is flanked to the W by reworked tuffs and is thus close to its original eruption level. Other reworked tuffs appear to be interbedded with the Passage Group sediments to the W, which are of marine and fluviatile origin. The presence of thin coals and limestones within the diatreme suggests that the environment round the tuff-ring consisted of swampy/shallow marine conditions. The Viewforth volcano may thus have erupted into shallow water and be of surtseyan type. The remainder of the diatremes appear to be the collapsed deposits of phreatomagmatic tuff-rings which had initial phreatic phases. Eruptions were initiated when magma rose along fissures and intruded thick piles of water-laden sediments. Some of the dykes fed sills at high levels, and diatremes formed from heating of ground and porewaters above these. Other magmas rose rapidly from depths of 70km or more carrying deep-seated xenoliths and xenocrysts and formed diatremes by magma:water interaction as they neared the surface.

The Heads of Ayr diatreme (Chapter 6) erupted into a shallow lacustrine/marginal marine environment in which cementstones and mudstones were accumulating. Reworking of the outer flanks of the tuff-ring occurred, although there is no evidence that the crater wall was ever breached. The tuffs contain variable proportions of lithic material, generally highest in the oldest deposits, as well as deep-seated xenoliths. Collapse occurred along ring faults and internal fractures, causing folding of the bedded outer flank tuffs. The volcano is thought to have originally been a phreatomagmatic tuff-ring, initiated by magma:water interaction at depth. Pore-water in poorly-consolidated sediments and surface lakes supplied water to cause

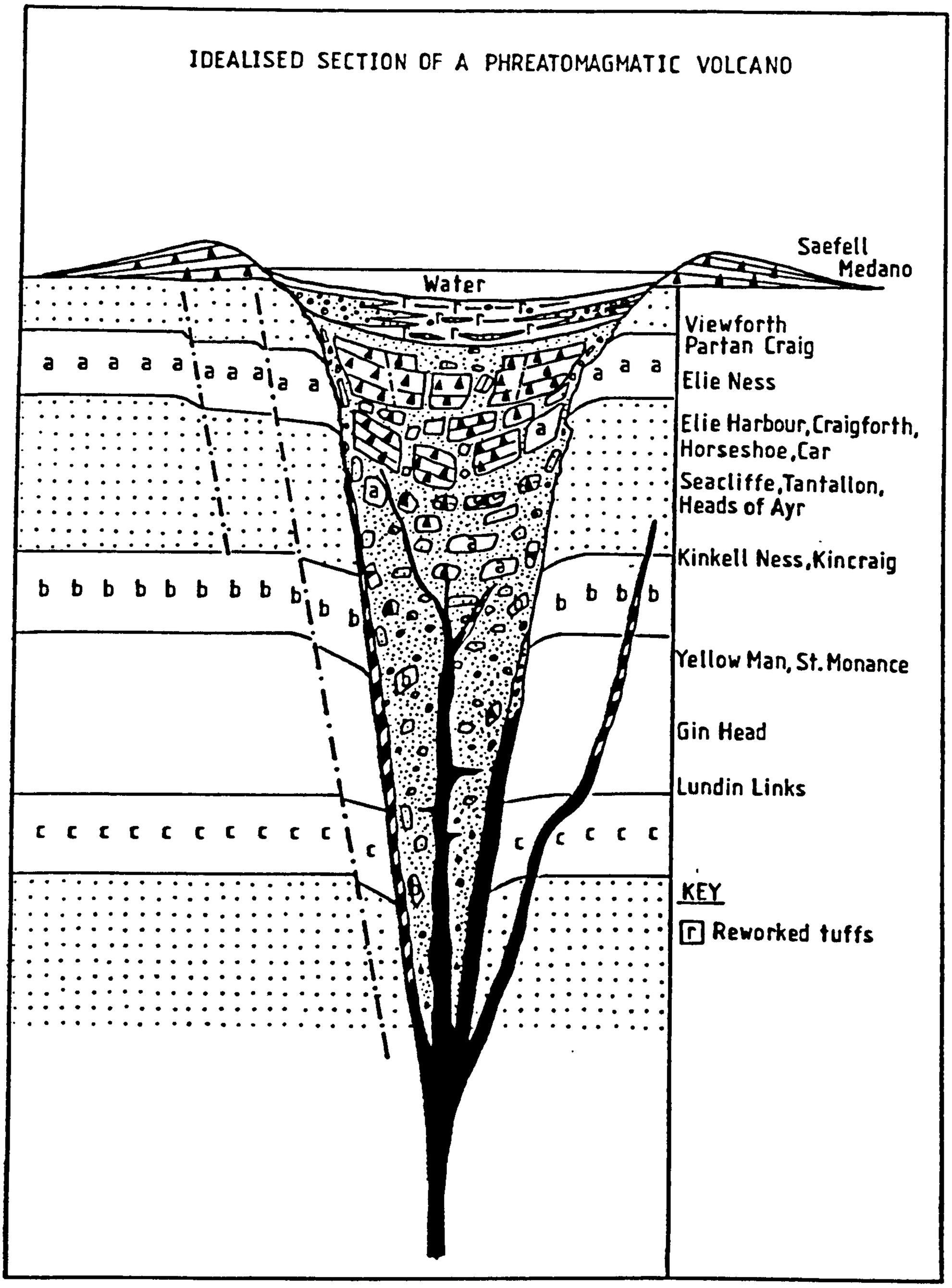

Fig. 7.5 Schematic section of a phreatomagmatic volcano showing the relative erosion levels exposed in each volcano studied. Relative levels were estimated purely on the basis of the type of diatreme infill, and are not quantitative measurements of the amount of collapse.

phreatomagmatic activity.

The relative erosion levels through the diatremes studied are shown schematically in Fig. 7.5 which is a composite, idealised cross-section through a diatreme. Comparisons between diatreme levels are purely qualitative and differences in internal structure and material depend on the erosion level, amount of collapse, size and duration of activity of any individual volcano.

7.5. Implications and Speculations

7.5.1 Recognition of ancient tuff sources

The present study has shown that detailed comparisons may be made between modern volcanoes and ancient, altered, eroded structures which are their commonly preserved remnants in the geological record. Such ancient structures provide information on diatreme processes which can never be directly studied in modern analogues. The recognition of the eruption type and original surface form of these diatremes is important since it indicates the former juxtaposition of magma with high-level or surface water. Water depth may also be qualitatively estimated from the morphology of the ash and the proportion of hyaloclastite to hyalotuff fragments.

Ash morphology may also be used to recognise phreatomagmatic products found interbedded in sedimentary sequences. Rapid alteration of unstable sideromelane glass and eventual replacement by calcite, chlorite or other minerals may preserve some of the original textures. Unreworked tuffs are most unlikely to be preserved in the geological record unless they occur within diatremes, so primary structures are of little use in determining the origin of distal tuffs.

7.5.2 Base-surge analogues

As well as occurring during phreatomagmatic volcanism, base-surges are generated by shallow nuclear explosions and during impact events which form craters. The lateral spread of radioactive fallout is greatly increased if base-surges

are generated, since they move horizontally at high velocities. If any water is vapourised during the explosion, its condensation removes heat from the surge and causes enhanced fallout because of clumping of moist particles.

Cratering events are not common on Earth but have greatly controlled the present topography of such planets as the Moon and Mercury. On meteorite impact, material is shock-heated, brecciating both meteorite and surface rocks. Hot gas from the volatilized meteorite and from heated material in the impact vicinity drives outward carrying comminuted ejecta (McKay & Morrison, 1971). Accretionary lapilli form within the surge by sintering of hot particles around a nucleus. The base-surge deposits form extensive breccia blankets around impact craters, some ejecta being hot enough to weld on deposition. Dunes and erosive channels associated with these deposits are analogous to structures found in terrestrial surge tuffs. McKay and Morrison (1971) argue that much of the regolith material found on the lunar surface is the product of impact crater induced surge deposition. Similar claims have been made for erosive channels on Mars (Reimers & Komar, 1979) which are thought to have been cut by base-surges. In this case the surges resulted from explosive activity when ascending magma contacted water derived from melting of the permafrost layers. Models of base-surges from terrestrial volcanoes may be adapted to the different gravity and atmospheric conditions on other planets and used to explain topographic features and distribution of materials on their surfaces.

7.5.3 Economic importance

Breccia pipes or diatremes are an important source of metals such as copper, gold and tin. The formation of explosive diatremes related to igneous intrusions generally involves phreatomagmatic activity rather than the exsolution of juvenile volatiles. Heated circulating groundwater systems above high-level intrusions are ideal environments for the generation of phreatic explosions and the formation of diatremes. Such breccia pipes are highly porous and form preferential sites for metal deposition

from hydrothermal solutions which have passed through the igneous body. The rapid alteration of breccia fragments favours their replacement by metal ores and is due to the continuous passage of groundwater through the rock and to the unstable nature of the chilled juvenile component. Alteration can take place very rapidly as at Taal Volcano, the Philippines, where breccia fragments were replaced by silica and pyrite in only 13 months (Wolfe, 1980). The great variety of lithic clast types often present in these breccias enhances the liklihood that at least one type will provide a preferential site for ore deposition.

Another class of economically important diatremes are kimberlite pipes, which are the major source of diamonds. Kimberlite magmas ascend relatively slowly, their yield strength allowing transport of deep-seated nodules (Sparks et al., 1977). At high crustal levels the magmas vesiculate freely and explosively interact with groundwater which has collected in joints and fissure systems utilised by the ascending magma. The exsolution of abundant CO_2 from these magmas aids the explosive activity and thoroughly alters the juvenile material. The high proportion of accessory lithic clasts in kimberlite pipes indicates that they probably terminated at the surface in a maar-type volcano, since diatreme enlargement by spalling favours the formation of collapse structures. This is confirmed by the existance of rare shallow craters underlain by kimberlite pipes in Tanzania (Edwards & Howkins, 1966). One such crater, Mwadui, contains kimberlite tuff, brecciated kimberlite and reworked kimberlitic sediments. The subsiding crater was filled with deltaic and lacustrine sediments, some of which contain diamonds. These sediments are thought to represent reworked products derived from the erosion of kimberlite tuffs surrounding the crater and kimberlite breccia within it.

Although some kimberlite pipes never reached the surface, similar to crypto-volcanic structures described in this report, most fed subaerial maar craters. It is suggested that base-surges from such craters might have deposited kimberlite tuffs some distance from the vent. Reworking of these tuffs, some of which must have been

diamond-bearing, formed the alluvial diamond deposits common in stable cratonic areas (Nixon, 1980). Where the subsequent erosion has been of minor extent, the recognition of kimberlite tuffs or their reworked equivalents might be used as an important guide to exploration for the source pipe.

CHAPTER 8
MAJOR THESIS CONCLUSIONS

Some of the important data chapter conclusions are briefly presented here, along with more general conclusions from the review and model chapters.

1. A threefold classification of explosive activity resulting from magma:water interaction has been adopted. Phreatic activity commonly forms maars which are underlain by large diatremes. Phreatomagmatic activity commonly forms tuff-rings which are underlain by moderately-sized diatremes. Surtseyan activity forms tuff-rings which are either underlain by small, poorly-developed diatremes, or have no diatreme beneath them.

2. The variety of products formed by the Medano tuff-ring resulted from variations in the depth of eruption focus and the amount of water interacting with the magma. The lithological similarity of all the Saefell tuffs reflects an essentially similar eruptive style throughout its activity, due to free access of water to the magma and less variation in the depth of eruption focus.

3. Surges were much more common during the Saefell activity than during the Medano activity, probably due to shallower explosions which resulted from water gaining access to the vent from the breached crater. Directed-blasts were important surge-forming mechanisms in both tuff-rings.

4. Scottish diatreme deposits undoubtedly represent the collapsed remnants of phreatomagmatic and phreatic volcanoes. The diatreme tuffs contain variable amounts of sediment, often making it impossible to determine whether they fed a maar or a tuff-ring.

5. Studies of diatremes at different erosion levels have allowed an idealised cross-section to be constructed. Where quantitative estimates of the level of collapse in a

diatreme cannot be made, this idealised section can be used to indicate the amount of collapse which has occurred relative to other diatremes of similar age and erosion level.

6. Diatreme processes are essentially the result of repeated explosions of varying magnitude which round and comminute large clasts. The overall effect of these blasts is to enlarge the diatreme and allow more material to subside into it. The repeated explosions may effect a crude size-sorting in the diatreme contents and result in gas-streaming at the pipe margins, rather than forming well-developed circulatory fluidized systems.

7. Base-surge deposits are relatively common in phreatomagmatic volcanoes and their structures indicate deposition by pulsatory, dissipative gravity flows. Surges are largely analogous to turbidity currents except that cooling of steam in surges results in the formation of regressive bedforms and plastering structures at the same time as flow power diminishes.Surge tuffs contain distinct sub-units which may be attributed to deposition from the head, body and tail of the flow.

8. Alteration of sideromelane to palagonite occurs rapidly in mild hydrothermal systems associated with crater thermal anomalies. After the cooling of intrusive magma palagonitization occurs much more slowly as a weathering process. Cation mobility during alteration of glass is probably a product of H^+ ion metasomatism and results in precipitation of authigenic minerals. In isolated pore spaces and vesicles these minerals grow under non-equilibrium conditions and some, especially zeolites, may take in large amounts of "foreign" cations. Alteration may also result in volume reduction of the tuffs, a factor which would aid post-volcanic subsidence.

9. Alteration rapidly seals pore spaces and indurates the tuffs allowing them to survive slow subsidence into

diatremes. Subsequent diagenesis is influenced by groundwater circulation from the country rocks, and by in situ alteration of unstable minerals. Most red tuffs studied contain high proportions of sedimentary material, the diagenesis of which resulted in in situ reddening of the entire rock.

10. Phreatomagmatic activity is purely a shallow crustal phenomenon associated with rocks containing groundwater. The occurrence of this type of volcanism indicates nothing about the mechanisms of magma ascent and little about magma composition and physical properties. Phreatomagmatic volcanoes are common, but products are volumetrically small and often buried beneath extensive lava flows. Preservation potential of maars and tuff-rings is slight because they commonly form and are reworked within active sedimentary environments. Ancient phreatomagmatic deposits are generally found within diatremes although it is thought that many tuffs interbedded with sediments may represent distal maar or tuff-ring products. Detailed petrographic examination of both altered and ancient tuffs by the present author has shown that phreatomagmatic tuffs may be recognised even when extensively reworked.

APPENDIX 1
GRAIN SIZE ANALYSIS

Thin section grain size analyses were determined by point counting after the method of Friedman (1958). The long axes of 350 grains were measured from each section. Fragments larger than 4mm were measured by grid point counting of slabs of the sampled tuffs.

The median, sorting and coarsest one percentile parameters were measured from cumulative/phi plots of grain size using the formulae of Inman (1952). In an attempt to convert the thin section grain size results to their sieve grain size equivalents the formulae of Harrell & Eriksson (1979) were used :-

Sieve Mdo = 0·121 + 1·03(X)

Sieve ϕ16 = 0·127 + 1·075(X)

Sieve ϕ84 = 0·452 + 0·895(X)

Sieve C(ϕ1) = 0·164 + 1·137(X)

(where X is the appropriate phi value measured from cumulative thin section grain size curves).

One of the drawbacks of these formulae is that they apply to rounded quartz grains in mineralogically mature sediments rather than irregular basaltic glass fragments in lithic-rich tuffs. Nevertheless, it is thought that the use of the formulae allows better comparisons to be made with published sieve analyses of pyroclastic deposits.

A more important drawback with the conversion of thin section volume % to sieve weight % values is the variable density of the fragments in tuffs. This is not thought to pose too great a problem in the case of the Recent tuff-rings (Chapters 2,3) where the tuffs largely comprise juvenile fragments. In the case of many of the diatreme deposits, however, their high lithic content means that conversion from volume % to weight % cannot be easily carried out. Grain size graphs of the diatreme deposits have thus been quoted as volume % and this factor must be taken into consideration when comparing them to sieved pyroclastics.

APPENDIX 2
ELECTRON MICROPROBE TECHNIQUES

Quantitative analyses were carried out on polished thin sections using a JEOL JX-A 50A microprobe fitted with a LINK 860 Series 2 Energy Dispersive System (E.D.S.). Operating details were as follows :- accelerating voltage, 20kV; beam current, 1nA; count time, 100s. Calibration standards used for major element analyses were :- Na - jadeite; Mg - MgO; Al - Al_2O_3; Si and Ca - wollastonite; K - orthoclase; Ti - TiO_2; Mn - rhodonite and Fe - metallic iron.

X-ray mapping was carried out using a LINK Digimap system with a picture count time of 200ms per spot and a line scan count time of 500ms. Raw data from the mapping was numerically enhanced to display the often low concentrations of elements present in basaltic glass. Backscattered electron image (B.E.I.) pictures were used to locate areas for mapping and proved of great use in detecting slight compositional variations within glass and mineral phases.

The microprobe was used in a scanning electron microscope mode to study the detailed morphology of the ash and its alteration products. Semi-quantitative analyses were carried out using the E.D.S. system to identify unknown phases which were then photographed.

REFERENCES

ABDEL-MONEM,A., WATKINS,N.D. and GAST,P.W., 1968. Volcanic stratigraphy and magnetic polarity history of the Canary Islands (abstract). Int. Ass. Volc. Tenerife.

ALEXANDER,W.R., 1980. A description of the geology of an area of Central Ayrshire, Scotland. Unpublished B.Sc. thesis, University of Edinburgh.

ALEXANDERSSON,T., 1972. The sedimentary xenoliths from Surtsey : turbidites indicating shelf growth. Surtsey Res. Prog. Rep. 6: 101-116.

AL-SALEH,S. and KHALAF,F.I., 1982. Surface textures of quartz grains from various Recent sedimentary environments in Kuwait. J. Sediment. Petrol. 52: 215-226.

ALLEN,J.R.L., 1982. Sedimentary Structures : their character and physical basis, Vol. 2. Developments in Sedimentology, 30B. Elsevier, Amsterdam.

BALLANCE,P.F., 1964. Streaked-out mud ripples below Miocene turbidites, Puriri Formation, New Zealand. J. Sediment. Petrol. 34: 91-101.

BELT,E.S., 1967. Sedimentology of Carboniferous Cementstone Facies, British Isles and Eastern Canada. J. Geol. 75: 711-721.

BONATTI,E., 1965. Palagonite hyaloclastites and alteration of volcanic glass in the ocean. Bull. Volcanol. 28: 257-269.

BOOTH,B., 1973. The Granadilla pumice deposit of Southern Tenerife, Canary Islands. Proc. Geol. Assoc. 84: 353-369.

CAMUS,G., BOIVIN,P., DE GOER de HERVE,A., GOURGAUD,A., KIEFFER,G., MERGOIL,J. and VINCENT,P.M., 1981. Le Capelinhos (Faial, Azores) vingt ans apres son eruption : le modele eruptif "Surtseyan" et les anneaux de tuffs hyaloclastiques. Bull. Volcanol. 44: 31-42.

CHAPMAN,N.A., 1974. Ultrabasic inclusions from the Coalyard Hill vent, Fife. Scott. J. Geol. 10:223-227.

CHRISTIANSEN,R.L. and PETERSON,D.W., 1981. Chronology of the 1980 eruptive activity of Mount St. Helens. U.S.G.S. Prof. Pap. 1250: 17-30.

CLOOS,H., 1941. Bau und Tatigkeit von Tuffschloten. Geol. Rdsch. 32: 703-800.

CLOUGH,C.T., BARROW,G., CRAMPTON,C.B., MAUFE,H.B., BAILEY, E.B. and ANDERSON,E.M., 1910. The geology of East Lothian, 2nd. edition. Mem. Geol. Surv. Gt. Br.

COE,K., 1966. Intrusive tuffs of West Cork, Ireland. Q. J. Geol. Soc. London. 122: 1-28.

COLEMAN,J.M., 1969. Brahmaputra River, channel processes and sedimentation. Sediment. Geol. 3: 129-239.

COLGATE,S.A. and SIGURGEIRSSON,T., 1973. Dynamic mixing of water and lava. Nature 244: 552-555.

COLLINSON,J., 1978. Alluvial sediments, in: Sedimentary environments and facies. H.G. Reading (ed.), Blackwell.

COLVINE,R.J.L., 1968. Pyrope from Elie, Fife. Scott. J. Geol. 4: 283-286.

CROWE,B.M. and FISHER,R.V., 1973. Sedimentary structures in base-surge deposits with special reference to cross-bedding, Ubehebe Craters, Death Valley, California. Bull. Geol. Soc. Am. 84: 663-682.

DEER,W.A., HOWIE,R.A. and ZUSSMAN,J., 1975. An introduction to the rock forming minerals. Longman, London.

EDWARDS,C.B. and HOWKINS J.B., 1966. Kimberlites in Tanganyika with special reference to the Mwadui occurrence. Econ. Geol. 61: 537-554.

EXNER,F.M., 1920. Zur Physik der dunen. Sitzungsb. der Akad. Wissensch. Wien. 2a, 129.

FISHER,R.V., 1977. Erosion by volcanic base-surge density currents : U-shaped channels. Bull. Geol. Soc. Am. 88: 1287-1297.

FISHER,R.V., 1979. Models for pyroclastic surges and pyroclastic flows. J. Volcanol. Geotherm. Res. 6: 305-318.

FISHER,R.V. and WATERS,A.C., 1970. Base-surge bed forms in maar volcanoes. Am. J. Sci. 268: 157-180.

FORSYTH,I.M., CHISHOLM,M.A., ELLIOT,R.W., FRANCIS,E.H. and WILSON,R.B., 1977. The geology of East Fife. Mem. Geol. Surv. Gt. Br.

FRANCIS,E.H., 1962. Volcanic neck emplacement and subsidence structures at Dunbar, SE Scotland. Trans. Roy. Soc. Edinb. 65: 41-58.

FRANCIS,E.H., 1968. Effect of sedimentation on volcanic processes, including neck-sill relationships, in the British Carboniferous. Int. Geol. Congr. 2: 163-174.

FRANCIS,E.H., 1970. Bedding in Scottish (Fifeshire) tuff-pipes and its relevance to maars and calderas. Bull. Volcanol. 34: 697-712.

FRANCIS,E.H., 1983 (in press). Magma and sediment 2 - problems of interpreting palaeovolcanics buried in the stratigraphic column. Q. J. Geol. Soc.

FRANCIS,E.H. and HOPGOOD,A.M., 1970. Volcanism and the Ardross Fault, Fife, Scotland. Scott. J. Geol. 6: 162-185.

FRANCIS,P.W. and THORPE,R.S., 1974. Significance of lithological and morphologic variations of pyroclastic cones. Bull. Geol. Soc. Am. 85: 927-930.

FURNES,H., 1974. Volume relations between palagonite and authigenic minerals in hyaloclastites, and its bearing on the rate of palagonitization. Bull. Volcanol. 38: 173-186.

FURNES,H., 1975. Experimental palagonitization of basaltic glasses of varied composition. Contrib. Mineral. Petrol. 50: 105-113.

FUSTER,J.M., ARANA,V., BRANDLE,J.L., NAVARRO,M., ALONSO,U. and APARICIO,A., 1968. Geology and volcanology of the Canary Islands, Tenerife. Inst. "Lucas Mallada" Madrid.

GRAHAM,A.M. and UPTON,B.G.J., 1978. Gneisses in diatremes, Scottish Midland Valley : petrology and tectonic implications. Q. J. Geol. Soc. London 135: 219-228.

GRIEVES,I., 1981. Aspects of the geology of some of the Lower Carboniferous volcanic pipes of North Berwick, Scotland. Unpublished B.Sc, thesis, University of Leeds.

GUTMANN,J.T., 1976. Geology of Crater Elegante, Sonora, Mexico. Bull. Geol. Soc. Am. 87: 1718-1729.

HAMILTON,W. and MYER,W.B., 1963. Menan Buttes, cones of glassy basalt in the Snake River Plain, Idaho. U.S.G.S. Prof. Pap. 450 E2: E114-118.

HARRELL,J.A. and ERIKSSON,K.A., 1979. Empirical conversion equations for thin-section and sieve derived size distribution parameters. J. Sediment. Petrol. 49: 273-280.

HARVEY,M.R., 1974. The geology of the older pyroclastic rocks of Deception Island. Unpublished Ph.D. thesis, University of Leeds.

HAWTHORNE,J.B., 1975. Model of a kimberlite pipe. Phys. Chem. Earth 9: 1-15.

HAY,R.L., 1966. Zeolites and zeolitic reactions in sedimentary rocks. Geol. Soc. Am. Sp. Pap 85.

HAY,R.L. and IIJIMA,I., 1968a. Petrology of palagonite tuffs of Koko Craters, Oahu, Hawaii. Contrib. Mineral. Petrol. 17: 141-154.

HAY,R.L. and IIJIMA, 1968b. Nature and origin of palagonite tuffs of the Honolulu Group on Oahu, Hawaii. Geol. Soc. Am. Mem. 116: 331-376.

HEARN,B.C.(Jr.), 1968. Diatremes with kimberlitic affinities in North-central Montana. Science 159: 622-625.

HEIKEN,G., 1971. Tuff-rings : examples from the Fort Rock-Christmas Lake Valley Basin, South-central Oregon. J. Geophys. Res. 76: 5615-5626.

HEIKEN,G., 1972a. Tuff-rings : examples from the Fort Rock-Christmas Lake Valley Basin, South-central Oregon. Unpublished Ph.D. thesis, University of California, Santa Barbera.

HEIKEN,G., 1972b. Morphology and petrography of volcanic ashes. Bull. Geol. Soc. Am. 83: 1961-1988.

HEIKEN,G., 1974. An atlas of volcanic ash. Smithson. Contrib. Earth Sci. 12.

HOBLITT,R.P., MILLER,C.D. and VALLANCE,J.W., 1981. Origin and stratigraphy of the deposit produced by the May 18 directed blast. U.S.G.S. Prof. Pap. 1250: 401-420.

HONNOREZ,J. and KIRST,P., 1975. Submarine basaltic volcanism : morphometric parameters for discriminating hyaloclastics from hyalotuffs. Bull. Volcanol. 39: 441-465.

JAHNS,R.H., 1959. Collapse depressions of the Pinacate volcanic field, Sonora, Mexico. Arizona Geol. Soc., Southern Arizona Guidebook 2: 165-184.

JAKOBSSON,S.P., 1968. The geology and petrography of the Westmann Islands : a preliminary report. Surtsey Res. Prog. Rep. 4: 113-129.

JAKOBSSON,S.P., 1978. Environmental factors controlling the palagonitization of the Surtsey tephra, Iceland. Bull. Geol. Soc. Denmark 27: 91-105.

JAKOBSSON,S.P., 1979. Outline of the petrology of Iceland. Jokull 29: 57-73.

KELLER,J., 1974. Quaternary maar volcanism near Karapinar in Central Anatolia. Bull. Volcanol. 38: 378-396.

KENNEDY,G.C. and NORDLIE,B.E., 1968. The genesis of diamond deposits. Econ. Geol. 63: 489-499.

KIENLE,J., KYLE,P.R., SELF,S., MOTYKA,R.J. and LORENZ,V., 1980. Ukinrek maars, Alaska, 1. April 1977 eruption sequence, petrology and tectonic setting. J. Volcanol. Geotherm. Res. 7: 11-38.

KJARTANSSON,G., 1967. Nokkrar nyrar C^{14} aldursakvardanir. Nattur. Fraed. 36, 3: 126-141.

KOKELAAR,B.P., 1982. Fluidization of wet sediments during the emplacement and cooling of various igneous bodies. Q. J. Geol. Soc. London. 139: 21-34.

KOKELAAR,B.P. and DURANT,G.P., 1982. The submarine eruption and erosion of Surtla (Surtsey), Iceland. J. Volcanol. Geotherm. Res. (in press).

KUENEN,P.H., 1964. Experimental abrasion of pebbles, 4 : eolian action. J. Geol. 69: 427-449.

KRINSLEY,D. and DONAHUE,J., 1968. Environmental interpretation of sand grain surface textures by electron microscopy. Bull. Geol. Soc. Am. 79: 743-748.

KRINSLEY,D. and DOORNKAMP,J.C., 1973. Atlas of quartz sand surface textures. Cambridge University Press, London.

LELIAVSKY,S., 1955. An introduction to fluvial hydraulics. Constable, London.

LORENZ,V., 1971. Collapse structures in the Permian of the Saar-Nahe area, Southwest Germany. Geol. Rdsch. 60: 924-948.

LORENZ,V., 1972. Sekundare Rotfarbung in Rotliegenden der Saar-Nahe-Senke, SW-Deutschland. Neues. Jb. Geol. Palaeont.(Mh). 6: 356-370.

LORENZ,V., 1973. On the formation of maars. Bull. Volcanol. 37: 183-204.

LORENZ,V., 1974a. Studies of the Surtsey tephra deposits. Surtsey Res. Prog. Rep. 7: 72-79.

LORENZ,V., 1974b. Vesiculated tuffs and associated features. Sedimentology 21: 273-291.

LORENZ,V., 1975. Formation of phreatomagmatic maar-diatreme volcanoes and its relevance to kimberlite diatremes. Phys. Chem. Earth 9: 17-27.

LORENZ,V., 1980. Explosive volcanism of alkalibasaltic to kimberlitic melts. Lithos 13: 217-219.

LORENZ,V. and BUCHEL,G., 1980. Zur Vulkanologie der Maare und Schlackenkegel der Westeifel. Mitt. Pollichia. 68: 29-100.

LORENZ,V., McBIRNEY,A.R. and WILLIAMS,H., 1970. An investigation of volcanic depressions 3: maars, tuff-rings, tuff-cones and diatremes. NASA Prog. Rep. NGR-38-003-012.

MacFARLANE,D.J. and RIDLEY,W.I., 1968. An interpretation of the gravity data for Tenerife, Canary Islands. Earth Planet. Sci. Lett. 4: 481-486.

MACHADO,F., PARSONS,W., RICHARDS,A.F. and MULFORD,J.W., 1962. Capelinhos eruption of Fayal Volcano, Azores 1957-58. J. Geophys. Res. 67: 3519-3529.

MARTIN,N.R., 1955. Lower Carboniferous Volcanism near North Berwick, Scotland. Bull. Geol. Surv. Gt. Br. 7: 90-99.

MATTSON,P. and ALVAREZ,W., 1973. Base surge deposits in Pleistocene volcanic ash near Rome. Bull. Volcanol. 37: 553-572.

McADAM,A.D., 1975. North Berwick, in: The Geology of the Lothians and SE Scotland. G.Y. Craig and P.Mcl. Duff. (eds), Scottish Academic Press.

McCALLUM,M.E., WOOLSEY,T.S. and SCHUMM,S.A., 1976. A fluidisation mechanism for subsidence of bedded tuffs in diatremes and related volcanic vents. Bull. Volcanol. 39: 512-527.

McGETCHIN,T.R. and ULLRICH,G.W., 1973. Xenoliths in maars and diatremes with inferences for the Moon, Mars and Venus. J. Geophys. Res. 78: 1833-1853.

McKAY,D.S. and MORRISON,D.A., 1971. Lunar breccias. J. Geophys. Res. 76: 5658-5669.

McGETCHIN,T.R., 1966. Geology of the Moses rock intrusion, San Juan County, Utah. U.S.G.S. Astrogeol. Studies Prog. Rep. B: 231-253.

MIDDLETON,G.V., 1966. Experiments on density and turbidity currents. Can. J. Earth Sci. 3: 523-546.

MIDDLETON,G.V. and HAMPTON,M.A., 1976. Subaqueous sediment transport and deposition by sediment gravity flows, in: Marine transport and environmental management. D.J. Stanley and D.J.P. Swift (eds.), Wiley.

MOORE,J.G., 1967. Base surge in Recent volcanic eruptions. Bull. Volcanol. 30: 337-363.

MOORE,J.G., NAKAMURA,K. and ALVAREZ,A., 1966. The 1965 eruption of Taal Volcano. Science 151: 955-960.

MOORE,J.G. and PECK,D.L., 1962. Accretionary lapilli in volcanic rocks of the western continental United States. J. Geol. 70: 182-193.

MOORE,J.G. and SISSON,T.W., 1981. Deposits and effects of the May 18 pyroclastic surge. U.S.G.S. Prof. Pap. 1250: 421-438.

MULLER,G. and VEYL,G., 1957. The birth of Nilahue; a maar-type volcano at Rininahue, Chile. Int. Geol. Congr. Rep. 20, Sect. 1: 375-396.

NAIRN,I.A., WOOD,C.P. and HEWSON,C.A.Y., 1979. Phreatic eruptions of Ruapehu : April 1975. N.Z. J. Geol. Geophys. 22: 155-173.

NAYUDU,Y.R., 1964. Palagonite tuffs (hyaloclastites) and the products of post-eruptive processes. Bull. Volcanol. 27: 391-401.

NELSON,L.S. and DUDA,P.M., 1982. Steam explosions of molten iron oxide drops : initiation at small pressurizations. Nature 296: 844-846.

NIXON,P.H., 1980. The morphology and mineralogy of diamond pipes. Publs. Geol. Dep. & Extension Service, Univ. West. Aust. 5: 32-47.

OLLIER,C., 1974. Phreatic eruptions and maars, in: Physical Volcanology. L. Civetta et al (eds.), Developments in Solid Earth Geophysics 6, Elsevier.

PEACOCK,M.A., 1926. The palagonite formation of Iceland. Geol. Mag. 63: 385-399.

REIMERS,C.E. and KOMAR,P.D., 1979. Evidence for explosive density currents on certain Martian volcanoes. Icarus 39: 88-110.

REINECK,H.E. and SINGH,I.B., 1973. Depositional sedimentary environments. Springer-Verlag.

RICHARDS,A.F., 1959. Geology of the Islas Revillagigedo, Mexico 1. Birth and development of Volcan Barcena, Isla San Benedicto. Bull. Volcanol. 22: 73-123.

RIDLEY,W.I., 1970. The petrology of the Las Canadas volcanoes, Tenerife, Canary Islands. Contrib. Mineral. Petrol. 26: 124-160.

SCHMID,R., 1981. Descriptive nomenclature and classification of pyroclastic deposits and fragments : recommendations of the I.U.G.S. Subcommission on the systematics of igneous rocks. Geology 9: 41-43.

SCHMINCKE,H., FISHER,R.V. and WATERS,A.C., 1973. Antidune and chute and pool structures in the base surge deposits of the Laacher See area, Germany. Sedimentology 20: 553-574.

SCHMINCKE,H., BREY,G. and STAUDIGEL,H., 1974. Craters of phreatomagmatic origin on Gran Canaria, Canary Islands. Naturwiss. 61: 125.

SELF,S., KIENLE,J. and HUOT,J.-P., 1980. Ukinrek Maars Alaska 2 : deposits and formation of the 1977 craters. J. Volcanol. Geotherm. Res. 7: 39-66.

SELF,S. and SPARKS,R.S.J., 1978. Characteristics of pyroclastic deposits formed by the interaction of silicic magma and water. Bull. Volcanol. 41: 196-212.

SHERIDAN,M.F., 1971. Particle size characteristics of pyroclastic tuffs. J. Geophys. Res. 76: 5627-5634.

SHERIDAN,M.F., BARBERI,F., ROSI,M. and SANTACROCE,R., 1981. A model for Plinian eruptions of Vesuvius. Nature 289: 282-285.

SHERIDAN,M.F. and UPDIKE, R.G., 1975. Sugarloaf Mountain tephra - a Pleistocene rhyolitic deposit of base-surge origin in Northern Arizona. Bull. Geol. Soc. Am. 86: 571-581.

SHOTTON,F.W. and WILLIAMS,R.E.G., 1971. Birmingham University Radiocarbon Dates 5. Radiocarbon 13: 150.

SIMPSON,J.E., 1972. A comparison between laboratory and atmospheric density currents. Q. J. Meterol. Soc. 95: 758-765.

SKIPPER,K., 1971. Antidune cross-stratification in a turbidite sequence, Chloridorme Formation, Gaspe, Quebec. Sedimentology 17: 51-68.

SPARKS,R.S.J., 1978. The dynamics of bubble formation and growth in magmas : a review and analysis. J. Volcanol. Geotherm. Res. 3: 1-37.

SPARKS,R.S.J., PINKERTON,H. and MACDONALD,R., 1977. The transport of xenoliths in magmas. Earth Planet. Sci. Lett. 35: 234-238.

SPARKS,R.S.J. and WALKER,G.P.L., 1977. The significance of vitric enriched air-fall ashes associated with crystal-enriched ignimbrites. J. Volcanol. Geotherm. Res. 2: 329-341.

STOKES,K.R., 1971. Further investigations into the nature of the materials chlorophaiite and palagonite. Mineralog. Mag. 38: 205-214.

STRAATEN,L.M.J.U.van, 1953. Rhythemic pattern on Dutch North Sea beaches. Geol. Mijnbouw 15e: 31-43.

TAZIEFFE,M., 1959. L'Eruption de 1957-1958 et la tectonique de Faial (Azores). Serv. Geol. Portugal Mem. 4: 71-88.

THORARINSSON,S., 1967. Surtsey - The new island in the North Atlantic. Viking Press.

THORARINSSON,S., EINARSSON,Th., SIGVALDASON,G. and ELISSON,G., 1964. The submarine eruption off the Vestmann Islands 1963-64 - a preliminary report. Bull. Volcanol. 27: 435-446.

TRYGGVASON,E., 1968. Result of precision levelling in Surtsey. Surtsey Res. Prog. Rep. 4: 149-157.

TURNER,P., 1980. Continental red beds. Developments in Sedimentology, 29. Elsevier, Amsterdam.

UPTON,B.G.J., 1982. Carboniferous to Permian volcanism in the stable foreland, in: Igneous rocks of the British Isles. D.S. Sutherland (ed.), Wiley.

WALKER,G.P.L., 1971. Grain size characteristics of pyroclastic deposits. J. Geol. 79: 696-714.

WALKER,G.P.L., 1973. Explosive volcanic eruptions - a new classification scheme. Geol. Rdsch. 62: 431-446.

WALKER,G.P.L. and CROASDALE,R., 1971. Characteristics of some basaltic pyroclasts. Bull. Volcanol. 35: 303-317.

WALKER,T.R., 1976. Diagenetic origin of continental red beds, in: The continental Permian of central west and south Europe. H. Falke (ed.), Riedel.

WATERS,A.C. and FISHER,R.V., 1971. Base-surges and their deposits : Capelinhos and Taal Volcanoes. J. Geophys. Res. 76: 5596-5614.

WHYTE,F., 1964. The Heads of Ayr vent. Trans. Geol. Soc. Glasgow 25: 72-97.

WILSON,L., 1980. Relationships between pressure, volatile content and ejecta velocity in three types of volcanic explosion. J. Volcanol. Geotherm. Res. 8: 297-313.

WILSON,L., SPARKS,R.S.J., WATKINS,N.D. and HUANG,T.C., 1978. The control of volcanic column heights by eruption energetics and dynamics. J. Geophys. Res. 83: 1829-1836.

WINKLER,H.G.F., 1978. The petrogenesis of metamorphic rocks. Springer-Verlag.

WOHLETZ,K.H. and SHERIDAN,M.F., 1979. A model of pyroclastic surge. Geol. Soc. Am. Spec. Pap. 180: 177-194.

WOLFE,J.A., 1980. Fluidisation versus phreatomagmatic explosions in breccia pipes. Econ. Geol. 75: 1105-1109.

WOMER,M.B., GREELY,R. and KING,J.S., 1980. The geology of Split Butte - A maar of the South-central Snake River Plain, Idaho. Bull. Volcanol. 43: 453-472.

WOOD,C.A. (in press). Encyclopaedia of volcanology.

WRIGHT,J.V. and WALKER,G.P.L., 1977. The ignimbrite source problem : significance of a co-ignimbrite lag-fall deposit. Geology 5: 729-732.

WRIGHT,J.V., SMITH,A.L. and SELF,S., 1980. A working terminology of pyroclastic deposits. J. Volcanol. Geotherm. Res. 8: 315-336.

INSERT KEY TO

SCOTTISH DIATREME MAPS

AND LOGS OF BEDDED TUFFS

KEY TO SCOTTISH DIATREME MAPS

Beach sand

Bedded tuff

Unbedded tuff

Tuffite

Collapsed bedded tuff

Country rock sediments

Cementstone

Red Basaltic Tuff Formation

Green Basaltic Tuff Formation

East Lothian country rocks

Basaltic intrusion

Basaltic breccia

Tuffisite

Tuffisitic breccia

Geological boundary

Inferred boundary

Fault

Bedding strike and dip

KEY TO LOGS OF BEDDED TUFFS

Volcanic bomb

Block impact sag

Blocks in tuff

Lapilli lens

Debris flow

Poorly-defined beds

Well-defined beds

Flaser bedding

Accretionary lapilli

Clast imbrication

Channel

Cross-bedding

Dune structure

Slump folds

Convolute bedding

Grain size

Ash tuff

Ash-lapilli tuff

Lapilli tuff

Lapilli-block tuff

Agglomerate

Very coarse agglomerate